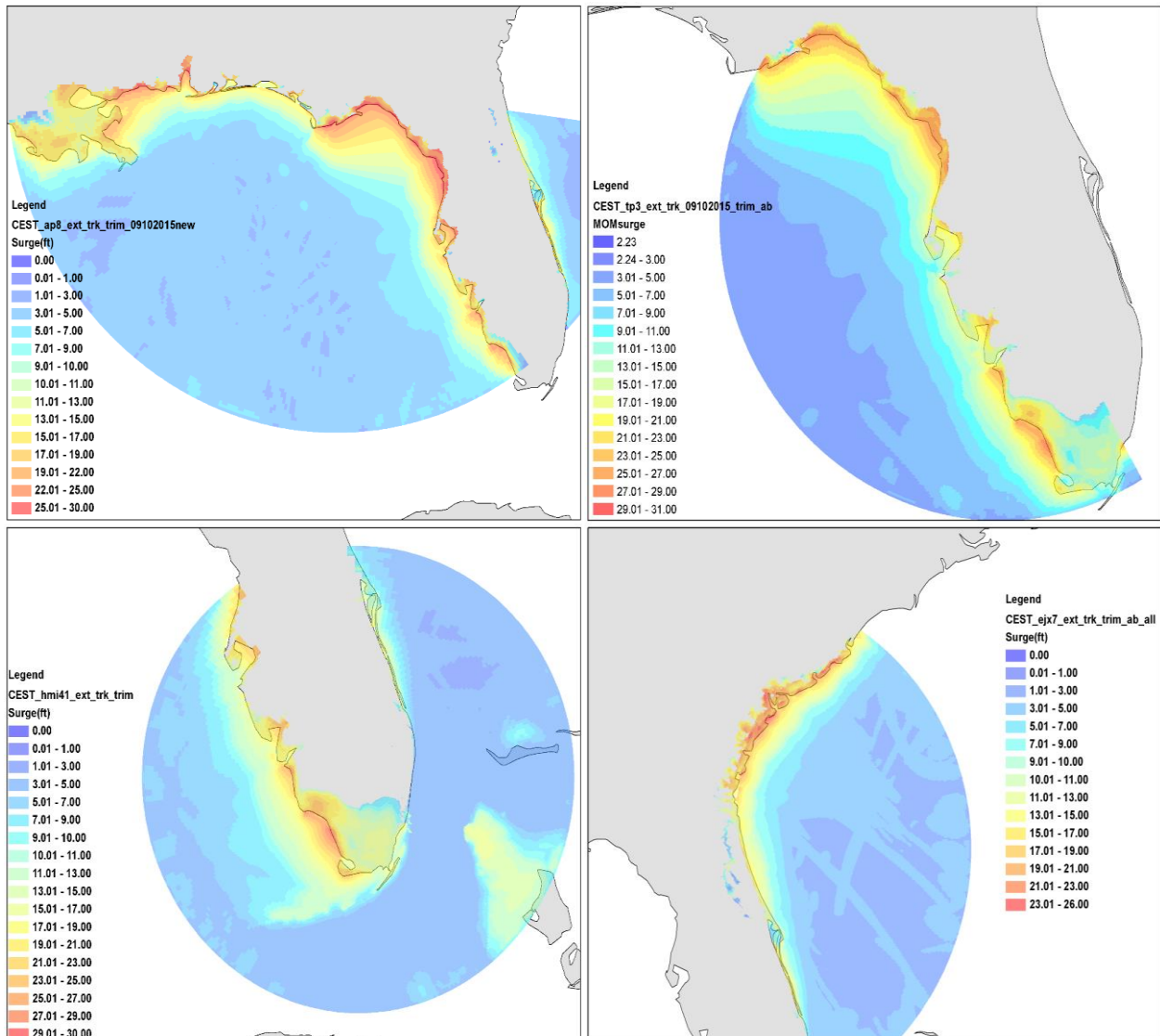


FLORIDA PUBLIC FLOOD LOSS MODEL V1.0

Submitted in compliance with the 2017 Standards of the
Florida Commission on Hurricane Loss Projection Methodology
Submitted on Feb. 29, 2020



Flood Model Identification

Name of Flood Model: Florida Public Flood Loss Model

Flood Model Version Identification: V1.0

Name of Modeling Organization: Florida International University

Street Address: Extreme Event Institute.

City, State, ZIP Code: Miami, Florida 33199

Mailing Address, if different from above: Same as above

Contact Person: Shahid S. Hamid

Phone Number: 305-348-2727

Fax: 305-348-1761

E-mail Address: hamids@fiu.edu

Date: Feb. 29, 2020

February 29, 2020

Chair, Florida Commission on Hurricane Loss Projection Methodology
c/o Donna Sirmons
Florida State Board of Administration
1801 Hermitage Boulevard, Suite 100
Tallahassee, FL 32308

Dear Commission Chairman:

I am submitting version 1.0 of Florida Public Flood Loss Model for review by the Commission. Enclosed are 8 bound copies of our submission document. The FPFLM model has been reviewed by professionals having credentials and/or experience in the areas of meteorology, hydrology, coastal surge, engineering, statistics and computer science; for compliance with the Standards, as documented by the expert certification forms G1-G5, G7. The actuarial forms and review will be submitted later.

Sincerely,



Shahid Hamid, Ph.D., CFA
Professor of Finance, and
Director, Laboratory for Insurance, Economic and Financial Research, Extreme Event Institute
RB 233, Department of Finance, College of Business
Florida International University
Miami, FL 33199
tel: 305 348 2727 fax: 305 348 4245

Statement of Compliance and Trade Secret Disclosure Items

The Florida Public Flood Loss Model 1.0 is intended to comply with each Standard of the 2017 Report of Activities released by the Florida Commission on Hurricane Loss Projection Methodology. The required disclosures, forms, and analysis are contained herein.

The source code for the loss model will be available for review by the Professional Team.

Flood Model Submission Checklist

A. Please indicate by checking below that the following has been included in your submission documentation to the Florida Commission on Flood Loss Projection Methodology.

Yes	No	Item
X		1. Letter to the Commission
X		a. Refers to the signed Expert Certification forms and states that professionals having credentials and/or experience in the areas of meteorology, hydrology, hydraulics, statistics, structural engineering, actuarial science, and computer/ information science have reviewed the model for compliance with the standards
X		b. States model is ready to be reviewed by the Professional Team
X		c. Any caveats to the above statements noted with a detailed explanation
X		1. Summary statement of compliance with each individual standard and the data and analyses required in the disclosures and forms
X		3. General description of any trade secret information the modeling organization intends to present to the Professional Team and the Commission
X		4. Flood Model Identification
X		5. Eight bound copies (duplexed)
X		6. Link e-mailed to SBA staff containing all required documentation that can be downloaded from a single ZIP file
	X	a. Submission document and Form AF-1, Zero Deductible Personal Residential Standard Flood Loss Costs in PDF format
X		b. PDF submission file supports highlighting and hyperlinking, and is bookmarked by standard, form, and section
X		c. Data file names include abbreviated name of modeling organization, standards year, and form name (when applicable)
	X	d. Forms VF-3, Flood Mitigation Measures Range of Changes in Flood Damage, AF-1, Zero Deductible Personal Residential Standard Flood Loss Costs, AF-2, Total Flood Statewide Loss Costs, AF-3, Personal Residential Standard Flood Loss Costs by ZIP Code, AF-4, Flood Output Ranges, and Form AF-6, Flood Probable Maximum Loss for Florida in Excel format
X		e. Forms VF-4, Coastal Flood Mitigation Measures, Mean Coastal Flood Damage Ratios and Coastal Flood Damage/\$1,000 (Trade Secret Item), VF-5, Inland Flood Mitigation Measures, Mean Inland Flood Damage Ratios and Inland Flood Damage/\$1,000 (Trade Secret Item), and AF-5, Logical Relationship to Flood Risk (Trade Secret Item) in Excel format if not considered as Trade Secret
X		7. All hyperlinks to the locations of forms are functional
X		8. Table of Contents
X		9. Materials consecutively numbered from beginning to end starting with the first page (including cover) using a single numbering system, including date and time in footnote
X		10. All tables, graphs, and other non-text items consecutively numbered using whole numbers, listed in Table of Contents, and clearly labeled with abbreviations defined
X		11. All column headings shown and repeated at the top of every subsequent page for forms and tables
X		12. Standards, disclosures, and forms in <i>italics</i> , modeling organization responses in non-italics
X		13. All graphs and maps conform to guidelines in II. Notification Requirements A.4.e
X		14. All units of measurement clearly identified with appropriate units used

Yes	No	Item
x		15. All forms included in submission appendix except Trade Secret Items. If forms designated as a Trade Secret Item are not considered as trade secret, those forms are to be included in the submission appendix
x		16. Hard copy documentation identical to electronic version
x		17. Signed Expert Certification Forms GF-1 to GF-8
x		18. All acronyms listed and defined in submission appendix

B. Explanation of “No” responses indicated above. (Attach additional pages if needed.)

The AF actuarial forms are not completed and reviewed by the project actuary. They will be submitted later.

Florida Public Flood Loss Model 1.0



Feb. 29, 2020

Model Name and Identification

Modeler Signature

Date

Contents

GENERAL FLOOD STANDARDS	21
GF-1 Scope of the Flood Model and Its Implementation.....	21
GF-2 Qualifications of Modeling Organization Personnel and Consultants Engaged in Development of the Flood Model.....	91
GF-3 Insured Exposure Location.....	99
GF-4 Independence of Flood Model Component	102
GF-5 Editorial Compliance.....	103
METEOROLOGICAL FLOOD STANDARDS	105
MF-1 Flood Event Data Sources.....	105
MF-2 Flood Parameters (Inputs).....	110
MF-3 Wind and Pressure Fields for Storm Surge.....	123
MF-4 Flood Characteristics (Outputs)	136
MF-5 Flood Probability Distributions.....	144
HYDROLOGICAL AND HYDRAULIC FLOOD Standards.....	146
HHF-1 Flood Parameters (Inputs).....	146
HHF-2 Flood Characteristics (Outputs).....	149
HHF-3 Modeling of Major Flood Control Measures.....	153
HHF-4 Logical Relationships Among Flood Parameters and Characteristics	156
STATISTICAL FLOOD STANDARDS	160
SF-1 Modeled Results and Goodness-of-Fit.....	160
SF-2 Sensitivity Analysis for Flood Model Output	172
SF-3 Uncertainty Analysis for Flood Model Output.....	174
SF-4 Flood Model Loss Cost Convergence by Geographic Zone	176
SF-5 Replication of Known Flood Losses	178
VULNERABILITY FLOOD STANDARDS	179
VF-1 Derivation of Personal Residential Structure Flood Vulnerability Functions	179
VF-2 Derivation of Personal Residential Contents Flood Vulnerability Functions.....	193
VF-3 Derivation of Personal Residential Time Element Flood Vulnerability Functions	199
VF-4 Flood Mitigation Measures.....	208
ACTUARIAL FLOOD STANDARDS.....	214
AF-1 Flood Modeling Input Data and Output Reports	214
AF-2 Flood Events Resulting in Modeled Flood Losses	224
AF-3 Flood Coverages.....	226
AF-4 Modeled Flood Loss Cost and Flood Probable Maximum Loss Level Considerations	228

AF-5 Flood Policy Conditions	231
AF-6 Flood Loss Outputs and Logical Relationships to Risk.....	233
COMPUTER/INFORMATION FLOOD STANDARDS.....	237
CIF-1 Flood Model Documentation.....	237
CIF-2 Flood Model Requirements	239
CIF-3 Flood Model Architecture and Component Design.....	240
CIF-4 Flood Model Implementation	241
CIF-5 Flood Model Verification	243
CIF-6 Flood Model Maintenance and Revision.....	246
CIF-7 Flood Model Security	249
APPENDICES	250
Expert Review Letter	250
Form GF-1: General Flood Standards Expert Certification	257
Form GF-2: Meteorological Flood Standards Expert Certification	258
Form GF-3: Hydrological and Hydraulic Flood Standards Expert Certification.....	259
Form GF-4: Statistical Flood Standards Expert Certification.....	259
Form GF-5: Vulnerability Flood Standards Expert Certification	261
Form GF-6: Actuarial Flood Standards Expert Certification.....	262
Form GF-7: Computer/Information Flood Standards Expert Certification.....	263
Form GF-8: Editorial Review Expert Certification	264
Form HHF-1: Historical Event Flood Extent and Elevation or Depth Validation Maps	265
Form HHF-2: Coastal Flood Characteristics by Annual Exceedance Probability	276
Form HHF-3: Coastal Flood Characteristics by Annual Exceedance Probabilities (Trade Secret Item)	283
Form HHF-4: Inland Flood Characteristics by Annual Exceedance Probability.....	298
Form HHF-5: Inland Flood Characteristics by Annual Exceedance Probabilities (Trade Secret Item)	302
Form SF-1: Distributions of Stochastic Flood Parameters (Coastal, Inland).....	311
Form SF-2: Examples of Flood Loss Exceedance Estimates (Coastal and Inland Combined).....	312
Form VF-1: Coastal Flood with Damaging Wave Action	313
Form VF-2: Inland Flood by Flood Depth.....	328
Form VF-3: Flood Mitigation Measures, Range of Changes in Flood Damage	343
Form VF-4: Coastal Flood Mitigation Measures, Mean Coastal Flood Damage Ratios and Coastal Flood Damage/\$1,000 (Trade Secret Item).....	348
Form VF-5: Inland Flood Mitigation Measures, Mean Inland Flood Damage Ratios and Inland Flood Damage/\$1,000 (Trade Secret Item)	356
Form AF-1: Zero Deductible Personal Residential Standard Flood Loss Costs.....	364
Form AF-2: Total Flood Statewide Loss Costs.....	364

Form AF-3: Personal Residential Standard Flood Loss Costs by ZIP Code..... 364
Form AF-4: Flood Output Ranges 364
Form AF-5: Logical Relationship to Flood Risk (Trade Secret Item) 364
Form AF-6: Flood Probable Maximum Loss for Florida..... 364
List of Acronyms 364

List of Figures

Figure 1. Process to assure continual agreement and correct correspondence of databases, data files, and computer source code to slides, technical papers, and modeling organization documents. 22

Figure 2. Florida Public Hurricane Loss Model domain. Threat zone is delineated by red line. . 24

Figure 3. Examples of simulated hurricane tracks. Track colors correspond to storm intensity: red – Cat 4, orange – Cat 3, yellow – Cat 2, light blue – Cat 1, dark blue – TS..... 26

Figure 4. Comparison between the modeled and observed Willoughby and Rahn (2004) *B* dataset. 27

Figure 5. Observed and expected distribution for *Rmax*. The x-axis is the radius in statute miles, and the y-axis is the frequency of occurrence..... 28

Figure 6. Tropical cyclones observed by TMI during the period 1 Jan 1998 to 31 Dec 2000. Each dot represents one TRMM observation. (From Lonfat et al, 2004)..... 30

Figure 7. TMI-based rainfall climatology. (Based on data from Lonfat et al, 2004). 31

Figure 8. The populated areas (red rectangles) along the Florida coast where severe storm surge flooding could occur when a large and intense hurricane makes landfall. The coverage of Light Detection And Ranging (LiDAR) data from the Florida Department of Emergency Management (FDEM) is also displayed. 32

Figure 9. Component diagram of FPFLM with the storm surge..... 33

Figure 10. Topologic errors in the shoreline dataset derived from the LiDAR surveys for Franklin County in Florida. 38

Figure 11. Four Florida Basins that used by CEST Model..... 41

Figure 12. Extent of six inland basins..... 45

Figure 13. Extent of five isolated area models 48

Figure 14. a) Pressure distribution based on Walton et al. (1989); b) Pressure distribution in terms of the breaking wave height..... 52

Figure 15. Tsunami surge pressure distribution, reproduced based on Palermo et al. (2013a)... 53

Figure 16. Tsunami and Coastal Flood (CF) water forces..... 54

Figure 17. Conversion of a tsunami fragility function to a surge fragility function..... 54

Figure 18. Example of Coastal Flood Fragility Curves 56

Figure 19. Fragility functions for tsunami and moderate coastal flood condition (CF mod): a) 1-story on-grade timber; b) 1-story on-grade reinforced masonry. Damage states 3 and 5 included.	64
Figure 20. Breaking wave dimensions, based on Kjeldsen and Myrhaug. (1978)	65
Figure 21. FPFLM Coastal flood (CF) vulnerability and USACE (2015) vulnerability relative to the ground elevation a) 1-story slab on-grade weak timber ,0.3 m FFE; b) 1-story slab on-grade strong masonry, 0 m FFE.....	66
Figure 22. FPFLM Coastal flood (CF) vulnerability, USACE (2015) vulnerability, and Hurricane Ivan 2004 NFIP claims-derived vulnerability relative to the ground elevation a) 1-story slab on-grade timber, 0.3 m FFE; b) 1-story slab on-grade reinforced masonry, 0 m FFE.....	68
Figure 23. Fitted curve based on USACE data. Two-story masonry, 2 ft FFE.	70
Figure 24. Inland and Coastal Flood Vulnerability Curves. One-story masonry, 2 ft FFE.	70
Figure 25. Two types of manufactured homes (MH)	71
Figure 26. Inland Flood vulnerability curves and existing flood depth-damage data.	72
Figure 27. Forces acting on an Untied MH.....	73
Figure 28. Forces acting on a Tied-down MH after the Friction force has been exceeded	74
Figure 29. Interactions among major flood model components.	77
Figure 30. Four Florida Basins that used by CEST Model.....	116
Figure 31. Axisymmetric rotational wind speed (mph) vs. scaled radius for $B = 1.38$, $\Delta eIP = 49.1$ mb.	126
Figure 32. Plot of pressure profile corresponding to the parameters used in the previous figure.	126
Figure 33. Analysis of 742 GPS dropsonde profiles launched from 2-4 km with flight-level winds at launch greater than hurricane force and with measured surface winds. Upper figure: Dependence of the ratio of 10 m wind speed (U10) to the mean boundary layer wind speed (MBL) on the scaled radius (ratio of radius of last measured wind (Rlmw) to the radius of maximum wind at flight level (RmaxFL). Lower figure: Surface wind factor (U10/MBL) dependence on maximum flight level wind speed (Vflmax, in units of miles per hour / 2.23).	128
Figure 34. Location of EGL3, HGL4, HGL5, and HGL6 basins for Hurricane Ike.....	130
Figure 35. Location of AP3, AP4, AP6, and AP7 basins for Hurricanes Ivan and Dennis.....	130
Figure 36. Extra Large domain EGM3 with Manning Coefficient.....	131

Figure 37. Observed and computed water levels at 4 NOAA tide gauges.	132
Figure 38. Observed and computed water levels at 4 stations established by Kennedy (replace with u,w,y,z).....	132
Figure 39. Computed peak storm tide heights for Hurricane Ivan.	134
Figure 40. Computed peak storm tide heights for Hurricane Dennis.	135
Figure 41. The flowchart illustrating coastal surge model with other components of the FPFLM.	139
Figure 42. Flowchart illustrating the inland flood model components of the FPFLM.	140
Figure 43. Sample plot of water surface elevation and discharge versus time in Broward County within Southeast Florida region.	157
Figure 44. Sample plot of water surface elevation and discharge versus time in Brevard County within East Florida region.....	157
Figure 45. Sample plot of water surface elevation and discharge versus time in Duval County within North Florida region.	158
Figure 46. Sample plot of water surface elevation and discharge versus time in Hillsborough County within Southwest Florida region.	158
Figure 47. Sample plot of water surface elevation and discharge versus time in Leon County within Panhandle region.....	159
Figure 48. Histogram of CVs for all zones combined.	162
Figure 49. Comparison of observed and modeled daily mean streamflow during model calibration for the Southeast Coasts (SEC) Basin.....	167
Figure 50. Comparison of observed and modeled daily mean streamflow during model validation for the Southeast Coasts (SEC) Basin.....	168
Figure 51. Scatter plots of observed peak surge heights versus simulated ones for Hurricane Andrew (HMI41 Basin with H*Wind). The purple solid line represents perfect simulations and the green dashed lines represent the boundaries of perfect simulations*(100±20)%. Both the computed and the observed peak surge heights are referenced to the NAVD88 vertical datum.	169
Figure 52. Comparison between the measured and the computed water levels at the NOAA stations during Hurricane Jeanne 2004: (A) TP3 Basin and (B) HMI41 Basin.....	170
Figure 53. Coastal flood vulnerability for residential structures.	181
Figure 54. Inland flood vulnerability for residential structures.	182

Figure 55. FPFLM Inland and Coastal flood vulnerability, a) 1-story slab on-grade reinforced masonry, 0 m FFE; b) 1-story slab on-grade reinforced masonry, 0.9 m FFE.	186
Figure 56. Content vulnerability for personal residential structures.....	194
Figure 57. Type 2 vulnerability function relating content damage to building damage.....	195
Figure 58. Transfer function of building to content vulnerability. Polynomial fit of empirical.	196
Figure 59. Content vulnerability function derivation.	196
Figure 60. Content vulnerability function. One-story on grade reinforced masonry 1 ft FFE. ..	197
Figure 61. Coastal flood time element vulnerability for personal residential structures.	200
Figure 62. Inland flood time element vulnerability for personal residential structures.....	201
Figure 63. Conceptual illustration of mitigated vs unmitigated vulnerability.	209
Figure 64. Pressure acting on elevated structure.	212
Figure 65. Flood maps for six inland basins during hurricane Katrina (2005).....	266
Figure 66. Flood maps for six inland basins during hurricane Ivan (2004).....	267
Figure 67. Flood maps for six inland basins during hurricane Jeanne (2004).....	268
Figure 68. Flood maps for six inland basins during hurricane Wilma (2005).....	269
Figure 69. Flood maps for six inland basins during tropical storm Fay (2008).....	270
Figure 70. Flood map for East Florida during unnamed storm May (2009).....	271
Figure 71. Flood map for Panhandle during unnamed storm July (2013).....	271
Figure 72. Flood maps for six inland basins during hurricane Dennis (2005).	272
Figure 73. Five grids generated for five Florida geographic regions.	276
Figure 74. High resolution (100 meters) ground elevation at Bay County for Panhandle grid. .	277
Figure 75. High resolution (100 meters) ground elevation at Dixie County for North Florida grid.	277
Figure 76. High resolution (100 meters) ground elevation at Sarasota County for South West Florida grid.....	278
Figure 77. High resolution (100 meters) ground elevation at Miami-Dade County for South East Florida grid.....	278

Figure 78. High resolution (100 meters) ground elevation at St. Lucie County for east Florida grid. 279

Figure 79. Color-coded contour showing the modeled flood extent and inundation depth corresponding to 0.01 annual exceedance probability at Bay County (Panhandle). 280

Figure 80. Color-coded contour showing the modeled flood extent and inundation depth corresponding to 0.01 annual exceedance probability at Dixie County (North Florida). 280

Figure 81. Color-coded contour showing the modeled flood extent and inundation depth corresponding to 0.01 annual exceedance probability at Sarasota County (South West Florida). 281

Figure 82. Color-coded contour showing the modeled flood extent and inundation depth corresponding to 0.01 annual exceedance probability at Miami-Dade County (South East Florida). 281

Figure 83. Color-coded contour showing the modeled flood extent and inundation depth corresponding to 0.01 annual exceedance probability at St. Lucie County (East Florida). 282

Figure 84. Modeled flood extent and inundation depth corresponding to 0.1 annual exceedance probability at Bay County (Panhandle). 283

Figure 85. Modeled flood extent and inundation depth corresponding to 0.02 annual exceedance probability at Bay County (Panhandle). 284

Figure 86. Modeled flood extent and inundation depth corresponding to 0.01 annual exceedance probability at Bay County (Panhandle). 284

Figure 87. Modeled flood extent and inundation depth corresponding to 0.002 annual exceedance probability at Bay County (Panhandle). 285

Figure 88. Modeled flood extent and inundation depth corresponding to 0.1 annual exceedance probability at Dixie County (North Florida). 286

Figure 89. Modeled flood extent and inundation depth corresponding to 0.02 annual exceedance probability at Dixie County (North Florida). 286

Figure 90. Modeled flood extent and inundation depth corresponding to 0.01 annual exceedance probability at Dixie County (North Florida). 287

Figure 91. Modeled flood extent and inundation depth corresponding to 0.002 annual exceedance probability at Dixie County (North Florida). 287

Figure 92. Modeled flood extent and inundation depth corresponding to 0.1 annual exceedance probability at Sarasota County (South West Florida). 288

Figure 93. Modeled flood extent and inundation depth corresponding to 0.02 annual exceedance probability at Sarasota County (South West Florida).....	289
Figure 94. Modeled flood extent and inundation depth corresponding to 0.01 annual exceedance probability at Sarasota County (South West Florida).....	289
Figure 95. Modeled flood extent and inundation depth corresponding to 0.002 annual exceedance probability at Sarasota County (South West Florida).....	290
Figure 96. Modeled flood extent and inundation depth corresponding to 0.1 annual exceedance probability at Miami-Dade County (South East Florida).	291
Figure 97. Modeled flood extent and inundation depth corresponding to 0.02 annual exceedance probability at Miami-Dade County (South East Florida).	291
Figure 98. Modeled flood extent and inundation depth corresponding to 0.01 annual exceedance probability at Miami-Dade County (South East Florida).	292
Figure 99. Modeled flood extent and inundation depth corresponding to 0.002 annual exceedance probability at Miami-Dade County (South East Florida).	292
Figure 100. Modeled flood extent and inundation depth corresponding to 0.1 annual exceedance probability at St. Lucie County (East Florida).....	293
Figure 101. Modeled flood extent and inundation depth corresponding to 0.02 annual exceedance probability at St. Lucie County (East Florida).....	294
Figure 102. Modeled flood extent and inundation depth corresponding to 0.01 annual exceedance probability at St. Lucie County (East Florida).....	294
Figure 103. Modeled flood extent and inundation depth corresponding to 0.002 annual exceedance probability at St. Lucie County (East Florida).....	295
Figure 104. Selected 10 locations within the study area.....	296
Figure 105. Modeled flood extent and depths in Southeast Florida Region (Broward County) for 0.01 exceedance probability.....	299
Figure 106. Modeled flood extent and depths in East Florida Region (Brevard County) for 0.01 exceedance probability.....	299
Figure 107. Modeled flood extent and depths in North Florida Region (Duval County) for 0.01 exceedance probability.....	300
Figure 108. Modeled flood extent and depths in Southwest Florida Region (Hillsborough County) for 0.01 exceedance probability.....	300
Figure 109. Modeled flood extent and depths in Panhandle Region (Leon County) for 0.01 exceedance probability.....	301

Figure 110. Flood maps for Southeast Florida Region (Broward County) corresponding to 0.1, 0.02, 0.01, and 0.002 annual exceedance probabilities.....	303
Figure 111. Flood maps for East Florida Region (Brevard County) corresponding to 0.1, 0.02, 0.01, and 0.002 annual exceedance probabilities.....	304
Figure 112. Flood maps for North Florida Region (Duval County) corresponding to 0.1, 0.02, 0.01, and 0.002 annual exceedance probabilities.....	305
Figure 113. Flood maps for Southwest Florida Region (Hillsborough County) corresponding to 0.1, 0.02, 0.01, and 0.002 annual exceedance probabilities.....	306
Figure 114. Flood maps for Panhandle Region (Leon County) corresponding to 0.1, 0.02, 0.01, and 0.002 annual exceedance probabilities.....	307
Figure 115. State of Florida By Region.	310
Figure 116. Coastal flood estimated damage vs inundation depth. All reference structures combined.....	314
Figure 117. Coastal flood estimated damage vs inundation depth, Reference Structure 1.	314
Figure 118. Coastal flood estimated damage vs inundation depth, Reference Structure 2.	315
Figure 119. Coastal flood estimated damage vs inundation depth, Reference Structure 3.	315
Figure 120. Coastal flood estimated damage vs inundation depth, Reference Structure 4.	316
Figure 121. Coastal flood estimated damage vs inundation depth, Reference Structure 5.	316
Figure 122. Coastal flood estimated damage vs inundation depth, Reference Structure 6.	317
Figure 123. Coastal flood estimated damage vs inundation depth, Reference Structure 7.	317
Figure 124. Coastal flood estimated damage vs inundation depth, Reference Structure 8.	318
Figure 125. Inland flood estimated damage vs inundation depth – All reference structures combined.....	329
Figure 126. Inland flood estimated damage vs inundation depth, Reference Structure 1.	329
Figure 127. Inland flood estimated damage vs inundation depth, Reference Structure 2.	330
Figure 128. Inland flood estimated damage vs inundation depth, Reference Structure 3.	330
Figure 129. Inland flood estimated damage vs inundation depth, Reference Structure 4.	331
Figure 130. Inland flood estimated damage vs inundation depth, Reference Structure 5.	331

Figure 131. Inland flood estimated damage vs inundation depth, Reference Structure 6.	332
Figure 132. Inland flood estimated damage vs inundation depth, Reference Structure 7.	332
Figure 133. Inland flood estimated damage vs inundation depth, Reference Structure 8.	333
Figure 134. Gulf of Mexico location.	344
Figure 135. St. Johns River location.	344
Figure 136. Elevations for the costal and inland locations from a Digital Elevation Map.	345
Figure 137. Mitigation measure: elevate equipment. One-story masonry home.	351
Figure 138. Mitigation measure: wet floodproof. One-story masonry home.	351
Figure 139. Mitigation measure: dry floodproof. One-story masonry home.	352
Figure 140. Mitigation measure: combined vs individual. One-story masonry home.	352
Figure 141. Mitigation measure: elevate floor. Two-story frame home.	353
Figure 142. Mitigation measure: elevate equipment. Two-story frame home.	353
Figure 143. Mitigation measure: wet flooproof. Two-story frame home.	354
Figure 144. Mitigation measure: combined vs individual. Two-story frame home.	354
Figure 145. Mitigation measure: flood openings. One-story frame home.	355
Figure 146. Mitigation measure: elevate equipment. One-story masonry home.	359
Figure 147. Mitigation measure: wet floodproof. One-story masonry home.	359
Figure 148. Mitigation measure: dry floodproof. One-story masonry home.	360
Figure 149. Mitigation measure: combined vs individual. One-story masonry home.	360
Figure 150. Mitigation measure: elevate floor. Two-story frame home.	361
Figure 151. Mitigation measure: elevate equipment. Two-story frame home.	361
Figure 152. Mitigation measure: wet flooproof. Two-story frame home.	362
Figure 153. Mitigation measure: combined vs individual. Two-story frame home.	362
Figure 154. Mitigation measure: flood openings. One-story frame home.	363

List of Tables

Table 1. Manning’s coefficients for various categories of land cover.....	39
Table 2. Basin description and statistics for Apalachicola Bay.....	42
Table 3. Basin description for Miami and Key.....	42
Table 4. Basin description and statistics for Tampa Bay.....	43
Table 5. Basin description and statistics for Jacksonville.....	43
Table 6. Summary of the generated hydro-network for the six inland basins.	46
Table 7. Rainfall Data Information for the Inland Basin.	46
Table 8. Tsunami fragility curves parameters per DS for timber and reinforced concrete residential structures (from Suppasri et al., 2013).....	50
Table 9. Definitions of three coastal flood conditions.....	51
Table 10. Mathematical description of the fragility conversion process.	55
Table 11. Qualitative description of six coastal flood damage states.	60
Table 12. Normal distribution parameters of the component physical damage based on qualitative description. One story slab on grade reinforced masonry structure.....	61
Table 13. Single Story Residence, No Basement, Building Characteristics (Table 55, USACE 2015).	68
Table 14. Single Story Residence, No Basement, Inundation Damage – Structure (Table 56, USACE 2015).	69
Table 15. Professional credentials.	95
Table 16. Inland Flood Model Data Sources.	108
Table 17. Manning’s coefficients for various categories of land cover.....	112
Table 18. Manning’s n – Overland Flow (McCuen et al., 1996).....	113
Table 19. Depression storage from SWMM User manual (Rossman, 2015).	114
Table 20. Soil Parameter values (Rawls et al., 1983).	114
Table 21. Manning’s n for Open Channel (Rossman, 2015).	114

Table 22. Basin description and statistics for Apalachicola Bay.....	121
Table 23. Basin description for Miami and Key.....	121
Table 24. Basin description and statistics for Tampa Bay.....	122
Table 25. Basin description and statistics for Jacksonville.....	122
Table 26. Basin description for Hurricane Ike with additional large Basin HGL6.	133
Table 27. Basin description for Hurricane Ivan with additional large Basin AP7.	134
Table 28. Basin description for Hurricane Dennis with additional large Basin AP7.	135
Table 29. Model performance statistics during historical flood events.....	150
Table 30. Flood control structures incorporated in the inland flood models.....	154
Table 31. 95% Confidence intervals for mean loss for all zones(based on 50,000) year simulation.	163
Table 32. Confidence Intervals for PML values.....	164
Table 33. Model performance statistics for the Southeast Coasts (SEC) Basin.	165
Table 34. Model performance statistics for the Southwest Florida (SWF) Basin.	165
Table 35. Model performance statistics for the St. Johns River (SJN) Basin.....	165
Table 36. Model performance statistics for the Northwest Florida (NWF) Basin.....	166
Table 37. Model performance statistics for the Suwannee River (SWN) Basin.	166
Table 38. Model performance statistics for the Kissimmee River (KIS) Basin.	166
Table 39. Summary statistics for subbasin-scale major parameters, forcing variable, and model output in the Southeast Coasts (SEC) Basin.	175
Table 40. NFIP claim and exposure datasets.....	183
Table 41. Hurricane events currently included in the NFIP database.....	184
Table 42. Available Flood Vulnerability Functions.	190
Table 43. Sample of NFIP claim data and damage ratio calculations.	195
Table 44. Distribution of component damage for different damage states, one story on-grade reinforced masonry structure.	210

Table 45. Expected damage ratios representing each damage states above and below mitigation heights, one story on-grade reinforced masonry structure.....	210
Table 46. Flood model results at 10 locations within five study area (unit is feet).....	297
Table 47. Chosen counties within each study area.	298
Table 48. Flood elevations from underlying grids within each region.	308
Table 49. Flood depths from underlying grids within each region.....	308

GENERAL FLOOD STANDARDS

GF-1 Scope of the Flood Model and Its Implementation

A. The flood model shall project loss costs and probable maximum loss levels for primary damage to insured personal residential property from flood events.

The Florida Public Flood Loss Model estimates loss costs and probable maximum loss levels from storm and rain fall events for insured residential properties.

B. The modeling organization shall maintain a documented process to assure continual agreement and correct correspondence of databases, data files, and computer source code to slides, technical papers, and modeling organization documents.

The FPFLM members follow the process specified in the flowchart of Figure 1 in order to assure continual agreement and correct correspondence of databases, data files, and computer source code to slides, technical papers, and FPFLM documents.

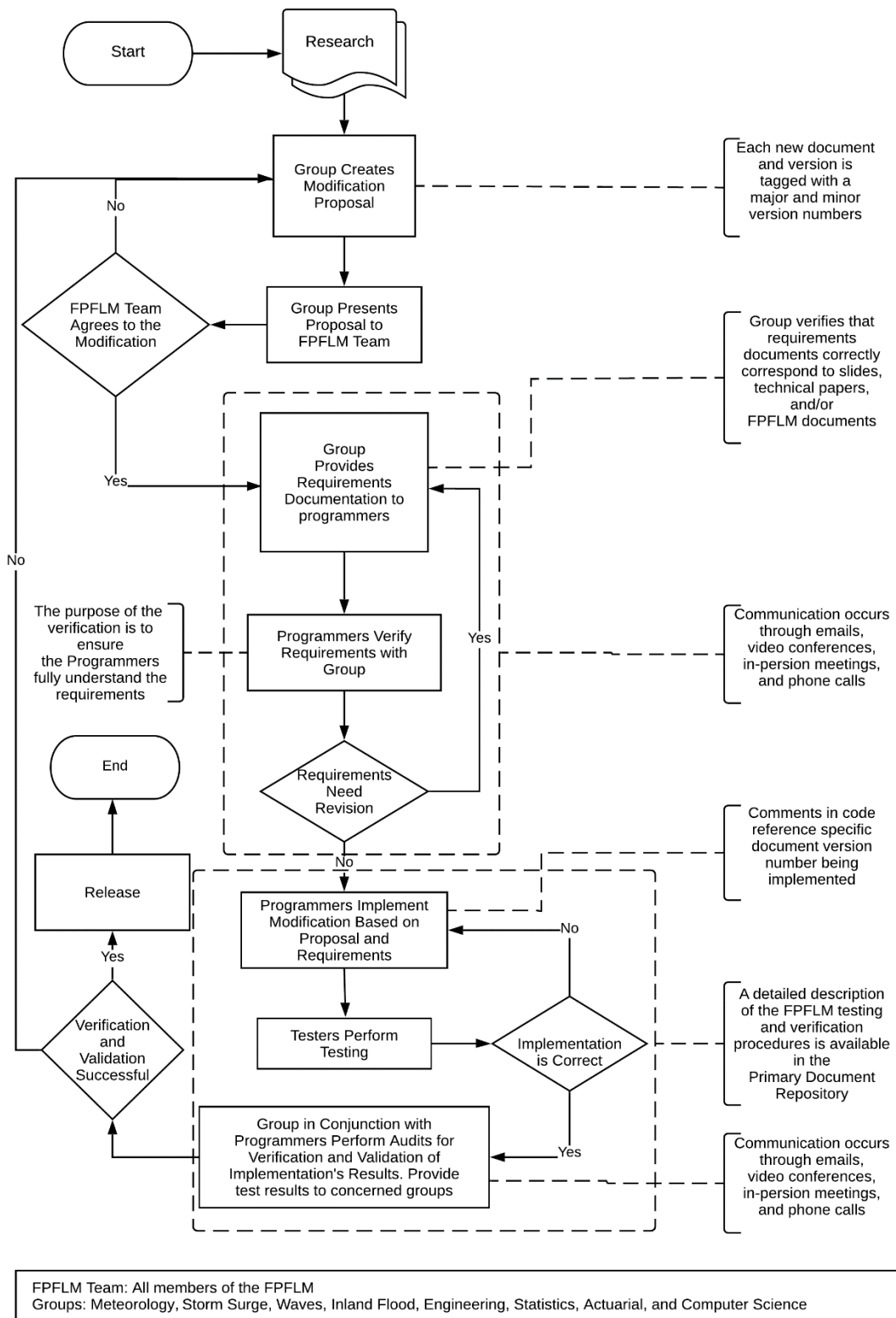


Figure 1. Process to assure continual agreement and correct correspondence of databases, data files, and computer source code to slides, technical papers, and modeling organization documents.
 FPFLM V1.0 Feb. 29, 2020

C. All software and data (1) located within the flood model, (2) used to validate the flood model, (3) used to project modeled flood loss costs and flood probable maximum loss levels, and (4) used to create forms required by the Commission in the Flood Standards Report of Activities shall fall within the scope of the Computer/Information Flood Standards and shall be located in centralized, model-level file areas.

All software and data used to validate the flood model, project modeled flood loss costs and flood PML, and used to create forms required by the Commission in the Flood Standards Report of Activities are located in centralized, model-level file area.

D. Differences between historical and modeled flood losses shall be reasonable, given available flood loss data.

Within the constraints of given available flood loss data the difference between historical and modeled flood losses are reasonable.

Disclosures

1. Specify the flood model version identification. If the flood model submitted for review is implemented on more than one platform, specify each flood model platform. Specify which platform is the primary platform and verify how any other platforms produce the same flood model output results or are otherwise functionally equivalent as provided for in the “Process for Determining the Acceptability of a Computer Simulation Flood Loss Model” in VI. Review by the Commission, I. Review and Acceptance Criteria for Functionally Equivalent Model Platforms.

The model name is Florida Public Flood Loss Model (FPFLM). The version identification is 1.0

2. Provide a comprehensive summary of the flood model. This summary should include a technical description of the flood model, including each major component of the flood model used to project loss costs and probable maximum loss levels for insured primary damage to personal residential property from flood events causing damage in Florida. Describe the theoretical basis of the flood model and include a description of the methodology, particularly the meteorology components, the hydrology and hydraulic components, the vulnerability components, and the insured flood loss components used in the flood model. The description should be complete and is not to reference unpublished work.

Meteorology Component

Storm Track and Intensity

The storm track model generates storm tracks and intensities on the basis of historical storm conditions and motions. The initial seeds for the storms are derived from the HURDAT2 database. For historical landfalling storms in Florida and neighboring states, the initial positions, intensities, and motions are taken from the track fix 36 hours prior to first landfall. For historical storms that do not make landfall but come within 62 sm (100 km) of the coast, the initial conditions are taken from the track fix 36 hours prior to the point at which the storm first comes within 62 sm of the coast (threat zone) and has a central pressure below 1005 mb. Small, uniform random error terms are added to the initial position, the storm motion change, and the storm intensity change. The initial conditions derived from HURDAT2 are recycled as necessary to generate thousands of years of stochastic tracks. After the storm is initiated, the subsequent motion and intensity changes are sampled from empirically derived probability distribution functions over the model domain. The model domain and threat zone are shown in Figure 2.

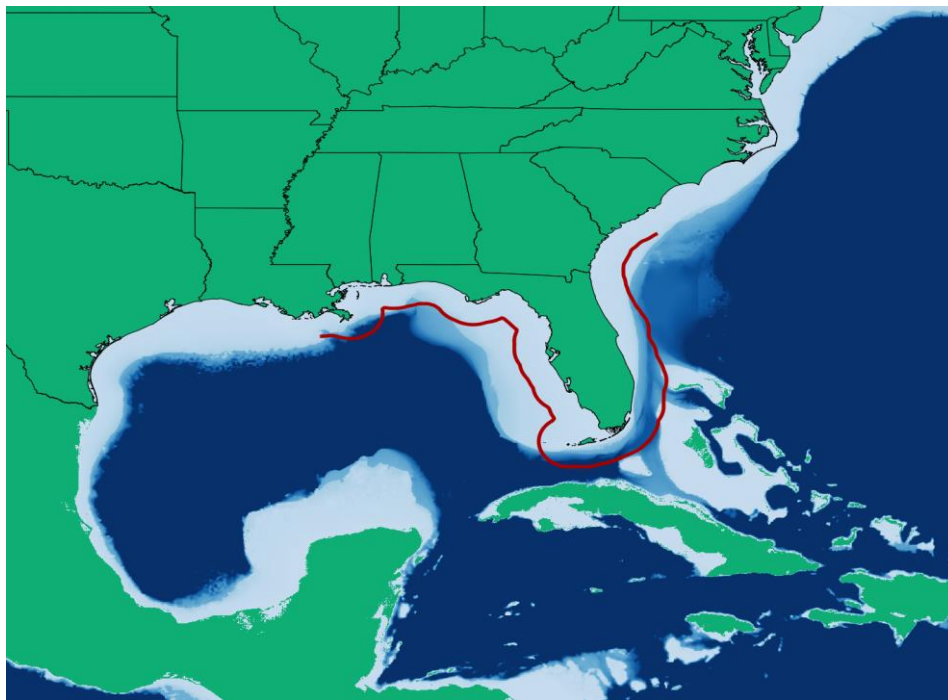


Figure 2. Florida Public Hurricane Loss Model domain. Threat zone is delineated by red line.

The time evolution of the stochastic storm tracks and intensity are governed by the following equations:

$$\begin{aligned}\Delta x &= \frac{c \cos(\theta) \Delta t}{\cos(y)} \\ \Delta y &= c \sin(\theta) \Delta t \\ \Delta p &= w \Delta t\end{aligned}$$

where (x, y) are the longitude and latitude of the storm, (c, θ) are the storm speed and heading (in conventional mathematical sense), p is central pressure, w is the rate of change in p , and Δt is the time step. The time step of the model is currently one hour. The change in storm speed and direction $(\delta c, \delta \theta)$ are sampled at every 24-hour interval from a probability distribution function (PDF). The intensity change after the initial 24 hours of track evolution is sampled every six hours

to capture the more detailed evolution over the continental shelf (shallow water). From the 24-hour change in speed and heading angle, we determine the speed and heading angle at each one-hour time step by assuming the storm undergoes a constant acceleration that gives the 24-hour sampled change in velocity. For changes in pressure, we first sample from a PDF of relative intensity changes, δr , for the six-hour period and then determine the corresponding rate of pressure change, w . The relative intensity is a function of the climatological sea surface temperatures and the upper tropospheric 100 mb temperatures. The PDFs of the changes ($\delta c, \delta \theta, \delta r$) depend on spatial location, as well as the current storm motion and intensity. These PDFs are of the form

$$PDF(\delta a) = A(\delta a, a, x, y)$$

where a is either c , θ , or r and are implemented as discrete bins that are represented by multi-dimensional matrices (arrays), $A(l, m, i, j)$. The indices (i, j) are the storm location bins. The model domain (100W to 70W, 15N to 40N) is divided into 0.5-degree boxes. The index m represents the bin interval that a falls into. That is, the range of all possible values of a are divided into discrete bins, the number of which depends on the variable, and the index m represents the particular bin a is in at the current time step. As with a , the range of all possible values of the change in a are also discretely binned. Given a set of indices (m, i, j) , which represent the current storm location and state, the quantity $A(l, m, i, j)$ represents the probability that the change in a , δa , will fall into the l 'th bin. When A is randomly sampled, one of the bins represented by the l index, e.g. l' , is chosen. The change of a is then assigned the midpoint value of the bin associated with l' . A uniform random error term equal to the width of bin l' is added to δa , so that δa may assume any value within the bin l' .

The PDFs described above were generated by parsing the HURDAT2 database and computing for each track the storm motion and relative intensity changes at every 24- and 6-hour interval, respectively, and then binning them. Once the counts are tallied, they are then normalized to obtain the distribution function. For intensity reports for which pressure is not available, a wind pressure relation developed by Landsea et al. (2004) is used. In cases where there is no pressure report for a track fix in the historical data but there are two pressure reports within a 24-hour period that includes the track fix, the pressures are derived by linear interpolation. Otherwise the pressure is derived by using the wind-pressure relation. Extra-tropical systems, lows, waves, and depressions are excluded. Intensity changes over land are also excluded from the PDFs. To ensure a sufficient density of counts to represent the PDFs for each grid box, counts from nearest neighbor boxes, ranging up to 2 to 5 grid units away (both north-south and east-west direction), are aggregated. Thus, the effective size of the boxes may range from 1.5 to 5.5 degrees but are generally a fixed size for a particular variable. The sizes of the bins were determined by finding a compromise between large bin sizes, which ensure a robust number of counts in each bin to define the PDF, and small bin sizes, which can better represent the detail of the distribution of storm motion characteristics. Detailed examinations of the distributions, as well as sensitivity tests, were done. Bin sizes need not be of equal width, and a nonlinear mapping function is used to provide unequal-sized bins. For example, most storm motion tends to be persistent, with small changes in direction and speed. Thus, to capture this detail, the bins are more fine-grained at lower speed and direction changes.

For intensity change PDFs, boxes which are centered over shallow water (defined to be less than 656 ft deep) are not aggregated with boxes over deeper waters. Deeper waters may have significantly higher ocean heat content, which can lead to more rapid intensification [see, for example, Shay et al. (2000); DeMaria et al. (2005); Wada and Usui (2007)].

In Figure 3 we show a sample of tracks generated by the stochastic track and intensity model.



Figure 3. Examples of simulated hurricane tracks. Track colors correspond to storm intensity: red – Cat 4, orange – Cat 3, yellow – Cat 2, light blue – Cat 1, dark blue – TS.

The pressure field for the model is based on the *Holland B* pressure profile (Holland, 1980). When a storm is initiated, the parameters for radius of maximum winds and *Holland B* are computed and appropriate error terms are added as described below. The *Holland B* term is modeled as follows:

$$B = 1.74425 - 0.007915Lat + 0.0000084DelP^2 - 0.005024Rmax$$

where *Lat* is the current latitude (degrees) of the storm center, *DelP* is the central pressure difference (mb), and *Rmax* is the radius of maximum winds (km). The random error term for the *Holland B* is modeled using a Gaussian distribution with a standard deviation of 0.286. Figure 4 shows a comparison between the Willoughby and Rahn (2004) *B* dataset and the modeled results (scaled to equal the 116 measured occurrences in the observed dataset). The modeled results with the error term have a mean of about 1.38 and are consistent with the observed results. The figure indicates excellent agreement between model and observations.

Distribution of the B parameter

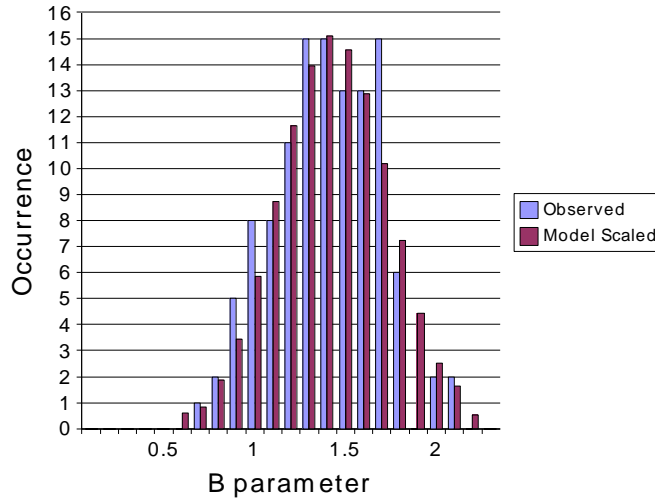


Figure 4. Comparison between the modeled and observed Willoughby and Rahn (2004) *B* dataset.

We developed an *Rmax* model using a landfall *Rmax* database, which includes more than 100 measurements for storms up to 2012. We have opted to model the *Rmax* at landfall rather than the entire basin for a variety of reasons. One is that the distribution of landfall *Rmax* may be different than that over open water. An analysis of the landfall *Rmax* database and the 1988–2007 DeMaria extended best track data shows that there appears to be a difference in the dependence of *Rmax* on central pressure (*Pmin*) between the two datasets (Demuth et al., 2006). The landfall dataset provides a larger set of independent measurements, more than 100 storms compared to about 31 storms affecting the Florida threat area region in the best track data. Since landfall *Rmax* is most relevant for loss cost estimation and has a larger independent sample size, we have chosen to model the landfall dataset.

We modeled the distribution of *Rmax* using a gamma distribution. Using the maximum likelihood estimation method, we found the estimated parameters for the gamma distribution, $\hat{k} = 4.76$ and $\hat{\theta} = 5.41$. With these estimated values, we show a plot of the observed and expected distribution in Figure 5. The *Rmax* values are binned in 5 sm intervals, with the *x*-axis showing the end value of the interval.

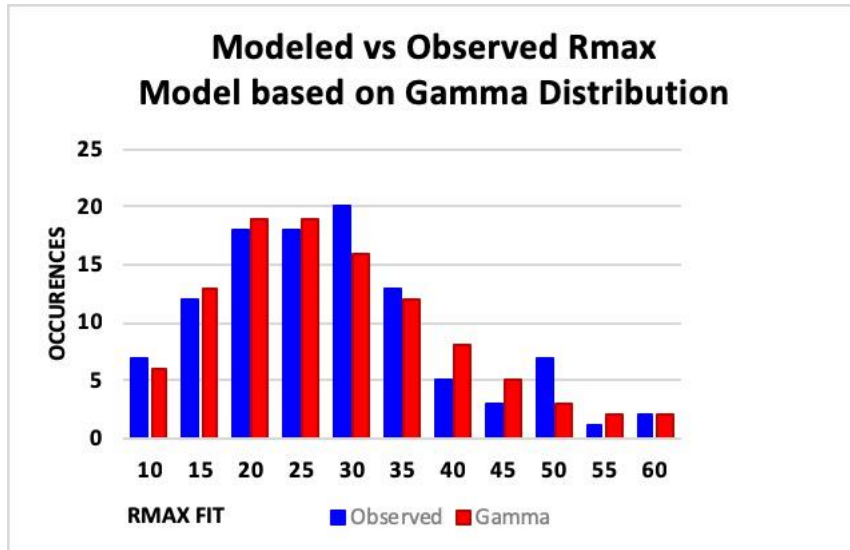


Figure 5. Observed and expected distribution for R_{max} . The x-axis is the radius in statute miles, and the y-axis is the frequency of occurrence.

An examination of the R_{max} database shows that intense storms, essentially Category 5 storms, have rather small radii. Thermodynamic considerations (Willoughby, 1998) also suggest that smaller radii are more likely for these storms. Thus, we model Category 5 ($DelP > 90$ mb, where $DelP = 1013 - P_{min}$ and P_{min} is the central pressure of the storm) storms using a gamma distribution, but with a smaller value of the θ parameter, which yields a smaller mean R_{max} as well as smaller variance. We have found that for Category 1–4 ($DelP < 80$ mb) storms there is essentially no discernable dependence of R_{max} on central pressure. This is further verified by looking at the mean and variance of R_{max} in each 10 mb interval. Thus, we model Category 1–4 storms with a single set of parameters. For a gamma distribution, the mean is given by $k\theta$, and variance is $k\theta^2$. For Category 5 storms, we adjust θ such that the mean is equal to the mean of the three Category 5 storms in the database: 1935 No Name, 1969 Camille, and 1992 Andrew. An intermediate zone between $DelP = 80$ mb and $DelP = 90$ mb is established where the mean of the distribution is linearly interpolated between the Category 1–4 value and the Category 5 value. As the θ value is reduced, the variance is likewise reduced. Since there are insufficient observations to determine what the variance should be for Category 5 storms, we rely on the assumption that variance is appropriately described by the rescaled θ , via $k\theta^2$.

For Category 5 and intermediate Category 4–5 storms, we use the property that the gamma cumulative distribution function is a function of $(k, x/\theta)$. Thus, by rescaling θ , we can use the same Gamma distribution with parameters described above, but just rescale x (R_{max}). The rescaled R_{max} will still have a gamma distribution but with different mean and variance.

The storms in the stochastic model will undergo central pressure changes during the storm life cycle. When a storm is generated, an appropriate R_{max} is sampled for the storm. To ensure the appropriate mean values of R_{max} as pressure changes, the R_{max} is rescaled every time step as necessary. As long as the storm has $DelP < 80$ mb, there is in effect no rescaling. In the stochastic storm generator, we limit the range of R_{max} from 4 sm to 120 sm.

Storm landfall and decay over land are determined by comparing the storm location (x,y) with a 0.6 sm resolution land-sea mask. This land mask is obtained from the U.S. Geological Survey (USGS) land use cover data, and inland bodies of water have been reclassified as land to avoid spurious landfalls. Landfall occurs every time the storm moves from an ocean point to a land point as determined by this land mask. During landfall, the central pressure is modeled by a filling model described in Vickery (2005) and is no longer sampled from the intensity change PDFs. The Vickery (2005) model basically uses an exponentially decaying, in time, function of the central pressure difference with the decay coefficients varying by region on the basis of historical data. The pressure filling model also takes into account the speed and size of the storm. When the storm exits to sea, the land-filling model is turned off and sampling of the intensity change PDFs begins again. A storm is dissipated when its central pressure exceeds 1011 mb.

Wind Field Model

The wind model is based on the slab boundary layer concept originally conceived by Ooyama (1969) and implemented by Shapiro (1983). Similar models based on this concept have been developed by Thompson and Cardone (1996), Vickery et al. (1995), and Vickery et al. (2000a). The model is initialized by a boundary layer vortex in gradient balance. Gradient balance represents a circular flow caused by balance of forces on the flow whereby the inward directed pressure gradient force is balanced by outward directed Coriolis and centripetal accelerations. The coordinate system translates with the hurricane vortex moving at velocity c . The vortex translation is assumed to equal the geostrophic flow associated with the large-scale pressure gradient. In cylindrical coordinates that translate with the moving vortex, equations for a slab hurricane boundary layer under a prescribed pressure gradient are

$$u \frac{\partial u}{\partial r} - \frac{v^2}{r} - fv + \frac{v}{r} \frac{\partial u}{\partial \phi} + \frac{\partial p}{\partial r} - K \left(\nabla^2 u - \frac{u}{r^2} - \frac{2}{r^2} \frac{\partial u}{\partial \phi} \right) + F(c, u) = 0 = \frac{\partial u}{\partial t}$$

$$u \left(\frac{\partial v}{\partial r} + \frac{v}{r} \right) + fu + \frac{v}{r} \frac{\partial v}{\partial \phi} - K \left(\nabla^2 v - \frac{v}{r^2} + \frac{2}{r^2} \frac{\partial u}{\partial \phi} \right) + F(c, v) = 0 = \frac{\partial v}{\partial t}$$

where u and v are the respective radial and tangential wind components relative to the moving storm; p is the sea level pressure, which varies with radius (r); f is the Coriolis parameter, which varies with latitude; ϕ is the azimuthal coordinate; K is the eddy diffusion coefficient; and $F(c,u)$, $F(c,v)$ are frictional drag terms. All terms are assumed to be representative of means through the boundary layer. The motion of the vortex is determined by the modeled storm track. The symmetric pressure field $p(r)$ is specified by the Holland (1980) pressure profile with the central pressure specified according to the intensity modeling in concert with the storm track. The model for the *Holland B* pressure profile and the radius of maximum wind are described above. The wind field is solved on a polar grid with a 0.1 R/R_{max} resolution. The input R_{max} is adjusted to remove a bias caused by a tendency of the wind field solution to place R_{max} one grid point radially outward from the input value. After the storm-relative wind components are derived, the storm translation motion vector is added to obtain the earth-relative wind.

Rain Model

The rain model provides estimates of the hourly rainfall accumulation due to tropical cyclones using the Atlantic Oceanographic & Meteorological Laboratory Hurricane Research Division (AOML/HRD) R-CLIPER rain algorithm for stochastic and historical storm events as input to the SWMM inland flood model. The rain amounts are estimated for select rain gauge locations that are used in the SWMM inland flood model. The rain model uses the storm track files to determine the location and intensity of the storms at hourly track intervals. The R-CLIPER algorithm requires the peak wind of the storm and the distance to the target location to the center of storm at one hour time intervals. The peak wind is estimated using a wind-pressure relation since the track file only includes central pressure (the track file is also input for the wind model). The distance from storm center to target location is estimated using the Haversine formula. A brief description of the R-CLIPER follows.

The R-CLIPER model is a statistical fit of observational rainfall climatology. R-CLIPER was initially based on U.S. rain gauge data, but has been updated using global satellite-based TRMM microwave imager (TMI) data.

TRMM rainfall data from 1 January 1998 to December 2002 were used to develop the rainfall climatology for R-CLIPER. These data include 3979 storm events over the globe. Figure 6 shows a subset (storms prior to 31 December 2000) of the storm event locations.

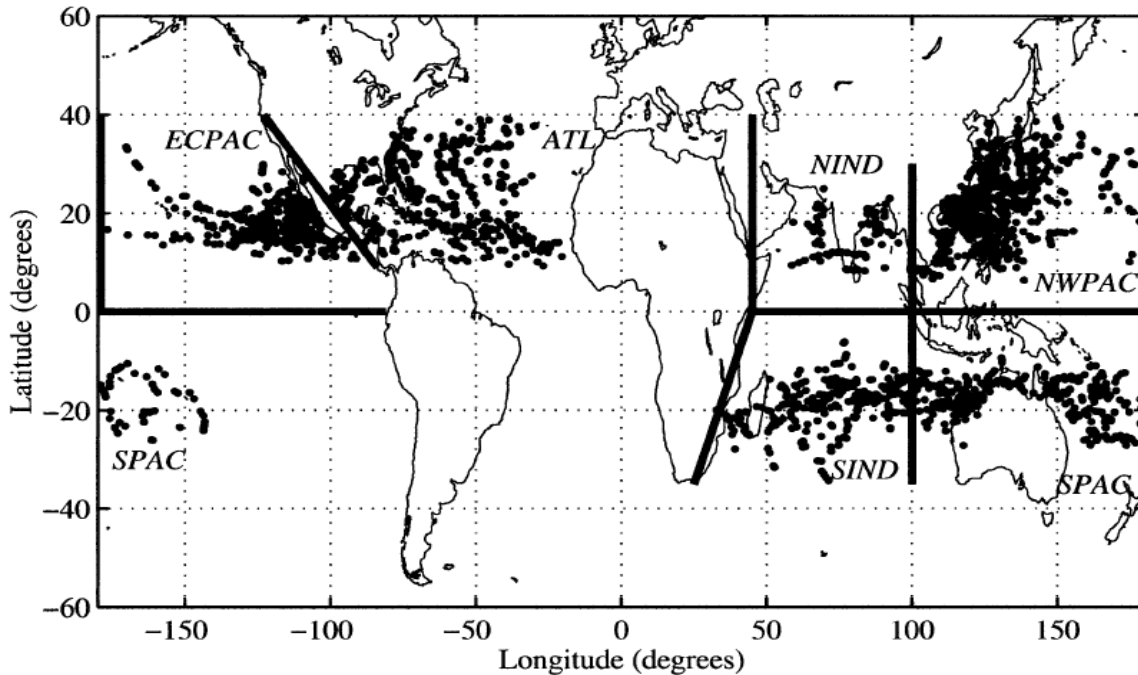


Figure 6. Tropical cyclones observed by TMI during the period 1 Jan 1998 to 31 Dec 2000. Each dot represents one TRMM observation. (From Lonfat et al, 2004).

The rainfall data were combined with operational best track data in order to link the rain data to characteristics of the associated storm. Lonfat et al (2004) showed that the azimuthally averaged rainfall of a storm depends strongly on the distance to storm center and the maximum intensity of the storm. Figure 7 shows the TMI-based rainfall climatology for different category of storms.

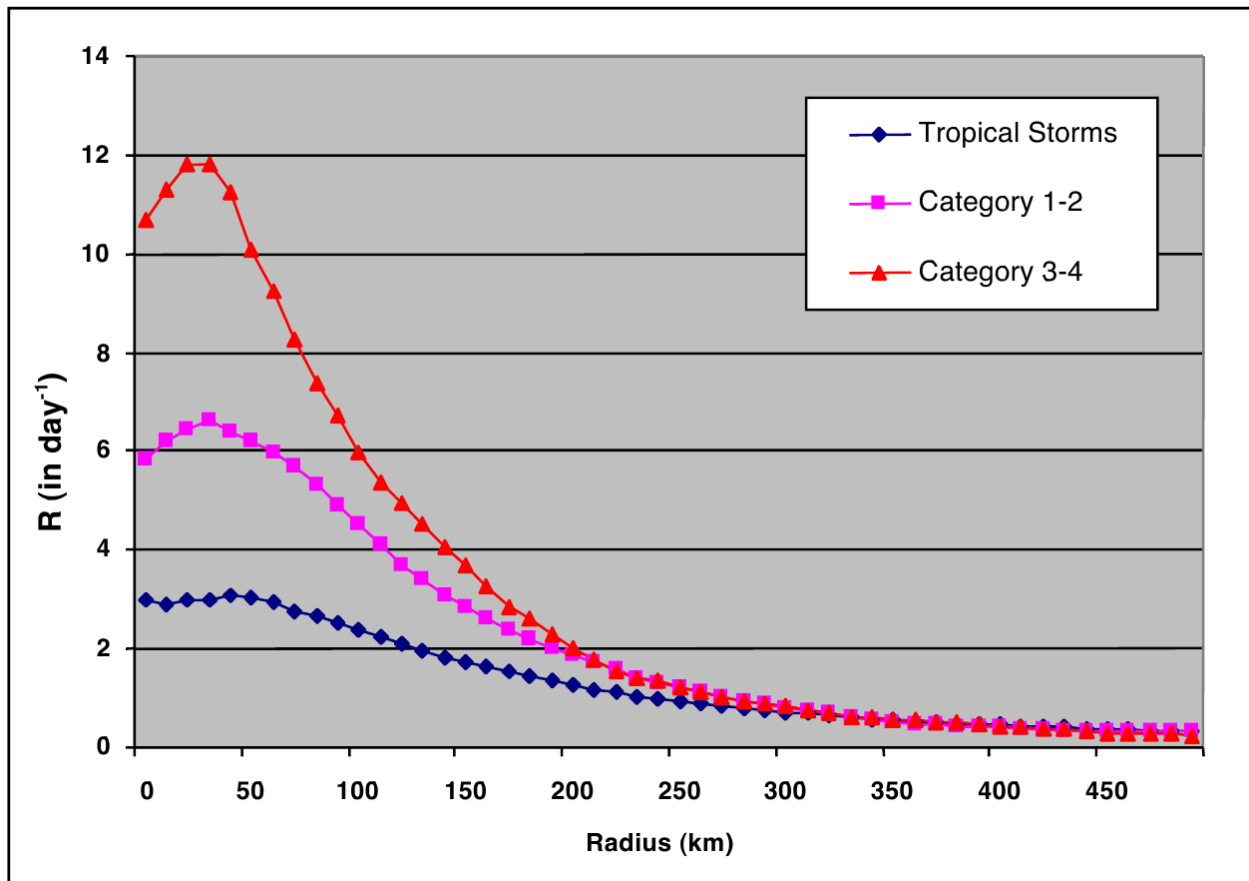


Figure 7. TMI-based rainfall climatology. (Based on data from Lonfat et al, 2004).

Thus, the R-CLIPER model uses a functional form which depends on the distance to storm center and maximum intensity (wind speed) of the storm. The function has the following form:

$$\begin{aligned}
 R(r) &= t_0 + (t_m - t_0)(r/R_{max}) & r < R_{max} \\
 &= t_m \exp(-(r - R_{max})/r_e) & r > R_{max}
 \end{aligned}$$

where R is rainfall rate, r is distance to storm center, R_{max} is radius of maximum winds, t_0 is rain at storm center, t_m is the rain at the radius of maximum winds, and r_e is the rain extent. The terms t_0 , t_m and r_e are determined by a regression equation as a function of the storm maximum intensity at a given instant of time based on the TMI climatology and best track data. The output is the mean rain rate at the target location. Due to the TMI measuring method, the rain rates are more representative of 3-hour averages.

Coastal Storm Surge Component

The State of Florida has the longest coastline in the nation and is the state most impacted by hurricanes based on historical records. Most of Florida's coastal areas are vulnerable to storm surge flooding because of low elevation. Several densely populated areas such as Miami, the

Florida Keys, Cape Coral, Tampa Bay, and Pensacola are extremely vulnerable to storm surge flooding because of their unique coastline configuration (Figure 8). Therefore, in addition to wind induced damage, it is essential to include the property damage caused by storm surge and storm wave in estimating the property damage from a hurricane.



Figure 8. The populated areas (red rectangles) along the Florida coast where severe storm surge flooding could occur when a large and intense hurricane makes landfall. The coverage of Light Detection And Ranging (LiDAR) data from the Florida Department of Emergency Management (FDEM) is also displayed.

The Coastal and Estuarine Storm Tide (CEST) model is used to compute storm surge parameters, which are the inputs of damage functions for estimating property loss from a hurricane, using the wind field data generated by the wind model of Florida Public Hurricane Loss Model (FPFLM) (Figure 9).

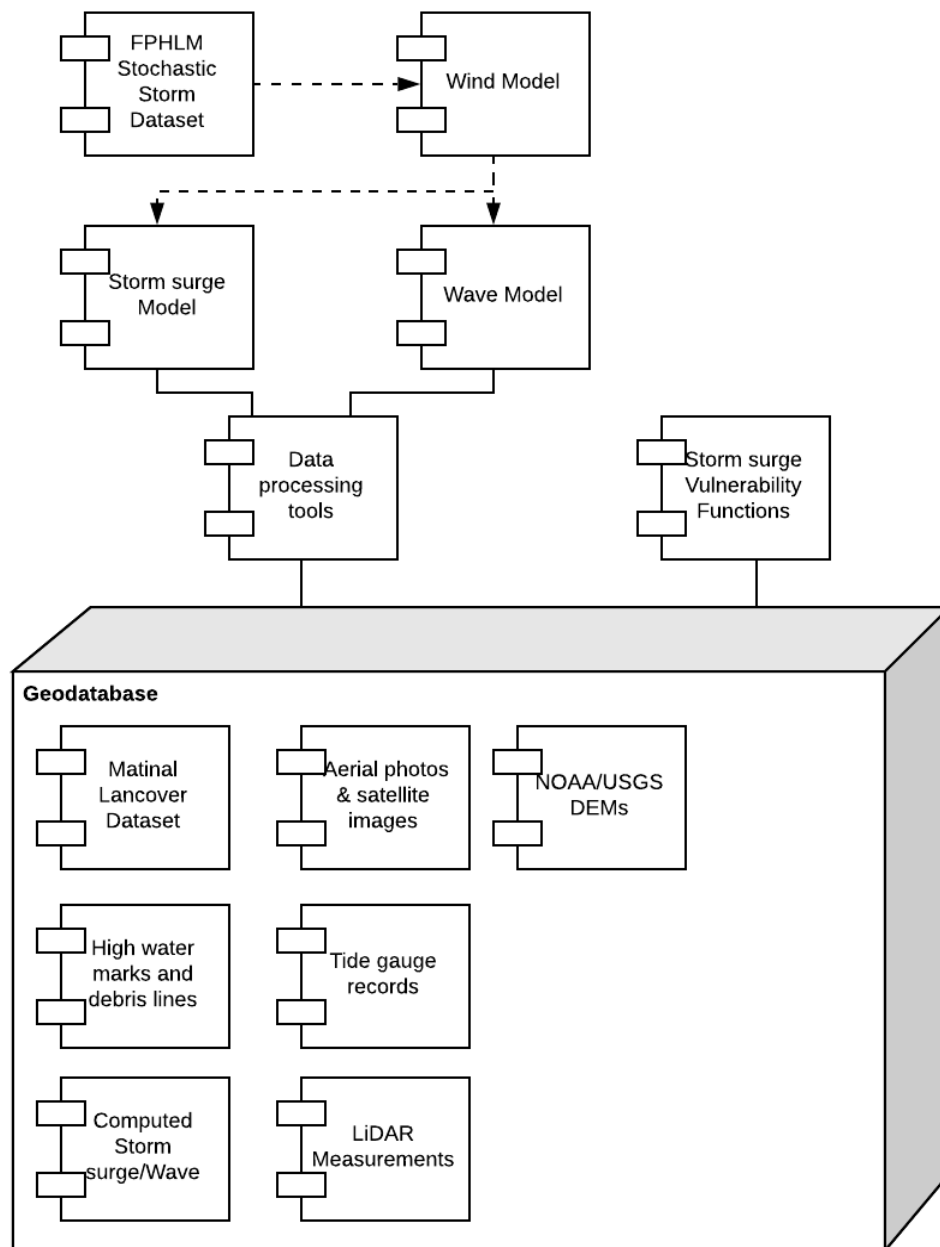


Figure 9. Component diagram of FPFLM with the storm surge.

Summary of CEST model

The National Hurricane Center (NHC) of National Weather Service (NWS) employs a numerical storm surge model, Sea, Lake, and Overland Surges from Hurricanes (SLOSH) to conduct real-time storm surge forecasts during the hurricane season to provide critical information for evacuation decision making in response to storms that threaten the US coastline. The CEST model which improves the physics and algorithm of SLOSH will be used to compute storm surges for

FHPLM (Zhang et al. 2013). The CEST model solves the continuity and full momentum equations which are forced by winds, atmospheric pressure drops, and astronomical tides or a time series of water levels at open boundaries. The depth-integrated 2D CEST model over orthogonal curvilinear grids was used to examine the effect of the basin size on the computation of storm surge.

Governing Equations

The 2D depth-integrated continuity equation in an x , y , and z coordinate system with the z -axis perpendicular to the still water level is:

$$\frac{\partial \zeta}{\partial t} + \frac{\partial HU}{\partial x} + \frac{\partial HV}{\partial y} = 0 \quad (1)$$

and the momentum equations along the x and y directions are:

$$\begin{aligned} \frac{\partial HU}{\partial t} + \frac{\partial HU^2}{\partial x} + \frac{\partial HUV}{\partial y} = fHV - g \frac{\partial}{\partial x} \left(\zeta + \frac{\Delta P_a}{\rho g} \right) \\ - \frac{\tau_b^x}{\rho} + \frac{\tau_s^x}{\rho} + A_h \frac{\partial^2 HU}{\partial x^2} + A_h \frac{\partial^2 HU}{\partial y^2} \end{aligned} \quad (2)$$

$$\begin{aligned} \frac{\partial HV}{\partial t} + \frac{\partial HUV}{\partial x} + \frac{\partial HV^2}{\partial y} = -fHU - g \frac{\partial}{\partial y} \left(\zeta + \frac{\Delta P_a}{\rho g} \right) \\ - \frac{\tau_b^y}{\rho} + \frac{\tau_s^y}{\rho} + A_h \frac{\partial^2 HV}{\partial x^2} + A_h \frac{\partial^2 HV}{\partial y^2} \end{aligned} \quad (3)$$

where, H is the water depth from the still water level to the bottom, ζ is the water surface elevation reference to the still water level, U and V are depth-integrated velocities along the x and y directions, f is the Coriolis parameter, g is the gravitational acceleration, ΔP_a is air pressure drop, ρ is the water density, A_h is the horizontal eddy diffusivity. The bottom friction forces τ_b^x and τ_b^y are given by a quadratic drag law:

$$\tau_b^x = \rho C_b \sqrt{U^2 + V^2} U \quad (4)$$

$$\tau_b^y = \rho C_b \sqrt{U^2 + V^2} V \quad (5)$$

where C_b is the coefficient based on the Chezy formula (LeMehaute 1976; Zhang et al. 2012b):

$$C_b = \frac{gn^2}{H^{1/3}} \quad (6)$$

where n is the Manning's coefficient. The surface wind stresses τ_s^x and τ_s^y are given by a similar formulation:

$$\tau_s^x = \rho_a C_s \sqrt{(U_a - U)^2 + (V_a - V)^2} (U_a - U) \quad (7)$$

$$\tau_s^y = \rho_a C_s \sqrt{(U_a - U)^2 + (V_a - V)^2} (V_a - V) \quad (8)$$

where ρ_a is the air density and U_a, V_a are the wind velocities at the 10-m height above the still water level along the x and y directions. C_s is the drag coefficient which is calculated using the modified formula of Large and Pond (1981) based on Powell et al. (2003).

$$C_s = \begin{cases} 0.00114 & \sqrt{U_a^2 + V_a^2} \leq 10 \\ (0.49 + 0.0065\sqrt{U_a^2 + V_a^2})10^{-3} & 10 < \sqrt{U_a^2 + V_a^2} \leq 38 \\ 0.003 & \sqrt{U_a^2 + V_a^2} > 38 \end{cases} \quad (9)$$

CEST Model Setup

The 2D CEST model is discretized on an orthogonal curvilinear grid based on the modified C-grid with velocity components on the four edges of a grid cell and the water depths at the center and four edges (Zhang et al. 2013). The radiation open boundary condition was employed to allow waves to propagate out of the model domain (Blumberg and Kantha 1983). In order to improve the computational efficiency and stability of the model, a semi-implicit scheme is employed to produce a discrete form of the control equations (Casulli and Chen 1992). The water pressure gradient and bottom friction items are solved implicitly and the remaining terms are treated explicitly. With varying cell sizes, the curvilinear grid is flexible in generating fine grid cells at the coast and coarse ones at the open ocean. The CEST model uses a mass-balanced algorithm based on accumulated water volume to simulate the wetting-drying process and includes the land cover effect into the overland flooding. The model can also run on conformal grids such as those used by SLOSH without modification of the numerical algorithms. The inputs and outputs of the CEST model are in Network Common Data Form

(NetCDF; <http://www.unidata.ucar.edu/software/netcdf/>). A set of tools in Matlab have been developed to convert input files created in ArcGIS (www.esri.com) into NetCDF files and to convert output NetCDF files into ArcGIS shapefiles for displaying and analyzing simulated surges.

The CEST model was verified by comparing calculated surges from historical storms such as Hurricanes Andrew, Camille, Hugo, and Wilma with field observations (Zhang et al. 2012b; Zhang et al. 2008). The measured maximum high water mark elevations from hurricanes Andrew, Camille, Hugo, and Wilma are about 5 m, 7 m, 6 m, and 5 m above NAVD88, respectively. The root mean square differences (RMSD) between computed and observed high water levels for these four hurricanes are 0.44 m, 0.58 m, 0.47 m, and 0.39 m, respectively. The CEST model has also been employed to perform preliminary real-time forecasts of storm surges based on advisory tracks for Hurricanes Isabel in 2003, Katrina in 2005, Hurricanes Irene in 2011, Hurricanes Isaac and Sandy in 2012. The comparison of computed surges with tidal gauge records and high water mark

measurements indicates that the model largely reproduced the inundation pattern generated by these hurricanes.

Topographic and bathymetric Data and Calculation of Grid Cell Elevation

The bathymetric and topographic data are required for calculating the water depths and elevations of the grid cells in a model basin. The topographic data used in this study mainly come from the US Geological Survey (USGS), and the bathymetric data come from NOAA. Water depths for grid cells at the open ocean were calculated based on the ETOPO1 global relief dataset from NOAA, which has a resolution of 1 arc minute (~1.8 km). Water depths for grid cells in coastal areas were interpolated from the U.S. coastal relief dataset from NOAA with a resolution of 3 arc second (~90 m) (http://www.ngdc.noaa.gov/mgg/gdas/gd_designagrid.html). The USGS 90 m, 30 m, 10 m, and 3 m digital elevation models (DEM) were used to calculate the elevation of grid cells on the land (<http://viewer.nationalmap.gov/viewer/>) in terms of the sizes of grid cells. USGS DEMs are periodically updated with new data from various federal, state, and local government agencies. For example, advances in airborne Light Detection And Ranging (LiDAR) technology in the past ten years have allowed for a rapid mapping of topology over a large area with a vertical resolution of 0.15 m and horizontal resolution of one meter (Zhang et al. 2012a). The State of Florida has completed LiDAR data collection for coastal areas vulnerable to surge flooding at a cost of \$25 million (Figure 8). Most of high-resolution topographic data have been incorporated into the DEMs created by USGS.

In order to support the National Tsunami Hazard Mitigation Program, the hurricane storm surge forecast, and to study the impacts of long-term sea-level rise on coastal ecosystems, NOAA has developed the integrated models of coastal reliefs for various areas along the US Atlantic and Gulf coasts in recent years (<http://www.ngdc.noaa.gov/mgg/coastal/>). The bathymetric and topographic data were merged and adjusted to a consistent vertical datum (e.g. NAVD88) in an integrated model of coastal relief, and important hydrological features such as main navigation channels are maintained.

The elevation of a CEST grid cell was calculated by averaging the pixel elevations of the digital bathymetric and topographic elevation models which are falling within the grid cell. All the topographic and bathymetric data were adjusted to NAVD 88 vertical datum before calculation. The following procedure was used to calculate the grid cell elevation and handle the overlaps between different bathymetric and topographic datasets.

(1) NOAA ETOPO1 global relief dataset was used to calculate the cell elevations of the model grid. In the deep ocean area that is covered by ETOPO1, but not covered by the bathymetric and topographic data with finer resolutions, a grid cell should include at least one data point from ETOPO1 for elevation calculation. If not, a new relief dataset with a pixel size of half the ETOPO1 pixel size was generated by interpolating ETOPO1 using the nearest neighbor method. The interpolation was conducted continuously by reducing the pixel size half every time until each grid cell in the deep ocean contains at least one data point from the interpolated relief dataset.

(2) NOAA coastal relief dataset was used to calculate the cell elevations and replace the elevations from ETOPO1 in the continental shelf and coastal areas. If the cell size of a model grid is less than

the pixel size of the coastal relief dataset. The new coastal relief dataset was generated for the calculation of the grid cell elevation using the same procedure to interpolating the ETOPO1 dataset.

(3) USGS 90 m, 30 m, 10 m, and 3 m DEMs were used to calculate the elevations of the model grid cells on the land. The model grid cells on the land and on the ocean were separated using the shoreline dataset extracted from the LiDAR surveys or digitized from the aerial photographs. The selection of 90 m, 30 m, 10 m, and 3 m DEMs were determined by the cell size of a model grid. A grid cell has to contain at least one data point from the DEM dataset used for the elevation calculation.

(4) NOAA integrated models of coastal reliefs were used to calculate and replace the depths of the grid cells in the coastal water. If the USGS DEMs on the land is older than the elevation data in the integrated model of coastal relief, the elevations of the grid cell on the land were also calculated and replaced.

(5) The water depths and elevations of the grid cell were updated using the most recent data which are often the LiDAR surveys provided by local government agencies through the flood map modernization program sponsored by the Federal Emergency Management Agency.

The high-quality shoreline dataset including the boundaries of the coastal lagoons, inlets, and barrier islands, and river streams is essential for separating the grid cells on the land and the ocean and preserving the connectivity of the coastal hydrological features. Fortunately, the digital shorelines can be extracted from the LiDAR surveys for coastal areas vulnerable to storm surge flooding in Florida. However, there are many topological errors such as dangles, intersections, and self-overlaps in the LiDAR shorelines (Figure 10). These errors were corrected through the manual editing in ArcGIS (www.esri.com) by setting up appropriate topological rules. The corrected shoreline vector data were converted into the polygons by adding lines connecting start and ending points and used to separate the land and ocean cells of a model grid.



Figure 10. Topologic errors in the shoreline dataset derived from the LiDAR surveys for Franklin County in Florida.

Calculation of Manning's Coefficients Using Land Cover Data

The CEST model uses the Chezy formula (LeMehaute 1976; Zhang et al. 2012b) with a Manning's roughness coefficient to calculate bottom stresses. The Manning's coefficients for ocean grid cells are computed by an empirical formula based on the water depth (H):

$$n_w = \begin{cases} 0.02 & 0 < H < 1 \text{ (m)} \\ 0.01/H + 0.01 & H \geq 1 \end{cases} \quad (10)$$

or set up to be constants, e.g.,

$$n_w = C \quad (11)$$

where C ranges from 0.01 to 0.03. Manning's coefficients for grid cells over the land were estimated according to the 2006 national land cover dataset (NLCD) created by the U.S. Geological Survey (USGS) (Fry et al. 2011). A modified table of Manning's coefficients (Table 1) corresponding to different land cover categories proposed by Mattocks and Forbes (2008) was employed in this study. Since the spatial resolution of NLCD is 30 m which is usually smaller than the cell size of a CEST grid, an average Manning's coefficient (n_a) for a grid cell was calculated using

$$n_a = \frac{\sum_{i=1}^N (n_i \alpha) + n_w \beta}{N \alpha + \beta} \quad (12)$$

where n_i is the Manning's coefficient value of a NLCD pixel within a model grid cell, α is the area of a NLCD pixel, N is the total number of NLCD pixels within a model cell, n_w is the Manning's coefficient for the oceanic area β that are not covered by NLCD pixels.

NLCD Class Number	NLCD Class Name	Manning Coefficient
11	Open Water	0.020
12	Perennial Ice/Snow	0.010
21	Developed Open Space	0.020
22	Developed Low Intensity	0.050
23	Developed Medium Intensity	0.100
24	Developed High Intensity	0.130
31	Barren Land (Rock/Sand/Clay)	0.090
32	Unconsolidated Shore	0.040
41	Deciduous Forest	0.100
42	Evergreen Forest	0.110
43	Mixed Forest	0.100
51	Dwarf Scrub	0.040
52	Shrub/Scrub	0.050
71	Grassland/Herbaceous	0.034
72	Sedge/Herbaceous	0.030
73	Lichens	0.027
74	Moss	0.025
81	Pasture/Hay	0.033
82	Cultivated Crops	0.037
90	Woody Wetlands	0.140
91	Palustrine Forested Wetland	0.100
92	Palustrine Scrub/Shrub Wetland	0.048
93	Estuarine Forested Wetland	0.100
94	Estuarine Scrub/Shrub Wetland	0.048
95	Emergent Herbaceous Wetlands	0.045
96	Palustrine Emergent Wetland (Persistent)	0.045
97	Estuarine Emergent Wetland	0.045
98	Palustrine Aquatic Bed	0.015
99	Estuarine Aquatic Bed	0.015

Table 1. Manning's coefficients for various categories of land cover.

Wind field computation

Both parametric models and time series of wind fields (H^*Wind) generated by the Hurricane Research Division of NOAA based on field measurements (Houston et al. 1999; Powell et al. 1998) can be used to compute wind stresses. H^*Wind provides snapshots of the wind field every 2-6 hours, but the instantaneous wind field is needed for storm surge computation by the model at

each time step. Thus, the wind fields between two adjacent H*Wind fields are generated using a bilinear interpolation in space and a linear interpolation in time based on the center positions of two H*Wind fields and the values of H*Wind fields. The parametric wind model used by the FPFLM was employed to estimate the hurricane wind field when H*Wind data were not available. To account for the terrain effect on the wind, two different drag coefficients are used to compute the wind field on the terrain and extreme shallow waters and the wind field on the ocean, which are referred to as lake wind and ocean wind, respectively. The effects of vegetation on the wind field have also been accounted for in a way similar to the SLOSH model (Jelesnianski et al. 1992). The wind speed is adjusted using a coefficient C_T based on the ratio of the surge water depth ($D=H+\zeta$) to the vegetation height (H_T):

$$C_T = \begin{cases} \frac{D}{H_T} & D < H_T \\ 1 & D \geq H_T \end{cases} \quad (13)$$

The effect of trees on the wind speed decreases based on this equation as the water submerges the vegetation gradually. In this study, the land areas covered by dense vegetation and development were classified into the "Tree" category and assigned an average vegetation height of 8 m, the same as the one used by SLOSH for the Florida basins. When a storm surge floods low-lying areas, it often forms a thin layer of water over land. An extinction coefficient C_E is applied to the wind speed to reduce its effect on the thin layer of water (Jelesnianski et al. 1992).

$$C_E = \begin{cases} \frac{D}{0.3} & D < 0.3 \text{ m} \\ 1 & D \geq 0.3 \text{ m} \end{cases} \quad (14)$$

Boundary Conditions

The ‘‘Sommerfield’’ radiation condition (Blumberg and Kantha 1983) was used at the open boundaries for a variable ϕ which can be either water level or velocity:

$$\frac{\partial \phi}{\partial t} + \hat{c} \frac{\partial \phi}{\partial n} = 0 \quad (15)$$

where \hat{c} is the velocity which includes wave propagation and advection. The water level elevation at the open boundary was generated using seven tidal constituents M2, S2, N2, K1, O1, K2, and Q1. These constituents were obtained from the U.S. Army Corps of Engineers’ (USACE) East Coast 2001 database of tidal constituents (Mukai et al. 2002).

Four Set of Florida Basins

There are totally 4 sets of basins established for the storm surge simulation covering the whole coastal area of Florida (Figure 11).

1. 3 Apalachicola Bay basin, AP7, AP8, and AP9, majorly covers the north and west Florida coastal areas, with different grid resolutions;
2. 3 Tampa Bay basin, TP2, TP3, and TP4, covers the west Florida coastal area, with different grid resolutions;
3. 3 South Florida basin, HMI4, HMI41, and HMI42, majorly covers the south Florida coastal area and Keys, with different grid resolutions;
4. 3 Florida Atlantic basin, EJX4, EJX5, and EJX6, covers the whole east Florida coastal area, with different grid resolutions.



Figure 11. Four Florida Basins that used by CEST Model.

The overlap area of the above four set basins is relatively large, sometime even half of the basin area. The reason is consideration between large domain size and fine resolution of the grid for the interesting area. It is necessary and interesting to examine the storm surges on the overlap area of different basins with same storm tracks. As the CEST model is robust, stable, consistent, and compatible, the computed surge at the same region with different basins should be similar and comparable.

Apalachicola Bay basins including AP7, AP8, and AP9

The AP8 and AP9 are the newly generated basins with the same semi-circle domain as AP7, which cover the all the north and west coastal area of Florida. The grid cell resolution for AP7, AP8, and AP9 is about 100, 350, and 1400 meters respectively along the coastal area (Table 2). The computational time for coarse resolution basin AP9 is only 0.5-1 minutes for a 4-days simulation, whereas AP8 and AP7 consume about 10-15 minutes and 2 hours to complete the same run, respectively.

Basin Name	AP7	AP8	AP9
Domain Description	CEST Basin	CEST Basin	CEST Basin
Size	Large	Large	Large
Resolution (m)*	100	350	1400
Dimension	772*710	387*356	99*91
Total Number of Cells	548,120	137,772	9,009
Time Step (s)	30	20	30
Computation Time** of 4 days (minutes)	120-130	10-15	0.5-1

Table 2. Basin description and statistics for Apalachicola Bay.

* The resolution of the model basin varies spatially. The resolution in the table represents the approximate edge size of a grid cell at the coastal area.

** Computational time was derived by recording the simulation time using a single processor in a Dell PC workstation with four 2.5 GHZ Intel Xeon processors and 12GB of RAM.

Miami and Key basins including HMI4, HMI41, and HMI42

The HMI4, HMI41, and HMI42 with the same circle domain cover the all the south coastal area of Florida with a grid cell resolution about 1,000, 300, and 150 meters respectively along the coastal area (Table 3). The coarse resolution grid HMI4 only takes 5-7 minutes to finish a 4-days simulation, whereas HMI41 and HMI42 consume around 25 minutes and 2 hours to complete the same run.

Basin Name	HMI4	HMI41	HMI42
Domain Description	CEST Basin	CEST Basin	CEST Basin
Size	Large	Large	Large
Resolution (m)	1000	300	150
Dimension	185*395	332*480	442*1216
Total Number of Cells	73,075	159,360	513,152
Time Step (s)	30	30	30
Computation Time of 4 days (minutes)	5-7	20-25	110-130

Table 3. Basin description for Miami and Key.

Tampa bay basins including TP2, TP3, and TP4

The TP2, TP3, and TP4 with the same semi-circle domain cover the all the west coastal area of Florida with grid cell resolution about 1,800, 450, and 230 meters respectively along the coastal area (Table 4). The computational time for coarse resolution basin TP2 is only 1 minutes for a 4-days simulation, whereas TP3 and TP4 consume about 10 minutes and 1 hour to complete the same run.

Basin Name	TP2	TP3	TP4
Domain Description	CEST Basin	CEST Basin	CEST Basin

Size	Large	Large	Large
Resolution (m)	1800	450	230
Dimension	80*106	314*418	626*834
Total Number of Cells	8,480	131,252	522,084
Time Step (s)	30	30	30
Computation Time of 4 days (minutes)	0.5-1	9-12	50-70

Table 4. Basin description and statistics for Tampa Bay.

Jacksonville basins including EJX4, EJX5, and EJX6

The EJX4, EJX5, and EJX6 with the same semi-circle domain cover the all the eastern coastal area of Florida with an area of 351,370 km² and a grid cell resolution about 2500, 600, and 300 meters respectively along the coastal area (Table 5). The computational time for coarse resolution basin EJX4 is only 1-2 minutes for a 4-days simulation, whereas EJX5 and EJX6 consume about 20 minutes and 2 hours to complete the same run.

Basin Name	EJX4	EJX5	EJX6
Domain Description	CEST Basin	CEST Basin	CEST Basin
Size	Large	Large	Large
Resolution (m)	2500	600	300
Dimension	104*106	410*418	818*834
Total Number of Cells	11,024	171,380	682,212
Time Step (s)	30	30	10
Computation Time of 4 days (minutes)	1-2	15-20	120-160

Table 5. Basin description and statistics for Jacksonville.

For each basin, all three updated grids with different grid size were verified and calibrated for historical hurricanes. The comparison of time series of water level showed that the CEST model can produce reasonable storm surge at selected NOAA tidal gauges with the H*WIND wind field. Considering the accuracy and computational time, the medium resolution grid AP8, TP3, HMI41, and EJX5 are finally selected for FPFLM project. As the massive High Performance Computes improve, the high resolution grids are going to employ into this project in the futures.

Wave Model

The wave model used is STWAVE, a US Army Corps of Engineers program for computing nearshore wave transformation. The model solves the spectral wave action equations over a regular grid, assuming steady-state conditions. From the STWAVE Manual (Massey et al., 2011):

“STWAVE (STeady-state spectral WAVE), a nearshore spectral wave model, was developed by the U.S. Army Engineer Research and Development Center (ERDC), Coastal and Hydraulics Laboratory (CHL) to accurately simulate nearshore wave propagation and transformation including refraction, shoaling, breaking, and wind-wave generation. Recently, CHL has further

enhanced STWAVE to include both half-plane and full-plane capabilities within a single executable; improved and streamlined file formats; and made it Earth System Modeling Framework (ESMF) compliant, which allows for easier coupling to other models. STWAVE now runs in serial mode as well as parallel in time or space on both personal computing (PC) and high-performance computing (HPC) systems”.

Assumptions made in STWAVE are:

- “1. Phase-averaged. STWAVE is based on the assumption that relative phases of the spectral components are random, and phase information is not tracked. In order to resolve detailed near-field reflection and diffraction patterns near coastal structures, a phase-resolving model should be applied.
2. Mild bottom slope and negligible wave reflection. Waves reflected from the shoreline or from steep bottom features are neglected.
3. Steady-state waves, currents, and winds. STWAVE is formulated as a steady-state model, which reduces computation time and is appropriate for wave conditions that vary more slowly than the time it takes for waves to transit the domain. For wave generation, the steady-state assumption means that the winds have remained steady sufficiently long for the waves to attain fetch-limited or full-developed conditions (waves are not limited by the duration of the winds).
4. Linear refraction and shoaling. STWAVE incorporates linear wave refraction, shoaling, and propagation, and thus, does not represent wave asymmetry or other nonlinear wave features. Model accuracy is reduced (e.g., underestimated wave heights) at large Ursell numbers.
5. Depth-uniform current. The wave-current interaction in the model is based on a current that is constant throughout the water column; the modification of refraction and shoaling due to strong vertical gradients is not represented.”
6. Linear radiation stress. Radiation stress is calculated based on linear wave theory”.

The present work does not use the full capabilities of STWAVE, but instead a subset to allow computation of tens of thousands of scenarios over the entire coastline of Florida. The model is run with directional capabilities, but only around the peak frequency. Computations are only made for a relatively short distance near the shoreline, and use parametric hindcast relations (Young and Verhagen, 1996) to provide the wave height and period at the offshore boundary. For nearshore locations, wave breaking uses Thornton and Guza (1983) relations instead of the standard depth-limited cutoff. Other than this, there are no changes to the model.

Inland Flood Component

The inland flood models have addressed the freshwater flooding scenarios within the state of Florida. The specific objective of this study is to predict stormwater led overland flooding during the rainfall events that will lead to flood loss at property locations. To compute the flood depths for different rainfall events, inland flood models have been developed using the US EPA Stormwater Management Model (SWMM 5.1), which is a process based, semi-distributed rainfall runoff model (Rossman, 2015). SWMM has been widely used in the study of hydrologic processes for runoff estimation and flood prediction (Abdul-Aziz and Al-Amin, 2016; Jiang et al., 2015) A brief description of the inland flood model is given below:

Model development for the inland basins

Basin delineation

The inland flood model for state of Florida has been discretized by six inland basins: Southeast Coasts Basin (SEC), Kissimmee River Basin (KIS), Southwest Florida Basin (SWF), St. Johns River Basin (SJN), Suwannee River Basin (SWN), and Northwest Florida Basin (NWF) (Figure 12). Extents of the six inland basins were developed using the watershed boundary datasets (previously known as Hydrologic Unit Codes) of U.S. Geological Survey (USGS).

Incorporation of hydro-network

In order to develop the hydro-network (e.g., subbasins, drainage links and nodes) for the inland basins by ArcGIS-ArcHydro tool, DEMs of 10m resolution (**Error! Hyperlink reference not valid.**) have been used. At first, six inland basins were split into smaller subbasins (Table 6. Summary of the generated hydro-network for the six inland basins Table 6). Areas having greater imperviousness (i.e., commercial, industrial areas) have been discretized by smaller subcatchments to provide inland flood model outputs at finer spatial resolutions. The stream networks (links and junctions), generated by ArcGIS-ArcHydro tool were then compared with the actual drainage network, obtained from National Hydrography dataset (NHD) of USGS, and modified accordingly if necessary.

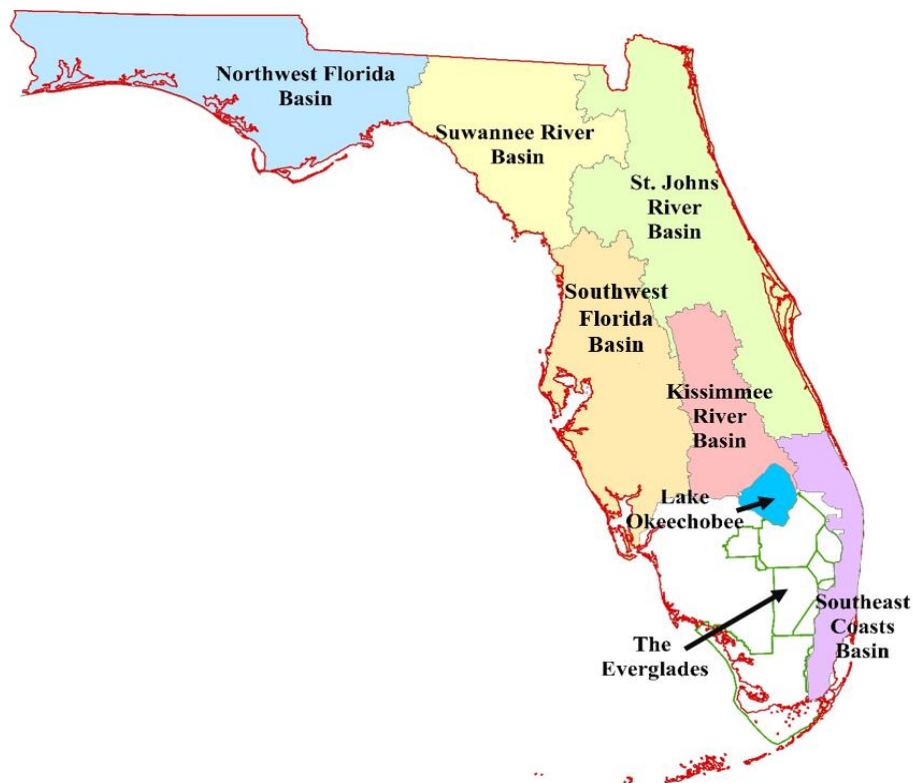


Figure 12. Extent of six inland basins.

Inland Basin Name	No. of Subbasins	Basin Area (km ²)	No. of Drainage Links	No. of Drainage Nodes
Southeast Coasts Basin (SEC)	333	7156	438	440
Kissimmee River Basin (KIS)	641	10267	641	649
Southwest Florida Basin (SWF)	703	28430	706	774
St. Johns River Basin (SJN)	766	28189	782	794
Suwannee River Basin (SWN)	337	18865	349	363
Northwest Florida Basin (NWF)	1055	29320	1066	1090

Table 6. Summary of the generated hydro-network for the six inland basins.

Incorporation of the hydro-meteorological information

Precipitation is the principal forcing variable for the rainfall-runoff process. We used hourly rainfall data in the six inland basin models. Rainfall data for available observed stations (Table 7) were assigned to each subbasin by creating Thiessen polygons. We incorporated spatially averaged monthly PET rates (mm/day) across all 2km X 2 km USGS grids falling within the respective basins.

Inland Basin	Number of Rainfall Stations	Source
SEC	71	South Florida Water Management District (SFWMD) and National Climatic Data Center (NCDC)
KIS	39	South Florida Water Management District (SFWMD)
SWF	96	Southwest Florida Water Management District (SWFWMD) and National Climatic Data Center (NCDC)
SJN	17	National Climatic Data Center (NCDC)
SWN	22	National Climatic Data Center (NCDC)
NWF	30	National Climatic Data Center (NCDC) and Florida Climate Center

Table 7. Rainfall Data Information for the Inland Basin.

Parameterization of subbasin properties

Subbasin properties such as the slope and imperviousness are required to develop the SWMM models for the inland basins. The percent slopes of the subbasins were extracted from the 10m DEM, whereas the land use information of the subbasins were obtained from the National Land Cover Database (NLCD) percent impervious raster dataset of NLCD 2006, and NLCD 2011 (Fry et al., 2011; Homer et al., 2015). The characteristic width, overland roughness coefficients, and depression storage depths were incorporated in the model in accordance with the recommended values mentioned in SWMM Reference Manual Volume I, Hydrology (Rossman and Huber, 2016).

Parameterization of groundwater and infiltration process

Aquifers incorporated in a SWMM model address vertical movement of water infiltrating from the subbasins that lie above them. These aquifers also account for the exchange of groundwater with the adjacent drainage system. SWMM only requires groundwater elevation information for the initial time step and it dynamically updates subsequent groundwater levels based on the provided rainfall data. The groundwater information were mainly obtained from USGS and DBHYDRO monitoring wells. Green-Ampt method was chosen for representing infiltration of water into the soil. The main parameters for the Green-Ampt model were the initial moisture deficit of the soil, the soil's hydraulic conductivity, and the suction head at the wetting front. For assigning the infiltration and aquifer parameters (porosity, wilting point, field capacity, etc.), soil type data obtained from the soil survey geographic (SSURGO) database (USDA-NRCS, 2015) and the recommended values mentioned in SWMM Reference Manual Volume I, Hydrology (Rossman and Huber, 2016) were used.

Incorporation of drainage network into inland flood model

Drainage system in SWMM is represented by a network of links (streams) connected at junction nodes. In natural system, nodes represent the confluence of surface channels, while the links represent the streams (rivers or canals). The invert elevations of nodes (elevation at channel bottom) are obtained from 10m DEM. The geometry of the stream links has been introduced by using the surveyed cross sections. When surveyed cross sections from corresponding water management districts were not available, we used 10m DEM to incorporate representative cross sections for streams.

Model simulation and performance evaluation

For calibration and validation of the inland flood models long term, continuous simulations were performed. The models were calibrated and validated with the daily mean observed streamflow at most major river reaches across the six inland basins. We used the Nash-Sutcliffe Efficiency (NSE) (Nash and Sutcliffe, 1970) and the ratio of the root-mean-square-error to the standard deviation of observations (RSR) metrics to evaluate the model performance.

Model development for the isolated areas

The six inland basins cover the entire state of Florida, except for the keys, isolated islands (e.g., Miami Beach), and the greater Everglades. Since it is quite difficult to develop the hydro-networks for such keys and isolated areas, we have developed separate SWMM models for the isolated areas without considering hydraulic routing. To compute the freshwater flooding depth in these isolated landmasses, five isolated area SWMM models named as East Coasts, Everglades, Keys, Southern Gulf Coasts, and Northern Gulf Coasts have been developed (Figure 13). These models have been discretized by a number of 300m X 300m blocks; each grid cell has been incorporated as a subbasin in the SWMM model. We have parameterized the subcatchment properties, infiltration parameters for these subbasins following the same approach that we adopted for the inland basins. The spatial resolution of rain gages for the isolated areas is 3km X 3km.



Figure 13. Extent of five isolated area models

Vulnerability Component

The engineering team of the FPFLM has several peer-reviewed publications, which have been either published (Baradaranshoraka et al., 2017; Baradaranshoraka et al., 2019) or are under review (Paleo-Torres et al., 2019; Pinelli et al., 2019). For the sake of clarity, and to provide a complete narrative describing the personal residential flood vulnerability model of the FPFLM, these papers have been combined, abridged and presented below. The subsequent disclosure responses in the VF standards will then refer as needed to this narrative.

Three main sections are presented below: development of vulnerability of residential structures to coastal flood, development of vulnerability of residential structures to inland flood, and development of manufactured housing to inland and coastal flood.

Vulnerability of site-built residential structures to Coastal Flood

Introduction and Background

In general, fragility and vulnerability functions are either empirical models derived from post-disaster damage assessments and/or claims data, engineering-based models derived from structural behavior principles, models based on expert opinion, or some combination of these three. Statistical analysis of the observed performance of structures, from large observational datasets are the basis of the empirical models. The development of engineering-based models requires an understanding of the loads, structural response and resistance, load path, and environmental uncertainties. Expert-based models rely on the consensus of opinions from a team of professionals with subject expertise. These expert opinions are commonly informed by a combination of personal observations, modeling and field data.

This report presents a semi-engineering approach, which adapts a procedure proposed in Barbato et al. (2013) to translate empirical tsunami fragility functions from Suppasri et al. (2013) into coastal flood fragility functions, based on engineering principles. Following Baradaranshoraka et al. (2019), the coastal flood fragility functions are translated into coastal flood vulnerability functions for different types of residential structures common in the state of Florida. Claims data and expert-based models are employed for validation.

The engineering team strategy was to adapt a large body of tsunami related building fragility curves, especially the work developed by Suppasri et al. (2013), to coastal flood, and to adapt the work of the US Army Corp of Engineers (USACE, 2006, 2015) for inland flood. The engineering model output consists of building vulnerability curves that estimate the mean building damage ratio as a function of inundation height relative to ground level (Baradaranshoraka et al., 2017). The building damage ratio is defined herein as the cost of repair of a damaged building divided by the replacement value of the building.

This report discusses the tsunami damage field dataset, the nonlinear translation of the tsunami fragilities to coastal flooding (surge) fragilities via force equivalency analysis, the quantification of the damage states, the conversion of coastal flood fragilities to vulnerability functions, and results and validation for a single family slab on grade timber and masonry structure using an independently derived model and claims data.

Tsunami Damage Dataset

The 2011 Great East Japan tsunami affected hundreds of thousands of buildings, including residential and commercial structures. Suppasri et al. (2013) used a dataset of more than 250,000 damaged buildings to develop empirical fragility functions related to the water inundation depth. These fragility functions are stratified by structural characteristics such as construction material and number of stories, resulting in one of the most comprehensive such studies ever conducted.

Suppasri et al. (2013) utilized information obtained by the Ministry of Land, Infrastructure and Transportation of Japan (MLIT) from post-disaster field surveys. The surveys information related the assessment of different levels of damage per building to the tsunami inundation depths at the structure's location. The data was grouped in 0.5 m increments of tsunami inundation depths. The MLIT classified the observed damage into six levels of severity, or physical Damage States (DS):

(1) minor damage, (2) moderate damage, (3) major damage, (4) complete damage, (5) collapse and (6) washed away. The MLIT classification of damage was based on observed physical damage in different structural and non-structural components of the buildings, and damage ratios dr_i can be assigned to each damage state DS_i (details in the next section). The buildings were classified according to their number of stories and their structural material, such as reinforced concrete, steel, timber and other materials. Based on the characteristic of the buildings and the damage states, Suppasri et al. (2013) used a least squares regression method and the lognormal cumulative distribution function to derive fragility functions for each damage state for the different building classes (BC). Equation ENG-1 describes the shape of the tsunami fragility functions resulting from regression analysis, where the function P is the probability of a damage ratio DR meeting or exceeding a damage state DS_i characterized by a damage ratio dr_i given a certain water inundation depth relative to ground level d_{s_j} at any given point, and a certain building class bc_l . Φ is the standard normal distribution function. The variables μ' and σ' are the mean and standard deviation for the lognormal function, specific to the building class and the damage state.

$$P(DR \geq dr_i | D_S = d_{s_j}, BC = bc_l) = \Phi \left[\frac{\ln d_{s_j} - \mu'}{\sigma'} \right] \quad [\text{ENG-1}]$$

Table 8 lists the parameters used as input in Equation ENG-1 to describe the tsunami fragility functions for timber and RC residential structures (Suppasri et al. 2013).

Structure		DS 1		DS 2		DS 3		DS 4		DS 5		DS 6	
		μ'	σ'										
Timber	1-	-1.73	1.15	-0.86	0.94	0.05	0.71	0.69	0.53	0.81	0.59	1.17	0.58
Timber	2-	-2.01	1.19	-0.87	0.91	0.04	0.74	0.78	0.52	0.95	0.57	1.36	0.47
Timber	3-	-2.19	1.32	-0.86	1.22	0.11	0.84	0.80	0.47	1.27	0.62	1.77	0.37
RC	1-story	-1.88	1.19	-0.82	1.06	0.16	0.82	0.89	0.84	1.66	0.90	2.42	0.87
RC	2-story	-2.26	1.25	-0.95	1.04	0.20	0.75	0.93	0.69	1.78	0.72	2.44	0.66
RC	3-story	-2.78	1.66	-0.98	1.02	0.15	0.66	1.14	0.80	2.35	0.79	2.71	0.50

Table 8. Tsunami fragility curves parameters per DS for timber and reinforced concrete residential structures (from Suppasri et al., 2013).

Coastal Flood Fragilities

The authors assume that the probability of meeting or exceeding a given damage state for residential structures in Japan is similar, but not identical, to the probability of meeting or exceeding the same damage state for a residential structure in Florida under water-induced forces of similar magnitudes. Under this assumption, the key element to translate the tsunami fragility curves into coastal flood fragility curves is the calculation of the different inundation depths that correspond to equivalent water loading forces for tsunami and surge. Deviations from this similar damage state assumption are then corrected in the model calibration stage through adjustments to the cost ratios assigned to the building components. The next section describes this water loading force equivalency calculation.

Coastal Flood and Tsunami Water Forces

The FPFLM coastal flood model considers the effect of different wave conditions during coastal flood. Storm surge waves (coastal flood) and tsunamis belong to the class of long gravity waves. The wavelengths of tsunamis are large in deep ocean and present small amplitudes, but as it approaches shallow waters, the tsunami slows down causing the wave to compress and increase in amplitude. Similar to tsunami waves, coastal flood waves amplify considerably in shallow waters and on wide continental shelves (Nirupama et al., 2006).

The conversion of the fragility functions from tsunami to coastal flood relies on the calculation of the different coastal flood and tsunami inundation depths that produce equivalent water-forces. The forces considered are the resultant lateral horizontal forces acting on the vertical walls of the structures. These forces vary depending on the severity of the wave state associated with the coastal flood condition. The FPFLM model discretizes the continuum of wave intensity relative to water depth into three coastal flood (CF) conditions: coastal flood with minor waves (CF1), with moderate waves (CF2), and with severe waves (CF3). Table 9 shows how the ratio of the wave height (H_w), distance from trough to crest, to still water inundation depth (d_s), H_w/d_s , defines the boundaries of the coastal flood conditions. Waves are assumed to break when the ratio is more than 0.78, (FEMA 2011).

Coastal Flood Conditions		Wave Height Range
CF1	Minor Waves	$0 < H_w/d_s \leq 0.3$
CF2	Moderate Waves	$0.3 < H_w/d_s \leq 0.6$
CF3	Severe Waves	$0.6 < H_w/d_s \leq 0.78$

Table 9. Definitions of three coastal flood conditions.

ASCE (2010) and FEMA (2011) recommend Equation ENG-2 to calculate the breaking wave load F_{wave} per unit length (l) on a vertical wall. This equation is from Walton et al. (1989), who reference Homma and Horikawa (1965). Figure 14-a shows the pressure diagram utilized to develop this equation through the calculation of the areas. The formula has two parts: a dynamic slamming load (first term) and a hydrostatic load (second term). Both terms assume a total affected depth at the wall of $2.2d_s$ (or $1.2d_s$ above the still water level) which results from the wave run-up and reflection. Dynamic pressure increases linearly from zero at the upper limit to the maximum value of $C_p \rho_w g d_s$ at the stillwater flood elevation (d_s), where C_p is a dimensionless dynamic pressure coefficient equal to 1.6, ρ_w is the density of saltwater and g is the gravitational acceleration constant. The dynamic pressure decreases linearly from its maximum value to zero at the toe of the wall.

$$F_{wave}/l = 1.1C_p\rho_wgd_s^2 + 2.4\rho_wgd_s^2 \quad \text{[ENG-2]}$$

Equation ENG-2 applies for breaking waves only, as described in FEMA (2011). It was necessary to modify Equation 2 to capture all three of the coastal flood conditions described in Table 9.

Considering a breaking wave height of $H_b = 0.78d_s$, and setting Equation ENG-2 in terms of H_b , the $1.2d_s$ above the stillwater level (Figure 14-a), due to the waves, is equivalent to $1.2H_b/0.78$

(Figure 14-b). The maximum value for the dynamic component in terms of H_b is equal to $C_p \rho_w g H_b / 0.78$ (Figure 14-b).

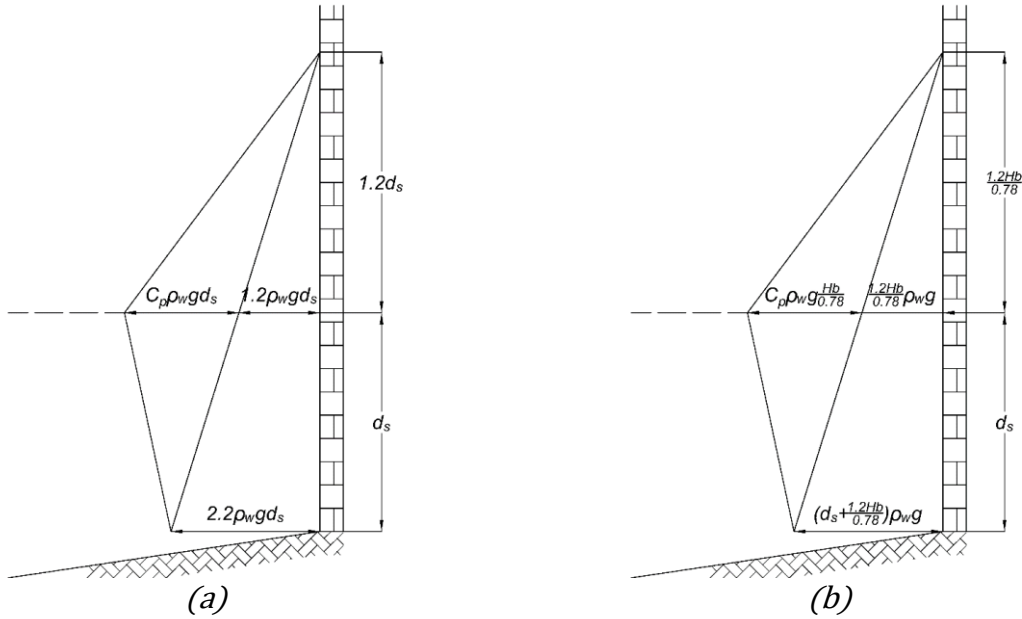


Figure 14. a) Pressure distribution based on Walton et al. (1989); b) Pressure distribution in terms of the breaking wave height.

Figure 14-b shows the pressure diagram presented in Figure 14-a, but here the terms affected by the dynamic effects of the wave are expressed in terms of the breaking wave height H_b . For a case of coastal flood with non-breaking waves, all of the assumptions are kept, but H_b is replaced by H_w . The calculation of the areas in Figure 14-b, but considering H_w instead of H_b results in Equation ENG-3, which now captures minor, moderate and severe wave states.

$$F_{CF} = F_{wave}/l = \frac{1}{2} C_p \rho_w g \frac{H_w}{0.78} \left(d_s + \frac{1.2 H_w}{0.78} \right) + \frac{1}{2} \rho_w g \left(d_s + \frac{1.2 H_w}{0.78} \right)^2 \quad [\text{ENG-3}]$$

For the case of breaking waves, i.e. $H_w = H_b = 0.78 d_s$, Equation ENG-3 reverts to the ASCE formula (Equation ENG-2), and for the case of no waves, it becomes the standard hydrostatic pressure of the still water depth. In this study, Equation ENG-3 is used to express the lateral horizontal forces acting on the structures due to coastal flood. The hydrostatic internal pressure of the water entering the structures is not subtracted from the resultant hydrodynamic external force. The model assumes that the water level inside the structure does not immediately reach d_s , with a worst-case scenario of a maximum d_s outside the structure and no water inside.

The tsunami water depth-force relationship is also needed for the development of the coastal flood fragility functions. Palermo et al. (2009), suggest Equation ENG-4 to estimate the tsunami surge force per unit length, where d_s in this case is the tsunami inundation depth, C_d is a drag coefficient and u is the flow velocity.

$$F_{ts}/l = \frac{1}{2} \rho_w g d_s^2 + \frac{1}{2} C_d \rho_w u^2 d_s \quad [\text{ENG-4}]$$

When C_d is taken as 2 (infinitely long walls) and u is assumed equal to $2\sqrt{gh}$, Equation ENG-4 becomes Equation 5. The City and County of Honolulu building code (CCH, 2000) suggests the use of Equation ENG-5 to estimate the tsunami surging force per unit length, generated by a bore-like wave based upon the results of Dames and Moore (1980). Palermo et al. (2013a) describe a triangular pressure distribution as the origin of Equation ENG-5, as illustrated Figure 15. In Equation ENG-5, d_s is the inundation depth, which is the hazard intensity metric adopted in this study.

$$F_{Tsu} = F_{ts}/l = 4.5\rho_wgd_s^2 \quad \text{[ENG-5]}$$

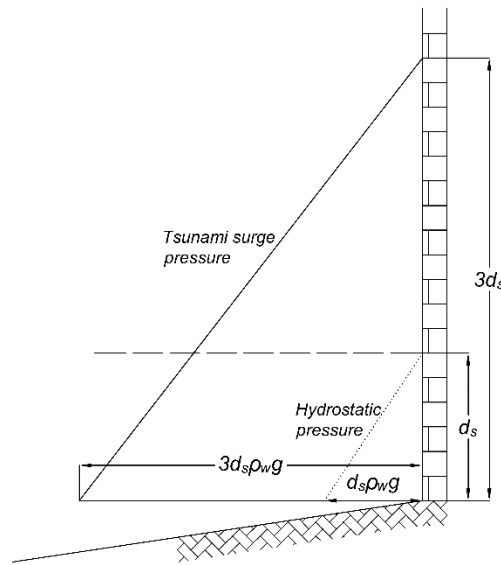


Figure 15. Tsunami surge pressure distribution, reproduced based on Palermo et al. (2013a).

Figure 16 presents the resultant water forces for tsunami (Equation ENG-5) and the three wave states being considered (Equation ENG-3 and Table 9). The coastal flood forces approach the tsunami forces as the severity of the wave increases. The upper limit value from Table 9 is assigned to each of the three different wave scenarios, i.e. H_w for minor waves is equal to $0.3d_s$, $0.6d_s$ for moderate waves, and $0.78d_s$ for severe waves (breaking waves).

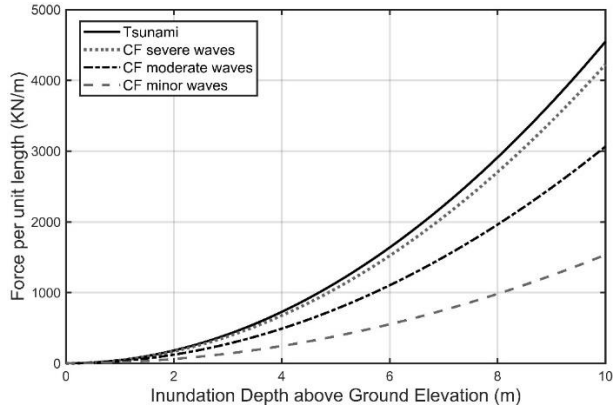


Figure 16. Tsunami and Coastal Flood (CF) water forces

Fragility function conversion

This study adapted the methodology in Barbato et al. (2013) for the conversion of tsunami fragility functions into coastal flood fragility functions via force equivalency. The procedure is conceptually illustrated in Figure 17, where d_s is the inundation depth, F is the lateral horizontal water forces exerted on a unit width of building, $P(DR \geq dr_i|F)$ is the fragility as a function of force, and $P(DR \geq dr_i|d_s)$ is the fragility as a function of inundation depth.

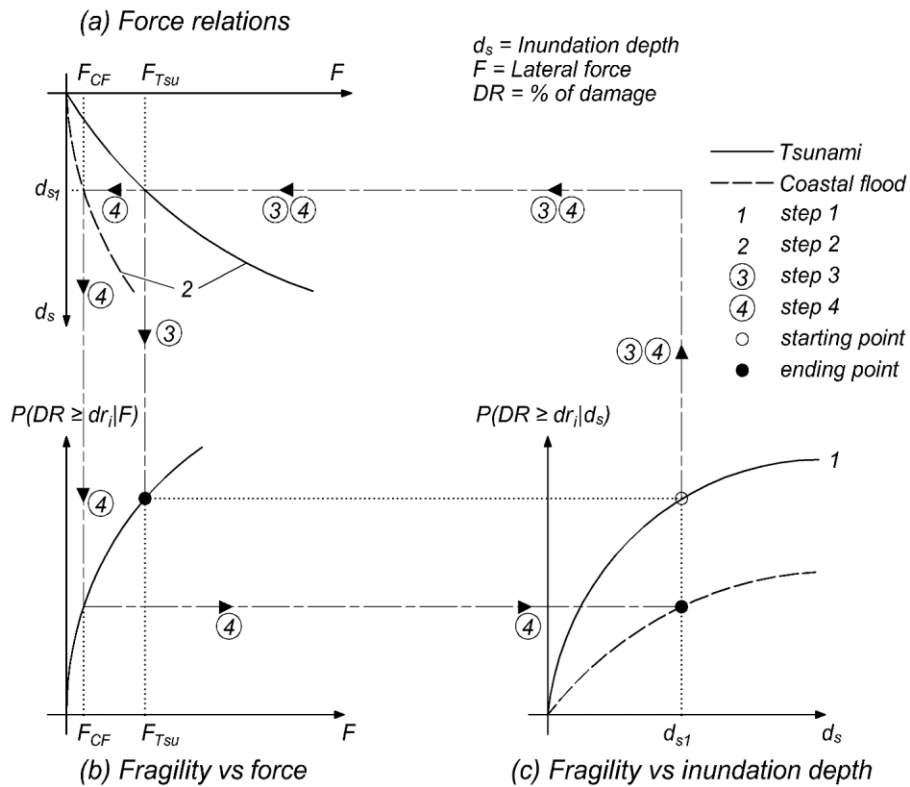


Figure 17. Conversion of a tsunami fragility function to a surge fragility function.

Table 10 conceptualizes mathematically the process described in Figure 17.

Tsunami Fragility function of $d_s \Rightarrow$ Tsunami Force function of d_s	Fragility function of $F \Rightarrow$ CF Force function of d_s	CF Fragility function of d_s
(from Eq. ENG - 1) $P(DR \geq dr_i d_s) = \Phi(d_s)$ (from Eq. ENG - 5) $x(d_s) = F_{Tsu}$	$P(DR \geq dr_i F) = \Phi(x^{-1}(F))$ (from Eq.3) $y(d_s) = F_{CF}$	$P(DR \geq dr_i d_s) = \Phi(x^{-1}(y(d_s)))$

Table 10. Mathematical description of the fragility conversion process.

The following walk-through of the procedure corresponding to Figure 17 illustrates the conversion of tsunami fragility for one damage state (DS) to fragility corresponding to one coastal flood condition for that same DS. In the full implementation of this method, fragility for each of the six tsunami DS (Table 8) is converted to the three coastal flood conditions (Table 9). This conversion is repeated for each building class (BC) considered. Each collection of six fragilities (per BC, per coastal flood condition) is then converted to a single vulnerability function that models mean damage ratio as a function of inundation depth (section 5).

Step 1: Initialize the conversion by selecting the tsunami fragility function (Equation ENG-1 and Table 8) to be converted. This produces the solid line in Figure 17-c, tsunami fragility as a function of inundation depth.

Step 2: Calculate the coastal flood force F_{CF} and tsunami force F_{Tsu} as a function of inundation depth d_s using Equations ENG-3 and ENG-5, respectively, to produce the force relations in Figure 17-a.

Step 3: Map tsunami fragility as a function of inundation depth to fragility as a function of force $P(DR \geq dr_i|F)$ by following the step 3 path in Figure 17. It is equivalent to plugging the inverse function of Equation ENG-5 into Equation ENG-1. This produces Figure 17-b. This expression of fragility is independent of the source of the force (tsunami or coastal flood), and provides the map for the final step.

Step 4: The desired coastal flood fragility as a function of inundation depth (Figure 17-c, dashed line) is now produced by following the step 4 path in Figure 17. This begins with tsunami fragility at a given inundation depth in Figure 17-c, and ends with the corresponding coastal flood fragility at that same inundation depth. This is repeated over a series of inundation depths to map tsunami fragility to coastal flood fragility as a function of inundation depth. It is equivalent to replacing the force F in the fragility equation $P(DR \geq dr_i|F)$ by its expression from Equation ENG-3.

From the above, each combination of building class (BC) and coastal flood condition (Table 9) results in a set of eight coastal flood fragility curves:

$$P\left(DR \geq dr_i \mid D_S = d_{s_j}, H_{w_j}/d_{s_j} \in CF_m, BC = bc_l\right) \equiv P(DR \geq dr_i | D_S, CF, BC) \text{ [ENG-6a]}$$

With index j varying between 0 and 6, with

$$P(DR \geq dr_0 = 0 | D_S, CF, BC) = 1 \quad \text{[ENG-6b]}$$

and

$$P(DR \geq dr_7 = dr_{\max} | D_S, CF, BC) = 0$$

[ENG-6c]

Where dr_{\max} can be greater than 100% due to the cost of debris removal and disposal. Figure 18 shows an example of a set of fragilities for the case of a one-story slab on grade reinforced masonry structure subject to coastal flood with severe waves.

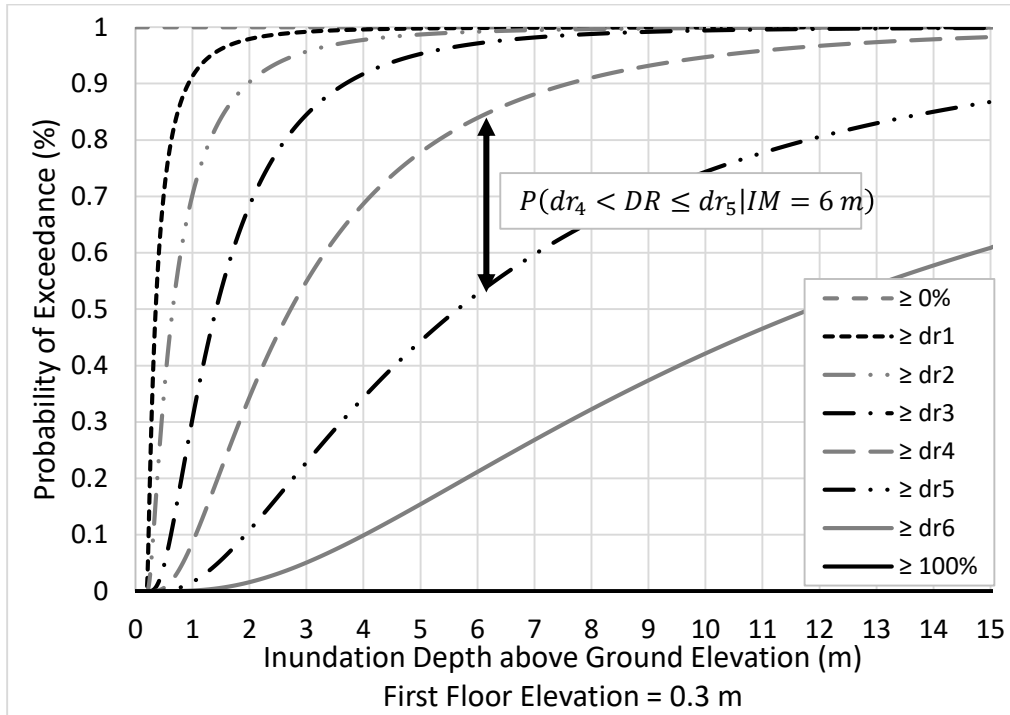


Figure 18. Example of Coastal Flood Fragility Curves

Quantification of The Damage States

Post event surveys discretize the continuum of damage by categorizing different discrete states. In the discretization process it is necessary to define a sufficient but limited number of damage states to cover the continuum of damage from no damage to extreme or total damage.

Prior to converting the coastal flood fragility functions (qualitative: damage state exceedence) to coastal flood vulnerability functions (quantitative: damage ratio), it is necessary to transform the physical descriptions of the damage states into monetary measures in terms of a cost ratio between the cost to repair or replace a component or building back to its original condition and the original cost of the entire building. The purpose of this section is to present a method to transform field observations of physical damage states into monetary-based damage states through cost analyses. The section presents a flexible, multi-component method to characterize and quantify the qualitative physical descriptions of the damage states. Section 5 will then demonstrate how the monetary description of the damage states is used to derive vulnerability curves from the fragility curves.

A critical component of this effort was the quantification of the damage states described in Suppasri et al. (2013). The first step was the characterization of the damage states based on the work of Friedland (2009) and Tomiczek et al. (2017). Friedland (2009) uses a component-by-component qualitative approach to develop a combined wind and water damage scale. Engineering judgment was used to develop this scale, based on the damage descriptions of HAZUS-MH Hurricane Model Residential Damage Scale (FEMA, 2015), which itself was developed following an approach similar to that used by Vann and MacDonald (1978). The components were the roof (roof cover, roof deck, roof structure), window/door, foundation, appurtenant structure, wall (wall cladding, wall structure), and structural damage, but it does not consider interior damage due to water intrusion. Friedland's proposed damage scale defined seven damage states starting from no damage to collapse. Each damage state for each component has a qualitative description. Pre-defined critical indicators determine the overall damage state. Tomiczek et al. (2017) modified the components into six categories, added damage to the interior, and classifies the damage into seven damage states. For each damage state and component, they provided damage descriptions approximately corresponding to those described by Friedland (2009) and assigned the overall damage state of a building based on the maximum of any individual component damage state. The FPFLM methodology uses a combination of the damage states defined in Tomiczek et al. (2017) and Suppasri et al. (2013).

The following six step methodology calculates the expected mean damage ratio for a specific damage state (dr_i). This approach requires a comprehensive description of damage states and corresponding repair tasks needed to restore the building to an undamaged condition.

Step 1: Break down a building into five components. They are:

1. Roof including roof cover, roof sheathing and soffits, and roof truss and wall connections
2. Exterior walls including wall structure and wall cover
3. Openings including garage doors, windows, doors, and sliders
4. Foundation works including site work, footing, slabs, piers or piles
5. Interior including the floor covering, ceilings, drywall, stairway, cabinets, plumbing, mechanical, and electric systems

Step 2: Provide a detailed qualitative physical description of each damage state (based on Suppasri et al., 2013; and Tomiczek et al., 2017). Each cell of Table 11 includes qualitative descriptions of the physical damages to each component for a given damage state. The first damage state represents zero damage ($dr_0 = 0\%$) to all components, and the last damage state represents 100% physical damage ($dr_7 = dr_{max} = 100\%$) to all components. These two are not included in Table 11.

Step 3: Allocate a normal distribution function of physical damage and its respective mean value and standard deviation to each description. The underlying concept of a fragility curve is the probability of meeting or exceeding a certain damage ratio. Therefore, the team decided to use the lower bound of physical damage in the qualitative description as the mean value of the assigned PDF of damage. For example, for DS2, the description states that "Significant amount of roof covering missing (greater than 40%)"; therefore, for DS2 40% is used as the mean value of the

normal distribution of roof damage. In order to define the standard deviation of each distribution for each damage state and component (σ_{DS_i, C_j}) the team used Equation ENG-7:

$$\sigma_{DS_i, C_j} = \left[\frac{(\mu_{DS_{i+1}, C_j} - \mu_{DS_{i-1}, C_j})}{6} \right] \quad [\text{ENG-7}]$$

where μ_{DS_{i+1}, C_j} is the allocated mean for the normal distribution of the next neighboring damage state for the same component and μ_{DS_{i-1}, C_j} is the allocated mean for the normal distribution of the previous neighboring damage state for the same component. The team chose to limit the distribution of the damage ratio within the two neighboring damage states, such that $(\mu_{DS_{i+1}, C_j} - \mu_{DS_{i-1}, C_j})$ is the range of the normal distribution. Since the tails of the normal distribution are unbounded, three standard deviations on each side of the mean (μ_{DS_i, C_j}) capture 99% of the probability ($\mu_{DS_i, C_j} \pm 3\sigma_{DS_i, C_j}$) that the normally distributed damage ratio is within a certain damage state (DS_i). Hence the denominator in Equation ENG-7. The assumptions behind allocating the mean and standard deviation of the normal distributions are based on engineering judgment, lessons learned from the FPFLM wind model, and descriptions of damage for each damage state included in Suppasri et al. (2013). Table 12 shows an example of the resulting distributions for each cell for the case of a one-story slab on grade reinforced masonry structure.

Step 4: Convert the normal distributions to beta distributions, which are bounded between 0% and 100%. Beta distributions are commonly used to represent the uncertainty in the probability of occurrence of an event over a bounded region (Morgan et al., 1992) and have been validated and employed in seismic economic losses studies (e.g. Dolce et al. 2006). Equations ENG-8 and ENG-9 calculate the parameters of a beta distribution (α and β):

$$\alpha = \left(\frac{1-\mu}{\sigma^2} - \frac{1}{\mu} \right) \times \mu^2 \quad [\text{ENG-8}]$$

$$\beta = \alpha \times \left(\frac{1}{\mu} - 1 \right) \quad [\text{ENG-9}]$$

Where μ is the mean value and σ is the standard deviation used in the normal distribution.

Step 5: Define the cost ratios for each component and for the total building. The cost ratio of a component (CR_j) is the ratio between the cost to repair or replace a component back to its original condition and the original cost of the entire building. The cost ratio of a building (CR_{Total}) is the summation of all CR_j .

The cost ratios are developed through a detailed cost analysis of different building types. The FPFLM team defined 72 different building types based on the number of stories (1-3 stories), structure type (timber or masonry), roof shapes, and roof cover, and elevated or on grade. A building has 76 components, and the cost of repair and replacement of these components for each building type is calculated using publicly available construction cost sources such as RSMMeans Residential Cost Data (2008a, 2012, 2015a), RSMMeans Square Foot Costs (2008b), and RSMMeans Contractor's Pricing Guide: Residential Repair and Remodeling Costs (2015b); as well as consultations with local general contractors who work in the business of constructing residential buildings in Florida (Baradaranshoraka ET AL. 2019). After calculating the cost ratio for each building type, the average for different number of stories, structure types, and building elevation

(elevated or on grade) is calculated. The cost variations in the roof cover and roof shape did not affect the results; therefore, they were not included in the building delineation. The CR_{Total} adds up to more than 100% due to the costs of removing the debris and preparing the site for the construction of a new component.

Step 6: Identify the mean and range of each damage ratio corresponding to each damage state using the damage PDFs and the cost ratios for each component for a certain building class (BC) and coastal flood condition (CF) and a Monte Carlo (MC) simulation via Equation ENG-10:

$$dr_i = E[DR|DS = ds_i, CF, BC] = \sum_{j=1}^5 E[PDR|DS = ds_i, CF, BC] \times CR_j \text{ [ENG-10]}$$

where dr_i is the expected monetary damage ratio at the i th damage state; $E[PDR|DS = ds_i, CF, BC]$ represents the expected physical damage ratio (PDR) of the j th component for the i th damage state.

A MC simulation produces the expected damage ratio and other statistical properties corresponding to each damage state. The simulation uses the distributions defined in Table 12, and the cost ratios from step 5 as input. The output is the expected damage ratio corresponding to each overall damage state. Each simulation randomly samples a physical damage value based on the assigned damage distributions for all damage states and components from Table 12, converting the distributions into sample data. Using Equation ENG-10 and the appropriate cost ratios from step 5, the expected damage ratio of each damage state is calculated. The total number of simulations is selected so that the results are within a margin of error equal to or less than 1% of all output means with a 95% confidence level (Palisade, 2015).

Component	Coastal Flood Damage States					
	DS 1	DS 2	DS 3	DS 4	DS 5	DS 6
Roof	Minor roof cover damage (greater than 20% of roof area); No roof sheathing or roof truss damage	Significant amount of roof covering missing (greater than 40%); Minor roof sheathing damage (greater than 20%); No roof truss damage	Extensive roof cover damage (greater than 60%); Significant roof sheathing damage (greater than 40%); Minor roof trusses damage (greater than 20%)	The majority of roof covering missing (greater than 80%); Extensive roof sheathing damage (greater than 60%); Many roof trusses damaged (greater than 50%)	Roof damage greater than 95%	Entire roof missing
Exterior Walls	Minor wall siding removal (greater than 20%) Small scratches; Cracks in breakaway wall	Wall siding has been removed from greater than 40% of multiple walls; Minor wall sheathing damage (greater than 20%); Minor cracks in many walls; Breakaways walls damaged or removed	Extensive damage to wall siding (60% of walls); Partial loss of wall sheathing caused by water or debris; Large and extensive cracks in most walls; Minor wall frame damage	Large holes due to floodborne debris; Extensive loss of wall sheathing; Repairable wall frame damage	Exterior wall damage greater than 95%	Overall wall system has collapsed
Interiors	Infiltration damage to floor covering & items below the first floor; Light damage to plumbing, mechanical and electric systems; Minor water damage to utility and cabinets	Water marks 0 to 0.6 m above the first floor; Significant interior damage, including plumbing and electrical systems; Dampness on greater than 25% of dry wall (Mold)	Water marks 0.6 to 1.2 m above the first floor; Water damage to interiors at high level; Interior stairway damaged or removed; Dampness on greater than 60% of dry wall (Mold)	Water marks 1.2 to 1.8 m above the first floor; Interior damage greater than 80%	Interior damage greater than 95%	Interior completely damaged
Foundation	Slight scour; Evidence of weathering on piles	Slab and piles experience extensive scour without apparent building damage	Slab and piles sustain significant scour with repairable structural damage; Moderate slab crack	Structure shifted off the foundation or overturning foundation; Piles: racking; Slab: undermining leads to significant deformation	Foundation damage greater than 95%	Buildings has collapsed
Openings	A few windows or doors are broken (glass only); Screens may be damaged or missing	Many windows are broken; Damage to frames of doors and windows	Extensive damage to openings	Damage to openings greater than 80%	Damage to openings greater than 95%	All openings damaged

Table 11. Qualitative description of six coastal flood damage states.

Source: Data from Tomiczek et al. (2017); Suppasri et al. (2013).

Coastal Flood Damage States						
Component	DS 1	DS 2	DS 3	DS 4	DS 5	DS 6
Roof	Roof cover ($\mu = 0.20$; $\sigma = 0.067$); Roof sheathing ($\mu = 1E-04$; $\sigma = 1E-04$); Roof truss ($\mu = 1E-04$; $\sigma = 1E-04$)	Roof cover ($\mu = 0.40$; $\sigma = 0.067$); Roof sheathing ($\mu = 0.20$; $\sigma = 0.067$); Roof truss ($\mu = 1E-04$; $\sigma = 1E-04$)	Roof cover ($\mu = 0.60$; $\sigma = 0.067$); Roof sheathing ($\mu = 0.40$; $\sigma = 0.067$); Roof truss ($\mu = 0.20$; $\sigma = 0.083$)	Roof cover ($\mu = 0.80$; $\sigma = 0.058$); Roof sheathing ($\mu = 0.60$; $\sigma = 0.092$); Roof truss ($\mu = 0.50$; $\sigma = 0.125$)	Roof cover ($\mu = 0.95$; $\sigma = 0.032$); Roof sheathing ($\mu = 0.95$; $\sigma = 0.065$); Roof truss ($\mu = 0.95$; $\sigma = 0.082$)	Roof cover ($\mu = 0.99$; $\sigma = 0.008$); Roof sheathing ($\mu = 0.99$; $\sigma = 0.008$); Roof truss ($\mu = 0.99$; $\sigma = 0.008$)
Exterior Walls	Wall cover ($\mu = 0.20$; $\sigma = 0.067$); Wall structure ($\mu = 0.10$; $\sigma = 0.033$)	Wall cover ($\mu = 0.40$; $\sigma = 0.067$); Wall structure ($\mu = 0.20$; $\sigma = 0.05$)	Wall cover ($\mu = 0.60$; $\sigma = 0.067$); Wall structure ($\mu = 0.40$; $\sigma = 0.067$)	Wall cover ($\mu = 0.80$; $\sigma = 0.058$); Wall structure ($\mu = 0.60$; $\sigma = 0.067$)	Wall cover ($\mu = 0.95$; $\sigma = 0.032$); Wall structure ($\mu = 0.80$; $\sigma = 0.065$)	Wall cover ($\mu = 0.99$; $\sigma = 0.008$); Wall structure ($\mu = 0.99$; $\sigma = 0.033$)
Interiors	Interior ($\mu = 0.20$; $\sigma = 0.067$)	Interior ($\mu = 0.40$; $\sigma = 0.067$)	Interior ($\mu = 0.60$; $\sigma = 0.067$)	Interior ($\mu = 0.80$; $\sigma = 0.058$)	Interior ($\mu = 0.95$; $\sigma = 0.032$)	Interior ($\mu = 0.99$; $\sigma = 0.008$)
Foundation	Foundation ($\mu = 0.20$; $\sigma = 0.067$)	Foundation ($\mu = 0.40$; $\sigma = 0.067$)	Foundation ($\mu = 0.60$; $\sigma = 0.067$)	Foundation ($\mu = 0.80$; $\sigma = 0.058$)	Foundation ($\mu = 0.95$; $\sigma = 0.032$)	Foundation ($\mu = 0.99$; $\sigma = 0.008$)
Openings	Openings ($\mu = 0.20$; $\sigma = 0.067$)	Openings ($\mu = 0.40$; $\sigma = 0.067$)	Openings ($\mu = 0.60$; $\sigma = 0.067$)	Openings ($\mu = 0.80$; $\sigma = 0.058$)	Openings ($\mu = 0.95$; $\sigma = 0.032$)	Openings ($\mu = 0.99$; $\sigma = 0.008$)

Table 12. Normal distribution parameters of the component physical damage based on qualitative description. One story slab on grade reinforced masonry structure.

Coastal Flood Vulnerability Function Development

Vulnerability and fragility curves are different simplified representations of a full set of damage information. The vulnerability curve is expressed as a building or component expected damage ratio for a specific hazard intensity measure, coastal flood condition, and building class $E[DR|IM, CF, BC]$:

$$E[DR|IM, CF, BC] = \int_0^{dr_{max}} dr f_{DR}(dr|IM, CF, BC) d(dr) \quad [ENG-11]$$

where dr is a specific damage ratio, dr_{max} is the maximum damage ratio, $f_{DR}(dr|IM, CF, BC)$ is the conditional probability density function (PDF) of dr given a particular intensity measure (IM), and the product $f_{DR}(dr|IM, CF, BC)d(dr)$ is the probability of occurrence of dr . A vulnerability curve is the plot of $E[DR|IM, CF, BC]$ as a function of IM . The damage ratio is the percentage of the building or component which is damaged as a function of IM . This percentage can be expressed as either a physical percentage or as a percentage of the value of the building (monetary damage). If this percentage is expressed as a physical damage dr_{max} would be equal to 100%. If it is expressed as monetary damage dr_{max} could exceed 100% due to the additional cost of removal and disposal. The total damage is the damage ratio times the building value.

Equation ENG-11 can be discretized using the total probability theorem in Equation ENG-12 (Rosseto et al., 2013):

$$E[DR|im_j < IM \leq im_{j+1}, CF, BC] \approx \sum_{i=0}^{k-1} E[dr_i < DR \leq dr_{i+1}] \times P(dr_i < DR \leq dr_{i+1}|im_j < IM \leq im_{j+1}, CF, BC) \quad [ENG-12]$$

where: $E[dr_i < DR \leq dr_{i+1}]$ is the building expected damage ratio (DR), within a damage ratio interval bounded by the damage states i (dr_i) and $i+1$ (dr_{i+1}); and, $P(dr_i < DR \leq dr_{i+1}|im_j < IM \leq im_{j+1}, CF, BC)$ represents the probability of occurrence of that damage ratio, given that the hazard intensity measure within a certain interval. That probability corresponds to the probability differences between adjacent fragilities for damage states i (dr_i) and $i+1$ (dr_{i+1}). To simplify notation, the paper refers to the hazard intensity measure interval ($im_j < IM \leq im_{j+1}$) as IM . In the current study with 8 fragilities, $k=7$.

Figure 18 illustrates the concept for a case with eight damage states, where the first damage state is the case of zero damage ($dr_0 = 0\%$), i.e. the upper horizontal line with 100% probability of exceedance and the last damage state is the case of 100% damage ($dr_7 = dr_{max} = 100\%$), i.e. the lower horizontal line with 0% probability of exceedance. As an example, Figure 18 shows the probability difference between the damage ratio corresponding to damage state 4 and 5 when the hazard intensity (inundation depth above ground elevation) is equal to 6 meters.

Ideally, if the PDF of damage were available, the correct solution for the $E[dr_i < DR \leq dr_{i+1}]$, at a certain IM , is the DR corresponding to the centroid of the interval of the PDF bounded by dr_i and dr_{i+1} . Typically, the PDFs of damage at any hazard intensity are unknown, and they are discretized in histograms, with constant values in each interval of damage. The number of fragility curves governs the discretization of the PDF into a histogram. If the number of fragility curves is

sufficiently high, the histogram can be a very good approximation of the actual PDF. This is generally the case when the fragilities are derived analytically or numerically, where any number of them can be generated. This is the case of the wind vulnerability model of the FPFLM, where an engineering component approach generates a 32-interval probability distribution histogram, with damage ratio intervals of 2% to 4%, evenly spaced (Pinelli et al., 2011). However, when the fragilities are based on the field surveys accessed for this study, the number of fragilities does not exceed 8, which results in a 7-interval histogram, unevenly spaced, with some damage ratio intervals as wide as 20%.

With a sufficiently high number of fragility curves, a mid-point assumption for the location of the centroid of the interval is reasonable. With few fragility curves, a mid-point assumption can introduce larger uncertainty and produce distortions of the model. For example, at low intensity of hazard, the difference in probabilities of exceedance between DS0 and DS1 is very large. If that difference is spread over a large interval (between dr_0 and dr_1), and the centroid of that interval is estimated to be at the interval mid-point, Equation ENG-12 will lead to an erroneously large value of the overall expected value of damage at that low intensity. Equation ENG-13 introduces an adjustment function f intended to minimize that distortion.

$$E[dr_i < DR \leq dr_{i+1}] = dr_i + (dr_{i+1} - dr_i) \times f(IM, dr_i) \quad [\text{ENG-13}]$$

where $f(IM, dr_i)$ is a function whose value should vary between zero and one depending on the hazard intensity, and whether dr_i is to the left or the right of the mean of the PDF.

The resulting Equation ENG-14 provides the translation of coastal flood fragility curves into coastal flood vulnerability curves.

$$E[DR|IM, CF, BC] = \sum_{i=0}^{k-1} \{ [dr_i + (dr_{i+1} - dr_i) \times f(IM)] \times [P(DR \geq dr_i|IM, CF, BC) - P(DR \geq dr_{i+1}|IM, CF, BC)] \} \quad [\text{ENG-14}]$$

The quantification of the damage states $[dr_i]$ values and the fragility curves $P(DR \geq dr_i|IM)$ values is critical to the translation process.

Equation ENG-15 was developed as the adjustment function $f(IM)$.

$$f(IM) = \left(\frac{1}{\sqrt{2\pi}} \int_{-\infty}^{\left(\frac{IM}{0.3048} - \mu\right)/\sigma} e^{-\frac{v^2}{2}} dv \right) (ul - ll) + ll \quad [\text{ENG-15}]$$

where μ and σ are equal to 2.0 for the weak models (older structures), and equal to 4.0 for the strong models (newer structures), ul (upper limit) equal to 1.0 and ll (lower limit) equal to -0.2, and v is a dummy variable of integration. IM must be input in meters. A Gaussian cumulative distribution function (CDF) is the basis for Equation 16 due to its flexibility and sigmoid behavior. The parameter values were based on expected behavior at low and high IM values.

Result and Validation

The building classes in the FPFLM library include timber and masonry structures with one to three stories, for both slab on grade and elevated structures. To reflect the evolution of building codes in Florida, a weak and strong version of each model was developed, and the differences in the vulnerability curves are based on the assigned probability of damage per component. This section presents model outputs for the weak version of a one-story slab on grade timber and the strong version of a one-story slab on grade reinforced masonry structure, as well as validation against an independently derived model and insured claims data.

Fragility functions

Figure 19 shows examples of the tsunami fragility functions and the resultant coastal flood fragility functions after the translation process described in Section 3. To avoid overcrowding the plots, the figure shows only the fragility functions for DS₃ (major damage) and DS₅ (collapse) for the case of tsunami and coastal flood with moderate waves. The coastal flood fragilities show lower probability of exceeding a given damage state at a given d_s than their equivalent tsunami fragilities, as expected.

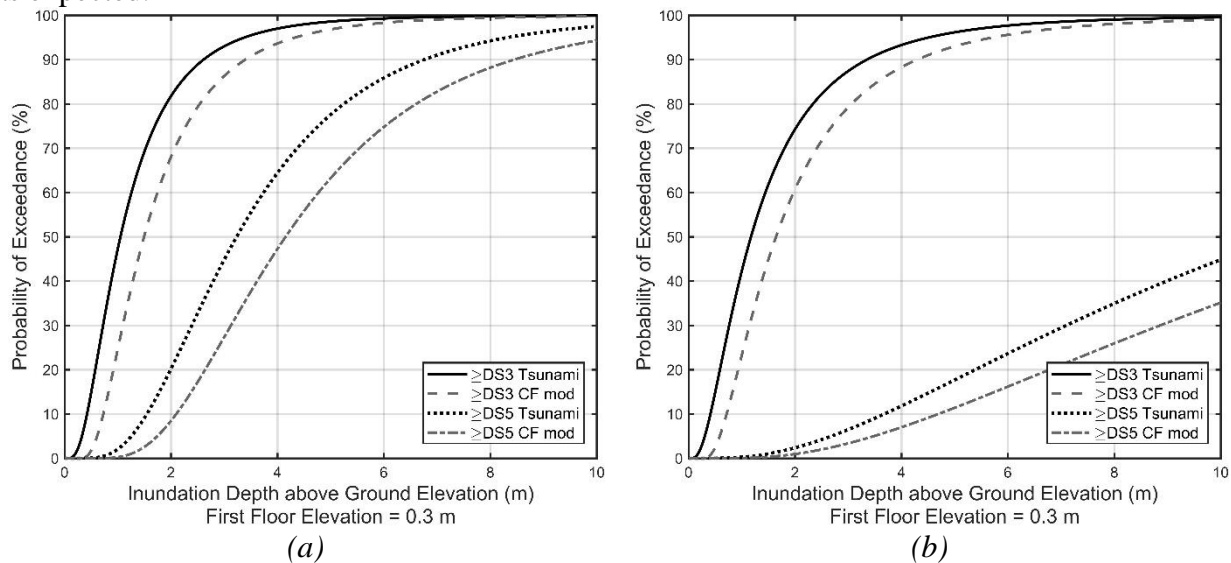


Figure 19. Fragility functions for tsunami and moderate coastal flood condition (CF mod): a) 1-story on-grade timber; b) 1-story on-grade reinforced masonry. Damage states 3 and 5 included.

Initiation of damage in the vulnerability curves

The first Floor Elevation (FFE) of a structure (above ground level) can vary depending on requirements related to building location and age of construction. The coastal flood vulnerability curves reflect this by initiating accumulation of damage when the wave crest reaches the FFE. The calculation of d_s when the wave crest reaches FFE is based on the diagram presented in Figure 20, from Kjeldsen and Myrhaug (1978), which illustrates the dimensions of a breaking wave in shallow water. The maximum height of the wave above the inundation depth is described by ηH_b , where η is equal to 0.7 (e.g. Peng, 2015; USACE, 2015). Equation ENG-16 calculates the inundation depth (d_{s0}) when the wave crest first reaches FFE. The breaking wave height H_b is

substituted by H_w for the case of minor or moderate waves. The term H_w/d_s depends on the severity of the coastal flood, defined in Table 9.

$$d_{s0} = \frac{FFE}{(1+0.7*\frac{H_w}{d_s})} \quad [\text{ENG-16}]$$

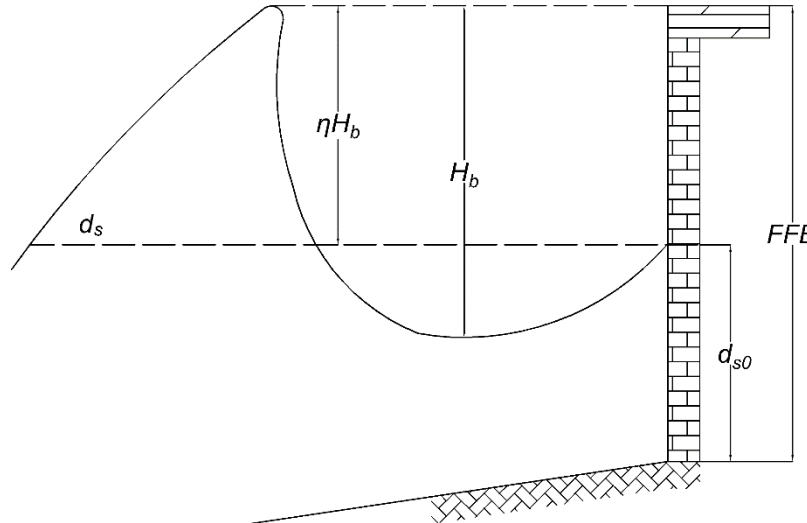


Figure 20. Breaking wave dimensions, based on Kjeldsen and Myrhaug. (1978)

Comparison with USACE model

Figure 21 presents the results from this study and the USACE (2015) vulnerability curves for wave (i.e. coastal flood) and inland flood. The USACE (2015) developed a set of vulnerability curves for different structures based on expert opinions informed in part by post-disaster damage assessments. The structures selected from the USACE report are a single-story timber frame house with slab foundation and FFE of 0.3 m above ground level, and a single-story reinforced masonry house with slab foundation and FFE of zero. The ages of these structures were described in USACE (2015), and correspond to an older (weak) timber model and a newer (strong) masonry model within the FPFLM model inventory.

USACE (2015) presents vulnerability curves for damage due to inland flood inundation (slow-rising flood) as a function of inundation depth, and damage due to coastal flood with waves as a function of wave height above FFE. The FPFLM model uses inundation depth at the hazard frame of reference for both flood and coastal flood with waves. It was therefore necessary to convert the USACE (2015) inland and coastal flood vulnerability curves to this same frame of reference, as described in Baradaranshoraka et al. (2019). The wave state in USACE (2015) is reported to be breaking waves. In Equation ENG-16, when substituting FFE by the wave crest plus FFE, it allows the conversion of the abscissas from wave height above FFE to d_s above ground using $H_w/d_s = 0.78$ (breaking waves). For the ordinate, the USACE (2015) report presents the results in terms of physical damage (up to 100%), while the FPFLM uses expected damage ratio. A factor equal to

the Building CR derived from the cost analyses was applied to the USACE values for each comparable structure.

Figure 21-a presents the USACE timber vulnerability model (severe waves and slow rising flood) along with the comparable FPFLM weak timber model (minor, moderate and severe waves). The USACE envelope of no waves and severe waves appears to bound the FPFLM outputs. The most relevant comparison is the ‘USACE wave’ and the ‘FPFLM CF severe waves’ as described in the legend. Both models show rapid damage accumulation with increasing inundation. The USACE model is more vulnerability that the FPFLM model, and the difference between models becomes larger with increasing inundation depth. Secondly, the ‘USACE flood’ and the ‘FPFLM CF minor waves’ show good agreement at low inundation levels where minor wave magnitudes are very small.

Figure 21-b presents the USACE masonry vulnerability model (severe waves and slow rising flood) along with the comparable FPFLM strong masonry model (minor, moderate and severe waves). Again, the most relevant comparison is the ‘USACE wave’ and the ‘FPFLM CF severe waves’ as the legend describes. The USACE results estimate more vulnerability, but shows close agreement with FPFLM within the first meter of inundation.

These comparisons show that the FPFLM model predicts less vulnerability than the USACE model for like structures subject to severe waves, with the difference between models increasing with inundation depth. While the USACE (2015) models are a valid source of comparison, they do not represent an ‘exact solution’, nor were they used in the development or calibration of the FPFLM models. One can judge the FPFLM and USACE model outputs to be different, but cannot assign superior performance to either, based on Figure 21 alone. The next section employs an analysis of National Flood Insurance Program (NFIP) claims data to complement Figure 21 with a record of actual losses.

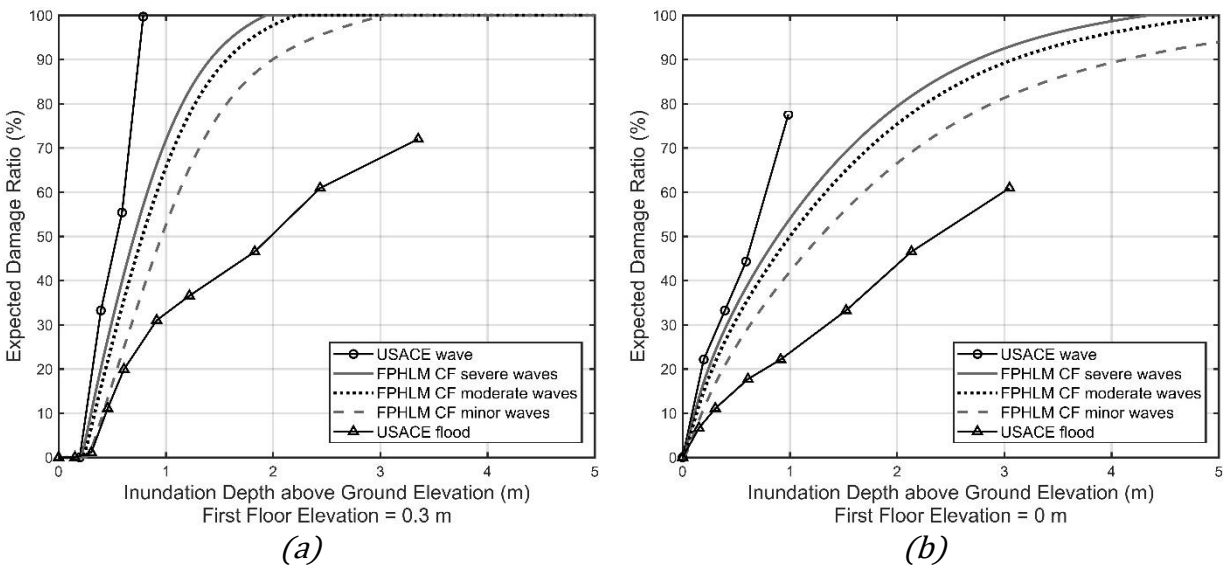


Figure 21. FPFLM Coastal flood (CF) vulnerability and USACE (2015) vulnerability relative to the ground elevation a) 1-story slab on-grade weak timber ,0.3 m FFE; b) 1-story slab on-grade strong masonry, 0 m FFE.

Validation against claims data

The Florida Office of Insurance Regulation provided NFIP claims data to the FPFLM team. The claims database contains more than 150,000 claims between July 1975 and January 2014 for 126 different events. The NFIP claims data were cross-referenced with tax appraiser databases at the county level. These efforts produced a more complete set of building descriptors for each policy in the NFIP (e.g. masonry or timber frame construction). The team analyzed the claims data locations and loss dates to associate a specific hazard to each claim. The following analysis focuses on the claims from Hurricane Ivan (2004) in the Florida Panhandle.

The FPFLM hazard teams employed FEMA water marks collected in post-Ivan studies to estimate a surge and wave height assignment to each NFIP Ivan claim based on its location. With the NFIP database enhanced with hazard data and building construction details, it is possible to produce empirical building vulnerability values to validate FPFLM outputs (Pinelli et al., 2019).

The NFIP Ivan claims were categorized by structure type to create subsets corresponding to single family residential slab on-grade single-story timber and masonry structures. This resulted in 132 individual claims for the timber structures, and 376 individual claims for the masonry structures. Each building damage claim was divided by the building value, also provided in the claims data, to produce a building damage ratio per claim. The claims were then binned by coastal flood inundation height using 0.25 m intervals. The mean damage ratio for a given inundation interval is the average of all claim damage ratios within the interval. Finally, the number of claims and the standard deviation among claims in each interval yield the 95% confidence interval for each claims-derived mean damage ratio.

Further stratification of the timber and masonry structure claims by age, FFE and wave severity were attempted, but this rendered the number of claims per stratification too low. Thus the mean damage ratios from claims data include multiple coastal flood conditions and FFE values, and both old (weak) and new (strong) construction.

Figure 22-a and Figure 22-b presents the same USACE (2015) and FPFLM timber and masonry model outputs utilized in Figure 21-a and Figure 21-b, respectively. In addition, the FPFLM strong timber and weak masonry model outputs were added given the mixed age of the claims data. All three coastal flood conditions were included for both weak and strong FPFLM model outputs (denoted 'all CF' in the legend), and the USACE model represents breaking waves. Finally, the claims-derived mean data damage ratios and their 95% confidence intervals were included. These confidence intervals provide a frame of reference regarding both the number of claims and their standard deviation at different inundation depth intervals.

The claims data mean damage ratios generally exhibit the expected trend of increased damage with increasing inundation depth. The exception is the highest inundation depth for timber claims data, where the comparatively large confidence interval indicates significant uncertainty due to few samples and a large standard deviation. Given the aggregation of age, FFE and wave state within the claims data, direct comparison of the claims data to any one of the six FPFLM model outputs or the USACE models is not appropriate. However, the 95% confidence intervals generally lie

within or partially overlap the swath of FPFLM model outputs over the available range of inundation depth, while the 95% confidence intervals diverge from the USACE models before reaching 1m of inundation. The NFIP claims data was not used to develop or calibrate the FPFLM vulnerability models. It is therefore encouraging that the claims data falls within the swath of FPFLM models for both timber and masonry, particularly at the higher inundation depths where the difference between the FPFLM and USACE models is more drastic.

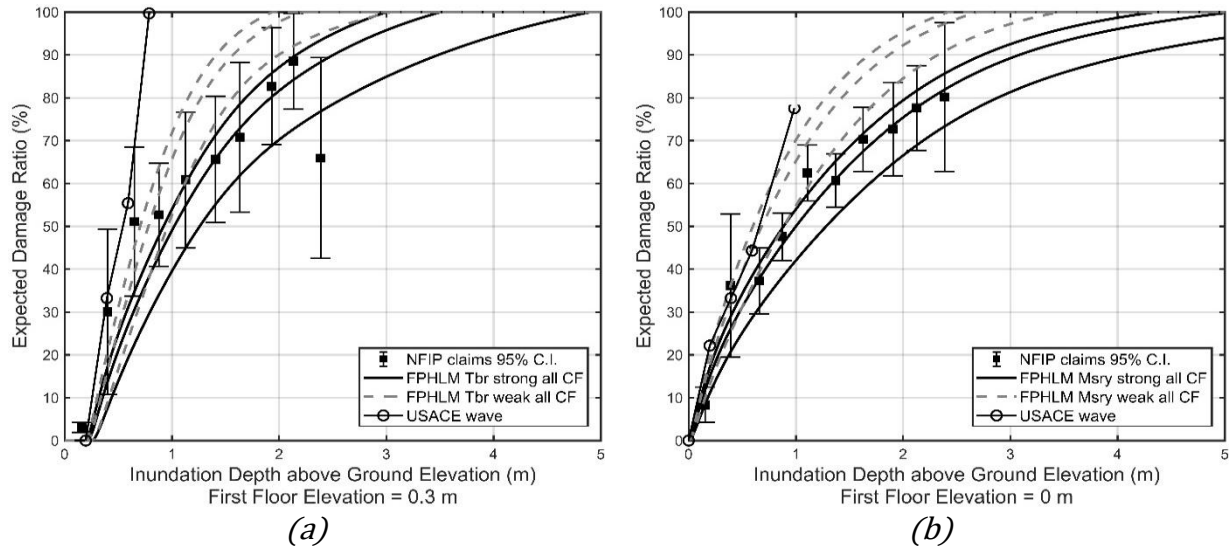


Figure 22. FPFLM Coastal flood (CF) vulnerability, USACE (2015) vulnerability, and Hurricane Ivan 2004 NFIP claims-derived vulnerability relative to the ground elevation a) 1-story slab on-grade timber, 0.3 m FFE; b) 1-story slab on-grade reinforced masonry, 0 m FFE.

Vulnerability of site-built residential structures to Inland Flood

The methodology to adapt tsunami fragility functions was not appropriate for the case of inland flooding. Therefore, the residential vulnerability functions for inland flood were developed separately from the vulnerability functions for coastal flood. The fundamental premise was to adapt the USACE (2015) inland flood vulnerability functions to account for varying FFE.

Table 13 and Table 14 present examples of the data used for the development of the Inland Flood vulnerability curves for residential buildings, based on USACE (2015).

	Most Likely	Minimum Damage	Maximum Damage
Stories	1	1	1
Foundation	Slab	Slab	Crawl Space
Age	15-30	0-10	Old – unknown codes
Structure	Wood frame	Masonry, reinforced per code	Wood frame
Height of Finished Floor Above Grade	1'-0"	0'-0"	3'-0"
Condition	Fair/Good	Good	Poor

Table 13. Single Story Residence, No Basement, Building Characteristics (Table 55, USACE 2015).

Flood Depth (ft)	Min (%)	Most Likely (%)	Max (%)
-1.0	0	0	0
-0.5	0	0	5
0.0	0	1	10
0.5	6	10	20
1.0	10	18	30
2.0	16	28	40
3.0	20	33	45
5.0	30	42	60
7.0	42	55	94
10	55	65	100

Table 14. Single Story Residence, No Basement, Inundation Damage – Structure (Table 56, USACE 2015).

For the case of timber structures, the most likely case was selected from the above tables, and for the case of masonry structures, the minimum damage case was selected. USACE (2015) provides information for one and two stories structures. For three-story residences, 90 percent of the two-story damage ratio was assumed to develop the vulnerability curves. The damage to two-story and three-story residences would be similar, but the total cost for the three-story residences is higher than that for two-story residences, thus, the damage ratio for three-story residences should be lower.

The adaptation of the USACE (2015) flood model to the FPFLM model consists of the following four steps:

Step 1:

Use the inundation damage curves for structural damage in USACE 2015 as the initial proxy. The reference level of USACE inundation damage curves is the finished floor elevation (FFE), while the FPFLM reference is ground level.

Step 2:

The FPFLM library of non-elevated models includes FFEs from zero to three feet in one-foot increments. To align the appropriate USACE model, the equivalent wetting depth is determined.

Step 3:

The reference level of the Inland flood damage curve is changed to ground level. The process is equivalent to shift the original curve with an offset equal to the FFE of the library model.

Step 4:

The shifted Inland flood damage curve is then fitted with a lognormal CDF function. The data from USACE, 2015 was only available up to 10 ft of inundation depth. To produce the curves up to 50 ft for the models, an extra point with a 100% damage was added. The inundation depth for this point was selected to ensure that the inland flood model remains less vulnerable than the coastal flood model for the same structure.

Figure 23 shows an example of the fitting result for the case of a two-story on grade reinforced masonry structure with a 2 ft FFE. Figure 24 shows the inland flood model for a one-story masonry with a 2 ft FFE, along with the models for the three coastal flood conditions. The reduced

vulnerability to inland flood relative to coastal flood is a consistent characteristic for all FPFLM models.

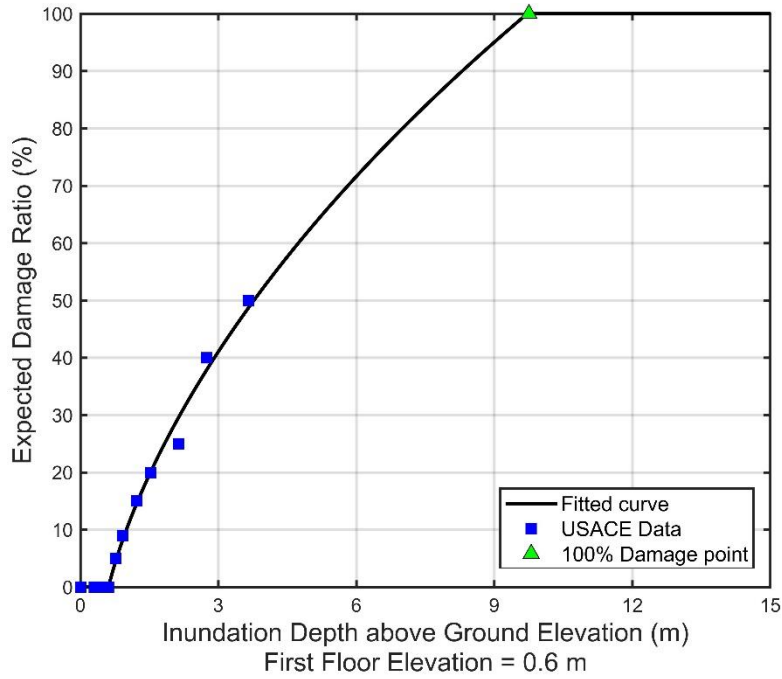


Figure 23. Fitted curve based on USACE data. Two-story masonry, 2 ft FFE.

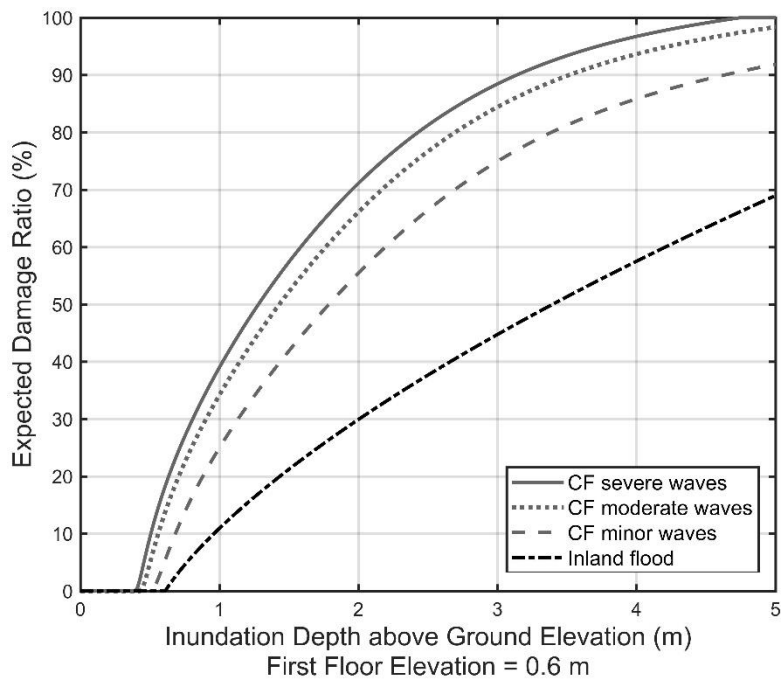


Figure 24. Inland and Coastal Flood Vulnerability Curves. One-story masonry, 2 ft FFE.

Vulnerability of manufactured housing to Inland and Coastal Flood

USACE reports (1992, 2006) provide vulnerability observations for manufactured homes subject to slow rising flood events. These observations are used as the basis of development for the manufactured housing (MH) vulnerability functions. The FPFLM model considers two foundation types (tied- and not tied-down), as illustrated in Figure 25.

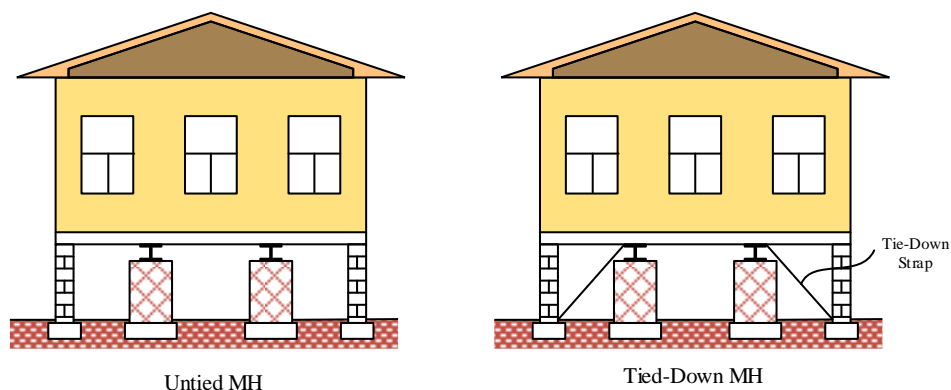


Figure 25. Two types of manufactured homes (MH)

The fundamental assumption, backed by field observation and experts, is that in most cases, water entering the living space of a manufactured home results in very rapid accumulation of damage of the structure. The damage does not necessarily indicate physical destruction of the structure, but rather the cost of repair exceeding the cost of replacement. Water entering the living space necessarily destroys the ground level contents, and more significantly results in the loss of floor level systems (e.g. electrical), the need for mold and corrosion remediation, and the likely replacement of the structural floor system due to warping. The associated cost typically approaches replacement cost. Thus, the floor elevation of manufactured homes is deemed to be a critical inundation depth.

Typical manufactured home construction sets the unit on a foundation elevated 2-3 feet above grade. Damage can also result from water approaching but not entering the elevated living space. If a home is not tied down, the rising water can displace the foundation, typically dry-stack masonry or concrete piers, causing shifting or collapse of the structure. This is mitigated if the structure is properly anchored.

USACE (1992) presents a comprehensive catalog of residential depth-damage functions used by Corps of Engineers district offices. These damage functions were derived based either upon National (or site-specific) flood damage records or upon synthetic flood damage estimates from residential and non-residential structure owners. This report provides a basis for the development of vulnerability functions for manufactured houses. USACE (2006) also provides a set of MH flood depth damage functions. Developing vulnerability functions based on observations allows the flexibility of using any well-documented source and reasonable judgement to make adjustments to fit the curves to the situation in the region of interest.

Figure 26 summarizes the available existing depth damage curves as a function of inundation depths relative to first floor. Untied houses are the weakest building type among manufactured homes. For this reason, the team used a normal CDF to fit the envelope of the existing dataset to

represent the damage function for this type of building (blue solid line in Figure 26). Equation ENG-17 shows the normal CDF used to fit the envelope, as a function of the inundation depth above the first floor elevation with μ equal to 0.276 and σ equal to 1.125; v is a dummy variable of integration. Tied-down manufactured homes are relatively more resistant against horizontal water forces, as compared to the untied structures. Thus, the generalized logistic function is used to fit the mean level of the available depth-damage curves and is deemed to be appropriate for the tied MH vulnerability function (blue dashed line in Figure 26). Equation ENG-18 shows the generalized logistic fit to the mean level, as a function of the inundation depth above the first floor elevation with the parameter α equal to 2.225.

$$f(d_{SFFE}) = \frac{1}{\sqrt{2\pi}} \int_{-\infty}^{\left(\frac{d_{SFFE}-\mu}{\sigma}\right)} e^{-\frac{v^2}{2}} dv \quad [\text{ENG-17}]$$

$$f(d_{SFFE}) = (1 + e^{-d_{SFFE}})^{-\alpha} \quad [\text{ENG-18}]$$

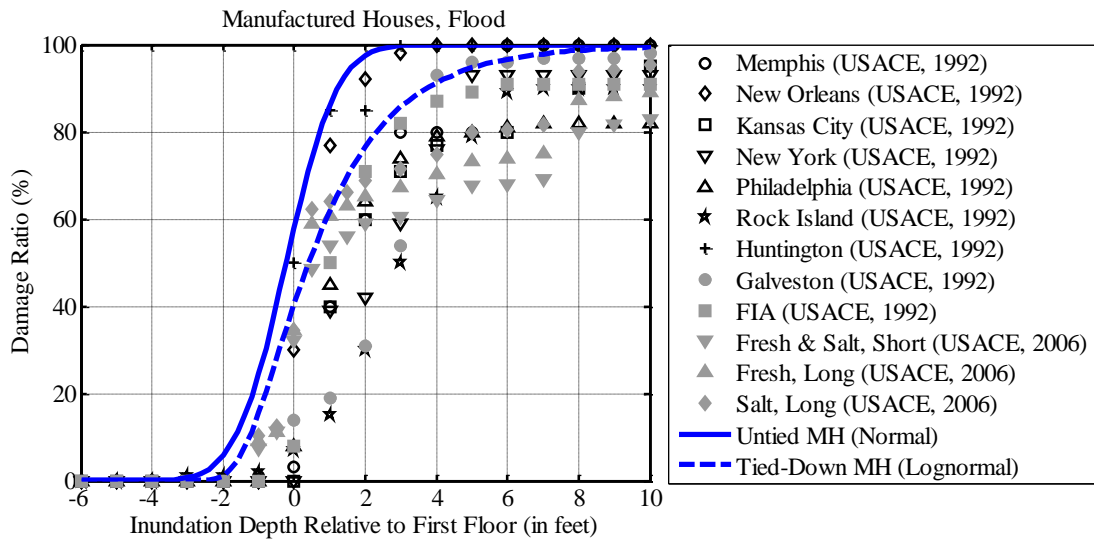


Figure 26. Inland Flood vulnerability curves and existing flood depth-damage data.

Depending on the FFE of the MH being modeled, the resulting vulnerability curves are shifted to reflect this elevation.

For the case of coastal flood with waves, the derived inland flood vulnerability curves are taken as the starting point and translated considering the wave heights and lateral forces. Since most of the damage to the manufactured homes is associated with water entering the living space, the presence of waves affects the inundation depth that initiates damage. The wave crest is considered to calculate the equivalent coastal flood inundation depth that produces the same damage ratio as the inland flood inundation depth, shifting the vulnerability functions to the left. Equation ENG-19 translates the inland flood inundation depth to coastal flood inundation depth for the flood conditions described in Table 9 according to the previously defined H_w/d_s values: 0.3 (minor waves), 0.6 (moderate waves) and 0.78 (severe waves).

$$d_{sCF}(d_{sIF}) = d_{sIF} * \left(1 - 0.7 * \frac{H_w}{d_s}\right) \quad [\text{ENG-19}]$$

Additionally, the inundation depth required to produce a horizontal force large enough to cause a sliding failure is calculated as a limit state, leading to a total loss of the house when the water reaches that inundation depth. Sliding or shear failure occurs when horizontal forces exceed the friction force or strength of the foundation. The building fails by sliding off its foundation, shear failure of components transferring loads to its foundation, or the foundation sliding. Figure 27 illustrates the forces acting on a manufactured house without ties for a generic manufactured home with dimensions L equal to 60 ft and W equal to 16 ft. The limit-state inundation depth is found when the coastal flood force is equal to the frictional force.

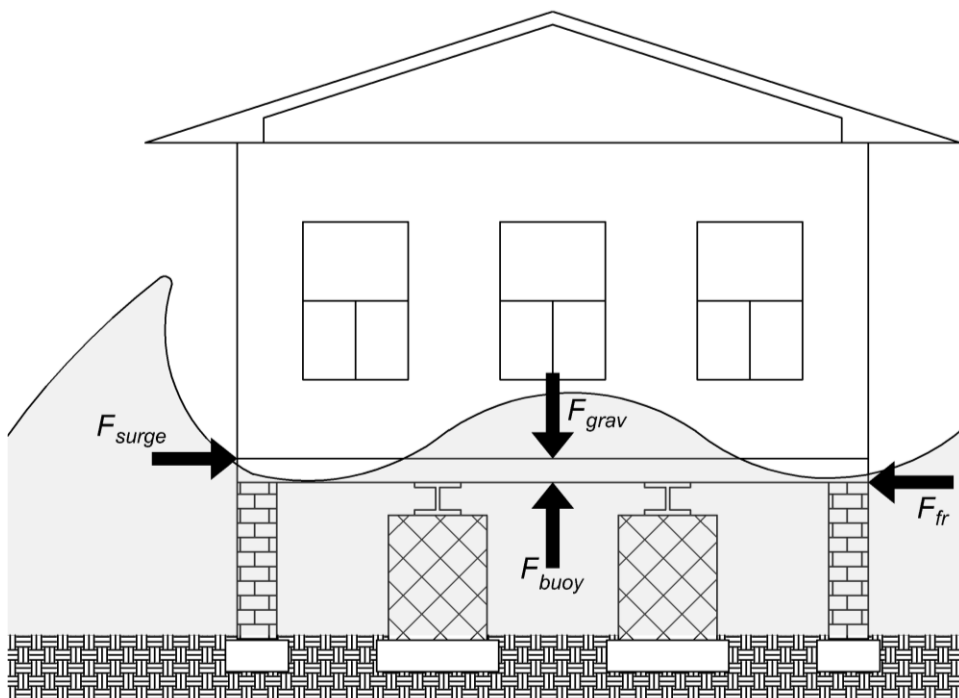


Figure 27. Forces acting on an Untied MH.

The surge force F_{surge} is calculated according to Figure 14b. The buoyancy force F_{buoy} is calculated according to Equation ENG-20, considering a saltwater unit weight γ equal to 64 pcf, and a Water Leakage Ratio (WLR) equal to zero. The Lowest Horizontal Structural Member (LHSM) is defined as the FFE minus the floor thickness (assumed to be equal to 1 ft).

$$F_{buoy}(d_s) = \begin{cases} \gamma * (d_s - LHSM) * (1 - WLR) * L * W, & d_s > LHSM \\ 0, & d_s \leq LHSM \end{cases} \quad [ENG-20]$$

The gravitational forces F_{grav} are calculated multiplying the floor area ($W*L$) by a dead load of 20 psf and a live load of 40 psf. Finally, the static frictional forces F_{fr} are defined by Equation ENG-21, where μ is the coefficient of friction equal to 0.2 for the case of the interaction of wood on metal under wet conditions (Cope, 2004), and the normal force F_n is the result of subtracting the buoyancy force from the gravitational loading.

$$F_{fr}(d_s) = \begin{cases} \mu * F_n(d_s), & F_n(d_s) > 0 \\ 0, & F_n(d_s) \leq 0 \end{cases} \quad [\text{ENG-21}]$$

For the same generic structure described for Figure 27, Figure 28 illustrates the forces acting on a manufactured house tied-down, after the coastal flood force has exceeded the frictional forces, and the buoyancy force has exceeded the gravitational loads. It is assumed that the tie-downs are not pre-tensioned. The behavior of a Tied-down Manufactured Housing is similar to the behavior previously described for a MH without ties, with the difference that once the frictional forces and/or gravitational loads are exceeded, the house does not slide until after the anchorage reaches its axial capacity. Therefore, the limit state inundation depth of a Tied-down MH is higher than the limit state inundation depth of a MH without ties.

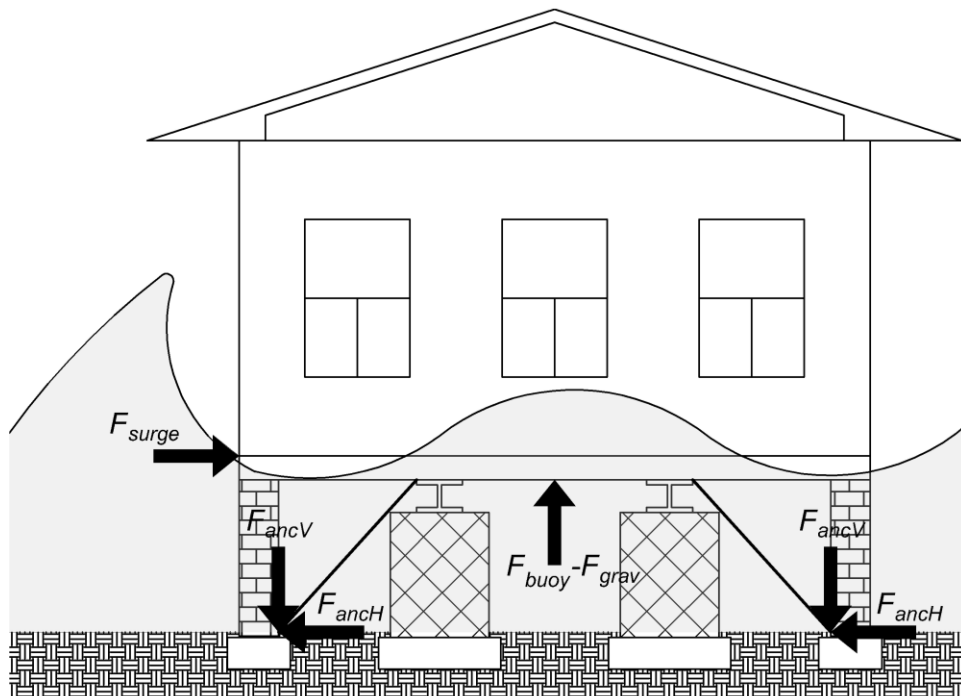


Figure 28. Forces acting on a Tied-down MH after the Friction force has been exceeded

The axial demand on the anchors comes from two components: an uplift vertical force, which originates when the buoyancy exceeds the gravitational loads, and a horizontal force, which originates when the surge exceeds the frictional forces; these combined forces result in an axial force in the inclined anchors. The vertical uplift force F_u acting on the anchors is the result of the buoyancy force minus the gravitational loads, and the horizontal force acting on the anchors, F_{surge} , is equal to the coastal flood force once the static frictional forces have been exceeded.

The uplift F_u actually pretensions all the 16 ties. If we assume them at 45-degree angle, from simple equilibrium, the vertical and horizontal components of the tie's axial loads are equal in magnitude, and the pre-tension axial force in each tie due to uplift is $F_{anc} = \sqrt{2\left(\frac{F_u}{16}\right)^2} =$

$\sqrt{2} \frac{F_u}{16}$. The lateral surge force F_{surge} is going to increase the tension in the “windward” ties and decrease the tension in the “leeward” ties. As long as $F_{surge} < F_u$, all the 16 anchors contribute to the resistance against sliding. But when $F_{surge} \geq F_u$, then the “leeward” ties lose their pretension and buckle, and the forces are distributed only on the 8 anchors in tension. This is also the case when there is no uplift (i.e. the buoyancy force is less than the gravity loads). Equation ENG-22 shows the resulting anchor’s demand when both vertical and horizontal loads are combined according to the 45-degree angle of installation.

According to FEMA P85, the recommended design axial load of 5-ft anchor ties installed at 45 degrees is 3150 lb. Recommended design loads are calculated applying statistical factors that result in a 10% lower exclusion limit. Assuming a normal distribution and a coefficient of variation of 0.2, the inferred mean axial capacity of the anchors, $F_{anc}(d_s)$, is equal to 4235 lb. The inundation depth that produces the anchor’s demand to be equal to its axial capacity becomes then the limit state for a tied-down MH.

$$F_{anc}(d_s) = \begin{cases} \frac{F_{surge}(d_s)}{\cos(45)*8}, & F_{buoy}(d_s) - (DL + LL) < 0 \\ \frac{F_{buoy}(d_s) - (DL + LL)}{\sin(45)*16} + \frac{F_{surge}(d_s)}{\cos(45)*16}, & F_{surge}(d_s) < F_{buoy}(d_s) - (DL + LL) \text{ [ENG-22]} \\ \frac{F_{buoy}(d_s) - (DL + LL)}{\sin(45)*8} + \frac{F_{surge}(d_s)}{\cos(45)*8}, & F_{surge}(d_s) \geq F_{buoy}(d_s) - (DL + LL) \end{cases}$$

ACTUARIAL COMPONENT

The actuarial component consists of a set of algorithms. The process involves a series of steps: rigorous check of the input data; selection and use of the relevant output produced by the coastal surge and inland flood hazard components; selection and use of the appropriate coastal and inland flood vulnerability functions for building structure, contents, and additional living expenses; running the actuarial algorithm to produce expected losses; aggregating the losses in a variety of manners to produce a set of expected annual flood losses; and produce probable maximum losses for various return periods. The expected losses can be reported by construction type (e.g., masonry, frame, manufactured homes), by geographic zone, county or ZIP Code, by rating territory, and combinations thereof.

Expected annual losses are estimated for individual policies in the portfolio. They are estimated for building structure, appurtenant structure, contents, and ALE on the basis of their exposures and by using the respective vulnerability functions for the construction types and hazard type. For each policy, losses are estimated for all the storms in the stochastic set by using appropriate damage functions and policy exposure data. The losses are then summed over all storms and divided by the number of years in the simulation to get the annual expected loss. These are aggregated at the ZIP Code, county, territory, geographic zone, or portfolio level and then divided by the respective level of aggregated exposure to get the loss costs. This is a computationally demanding method. Each portfolio must be run through the entire stochastic set of storms.

The distribution of losses is driven by both the distribution of damage ratios generated by the engineering component and by the distribution of inundation depth generated by the coastal and the hydrology components. The meteorology component uses up to 50,000 year simulations to generate a stochastic set of storms. For each location grid the coastal surge and inland flood models produce flood depth which is applied to the appropriate vulnerability function to generate damages. The vulnerability component outputs are used as input in the actuarial model.

The starting point for the computations of personal residential losses is the vulnerability function. Appropriate vulnerability matrices are applied separately for building structure, content, appurtenant structure, and ALE. The ground up loss is computed, the appropriate deductibles and limits are applied, and the loss net of deductible is calculated. The expected losses are then adjusted by the appropriate expected demand surge factor. The demand surge factors are estimated by a separate model and applied appropriately to each storm in the stochastic set.

After the losses are adjusted for demand surge, they are summed across all structures of the type in the grid and also across the grids to get expected aggregate portfolio loss. The model can process any combination of policy type, construction type, deductibles, coverage limits, etc.

Another function of the actuarial algorithms is to produce estimates of the probable maximum loss for various return periods. The PML is produced non-parametrically using order statistics of simulated annual losses. Suppose the model produces N years of simulated annual losses. The annual losses L are ordered in increasing order so that $L(1) \leq L(2) \leq \dots \leq L(N)$. For a return period of Y years, let $p = 1 - 1/Y$. The corresponding PML for the return period Y is the p th quantile of the ordered losses. Let $k = (N) * p$. If k is an integer, then the estimate of the PML is the k th order statistic, $L(k)$, of the simulated losses. If k is not an integer, then let $k^* =$ the smallest integer greater than k , and the estimate of the p th quantile is given by $L(k^*)$.

3. Provide a flowchart that illustrates interactions among major flood model components.

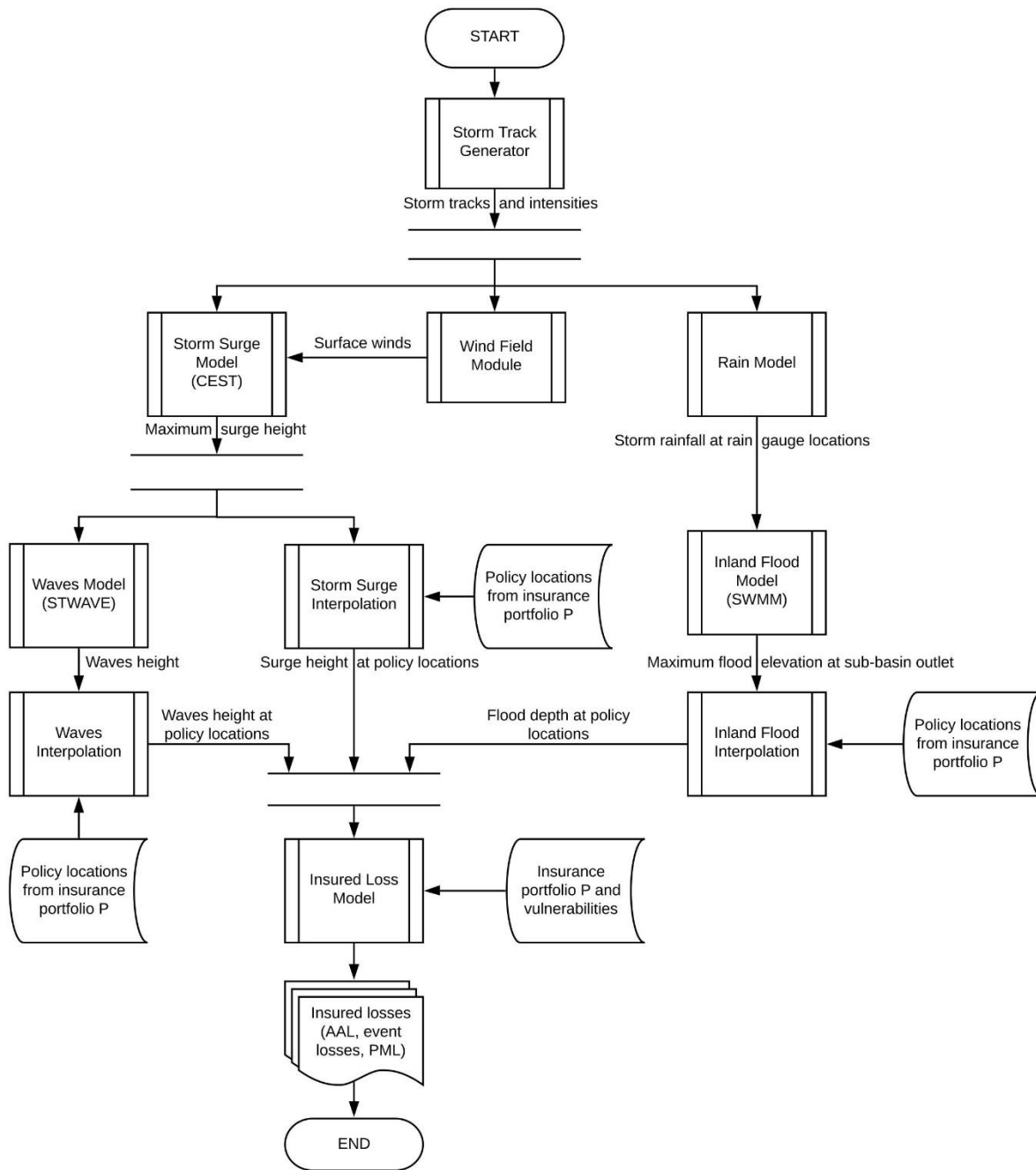


Figure 29. Interactions among major flood model components.

4. Provide a comprehensive list of complete references pertinent to the submission by flood standard grouping using professional citation standards.

References

Meteorology

FPFLM V1.0 Feb. 29, 2020

- Darling, R. W. (1991). Estimating probabilities of hurricane wind speeds using a large scale empirical model. *Journal of Climate*, 4, 1035-1046.
- DeMaria, M., & Kaplan, J. (1995). Sea surface temperature and the maximum intensity of Atlantic tropical cyclones. *Journal of Climate*, 7, 1324-1334.
- DeMaria, M., Mainelli, M., Shay, L. K., Knaff, J. A., & Kaplan, J. (2005). Further improvements to the statistical hurricane intensity prediction scheme. *Weather and Forecasting*, 20, 531-543.
- DeMaria, M., Pennington, J., & Williams, K. (2002). *Description of the Extended Best track file (EBTRK1.4) version 1.4*. Retrieved 2002, from <ftp://ftp.cira.colostate.edu/demaria/ebtrk/>
- Demuth, J., DeMaria, M., & Knaff, J. A. (2006). Improvement of advanced microwave sounder unit tropical cyclone intensity and size estimation algorithms. *Journal of Applied Meteorology*, 45, 1573-1581.
- Franklin, J. L., Black, M. L., & Valde, K. (2003). GPS dropwindsonde wind profiles in hurricanes and their operational implications. *Weather and Forecasting*, 18, 32– 44.
- Ho, F. P., Su, J. C., Hanevich, K. L., Smith, R. J., & Richards, F. P. (1987). *Hurricane Climatology for the Atlantic and Gulf Coasts of the United States*. NOAA Technical Report NWS 38. Maryland: Silver Spring.
- Holland, G. J. (1980). An analytic model of the wind and pressure profiles in hurricanes. *Monthly Weather Review*, 108, 1212-1218.
- Kanamitsu, M., Ebisuzaki, W., Woollen, J., Yang, S.-K., Hnilo, J. J., Fiorino, M., et al. (2002). NCEP-DEO AMIP-II Reanalysis (R-2). *Bulletin of the American Meteorological Society*, 83, 1631-1643.
- Landsea, C. W. (2004). The Atlantic hurricane database re-analysis project- documentation for 1850-1910 alterations and additions to the HURDAT database. In R. Murnane, & K. Liu, *Hurricanes and Typhoons: Past, Present, and Future* (pp. 178-221). Columbia University Press.
- Landsea, C. W., Pielke Jr, R. A., Mestas-Nuñez, A. M., & Knaff, J. A. (1999). Atlantic basin hurricanes: Indices of climatic changes. *Climatic Change*, 42, 89-129.
- Large, W. G., & Pond, S. (1981). Open ocean momentum flux measurements in moderate to strong winds. *Journal of Physical Oceanography*, 11, 324-336.
- Lonfat, M., F.D. Marks, and S.S. Chen 2004: Precipitation Distribution in Tropical Cyclones Using the Tropical Rainfall Measuring Mission (TRMM) Microwave Imager: A Global Perspective, *Monthly Weather Review*, v. **132**, p. 1645.

- Lonfat, M., Rogers, R., Marchok, T., & Marks, F. D. (2007). A Parametric Model for Predicting Hurricane Rainfall. *Monthly Weather Review*, *135*, 3086-3097.
- Marks, F. D., Atlas, D., & Willis, P. T. (1993). Probability-matched Reflectivity-Rainfall relations for a Hurricane from Aircraft Observations. *Journal of Applied Meteorology*, *32*, 1134-1141.
- Neumann, C. J., Jarvinen, B. R., McAdie, C. J., & Hammer, G. R. (1999). *Tropical Cyclones of the North Atlantic Ocean, 1871-1998*. National Oceanic and Atmospheric Administration.
- Ooyama, K. V. (1969). Numerical simulation of the life cycle of tropical cyclones. *Journal of the Atmospheric Sciences*, *26*, 3-40.
- Pennington, J., DeMaria, M., & Williams, K. (2000). *Development of a 10-year Atlantic basin tropical cyclone wind structure climatology*. Retrieved from www.bbsr.edu/rpi/research/demaria/demaria4.html
- Powell, M. D. (1980). Evaluations of diagnostic marine boundary layer models applied to hurricanes. *Monthly Weather Review*, *108*, 757-766.
- Powell, M. D. (1982). The transition of the Hurricane Frederic boundary layer wind field from the open Gulf of Mexico to landfall. *Monthly Weather Review*, *110*, 1912-1932.
- Powell, M. D. (1987). Changes in the low-level kinematic and thermodynamic structure of Hurricane Alicia (1983) at landfall. *Monthly Weather Review*, *115*(1), 75-99.
- Powell, M. D., & Abernethy, S. D. (2001). Accuracy of United States tropical cyclone landfall forecasts in the Atlantic basin 1976-2000. *Bulletin of the American Meteorological Society*, *82*, 2749-2767.
- Powell, M. D., & Houston, S. H. (1996). Hurricane Andrew's Landfall in South Florida. Part II: Surface Wind Fields and Potential Real-time Applications. *Weather and Forecasting*, *11*, 329-349.
- Powell, M. D., & Houston, S. H. (1998). Surface wind fields of 1995 Hurricanes Erin, Opal, Luis, Marilyn, and Roxanne at landfall. *Monthly Weather Review*, *126*, 1259-1273.
- Powell, M. D., & Reinhold, T. A. (2007). Tropical cyclone destructive potential by integrated kinetic energy. *Bulletin of the American Meteorological Society*, *88*, 513-526.
- Powell, M. D., Bowman, D., Gilhousen, D., Murillo, S., Carrasco, N., & St. Fleur, R. (2004). Tropical Cyclone Winds at Landfall: The ASOS-CMAN Wind Exposure Documentation Project. *Bulletin of the American Meteorological Society*, *85*, 845-851.
- Powell, M. D., Dodge, P. P., & Black, M. L. (1991). The landfall of Hurricane Hugo in the Carolinas. *Weather and Forecasting*, *6*, 379-399.

Powell, M. D., Houston, S. H., & Ares, I. (1995). Real-time Damage Assessment in Hurricanes. *21st AMS Conference on Hurricanes and Tropical Meteorology*, (pp. 500-502). Miami, Florida.

Powell, M. D., Houston, S. H., & Reinhold, T. (1996). Hurricane Andrew's landfall in south Florida. Part I: Standardizing measurements for documentation of surface wind fields. *Weather and Forecasting*, *11*, 304-328.

Powell, M. D., Houston, S. H., Amat, L. R., & Morisseau-Leroy, N. (1998). The HRD real-time hurricane wind analysis system. *Journal of Wind Engineering and Industrial Aerodynamics*, *77* & *78*, 53-64.

Powell, M. D., Murillo, S., Dodge, P., Uhlhorn, E., Gamache, J., Cardone, V., et al. (2010). Reconstruction of Hurricane Katrina's wind fields for storm surge and wave hindcasting. *Ocean Engineering*, *37*, 26-36.

Powell, M. D., Reinhold, T. A., & Marshall, R. D. (1999). GPS sonde insights on boundary layer wind structure in hurricanes. In A. Larsen, G. L. Larose, F. M. Livesey, M. D. Powell, T. A. Reinhold, & R. D. Marshall (Eds.), *Wind Engineering into the 21st Century*. Rotterdam: A.A. Balkema.

Powell, M. D., Soukup, G., Cocke, S., Gulati, S., Morisseau-Leroy, N., Hamid, S., et al. (2005). State of Florida Hurricane Loss Projection Model: Atmospheric Science Component. *Journal of Wind Engineering and Industrial Aerodynamics*, *93*, 651-674.

Powell, M. D., Uhlhorn, E., & Kepert, J. (2009). Estimating maximum surface winds from hurricane reconnaissance aircraft. *Weather and Forecasting*, *24*, 868-883.

Powell, M. D., Vickery, P. J., & Reinhold, T. (2003). Reduced drag coefficient for high wind speeds in tropical cyclones. *Nature*, *422*, 279-283.

Reynolds, R. W., Rayner, N. A., Smith, T. M., Stokes, D. C., & Wang, W. (2002). An improved in situ and satellite SST analysis for climate. *Journal of Climate*, *15*, 1609-1625.

Shapiro, L. (1983). The asymmetric boundary layer flow under a translating hurricane. *Journal of the Atmospheric Sciences*, *40*, 1984-1998.

Shay, L. K., Goni, G. j., & Black, P. G. (2000). Effects of a warm oceanic feature on Hurricane Opal. *Monthly Weather Review*, *125*(5), 1366-1383.

Thompson, E. F., & Cardone, V. J. (1996). Practical modeling of hurricane surface wind fields. *Journal of Waterway, Port, Coastal, and Ocean Engineering*, *122*, 195-205.

Vickery, P. J. (2005). Simple empirical models for estimating the increase in the central pressure of tropical cyclones after landfall along the coastline of the United States. *Journal of Applied Meteorology*, *44*, 1807-1826.

Vickery, P. J., & Skerlj, P. F. (2000). Elimination of exposure D along the hurricane coastline in ASCE 7. *Journal of Structural Engineering*, 126, 545-549.

Vickery, P. J., & Skerlj, P. F. (2005). Hurricane gust factors revisited. *Journal of Structural Engineering*, 131, 825-832.

Vickery, P. J., & Twisdale, L. A. (1995). Wind field and filling models for hurricane wind speed predictions. *Journal of Structural Engineering*, 121, 1700-1709.

Vickery, P. J., Skerlj, P. F., & Twisdale, L. A. (2000a). Simulation of hurricane risk in the United States using an empirical storm track modeling technique. *Journal of Structural Engineering*, 126, 1222-1237.

Vickery, P. J., Skerlj, P. F., Steckley, A. C., & Twisdale, L. A. (2000b). A hurricane wind field model for use in simulations. *Journal of Structural Engineering*, 126, 1203-1222.

Vickery, P. J., Wadhera, D., Powell, M. D., & Chen, Y. (2009). A hurricane boundary layer and wind field model for use in engineering applications. *Journal of Applied Meteorology and Climatology*, 48, 381-405.

Wada, A., & Usui, N. (2007). Importance of tropical cyclone intensity and intensification in the Western North Pacific. *Journal of Physical Oceanography*, 63, 427-447.

Willoughby, H. E. (1998). Tropical cyclone eye thermodynamics. *Monthly Weather Review*, 126, 3053-3067.

Willoughby, H. E., & Rahn, M. E. (2004). Parametric Representation of the Primary Hurricane Vortex. Part I: Observations and Evaluation of the Holland (1980) Model. *Monthly Weather Review*, 132, 3033-3048.

Willoughby, H. E., & Shoreibah, M. D. (1982). Concentric eyewalls, secondary wind maxima, and the evolution of the hurricane vortex. *Journal of the Atmospheric Sciences*, 39, 395-411.

Surge

Blumberg, A., & Kantha, L. (1983). Open boundary condition for circulation models. *Journal of Hydraulic Engineering*, 112, 237-255

Casulli, V., & Chen, R.T. (1992). Semi-implicit finite difference method for three-dimensional shallow water flow. *International Journal for Numerical Methods in Fluids*, 15, 629-648

Conver, A., Sepanik, J., Louangsaysongkham, B., & Miller, S. (2010). Sea, Lake, and Overland Surges from Hurricanes (SLOSH) Basin Development Handbook v2.2. In (p. 76): Meteorological Development Lab, The National Weather Service

- Freeman, J.C., Baer, L., & Jung, C.H. (1957). The Bathystrophic storm tide. *Journal of Marine Research*, 16, 12-22
- Fry, J., Xian, G., Jin, S., Dewitz, J., Homer, C., Yang, L., Barnes, C., Herold, N., & Wickham, J. (2011). Completion of the 2006 National Land Cover Database for the Conterminous United States. *Photogrammetric Engineering and Remote Sensing*, 77, 858-864
- Glahn, B., Taylor, A., Kurkowski, N., & Shaffer, W.A. (2009). The role of the SLOSH model in National Weather Service storm surge forecasting. *National Weather Digest*, 33, 3-14
- Houston, S.H., Shaffer, W.A., Powell, M.D., & Chen, J. (1999). Comparisons of HRD and SLOSH surface wind fields in hurricanes: implications for storm surge and wave modeling. *Weather and Forecasting*, 14, 671-686
- Jelesnianski, C.P., Chen, J., & Shaffer, W.A. (1992). SLOSH: Sea, lake and overland surges from hurricanes. In (p. 71). Washington, D.C.: NOAA
- Kennedy, A.B., Gravois, U., Zachry, B.C., Westerink, J.J., Hope, M.E., Dietrich, J.C., Powell, M.D., Cox, A.T., Luettich, R.A., & Dean, R.G. (2011). Origin of the Hurricane Ike forerunner surge. *Geophysical Research Letters*, 38
- Large, W.G., & Pond, S. (1981). Open ocean momentum flux measurements in moderate to strong winds. *Journal of Physical Oceanography*, 11, 324-481
- LeMehaute, B. (1976). *An introduction to hydrodynamics and water waves*. New York, USA: Springer-Verlag
- Mattocks, C., & Forbes, C. (2008). A real-time, event-triggered storm surge forecasting system for the state of North Carolina. *Ocean Modelling*, 25, 95-119
- Liu, H., Zhang, K., Li, Y., and Xie, L. (2013) Numerical study of the sensitivity of mangroves in reducing storm surge and flooding to hurricane characteristics in southern Florida. *Continental Shelf Research* . 64:51–65.
- Morey, S.L., Baig, S., Bourassa, M.A., Dukhovskoy, D.S., & O'Brien, J.J. (2006). Remote forcing contribution to storm-induced sea level rise during Hurricane Dennis. *Geophysical Research Letters*, 33
- Mukai, A.Y., Westerink, J.J., Luettich, R.A., & Mark, D. (2002). Eastcoast 2001, A Tidal Constituent Database for Western North Atlantic, Gulf of Mexico, and Caribbean Sea. In (p. 23). Vicksburg, Mississippi: U.S. Army Corps of Engineers
- Powell, M.D., Houston, S.H., Amat, L.R., & Morisseau-Leroy, N. (1998). The HRD real-time hurricane wind analysis program. *Journal of Wind Engineering and Industrial Aerodynamics*, 77&78, 53-64

Powell, M.D., Vickery, P.J., & Reinhold, T.A. (2003). Reduced drag coefficient for high wind speeds in tropical cyclones. *Nature*, 422, 279-283

Zhang, K., Cui, Z., & Houle, H. (2012a). Airborne LiDAR Remote Sensing and its Application. In C. Yang, & J. Li. (Eds.), *Advances in Mapping from Aerospace Imagery: Techniques and Applications* (pp. 33-67). Boca Raton: CRC Press

Zhang, K., Li, Y., Lui, H., Rhome, J., & Forbes, C. (2013). Transition of the Coastal and Estuarine Storm Tide Model to an operational forecast model: A case study of Florida. *Weather and Forecasting*, DOI:10.1175/WAF-D-12-00076.1

Zhang, K., Liu, H., Li, Y., Xu, H., Shen, J., Rhome, J., & Smith III, T.J. (2012b). The role of mangroves in attenuating storm surges. *Estuarine, Coastal, and Shelf Science*, 102-103, 11-23

Zhang, K., Xiao, C., & Shen, J. (2008). Comparison of the CEST and SLOSH models for storm surge flooding. *Journal of Coastal Research*, 24, 489-499

DiGiano, F.A., Adrian, D.D., Mangarella, P.A., 1976. Short Course Proceedings: Applications of Stormwater Management Models, 1976 - Google Books.

FEMA, 2005. Hurricane Jeanne rapid response Florida riverine high water mark (RHWM) collection, Federal Emergency Management Agency. Atlanta, GA.

Gesch, D.B., Oimoen, M.J., Evans, G.A., 2014. Accuracy assessment of the U.S. Geological Survey National Elevation Dataset, and comparison with other large-area elevation datasets: SRTM and ASTER, U.S. Geological Survey. Reston, Virginia.
<https://doi.org/10.3133/ofr20141008>

McCuen, R.H., Johnson, P.A., Ragan, R.M., 1996. Highway hydrology - Hydraulic Design Series No. 2, FHWA-SA-96-067. <https://doi.org/PNR61>

Rawls, W.J., Brakensiek, D.L., Miller, N., 1983. Green-ampt infiltration parameters from soils data. *J. Hydraul. Eng.* 109, 62–70. [https://doi.org/10.1061/\(ASCE\)0733-9429\(1983\)109:1\(62\)](https://doi.org/10.1061/(ASCE)0733-9429(1983)109:1(62))

Rossman, L. a., 2015. Storm Water Management Model User's Manual Version 5.1. United States Environ. Prot. Agency 353. <https://doi.org/PNR61>

Wave

Bunya, S., Dietrich, J.C., Westerink, J.J., Ebersole, B.A., Smith, J.M., Atkinson, J.H., Jensen, R., Resio, D.T., Luettich, R.A., Dawson, C., Cardone, V.J., Cox, A.T., Pweoll, M.D., Westerink, H.J., and Roberts, H.J. (2010). "A high-resolution coupled riverine flow, tide, wind, wind wave, and storm surge model for Southern Louisiana and Mississippi. Part I: Model development and validation". *Monthly Weather Review* 138(2), 345-377.

Massey, T.C., Anderson, M.E., Smith, J.M., Gomez, J., and Jones, R. (2011). *STWAVE: Steady-State Spectral Wave model. User's Manual for STWAVE, Version 6.0*. Report ERDC/CHL SR-11-1, US Army Corps of Engineers.

Thornton, E.B., and Guza, R.T. (1983). "Transformation of wave height distribution". *J. Geophys. Res.-Oceans* 88(C10), 5925-5938.

Young, I.R., and Verhagen, L.A. (1996). "The growth of fetch limited waves in water of finite depth. 1. Total energy and peak frequency". *Coastal Engineering* 29(1-2), 47-48.

FEMA, 2005. Hurricane Jeanne rapid response Florida riverine high water mark (RHWM) collection, Federal Emergency Management Agency. Atlanta, GA.

Abdul-Aziz, O.I., Al-Amin, S., 2016. Climate, land use and hydrologic sensitivities of stormwater quantity and quality in a complex coastal-urban watershed. *Urban Water J.* 13, 302–320. <https://doi.org/10.1080/1573062X.2014.991328>.

Inland Flood

Abdul-Aziz, O.I., Al-Amin, S., 2016. Climate, land use and hydrologic sensitivities of stormwater quantity and quality in a complex coastal-urban watershed. *Urban Water J.* 13, 302–320. <https://doi.org/10.1080/1573062X.2014.991328>.

Fry, J. A., Xian, G., Jin, S., Dewitz, J. A., Homer, C. G., Yang, L., Barnes, C. A., Herold, N. D., & Wickham, J.D., 2011. Completion of the 2006 National land cover database for the conterminous United States. *Photogramm. Eng. Remote Sens.* 77(9), 858-864.

Homer, C., Dewitz, J., Yang, L., Jin, S., Danielson, P., Xian, G., Coulston, J., Herold, N., Wickham, J., Megown, K., 2015. Completion of the 2011 National land cover database for the conterminous United States—Representing a decade of land cover change information. *Photogramm. Eng. Remote Sens.* 81(5), 345-354.

Jiang, L., Chen, Y., Wang, H., 2015. Urban flood simulation based on the SWMM model. *IAHS-AISH Proc. Reports* 368, 186–191. <https://doi.org/10.5194/piahs-368-186-2015>

Nash, J.E., Sutcliffe, J. V, 1970. River flow forecasting through conceptual models PART I-A Discussion of principles*. *J. Hydrol.* 10, 282–290.

Rossman, L.A., Huber, W.C., 2016. *Storm Water Management Model Reference Manual Volume I – Hydrology (revised) (EPA/600/R-15/162A)*. U.S. Environ. Prot. Agency I, 231.

USDA (United States Department of Agriculture), NRCS (Natural Resources Conservation Service), 2015. Soil survey geographic (SSURGO) database for Florida – June 2012. <http://www.fgdl.org/metadataexplorer/explorer.jsp>.

USGS (United States Geological Survey), 2016a. The national map. FPFLM V1.0 Feb. 29, 2020

USGS (United States Geological Survey), 2016b. National elevation dataset (NED).
<https://lta.cr.usgs.gov/NED>.

USGS (United States Geological Survey), 2016c. Evapotranspiration information and data.
<https://fl.water.usgs.gov/et/>.

Moriasi, D. N., Arnold, J. G., Van Liew, M. W., Bingner, R. L., Harmel, R. D., Veith, T. L., 2007. Model evaluation guidelines for systematic quantification of accuracy in watershed simulations. *Trans. ASABE*. 50(3), 885-900. <https://pubag.nal.usda.gov/catalog/9298>.

Nash, J. E., Sutcliffe, J. V., 1970. River flow forecasting through conceptual models part I—A discussion of principles. *J. Hydrol.* 10(3), 282-290. [https://doi.org/10.1016/0022-1694\(70\)90255-6](https://doi.org/10.1016/0022-1694(70)90255-6).

Rossman, L. A., 2015. Storm Water Management Model user's manual, version 5.1, report EPA-600/R-14/413b. National risk management research laboratory, office of research and development, U.S. Environmental Protection Agency. Cincinnati, OH, USA.
<http://nepis.epa.gov/Exe/ZyPDF.cgi?Dockey=P100N3J6.TXT>.

Abdul-Aziz, O. I., Al-Amin, S., 2015. Climate, land use and hydrologic sensitivities of stormwater quantity and quality in a complex coastal-urban watershed. *Urban Water J.* 13(3), 302-320. <https://doi.org/10.1080/1573062X.2014.991328>.

Rawls, W.J., Brakensiek, D.L., Miller, N., 1983. Green-ampt infiltration parameters from soils data. *J. Hydraul. Eng.* 109, 62–70. [https://doi.org/10.1061/\(ASCE\)0733-9429\(1983\)109:1\(62\)](https://doi.org/10.1061/(ASCE)0733-9429(1983)109:1(62))

Rossman, L.A., Huber, W.C., 2016. Storm Water Management Model Reference Manual Volume I – Hydrology (revised) (EPA/600/R-15/162A). U.S. Environ. Prot. Agency I, 231.

USDA (United States Department of Agriculture), NRCS (Natural Resources Conservation Service), 2015. Soil survey geographic (SSURGO) database for Florida – June 2012.
<http://www.fgdl.org/metadataexplorer/explorer.jsp>.

USDA, 2020. National Resources Conservation Service Soils: Published Soil Surveys for Florida.
<https://www.nrcs.usda.gov/wps/portal/nrcs/surveylist/soils/survey/state/?stateId=FL>.

USDA, 2018. United States Department of Agriculture.
<https://nassgeodata.gmu.edu/CropScape/>.

FEMA, 2005. Hurricane Jeanne rapid response Florida riverine high water mark (RHWM) collection, Federal Emergency Management Agency. Atlanta, GA.

Moriasi, D. N., Arnold, J. G., Van Liew, M. W., Bingner, R. L., Harmel, R. D., Veith, T. L., 2007. Model evaluation guidelines for systematic quantification of accuracy in watershed simulations. *Trans. ASABE*. 50(3), 885-900. <https://pubag.nal.usda.gov/catalog/9298>.

Nash, J. E., Sutcliffe, J. V., 1970. River flow forecasting through conceptual models part I—A discussion of principles. *J. Hydrol.* 10(3), 282-290. [https://doi.org/10.1016/0022-1694\(70\)90255-6](https://doi.org/10.1016/0022-1694(70)90255-6).

Rossmann, L. A., 2015. Storm Water Management Model user's manual, version 5.1, report EPA- 600/R-14/413b. National risk management research laboratory, office of research and development, U.S. Environmental Protection Agency. Cincinnati, OH, USA. <http://nepis.epa.gov/Exe/ZyPDF.cgi?Dockkey=P100N3J6.TXT>.

Rossmann, L.A., Huber, W.C., 2016. Storm Water Management Model Reference Manual Volume I – Hydrology (revised) (EPA/600/R-15/162A). U.S. Environ. Prot. Agency I, 231.

FEMA, 2005. Hurricane Jeanne rapid response Florida riverine high water mark (RHWM) collection, Federal Emergency Management Agency. Atlanta, GA.

Vulnerability

ASCE (American Society of Civil Engineers). (2010). “Minimum design loads for buildings and other structures.” ASCE/SCI 7-10, New York.

Baradaranshoraka, M., Pinelli, J. P., Gurley, K., Peng, X., and Zhao, M. (2017). Hurricane wind versus storm surge damage in the context of a risk prediction model. *Journal of Structural Engineering*, 143(9), 04017103.

Baradaranshoraka, M., Pinelli, J. P., Gurley, K., Peng, X., Zhao, M., and Paleo-Torres, A. (2019). “Characterization of Coastal Flood Damage States for Residential Buildings.” *ASCE-ASME J. Risk Uncertainty Eng. Syst., Part A: Civ. Eng.*, 10.1061/AJRUA6.0001006.

Barbato, M., Petrini, F., Unnikrishnan, V. U., and Ciampoli, M. (2013). “Performance-Based Hurricane Engineering (PBHE) framework.” *Structural Safety*, 45, 24-35.

CCH. (2000). "City and County of Honolulu Building Code (CCH)." Chapter 16. Article 11. Department of Planning and Permitting of Honolulu HawaiiHonolulu, HI.

Dames and Moore (1980). "Design and construction standards for residential construction in tsunami-prone areas in Hawaii." Prepared for the Federal Emergency Management Agency, by Dames & Moore, Washington, DC, USA.

Dolce, M., Kappos, A., Masi, A., Penelis, G., and Vona, M. (2006). "Vulnerability assessment and earthquake damage scenarios of the building stock of Potenza (Southern Italy) using Italian and Greek methodologies." *Engineering Structures*, 28(3), 357-371.

FEMA. (2003). Coastal Construction Manual (3 vols.). 3rd ed. (FEMA 55). Federal Emergency Management Agency, Jessup, Md.

FEMA. (2011). "Coastal construction manual." FEMA P-55, Washington, DC.

FEMA (2015). *Hazus 2.1 Hurricane Model Technical Manual*. Department of Homeland Security. Last updated January 29, 2015.

FGDL (Florida Geographic Data Library). (2012). "Florida Digital Elevation Model (DEM) mosaic - 5-meter cell size - elevation units centimeters."
https://www.fgdl.org/metadata/fgdl_html/flidar_mosaic_cm.htm (Jun. 7, 2019).

Friedland, C. J. (2009). "Residential building damage from hurricane storm surge: Proposed methodologies to describe, assess and model building damage." Ph.D. dissertation, Dept. of Civil and Environmental Engineering, Louisiana State Univ., Baton Rouge, LA.

Hamid, S., Pinelli, J.-P., Cheng, S.-C., and Gurley, K., (2011) "Catastrophe Model Based Assessment of Hurricane Risk and Estimates of Potential Insured Losses for the State of Florida," ASCE Natural Hazard Review, November 2011, Vol. 12, No. 4, pp. 171-183.

Hom-ma, M., and Horikawa, K. (1965). "Experimental study on total wave force against sea wall". *Coastal Engineering in Japan* 8, 119-124.

Kjeldsen, S.P., Myrhaug, D. (1978). "Kinematics and dynamics of breaking waves." *Technical Report. River and Harbour Laboratory (NHL)* — The Norwegian Institute of Technology.

Li, Y., van de Lindt, J. W., Dao, T., Bjarnadottir, S., and Ahuja, A. (2012). "Loss analysis for combined wind and surge in hurricanes." *Nat. Hazards Rev.*, 10.1061/(ASCE)NH.1527-6996.0000058, 1–10.

Masoomi, H., van de Lindt, J. Ameri, M., Do, T., and Webb, B. (2018). " Combined Wind-Wave-Surge Hurricane-Induced Damage Predictions for buildings." *Journal of Structural Engineering*, 10.1061/(ASCE)ST.1943-541X.0002241.

Morgan, M. G., Henrion, M., and Small, M. (1992). Uncertainty: a guide to dealing with uncertainty in quantitative risk and policy analysis. *Cambridge university press*.

Nadal, N. C., Zapata, R. E., Pagán, I., López, R., and Agudelo, J. (2009). "Building damage due to riverine and coastal floods." *Journal of Water Resources Planning and Management*, 136(3), 327-336.

Nirupama, N., Murty, TS, Nistor, I., and Rao, AD. (2006). "A Review of Classical Concepts on Phase and Amplitude Dispersion: Application to Tsunamis." In: Indian Ocean Tsunami, Eds: Murty, Aswathanarayana, Nitupama, A.A. Balkema Publication, The Netherlands, p63-72.

Paleo-Torres, A., Gurley, K., Pinelli, J. P., Baradaranshoraka, M., Zhao, M., Suppasri, A., and Peng, X. (2019). "Vulnerability of Florida residential structures to hurricane induced coastal flood." *Engineering Structures*, *submitted*.

Palermo, D., Nistor, I., Nouri, Y., and Cornett, A., (2009). "Tsunami loading of near-shoreline structures: a primer." *Canadian Journal of Civil Engineering*, 36(11), 1804–1815.

Palermo D., Nistor I., Saatcioglu M. (2013a). "Tsunami Loads on Infrastructure." In: Bobrowsky P.T. (eds) *Encyclopedia of Natural Hazards. Encyclopedia of Earth Sciences Series*. Springer, Dordrecht.

Palermo, D., Nistor, I., Al-Faesly, T., and Cornett, A. (2013b). "Impact of tsunami forces on structures: The University of Ottawa Experience." *Science of Tsunami Hazards: Journal of the Tsunami Society International*, V. 32, No. 2, pp. 58-76

Palisade (2015, June 08). How Many Iterations Do I Need? Palisade Knowledge Based. Retrieved from <http://kb.palisade.com/index.php?pg=kb.page&id=125>

Peng, X. (2015). *Modeling Vulnerability of Residential Buildings to Multiple Hazards* (Doctoral dissertation). University of Florida.

Pinelli, J. P., Pita, G., Gurley, K., Torkian, B., Hamid, S., and Subramanian, C. (2011). "Damage characterization: application to Florida public hurricane loss model." *Natural Hazards Review*, 12(4), 190-195.

Pinelli, J. P., Da Cruz, J., Hasanain, A., Gurley, K., Paleo-Torres, A., Baradaranshoraka, M., Cocke, S., and Shin, D.W. (2019). "Data management for the development, validation, calibration and operation of a hurricane vulnerability model." *International Journal of Disaster Risk Science*, *submitted*.

RSMeans. (2008a). *RSMeans Residential Cost Data*. Robert S Means Co; 27th edition (October 31, 2007).

RSMeans. (2008b). *RSMeans Square Foot Costs*. R.S. Means Company; 29th edition (October 31, 2007).

RSMeans. (2012). *RSMeans Residential Cost Data*. Robert s Means Co; 31 edition (October 31, 2011).

RSMeans. (2015a). *RSMeans Residential Cost Data*. R.S. Means Company; 34 Annual edition (October 27, 2014).

RSMeans. (2015b). *RSMeans Contractor's Pricing Guide: Residential Repair & Remodeling Costs*. Robert S Means Co (November 24, 2014).

Suppasri, A., Mas, E., Charvet, I., Gunasekera, R., Imai, K., Fukutani, Y., Abe, Y., and Imamura, F. (2013). "Building damage characteristics based on surveyed data and fragility curves of the 2011 Great East Japan tsunami." *Natural Hazards*, 66(2), 319-341.

Tomiczek, T., Kennedy, A., and Rogers, S. (2014). "Collapse limit state fragilities of wood-framed residences from storm surge and waves during Hurricane Ike." *J. Waterway, Port, Coastal, Ocean Eng.*, 10.1061/(ASCE)WW.1943-5460.0000212, 43–55.

Tomiczek, T., Kennedy, A., Zhang, Y., Owensby, M., Hope, M. E., Lin, N., & Flory, A. (2017). Hurricane damage classification methodology and fragility functions derived from Hurricane Sandy's effects in Coastal New Jersey. *Journal of Waterway, Port, Coastal, and Ocean Engineering*, 143(5), 04017027.

USACE (2006). "Depth-damage relationships for structures, contents, and vehicles and content-to-structure value ratios (CSV) in support of the Donaldsonville to the Gulf, Louisiana, Feasibility Study." US Army Corps of Engineers (USACE), New Orleans District, Louisiana.

USACE (2015). "US North Atlantic Coast Comprehensive Study: Resilient Adaptation to Increasing Risk." Physical Damage Function Summary Report, Washington, DC: USACE.

Vann, P.W., and J.R. McDonald (1978), "An Engineering Analysis: Mobile Homes in Windstorms", Report prepared for Disaster Preparedness Staff, National Weather Service, NOAA, Silver Spring, MD, *Institute for Disaster Research*, Lubbock, TX.

Walton, T.L., Ahrens, J.P., Truitt, C.L., and Dean, R.G. (1989). Criteria for evaluating coastal flood-protection structures. Technical Report. Washington, DC: USACE.

Actuarial Standards

Hogg, R. V., & Klugman, S. (1984). *Loss Distributions*. New York: Wiley.

Klugman, S., Panjer, H., & Willmot, G. (1998). *Loss Models: From Data to Decisions*. New York: Wiley.

Wilkinson, M. E. (1982). Estimating Probable Maximum Loss with Order Statistics. *Casualty Actuarial Society, LXIX*, pp. 195-209.

Statistical

Moriasi, D. N., Arnold, J. G., Van Liew, M. W., Bingner, R. L., Harmel, R. D., Veith, T. L., 2007. Model evaluation guidelines for systematic quantification of accuracy in watershed simulations. *Trans. ASABE*. 50(3), 885-900. <https://pubag.nal.usda.gov/catalog/9298>.

Nash, J. E., Sutcliffe, J. V., 1970. River flow forecasting through conceptual models part I—A discussion of principles. *J. Hydrol.* 10(3), 282-290. [https://doi.org/10.1016/0022-1694\(70\)90255-6](https://doi.org/10.1016/0022-1694(70)90255-6).

Rossman, L. A., 2015. Storm Water Management Model user's manual, version 5.1, report EPA-600/R-14/413b. National risk management research laboratory, office of research and development, U.S. Environmental Protection Agency. Cincinnati, OH, USA.
<http://nepis.epa.gov/Exe/ZyPDF.cgi?Dockey=P100N3J6.TXT>.

Abdul-Aziz, O. I., Al-Amin, S., 2015. Climate, land use and hydrologic sensitivities of stormwater quantity and quality in a complex coastal-urban watershed. Urban Water J. 13(3), 302-320. <https://doi.org/10.1080/1573062X.2014.991328>.

5. Provide a list and description of any potential interim updates to underlying data relied upon by the flood model. State whether the time interval for the update has a possibility of occurring during the period of time the flood model could be found acceptable by the Commission under the review cycle in this Flood Standards Report of Activities.

None.

6. Identify and describe the modeling-organization-specified, predetermined, and comprehensive exposure dataset used for projecting personal residential flood loss costs and flood probable maximum loss levels.

The exposures in this file were sourced from:

- NFIP's 2012 exposure file for Florida,
- The 2019 exposures of a manufactured home insurer whose policies include flood coverage, and
- Post-2012 construction for frame and masonry owners policies located in coastal ZIP codes as reported to the modeler by the Florida OIR for 2019 stress testing.

Properties from the latter two sources were assumed to be insured to value. The NFIP policies were matched to county tax assessor (TA) databases in order to determine the current property value. For unmatched exposures the building limit was assumed to be the property value.

GF-2 Qualifications of Modeling Organization Personnel and Consultants Engaged in Development of the Flood Model

A. Flood model construction, testing, and evaluation shall be performed by modeling organization personnel or consultants who possess the necessary skills, formal education, and experience to develop the relevant components for flood loss projection methodologies.

The model was developed, tested, and evaluated by a multi-disciplinary team of professors and experts in the fields of hydrology, coastal surge, coastal engineering, meteorology, structural engineering, computer science, statistics, finance, and actuarial science. The experts work primarily at Florida International University, Florida Institute of Technology, Florida State University, University of Florida, West Virginia University, University of Miami, Notre dame University, Hurricane Research Division of NOAA, and AMI Risk Consultants.

B. The flood model and flood model submission documentation shall be reviewed by modeling organization personnel or consultants in the following professional disciplines with requisite experience: hydrology and hydraulics (advanced degree or licensed Professional Engineer(s) with experience in coastal and inland flooding), meteorology (advanced degree), statistics (advanced degree), structural engineering (licensed Professional Engineer(s) with experience in coastal and inland flooding), actuarial science (Associate or Fellow of Casualty Actuarial Society or Society of Actuaries), and computer/information science (advanced degree or equivalent experience and certifications). These individuals shall certify Expert Certification Forms GF-1 through GF-7 as applicable.

The model has been reviewed by modeler personnel and consultants in the required professional disciplines. These individuals abide by the standards of professional conduct as adopted by their profession.

Disclosures

1. Organization Background

A. Describe the ownership structure of the modeling organization engaged in the development of the flood model. Describe affiliations with other companies and the nature of the relationship, if any. Indicate if the organization has changed its name and explain the circumstances.

The model was developed independently by a multi-disciplinary team of professors and experts. The lead university is the Florida International University. The model was commissioned by the Florida Office of Insurance Regulation.

B. If the flood model is developed by an entity other than the modeling organization, describe its organizational structure and indicate how proprietary rights and control over the flood model and its components are exercised. If more than one entity is involved in the development of the flood model, describe all involved.

The wave program STWAVE was developed by the US Army Corps of Engineers, which is a branch of the US Federal government. All components of the model are freely available, including source code. It may be used without needing additional rights or compensation.

The Florida Office of Insurance Regulation (OIR) contracted and funded Florida International University to develop the Florida Public Flood Loss Model. The model is based at the Laboratory for Insurance, Financial and Economic Research, which is part of the Extreme Event Institute at Florida International University. The OIR did not influence the development of the model. The model was developed independently by a team of professors, experts, and graduate students working primarily at Florida International University, Florida Institute of Technology, Florida State University, University of Florida, West Virginia University, Notre Dame University, University of Miami, Hurricane Research Division of NOAA, and AMI Risk Consultants. The copyright for the model belongs to OIR.

The coastal flood surge model, Coastal and Estuarine Storm Tide (CEST) model, was developed by FPFLM project experts at Florida International University. The coastal flood model uses the wave program STWAVE for modeling the wave part of the coastal flood. This was developed by the US Army Corps of Engineers, which is a branch of the US Federal government. All components of the model are freely available, including source code. It may be used without needing additional rights or compensation.

The inland flood model was developed by using the FEMA certified, well-established hydrologic modeling platform called storm water management model (SWMM). The platform was originally developed by the U.S. Environmental Protection Agency (EPA) (<http://www.epa.gov/nrmrl/wswrd/wq/models/swmm/>). SWMM is a one-dimensional, process-based hydrologic model that links climate, land use, and surface and subsurface hydrologic processes. All components of the model are freely available, including source codes. It is freely available online for use without needing additional rights or compensations.

C. If the flood model is developed by an entity other than the modeling organization, describe the funding source for the development of the flood model.

The model was funded by the state legislature at the request of the Florida Office of Insurance Regulation.

D. Describe any services other than flood modeling provided by the modeling organization.

The modeling organization provides hurricane wind loss modeling service.

E. Indicate if the modeling organization has ever been involved directly in litigation or challenged by a governmental authority where the credibility of one of its U.S. flood model versions for projection of flood loss costs or flood probable maximum loss levels was disputed. Describe the nature of each case and its conclusion.

None.

2. Professional Credentials

A. Provide in a tabular format (a) the highest degree obtained (discipline and university), (b) employment or consultant status and tenure in years, and (c) relevant experience and responsibilities of individuals currently involved in the acceptability process or in any of the following aspects of the flood model:

1. Meteorology

2. Hydrology and Hydraulics

3. Statistics

4. Vulnerability

5. Actuarial Science

6. Computer/Information Science

Key Personnel	Degree/ Discipline	University	Employment Status	Tenure	Experience
Meteorology					
Dr. Steve Cocke	Ph.D. Physics	Univ. Texas Austin	Scholar/Scientist FSU, Dept of Meteorology	24	Meteorology track, intensity, roughness models
Dr. Dongwook Shin	Ph.D. Meteorology	Florida State University	FSU/COAPS, Associate Research Scientist	19	Meteorology
Bachir Annane	M.S. Meteorology, M.S. Mathematics	Florida State University	Meteorologist, Univ. of Miami	26	Meteorology
Coastal Flood					

Key Personnel	Degree/ Discipline	University	Employment Status	Tenure	Experience
Dr. Yuepeng Li	Ph. D. Marine Science	The College of William and Mary	Research Scientist IHRC FIU	10	Storm Surge, coastal flooding, marine science
Dr. Keqi Zhang	Ph. D. Marine Science	University of Maryland	Professor of Earth and Environment, FIU	22	Lidar, Storm Surge, coastal flooding, marine science
Andrew Kennedy	Ph.D. Mechanical Engineering	Monash Univ., Australia	Professor, Dept. of Civil & Environmental Engineering & Earth Sciences	12	Waves, Surge, Coastal Science & Engineering
Inland Flood					
Dr. Omar I. Abdul- Aziz	Ph.D. in Civil Engineering	University of Minnesota, Twin Cities	Associate Professor, Civil and Environmental Engineering, West Virginia University	10	Hydrologic and hydraulic modeling
Erfanul Huq	M.S. in Environmental Engineering	Washington State University, Tri- Cities	Doctoral candidate, Civil Engineering, West Virginia University	6	Hydrologic and hydraulic modeling
Mahmood Khan	M.S. in Water Resources Engineering	Bangladesh University of Engineering and Technology	Doctoral student, Civil Engineering, West Virginia University	5	Hydrologic and hydraulic modeling
Mehedi Hasan Tarek	M.S. in Civil Engineering	Bangladesh University of Engineering and Technology	Doctoral student, Civil Engineering, West Virginia University	3	Hydrologic and hydraulic modeling
Statistics					
Dr. S. Gulati	Ph.D. Statistics	University of South Carolina	Professor, Statistics , FIU	29	Served on the Flori da Commission on Hurricane Loss Proj ection Methodology 2000 –2008; Previous statistician for Florida Public Hurricane Loss Model (FPFLM)
Dr. B. M. Golam Kibria	Ph.D. Statistics	University of Western Ontario	Professor of Statistics, FIU	20	Statistician for Florida Public Hurricane Loss Model (FPFLM) since 2006
Dr. Wensong Wu	Ph.D. Statistics	University of South Carolina	Associate Professor, Statistics, FIU	9	Statistician for Florida Public Hurricane Loss Model (FPFLM) since 2015
Engineering					
Dr. Jean-Paul Pinelli	Ph.D. Civil Engineering	Georgia Tech	Professor, CE Florida Institute of Technology	25	Vulnerability model development

Key Personnel	Degree/ Discipline	University	Employment Status	Tenure	Experience
Dr. Kurt Gurley	Ph.D. Civil Engineering	University of Notre Dame	Professor, University of Florida	23	Vulnerability model development
Andres Paleo-Torres	M.S. Civil Eng.	Autonomous University of Yucatan	Ph.D. Candidate, University of Florida	2	Vulnerability model development
Actuarial/Finance					
Dr. Shahid Hamid Project Manager, PI	Ph.D. Economics (Financial), CFA	University of Maryland	Professor of Finance Florida International University	32	Insurance and finance
Gail Flannery	FCAS, Actuary	CAS	VP, AMI Risk Consultants	35	Reviewer, demand surge, actuarial analysis
Aguedo Ingco	FCAS, Actuary	CAS	President, AMI Risk Consultants	45	Reviewer, demand surge
Computer Science					
Dr. Shu-Ching Chen	Ph.D. Electrical and Computer Engineering	Purdue University	Professor of Computer Science, FIU	20	Software and database development
Dr. Mei-ling Shyu	Ph.D. Electrical and Computer Engineering	Purdue University	Professor of Electrical and Computer Engineering, University of Miami	20	Software quality assurance
Raul Garcia	M.S. Computer Science	Georgia Institute of Technology	Research Specialist II, FIU	10	Software and database development
Diana Machado	M.S. Computer Science	Georgia Institute of Technology	Research Specialist II, FIU	9	Software and database development
Yudong Tao	B.S. Microelectronics	Fudan University	Ph.D. Candidate in Electrical and Computer Engineering, UM	5	Software and database development
Anchen Sun	B.S. Marine and Atmosphere Science/Computer Science	University of Miami	Master in Electrical and Computer Engineering, University of Miami	1	Software and database development
Mario Jacas	B.S. Nuclear Engineering	Higher Institute of Nuclear Technologies and Applied Sciences	Master in Computer Science, FIU	1	Software and database development
Daniel Martinez	High School	Florida International University	Student assistant in the DMIS lab, FIU	2	Information management systems
Christian Morerya	High School	Florida International University	IHRC Student Research Assistant, FIU	1	Software and database development

Table 15. Professional credentials.

B. Provide visual business workflow documentation connecting all personnel related to flood model design, testing, execution, maintenance, and decision-making.

3. Independent Peer Review

A. Provide reviewer names and dates of external independent peer reviews that have been performed on the following components as currently functioning in the flood model:

1. Meteorology

2. Hydrology and Hydraulics

3. Statistics

4. Vulnerability

5. Actuarial Science

6. Computer/Information Science

The peer review for the coastal flood model was provided in February 2020 by Arthur Taylor, Physical Scientist and SLOSH modeling POC, NOAA, NWS, Meteorological Development Lab.

The peer review for the meteorology component was provided by dr. Gary Barnes, professor of meteorology at University of Hawaii in 2007. The current version was reviewed by modeler personnel.

B. Provide documentation of independent peer reviews directly relevant to the modeling organization responses to the flood standards, disclosures, or forms. Identify any unresolved or outstanding issues as a result of these reviews.

The written independent review by Arthur Taylor and Gary Barnes are presented in the appendix. No unresolved outstanding issues remain after the review.

C. Describe the nature of any on-going or functional relationship the organization has with any of the persons performing the independent peer reviews.

Arthur Taylor and Gary Barnes have no on-going or functional relationship to FIU or the modeling organization, other than as an independent reviewer. They did not take part in the development or testing of the model.

4. Provide a list of rating agencies and insurance regulators that have reviewed the flood model. Include the dates and purpose of the reviews.

None.

5. Provide a completed Form GF-1, General Flood Standards Expert Certification. Provide a link to the location of the form [insert hyperlink here].

See [Form GF-1](#).

6. Provide a completed Form GF-2, Meteorological Flood Standards Expert Certification. Provide a link to the location of the form [insert hyperlink here].

See [Form GF-2](#).

7. Provide a completed Form GF-3, Hydrological and Hydraulic Flood Standards Expert Certification. Provide a link to the location of the form [insert hyperlink here].

See [Form GF-3](#).

8. Provide a completed Form GF-4, Statistical Flood Standards Expert Certification. Provide a link to the location of the form [insert hyperlink here].

See [Form GF-4](#).

9. Provide a completed Form GF-5, Vulnerability Flood Standards Expert Certification. Provide a link to the location of the form [insert hyperlink here].

See [Form GF-5](#).

10. Provide a completed Form GF-6, Actuarial Flood Standards Expert Certification. Provide a link to the location of the form [insert hyperlink here].

N/A

11. Provide a completed Form GF-7, Computer/Information Flood Standards Expert Certification. Provide a link to the location of the form [insert hyperlink here].

See [Form GF-7](#).

GF-3 Insured Exposure Location

- A. ZIP Codes used in the flood model shall not differ from the United States Postal Service publication date by more than 48 months at the date of submission of the flood model. ZIP Code information shall originate from the United States Postal Service.**

The FPFLM uses ZIP Code data exclusively from a third-party developer, which bases its information on the ZIP Code definitions issued by the United States Postal Service. The version we used has a USPS vintage of April 2017.

- B. Horizontal location information used by the modeling organization shall be verified by the modeling organization for accuracy and timeliness and linked to the personal residential structure where available. The publication date of the horizontal location data shall be no more than 48 months prior to the date of submission of the flood model. The horizontal location information data source shall be documented and updated.**

The FPFLM uses commercial software to geo-locate the personal residential structures, and it was verified for accuracy and timeliness

- C. If any hazard or any flood model vulnerability components are dependent on databases pertaining to location, the modeling organization shall maintain a logical process for ensuring these components are consistent with the horizontal location database updates.**

- D. Geocoding methodology shall be justified.**

The FPFLM uses an enterprise class geocoding engine for converting street addresses to latitude and longitude values.

- E. Use and conversion of horizontal and vertical projections and datum references shall be consistent and justified.**

Disclosures

- 1. List the current location databases used by the flood model and the flood model components to which they relate. Provide the effective dates corresponding to the location databases.**

The Insured Loss Module of the FPFLM uses two location databases: The U.S. ZIP Code Database from zip-codes.com effective April 2017 and the Esri StreetMap Premium North America locators effective March 2018.

2. Describe in detail how invalid ZIP Codes, parcels, addresses, and other location information are handled.

When a valid street address or coordinates are not available for an exposure, the policy is not modeled. Clients are notified of unmodeled policies because of missing location information.

Invalid ZIP Codes are corrected using the value returned by the geocoding engine provided that the street address of the exposure is valid.

3. Describe any methods used for subdividing or disaggregating the location input data and the treatment of any variations for populated versus unpopulated areas.

The FPFLM does not subdivide or disaggregate the location input data.

4. Describe the data, methods, and process used in the flood model to convert between street addresses and geocode locations (latitude-longitude).

The FPFLM uses the REST API of the ArcGIS Server with the esri StreetMap Premium for ArcGIS locators to geocode street addresses. A request containing the given street address, city, state, and ZIP Code is sent to the server. The server processes the request and sends a response containing the status, the location, and the standardized address. The location and address fields of the response are empty when the status is unmatched.

5. Describe the use of geographic information systems (GIS) in the process of converting among street address and geocode locations, and the generation of insured exposure locations.

The FPFLM uses the GIS software tool mentioned above to convert street addresses of exposure locations to longitude and latitude.

6. List and provide a brief description of each database used in the flood model for determining geocode location.

The esri StreetMap Premium North America locators data files include all necessary information for determining geocode locations.

7. Describe the process for updating flood model geocode locations as location databases are updated.

The locators data files are downloaded from the vendor and updated annually.

8. Describe in detail the methods by which ground elevation data at the insured exposure location (e.g., building) is associated with the location databases and how this associated data is used in the flood model.

All building locations have a latitude and longitude associated with them. These locations in the exposure dataset are mapped onto corresponding grid locations in the wave model, or to a null grid if they are not in the wave grids (e.g. inland flooding). The grid locations are then saved to a file, and each location is queried for each run of the wave model to determine wave properties at the insured location.

Exposure addresses are first geocoded using the method described above. The longitude and latitude information is then used to create a collection of points neighboring the query point. The elevation at each of the points is extracted from a Digital Elevation Map using the Python API of a service published in a local ArcGIS Server instance. Finally a heuristic is used to compute the ground elevation and the exposure location from the collection of ground elevations.

9. For each parameter used in the flood model, provide the horizontal and vertical projections and datum references, if applicable. If any horizontal or vertical datum conversions are required, provide conversion factors and describe the conversion methodology used.

The STWAVE model runs in (x,y) meters coordinates. Each point on the STWAVE grids is converted into geographical space with coordinates latitude, longitude (both NAD83), and elevation (NAVD88) using Matlab coordinate transformation routines. Topography, bathymetry, Manning's n and all other appropriate properties are determined in geographic coordinates at the grid locations, and then used in the model.

GF-4 Independence of Flood Model Component

The meteorology, hydrology and hydraulics, vulnerability, and actuarial components of the flood model shall each be theoretically sound without compensation for potential bias from other components.

The meteorology, coastal surge, hydrology, vulnerability, and actuarial components of the model are theoretically sound and were developed independently before being integrated. The model components were tested individually.

+

GF-5 Editorial Compliance

The flood model submission and any revisions provided to the Commission throughout the review process shall be reviewed and edited by a person or persons with experience in reviewing technical documents who shall certify on Form GF-8, Editorial Review Expert Certification, that the flood model submission has been personally reviewed and is editorially correct.

The current submission document has been reviewed and edited by persons who are qualified to perform such tasks. Future revisions and related documentation will likewise be reviewed and edited by the qualified individual listed in Form GF-8.

Disclosures

- 1. Describe the process used for document control of the flood model submission. Describe the process used to ensure that the paper and electronic versions of specific files are identical in content.***

All submission document revisions are passed to the Editor prior to inclusion in the document. The editor is responsible for the electronic version of the document and the technical software issues. Several Microsoft Word tools are utilized to automate the process of formatting and editing the document. For example, we used Source Manager for APA-style bibliographies, consistent formatting via styles for standards, forms and disclosures, cross-references to cite figures and tables, and multi-level lists to ensure consistent numbering. In addition, Microsoft Word's track changes tool is used to keep track of modifications to the document since the initial submission. An export filter to PDF format is used to export the document directly to PDF format, which subsequently is printed directly to paper via a printer. The PDF and printed document should be identical barring unforeseen bugs in the PDF export plug-in or PDF printing software.

- 2. Describe the process used by the signatories on the Expert Certification Forms GF-1 through GF-7 to ensure that the information contained under each set of flood standards is accurate and complete.***

Each signatory was responsible for doing a final review of the standards related to their expertise prior to submission to verify the accuracy and completeness of the information in the submission document. A technical editor performs a thorough edit of the document. All signatories were required to proof-read a PDF version of the document to ensure accuracy and completeness. On-site meetings were held to perform a thorough review of the final version of the document.

- 3. Provide a completed Form GF-8, Editorial Review Expert Certification. Provide a link to the location of the form [insert hyperlink here].***

See [Form GF-8](#).

METEOROLOGICAL FLOOD STANDARDS

MF-1 Flood Event Data Sources

A. The modeling of floods in Florida shall involve meteorological, hydrological, hydraulic, and other relevant data sources required to model coastal and inland flooding.

The flood model uses a large volume of meteorological, hydrological, hydraulic and other relevant data sources to estimate potential coastal and inland flooding.

B. The flood model shall incorporate relevant data sources in order to account for meteorological, hydrological, and hydraulic events and circumstances occurring either inside or outside of Florida that result in, or contribute to, flooding in Florida.

The coastal surge model CEST simulate the coastal surge induced by hurricanes making landfall along or near Florida coastal region. In other word, even the hurricanes made landfall at George or Louisiana, the CEST model still can simulate the surge induced by hurricane wind along Florida coastal region.

The hydrological conditions prevailing outside the state of Florida have been taken care of by introducing upstream boundary conditions. For example, the Apalachicola River originates in Georgia and flows through Florida on its way to Gulf of Mexico. The streamflow contributed to the Apalachicola River by the runoff generated within the watersheds in Georgia was introduced in the Northwest Florida Basin model as upstream boundary conditions.

C. Coastal and inland flood model calibration and validation shall be justified based upon historical data consistent with peer reviewed or publicly developed data sources.

For the coastal flooding team, there are three types data are used to calibrate and validate the coastal surge model. First is water elevation time series data (<https://tidesandcurrents.noaa.gov/>) along Florida coastal region. The water elevation data was directly downloaded from National Oceanic and Atmospheric Administration (NOAA), Units: Meters, Timezone: GMT, Datum: MSL, Interval 1 hour or 6 min (if available). Second is the High Water Mark (HWM) data, the reports, published by United States Geological Survey (USGS) or Federal Emergency Management Agency (FEMA) related to each historical hurricanes required by standards, are extracted or digitalized. For the High Water Mark (HWM) data, data above NAVD88 are used. Third is the Inundation maps or debris line, (<https://www.fema.gov/hurricane-ivan-surge-inundation-maps>)

Consistent with scientific and technical literature, for coastal surge model, the time series of water elevation are all compared at vertical datum Mean Sea Level (MSL). For the High Water Mark (HWM) data, data above NAVD88 are used.

The inland flood models have been calibrated and validated by the daily mean historical observed streamflow data obtained from USGS, and South Florida Water Management District.

D. Any trends, weighting, or partitioning shall be justified and consistent with current scientific and technical literature.

We conduct no trending, weighting, or partitioning.

Disclosures

1. Specify relevant data sources, their release dates, and the time periods used to develop and implement flood frequencies for coastal and inland flooding into the flood model.

For the coastal flooding team, the flood control measures information are collected from different federal and state agents, U.S. Army Corps of Engineers, Federal Emergency Management Agency, from National Oceanic and Atmospheric Administration, and Florida Division of Emergency Management.

For the historical hurricanes data, the following reports are used to calibrate or validate the coastal surge model.

Mitchell H.Murray (1992). Storm-Tide Elevations Produced by Hurricane Andrew Along the Southern Florida Coasts. U.S Geological Survey Open-File Report 96-116.

Michael Baker Jr., Inc. Alexandria, VA (1995). Hurricane Opal Florida Panhandle Wind and Water Line Survey.

U.S. Army Corps of Engineers, Mobile District, Coastal, Hydrology, and Hydraulic Design Section in cooperation with the United States Geological Survey; Alabama, Florida, and Mississippi Districts (1998). Hurricane Georges Storm Surge September.

U.S. Army Corps of Engineers Jacksonville District (1998). South Florida High Water Marks – Post Georges.

U.S. Department of Commerce National Ocean Service Center for Operational Products and Services (2004). Hurricane CHARLEY Preliminary Water Levels Report.

URS Group, Inc. 200 Orchard Ridge Drive Suite 101 Gaithersburg, MD 20878 (2005). Hurricane Frances Rapid Response Florida Coastal High Water Mark (CHWM) Collection FEMA-1545-DR-FL.

NOAA National Oceanic and Atmospheric Administration(2004). Hurricane FRANCES Preliminary water Levels report.

Mobile District Engineering Division Hydrology and Hydraulics Branch (2004). Tide Gage Data for Hurricane Ivan.

NOAA National Oceanic and Atmospheric Administration(2004). Hurricane IVAN Preliminary Water Levels Report.

URS Group, Inc. 200 Orchard Ridge Drive Suite 101 Gaithersburg, MD 20878 (2004). Hurricane Ivan Rapid Response Alabama and Mississippi Coastal High Water Mark (CHWM) Collection FEMA-1549-DR-AL & 1550-DR-MS.

URS Group, Inc. 200 Orchard Ridge Drive Suite 101 Gaithersburg, MD 20878 (2004). Hurricane Ivan Rapid Response Florida Coastal High Water Mark (CHWM) Collection FEMA-1551-DR-FL.

URS Group, Inc. 200 Orchard Ridge Drive Suite 101 Gaithersburg, MD 20878 (2004). Hurricane Jeanne Rapid Response Florida Riverine High Water Mark (RHWM) Collection FEMA-1561-DR-FL.

NOAA National Oceanic and Atmospheric Administration (2004).Hurricane Jeanne Preliminary Water Levels Report.

RS Group, Inc. 200 Orchard Ridge Drive Suite 101 Gaithersburg, MD 20878 (2004). Hurricane Dennis Rapid Response Florida Coastal High Water Mark (CHWM) Collection FEMA-1595-DR-FL.

NOAA National Oceanic and Atmospheric Administration (2005). Hurricane Dennis Preliminary Water Levels.

Mark E. Luther, Clifford R. Merz, Jeff Scudder, Stephen R. Baig, LT Jennifer Pralgo, Douglas Thompson, Stephen Gill & Gerald Hovis (2007). Water Level Observations for Storm Surge.

URS Group, Inc. 200 Orchard Ridge Drive Suite 101 Gaithersburg, MD 20878 (2006). Final Coastal High Water Mark Collection for Hurricane Wilma in Florida FEMA-1609-DR-FL, Task Order 460.

NOAA National Oceanic and Atmospheric Administration (2005).Hurricane Wilma Preliminary Water Levels Report.

Thomas J. Smith III, Gordon H. Anderson, and Ginger Tiling (2005). A Tale of Two Storms: Surges and Sediment Deposition from Hurricanes Andrew and Wilma in Florida's Southwest Coast Mangrove Forests.

Lars E. Soderqvist and Michael J. Byrne (2005). Monitoring the Storm Tide of Hurricane Wilma in Southwestern Florida.

Inland flood model data sources with release dates and time periods are tabulated below:

Data type	Data source	Release date	Time periods used
Elevation	National Elevation Dataset	2016	2016
Rainfall	National Climatic Data Centre (NCDC), South Florida Water Management District, Southwest Florida Water Management District	2004-2013	2004-2013
Evapotranspiration (ET)	U.S. Geological Survey	2015	2004-2013
Percent Imperviousness	National Land Cover Database (NLCD)	2015	2006, 2011
Percent Slope	National Elevation Dataset	2014	2014
Soil properties	Soil survey geographic (SSURGO) database		
Stream Geometry	South Florida Water Management District Southwest Florida Water Management District St. Johns River Water Management District National Elevation Dataset	2014	2014
Groundwater Level	U.S. Geological Survey	2004-2013	2004-2013
Streamflow	U.S. Geological Survey	2004-2013	2004-2013
Water Level	U.S. Geological Survey	2004-2013	2004-2013

Table 16. Inland Flood Model Data Sources.

2. Where the flood model incorporates modification, partitioning, or adjustment of the historical data leading to differences between modeled climatological and historical data, justify each modification and describe how it is incorporated.

For the coastal flooding team, the depth or elevation data are all converted to NAVD88. If the vertical datum of DEM or bathymetry data are National Geodetic Vertical Datum of 1929 (NGVD 29), the tool Vertcon 2.1 is used to compute the difference in orthometric height between the North American Vertical Datum of 1988 (NAVD 88) and the National Geodetic Vertical Datum of 1929 (NGVD 29) for a given location specified by latitude and longitude. This tool is developed by NOAA, and can be downloaded from https://www.ngs.noaa.gov/PC_PROD/VERTCON/.

The inland flood models have been developed based on the published dataset, without any modification or adjustment to the original data.

3. Describe any assumptions or calculations used in the flood model relating to future conditions (e.g., sea level rise, changes in precipitation patterns, changes in storm frequency or severity).

The sea level rise is not considered in the coastal flooding model, while The coastal flooding model doesn't directly simulate changes in precipitation patterns, storm frequency or severity, until meteorology model includes these effect.

4. If precipitation is explicitly modeled for either inland or coastal flooding, then describe the underlying data and how they are used as inputs to the flood model.

Rain is explicitly modeled using a rain model as described in Standard GF-1.2. The modeled rain rates are based on a regression against TRMM satellite rainfall estimates and are a function of the maximum intensity of the storm at a given point in time and distance to the center of the storm. Hourly estimated rainfall is produced by the rain model using historical or stochastic track information and the SWMM flood model rain gauge locations.

5. Provide citations to all data sources used to develop and support bottom friction for storm surge modeling, including publicly developed or peer reviewed information.

Mattocks, C., & Forbes, C. (2008). A real-time, event-triggered storm surge forecasting system for the state of North Carolina. *Ocean Modelling*, 25, 95-119

Zhang, K., Li, Y., Lui, H., Rhome, J., & Forbes, C. (2013). Transition of the Coastal and Estuarine Storm Tide Model to an operational forecast model: A case study of Florida. *Weather and Forecasting*, DOI:10.1175/WAF-D-12-00076.1

Zhang, K., Liu, H., Li, Y., Xu, H., Shen, J., Rhome, J., & Smith III, T.J. (2012b). The role of mangroves in attenuating storm surges. *Estuarine, Coastal, and Shelf Science*, 102-103, 11-23

6. State whether the model includes flooding other than coastal and inland flooding. State whether the other flooding types are independent of the minimum required sub-perils of coastal and inland flooding.

For the coastal flooding model, the surge induced by hurricane wind is simulated combined with the tide. No other flooding components are included, like the flooding caused by breaking water supplying line.

MF-2 Flood Parameters (Inputs)

A. The flood model shall be developed with consideration given to flood parameters that are scientifically appropriate for modeling coastal and inland flooding. The modeling organization shall justify the use of all flood parameters based on information documented in current scientific and technical literature.

The coastal surge model CEST includes several parameters, such as surface wind drag, bottom Manning's Coefficient, parameters and equations to calculate tidal elevation at open boundary, and other parameters. All these parameters are from scientific and technical literatures like papers or reports. All the detailed information are presented at GF-1 and disclosures of MF-1 and MF-2.

The inland flood models have been developed using EPASWMM 5.1. Inland flood model parameters were estimated based on the SWMM input requirements. All these parameters are incorporated from scientific and technical literatures.

B. Differences in the treatment of flood parameters between historical and stochastic events shall be justified.

In order to keep the consistency of the historical and stochastic events, all the parameters in the coastal surge model CEST are same. In other word, there is no difference of surface drag, bottom friction, depth, elevation, or other parameters between historical and stochastic events.

The same inland flood model parameters were used for both the historical and stochastic events.

C. Grid cell size(s) used in the flood model shall be justified.

For the coastal flooding model, there are four sets of basins with different grid cell size are established for coastal surge model covering the whole Florida region, Apalachicola Bay basins including AP7, AP8, and AP9; Miami and Key basins including HMI4, HMI41, and HMI42; Tampa bay basins including TP2, TP3, and TP4; Jacksonville basins including EJX4, EJX5, and EJX6. Through calibrations and verifications for different cell size, the medium grid cell size (300 – 500 meters) are the optimal choice considering both accuracy and computational efficiency. The detail basin description and statistics are presented in Disclosure 12.

The grid resolution is 40 meters, which was selected due to the resolution of data available. The coastal bathymetry data is 3 arc second data which is approximately 90 meters resolution and the onshore data was 1/3 arc second or 10 meter resolution. Therefore, higher resolution onshore is possible, yet would not be necessary for resolving the offshore features considering the input conditions to also be coarser. Sensitivity tests were performed using 20m resolution data, and the results were almost identical to those using the 40m resolution. Because a 20m model would take 4 times longer to run, and the wave model already takes weeks to run the entire stochastic system. In the hydrological models like SWMM, the model domain is discretized by a number of subcatchments. The size (area) of the subcatchments of six inland basin models were chosen based

on the topography, drainage pattern and land use of the watersheds. The isolated area models were discretized by a uniform 300m X 300m blocks.

Disclosures

1. **For coastal and inland flood model components, identify and justify the various flood parameters used in the flood model.**

Surface wind drag

The CEST model uses C_s the drag coefficient which is calculated using the modified formula of Large and Pond (1981) based on Powell et al. (2003).

$$C_s = \begin{cases} 0.00114 & \sqrt{U_a^2 + V_a^2} \leq 10 \\ (0.49 + 0.0065\sqrt{U_a^2 + V_a^2})10^{-3} & 10 < \sqrt{U_a^2 + V_a^2} \leq 38 \\ 0.003 & \sqrt{U_a^2 + V_a^2} > 38 \end{cases}$$

Calculation of Manning's Coefficients Using Land Cover Data

The CEST model uses the Chezy formula (LeMehaute 1976; Zhang et al. 2012b) with a Manning's roughness coefficient to calculate bottom stresses. The Manning's coefficients for ocean grid cells are computed by an empirical formula based on the water depth (H):

$$n_w = \begin{cases} 0.02 & 0 < H < 1 \text{ (m)} \\ 0.01/H + 0.01 & H \geq 1 \end{cases}$$

or set up to be constants, e.g.,

$$n_w = C$$

where C ranges from 0.01 to 0.03. For 4 Florida basins, C = 0.015 on the water cell is used. Manning's coefficients for grid cells over the land were estimated according to the 2006 national land cover dataset (NLCD) created by the U.S. Geological Survey (USGS) (Fry et al. 2011). A modified table of Manning's coefficients (Table 17) corresponding to different land cover categories proposed by Mattocks and Forbes (2008) was employed in this study. Since the spatial resolution of NLCD is 30 m which is usually smaller than the cell size of a CEST grid, an average Manning's coefficient (n_a) for a grid cell was calculated using

$$n_a = \frac{\sum_{i=1}^N (n_i \alpha) + n_w \beta}{N\alpha + \beta}$$

where n_i is the Manning's coefficient value of a NLCD pixel within a model grid cell, α is the area of a NLCD pixel, N is the total number of NLCD pixels within a model cell, n_w is the Manning's coefficient for the oceanic area β that are not covered by NLCD pixels.

NLCD Class Number	NLCD Class Name	Manning Coefficient
11	Open Water	0.020

12	Perennial Ice/Snow	0.010
21	Developed Open Space	0.020
22	Developed Low Intensity	0.050
23	Developed Medium Intensity	0.100
24	Developed High Intensity	0.130
31	Barren Land (Rock/Sand/Clay)	0.090
32	Unconsolidated Shore	0.040
41	Deciduous Forest	0.100
42	Evergreen Forest	0.110
43	Mixed Forest	0.100
51	Dwarf Scrub	0.040
52	Shrub/Scrub	0.050
71	Grassland/Herbaceous	0.034
72	Sedge/Herbaceous	0.030
73	Lichens	0.027
74	Moss	0.025
81	Pasture/Hay	0.033
82	Cultivated Crops	0.037
90	Woody Wetlands	0.140
91	Palustrine Forested Wetland	0.100
92	Palustrine Scrub/Shrub Wetland	0.048
93	Estuarine Forested Wetland	0.100
94	Estuarine Scrub/Shrub Wetland	0.048
95	Emergent Herbaceous Wetlands	0.045
96	Palustrine Emergent Wetland (Persistent)	0.045
97	Estuarine Emergent Wetland	0.045
98	Palustrine Aquatic Bed	0.015
99	Estuarine Aquatic Bed	0.015

Table 17. Manning’s coefficients for various categories of land cover.

The only adjustable parameter in the wave model is the Manning’s n coefficient. These are taken from the NCLD 2011 database. Land use/land cover values are converted into Manning’s n following Bunya et al. (2010).

To develop the inland flood models, the watersheds within the state of Florida were discretized into a number of subcatchments using the ArcGIS platform. The details of the model development are described in GF-1 and data sources are provided in MF-1. The major parameters for the inland flood models were estimated as given below:

Subcatchment Properties

Subcatchment Width

We estimated sub-catchment characteristic width according to DiGiano et al., 1976 with the following formula:

$$W = L + 2L(1 - Z) \quad (1)$$

where,

L = length of the main drainage channel

Z = skew factor= A_m/A

A_m = larger of the two areas on each side of the channel

A = subbasin area

Manning's Roughness Coefficient, n

The overland flow roughness of each subcatchment was calculated based on the land use and Manning's n . Following table is the roughness values for the overland flow:

Surface	n
Smooth asphalt	0.011
Smooth concrete	0.012
Ordinary concrete lining	0.013
Good wood	0.014
Brick with cement mortar	0.014
Vitrified clay	0.015
Cast iron	0.015
Corrugated metal pipes	0.024
Cement rubble surface	0.024
Fallow soils (no residue)	0.05
Cultivated soils	
Residue cover < 20%	0.06
Residue cover > 20%	0.17
Range (natural)	0.13
Grass	
Short, prairie	0.15
Dense	0.24
Bermuda grass	0.41
Woods	
Light underbrush	0.40
Dense underbrush	0.80

Table 18. Manning's n – Overland Flow (McCuen et al., 1996).

Depression Storage

The reference values of depression storage are given below:

Land Use	Depression Storage
Impervious surfaces	0.05 - 0.10 inches
Lawns	0.10 - 0.20 inches
Pasture	0.20 inches

Forest litter 0.30 inches
Table 19. Depression storage from SWMM User manual (Rossman, 2015).

Soil Properties

Soil parameter values used for Green-Ampt infiltration formula are as follows:

Soil type	Porosity	Effective porosity	Suction head (mm)	Hydraulic Conductivity (mm/hr)
Sand	0.437	0.417	49.5	117.8
Loamy Sand	0.437	0.401	61.3	29.9
Sandy Loam	0.453	0.412	110.1	10.9
Loam	0.463	0.434	88.9	3.4
Silt Loam	0.501	0.486	166.8	6.5
Sandy Clay loam	0.398	0.330	218.5	1.5
Clay loam	0.464	0.309	208.8	1.0
Silty clay loam	0.471	0.432	273.0	1.0
Sandy clay	0.430	0.321	239.0	0.6
Silty clay	0.479	0.423	292.2	0.5
Clay	0.475	0.385	316.3	0.3

Table 20. Soil Parameter values (Rawls et al., 1983).

Channel Roughness

Channel Type	Manning n
Lined Channels	
- Asphalt	0.013 - 0.017
- Brick	0.012 - 0.018
- Concrete	0.011 - 0.020
- Rubble or riprap	0.020 - 0.035
- Vegetal	0.030 - 0.40
Excavated or dredged	
- Earth, straight and uniform	0.020 - 0.030
- Earth, winding, fairly uniform	0.025 - 0.040
- Rock	0.030 - 0.045
- Unmaintained	0.050 - 0.140
Natural channels (minor streams, top width at flood stage < 100 ft.)	
- Fairly regular section	0.030 - 0.070
- Irregular section with pools	0.040 - 0.100

Table 21. Manning's n for Open Channel (Rossman, 2015).

2. For coastal and inland flood model components, describe the dependencies among flood model parameters and specify any assumed mathematical dependencies among these parameters.

The parameters used in the coastal surge model are from previous independent literatures.

The inland flood models were parameterized based on the guidelines of SWMM reference manual and scientific literatures.

3. For coastal and inland flood model components, describe the dependencies that exist among the flood model components.

There is no direct interaction between coastal and inland flood model components. The coastal and inland flood model components are performed at different platforms and grids. If the same locations are both flooded by coastal and inland components, the maximum inundation depth will be used.

Wave properties do not affect wind, surge, or inland flood properties. Wave properties rely on surge levels, local bathymetry and topography, winds, and land cover.

The inland flood and coastal flood models are independent models. No dependencies exist between the coastal and inland flood model components.

4. Identify whether physical flood parameters are modeled as random variables, functions, or fixed values for the stochastic flood event generation. Provide rationale for the choice of parameter representations.

All the coastal surge model parameters are from scientific literatures and technical reports. There are almost fixed values, or calculated from equations presented in the previous literatures. All the values and equations are presented in Section GF-1, MF-1, and MF-2.

The inland flood model parameters are fixed values for the stochastic flood event generation. We introduced stochastic rainfall events as an input to the inland flood model to generate the stochastic flood events.

5. Describe if and how any physical flood parameters are treated differently in the historical and stochastic flood event sets, and provide rationale.

In the flood models the same physical parameters were used for the historical and stochastic flood events.

6. If there is explicit modeling of precipitation-driven flooding, then describe how rainfall extent, duration, and rate are modeled. If the effects of precipitation are implicitly incorporated into the flood model, describe the method and implementation.

The rain model uses the R-CLIPER rain algorithm which determines the rainfall extent and rain rate for a target location. Rainfall duration is included since the rain model incorporates track

motion information obtained from the input track file. More details on the rain model can be found in Standard GF-1.2.

7. For coastal flood analyses, describe how the coastline is segmented (or partitioned) in determining the parameters for flood frequency used in the flood model.

There are totally 4 set of basins established for the storm surge simulation covering the whole coastal area of Florida (Figure 30).

1. Apalachicola Bay basin, AP8, majorly covers the north and west Florida coastal areas;
2. Tampa Bay basin, TP3, covers the west Florida coastal area;
3. South Florida basin, HMI41, majorly covers the south Florida coastal area and Keys;
4. Florida Atlantic basin, EJX5, covers the whole east Florida coastal area.

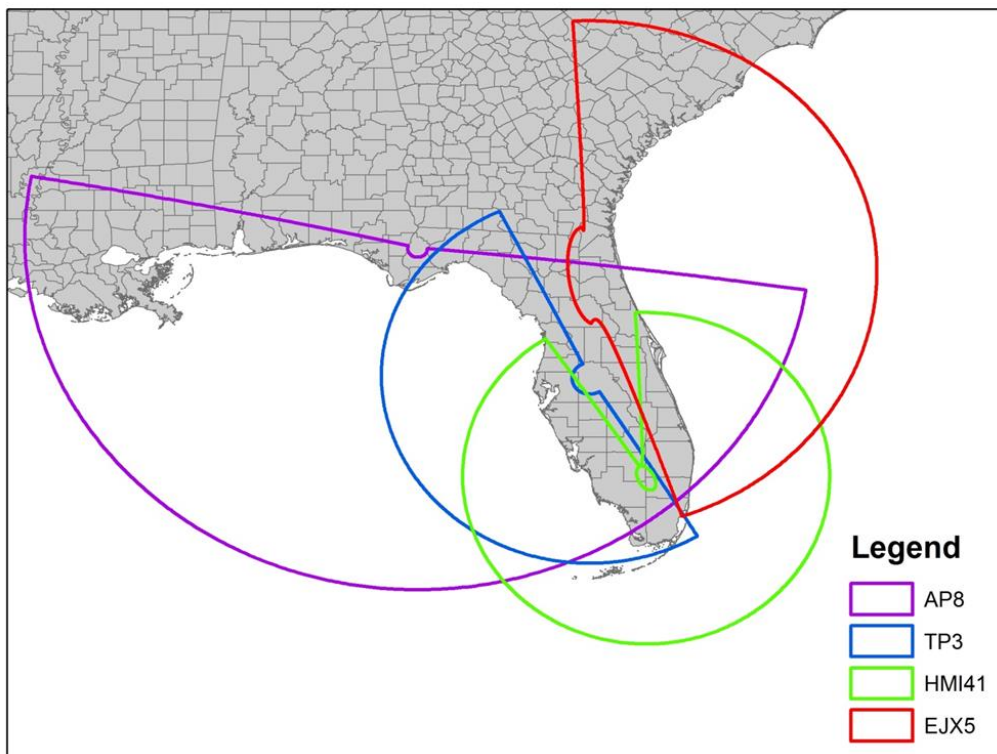


Figure 30. Four Florida Basins that used by CEST Model.

The overlap area of the above four set basins is relatively large, sometime even half of the basin area. The reason is consideration between large domain size and fine resolution of the grid for the interesting area.

For the wave model, 116 subgrids were partitioned around the state in areas likely to be impacted by wave action, including open coasts, inlets, bays, and wetlands. Areas not likely impacted by substantial wave action were not modeled for waves.

8. For coastal flooding, describe how astronomical tides are incorporated and combined with storm surge to obtain storm tide.

In the tide simulation, a Dirichlet-type (clamped) condition is generally used at the open boundary, where the surface elevation is set to the specific known value as follows:

$$\zeta = \widehat{\zeta}$$

where $\widehat{\zeta}$ is elevation specified at the open boundary.

In case of including astronomical tide simulation, initial transients are damped by bottom friction and there are no internal flows driven by atmospheric or wind forcing (Bills, 1991). As an open boundary condition for tide elevation, the equilibrium tidal potential is expressed as follows (Reid,1990):

$$\zeta(\phi, \lambda, t) = \sum_{n,j} C_{jn} f_{jn}(t_0) L_j(\phi) \cos \left[\frac{2\pi(t-t_0)}{T_{jn}} + j\lambda + v_{jn}(t_0) \right]$$

where t is time relative to t_0 (the reference time),

C_{jn} is a constant characterizing the amplitude of a tidal constituent n of species j,

f_{jn} is the time-dependent nodal factor,

v_{jn} is the time-dependent astronomical argument,

j = 0, 1, 2 are the tidal species (j=0 declinational; j=1 diurnal, j=2 semidiurnal),

$$L_0 = 3 \sin^2 \phi, L_1 = \sin(2\phi), L_2 = \cos^2 \phi$$

T_{jn} is the period of a constituent n for species j.

At the open boundaries, the tidal elevation generated by seven constituents (M2, S2, N2, K1, O1, K2, and Q1) are specified.

9. Describe if and how any flood parameters change or evolve during an individual flood life cycle (e.g., astronomical tide, representation of Manning's roughness varying with flood depth).

For the coastal flooding model, during an individual flood life cycle, the inundation depth changes with surge propagate on the land. To account for the terrain effect on the wind, two different drag coefficients are used to compute the wind field on the terrain and extreme shallow waters and the wind field on the ocean, which are referred to as lake wind and ocean wind, respectively. The effects of vegetation on the wind field have also been accounted for in a way similar to the SLOSH model (Jelesnianski et al. 1992). The wind speed is adjusted using a coefficient C_T based on the ratio of the surge water depth ($D=H+\zeta$) to the vegetation height (H_T):

$$C_T = \begin{cases} \frac{D}{H_T} & D < H_T \\ 1 & D \geq H_T \end{cases}$$

The effect of trees on the wind speed decreases based on this equation as the water submerges the vegetation gradually. In this study, the land areas covered by dense vegetation and development were classified into the "Tree" category and assigned an average vegetation height of 8 m, the same as the one used by SLOSH for the Florida basins. When a storm surge floods low-lying areas, it often forms a thin layer of water over land. An extinction coefficient C_E is applied to the wind speed to reduce its effect on the thin layer of water (Jelesnianski et al. 1992).

$$C_E = \begin{cases} \frac{D}{0.3} & D < 0.3 \text{ m} \\ 1 & D \geq 0.3 \text{ m} \end{cases}$$

The flood parameters used in the wave model do not evolve or change over any surge event.

Inland flood model physical parameters are assigned as fixed values throughout the simulation periods of the flood events. Therefore, flood parameters don not change or evolve during the life cycle of an individual flood event.

10. For coastal modeling, describe any wave assumptions, calculations or proxies and their impact on flood elevations.

Waves at the offshore boundary are assumed to be a steady-state snapshot at the time of max surge, or max wind, so that more tractable systems can be solved. Wave heights at the offshore boundary (usually several km offshore) are computed from depth-dependent hindcasts using analytic wind-wave relations of Young and Verhagen (1996, [Coastal Engineering](#) 27(1-2):47-78) Wave setup is computed as a fixed fraction (0.1) of the significant wave height at the offshore boundary. Wave transformation in the nearshore and overland is computed for directional waves but with one frequency only to keep run times tractable. Wave heights around the insured are largely depth-limited and depend much more on the local flooded water depths.

11. Provide the source, resolution, datum, and accuracy of the topography and bathymetry throughout the flood model domain.

The elevation of a CEST grid cell was calculated by averaging the pixel elevations of the digital bathymetric and topographic elevation models which are falling within the grid cell. All the topographic and bathymetric data were adjusted to NAVD 88 vertical datum before calculation. The following procedure was used to calculate the grid cell elevation and handle the overlaps between different bathymetric and topographic datasets.

(1) NOAA ETOPO1 global relief dataset was used to calculate the cell elevations of the model grid. In the deep ocean area that is covered by ETOPO1, but not covered by the bathymetric and topographic data with finer resolutions, a grid cell should include at least one data point from ETOPO1 for elevation calculation. If not, a new relief dataset with a pixel size of half the ETOPO1 pixel size was generated by interpolating ETOPO1 using the nearest neighbor method. The

interpolation was conducted continuously by reducing the pixel size half every time until each grid cell in the deep ocean contains at least one data point from the interpolated relief dataset.

(2) NOAA coastal relief dataset was used to calculate the cell elevations and replace the elevations from ETOPO1 in the continental shelf and coastal areas. If the cell size of a model grid is less than the pixel size of the coastal relief dataset. The new coastal relief dataset was generated for the calculation of the grid cell elevation using the same procedure to interpolating the ETOPO1 dataset.

(3) USGS 90 m, 30 m, 10 m, and 3 m DEMs were used to calculate the elevations of the model grid cells on the land. The model grid cells on the land and on the ocean were separated using the shoreline dataset extracted from the LiDAR surveys or digitized from the aerial photographs. The selection of 90 m, 30 m, 10 m, and 3 m DEMs were determined by the cell size of a model grid. A grid cell has to contain at least one data point from the DEM dataset used for the elevation calculation.

(4) NOAA integrated models of coastal reliefs were used to calculate and replace the depths of the grid cells in the coastal water. If the USGS DEMs on the land is older than the elevation data in the integrated model of coastal relief, the elevations of the grid cell on the land were also calculated and replaced.

(5) The water depths and elevations of the grid cell were updated using the most recent data which are often the LiDAR surveys provided by local government agencies through the flood map modernization program sponsored by the Federal Emergency Management Agency.

The high-quality shoreline dataset including the boundaries of the coastal lagoons, inlets, and barrier islands, and river streams is essential for separating the grid cells on the land and the ocean and preserving the connectivity of the coastal hydrological features. Fortunately, the digital shorelines can be extracted from the LiDAR surveys for coastal areas vulnerable to storm surge flooding in Florida.

Two major sources of bathymetry and topography data are used for wave grids. For bathymetry, The National Centers for Environmental Information (NCEI) 3 arc second data (~90 meter resolution) coastal relief model is used, with sea level datum converted to NAVD88 and NAD83 horizontal datum. For topography above sea level, the United States Geological Survey National Elevation Dataset 1/3 arc second (~10 meter resolution) is used with NAVD88 vertical datum and NAD83 horizontal datum. Both sources are interpolated to create wave grids.

The details of topography dataset are provided below for the inland flood model:

Source: USGS National Elevation Dataset (NED)

Horizontal Resolution: 1/3-arc-second DEM has a ground spacing of approximately 10 meters north-south, but the spacing varies towards east-west direction depending on the latitude.

Datum: North American Datum of 1983 (NAD 1983)

Horizontal Accuracy: In most cases, the horizontal accuracy of seamless DEM coverage produced from 3DEP technologies is expected to be 1 meter or better (Gesch et al., 2014).

Vertical Datum: North American Vertical Datum of 1988 (NAVD 1988).

Vertical Accuracy: The relative vertical accuracy of the 1/3-arc-second DEM dataset is 0.81 meter (Gesch et al., 2014).

The surveyed bathymetry of the canals and rivers were obtained from the South Florida Water Management District (SFWMD), Southwest Florida Water Management District (SWFWMD) and St Johns River Water Management District (SJRWMD). If surveyed bathymetry data were unavailable, we used NED data to extract the river cross-sections. The North American Vertical Datum of 1988 (NAVD1988) was used as the reference datum for the bathymetry data throughout the inland flood models.

12. Describe the grid geometry used in the coastal flood model.

There are 4 sets of basins are established for coastal surge model,

- a) Apalachicola Bay basins including AP7, AP8, and AP9,
- b) Miami and Key basins including HMI4, HMI41, and HMI42,
- c) Tampa bay basins including TP2, TP3, and TP4,
- d) Jacksonville basins including EJX4, EJX5, and EJX6.

For each basin, at least three grids were established with same cover area but with fine, medium, and coarse size of grid cell. The purpose for these three different resolution basins is to consider the consummation of the computational time.

Apalachicola Bay basins including AP7, AP8, and AP9

The AP8 and AP9 are the new generated basins with the same semi-circle domain as AP7, which cover the all the north and west coastal area of Florida. The grid cell resolution for AP7, AP8, and AP9 is about 100, 350, and 1400 meters respectively along the coastal area (Table 22). The computational time for coarse resolution basin AP9 is only 0.5-1 minutes for a 4-days simulation, whereas AP8 and AP7 consume about 10-15 minutes and 2 hours to complete the same run, respectively.

Basin Name	AP7	AP8	AP9
Domain Description	CEST Basin	CEST Basin	CEST Basin
Size	Large	Large	Large
Resolution (m)*	100	350	1400
Dimension	772*710	387*356	99*91
Total Number of Cells	548,120	137,772	9,009
Time Step (s)	30	20	30

Computation Time* of 4 days (minutes)	120-130	10-15	0.5-1
---------------------------------------	---------	-------	-------

Table 22. Basin description and statistics for Apalachicola Bay.

* The resolution of the model basin varies spatially. The resolution in the table represents the approximate edge size of a grid cell at the coastal area.

* Computational time was derived by recording the simulation time using a single processor in a Dell PC workstation with four 2.5 GHZ Intel Xeon processors and 12GB of RAM.

Miami and Key basins including HMI4, HMI41, and HMI42

The HMI4, HMI41, and HMI42 with the same circle domain cover the all the south coastal area of Florida with a grid cell resolution about 1,000, 300, and 150 meters respectively along the coastal area (Table 23). The coarse resolution grid HMI4 only takes 5-7 minutes to finish a 4-days simulation, whereas HMI41 and HMI42 consume around 25 minutes and 2 hours to complete the same run.

Basin Name	HMI4	HMI41	HMI42
Domain Description	CEST Basin	CEST Basin	CEST Basin
Size	Large	Large	Large
Resolution (m)	1000	300	150
Dimension	185*395	332*480	442*1216
Total Number of Cells	73,075	159,360	513,152
Time Step (s)	30	30	30
Computation Time of 4 days (minutes)	5-7	20-25	110-130

Table 23. Basin description for Miami and Key.

Tampa bay basins including TP2, TP3, and TP4

The TP2, TP3, and TP4 with the same semi-circle domain cover the all the west coastal area of Florida with grid cell resolution about 1,800, 450, and 230 meters respectively along the coastal area (Table 24). The computational time for coarse resolution basin TP2 is only 1 minutes for a 4-days simulation, whereas TP3 and TP4 consume about 10 minutes and 1 hour to complete the same run.

Basin Name	TP2	TP3	TP4
Domain Description	CEST Basin	CEST Basin	CEST Basin
Size	Large	Large	Large
Resolution (m)*	1800	450	230
Dimension	80*106	314*418	626*834
Total Number of Cells	8,480	131,252	522,084
Time Step (s)	30	30	30
Computation Time* of 4 days (minutes)	0.5-1	9-12	50-70

Table 24. Basin description and statistics for Tampa Bay.

Jacksonville basins including EJX4, EJX5, and EJX6

The EJX4, EJX5, and EJX6 with the same semi-circle domain cover the all the eastern coastal area of Florida with an area of 351,370 km² and a grid cell resolution about 2500, 600, and 300 meters respectively along the coastal area (Table 25). The computational time for coarse resolution basin EJX4 is only 1-2 minutes for a 4-days simulation, whereas EJX5 and EJX6 consume about 20 minutes and 2 hours to complete the same run.

Basin Name	EJX4	EJX5	EJX6
Domain Description	CEST Basin	CEST Basin	CEST Basin
Size	Large	Large	Large
Resolution (m)*	2500	600	300
Dimension	104*106	410*418	818*834
Total Number of Cells	11,024	171,380	682,212
Time Step (s)	30	30	10
Computation Time* of 4 days (minutes)	1-2	15-20	120-160

Table 25. Basin description and statistics for Jacksonville.

The wave model used 116 separate regular 40m grids of varying coverage that together cover all relevant nearshore areas.

MF-3 Wind and Pressure Fields for Storm Surge

A. Modeling of wind and pressure fields shall be employed to drive storm surge models due to tropical cyclones.

The wind and pressure fields for tropical cyclones are modeled and are used to drive the storm surge models.

B. The wind and pressure fields shall be based on current scientific and technical literature or developed using scientifically defensible methods.

The wind and pressure fields are based on methods that are published in accepted scientific and technical literature.

C. The modeling of wind and pressure fields that drive coastal flood models shall be conducted over a sufficiently large domain that storm surge height is converged.

Tests were performed with varying domain sizes to ensure convergence is achieved for storm surge height.

D. The features of modeled wind and pressure fields shall be consistent with those of historical storms affecting Florida.

The wind and pressure fields are consistent with historical storms affecting Florida.

Disclosures

1. Describe the modeling of the wind and pressure fields for tropical cyclones. State and justify the choice of the parametric forms and the parameter values.

The wind model and simulated pressure fields are described in Standard GF-1.2. A description and justification of the parameters used in the model are described below.

Tropical cyclone parameters used in the model include storm track (translation speed and direction of the storm), radius of maximum wind (R_{max}), Holland surface pressure profile parameter (B), the minimum central sea level pressure (P_{min}), and the pressure decay as a function of time after landfall.

The storm initial position and motion are modeled using the HURDAT2 database. Initial storm positions and motion changes derived from HURDAT2 are modified by the addition of small uniform random error terms. Subsequent storm motion change and intensity are obtained by sampling from empirically derived PDFs as described in Standard GF-1.2.

For pressure decay we use the Vickery (2005) decay model. Vickery developed the model on the basis of pressure observations in HURDAT and NWS-38 (Ho et al., 1987), together with R_{max} and storm motion data as described in the publication.

The radius of maximum winds at landfall is modeled by fitting a gamma distribution to a comprehensive set of historical data published in NWS-38 by Ho et al. (1987) and supplemented by the extended best track data of DeMaria (Pennington et al., 2000), the HURDAT Reanalysis Project (Landsea et al., 2004), NOAA HRD research flight data, and NOAA-AOML-HRD H*Wind analyses (Powell & Houston, 1996; Powell et al., 1996; Powell & Houston, 1998; Powell et al., 1998).

Additional research was used to construct a historical landfall R_{max} - P_{min} database using existing literature (Ho et al., 1987), extended best track data, HRD Hurricane field program data, and the H*Wind wind analysis archive (Demuth et al., 2006). We developed an R_{max} model using the compiled landfall R_{max} database, which includes more than 100 measurements for hurricanes up to 2012. We have opted to model the R_{max} at landfall rather than the entire basin for a variety of reasons. One is that the distribution of landfall R_{max} may be different than that over open water. An analysis of the landfall R_{max} database and the 1988–2007 extended best track data shows that there appears to be a difference in the dependence of R_{max} on central pressure (P_{min}) between the two datasets (Demuth et al., 2006). The landfall dataset provides a larger set of independent measurements (more than 100 storms compared to about 31 storms affecting the Florida threat area region in the best track data). Since landfall R_{max} is most relevant for loss cost estimation and has a larger independent sample size, we have chosen to model the landfall dataset. Since R_{max} is nonnegative and skewed, we model the distribution using a gamma distribution. As described in Standard GF-1.2, the maximum likelihood estimates of the parameters of the gamma distribution were obtained and was found to be a good fit.

Recent research results by Willoughby and Rahn (2004) based on the NOAA-AOML-HRD annual hurricane field program and Air Force reconnaissance flight-level observations are used to create a model for the “Holland B ” parameter. Ongoing research on the relationship between horizontal surface wind distributions (based on Stepped Frequency Microwave Radiometer observations) to flight level distributions (Powell et al., 2009) is used to correct the flight-level R_{max} to a surface R_{max} when developing a relationship for the Holland B term. We multiply the flight-level R_{max} from the Willoughby and Rahn (2004) dataset by 0.815 to estimate the surface R_{max} (based on SFMR, flight-level maxima pair data). This adjustment keeps the Holland pressure profile parameter consistent with a surface R_{max} and because of the negative term in the equation produces a larger value of B than if a flight-level value of R_{max} were used. This is consistent with the concept of a stronger radial pressure gradient for the mean boundary layer slab than at flight level (due to the warm core of the storm), which agrees with GPS dropsonde wind profile observations showing boundary layer winds that are stronger than those at the 10,000 ft flight level, which is the level for most of the B data in Willoughby and Rahn (2004). The B adjustment for a surface R_{max} produces an overall stronger surface wind field than if B were not adjusted. In addition, surface pressures from the “best track” information on HURDAT are used to associate a particular flight-level pressure profile B with a surface pressure. A regression model for B was obtained as described in Standard GF-1.2. The random error term for the B parameter is modeled

a normal distribution with zero mean. A comparison of modeled and fitted values of B can be found in Standard GF-1.2.

HRD wind modeling research initiated by Ooyama (1969) and extended by Shapiro (1983) has been used to develop the HRD wind field model. This model is based on the concept of a slab boundary layer model, a concept pioneered at NOAA-AOML-HRD and now in use by other modelers for risk applications (Thompson & Cardone, 1996; Vickery & Twisdale, 1995; Vickery et al., 2000b). The HURDAT2 historical database is used to develop the track and intensity model. Historical data used for computing the potential intensity is based on the National Centers for Environmental Prediction (NCEP) sea surface temperature archives and the NCEP reanalysis for determining the upper tropospheric outflow temperatures. Monthly geographic distributions of climatological sea surface temperatures (Reynolds et al., 2002) and upper tropospheric outflow temperatures (Kanamitsu et al., 2002) are used to determine physically realistic potential intensities that help to bound the modeled intensity.

2. Provide the historical data used to estimate parameters and to develop stochastic storm sets.

The historical data used to estimate parameters and develop stochastic storm sets are provided in the previous disclosure. For the current version of the flood model, the version of HURDAT2 that was used is the May 1, 2018 version.

3. Provide a rotational (y-axis) versus radial (x-axis) plot of the average or default wind and pressure fields for tropical cyclones. Provide such plots for non-tropical cyclones, if non-tropical cyclones are modeled explicitly.

See Figure 31 and Figure 32.

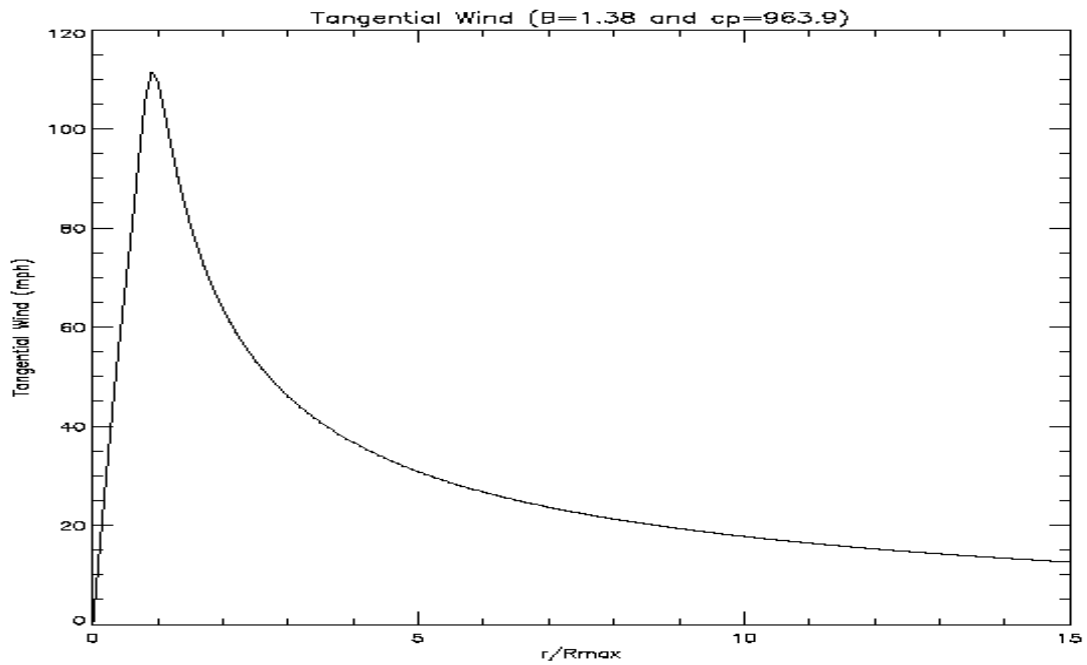


Figure 31. Axisymmetric rotational wind speed (mph) vs. scaled radius for B = 1.38, DelP = 49.1 mb.

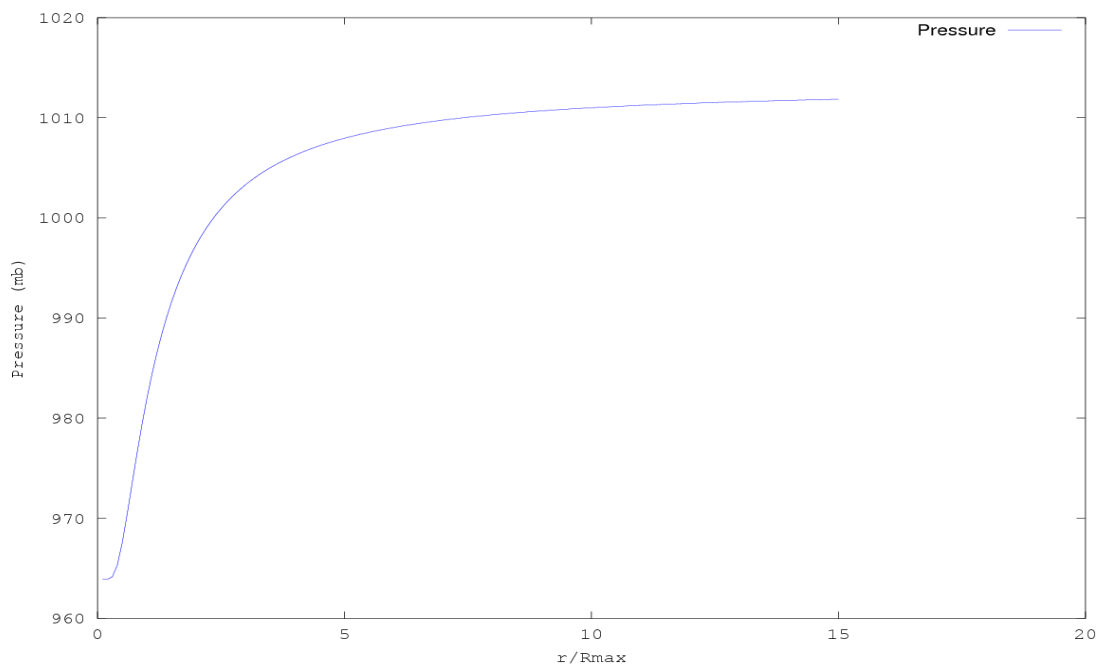


Figure 32. Plot of pressure profile corresponding to the parameters used in the previous figure.

4. If windfields are modeled above the surface and translated to the surface to drive storm surge, then describe this translation; e.g., via planetary boundary layer models or empirical surface wind reduction factors and inflow angles. Discuss the associated uncertainties.

The windfield is not modeled above the surface, but as a mean slab surface layer. The conversion of the mean layer wind to the 10 m wind, and associated uncertainties for the conversion, are described below.

The mean boundary layer winds computed by the model are adjusted to the surface using results from Powell et al. (2003), which estimated a mean surface wind factor of 77.5% on the basis of over 300 GPS sonde wind profile observations in hurricanes. The surface wind factor is based on the ratio of the surface wind speed at 10 m to the mean wind speed for the 0–500 m layer (mean boundary layer wind speed or MBL) published in Powell et al. (2003). This ratio is far more relevant to a slab boundary layer model than using data based on higher, reconnaissance aircraft flight levels. The depth of the slab boundary layer model is assigned a value of 450 m, which is the level of the maximum mean wind speed from GPS sonde wind profiles published in Powell et al. (2003). The uncertainty of the surface wind factor is ~8%, based on the standard deviation of the measurements, but no attempt is made to model this uncertainty. No radial distance from center or intensity dependent variation of reduction factor is used at this time because of a lack of dependency on these quantities based on examination of GPS dropsonde data (see Figure 33).

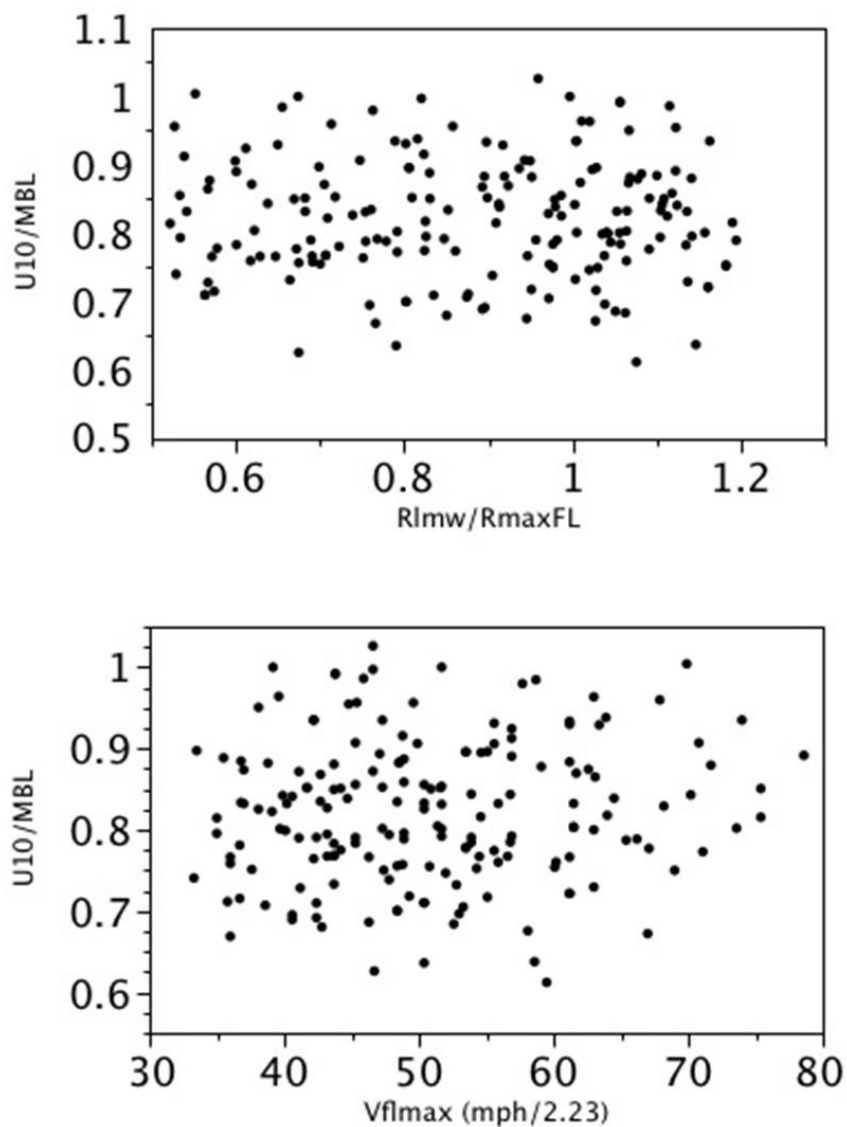


Figure 33. Analysis of 742 GPS dropsonde profiles launched from 2-4 km with flight-level winds at launch greater than hurricane force and with measured surface winds. Upper figure: Dependence of the ratio of 10 m wind speed (U10) to the mean boundary layer wind speed (MBL) on the scaled radius (ratio of radius of last measured wind (Rlmw) to the radius of maximum wind at flight level (RmaxFL)). Lower figure: Surface wind factor (U10/MBL) dependence on maximum flight level wind speed (Vflmax, in units of miles per hour / 2.23).

5. Describe how storm translation is accounted for when computing surface windfields.

The incorporation of storm translation in the wind model is described in Standard GF-1.2.

6. Describe how storm surge due to non-tropical cyclones is accounted for in the flood model. If it is not accounted for, explain why.

Non-tropical cyclones are currently not accounted for in the model. There is only one non-tropical event that has produced potentially significant storm surge in Florida in recorded history, the so-called “Storm of the Century” in March, 1993. An examination of NFIP claims data reveal that the cause of loss, whether surge versus accumulation of rainfall, is highly unreliable. Thus we do not have sufficient or reliable data to attempt to model non-tropical cyclone surge events or even assess whether those losses might be associated with surge only. In addition, we have examined inundation estimates from SLOSH Maximum of Maximums (MoM) simulation output from NHC combined with high resolution LIDAR DEM data (a detailed data set provided by the Florida Division of Emergency Management), and found that there are very few locations in Florida that are susceptible to flood due to surge for tropical cyclones below hurricane strength. Since non-tropical cyclones in Florida are generally much weaker than hurricanes, we cannot conclude that there will be significant surge due to non-tropical events.

7. Describe and justify the averaging time of the windspeeds used to drive the storm surge model.

The wind fields generated by the wind model are assumed to be 10 minute averaged winds. The wind model does not incorporate the effects of short gusts or other transitory turbulence, so shorter averaging times would not be appropriate for representing the wind field. For longer averaging times, the effects of storm motion would impact the wind speeds and thus not be appropriate.

8. Describe the process for verifying storm surge height convergence as a function of domain size.

In order to verify the storm surge height convergence as different domain sizes, two basins, HGL and AP, with larger sizes were generated to simulate Hurricane Ike, Ivan, and Dennis (Figure 34 and Figure 35). The purpose of these two large domains is to further examine the effect of domain size on computing storm surge. The extra-large domain EGM3 is the largest domain for Gulf of Mexico (Figure 36).

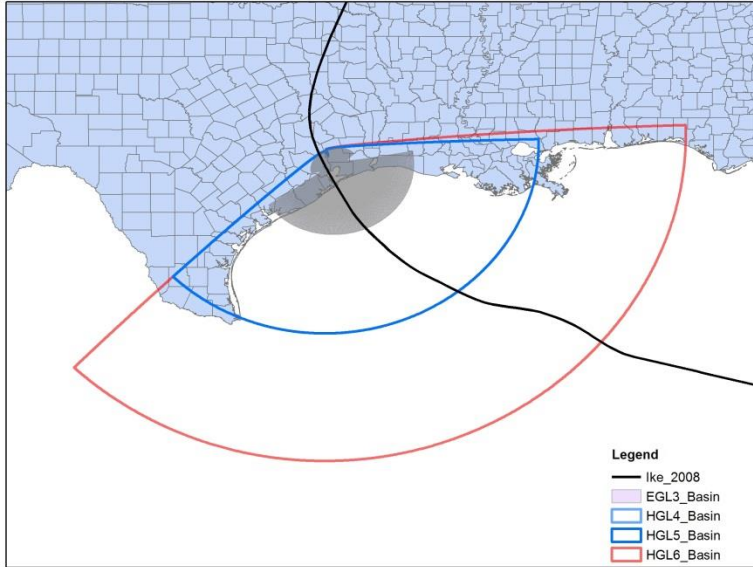


Figure 34. Location of EGL3, HGL4, HGL5, and HGL6 basins for Hurricane Ike.

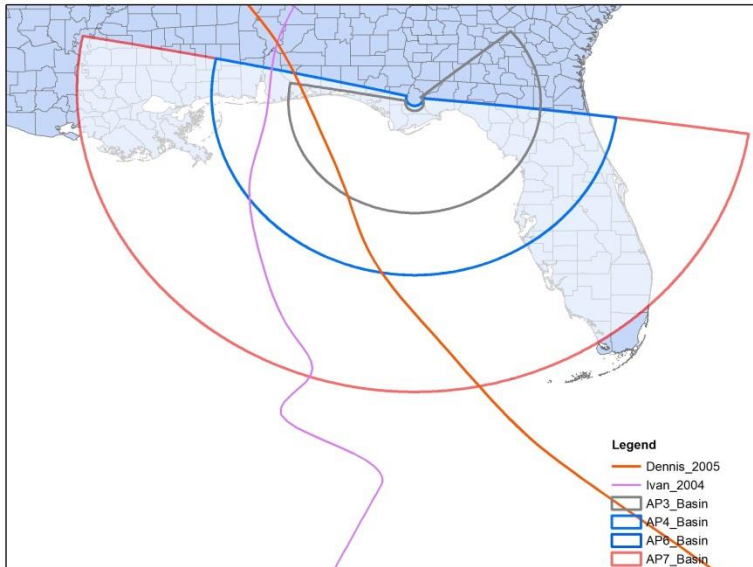


Figure 35. Location of AP3, AP4, AP6, and AP7 basins for Hurricanes Ivan and Dennis.

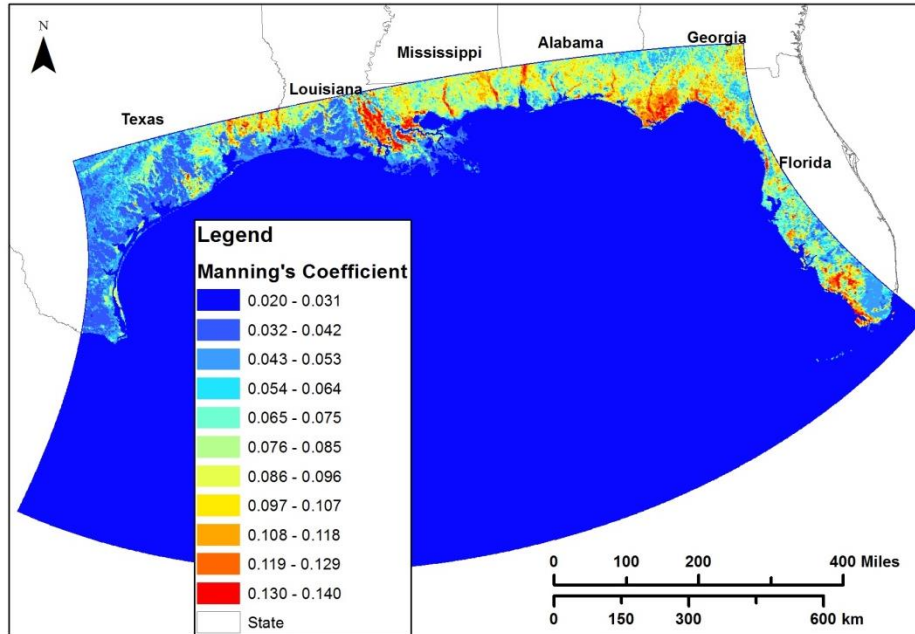


Figure 36. Extra Large domain EGM3 with Manning Coefficient.

Figure 34 Shows the domain size for the new generated basin HGL6 for Hurricane Ike with EGL3, HGL4, and HGL5 basins. The HGL6 basin spans the whole Texas coast and west coast of Florida, covering 682,000 km² and with an averaged cell size of 200 m on the land. The HGL6 basin covers much more area than the HGL5, but with the same resolution of HGL5 (Table 26).

Comparison of observed and computed storm tides of Hurricane Ike indicates that the HGL6 basin produces storm surge agreeing better with observations than other basins (Figure 37 and Figure 38). The largest EGM3 basin over-predicts peak storm tides at stations Galveston Bay Entrance, Galveston Pier 21, Y, W, and Z. The HGL6 basin generates better peak storm surges at the above 5 stations. The shape of storm tide from HGL6 is also comparable with the shape of observed storm tide. The largest basin EGM3, the large basin HGL6, and intermediate size basins HGL4 and HGL5 capture the forerunners from IKE, thus, produce storm tides matching better with field observations. It appears that the high-resolution HGL6 produces the storm tide which agrees with observed storm tide best (Table 26).

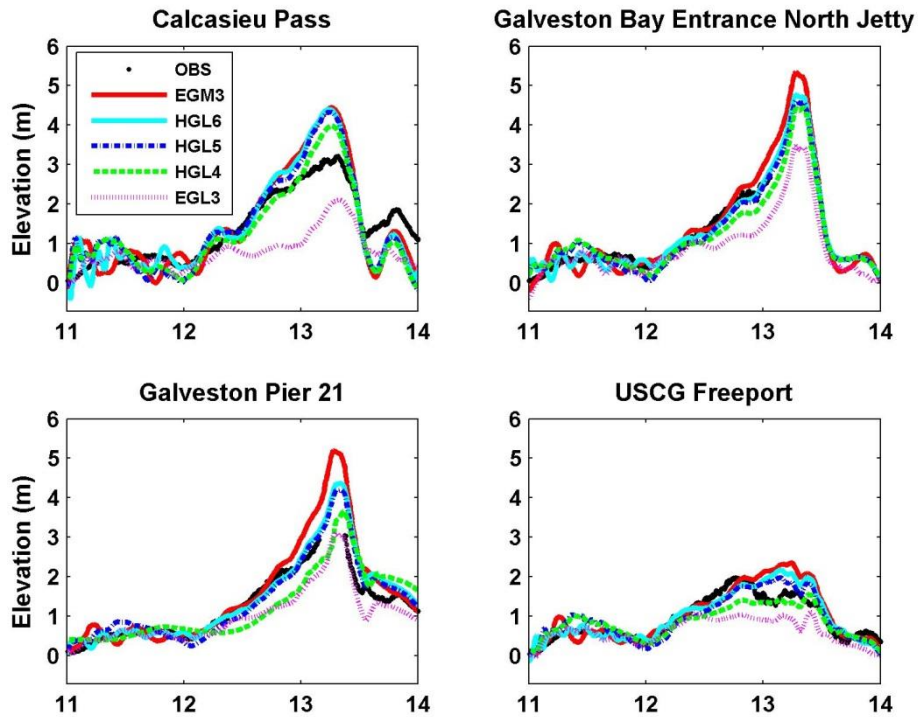


Figure 37. Observed and computed water levels at 4 NOAA tide gauges.

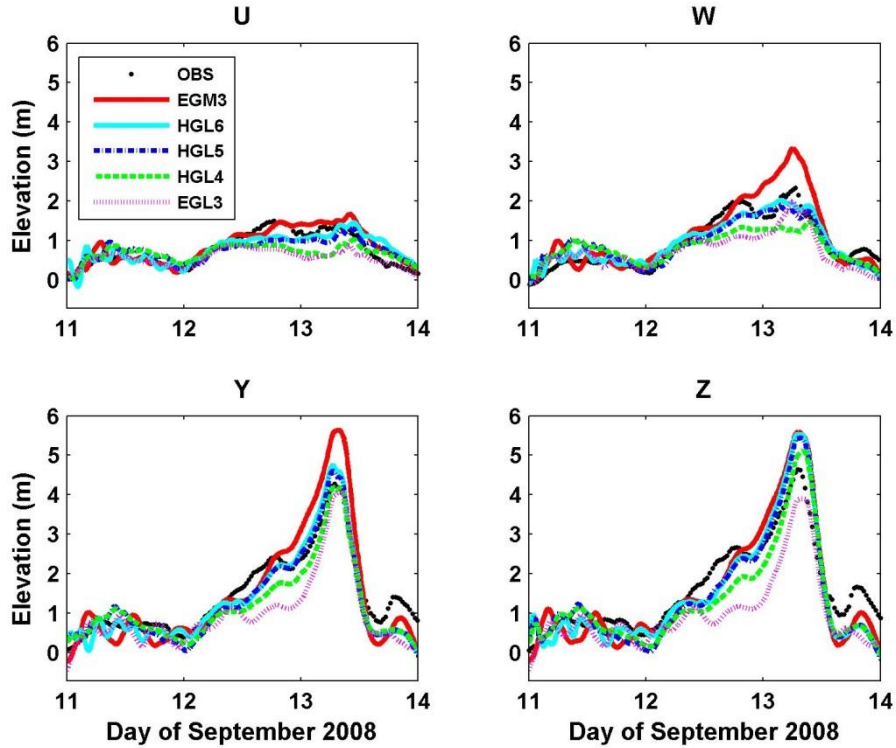


Figure 38. Observed and computed water levels at 4 stations established by Kennedy (replace with u, w, y, z).

Basin Name	EGL3	HGL4	HGL5	HGL6	EGL3
Description	SLOSH Basin	CEST Basin	CEST Basin	CEST Basin	SLOSH Basin
Size	Small	Medium	Medium	Large	Extra Large
Resolution (m)*	700	1,200	200	200	2,700
Dimension	243*192	251*172	998*682	1143*694	329*569
Total Number of Cells	46,656	43,172	680,636	793,242	187,201
Time Step (s)	30	30	30	30	30
Computation Time* of 4 days (minutes)	3-5	3-4	105-120	170-180	38-45
RMSD (m, Andrew)	0.69	0.54	0.41	0.41	0.42
RMSD (m, NOAA)	0.70	0.46	0.42	0.40	0.37

Table 26. Basin description for Hurricane Ike with additional large Basin HGL6.

Figure 35 Shows the domain size for the new generated basin AP7 with AP3, AP4, and AP6 basins. The AP7 basin spans the almost whole Florida coast and west coast of Louisiana, covering 564,000 km² and with an averaged cell size of 200 m on the land. The AP7 basin covers a larger area than the AP6, but with the same resolution (Table 27, Table 28).

Comparison of observed and computed storm tides of Hurricane Ivan indicates that the peak storm tides from AP7 have the best agreement with the observed ones at all stations (Figure 39). The shapes of storm tides from AP7 are most similar to the shapes of observed ones.

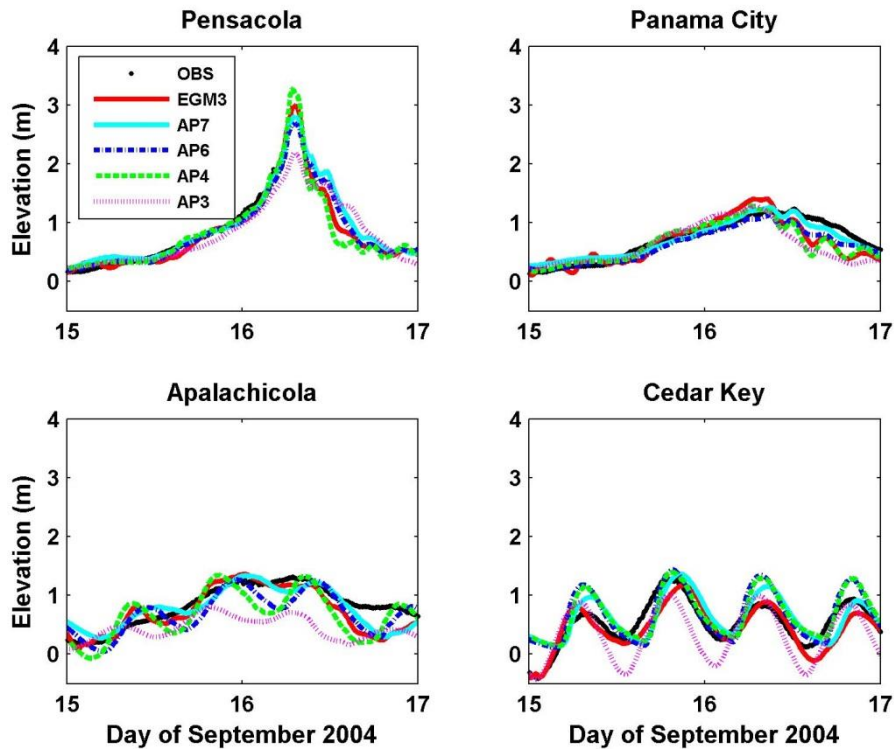


Figure 39. Computed peak storm tide heights for Hurricane Ivan.

Basin Name	AP3	AP4	AP6	AP7	EGM3
Description	SLOSH Basin	CEST Basin	CEST Basin	CEST Basin	SLOSH Basin
Size	Small	Medium	Medium	Large	Extra Large
Resolution (m)*	400	400	100	100	2,700
Dimension	142*226	167*179	662*710	772*710	329*569
Total Number of Cells	32,092	29,893	470,020	548,120	187,201
Time Step (s)	30	30	30	30	30
Computation Time* of 4 days (minutes)	2-3	3-5	92-100	120-130	46-50
RMSD (m, NOAA)	0.36	0.25	0.21	0.17	0.19

Table 27. Basin description for Hurricane Ivan with additional large Basin AP7.

Comparison of observed and computed storm tides of Hurricane Dennis indicates that the peak storm tides from AP7 have the best agreement with the observed ones for stations Pensacola, Panama City, and Apalachicola (Figure 40 and Table 28). The shapes of storm tides from AP7 are most similar to the shapes of observed ones. The difference between computed and observed storm tides at Cedar Key is relatively large, probably due to the complicated bathymetry around this station. There is a possibility to improve the simulation through adjustment of topographic and bathymetric data around this area.

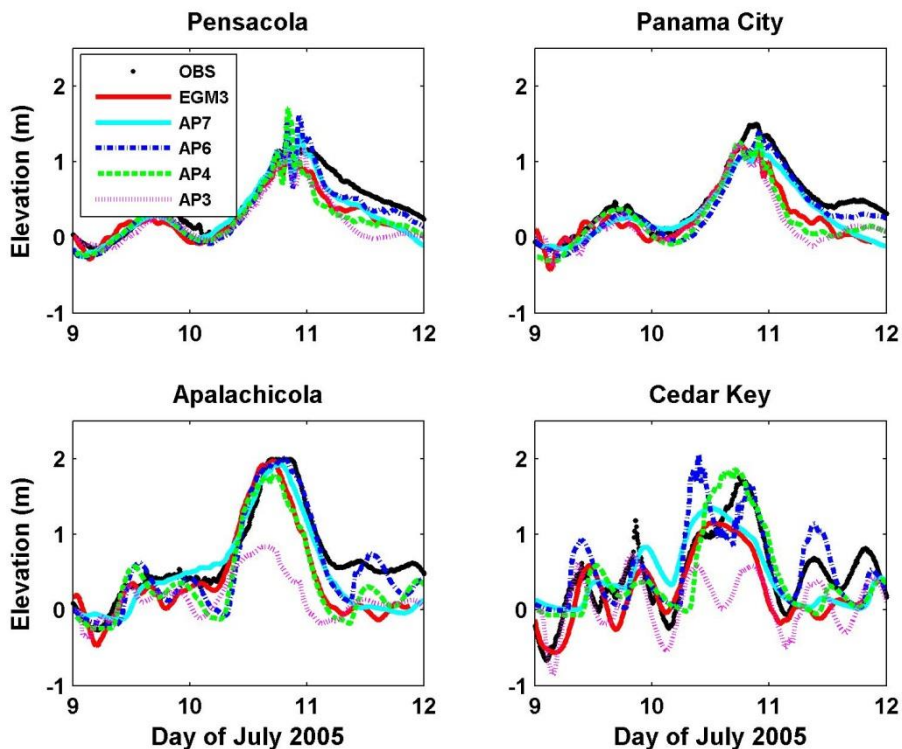


Figure 40. Computed peak storm tide heights for Hurricane Dennis.

Basin Name	AP3	AP4	AP6	AP7	EGM3
Description	SLOSH Basin	CEST Basin	CEST Basin	CEST Basin	SLOSH Basin
Size	Small	Medium	Medium	Large	Extra Large
Resolution (m)	400	400	100	100	2,700
Dimension	142*226	167*179	662*710	772*710	329*569
Total Number of Cells	32,092	29,893	470,020	548,120	187,201
Time Step (s)	30	30	30	30	30
Computation Time of 4 days (minutes)	2-3	3-4	85-95	110-120	35-40
RMSD (m, NOAA)	0.39	0.27	0.25	0.22	0.27

Table 28. Basin description for Hurricane Dennis with additional large Basin AP7.

The effect of the basin size on storm tide computation is examined by two new large basins HGL6 and AP7. With the proper domain size and resolution, CEST can capture the forerunner and produce peak surges comparable with observations. The utilization of the large basins with a high-resolution grid improves the simulation accuracy, but increases computation time by 20-30% in comparison of the usage of intermediate size basins. It took one processor about 120 minutes to complete a 4 day simulation on the large size CEST basin, and 95 minutes on the intermediate size CEST basin.

MF-4 Flood Characteristics (Outputs)

A. Flood extent and elevation or depth generated by the flood model shall be consistent with observed historical floods affecting Florida.

For the coastal surge model, there is separated document to present the flood extent and elevation comparison between observed and computed for historical hurricanes. One component is the High Water Mark (HWM) data, the reports, published by United States Geological Survey (USGS) or Federal Emergency Management Agency (FEMA) related to each historical hurricanes required by standards, are extracted or digitalized. For the High Water Mark (HWM) data, data above NAVD88 are used.

The inland flood models have been developed using US EPA SWMM and calibrated and validated with observed stream flow data (Please see SF-1 for details). Based on the calibrated model output, we estimated the flooding extent and depth for different rainfall events.

B. Methods for deriving flood extent and elevation or depth shall be scientifically defensible and technically sound.

For the coastal surge model, there are three outputs related to the flood extent and elevation or depth can be used to derive the flood extent and elevation or depth.

1. storm*_env.nc: maximum surge height (m) at each grid location;
2. storm*_mwspd_r_el: maximum wind speed associated surge (m);
3. storm*_first_t.nc: time of first inundation (m).

The maximum surge height (m) at each grid location (Envelop) can be directly used to extract maximum flood extent and elevation caused by hurricane surge tide. The flooding depth can derived from the elevation minus the ground elevation extracted from high resolution Lidar data. The rest two outputs can be used to estimate the flooding duration and moment.

The flood extents and depths have been derived at every 1 km by 1km blocks within the six inland basins. The predicted flood elevations at subbasin outlets were interpolated to these blocks by inverse distance weighing approach to compute flood depths.

C. Methods for modeling or approximating wave conditions in coastal flooding shall be scientifically defensible and technically sound.

The wave model uses the well-known program STWAVE to compute wave heights and directions on a 40 meter grid that covers the coast of Florida with insurable properties.

D. Modeled flood characteristics shall be sufficient for the calculation of flood damage.

For the coastal surge model, each simulation (both historical and stochastic storm events), 8 surge and wind related information are directly output in NETCDF format:

1. storm*_env.nc: maximum surge height (m) at each grid location;
2. storm*_hwm_r_wind.nc: maximum surge height associated wind (m/s);
3. storm*_msurge_t.nc: time of maximum surge (s);
4. storm*_mwpsd.nc: maximum wind speed(m/s);
5. storm*_mwspd_r_el: maximum wind speed associated surge (m);
6. storm*_mwspd_t.nc: time of maximum wind speed (m/s);
7. storm*_first_t.nc: time of first inundation (m);
8. storm*_first_w.nc: wind speed at that time (m/s).

These information are required by engineering team, and are sufficient to calculate the flood damage.

The inland flood damage during a flood event is estimated from the inland flood model predicted flood depths at the inundated locations for the respective flood event.

Disclosures

- 1. Demonstrate that the coastal flood model component incorporates flood parameters necessary for simulating storm-surge-related flood damage in Florida. Provide justification for validation using any historical events not specified in Form HHF-1, Historical Event Flood Extent and Elevation or Depth Validation Maps.**

For the coastal surge model, each simulation (both historical and stochastic storm events), 8 surge and wind related information are directly output in NETCDF format:

1. storm*_env.nc: maximum surge height (m) at each grid location;
2. storm*_hwm_r_wind.nc: maximum surge height associated wind (m/s);
3. storm*_msurge_t.nc: time of maximum surge (s);
4. storm*_mwpsd.nc: maximum wind speed(m/s);
5. storm*_mwspd_r_el: maximum wind speed associated surge (m);
6. storm*_mwspd_t.nc: time of maximum wind speed (m/s);
7. storm*_first_t.nc: time of first inundation (m);
8. storm*_first_w.nc: wind speed at that time (m/s).

In addition to the historical events not specified in Form HHF-1, there are several other storm events are also simulated, like hurricane Katrina, Ike, Rita, Nate, Hermine, and Irma. All these historical event flood extent and elevation validation maps are presented in separated documents.

- 2. For coastal flooding, describe how the presence, size, and transformation of waves are modeled or approximated.**

Waves are modeled using the US Army Corps of Engineers program, STWAVE. The program was modified slightly to include bulk Thornton and Guza (1983, Journal of Geophysical Research – Oceans, 88(C10), 5925-5938) type wave breaking rather than a strict depth-dependent limit. Other than this, there are no modifications to the program. Waves are computed on 116 subgrids using local topobathy, provided surge levels, local land use/land cover data, and provided winds as input. Wave heights and periods at the offshore boundaries are computed using maximum winds over each storm and either the maximum surge, or the surge at time of maximum wind. Constant wave parameters are applied

3. For coastal modeling, describe if and how the flood model accounts for flood velocity, flood duration, flood-induced erosion, floodborne debris, salinity, and contaminated floodwaters.

CEST model directly simulated flood velocity, and can output the flood duration for each storm at given locations. However, flood-induced erosion, floodborne debris, salinity, and contaminated floodwaters are not considered in the current model.

4. Describe if and how the coincidence and interaction of inland and coastal flooding is modeled.

The inland and coastal flooding are separately simulated, and there is no interaction between the two models right now. The coastal and inland flood model components are performed at different platforms and grids. If the same locations are both flooded by coastal and inland components, the maximum inundation depth will be used.

5. Provide a flowchart illustrating how the characteristics of each flood model component are utilized in other components of the flood model.

Figure 41 presents the flowchart illustrating coastal surge model with other components of the FPFLM.

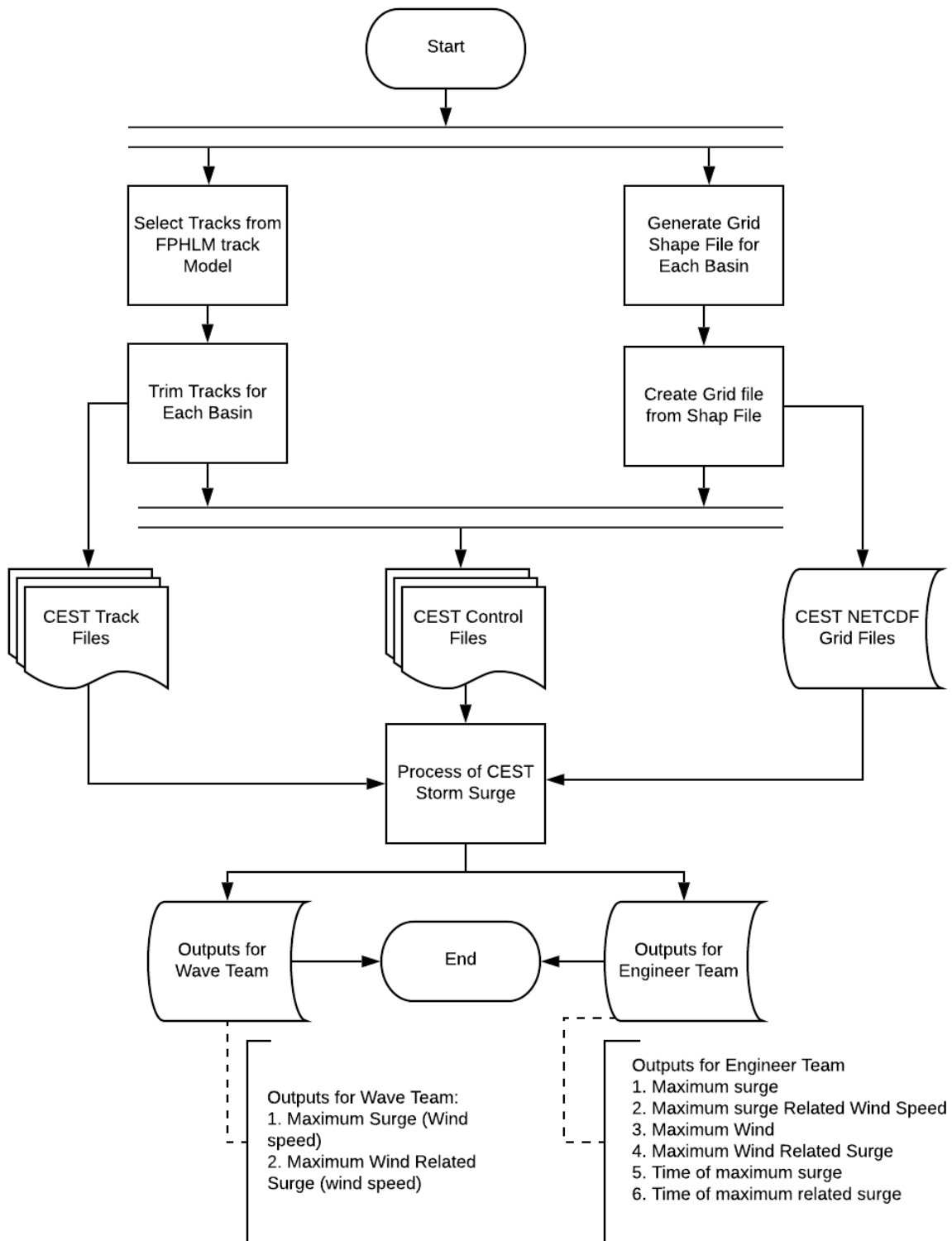


Figure 41. The flowchart illustrating coastal surge model with other components of the FPFLM.

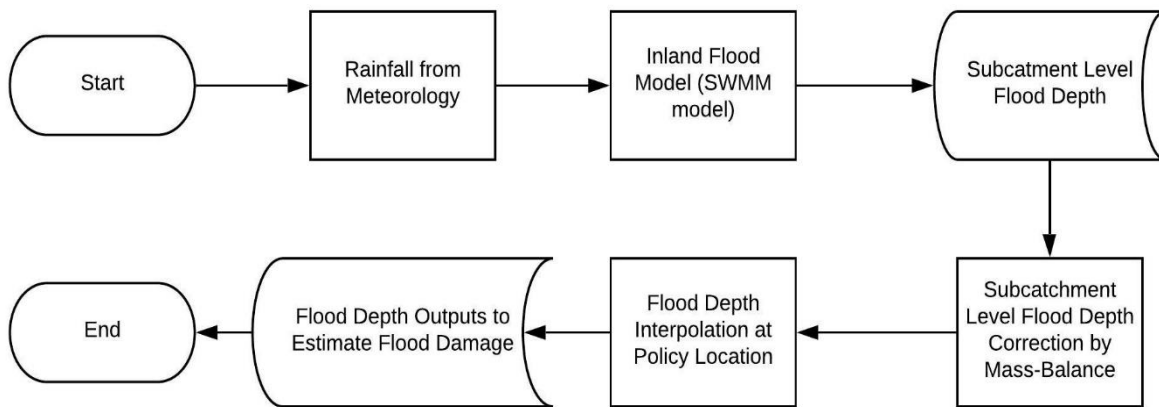


Figure 42. Flowchart illustrating the inland flood model components of the FPFLM.

6. Describe and justify the appropriateness of the databases and methods used for the calibration and validation of flood extent and elevation or depth.

For the coastal flooding team, there are three types data are used to calibrate and validate the coastal surge model. First is water elevation time series data (<https://tidesandcurrents.noaa.gov/>) along Florida coastal region. The water elevation data was directly downloaded from National Oceanic and Atmospheric Administration (NOAA), Units: Meters, Timezone: GMT, Datum: MSL, Interval 1 hour or 6 min (if available). Second is the High Water Mark (HWM) data, the reports, published by United States Geological Survey (USGS) or Federal Emergency Management Agency (FEMA) related to each historical hurricanes required by standards, are extracted or digitalized. For the High Water Mark (HWM) data, data above NAVD88 are used. Third is the Inundation maps or debris line, (<https://www.fema.gov/hurricane-ivan-surge-inundation-maps>)

Consistent with scientific and technical literature, for coastal surge model, the time series of water elevation are all compared at vertical datum Mean Sea Level (MSL). For the High Water Mark (HWM) data, data above NAVD88 are used.

For the historical hurricanes data, the following reports are used to calibrate or validate the coastal surge model.

Mitchell H.Murray (1992). Storm-Tide Elevations Produced by Hurricane Andrew Along the Southern Florida Coasts. U.S Geological Survey Open-File Report 96-116.

Michael Baker Jr., Inc. Alexandria, VA (1995). Hurricane Opal Florida Panhandle Wind and Water Line Survey.

U.S. Army Corps of Engineers, Mobile District, Coastal, Hydrology, and Hydraulic Design Section in cooperation with the United States Geological Survey; Alabama, Florida, and Mississippi Districts (1998). Hurricane Georges Storm Surge September.

U.S. Army Corps of Engineers Jacksonville District (1998). South Florida High Water Marks – Post Georges.

U.S. Department of Commerce National Ocean Service Center for Operational Products and Services (2004). Hurricane CHARLEY Preliminary Water Levels Report.

URS Group, Inc. 200 Orchard Ridge Drive Suite 101 Gaithersburg, MD 20878 (2005). Hurricane Frances Rapid Response Florida Coastal High Water Mark (CHWM) Collection FEMA-1545-DR-FL.

NOAA National Oceanic and Atmospheric Administration(2004). Hurricane FRANCES Preliminary water Levels report.

Mobile District Engineering Division Hydrology and Hydraulics Branch (2004). Tide Gage Data for Hurricane Ivan.

NOAA National Oceanic and Atmospheric Administration(2004). Hurricane IVAN Preliminary Water Levels Report.

URS Group, Inc. 200 Orchard Ridge Drive Suite 101 Gaithersburg, MD 20878 (2004). Hurricane Ivan Rapid Response Alabama and Mississippi Coastal High Water Mark (CHWM) Collection FEMA-1549-DR-AL & 1550-DR-MS.

URS Group, Inc. 200 Orchard Ridge Drive Suite 101 Gaithersburg, MD 20878 (2004). Hurricane Ivan Rapid Response Florida Coastal High Water Mark (CHWM) Collection FEMA-1551-DR-FL.

URS Group, Inc. 200 Orchard Ridge Drive Suite 101 Gaithersburg, MD 20878 (2004). Hurricane Jeanne Rapid Response Florida Riverine High Water Mark (RHWM) Collection FEMA-1561-DR-FL.

NOAA National Oceanic and Atmospheric Administration (2004).Hurricane Jeanne Preliminary Water Levels Report.

RS Group, Inc. 200 Orchard Ridge Drive Suite 101 Gaithersburg, MD 20878 (2004). Hurricane Dennis Rapid Response Florida Coastal High Water Mark (CHWM) Collection FEMA-1595-DR-FL.

NOAA National Oceanic and Atmospheric Administration (2005). Hurricane Dennis Preliminary Water Levels.

Mark E. Luther, Clifford R. Merz, Jeff Scudder, Stephen R. Baig, LT Jennifer Pralgo, Douglas Thompson, Stephen Gill & Gerald Hovis (2007). Water Level Observations for Storm Surge.

URS Group, Inc. 200 Orchard Ridge Drive Suite 101 Gaithersburg, MD 20878 (2006). Final Coastal High Water Mark Collection for Hurricane Wilma in Florida FEMA-1609-DR-FL, Task Order 460.

NOAA National Oceanic and Atmospheric Administration (2005).Hurricane Wilma Preliminary Water Levels Report.

Thomas J. Smith III, Gordon H. Anderson, and Ginger Tiling (2005). A Tale of Two Storms: Surges and Sediment Deposition from Hurricanes Andrew and Wilma in Florida's Southwest Coast Mangrove Forests.

Lars E. Soderqvist and Michael J. Byrne (2005). Monitoring the Storm Tide of Hurricane Wilma in Southwestern Florida.

FEMA and URS, 1595-DR-FL (2005) Hurricane Dennis Rapid Response Florida Coastal High Water Mark (CHWM) Collection.

Wang, R. and Manausa, M. (2005) Hurricane Ivan Characteristics and Storm Tide Elevation. *Sponsored by Florida Department of Environmental Protection.*

The inland flood models have been developed using US EPA SWMM and calibrated and validated with observed stream flow data (details in SF-1). Based on the calibrated model output, we estimated the flooding extent and depth for the historical flood events. High water mark of the hurricane Jeanne 2004 (FEMA, 2005) is the only available observed flood depth record, which was used to evaluate the inland flood model predicted flood depths.

7. Describe any variations in the treatment of the flood model flood extent and elevation or depth for stochastic versus historical floods, and justify this variation.

There is not variations in the treatment of flood model flood extent and elevation or depth for the stochastic versus historical floods.

8. Provide a completed Form HHF-2, Coastal Flood Characteristics by Annual Exceedance Probability. Provide a link to the location of the form [insert hyperlink here].

See the Form [HHF-2](#).

9. Describe the effects of storm size, bathymetry, and windspeed on storm surge height for the coastal flood model.

For the coastal surge model, we conducted the study to provide the first analysis of the modeling sensitivity runs on the relationship between storm size and storm surge heights. Storm surge height

is calculated the Radius of Maximum Wind (RMW) with 20 and 35 miles. The results indicates that the storm sizes correlated with storm surge heights.

Storm surge heights are calculated from CEST at four different bathymetry Basins, Apalachicola Bay Basin (AP3) with 0.5, 1.0, 1.5, and 2.0 times of the original depth. It is indicated that the bathymetry correlated with storm surge heights. Shallower bathymetry may generate higher surge than the deeper.

We also conduct the CEST simulations for nine different hurricane forward direction at AP3 basin. For each different forwarding direction, simulations will include 80 mph (Wind 1), 100 mph (Wind 2), 120 mph (Wind 3), and 140 mph (Wind 4) maximum onshore wind speeds with the exactly same initial surge tide level, and same hurricane track information, same grid setup, same time step, and same Manning coefficient. In other word, only the onshore wind speed varied, and all other factors held constant. It is obvious that the higher windspeed will produce higher surge at most cases.

The detailed information is presented in separated documentation.

Wave heights and periods at the offshore wave boundaries increase with wind speed, fetch, and depth according to Young and Verhagen (1996, [Coastal Engineering](#) 27(1-2):47-78) hindcast relations, and to computed bulk setup. Wave properties are not impacted by wind duration, as steady-state relations are used.

10. Describe the effects of windspeed, depth, fetch, and wind duration on locally generated wave heights or wave proxies for the coastal flood model.

Wave heights and periods at the offshore wave boundaries increase with wind speed, fetch, and depth according to Young and Verhagen (1996, [Coastal Engineering](#) 27(1-2):47-78) hindcast relations, and to computed bulk setup. Wave properties are not impacted by wind duration, as steady-state relations are used.

MF-5 Flood Probability Distributions

A. Flood probability, its geographic variation, and the associated flood extent and elevation or depth shall be scientifically defensible and shall be consistent with flooding observed for Florida.

For the coastal flooding model, time series of water elevation along Florida coastal region and High Water Mark caused by hurricane surge are used to calibrate and validate the coastal surge model. These two data sets are scientifically defensible to validate the computed flood extent and elevation with the observed.

The inland flood models were calibrated and validated with mean daily streamflow observations in the most major stream reaches within the state of Florida. Using streamflow data in calibrating flood models is a common practice in hydrologic modeling (Abdul-Aziz and Al-Amin, 2016).

B. Flood probability distributions for storm tide affected areas shall include tropical, and if modeled, non-tropical events.

Using tropical storm Fay as an example, we also conduct the coastal surge simulations for all four Florida basins. The results indicate that the surges induced by tropical storm are not significant. The non-tropical events are not simulated.

C. Probability distributions for coastal wave conditions, if modeled, shall arise from the same events as the storm tide modeling.

Wave conditions arise from the same probability distribution as is used for the storm tide modeling.

D. Any additional probability distributions of flood parameters and modeled characteristics shall be consistent with historical floods for Florida resulting from coastal and inland flooding.

The coastal surge model parameters are from scientific literatures and technical reports. There are almost fixed values, or calculated from equations presented in the previous literatures. All the values and equations are presented in Section GF-1, MF-1, and MF-2. There is no probability distributions used in coastal surge model.

The inland flood models are deterministic models, therefore, probability distributions were not used in the parameterization.

Disclosures

1. Describe how non-tropical and tropical event coastal storm tide flood probability distributions are combined, if applicable. Provide an example demonstrating the process.

For the current coastal surge model setup, there is no non-tropical event simulation.

2. Provide the rationale for each of the probability distributions used for relevant flood parameters and characteristics.

The coastal surge model parameters are from scientific literatures and technical reports. There is no probability distributions used in coastal surge model.

Since the inland flood models are deterministic models, probability distributions were not used in parameterizing flood parameters.

3. Demonstrate that simulated flood elevation or depth frequencies are consistent with historical frequencies.

The historical hurricane events calibrations and validations are presented in separated documents. The results indicate that the simulated flood elevation frequencies are consistent with historical frequencies.

The comparison of historical observations and corresponding model predicted streamflow is documented in SF-1. The values of model performance metrics indicate that model predictions are consistent with historical streamflow frequencies.

HYDROLOGICAL AND HYDRAULIC FLOOD Standards

HHF-1 Flood Parameters (Inputs)

- A. Treatment of land use and land cover (LULC) effects shall be consistent with current scientific and technical literature. Any LULC database used shall be consistent with the National Land Cover Database (NLCD) 2006 or later. Use of alternate datasets shall be justified.***

In order to parameterize the land use/cover features of the inland flood models, National Land Cover Database (NLCD) of 2006 and 2011 have been used. This is a high-resolution (30 m) land cover database that covers not only Florida, but also the entire United States. Details of the parameterization have been described in GF-1, MF-2 and HHF-1.

- B. Treatment of soil effects on inland flooding shall be consistent with current scientific and technical literature.***

Soil and aquifer properties (porosity, saturated hydraulic conductivity, etc.) in the inland flood models have been incorporated based on the Soil Survey Geographic Database (SSURGO) from United States Department of Agriculture (USDA); scientific and technical literatures were explored as well. Details of the soil properties estimation have been described in GF-1, MF-2 and HHF-1.

Disclosures

- 1. For inland flood analyses associated with riverine and lacustrine flooding, describe how the rivers, lakes, and associated floodplains are segmented (or partitioned) in determining the parameters for flood frequency used in the flood model.***

In the inland flood SWMM models, the rivers are represented as a system of connected link (streams) and nodes (confluence/bifurcation). Lakes which significantly influence the streamflow of the major rivers within the same drainage network have been taken into account; lake bathymetry information were collected from St. Johns River Water Management District and South Florida Water Management District. However, the inland flood model does not account for lacustrine flooding.

- 2. For inland flood analyses associated with surface water flooding, describe how the affected area is segmented (or partitioned) in determining the parameters for flood frequency used in the flood model.***

The inland flood models have been segmented based on the USGS hydrologic unit boundary. The details of the model partitioning and parameterization have been described in GF-1 and MF-2.

3. Describe any assumptions or calculations used in the inland flood model relating to initial and boundary conditions (e.g., groundwater levels, lake levels, river discharges, tides, soil moisture).

Boundary conditions have been introduced into the inland flood models by incorporating observed streamflow time series (upstream boundary condition) and observed water level time series (downstream boundary condition). No assumptions or calculations were made to apply boundary conditions in the inland flood models.

4. Provide the grid resolution or other area partitioning used to model the inland flood extent and depth and how the hydrological and hydraulic characteristics are determined on these scales.

DEMs of 10 m spatial resolution have been used to develop the inland flood models. The details of hydro-network (e.g., subcatchments, drainage links and nodes) development have been described in GF-1. Since the urban areas (i.e., higher impervious areas) are more prone to flood hazards, we discretized them into smaller subcatchments to provide inland flood model outputs at finer spatial resolution. Determination of the hydrological and hydraulic characteristics of the inland flood models have been described in GF-1 and MF-2.

5. Describe any assumptions or calculations used in the inland flood model relating to flood-induced erosion or topographic changes.

In developing the inland flood models, no assumptions or calculations have been considered for flood-induced erosion or topographic changes.

6. Provide citations to all data sources used to develop and support the land-use evaluation methodology, including publicly-developed or peer-reviewed information.

The land use/cover information for the inland flood models were obtained from percent impervious raster dataset of the National Land Cover Database (NLCD) for 2006 and 2011 (Fry et al., 2011; Homer et al., 2015). Based on land use of the subcatchments, overland roughness coefficients and depression storage depth were incorporated in the models in accordance with the recommended values mentioned in SWMM Reference Manual Volume I, Hydrology (Rossman and Huber, 2016).

7. Provide the collection and publication dates of the LULC and soil data used in the flood model, and justify the applicability and timeliness of the data for Florida.

We used the 30 m NLCD percent impervious surface dataset for 2006 and 2011 in order to incorporate land use features in the inland flood models. The SSURGO data used for determination

of soil properties were published for Florida by National Resources Conservation Service Soils (USDA, 2018) and the web soil survey details for Florida were available in 2005 (USDA, 2020).

8. Describe the methodology used to convert LULC information into a spatial distribution of hydrological parameters, including roughness coefficients, throughout the flood model domain.

In order to represent an inland basin on SWMM platform, it was divided into various subbasins. Spatially averaged LULC information for a subbasin was used to determine overland hydrological parameters such as roughness coefficients and depression storage depths in regards to the recommended values in SWMM reference manual (Rossman and Huber, 2016).

9. Describe the methods used to account for soil infiltration and percolation rates and soil moisture conditions in the inland flood model, if applicable. Provide citations to all data sources used to develop and support the soil infiltration and percolation rates and soil moisture conditions methodology, including publicly-developed or peer-reviewed information.

Green-Ampt method was chosen for representing infiltration of water into the soil for the inland flood models. Main parameters for the Green-Ampt method are initial moisture deficit of the soil, soil's saturated hydraulic conductivity, and soil suction head at the wetting front. These infiltration parameters along with the aquifer parameters (e.g., porosity, wilting point, field capacity, etc.) were assigned based on soil type data obtained from the SSURGO database (USDA-NRCS, 2015), SWMM Reference Manual Volume I, Hydrology (Rossman and Huber, 2016), and infiltration parameters reported by Rawls et al. (1983). Details of model development and data sources have been described in GF-1 and MF-2.

HHF-2 Flood Characteristics (Outputs)

A. Flood extent and elevation or depth generated by the flood model shall be consistent with observed historical floods affecting Florida.

The required database for evaluating the consistency between the observed and inland flood model predicted flood depth and extent during historical flood events is not available. Flood depths and extent generated by inland flood models have been compared with the observed high water marks during hurricane Jeanne (2004), which is the only available location-specific historical flood depth observations.

B. Methods for deriving flood extent and depth shall be scientifically defensible and technically sound.

The flood extents and depths have been derived at every 1 km by 1km blocks within the six inland basins. The predicted flood elevations at subbasin outlets were interpolated to these blocks to compute flood depths.

C. Modeled flood characteristics shall be sufficient for the calculation of flood damage.

Inland flood damage is estimated by the model predicted flood depths at the flood prone locations.

Disclosures

1. Provide comparisons of the modeled and historical flood extents and elevations or depths for the storm events listed in Form HHF-1, Historical Event Flood Extent and Elevation or Depth Validation Maps. For any storms where sufficient data are not available, the modeling organization may substitute an alternate historical storm of their choosing. Describe how each substituted storm provides similar coastal and inland flooding characteristics to the storm being replaced.

The inland flood models were calibrated and validated with observed daily mean streamflow in the major stream reaches within the state of Florida (documented in SF-1). However, the appropriate database for investigating the consistency between observed and model predicted flood depths and extents during the historical hurricane events is not available. There are only a few high water mark observations available during hurricane Jeanne (FEMA, 2005). The high water mark observations recorded during hurricane Jeanne fall within the model predicted flood extents, which indicate reasonable prediction of flood extents. On an average, the observed flood depth during hurricane Jeanne (2004) was 73 cm, while the modeled average flood depth is 41 cm.

2. Demonstrate that the inland flood model component incorporates flood parameters necessary for simulating inland flood damage and accommodates the varied geographic, geologic, hydrologic, hydraulic, and LULC conditions in Florida. Provide justification for validation using any historical events not specified in Form HHF-1, Historical Event Flood Extent and Elevation or Depth Validation Maps.

The inland flood models have been developed based on the published dataset and scientific literatures while following guidelines in the SWMM Reference Manual (Rossman 2015) Details of model development are documented in GF-1, MF-1, and MF-2.

3. For each of the storm events in Form HHF-1, Historical Event Flood Extent and Elevation or Depth Validation Maps, resulting in inland flooding, provide a comparison of the modeled flood flow to recorded flow data from selected United States Geological Survey (USGS) or Florida Water Management District (FWMD) gauging stations. Provide the rationale for gauging station selections.

The long-term model performance evaluation of six inland basins have been documented in the disclosures of SF-1. Model performance was evaluated by the Nash-Sutcliffe Efficiency (*NSE*) (Nash and Sutcliffe, 1970) and the ratio of the root-mean-square error to the standard deviation of observations (*RSR*) (Moriassi et al., 2007). Similar to coefficient of determination (R^2), *NSE* measures goodness-of-fit for a hydrological model. To demonstrate how the inland flood models perform during the historical flood events, the comparison of observed and model predicted streamflow in the Hillsboro Canal of Southeast Coasts Basin (SEC) is presented as an example in the Table 29:

Historical Event	NSE	RSR
Hurricane Katrina (2005)	0.73	0.50
Hurricane Ivan (2004)	0.68	0.56
Hurricane Jeanne (2004)	0.77	0.47
Hurricane Wilma (2004)	0.90	0.31
Tropical Storm Fay (2008)	0.86	0.37
Unnamed Storm (May 2009)	0.95	0.24
Unnamed Storm (July 2013)	0.77	0.47
Hurricane Dennis (2005)	0.96	0.20

Table 29. Model performance statistics during historical flood events.

4. Identify all hydrological and hydraulic variables that affect the flood extent, elevation, depth, and other flood characteristics.

The dominant hydrologic and hydraulic variables that affect the flood characteristics include:

- subcatchment width,
- watershed slope
- saturated hydraulic conductivity
- overland roughness

- channel roughness

The details of parameterization and data sources are documented in GF-1, MF-1, and MF-2.

5. For inland flood modeling, describe if and how the flood model accounts for flood velocity, flood duration, flood-induced erosion, floodborne debris, and contaminated floodwaters.

Flood damage caused by inland flooding is computed from model predicted flood depths at policy locations. Flood velocity, duration, flood induced erosion, etc. are not considered for estimation of the inland flood damage.

6. Describe the effect of any assumptions or calculations relating to initial and boundary conditions on the flood characteristics.

Boundary conditions have been introduced into the inland flood models by incorporating observed streamflow time series (upstream boundary condition) and observed water level time series (downstream boundary condition). No assumptions or calculations were made to apply boundary conditions in the inland flood models (documented in HHF-1).

7. Describe and justify the appropriateness of the databases and methods used for the calibration and validation of flood extent and elevation or depth.

The appropriate database for calibrating and validating the flood extent and depth for the storms listed in the Form HHF-1 is not available. The inland flood model predicted flood outputs were evaluated based on a few high water mark observations during hurricane Jeanne that occurred on 2004.

8. Describe any variations in the treatment of the flood model flood extent and elevation or depth for stochastic versus historical floods, and justify this variation.

Similar approach is adopted to compute flood depths for stochastic and historical floods.

9. Provide a completed Form HHF-1, Historical Event Flood Extent and Elevation or Depth Validation Maps. Provide a link to the location of the form [insert hyperlink here].

See [Form HHF-1](#).

10. Provide a completed Form HHF-4, Inland Flood Characteristics by Annual Exceedance Probability. Provide a link to the location of the form [insert hyperlink here].

See [Form HHF-4](#).

HHF-3 Modeling of Major Flood Control Measures

A. The flood model's treatment of major flood control measures and their performance shall be consistent with available information and current state-of-the-science.

We have incorporated several flood control measures in the inland flood models. Information of these control structures required to be included in the models were collected from South Florida Water Management District (SFWMD). List of the flood control measures and the methodology of incorporating them have been included in the disclosures of this standard.

B. The modeling organization shall have a documented procedure for reviewing and updating information about major flood control measures and if justified, shall update the flood model flood control databases.

Structural information of the flood control measures and time series of their real-time gate opening information were obtained from SFWMD and they were included in the inland flood models in reference to user manual of EPA SWMM 5.1 (Rossman, 2015).

C. Treatment of the potential failure of major flood control measures shall be based upon current scientific and technical literature, empirical studies, or engineering analyses.

In order to simulate the effects of potential failure of flood control measures in the inland flood models, full failure of these control structures were assumed.

Purpose: Major flood control measures are those measures undertaken outside the building footprint and on a larger scale, to reduce the presence, depth or energy of flow or waves that affect personal residential structures. The presence of major flood control measures can reduce the flood damage to buildings. The failure of major flood control measures during a flooding event can cause damage to buildings equal to or in excess of the damage that would occur if the measures were not present. The evaluation of impacts of major flood control measures may include, but not be limited to, considering dams, levees, and floodwalls, and the associated location, dimensions, strength, and performance thereof.

Relevant [Form: GF-3](#), Hydrological and Hydraulic Flood Standards Expert Certification

Disclosures

1. List the major flood control measures incorporated in the flood model and the sources of all data employed.

We incorporated several major flood control structures in the inland flood models (Table 30). Structural information (e.g., number of gates, gate size, etc.) of these structures along with their
FPFLM V1.0 Feb. 29, 2020

real time gate opening data were collected from DBHYDRO, the environmental database of SFWMD.

Control Structure ID	Type	Location	Watershed	Data Source
S-65	Spillway	Canal C-38 at Lake Kissimmee	Kissimmee River Basin	SFWMD
S-61	Spillway	Canal C-35 at Lake Tohopekaliga	Kissimmee River Basin	SFWMD
S-68	Spillway	Canal C-41A at Lake Istokpoga	Kissimmee River Basin	SFWMD
S-67	Spillway	Lake Istokpoga canal	Kissimmee River Basin	SFWMD
S-65E	Spillway	Canal C-38 at Lake Okeechobee	Kissimmee River Basin	SFWMD
S-84	Spillway	Canal C-41A at Lake Okeechobee	Kissimmee River Basin	SFWMD
S-49	Spillway	C-24 Canal	Southeast Coasts Basin	SFWMD
S-46	Spillway	Loxahatchee Slough Canal	Southeast Coasts Basin	SFWMD
S-155	Spillway	West Palm Beach Canal	Southeast Coasts Basin	SFWMD
G-56	Spillway	Hillsboro Canal	Southeast Coasts Basin	SFWMD
G-54	Spillway	North New River Canal	Southeast Coasts Basin	SFWMD
S-26	Spillway	Miami River	Southeast Coasts Basin	SFWMD

Table 30. Flood control structures incorporated in the inland flood models.

2. Describe the methodology to account for major flood control measures in the flood model and indicate if these measures can be set (either to on or off) in the flood model.

The control structures incorporated in the inland flood models are spillways (Table 1). Structural information (e.g., number of gates, gate size, crest elevation, etc.) and real time gate opening data of these structures were collected from the DBHYDRO database of SFWMD. In reference to the user manual of EPA SWMM 5.1 (Rossman, 2015), the gate opening information were incorporated as ‘fraction open’, i.e., ratio of gate opening over gate height in the models. These flood control measures can be set off, i.e., gates of the control structures can be kept fully open by setting the value of ‘fraction open’ equal to 1. Other non-zero values (less than 1) of ‘fraction open’ indicate that the gates are partially open, i.e., the flood control measures have been set on; Zero values of ‘fraction open’ means the gates are fully closed.

3. Describe if and how major flood control measures that require human intervention are incorporated into the flood model.

Operation of most of the control structures included in the inland flood models are automatically controlled. There are a few structures that require manual operations. As previously mentioned, we incorporated real time gate opening information for these controls structures which took care of the required human interventions.

4. Describe and justify the methodology used to account for the potential failure or alteration of major flood control measures in the flood model and if the level of failure can be adjusted in the flood model.

In order to account for potential failure of the flood control measures in the inland flood model, the control structures were turned off, i.e., unrestrained open channel flows were simulated. We, therefore, assumed full failure of the flood control measures and the level of failure cannot be adjusted.

5. Provide an example of the flood extent and elevation or depth showing the potential impact of a major flood control measure failure.

We are in the process of modeling the impact of failure of a major flood control measure in the Southeast Coasts Basin. The flood depth and extent maps under potential failure of the control structure will be addressed later.

HHF-4 Logical Relationships Among Flood Parameters and Characteristics

A. At a specific location, water surface elevation shall increase with increasing terrain roughness at that location, all other factors held constant.

The terrain roughness impedes the passage of overland flow. Therefore, a location with higher terrain roughness will slow down the movement of overland flow allowing more water to accumulate over the ground surface. Thus if all other factors are held constant, the water surface elevation over the ground surface will increase with the increase in terrain roughness.

B. Rate of discharge shall increase with increase in steepness in the topography, all other factors held constant.

For the inland flood models the stream discharge increases as the steepness of the topography (watershed slope) increases.

C. Inland flood extent and depth associated with riverine and lacustrine flooding shall increase with increasing discharge, all other factors held constant.

With the increasing discharge while all other factors are held constant, the volume of water will increase in the streams. The additional volume of water will increase water depth in the channels. Therefore increased discharge enhances the likelihood of stream overflowing and the corresponding enlargement of flooding extent.

D. The coincidence of storm tide and inland flooding shall not decrease the flood extent and depth, all other factors held constant.

In case of coincidence of inland and coastal flood at a location, the maximum inundation depth will be considered to estimate flood damage. Therefore, if inland flooding and storm tide co-occur, flooding extent and depth will not decrease assuming all other factors are held constant.

Disclosures

1. Provide a sample graph of water surface elevation and discharge versus time associated with inland flooding for modeling-organization-defined locations within each region in Florida identified in Figure 115 Discuss how the flood characteristics exhibit logical relationships.

The sample graphs of water surface elevation and discharge versus time within each region is given below:

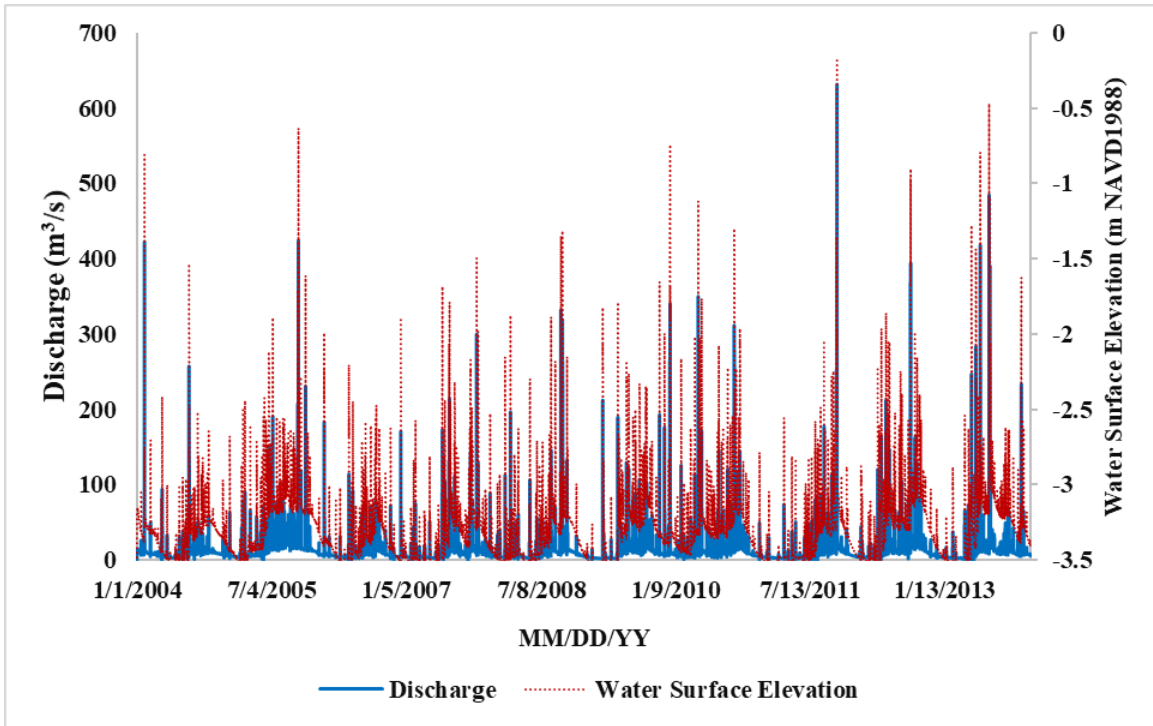


Figure 43. Sample plot of water surface elevation and discharge versus time in Broward County within Southeast Florida region.

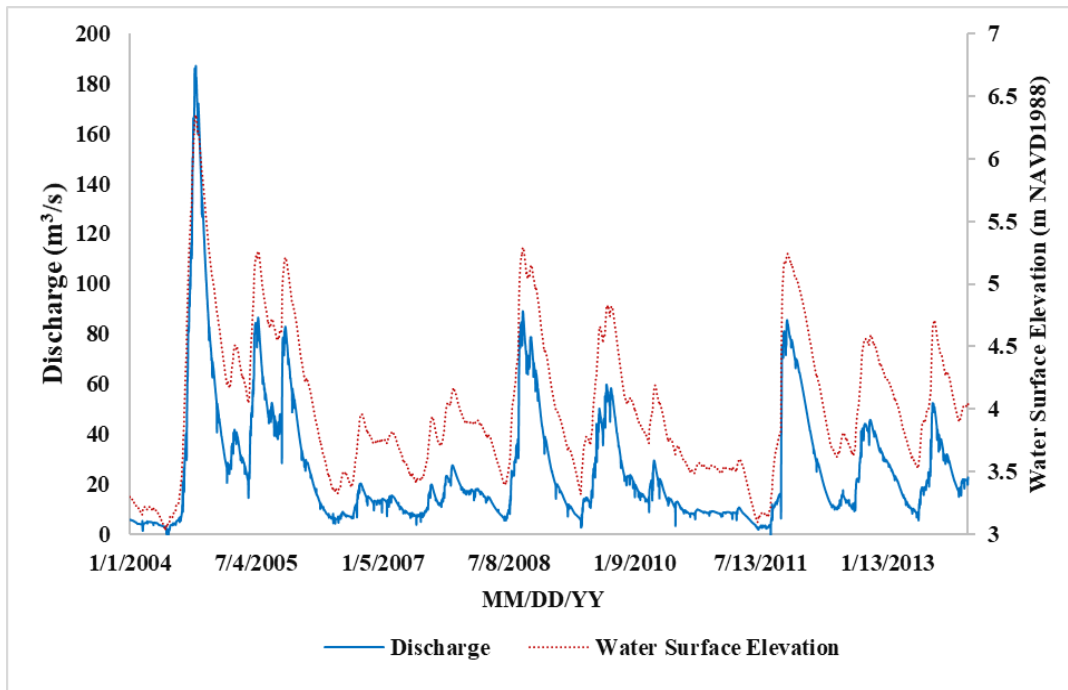


Figure 44. Sample plot of water surface elevation and discharge versus time in Brevard County within East Florida region.

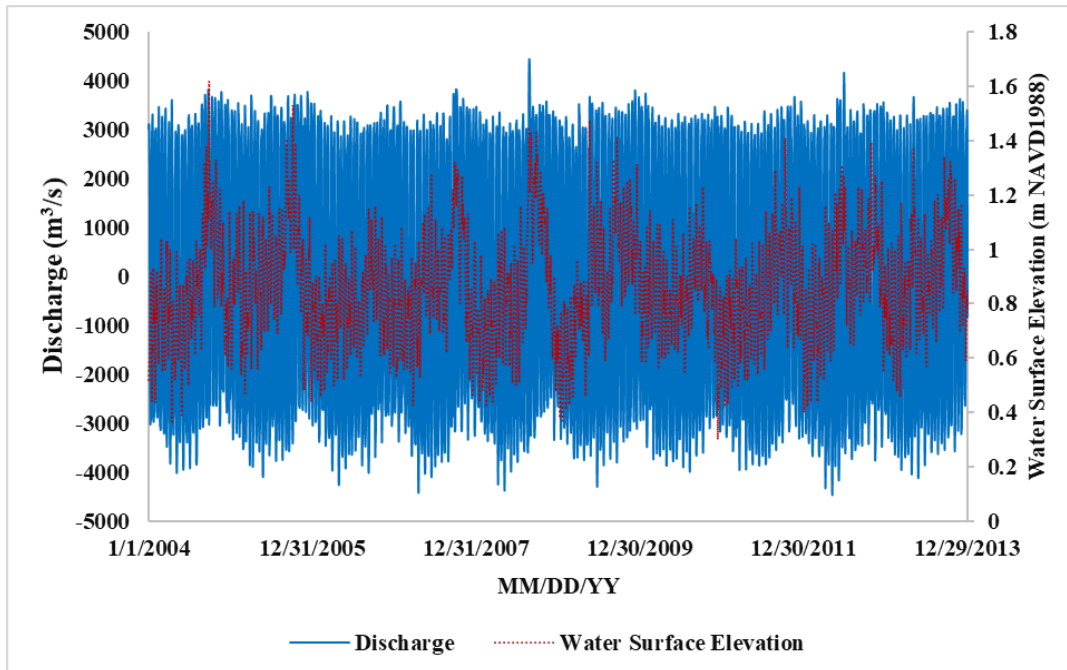


Figure 45. Sample plot of water surface elevation and discharge versus time in Duval County within North Florida region.

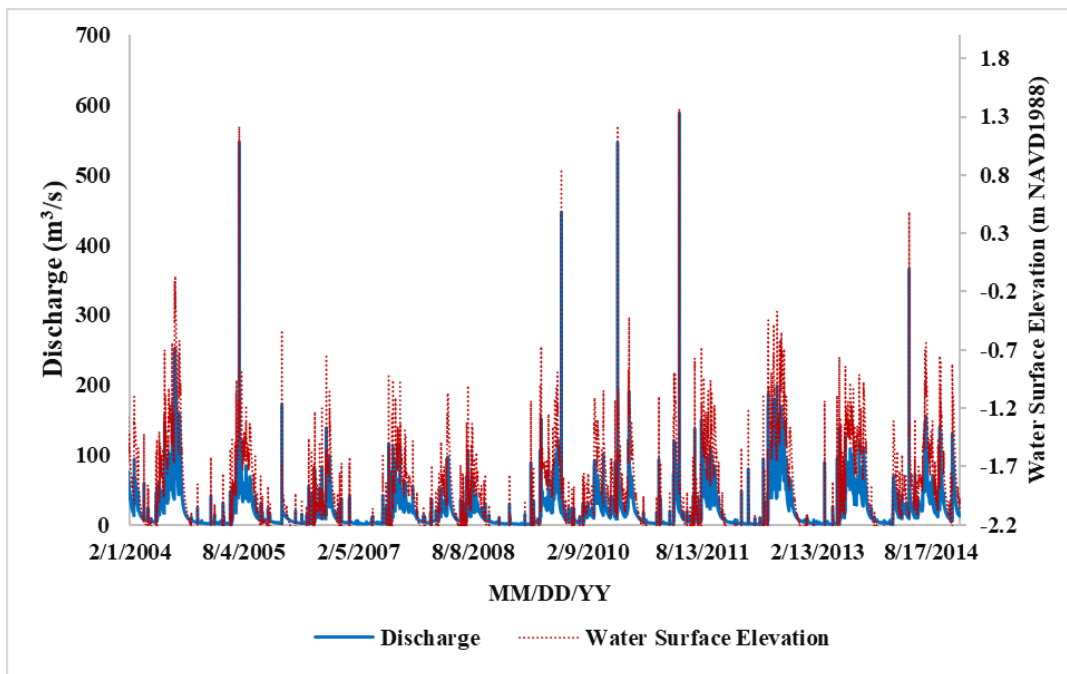


Figure 46. Sample plot of water surface elevation and discharge versus time in Hillsborough County within Southwest Florida region.

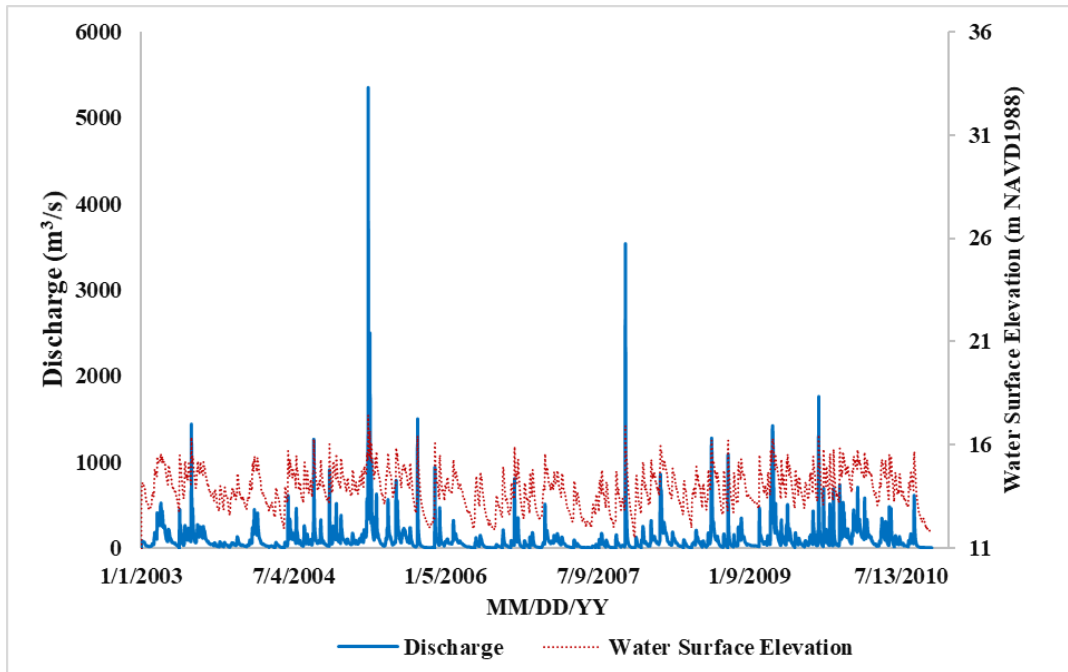


Figure 47. Sample plot of water surface elevation and discharge versus time in Leon County within Panhandle region.

The plots of water surface elevation and discharge versus time exhibit the increasing nature of water surface elevation with increasing stream discharge. Therefore, the inland flood model predicted flooding depth and extent will increase with the increasing river discharge.

2. Describe the analysis performed in order to demonstrate the logical relationships in this standard.

In SWMM model, a subcatchment is conceptualized as a rectangular surface having a uniform slope S and a width W draining to a single channel outlet (Rossman and Huber, 2016). Assuming flow across the subcatchment surface behaves like uniform flow within a rectangular channel, volumetric flow rate Q (cms) is computed as:

$$Q = \frac{1}{n} * R_x^{\frac{2}{3}} A_x S^{\frac{1}{2}} \quad (1)$$

where

- n = roughness coefficient
- S = average slope of subcatchment
- A_x = subcatchment area
- R_x = hydraulic radius

Equation 1 implies that the discharge will increase with increasing steepness (i.e., slope) of the overland surface.

STATISTICAL FLOOD STANDARDS

SF-1 Modeled Results and Goodness-of-Fit

A. The use of historical data in developing the flood model shall be supported by rigorous methods published in current scientific and technical literature.

B. Modeled results and historical observations shall reflect statistical agreement using current scientific and statistical methods for the academic disciplines appropriate for the various flood model components or characteristics.

Disclosures

1. Provide a completed Form SF-1, Distributions of Stochastic Flood Parameters (Coastal, Inland). Identify the form of the probability distributions used for each function or variable, if applicable. Identify statistical techniques used for estimation and the specific goodness-of-fit evaluations applied along with appropriate metrics. Describe whether the fitted distributions provide a reasonable agreement with available historical data. Provide a link to the location of the form [insert hyperlink here].

The inland flood models are mechanistic and deterministic in nature which have been developed using the EPA Storm Water Management Model (SWMM) 5.1 (Rossman, 2015). Therefore, no probability distributions were fitted to any variables/parameters. The models were calibrated and validated with daily mean observed streamflow at most of the major streams across the state of Florida. Model performance evaluations were done by the Nash-Sutcliffe Efficiency (*NSE*) (Nash and Sutcliffe, 1970) and the ratio of the root-mean-square error to the standard deviation of observations (*RSR*). Similar to coefficient of determination (R^2), *NSE* measures goodness-of-fit for a hydrological model. *NSE* was computed as:

$$NSE = 1 - \frac{\sum_{i=1}^N (Y_{i,obs} - Y_{i,mod})^2}{\sum_{i=1}^N (Y_{i,obs} - Y_{mean,obs})^2}$$

where N is the total number of observations; $Y_{i,mod}$ and $Y_{i,obs}$ are the i -th model prediction and the corresponding observation, respectively; and $Y_{mean,obs}$ is the mean of all observations. $NSE = 1.0$ indicates a perfect model that has predictions exactly matching with the respective observations. $NSE < 0$ indicates a model that is a worse predictor than the mean of all observations as an alternative model. As per Moriasi et al. (2007), $NSE = 0.75-1.00$ for a very good model; $NSE = 0.65-0.75$ for a good model; and $NSE = 0.50-0.65$ for a satisfactory model. *RSR* is an error index statistics which was computed as:

$$RSR = \frac{\sqrt{\sum_{i=1}^N (Y_{i,mod} - Y_{i,obs})^2 / N}}{\sigma_{obs}}$$

where N is the total number of observations; $Y_{i,mod}$ and $Y_{i,obs}$ are the i -th model prediction and the corresponding observation, respectively; and σ_{obs} is the standard deviation of observations. As per Moriasi et al. (2007), $RSR = 0.00-0.50$ for a very good model; $RSR = 0.50-0.60$ for a good model; and $RSR = 0.60-0.70$ for a satisfactory model.

Link to [Form SF-1](#).

2. Provide the date of loss of the insurance claims data used for validation and verification of the flood model.

The validation of the flood model is based on the 2004 hurricanes and the 2004 NFIP PR exposure data.

3. Provide an assessment of uncertainty in flood probable maximum loss levels and in flood loss costs for flood output ranges using confidence intervals or other scientific characterizations of uncertainty.

While the model does not automatically produce confidence intervals for the output ranges, the data do allow for the calculation of confidence intervals. We calculated the mean and the standard deviation of the losses for each zone, and it was found that the standard errors were within 5% of the means for all zones but zone number 19. We also calculated the coefficient of variation (CV) for all zones and drew a histogram which is provided in Figure 48. The range of the CVs was between 2.26 and 13.15. Finally, we computed 95% confidence intervals for the average loss for each zone are reproduced in Table 31.

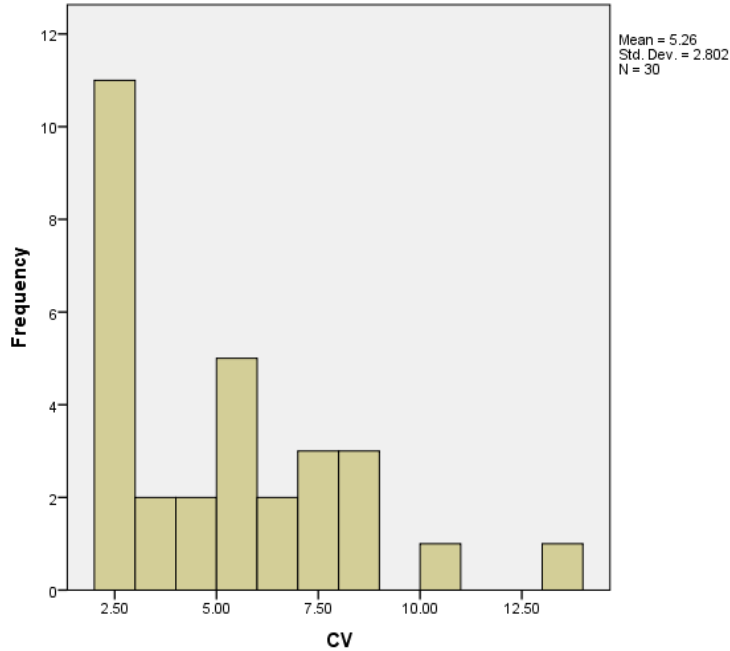


Figure 48. Histogram of CVs for all zones combined.

Zone	Zone Name	Average Loss	Stdev_Loss	LCL	UCL
1	Pensacola	2807002.75	20705144.00	2625514.16	2988491.34
2	Navarre	2881344.00	22982098.00	2679897.03	3082790.97
3	Ft Walton Beach	4334651.50	38455812.00	3997571.45	4671731.55
4	Grayton Beach	3670693.25	27213548.00	3432155.98	3909230.52
5	Panama City Beach	8605574.00	58600044.00	8091921.97	9119226.03
6	Mexico Beach	996209.44	8768097.00	919353.68	1073065.20
7	Carrabelle	2182019.00	11793354.00	2078645.69	2285392.31
8	St Marks	1772279.75	7535590.00	1706227.39	1838332.11
9	Steinhatchee	696801.19	1853575.88	680553.88	713048.50
10	Cedar Key	1158911.63	5806981.00	1108011.19	1209812.06
11	Hernando Beach	14268905.00	72242064.00	13635675.39	14902134.61
12	Clearwater	73362352.00	361482400.00	70193819.06	76530884.94
13	Sarasota	17595240.00	95342440.00	16759526.67	18430953.33
14	Port Charlotte	5466171.00	59378388.00	4945696.48	5986645.52
15	Cape Coral	22081056.00	147291520.00	20789988.90	23372123.10
16	Naples	9715971.00	77756984.00	9034400.98	10397541.02
17	Key West	18706054.00	69497808.00	18096878.85	19315229.15
18	Key Largo	18658510.00	46307284.00	18252608.76	19064411.24
19	Homestead	7258848.50	95446080.00	6422226.72	8095470.28
20	Miami	15252093.00	77403904.00	14573617.87	15930568.13
21	Ft Lauderdale	6831347.50	18792946.00	6666620.07	6996074.93
22	Delray Beach	2144246.50	5768874.00	2093680.09	2194812.91
23	N Palm Beach	2113020.25	6241800.00	2058308.46	2167732.04
24	Stuart	3121143.50	8722741.00	3044685.30	3197601.70
25	Vero Beach	13302215.00	39736452.00	12953909.64	13650520.36
26	Melbourne	56096964.00	126897272.00	54984660.37	57209267.63

27	Titusville	2570429.50	7327068.50	2506204.91	2634654.09
28	New Smyrna Beach	12687268.00	35145776.00	12379201.69	12995334.31
29	St Augustine Beach	17132226.00	52388148.00	16673023.64	17591428.36
30	Atlantic Beach	24370284.00	65827172.00	23793283.40	24947284.60

Table 31. 95% Confidence intervals for mean loss for all zones(based on 50,000) year simulation.

As far as uncertainties for probable maximum loss, we use the we use the well-known result from nonparametric statistics (see Section 3.2 of Practical Nonparametric Statistics by WJ Conover) that for any $1 \leq j \leq N$, the probability that

$$P(\text{PML}_p < X_{(j)}) = \sum_{i=1}^{j-1} \frac{N!}{i!(N-i)!} p^i (1-p)^{N-i}$$

Here PML_p refers to the probable maximum loss corresponding to the p th percentile (return period $\frac{1}{1-p}$)

The above implies that for some $r < s \leq N$,

$$\begin{aligned} & p(X_{(r)} < \text{PML}_p < X_{(s)}) \\ &= p(\text{PML}_p < X_{(s)}) - p(\text{PML}_p < X_{(r)}) \\ &= \sum_{i=1}^{s-1} \binom{N}{i} p^i (1-p)^{N-i} - \sum_{i=1}^{r-1} \binom{N}{i} p^i (1-p)^{N-i} \\ &= \sum_{i=r}^{s-1} \binom{N}{i} p^i (1-p)^{N-i} \approx 0.95 \end{aligned}$$

Hence to construct an exact $(1-\alpha)100\%$ confidence interval for PML_p , we need to find r and s with $r < s$ (done through a numerical search) such that

$$\sum_{i=r}^{s-1} \frac{N!}{i!(N-i)!} p^i (1-p)^{N-i} \approx 1-\alpha.$$

If the solution from the computer search is not unique, the pair of r and s that minimizes $s-r$ is selected to give the narrowest interval.

However, for large samples, approximate 95% confidence interval of PML_p is given by (X_r, X_s) using a binomial approximation. The large sample approximation assumes normality to obtain r and s as

$$\begin{aligned} r &= Np - 1.96\sqrt{Np(1-p)} \\ s &= Np + 1.96\sqrt{Np(1-p)} \end{aligned}$$

Since for our modeled losses, we use 50,000 simulation years, we can easily use the binomial approximation and compute confidence intervals for probable maximum loss. Applying the approximation to the PML values for the estimated flood loss data in Form SF-2, we obtain confidence intervals for the PML values as shown in Table 32.

Return Period (Years)	Probability of Exceedance	Estimated PML	Lower Confidence Limit for PML	Upper Confidence Limit for PML
Top Event	NA	\$23,111,003,598	NA	NA
10000	0.01%	\$12,919,512,938	\$10584208352	\$16951885209
5000	0.02%	\$10,584,208,352	\$9270771929	\$12919512938
2000	0.05%	\$8,230,378,121	\$6974483560	\$9808060850
1000	0.10%	\$6,231,934,694	\$5640278641	\$6914143147
500	0.20%	\$4,675,158,380	\$4257942187	\$5131864687
250	0.40%	\$3,369,852,487	\$3040190140	\$3629444795
100	1.00%	\$1,946,091,874	\$1871258702	\$2066301116
50	2.00%	\$1,316,941,577	\$1277204547	\$1366749173
20	5.00%	\$790,411,775	\$771982988	\$805465369
10	10.00%	\$535,246,191	\$526381889	\$545331325
5	20.00%	\$283,298,648	\$278370726	\$289478630

Table 32. Confidence Intervals for PML values.

4. Justify any differences between the historical and modeled results using current scientific and statistical methods in the appropriate disciplines.

As per Moriasi et al. (2007), $NSE = 0.75-1.00$ for a very good model; $NSE = 0.65-0.75$ for a good model; and $NSE = 0.50-0.65$ for a satisfactory model. Moriasi et al. (2007) also outlined the recommended RSR values for model performance evaluation. $RSR = 0.00-0.50$ for a very good model; $RSR = 0.50-0.60$ for a good model; and $RSR = 0.60-0.70$ for a satisfactory model. For the six inland flood models, NSE and RSR ranged between 0.62-0.96 and 0.20-0.61, respectively (Table 33-Table 38). These metrics values are confirmatory of good prediction performance of the inland flood models.

Station	Calibration period	Validation period	NSE		RSR	
			Calibration	Validation	Calibration	Validation
C-24 Canal at spillway S49	01/01/2006-12/31/2008	01/01/2009-12/31/2013	0.93	0.93	0.27	0.27
Loxahatchee Slough Canal at spillway S46	01/01/2004-12/31/2008	01/01/2009-12/31/2013	0.79	0.84	0.46	0.40
West Palm Beach Canal at spillway S155	01/01/2005-12/31/2008	01/01/2009-12/31/2013	0.79	0.85	0.46	0.39

Hillsboro Canal at spillway G56	01/01/2004-12/31/2008	01/01/2009-12/31/2013	0.76	0.82	0.49	0.42
North New River Canal at spillway G54	01/01/2004-12/31/2008	01/01/2009-12/31/2013	0.89	0.80	0.32	0.45
Miami River at spillway S26	01/01/2006-12/09/2008	01/01/2009-10/03/2011	0.84	0.75	0.40	0.50

Table 33. Model performance statistics for the Southeast Coasts (SEC) Basin.

Station	Calibration period	Validation period	NSE		RSR	
			Calibration	Validation	Calibration	Validation
Myakka River	01/01/2004-12/31/2009	01/01/2010-12/31/2014	0.69	0.7	0.55	0.55
Peace River	01/01/2004-12/31/2009	01/01/2010-12/31/2014	0.83	0.86	0.41	0.37
Withlacoochee River	01/01/2004-12/31/2009	01/01/2010-12/31/2014	0.82	0.65	0.48	0.58
Hillsborough River	01/01/2004-12/31/2009	01/01/2010-12/31/2014	0.7	0.83	0.55	0.41
Alafia River	01/01/2004-12/31/2009	01/01/2010-12/31/2014	0.72	0.76	0.49	0.47
Little Manatee River	01/01/2004-12/31/2009	01/01/2010-12/31/2014	0.68	0.80	0.56	0.45

Table 34. Model performance statistics for the Southwest Florida (SWF) Basin.

Station	Calibration period	Validation period	NSE		RSR	
			Calibration	Validation	Calibration	Validation
St. Johns River near Melbourne	01/01/2004-12/31/2008	01/01/2009-12/31/2013	0.78	0.66	0.47	0.58
St. Johns River near DeLand	01/01/2004-12/31/2008	01/01/2009-12/31/2013	0.78	0.62	0.47	0.61
St. Johns River near Satsuma	01/01/2004-12/31/2008	01/01/2009-12/31/2013	0.69	0.67	0.56	0.57
St. Johns River at Jacksonville	01/01/2004-12/31/2008	01/01/2009-12/31/2013	0.78	0.7	0.46	0.54

Table 35. Model performance statistics for the St. Johns River (SJN) Basin.

Station	Calibration period	Validation period	NSE		RSR	
			Calibration	Validation	Calibration	Validation
Escambia River	10/01/2012-09/30/2014	10/01/2014-09/30/2016	0.91	0.96	0.3	0.2
Apalachicola River	01/01/2009-12/31/2010	01/01/2012-12/31/2013	0.94	0.89	0.25	0.33

Oclocknee River	01/01/2009- 12/31/2010	01/01/2013- 12/31/2014	0.88	0.88	0.44	0.45
Choctawhatchee River	01/01/2009- 12/31/2010	01/01/2011- 12/31/2012	0.94	0.86	0.25	0.37

Table 36. Model performance statistics for the Northwest Florida (NWF) Basin.

Station	Calibration period	Validation period	NSE		RSR	
			Calibration	Validation n	Calibration	Validation
Confluence of three Rivers	01/01/2004- 12/31/2005	01/01/2006- 12/31/2007	0.93	0.92	0.26	0.26
Outlet of Suwannee River	01/01/2004- 12/31/2005	01/01/2006- 12/31/2007	0.8	0.92	0.45	0.26

Table 37. Model performance statistics for the Suwannee River (SWN) Basin.

Station	Calibration period	Validation period	NSE		RSR	
			Calibration	Validation n	Calibration	Validation
Shingle Creek at Campbell	1/1/2004- 12/31/2008	01/01/2009- 12/31/2013	0.71	0.74	0.54	0.51
Reedy Creek near Loughman	1/1/2004- 12/31/2008	01/01/2009- 12/31/2013	0.76	0.71	0.49	0.53
Arbuckle Creek near De Soto City	1/1/2004- 12/31/2008	01/01/2009- 12/31/2013	0.71	0.73	0.53	0.51
Kissimmee River near Basinger	1/1/2004- 12/31/2008	01/01/2009- 12/31/2013	0.8	0.74	0.44	0.51
Fisheating Creek at Palmade	1/1/2004- 12/31/2008	01/01/2009- 12/31/2013	0.74	0.7	0.53	0.55

Table 38. Model performance statistics for the Kissimmee River (KIS) Basin.

5. Provide graphical comparisons of modeled and historical data and goodness-of-fit evaluations. Examples to include are flood frequencies, flow, elevations or depths, and available damage.

The inland flood models were calibrated and validated with daily mean observed streamflow at many major streams of the state of Florida. Figure 49 and Figure 50 depict comparisons of modeled vs. observed streamflow during model calibration and validation for the Southeast Coasts (SEC) Basin of southeast Florida. Table 33-Table 38 outlined mode performance evaluation statistics (*NSE* and *RSR*) for all of the six inland flood models in the State of Florida.

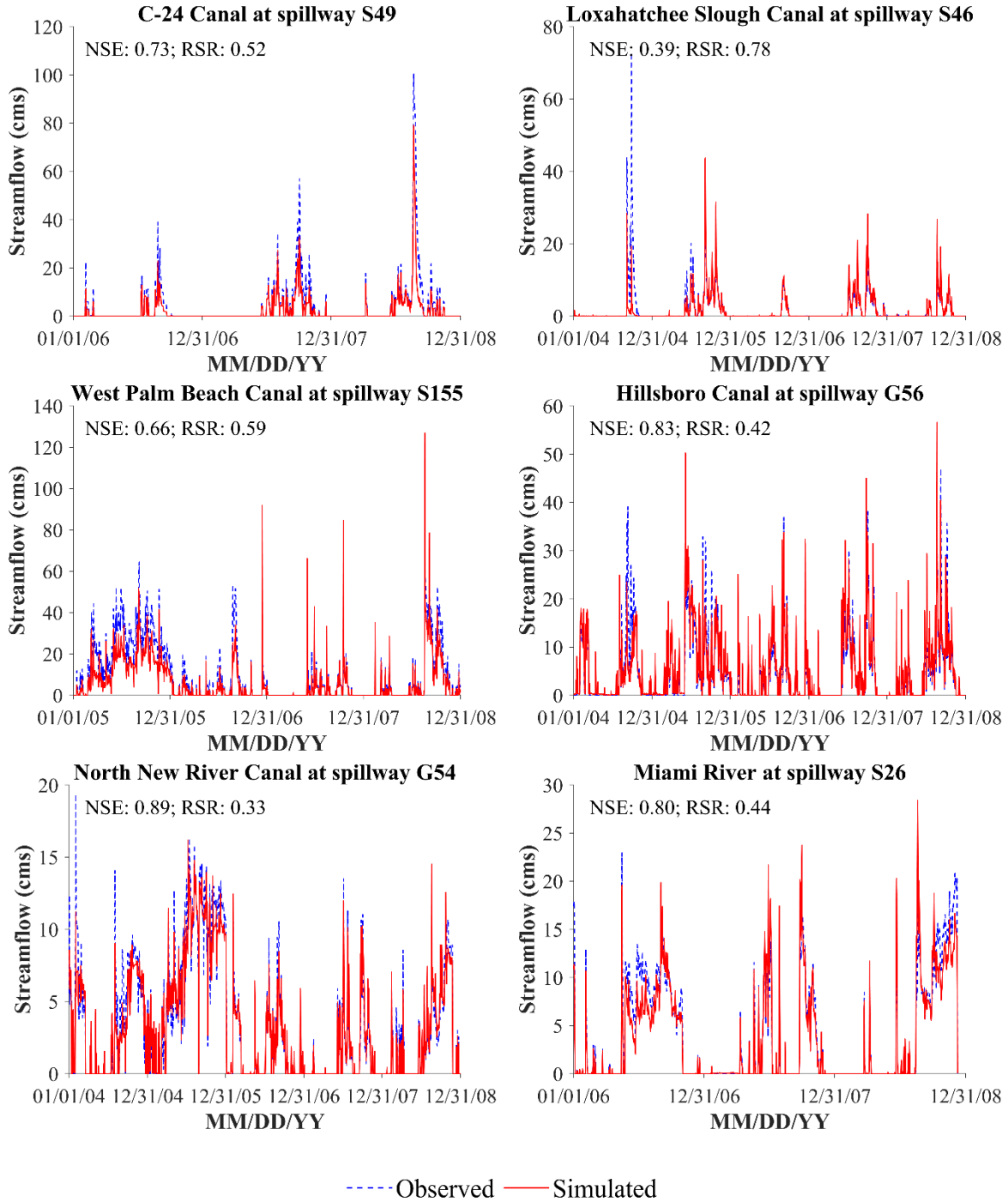


Figure 49. Comparison of observed and modeled daily mean streamflow during model calibration for the Southeast Coasts (SEC) Basin.

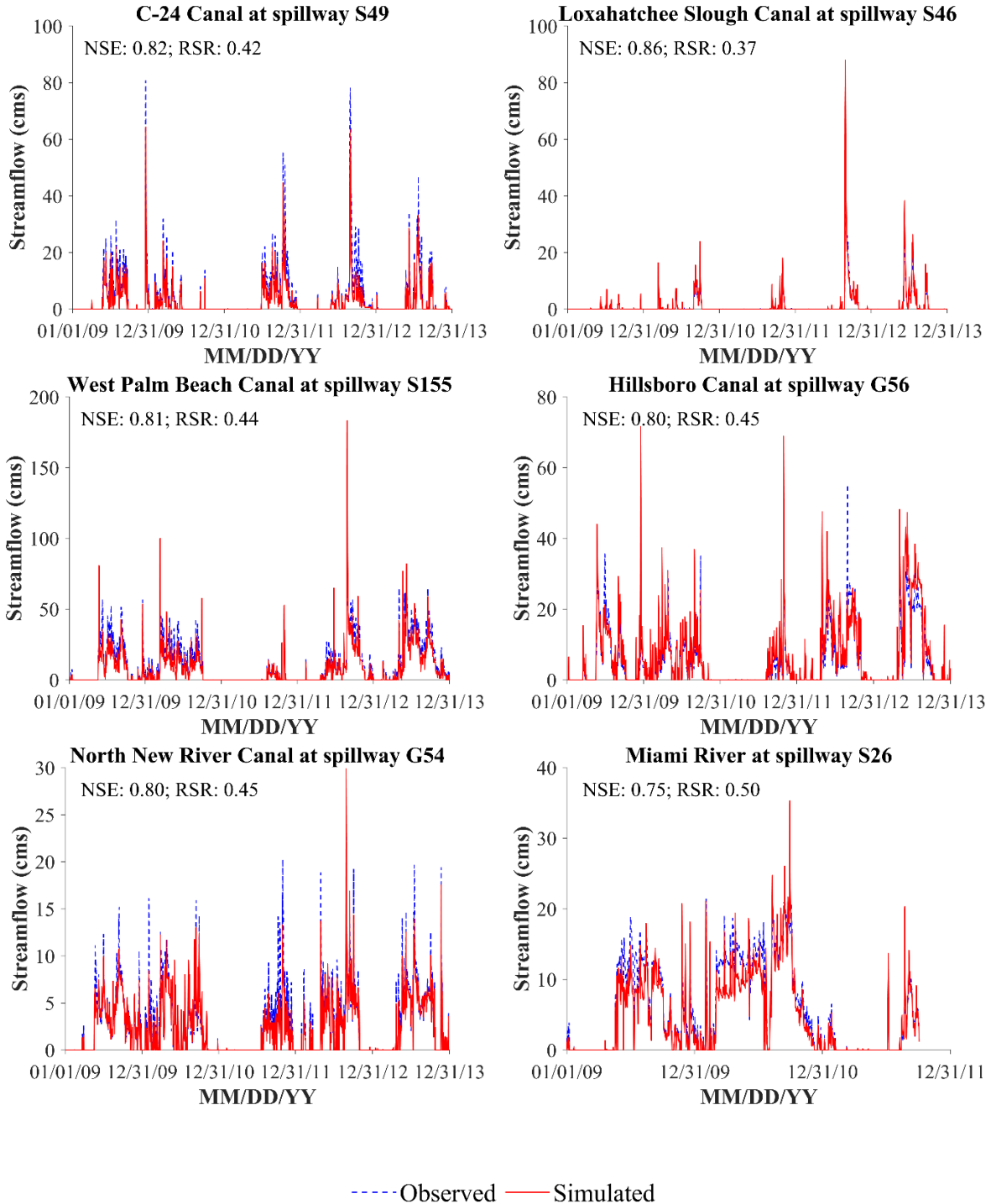


Figure 50. Comparison of observed and modeled daily mean streamflow during model validation for the Southeast Coasts (SEC) Basin.

In addition to running validation studies on the inland flood model we also ran some validation studies using storm surge modeling. This was done by considering a calibration study of the modeled storm surge with the historical storm surge. A total of 4 set of basins were established for

the storm surge calibration of historical hurricanes, covering the whole coastal area of Florida. The basins are as follows:

1. Apalachicola Bay basin, AP8, covering the northwest Florida coastal area;
2. Tampa Bay basin, TP3, covering the west Florida coastal area;
3. South Florida basin, HMI41, covering the south Florida coastal area with Florida Keys;
4. Florida Atlantic basin, EJX7, covering the east Florida coastal area.

We chose the basins as they all have already been calibrated for several historical hurricanes using H*Wind model. The historical hurricanes selected for the FPFLM-CEST validation are Andrew (1992), Frances (2004), Ivan (2004), Jeanne (2004), Katrina (2005), Wilma (2005), and also tropical storm Fay (2008). The storm surge calibration of historical hurricanes compares the observed and the computed High Water Marks (HWMs). Figure 51 depicts the scatter plot of observed HWMs versus simulated ones for Hurricane Andrew at HMI41 Basin with H*Wind. In addition to the HWMs, the time series of water level elevations recorded at several NOAA tidal gauges coasts were selected for model-data comparison. Figure 52 depicts the graphical comparison for Hurricane Jeanne 2004 at TP3 Basin and HMI41 Basin. Other results and figures can be found in [Form HHF-1](#).

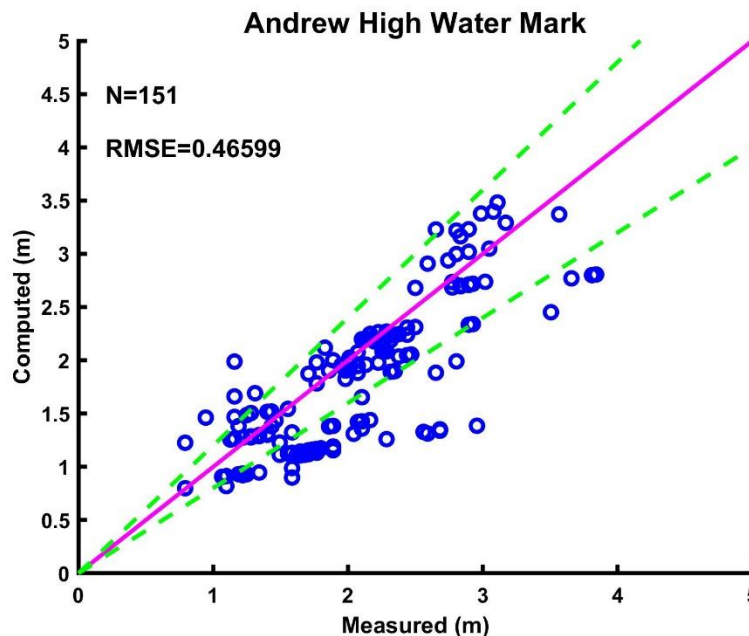


Figure 51. Scatter plots of observed peak surge heights versus simulated ones for Hurricane Andrew (HMI41 Basin with H*Wind). The purple solid line represents perfect simulations and the green dashed lines represent the boundaries of perfect simulations*(100±20)%. Both the computed and the observed peak surge heights are referenced to the NAVD88 vertical datum.

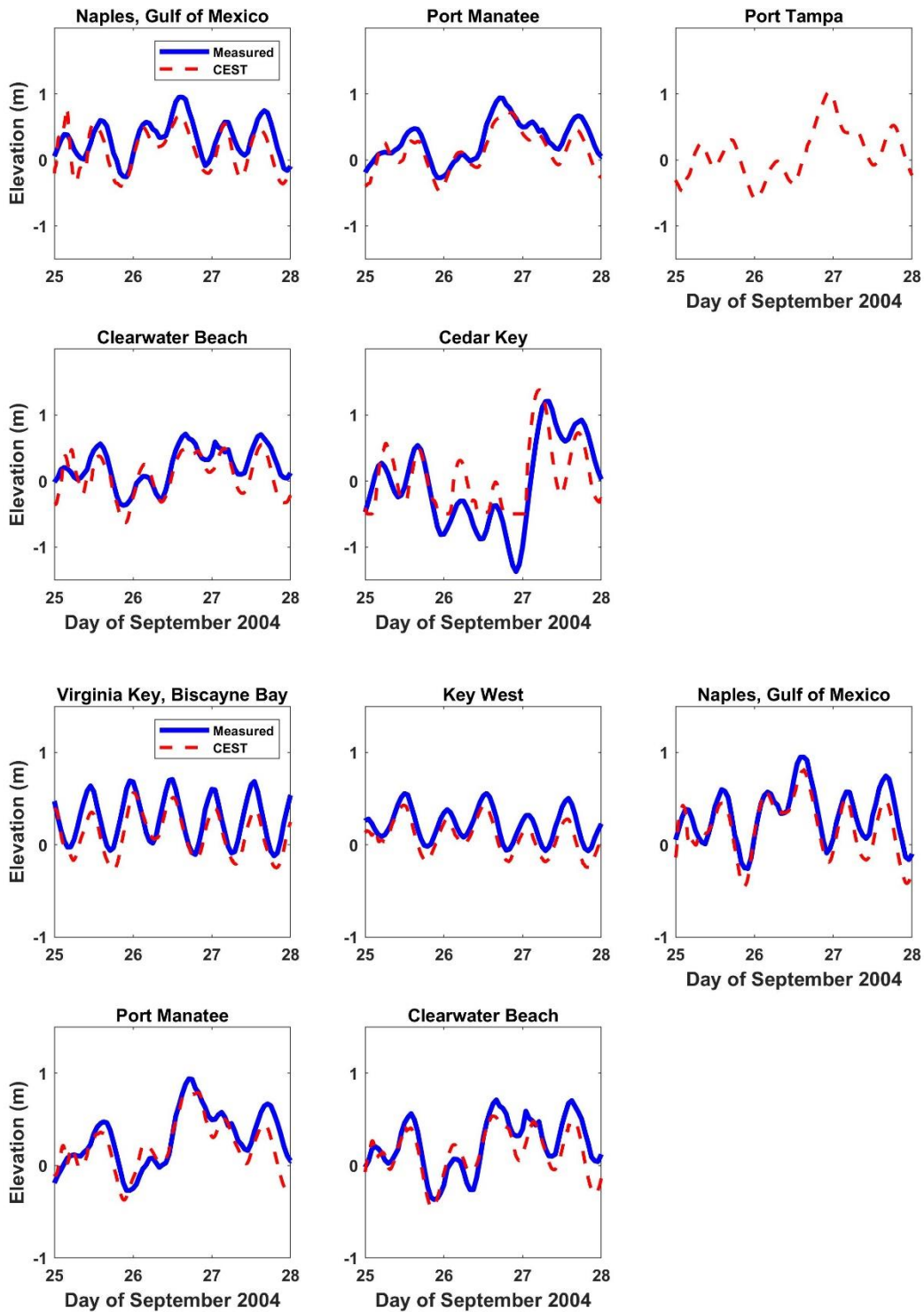


Figure 52. Comparison between the measured and the computed water levels at the NOAA stations during Hurricane Jeanne 2004: (A) TP3 Basin and (B) HMI41 Basin.

6. Provide a completed Form SF-2, Examples of Flood Loss Exceedance Estimates (Coastal and Inland Combined). Provide a link to the location of the form [insert hyperlink here].

Link to [Form SF-2](#).

SF-2 Sensitivity Analysis for Flood Model Output

The modeling organization shall have assessed the sensitivity of temporal and spatial outputs with respect to the simultaneous variation of input variables using current scientific and statistical methods in the appropriate disciplines and shall have taken appropriate action.

Disclosures

1. Identify the most sensitive aspects of the flood model and the basis for making this determination.

We computed monthly and annual runoff sensitivities for the Southeast Coasts Basin of southeast Florida, as an example, to identify the most sensitive aspects of inland flood model. Reference percent changes were applied to rainfall, potential evapotranspiration (PET), and imperviousness for the baseline 10-year period of 2004-2013 in this concern. These variables and parameter for the sensitivity analyses were chosen with reference to findings of Abdul-Aziz and Al-Amin (2015) on Miami River Basin in southeast Florida. The reference change scenarios were formed based on the potential future changes in climate and percent impervious surface. The baseline values for rainfall, PET, and imperviousness were perturbed from -30 to +30% (with an increment of 5%) to address the overall range of anticipated changes in climate and land cover. Runoff percent changes were computed for both individual (one-at-a-time) and concurrent (two-at-a-time) changes in rainfall, PET, and imperviousness.

The 10-year mean monthly runoffs in the Southeast Coasts Basin showed notably different sensitivities in response to standalone -30 to +30% changes in rainfall. Higher runoff sensitivities (-52 to +67% changes) were witnessed during the wet season months, i.e., June-September due to substantially high rainfall depth and increased number of rainfall events. Runoff sensitivities to rainfall were substantially lower in the dry season (November-April) than that in the wet season with -46 to +59% changes. Annual basin runoff varied from -48 to +59% under -30 to +30% changes in rainfall. Individual changes in PET of -30 to +30% also produced higher monthly runoff sensitivities of -16 to +27% in the wet season than the dry season. For the dry season months, runoff sensitivity to changing PET ranged from -10 to +18%. Annual basin runoff sensitivities to changing PET were +20 to -12%. Monthly runoff sensitivities to imperviousness were higher in the dry season than that in the wet season. Subject to -30 to +30% changes in imperviousness, monthly runoff during dry season months varied from -27 to +26%; wet season runoff sensitivities ranged from -17 to +17%. Annual runoff sensitivities to changing imperviousness were -16 to +16%. Therefore, the individual sensitivity results clearly represent rainfall as the most dominant driver of inland flood model outputs, i.e., flood depths.

2. Identify other input variables that impact the magnitude of the output when the input variables are varied simultaneously. Describe the degree to which these sensitivities affect output results and illustrate with an example.

As mentioned in disclosure 1, we also quantified runoff sensitivities under simultaneously changing climate and land cover in the Southeast Coasts Basin. Concurrent changes in these drivers produced stronger non-linear responses of annual basin runoff than the linear summation of their standalone individual impacts. For example, when impacts of standalone +30% changes in rainfall and imperviousness (runoff increase of 58% and 17% respectively) were summed, it was 5% points higher than the impact of simultaneous and similar changes in these variables on annual runoff. Concurrent 30% increase in rainfall and 30% decrease in PET produced the maximum increase in annual basin runoff of 85%, which was 6% points higher than the algebraic summation of their standalone individual contributions. However, in case of simultaneous PET-imperviousness changes, the runoff responses were almost identical to their aggregated, isolated impacts. Therefore, under synergic effects of concurrently changing rainfall-PET and rainfall-imperviousness, stronger non-linear responses of the inland flood model are generally anticipated.

3. Describe how other aspects of the flood model may have a significant impact on the sensitivities in output results and the basis for making this determination.

Based on the sensitivity results for the Southeast Coasts Basin (disclosure 1), as an example, PET and imperviousness may also have a controlling impact on sensitivity of the inland flood model outputs.

4. Describe and justify action or inaction as a result of the sensitivity analyses performed

Sensitivity analyses for rainfall, PET, and imperviousness for the Southeast Coasts Basin, as an example, helped to understand the relative role of these crucial drivers on inland flood model response. For the other five inland basins, due considerations were given in data collection for these variables and parameter since they can significantly affect the model outputs.

SF-3 Uncertainty Analysis for Flood Model Output

The modeling organization shall have performed an uncertainty analysis on the temporal and spatial outputs of the flood model using current scientific and statistical methods in the appropriate disciplines and shall have taken appropriate action. The analysis shall identify and quantify the extent that input variables impact the uncertainty in flood model output as the input variables are simultaneously varied.

Disclosures

- 1. Identify the major contributors to the uncertainty in flood model outputs and the basis for making this determination. Provide a full discussion of the degree to which these uncertainties affect output results and illustrate with an example.**

Uncertainty in a dataset can be quantified based on its coefficient of variation (ratio of standard deviation over mean) and relative standard error (ratio of coefficient of variation over square root of sample size). Table 1 summarizes mean, standard deviation, coefficient of variation, standard error (ratio of standard deviation over square root of sample size), and relative standard error of subbasin-scale major variables/parameters and runoff (i.e., flood depth) for inland flood model in the Southeast Coasts Basin, as an example. The major contributors of uncertainty in model output are saturated hydraulic conductivity of soil, percent imperviousness, subbasin slope, and groundwater exchange coefficient (*AI*). For these parameters, coefficient of variation and relative standard error ranged between 38.2 to 84.9%, and 2.1 to 4.7%, respectively. Uncertainty in these parameters resulted in coefficient of variation and relative standard error of 75% and 4.1%, respectively, for subbasin-scale 10-year mean annual runoff volume during 2004-2013.

Parameter/Variable	Mean	Standard deviation	Coefficient of variation (%)	Standard error	Relative standard error (%)
Roughness coefficient of impervious subarea	0.02	2.1×10^{-3}	13.01	1.1×10^{-4}	0.71
Roughness coefficient of pervious subarea	0.13	0.04	31.05	2.3×10^{-3}	1.70
Depression storage depth of impervious subarea (mm)	2.08	0.29	13.89	0.02	0.76
Depression storage depth of pervious subarea (mm)	5.80	1.16	19.98	0.06	1.09
Saturated hydraulic conductivity (mm/hr)	10.30	3.93	38.18	0.22	2.09
Imperviousness (%)	27.09	17.23	63.61	0.94	3.49
Subbasin slope (%)	1.10	0.94	84.90	0.05	4.65
Soil porosity	0.46	0.02	3.77	9.5×10^{-4}	0.21
Groundwater exchange coefficient, AI	0.01	0.01	47.39	3.5×10^{-4}	2.60

Mean annual rainfall depth (mm)	1346.41	129.50	9.62	7.10	0.53
Mean annual runoff volume (m ³)	5477023.58	4109577.69	75.03	225203.47	4.11

Table 39. Summary statistics for subbasin-scale major parameters, forcing variable, and model output in the Southeast Coasts (SEC) Basin.

2. Describe how other aspects of the flood model may have a significant impact on the uncertainties in output results and the basis for making this determination.

For the Southeast Coasts Basin, as an example, other subbasin-scale variable/parameters that contributed to uncertainty in inland flood model output are roughness coefficients (for pervious and impervious subarea), depression storage depths (for pervious and impervious subarea), soil porosity, and 10-year mean annual rainfall for 2004-2013. For these parameters and variable, coefficient of variation and relative standard error ranged between 3.8 to 31.1%, and 0.2 to 1.7%, respectively.

3. Describe and justify action or inaction as a result of the uncertainty analyses performed.

Identification of the major and minor contributors of uncertainty in the inland flood model for the Southeast Coasts Basin, as an example, also aided in parameterization for different subbasins across the five other inland basins. Due considerations were given to conceptualization of the local hydrological settings and availing of appropriate data sources, while incorporating those parameters and variable to inland flood model for the five basins.

SF-4 Flood Model Loss Cost Convergence by Geographic Zone

At a modeling-organization-determined level of aggregation utilizing a minimum of 30 geographic zones encompassing the entire state, the contribution to the error in flood loss cost estimates attributable to the sampling process shall be negligible for the modeled coastal and inland flooding combined.

The error in the zone level loss costs induced by the sampling process can be quantified by computing standard errors for the zone level loss costs. These loss costs have been computed for 30 zones in the state of Florida using 50,000 years of simulation. The results indicate that the standard errors are less than 5% of the average loss cost estimates for 29 zones and less than 6% for one of the zones.

Disclosures

- 1. Describe the sampling plan used to obtain the average annual flood loss costs and flood output ranges. For a direct Monte Carlo simulation, indicate steps taken to determine sample size. For an importance sampling design or other sampling scheme, describe the underpinnings of the design and how it achieves the required performance.***

Our aim was to achieve convergence using 30 geographic zones. Geographic zones for the model were defined by a selection of coastal locations along the Florida coast. Each zone was determined by proximity to a specified coastal location. A policy was determined to be in a zone if the policy was closer to the specified zone coastal location than any other zonal coastal location. The basic procedure to determine the zone for a given policy was to loop through all of the specified zone locations and choose the one that was closest by distance.

Once we determined the zones, the number of simulation years was determined through the following process:

The average loss due to flood, \bar{x}_Y , and standard deviation S_Y , were determined for each zone Y using an initial run of 10,000-year simulation. Then the maximum error of the estimate will be 5% of the estimated mean loss cost, if the number of simulation years for county Y is:

$$N_Y = \left(\frac{S_Y}{0.05\bar{X}_Y} \right)^2$$

Based on the initial 10,000-year simulation run, the minimum number of years required is $N_Y = 72,540$

for Zone 19, which had the highest number of years required of all the zones. However using 72,540 years significantly increases the computational time required to run the model. As a result, the team members decided that it was best to use 50,000 years to generate losses as this keeps the computational time reasonable and the standard errors for all but one zone are less than 5% of the

estimated mean loss. Even for the zone 19, the standard error is 5.9% of the estimated mean loss which is not significantly higher than 5%.

2. Describe the nature and results of the convergence tests performed to validate the expected flood loss projections generated. If a set of simulated flood events or simulation trials was used to determine these flood loss projections, specify the convergence tests that were used and the results. Specify the number of flood events or trials that were used.

Losses were generated for 50,000 for each zone and the mean \bar{x}_Y and the standard deviation S_Y of these losses were computed. The standard error was then computed as $\frac{S_Y}{\sqrt{50,000}}$ for each zone and verified to be within 5% of the mean for all zones except for zone 19 where it is found to be 5.9% of the mean loss.

SF-5 Replication of Known Flood Losses

The flood model shall estimate incurred flood losses in an unbiased manner on a sufficient body of past flood events, including the most current data available to the modeling organization. This standard applies to personal residential exposures. The replications shall be produced on an objective body of flood loss data by county or an appropriate level of geographic detail.

Due to the lack of a sufficient body of claims data for flood losses, extensive statistical tests were not conducted to validate the model losses. A tabular comparison of the modeled vs. actual flood insured loss costs will be provided.

Disclosure

- 1. Describe the nature and results of the analyses performed to validate the flood loss projections generated for personal residential losses. Include analyses for the events listed in Form HHF-1, Historical Event Flood Extent and Elevation or Depth Validation Maps.***

Will be provided.

VULNERABILITY FLOOD STANDARDS

VF-1 Derivation of Personal Residential Structure Flood Vulnerability Functions

A. Development of the personal residential structure flood vulnerability functions shall be based on two or more of the following: (1) rational structural analysis, (2) post-event site investigations, (3) technical literature, (4) expert opinion, (5) laboratory or field testing, and (6) insurance claims data. Personal residential structure flood vulnerability functions shall be supported by historical and other relevant data.

The development of the coastal flood vulnerabilities is based on a semi-engineering approach, which translates empirical tsunami fragility functions into coastal flood fragility functions, based on engineering principles. The coastal flood fragility functions translate into coastal flood vulnerability functions for different types of residential structures common in the state of Florida. The characterization of the damage states corresponding to each fragility function, based on a detailed cost analysis provides the basis for the translation of the fragilities into vulnerabilities.

The inland flood vulnerabilities are derived from the work of the US Army Corp of Engineers (USACE) vulnerability curves, based on expert opinion.

Claims data and expert-based models validated both the coastal and inland flood models.

B. The derivation of personal residential structure flood vulnerability functions and their associated uncertainties shall be theoretically sound and consistent with fundamental engineering principles.

The conversion of the fragility functions from tsunami to coastal flood relies on the calculation of the different inundation depths that produce equivalent water-forces. The forces considered are the resultant lateral horizontal forces acting on the vertical walls of the structures. Both the tsunami and the coastal flood water depth-force relationships needed for the development of the coastal flood fragility functions were adopted from well-recognized engineering literature.

Uncertainties in the derivation of the tsunami fragility functions used in the derivation result from the empirical development of these functions. The tsunami fragility uncertainties transfer to the coastal flood fragility curves. The FPFLM team estimated these uncertainties involved in the conversion from coastal flood fragility curves to coastal flood vulnerability curves, including the uncertainty attached to the damage states quantification.

The FPFLM inland flood model is adapted from the USACE work, which is based on expert opinion, informed by engineering principles.

C. Residential building stock classification shall be representative of Florida construction for personal residential structures.

A detailed exposure study defined the most prevalent construction types and characteristics in the Florida residential building stock. The corresponding models represent each of the identified common structural types. In the case of the residential model, the models include differing wall types (wood and masonry) of varying strengths (weak or strong), and one to three story houses, as applicable, as well as manufactured homes.

D. The following flood characteristics shall be used in the derivation of personal residential structure flood vulnerability functions: depth above ground, and in coastal areas, damaging wave action.

The vulnerability functions for all personal residential models (site-built residential, and manufactured homes,) are derived as a function of inundation depth. In coastal areas, these depth-to-damage functions incorporate damaging wave action.

E. The following primary building characteristics shall be used or accounted for in the derivation of personal residential structure vulnerability functions: lowest floor elevation relative to ground, foundation type, construction materials, and year of construction.

The various personal residential models reflect the construction materials, timber or masonry, as well as the lowest floor elevation relative to ground, and the foundation type (slab on grade or elevated). The structural models also allow the representation of year of construction. Two models exist for each structural type: weak construction, and strong construction. For example, each model for wood frame homes has weak and strong versions. The assignment of a given strength level depends on the age of the home being modeled and the available information on construction practice in that region of the state in that era of construction. Separate models also exist for manufactured housing constructed based on pre- and post-1994 HUD regulations and for different flood conditions. Lowest floor elevation relative to ground is explicitly represented for each model type in 1 foot increments. For example, the weak timber frame on-grade models include separate outputs for 0, 1, 2 and 3 foot lowest floor elevations.

F. Flood vulnerability functions shall be separately derived for personal residential building structures and manufactured homes.

Flood vulnerability functions were separately derived for personal residential building structures and manufactured homes. As described in detail within, personal residential building structure vulnerability functions are derived based on an adaptation of tsunami fragility functions to reflect coastal flood forces. Manufactured home vulnerability functions are adapted from USACE reports.

Disclosures

- 1. Provide a flowchart documenting the process by which the personal residential structure flood vulnerability functions are derived and implemented.***

The flow charts below summarize the procedure used to develop the coastal flood and the inland flood vulnerability functions for the different structural types of personal residential buildings.

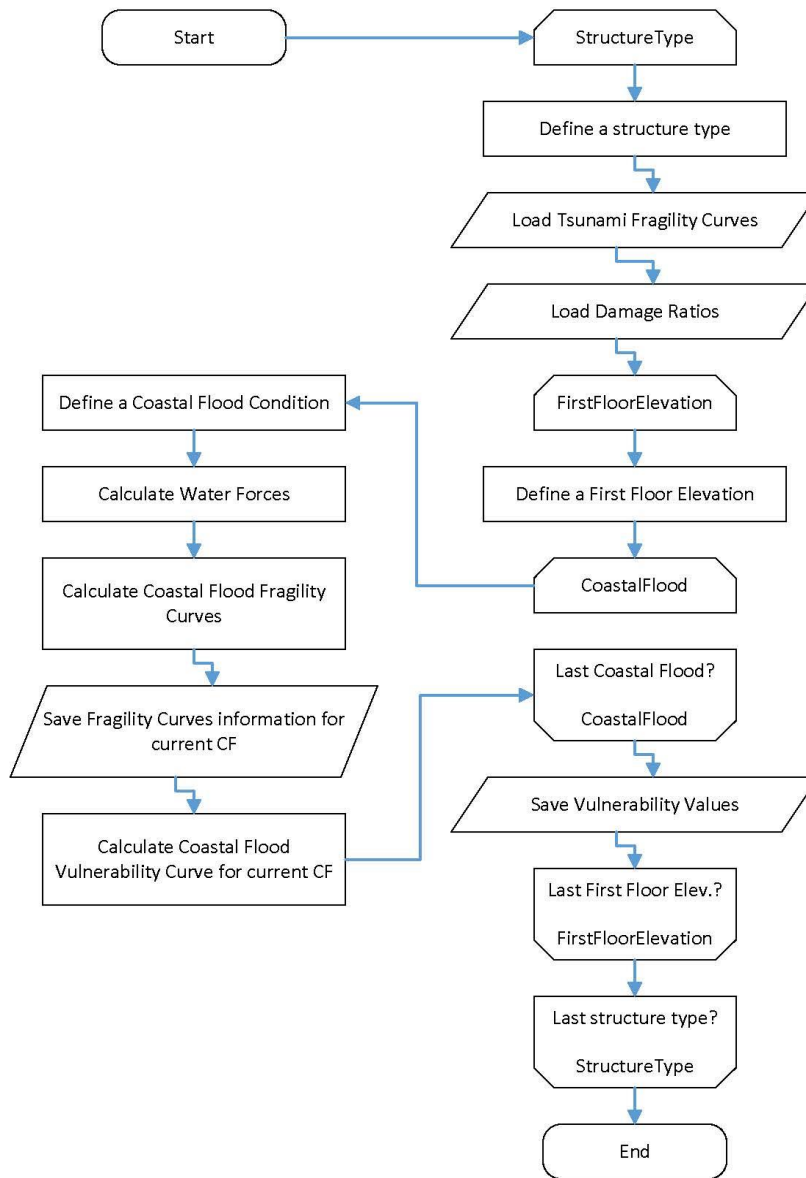


Figure 53. Coastal flood vulnerability for residential structures.

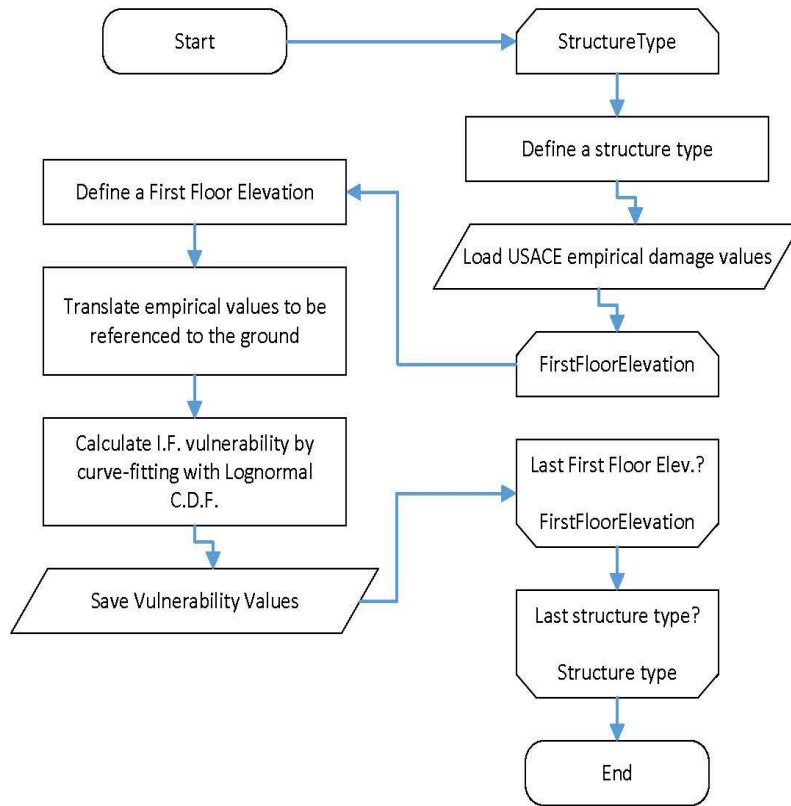


Figure 54. Inland flood vulnerability for residential structures.

2. Describe the assumptions, data, methods, and processes used for the development of the personal residential structure flood vulnerability functions.

Site-Built Homes

The assumptions, data, methods and processes used for the development of the personal residential structure coastal flood vulnerability functions are detailed in the GF-1 Disclosure 2 standard under the section entitled: **Vulnerability of site-built residential structures to Coastal Flood.**

The assumptions, data, methods and processes used for the development of the personal residential structure inland flood vulnerability functions are detailed in the GF-1 Disclosure 2 standard under the section entitled: **Vulnerability of site-built residential structures to Inland Flood.**

Manufactured Homes

The assumptions, data, methods and processes used for the development of the manufactured home structure coastal and inland flood vulnerability functions are detailed in the GF-1 Disclosure 2

standard under the section entitled: **Vulnerability of manufactured housing to Inland and Coastal Flood.**

- 3. As applicable, describe the nature and extent of actual insurance claims data used to develop the personal residential structure flood vulnerability functions. Describe in detail what is included, such as, number of policies, number of insurers, dates of loss, and number of units of dollar exposure, separated into personal residential building structures and manufactured homes.**

NFIP claims database

FLOIR provided the National Flood Insurance program (NFIP) claims and exposure portfolios to the FPFLM team. The claims database contains 153,751 claims between July 1975 and January 2014 for 126 different events. The NFIP exposure portfolios exist for each year from 1992 to 2012. The hazard team combined the exposure portfolios into one file containing all policies between 1992 and 2012. They also analyzed the claims data locations and dates to associate a specific hazard to a given claim. From these datasets, a trial dataset of 58551 personal residential claims from the twelve storms with the most claims were chosen for validating the FPFLM. NFIP has a very limited number of claims for manufactured homes in Florida. The specifics for each dataset are provided in Table 40. The twelve storms are listed in Table 41.

The coastal flood and wave teams provided hazard information for all 12 storms, but the inland flood team was able to provide hazard outputs only for the post 1999 storms (Irene, Charlie, Francis, Jeanne, Dennis, Wilma, Ivan, and Katrina).

The NFIP claim files contain information such as the date of loss, policy number, physical address, cause of damage, total property value, financial damage to building and contents, and replacement cost. Fields are present in the files for structural information such as exterior wall type and foundation type, but do not contain values for 97% of the claims. The exposure files contain policy number, flood zone, address, original construction date, base flood elevation, and other data, but no structural building information.

Description	Number of Records
NFIP Exposure Portfolios (by year, 1992-2012)	~ 22 million
NFIP Claims Portfolio (all events)	153,751
NFIP Claims Portfolio (8 events)	43,552
NFIP Claims Portfolio (12 events)	58,551

Table 40. NFIP claim and exposure datasets.

Building use (code)	Storm name	Building use (quantity)	Property Value (total)	Manufactured Homes (quantity)
	Andrew	2122	\$ 498,423,966	0

01 – Main House/Building	Charley	824	\$ 185,651,732	0
	Dennis	1885	\$ 219,463,483	0
	Elena	5151	\$ 404,763,826	0
	Frances	2923	\$ 5,591,654,970	0
	Georges	2422	\$ 27,539,250,986	0
	Irene	10626	\$1,399,127,662,709	1
	Ivan	3733	\$ 20,323,497,987	0
	Jeanne	2176	\$ 378,586,379	0
	Katrina	4173	\$ 5,170,407,511	0
	Opal	2946	\$ 361,648,781	0
	Wilma	5027	\$ 751,551,640	0
02 – Detached Guest House	Andrew	403	\$ 135,387,754	0
	Charley	493	\$ 1,436,111,215	6
	Dennis	1199	\$ 3,467,182,836	0
	Elena	371	\$ 42,581,009	0
	Frances	711	\$ 2,016,828,955	4
	Georges	953	\$ 27,312,215,303	0
	Irene	1585	\$ 108,212,199,325	0
	Ivan	3271	\$ 5,618,068,371	0
	Jeanne	596	\$ 346,335,534	16
	Katrina	695	\$ 137,580,927	0
	Opal	2476	\$ 17,732,382,487	0
	Wilma	1746	\$ 8,328,694,934	0
06 – Poolhouse/Club house/Other Recreational	Andrew	0	\$ -	0
	Charley	0	\$ -	0
	Dennis	8	\$ 780,522	0
	Elena	0	\$ -	0
	Frances	5	\$ 566,350	0
	Georges	0	\$ -	0
	Irene	4	\$ 241,865	0
	Ivan	18	\$ 2,311,141	0
	Jeanne	3	\$ 850,936	0
	Katrina	4	\$ 383,529	0
	Opal	0	\$ -	0
	Wilma	2	\$ 184,162	0
Total		58551	\$ 1,635,343,451,125	27

Table 41. Hurricane events currently included in the NFIP database.

4. Summarize post-event site investigations, including the sources, and provide a brief description of the resulting use of these data in the development or validation of personal residential structure flood vulnerability functions.

Tsunami damage dataset

The FPFLM team adopted a semi-engineering approach, which adapts a procedure proposed in Barbato et al. (2013) to translate empirical tsunami fragility functions from Suppasri et al. (2013) into coastal flood fragility functions, based on engineering principles. The tsunami fragilities are the result of a post-event field investigation. See GF-1 Disclosure 2 standard under the section entitled: **Vulnerability of site-built residential structures to Coastal Flood, Section 2.**

describes the resulting data, section 3 describe the use of these data, and section 6 presents an example of its use for model validation.

US Army Corps of Engineers Vulnerability Curves.

US Army Corps of Engineers (USACE, 2015) developed a set of vulnerability curves for different structures based on expert opinions informed in part by post-disaster damage assessments. See GF-1 standard Disclosure 2 under the section entitled: **Vulnerability of site-built residential structures to Coastal Flood, Section 6.3** describes the USACE data, and how it was use for validation of the coastal flood vulnerabilities. GF-1 standard Disclosure 2 under the section entitled: **Vulnerability of site-built residential structures to Inland Flood** describes its use in the development of inland flood vulnerabilities.

FEMA Estimates of Flood Elevations for Hurricane Ivan

There are relatively few observations of flood elevation and wave conditions for historical flood events, particularly at the resolution of claims data. For Hurricane Ivan (2004), FEMA has published some resources on flood elevation for this event. These include high water marks, flood surge height contours and an inundation map (available at <https://www.fema.gov/geographic-information-systems-data> as of 10/22/19). High water marks along with engineering judgment form the basis for the flood contour lines. The inundation maps indicate all locations that experienced flooding, regardless of surge height. These data are highly correlated to observed flood damage. The FPFLM team derived estimated surge heights at NFIP claims data locations for Ivan by using an interpolation algorithm between the closest points to the FEMA surge contour elevations and the target claim location. The method used an inverse distance squared weighting method when the target location was between two contours, and a nearest neighbor extrapolation otherwise. The domain of the FEMA data, which covers 3 counties, Escambia, Okaloosa and Santa Rosa, was divided into zones, so that interpolation was not done across contours that were in separate regions divided by dry land masses.

The FEMA data combined with the NFIP database described in Disclosure 3, enhanced with building construction details from the tax appraiser databases, was used to validate the FPFLM outputs as described in GF-1 standard Disclosure 2 under the section entitled: **Vulnerability of site-built residential structures to Coastal Flood, Section 6.4** .

5. Describe how the personal residential structure flood vulnerability functions incorporate depth of flooding (above ground and above lowest floor) and damaging wave action (in coastal areas). For coastal areas, define the thresholds indicating the presence of damaging wave action for personal

residential building structures and manufactured homes. Describe the area over which vulnerability functions for damaging wave action or wave proxies are applied.

The vulnerability functions are derived as a function of hazard intensity in the form of flood depth above ground. Vulnerability outputs for any given structural model include results for each or several first floor elevations (FFE) above ground. For example, the model representing one-story masonry on-grade construction includes outputs for 0, 1, 2, and 3 foot FFE. For each FFE, vulnerability as a function of flood depth above ground is derived for four separate hydrologic states: slow rising flood – no waves, flood with minor waves, flood with moderate waves, and flood with severe waves. Thus, the one-story masonry on-grade model vulnerability is represented by 16 possible outputs as a function of flood depth above ground. These consist of four possible FFEs, each with four possible hydrologic states. Figure 55 shows a comparison of Inland and Coastal Flood vulnerability results for a one-story slab on-grade reinforced masonry structure at 0 and 3 ft FFEs.

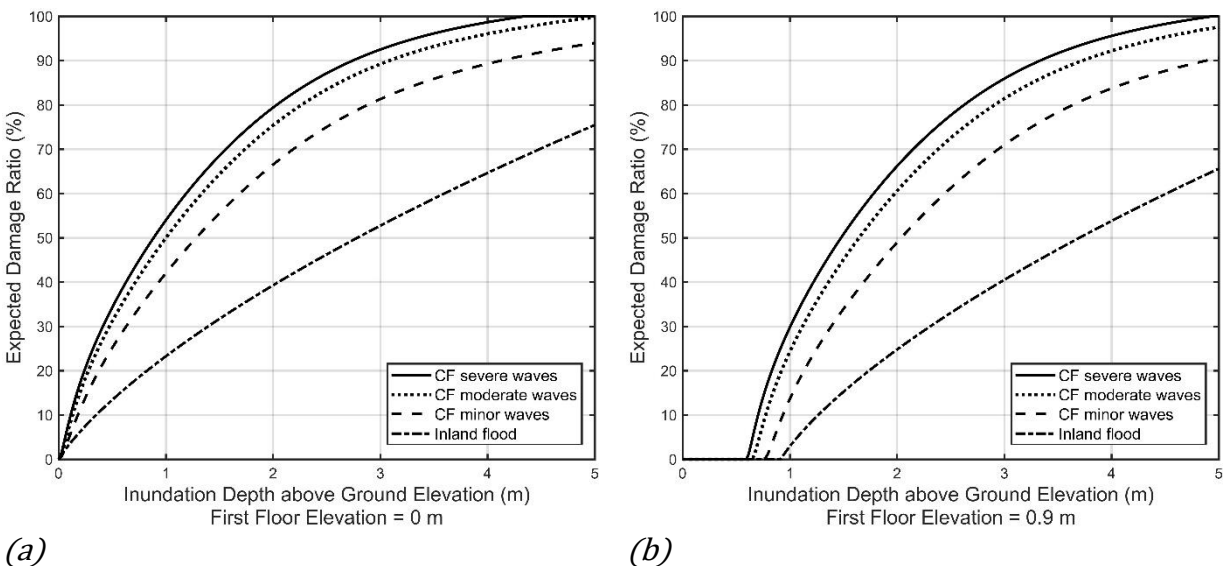


Figure 55. FPFLM Inland and Coastal flood vulnerability, a) 1-story slab on-grade reinforced masonry, 0 m FFE; b) 1-story slab on-grade reinforced masonry, 0.9 m FFE.

The thresholds indicating the presence of damaging wave action is not specified within the vulnerability model. Rather, the inland flood, surge and wave hazard model outputs are used to assign one of the four hydrologic states to a given structure. This assignment then dictates which of the four separate vulnerability functions (one for each hydrologic state) to select to model damage.

6. State if the following flood characteristics are considered in the development of the personal residential structure flood vulnerability functions, and if so, how; if not, explain why:

a. Flood velocity,

- b. Flood duration,**
- c. Flood-induced erosion,**
- d. Flood-borne debris,**
- e. Salinity (saltwater versus freshwater flooding), and**
- f. Contaminated floodwaters.**

The FPFLM flood vulnerabilities does not explicitly include any of the above parameters. The hazard models for coastal and inland floods do not quantify these parameters. They provide flood depth and wave height. However, the descriptions of the coastal flood damage states (Table 11, located in GF-1 standard Disclosure 2 under the section entitled: **Vulnerability of site-built residential structures to Coastal Flood** does qualitatively include damage from flood-borne debris. Additionally, all field data that was utilized implicitly includes flood-borne debris, erosion, velocity and salinity. This applies to both the tsunami fragility functions used as the basis of the coastal flood model and the NFIP claims data used for validation.

7. Describe how the personal residential structure flood vulnerability functions incorporate the following primary building characteristics:

- a. Lowest floor elevation relative to ground,**
- b. Foundation type,**
- c. Primary construction materials, and**
- d. Year of construction.**

Lowest floor elevation: As discussed in Disclosure 5, any given structural model is derived separately for a series of first floor elevations (FFE). This is not a simple shift of the same vulnerability curve. For example, the 3 ft FFE output is not equivalent to shifting the 1 ft FFE curve by 2 feet. Rather, the combination of flood depth and wave state at which a structure will begin to experience wetting of the FFE is explicitly calculated.

Foundation type: on-grade and elevated foundation types are modeled separately. The vulnerability of the foundation type is incorporated within the building vulnerability via the component cost analysis described in Section 4 of the Vulnerability Development description above.

Primary construction materials: Models were derived separately for timber frame and masonry construction materials. The tsunami fragilities based on field data were stratified by material type.

Thus conversion to coastal flood models were thus separately performed based on material type. Timber frame models are more vulnerable than masonry models, all other parameters equal (number of stories, age, FFE, hazard intensity).

Year of construction: For both material types (timber frame and masonry), a weak and strong version of these models was derived to reflect changes in construction methods over time. The current level of granularity in the model uses 2002 as the separation date between weak (older) and strong (newer) models, as this reflects the statewide adoption of the Florida Building Code. Weak and strong models differ by the assignment of damage ratios during the conversion from coastal flood fragility to coastal flood vulnerability.

8. State if the following building characteristics are considered in the development of the personal residential structure flood vulnerability functions, and if so, how; if not, explain why:

a. Number of stories,

Yes. The FPFLM provides separate on-grade and elevated 1, 2, and 3 story structures. This is stratification by story was included within the tsunamic fragility dataset.

b. Use of each story (e.g., habitable space, parking, storage, other),

No. No field or claim data was available to validate the incorporation of this parameter.

c. Presence of basement,

No. A modification to incorporate basements was investigated but not developed. During the initial investigation, NFIP claims data were analyzed to identify a target nominal difference in damage between like structures with and without basement (e.g. one story single family on-grade). The claims data were stratified accordingly and damage ratios (ratio of claim to building value) produced for single family structures, with and without basement. The resultant frequency of claims as a function of damage ratio were essentially identical for no-basement and with-basement. Given that the vulnerability model output is a damage ratio, development of a separate basement model was not justified or necessary since the claims analysis reveals that the target output should be the same. This is not a statement that a house without a basement and an identical house with a basement would suffer the same nominal loss at the same location for the same event. On the contrary, the house with basement would suffer a larger loss. However, the building value of the house with basement is necessarily larger than the identical house without basement. As such, the larger nominal loss for the house with basement is proportionally offset by the larger building value, thus the equivalent damage ratios observed in the NFIP claims analysis. Finally, the NFIP claims data shows that only ~ 0.6% of the single family homes in Florida have a basement.

d. Replacement value of building,

Yes. The building replacement value is the denominator of the damage ratio.

e. Structure value by story,

No. No field or claim data is available to validate the incorporation of this parameter

f. Square footage of living area, and

Yes. The cost analysis includes consideration of the square footage. The replacement values of a home is partially a function of the square footage.

g. Other construction characteristics, as applicable.

None.

9. Describe the process by which local construction practices, statewide and county building code, and floodplain management regulation adoption and enforcement are considered in the development of personal residential structure flood vulnerability functions.

The influence of construction practices, building codes and floodplain management regulations are incorporated within the personal residential structure flood vulnerability functions by two characteristics: first floor elevation relative to ground and model strength.

As described in Disclosures 5 & 7, each structural model is developed for each of multiple FFEs in increments of 1 foot. During model execution, the model with the appropriate FFE is assigned based on one of two possible scenarios. The first scenario accesses the NFIP exposure data field that defines the FFE relative to NAVD 88. A 5m DEM map from the Florida Geographic Data Library (FGDL, 2012) is used to convert this FFE to the local ground elevation frame of reference. This then directly defines the appropriate FFE option. The second scenario is engaged if the first scenario fails, either because the NFIP data field is not filled in, or if the resultant FFE relative to ground is not realistic (e.g. negative or positive 20 feet). In such cases, local base flood elevation (BFE) is used in the process of assigning a particular FFE to a given property. The address and age of the property in the exposure is used to determine whether that structure was built before or after BFE maps were assigned to that region. If built after, the FFE is assigned to BFE (referenced to local elevation) plus one foot. If built before, the FFE is assigned one foot above ground. This same process is also used to delineate on-grade vs elevated structures.

The age of the property is used to assign a strength of either weak or strong (as described in Disclosure 7d - year of construction) to delineate between pre- and post-2002 Florida Building Code statewide enforcement.

10. Provide the total number of personal residential structure flood vulnerability functions available for use in the flood model. Describe which structure flood

vulnerability functions are used for personal residential building structures, manufactured homes, condo unit owners, and apartment renters.

Residential on-grade	2 Models: Timber Masonry	2 Strengths: Weak Strong	3 Stories: 1-story 2-story 3-story	4 FFE Elevations: 0 ft 1 ft 2 ft 3 ft	4 Flood conditions: I.F. C.F. minor waves C.F. moderate waves C.F. severe waves	192
Residential elevated	2 Models: Timber Masonry	2 Strengths: Weak Strong	2 Stories: 1-story 2-story	9 FFE Elevations: 4 ft 5 ft 6 ft 7 ft 8 ft 9 ft 10 ft 11 ft 12 ft	4 Flood conditions: I.F. C.F. minor waves C.F. moderate waves C.F. severe waves	288
Manufactured housing		2 Strengths: No Tied down Tied down		8 FFE Elevations: 1 ft 2 ft 3 ft 4 ft 5 ft 6 ft 7 ft 8 ft	4 Flood conditions: I.F. C.F. minor waves C.F. moderate waves C.F. severe waves	64
Total						544

Table 42. Available Flood Vulnerability Functions.

Different personal residential structure flood vulnerability functions are used for various building classes of personal residential building structures, and manufactured homes, as the above Table 42 details.

The personal residential structure flood vulnerability functions used for condo unit owners are the personal residential structure flood vulnerability functions for personal residential buildings.

The apartment unit renters are only insured for contents damage. This is addressed in disclosure 5 of Standard VF-2.

11. Describe the assumptions, data, methods, and processes used to develop personal residential structure flood vulnerability functions when:

a. personal residential construction types are unknown, or

b. one or more primary building characteristics are unknown, or

c. building input characteristics are conflicting.

The parameters defining an FPFLM personal residential vulnerability model for site-built structures, for a given hydrological state or flood condition are the construction type (i.e. exterior wall type), strength (weak or strong) based on year built, number of stories, building type (on grade or elevated), and first floor elevation (FFE).

The NFIP exposure data is the main source of input for the flood model. As described in disclosure 3, data regarding building characteristics might be missing in the NFIP data set, including construction type, number of stories, and FFE. To make up for the missing, i.e. unknown data, the FPFLM team assigns the missing parameters based on available statistics. These statistics can vary by era and by location, and the FPFLM team has already compiled them for the wind model from the county property tax appraiser databases, and the history of the building code, and complemented them with statistics from NFIP.

For the single family manufactured homes, the weighting scheme will be the same as the one currently used in the wind model, using the same stats.

If building input characteristics are conflicting, the FPFLM team developed a set of rules to resolve the conflict.

12. Describe similarities and differences in how the personal residential structure flood vulnerability functions are developed and applied for coastal and inland flooding.

The personal residential structure flood vulnerability functions were developed for coastal and inland flooding using entirely different methodologies. Coastal flood vulnerabilities were derived by translation of tsunami fragility functions to coastal flood vulnerability functions as described in the GF-1 Disclosure 2 standard under the section entitled: **Vulnerability of site-built residential structures to Coastal Flood**, with example outputs provided in Figure 21, Figure 22, Figure 24, and Figure 55.

Inland flood vulnerabilities were derived by adapting USACE (2015) flood vulnerabilities as described in the GF-1 Disclosure 2 standard under the section entitled: **Vulnerability of site-built residential structures to Inland Flood**, with example outputs provided in Figure 23, Figure 24 and Figure 53.

13. Provide a completed Form VF-1, Coastal Flood with Damaging Wave Action. Provide a link to the location of the form [insert hyperlink here].

See [Form VF-1](#).

14. Provide a completed Form VF-2, Inland Flood by Flood Depth. Provide a link to the location of the form [insert hyperlink here].

See [Form VF-2](#).

VF-2 Derivation of Personal Residential Contents Flood Vulnerability Functions

A. Development of the personal residential contents flood vulnerability functions shall be based on some combination of the following: (1) post-event site investigations, (2) technical literature, (3) expert opinion, (4) laboratory or field testing, and (5) insurance claims data. Contents flood vulnerability functions shall be supported by historical and other relevant data.

The development of the personal residential contents flood vulnerabilities is based on insurance claims data, informed by expert opinion.

B. The relationship between personal residential structure and contents flood vulnerability functions shall be reasonable.

The relationship between the modeled personal residential structure and the contents flood vulnerability functions is reasonable, on the basis of the relationship between historical structure and contents flood losses.

Disclosures

1. Provide a flowchart documenting the process by which the personal residential contents flood vulnerability functions are derived and implemented.

The flow chart below summarizes the procedure used to develop the flood contents vulnerability functions for the different types of personal residential buildings.

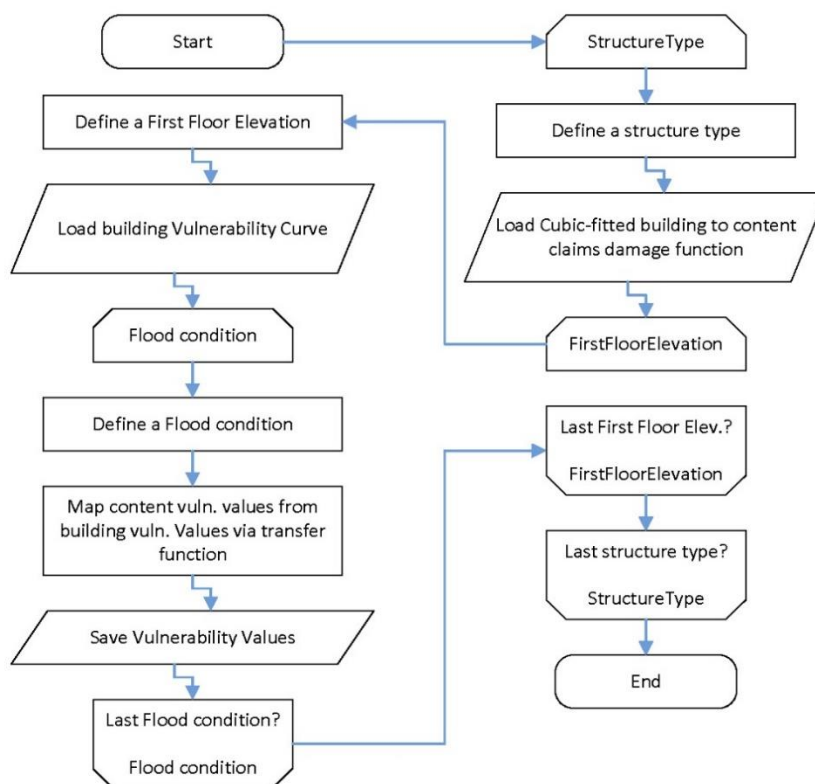


Figure 56. Content vulnerability for personal residential structures.

2. Describe the relationship between personal residential contents and personal residential structure flood vulnerability functions.

The personal residential contents flood vulnerability functions were derived from the personal residential structure flood vulnerability functions, in a 3-step process described in disclosure 3, based on claim data. This insures consistency between the two types of functions.

3. Describe any assumptions, data, methods, and processes used to develop and validate the personal residential contents flood vulnerability functions.

NFIP claims data is used for the development of the coastal and inland flood model content damage vulnerabilities. For each claim, the building damage ratio (building damage to building value) and content damage ratio (content damage to content value) were calculated using the available information in the NFIP claim data. NFIP reports the building property value, building coverage and the content coverage. To calculate the content value, a factor resulting from the ratio between the building property value and the building coverage is applied to the content coverage. Table 43 shows a sample subset of the NFIP claims data (first five columns), and the values calculated from this data and appended (last three columns, grey shaded). In any row: Content value = Content

coverage * (Building value/Building coverage); Building damage ratio = Building damage / Building value; Content damage ratio = Content damage / Content value.

Building damage (\$)	Content damage (\$)	Building value (\$)	Building coverage (\$)	Content coverage (\$)	Content value (\$)	Building damage ratio (%)	Content damage ratio (%)
33,646	2,222	164,939	250,000	100,000	65,976	20.40	3.37
23,194	0	101,435	121,000	44,100	36,969	22.87	0.00
61,988	52,706	249,097	250,000	100,000	99,639	24.89	52.90
42,631	6,400	232,790	250,000	100,000	93,116	18.31	6.87
48,249	6,766	123,105	125,000	50,000	49,242	39.19	13.74

Table 43. Sample of NFIP claim data and damage ratio calculations.

For all claims, the building and content damage ratios are paired, where the x-axis refers to the building damage ratio and the y-axis to the content damage ratio. Discrete building damage ratio intervals are defined along the x-axis. Within each interval, the average of the data along both axes yields the coordinates of the empirical building to content relationship. The result is illustrated in Figure 57, where the size of the intervals is 2.5% along the x-axis. The contents damage ratio is thus a function of the building damage ratio, rather than a direct function of the hazard intensity. This is referred to as a type 2 vulnerability function. The database used corresponds to the twelve-storm claim database described in standard VF-1.

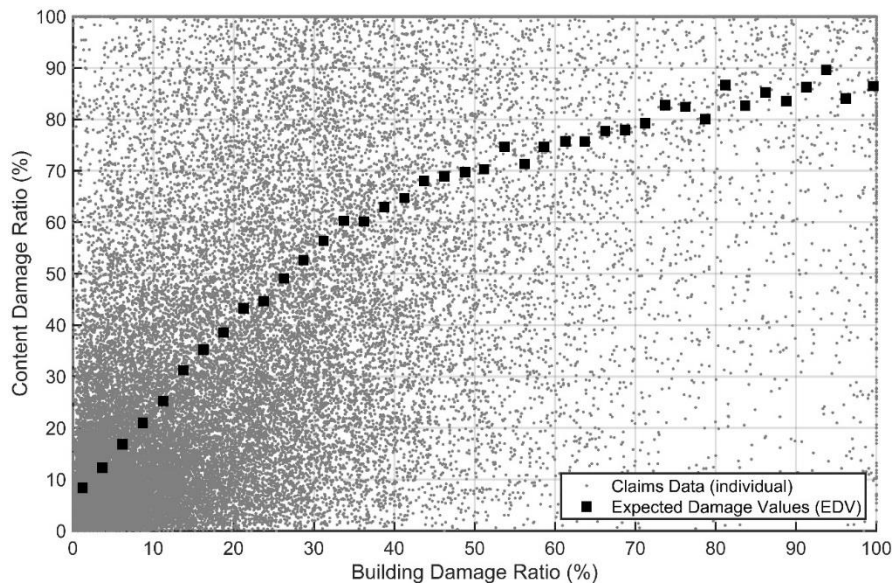


Figure 57. Type 2 vulnerability function relating content damage to building damage.

The empirical type 2 content vulnerability function was fitted with a 3-order polynomial as illustrated in Figure 58. The resulting polynomial equation (Equation 1) becomes the transfer function to obtain the content vulnerability function as a function of building vulnerability. The coefficient of determination R^2 of the 3-order polynomial with respect to the expected values is 0.9938.

$$cont(bldg) = 1.26bldg^3 - 2.95bldg^2 + 2.58bldg \quad [1]$$

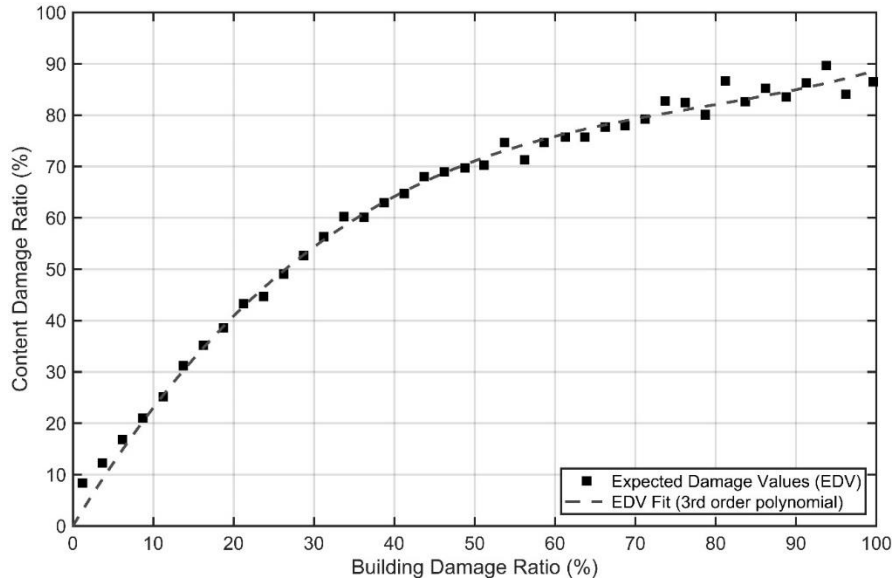


Figure 58. Transfer function of building to content vulnerability. Polynomial fit of empirical.

The transfer function converts the building vulnerability to the content vulnerability at the same inundation depth. This mapping procedure is illustrated in Figure 59, where the transfer function is Equation 1.

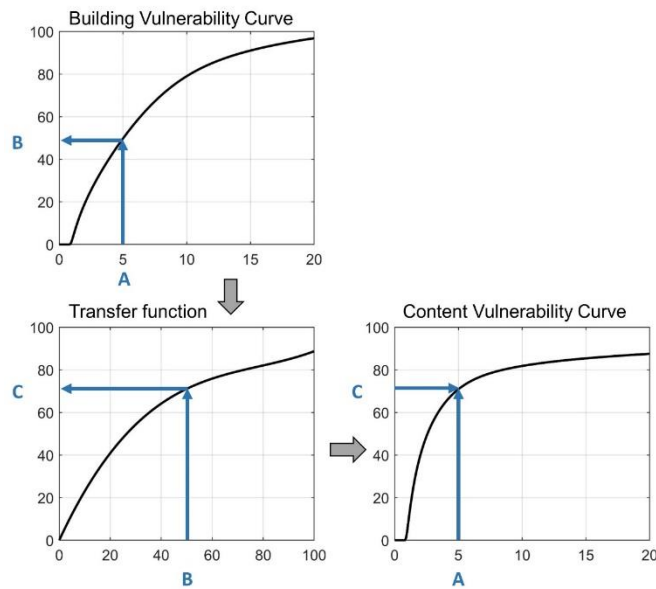


Figure 59. Content vulnerability function derivation.

This procedure ensures compatibility between the building vulnerability model, the claims data, and the resulting content vulnerability model. Figure 60 presents an example of content vulnerability function for the case of a one-story on grade reinforced masonry structure with 1 foot first floor elevation. All the flood conditions are presented.

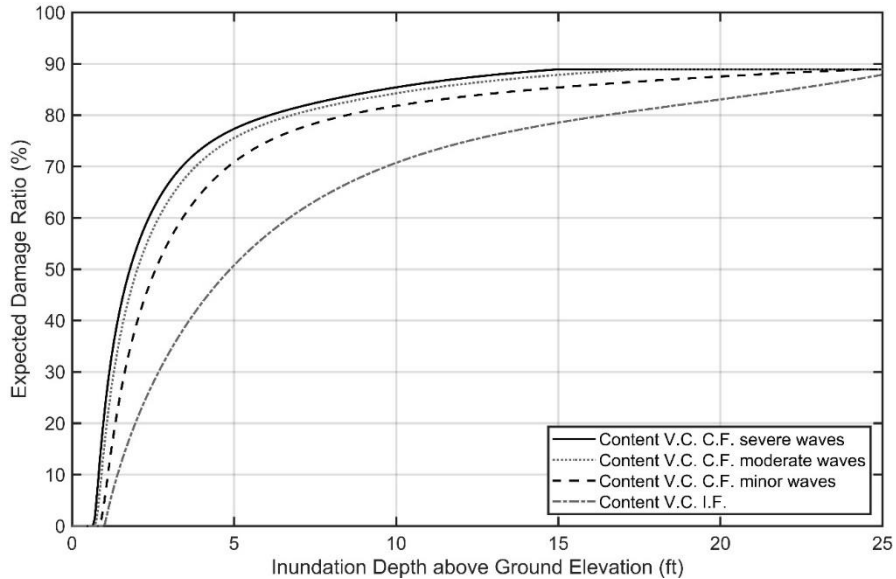


Figure 60. Content vulnerability function. One-story on grade reinforced masonry 1 ft FFE.

4. As applicable, describe the nature and extent of actual insurance claims data used to develop the personal residential contents flood vulnerability functions. Describe in detail what is included, such as, number of policies, number of insurers, dates of loss, and number of units of dollar exposure, separated into personal residential building structures and manufactured homes.

The actual insurance claims data used to develop the personal residential contents flood vulnerability functions is described in disclosure 3 of Standard VF-1.

5. Provide the total number of personal residential contents flood vulnerability functions available for use in the flood model. Describe whether different contents flood vulnerability functions are used for personal residential building structures, manufactured homes, unit location for condo owners and apartment renters, and various building classes.

A content vulnerability function was produced for each of the building vulnerability functions listed in disclosure 10 of standard VF-1. Since each building vulnerability function is unique, its corresponding content vulnerability function is unique.

6. Describe any relationships between flood characteristics and personal residential contents flood vulnerability functions.

Since the contents flood vulnerability functions are derived from the building vulnerability functions, as described in disclosure 3, the relationship between flood characteristics and personal residential contents flood vulnerability functions are the same as those with personal residential

building flood vulnerability functions. These relationships are described in disclosure 2 of Standard VF-1.

- 7. State the minimum threshold, if any, at which personal residential contents flood damage is calculated (e.g., personal residential contents flood damage is estimated for personal residential structure damage greater than x percent or flood depth greater than y inches). Provide documentation of assumptions and available validation data to verify the approach used.**

The content loss is initiated at the inundation depth consistent with the initiation of building damage. This corresponds to the inundation depth at which water reaches the FFE. This depth is dependent on the flood condition, as illustrated in Figure 60, where content damage is initiated at an inundation depth lesser than the FFE for the coastal flood conditions (due to waves reaching FFE) and at inundation depth equal to FFE for inland flood. See also disclosure 5 in standard VF-1 and disclosure 2 in standard GF-1.

- 8. Describe similarities and differences in how personal residential contents flood vulnerability functions are developed and applied for coastal and inland flooding.**

Both coastal and inland flood vulnerability functions are derived from the building vulnerability functions using the same transfer function (see disclosure 3).

- 9. Describe the assumptions, data, methods, and processes used to develop personal residential contents flood vulnerability functions when:**
 - a. personal residential construction types are unknown, or**
 - b. one or more primary building characteristics are unknown, or**
 - c. building input characteristics are conflicting.**

The assumptions, data, methods, and processes are the same as those described in disclosure 11 of standard VF-1.

VF-3 Derivation of Personal Residential Time Element Flood Vulnerability Functions

A. Development of the personal residential time element flood vulnerability functions shall be based on one or more of the following: (1) post-event site investigations, (2) technical literature, (3) expert opinion, (4) laboratory or field testing, and (5) insurance claims data.

The development of the personal residential time element flood vulnerability functions is based on expert opinion, informed by insurance claims data for wind.

B. The relationship among personal residential structure, contents, and time element flood vulnerability functions shall be reasonable.

The relationship between the modeled personal residential structure, contents, and time element flood vulnerability functions is reasonable, on the basis of similar relationship for wind losses.

Disclosures

1. Provide a flowchart documenting the process by which the personal residential time element flood vulnerability functions are derived and implemented.

The flow chart below *Error! Reference source not found.* summarizes the procedure used to develop the flood time element vulnerability functions for the different types of personal residential buildings.

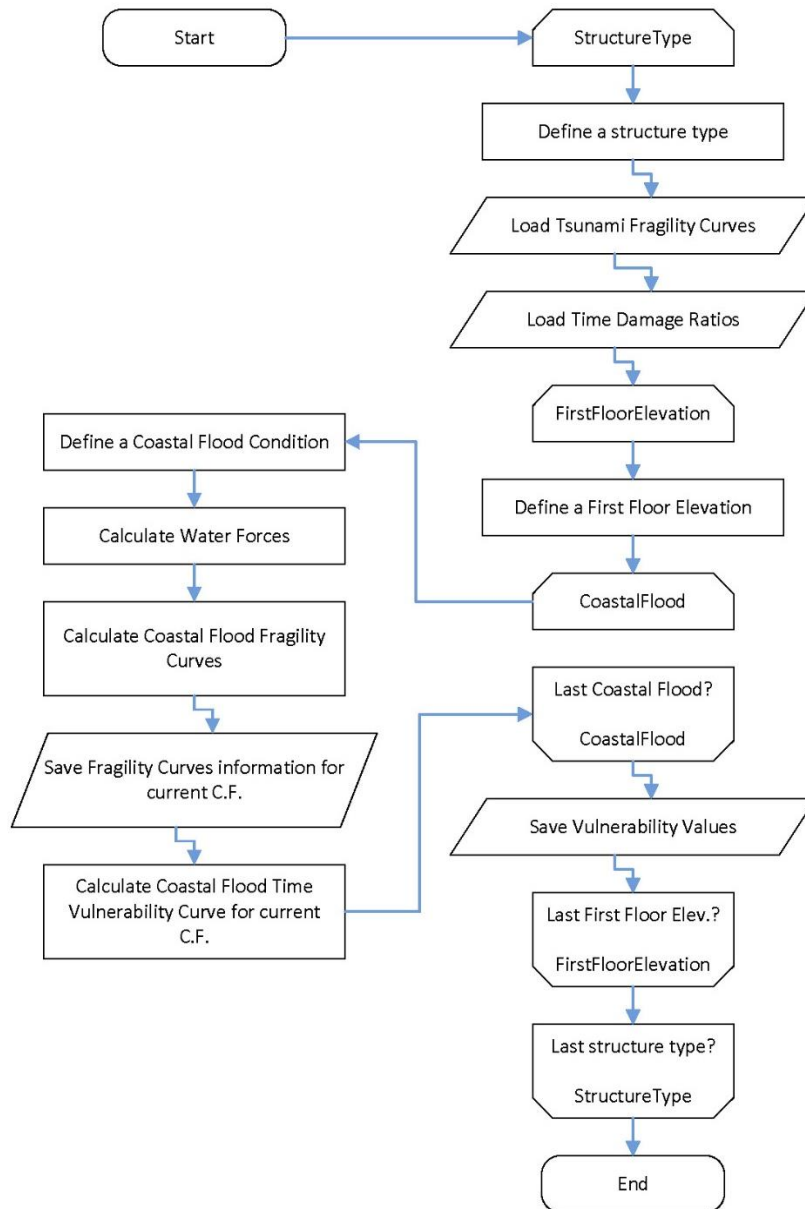


Figure 61. Coastal flood time element vulnerability for personal residential structures.

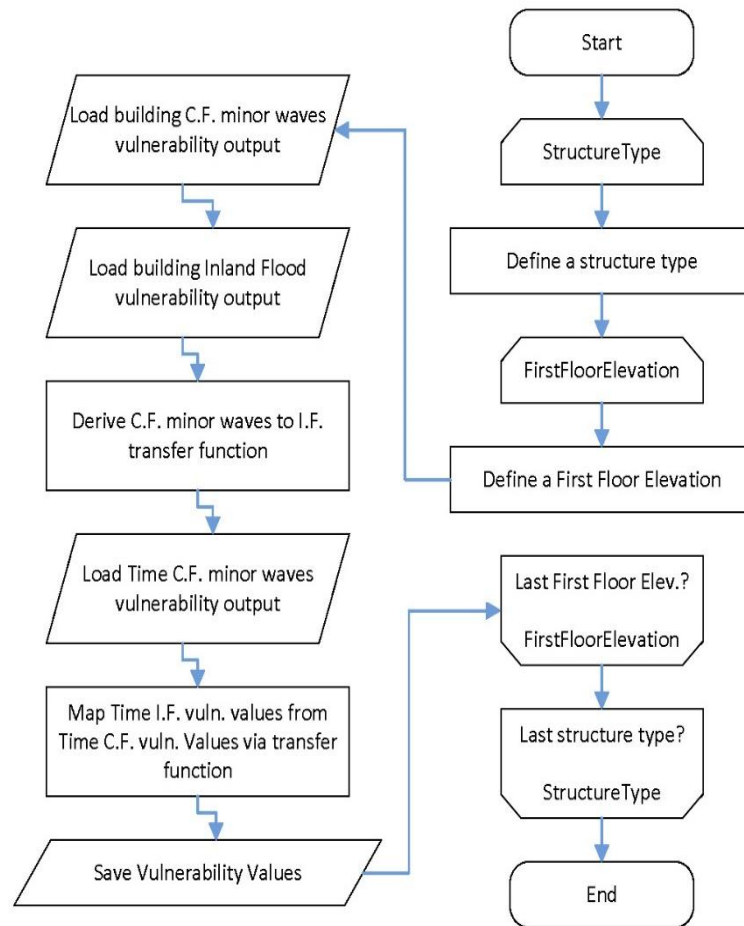


Figure 62. Inland flood time element vulnerability for personal residential structures.

2. Describe the assumptions, data, methods, and processes used to develop and validate personal residential time element flood vulnerability functions.

Development of coastal flood time element vulnerability

The definition of the time an event forces a house occupant to live outside their dwelling controls the methodology for calculating additional living expenses (ALE). The ALE ratio is a percentage of the ALE coverage, as follows:

$$\text{ALE Ratio (ALER)} = \frac{\text{Cost of living outside a dwelling}}{\text{Total ALE coverage}} \cong \frac{\text{Time of living outside a dwelling for a specific event}}{\text{Maximum amount of time allowed by the ALE coverage}} \quad [1]$$

In Eq. 1 the *cost* of living outside a dwelling is approximated by the *time* spent living outside the dwelling. It is reasonable to assume that the time an owner is forced to live outside their house is

directly related to the time it takes to repair a house, which is directly linked to the damage itself. The following section explains the relationship between building damage and time of repair.

Developing the ALE vulnerability functions, which express the expected ALE ratio for a given hazard intensity, starts with the building fragility functions, which are the basis for the building damage vulnerability functions as well. Disclosure 2 of Standard GF-1 documents the fragility to vulnerability function conversion. In the case of the ALE, the fragility functions express the probability of meeting or exceeding a specific ALE ratio instead of the expected damage ratio. For the case of the building:

Fragility function:

$$P(\text{DR} \geq \text{dr}_i | \text{IM}) = \int_{\text{dr}_i}^{\text{dr}_{\max}} f_{\text{DR}}(\text{dr} | \text{IM}) d(\text{dr}) \rightarrow \text{Vulnerability function: } E[\text{DR} | \text{IM}] = \sum_{i=1}^k \frac{\text{dr}_i + \text{dr}_{i+1}}{2} \cdot \begin{cases} 1 - P(\text{DR} \geq \text{dr}_{i+1} | \text{IM}) & i = 1 \\ P(\text{DR} \geq \text{dr}_i | \text{IM}) - P(\text{DR} \geq \text{dr}_{i+1} | \text{IM}) & 1 < i \leq k - 1 \\ P(\text{DR} \geq \text{dr}_i | \text{IM}) & i = k \end{cases} \quad [2]$$

For the case of ALE, the equations are the same with the difference that all the damage ratios (DR) will change to ALE ratios (ALER) and the damage ratio representing each damage state (dr_i) will change to the ALE ratio representing each damage state (aler_i). The methodology for calculating the values for ALER and aler_i are explained in the next sections. The methodology described for the development of building damage fragility function to vulnerability function is adapted to the case of ALE. Each damage state (DS_i) is associated with an average time occupants are forced outside their dwelling and an ALE ratio. The fragility function for each building damage state can then be reformulated to give the probability of meeting or exceeding the assigned ALE ratio. The resulting set of ALE fragility functions yields an ALE vulnerability function. The conversion method between fragilities and vulnerability is the same as the one explained in disclosure 2 of Standard GF-1.

The first step of the ALE fragility function development is to identify the average time the occupants are forced outside their dwelling. This time is divided into two categories, the delay time and the repair time.

Delay time

The delay time is up to the point that repairs start. It has three components:

- Evacuation time, whether mandatory or not, previous to the event.
- The event time, which is the time it takes for the hurricane to pass over the house location.
- Processing time, which is an accumulation of all tasks that need to be done before the repairs can start. Some of the tasks include adjusters visiting for assessment, finding a contractor, accessibility (e.g., infrastructure integrity), claim processing time, and many other factors.

For each time and damage state, using engineering judgment, the FPFLM team selected different statistical distributions. The delay time is not building specific; therefore, the same delay times are used for all residential building types. The basis of the engineering judgment is:

- For the evacuation time, it was assumed that the damage states were correlated to the hurricane magnitude. It was assumed that on average, the higher damage states happen during a more extreme hurricane event. Therefore, the higher the damage state, the bigger the mean values of the distributions for evacuation time (e.g., the mean value of the distribution of the evacuation time for damage state 1 and 2 is one day and for damage state 5 and 6 is three days).
- For the event time, it was assumed that regardless of the damage state, on average, it would take a whole day for the hurricane to pass a location.
- For the processing time, it was assumed that the bigger the damage state, the bigger the damage, and therefore the more time it would take to process such a building.

The values of the delay time mean values (μ) and standard deviation (σ) for various damage states are used for the development of the ALE model. The mean value and standard deviation stated for each delay time and damage state are then used to calculate beta distribution parameters α and β .

Repair time

The repair time is from the time the repair starts until the owner can re-occupy the structure. This includes the time to repair or remove and replace the damaged components. For the repair time, similar to the cost analysis, the team performed an analysis to see how long it will take to repair various components of different typical houses. This started with 36 different building types based on the number of stories (1–3 stories), structure type (timber or masonry), roof types (hip or gable), and roof cover (shingles, tiles, or metal). A building has 17 components, and the time to completely repair these components for each building type is calculated using publicly available construction cost and repair sources such as RSMeans Residential Cost Data 2015 (RSMeans, 2015b) and RSMeans Contractor’s Pricing Guide Residential Repair & Remodeling Costs 2015 (RSMeans, 2015a). The component repair times are then averaged based on the number of stories and structure type. The structure type does not influence the component repair time; therefore, the selecting factor was the number of stories. The summation of the repair times of each component will be the total repair time.

Eq. 3 shows how the repair time of each damage state is calculated:

$$\text{Repair time}_i = \sum_{j=1}^k E[\text{PDR}|\text{DS} = \text{ds}_i] \times \text{RT}_j \quad [3]$$

Where

- Repair time_i = repair time (in days) at the i th damage state;
- $E[\text{PDR}|\text{DS} = \text{ds}_i]$ = the expected physical damage ratio (PDR) of the j th component for the i th damage state;
- RT_j = time of repair of the j th component.

Eq. 3 shows the relationship between the physical damage and the repair time of a component for a specific damage state. The time to repair a partially damaged component is the percentage the component has been damaged multiplied by the total time it takes to completely repair that given component. The procedure to calculate $E[PDR|DS = ds_i]$ is the same as in disclosure 2 of Standard GF-1.

ALE ratio representing each damage state ($aler_i$)

The next step is to assign an ALE ratio to each damage state, which is the summation of the repair time of each component plus the delay time of that specific damage state.

The ALE ratio of a given damage state ($aler_i$) can be defined as:

$$aler_i = \frac{\text{Delay Time}_i + \text{Repair Time}_i}{\text{Maximum Delay Time} + \text{Maximum Repair Time}} = \frac{\text{Delay Time}_i + \text{Repair Time}_i}{\text{Maximum Additional Living Time}} \quad [4]$$

Where

- Delay Time_{*i*} = summation of the different components of the delay time of the *i*th damage state;
- Repair Time_{*i*} = repair time of the *i*th damage state (using Eq. 3);
- Maximum Delay Time = maximum delay time used in the model. This is the summation of the 95% percentile of different components of the damage state 6 delay time;
- Maximum Repair Time = maximum time it takes to repair the house. This is total time of repair;
- Maximum Additional Living Time = summation of the two maximum delay and repair times. This is equal to the ALE coverage.

The model uses a Monte Carlo simulation to calculate the ALE ratio that characterizes each damage state ($aler_i$). The simulation uses the physical damage distributions, delay time distributions, and repair time distributions as input to Eq. 4, and the output is the expected ALE ratio corresponding to each damage state. In each simulation run, the simulation randomly samples a physical damage value based on the assigned damage distributions for all damage states and components, as well as randomly sampling an evacuation, event, and processing time based on the assigned delay time distributions for all damage states, converting the distributions into sample data. For each simulation, using Eq. 3 and the appropriate time of completely repairing a component, the repair time is calculated. The calculated repair time in addition to the sampled delay times are used in Eq. 4 to calculate the expected ALE ratio corresponding to each overall damage state. The Monte Carlo simulation performs these process for a total of 100,000 simulations. The mean value of all simulations is used as the ALE ratio of a given damage state ($aler_i$). In each simulation, if the repair time is zero, the processing time is changed to zero; however, the evacuation and event time can be nonzero and cause ALE.

Converting ALE fragility functions into ALE vulnerability functions

This conversion uses the same approach as converting the building fragility to vulnerability functions. Eq. 5 is similar to Eq. 1, converted from building damage to ALE:

$$E[\text{ALER}|\text{IM}] = \sum_{i=1}^k \frac{\text{aler}_i + \text{aler}_{i+1}}{2} \cdot \begin{cases} 1 - P(\text{ALER} \geq \text{aler}_{i+1}|\text{IM}) & i = 1 \\ P(\text{ALER} \geq \text{aler}_i|\text{IM}) - P(\text{ALER} \geq \text{aler}_{i+1}|\text{IM}) & 1 < i \leq k - 1 \\ P(\text{ALER} \geq \text{aler}_i|\text{IM}) & i = k \end{cases} \quad [5]$$

Where

- $E[\text{ALER}|\text{IM}]$ = expected ALE ratio for a given hazard intensity (IM),
- aler_i = expected ALE ratio representing damage state i . This is calculated using the Monte Carlo simulation explained above. For $i = k$ the aler_{i+1} is equal to 1;
- $P(\text{ALER} \geq \text{aler}_i|\text{IM})$ = probability of occurrence or exceedance of damage state i at a given hazard intensity (IM). This is equal to the fragility curve value of damage state i at a given hazard intensity (IM).

For any given damage state, characterized by a damage ratio and an ALE ratio, the probability of exceeding the ALE ratio is the same as the probability of exceeding the damage ratio. Therefore, the ALE and building damage fragility functions are identical. However, the resulting vulnerability functions differ.

Development of inland flood time element vulnerability

The inland flood building vulnerability curves were derived following a different procedure than the coastal flood, as explained in standard GF-1 disclosure 2. Therefore, the methodology for coastal flood time element vulnerability (section 2.1 above) cannot be applied for inland flood time element vulnerability. The inland flood time element vulnerability is derived by applying a transfer function to the minor wave coastal flood time element vulnerability. The transfer function is the ratio of inundation depth of the inland flood building vulnerability function to the inundation depth of the minor wave coastal flood building vulnerability function at a series of discrete damage ratios. This transfer function is then used to map the minor wave coastal flood time element vulnerability to the inland flood time element vulnerability. This transfer function and resulting time element vulnerability is unique for each of the 544 building type variations listed in Table 42 in standard VF-1, disclosure 10.

3. Describe the relationships among personal residential structure, contents, and time element vulnerability functions.

The building vulnerability functions are derived based on fragility functions. The content vulnerability functions are indirectly derived from the fragility functions, because these are derived based on the building vulnerability functions along with the relation between building and content damage ratios from claim data. The time element vulnerability functions are derived by either directly using the same fragility functions as the building vulnerability (coastal flood, section 2.1 disclosure 2) or by mapping (inland flood, section 2.2, disclosure 2).

- 4. As applicable, describe the nature and extent of actual insurance claims data used to develop the personal residential time element flood vulnerability functions. Describe in detail what is included, such as number of policies, number of insurers, dates of loss, and number of units of dollar exposure, separated into personal residential building structures and manufactured homes.**

Since NFIP does not cover time related expenses, there is no NFIP claim data related to time related expenses.

- 5. Provide the total number of personal residential time element flood vulnerability functions available for use in the flood model. Describe whether different time element flood vulnerability functions are used for personal residential building structures, manufactured homes, unit location for condo owners and apartment renters, and various building classes.**

A time element vulnerability function was produced for each of the building vulnerability functions listed in disclosure 10 of standard VF-1. The time element vulnerability functions used for condo unit owners and apartment unit renters are the time element vulnerability functions for personal residential buildings, as explained in disclosure 10 of standard V-1.

- 6. Describe similarities and differences in how personal residential time element flood vulnerability functions are developed and applied for coastal and inland flooding.**

See Disclosure 2. Section 2.1 describes coastal flood time element functions, and section 2.2 describes inland flood time element functions.

- 7. Describe whether and how personal residential structure classification and characteristics, and flood characteristics, are incorporated into the personal residential time element flood vulnerability functions.**

A time element vulnerability function was produced for each of the building vulnerability functions listed in disclosure 10 of standard VF-1. Thus, all structure classification and characteristics, and flood characteristics are incorporated into the time element functions in the same manner as they are incorporated in the structure vulnerability functions.

- 8. Describe whether and how personal residential time element flood vulnerability functions take into consideration the damage to local and regional infrastructure, or personal residential time element vulnerability resulting from a governmental mandate associated with flood events (e.g., evacuation and re-entry mandates).**

Time element losses for personal residential buildings are based on estimation of delay and repair times of damage to the structure. These times take indirectly into account potential damage to the infrastructure. For example more severe flood events results in more delay time, in part due to possible damage to infrastructure.

9. Describe the assumptions, data, methods, and processes used to develop personal residential time element flood vulnerability functions when:

- a. personal residential construction types are unknown, or**
- b. one or more primary building characteristics are unknown, or**
- c. building input characteristics are conflicting.**

The assumptions, data, methods, and processes are the same as those described in disclosure 11 of standard VF-1.

VF-4 Flood Mitigation Measures

- A. Modeling of flood mitigation measures to improve flood resistance of personal residential structures, the corresponding effects on flood vulnerability, and their associated uncertainties shall be theoretically sound and consistent with fundamental engineering principles. These measures shall include design, construction, and retrofit techniques that affect the flood resistance or flood protection of personal residential structures. The modeling organization shall justify all flood mitigation measures considered by the flood model.**

The modeled flood mitigation measures improve the resistance of personal residential structures and reduce their vulnerability relative to their like-structure without the mitigation measures. Engineering principles were employed to develop and implement the mitigation measures.

- B. Application of flood mitigation measures that affect the performance of personal residential structures and the damage to contents shall be justified as to the impact on reducing flood damage whether done individually or in combination.**

The mitigation measures described in disclosure 2 may be implemented individually or in combination. Reductions in building vulnerability result in a reduction in content damage.

Disclosures

- 1. Provide a completed Form VF-3, Flood Mitigation Measures, Range of Changes in Flood Damage. Provide a link to the location of the form [insert hyperlink here].**

Link to [Form VF-3](#).

- 2. Provide a description of all flood mitigation measures used by the flood model, whether or not they are listed in Form VF-3, Flood Mitigation Measures, Range of Changes in Flood Damage.**

Fundamentally, the implementation of a given mitigation measure results from an adjustment to the damage ratios (see standard GF-1, disclosure 2) assigned to those components influenced by the mitigation measure to reflect a reduced probability of damage to the affected components. The methodology considers the influence of mitigation measures before and after the water inundation depth overcomes the given mitigation. When inundation has not yet reached the height of the mitigation, the adjusted damage ratios are employed. When inundation has reached the height of the mitigation, the model transitions to the unmitigated damage ratios. Figure 63 shows a conceptual comparison of mitigated and unmitigated vulnerability. The mitigation reduces but does not eliminate damage, and the mitigation is effective until the inundation height overcomes it.

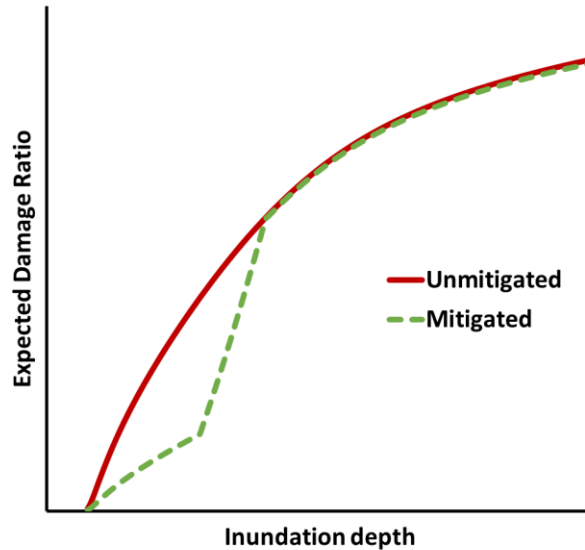


Figure 63. Conceptual illustration of mitigated vs unmitigated vulnerability.

The model currently considers the following mitigation measures, described in detail below: elevating utilities, wet floodproofing, dry floodproofing, flood openings, and elevated structure.

Elevating Utilities

This mitigation considers elevating or otherwise protecting the equipment and utilities to a specified height. The equipment and utilities are mechanical, electrical and plumbing used within or on the exterior of a building. The mitigation measures for equipment and utility include elevating or protecting for 1, 2, or 3 feet.

The method implements the effect of mitigation by using a combination of the original interior damage distributions and a modified interior damage distributions. The modified interior damage distributions are used for water height lower than the mitigation height; the original distributions are used for water height above the mitigation height. However, considering the costs associated with elevating the equipment, the cost ratios are slightly different (less than 1%). For illustration, Table 44 shows the damage distributions of three subcomponents for the case of a 1-story single family on grade reinforced masonry (strong) structure. Notice that only the utilities component is affected due to this mitigation measure. The water level relative to the mitigation height is used to determine whether the top row or bottom row assignment is employed when creating the vulnerability function. Using these distributions with the cost ratios for each component for a certain building type yields the Damage Ratio per Damage state, for the cases when the water is below and above the mitigation height.

Table 45 shows the damage ratio representing each damage state for water level below the mitigation height and above the mitigation height for the case of a one story on-grade masonry structure. When the water reaches the mitigation height, a transition occurs from using the mitigated DR to using the unmitigated DR, as illustrated conceptually in Figure 63.

Elevating utilities	DS1	DS2	DS3	DS4	DS5	DS6
Water above mitigation height	Interior: Normal ($\mu=0.2, \sigma=0.07$)	Interior: Normal ($\mu=0.4, \sigma=0.07$)	Interior: Normal ($\mu=0.6, \sigma=0.07$)	Interior: Normal ($\mu=0.8, \sigma=0.06$)	Interior: Normal ($\mu=0.95, \sigma=0.03$)	Interior: Normal ($\mu=0.99, \sigma=0.01$)
	Utilities: Normal ($\mu=0.2, \sigma=0.07$)	Utilities: Normal ($\mu=0.4, \sigma=0.07$)	Utilities: Normal ($\mu=0.6, \sigma=0.07$)	Utilities: Normal ($\mu=0.8, \sigma=0.06$)	Utilities: Normal ($\mu=0.95, \sigma=0.03$)	Utilities: Normal ($\mu=0.99, \sigma=0.01$)
	Foundation: Normal ($\mu=0.2, \sigma=0.07$)	Foundation: Normal ($\mu=0.4, \sigma=0.07$)	Foundation: Normal ($\mu=0.6, \sigma=0.07$)	Foundation: Normal ($\mu=0.8, \sigma=0.06$)	Foundation: Normal ($\mu=0.95, \sigma=0.03$)	Foundation: Normal ($\mu=0.99, \sigma=0.01$)
Water below mitigation height	Interior: Normal ($\mu=0.2, \sigma=0.07$)	Interior: Normal ($\mu=0.4, \sigma=0.07$)	Interior: Normal ($\mu=0.6, \sigma=0.07$)	Interior: Normal ($\mu=0.8, \sigma=0.06$)	Interior: Normal ($\mu=0.95, \sigma=0.03$)	Interior: Normal ($\mu=0.99, \sigma=0.01$)
	Utilities: No damage	Utilities: No damage				
	Foundation: Normal ($\mu=0.2, \sigma=0.07$)	Foundation: Normal ($\mu=0.4, \sigma=0.07$)	Foundation: Normal ($\mu=0.6, \sigma=0.07$)	Foundation: Normal ($\mu=0.8, \sigma=0.06$)	Foundation: Normal ($\mu=0.95, \sigma=0.03$)	Foundation: Normal ($\mu=0.99, \sigma=0.01$)

Table 44. Distribution of component damage for different damage states, one story on-grade reinforced masonry structure.

Structure type	Expected damage ratio	dr ₁	dr ₂	dr ₃	dr ₄	dr ₅	dr ₆	dr _{max}
1st-M	Water above mitigation height	19.9%	40.7%	62.5%	84.7%	103.3%	108.2%	109.2%
	Water below mitigation height	14.1%	29.4%	45.8%	62.7%	77.6%	81.4%	

Table 45. Expected damage ratios representing each damage states above and below mitigation heights, one story on-grade reinforced masonry structure.

Wet floodproofing

Wet floodproofing does not protect against hydrodynamic forces from moving water. Rather, the interior of the dwelling is constructed using materials that are less susceptible to water damage and can recover from wetting with minimal need for replacement (e.g. tile flooring rather than wood).

After consulting with a Florida local contractor, common practice for wet floodproofing a masonry home consists of:

1. waterproofing the interior block with paint to eliminate the possibility of mold growing on the interior masonry;
2. using non-wood (e.g., metal) furring strip boards
3. using cement boards instead of drywall;
4. using plastic or vinyl base boards;
5. using tile or terrazzo flooring;
6. elevating mechanical equipment;

7. using PVC or composite frames for the opening
8. Placing electric plugs above 3 or 4 ft.

The extra cost of the first four measures to mitigate the interior walls is \$5.75 per sq.ft of wall. The cost of using tile or terrazzo vs. hardwood is the same. The cost of elevating mechanical equipment is \$500 per unit. Using PVC or composite frames is slightly cheaper than wood frames. And the cost of placing the electric plugs at a higher elevation is the same as lower elevations. Since all these mitigation measures are performed on the interior, the calculated costs will be added to the interior section of the cost analysis. Also, since the mitigation measures are performed only on the first floor, all extra cost (repair and replacement) are added to the cost analysis of the first floor. However, given that these extra costs change the cost analysis of the entire building, regardless of the number of stories of the building, the cost ratio of all the components change. The cost of mitigating interior components increases the ratio of interior cost to cost of the entire house. These modifications do not add to the strength of a building but reduce the need to replace some components and therefore results in less loss for the building.

Following the procedure explained in section 2.1, damage distributions are altered for the components influenced by wet floodproofing (interior and utilities).

Dry floodproofing

Dry floodproofing is a method that makes the dwelling watertight from the ground level up to a designated height (1, 2, 3 feet) via use of waterproof coatings or membranes, water tight gates around low entryways, and protecting utilities to that same height. According to FEMA 551, common practice for dry floodproofing a structure consists of:

1. Waterproofing a concrete block or brick-faced wall by applying a polyethylene sheet or other impervious material and covering with a facing material such as brick;
2. Acrylic latex wall coating;
3. Caulking/sealant – a high performance electrometric “urethane” sealant is recommended.

Since the mitigation measures are performed only on the first floor, all extra cost (repair and replacement) are added to the cost analysis of the first floor. Given that the mitigation costs change the cost analysis of the entire building, regardless of the number of stories of the building, the cost ratio of all the components changes.

Following the procedure explained in section 2.1, damage distributions are altered for the affected components. For the case of dry floodproofing, when the water is below the mitigation height, the interior and the utilities components are considered to be undamaged.

Flood Openings in foundation wall

Flood openings are used as a mitigation measure where the water is allowed to flow in and out of an elevated foundation. The procedure to model this mitigation measure is similar to the ones described for the previous cases. As seen in Table 44, the foundation is one of the components

considered. The flood openings mitigation is reflected by reducing the mean of the pdf of damage of the foundation relative to the unmitigated case.

Elevated structure

Elevated residential structures are a common in coastal regions. The methodology to develop personal residential vulnerability functions for elevated structures is the same as described in standard GF-1 disclosure 2, where tsunami fragility curves are used as a basis and then translated into coastal flood fragility functions via force equivalency calculations. With the damage states quantification, the vulnerability functions are derived from the fragility functions. The only difference in the procedure (with respect to on grade structures) is in the way the forces are calculated. Instead of directly using the coastal flood force equations, only the pressure acting on the superstructure is integrated to calculate the resulting lateral force acting on the elevated structure, as shown (shaded) in Figure 64. Damage begins to accumulate at the inundation height associated with wave crest reaching the lowest horizontal structural member, followed by rapid accumulation of damage with increasing depth due to larger wave forces at deeper inundation depths.

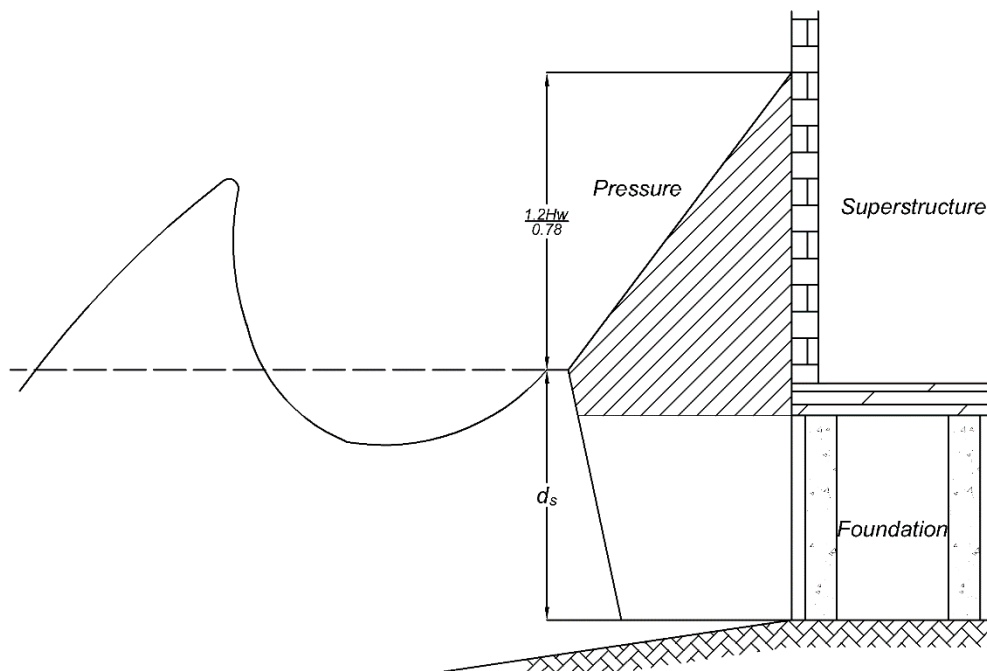


Figure 64. Pressure acting on elevated structure.

Combined mitigation: utility equipment elevated 2 feet and wet floodproofing 2 feet

Combining mitigations is a matter of implementing more than one mitigation method within the model simultaneously. The combinations performed involve wet floodproofing and elevated utility equipment from 1 to 3 feet. The resultant combination is derived by selecting the appropriate

distributions for utilities and interior. The resultant combined mitigation is not a linear superposition of individual mitigations.

3. Describe how personal residential time element losses are affected by performance of flood mitigation measures. Identify any assumptions.

Standard VF-3 explains that time element losses are related to structure damage. Therefore, any given mitigation that reduces structure damage will reduce time element losses.

4. Describe how personal residential structure and contents damage and their associated uncertainties are affected by flood mitigation measures. Identify any assumptions.

The implementation of mitigation measures directly influences one or more components of the structure damage as discussed in Disclosure 2. Standard VF-2 explains that content damage is a function of structure damage. Therefore any given mitigation that reduces structure damage will reduce content damage.

5. Describe how the effects of multiple flood mitigation measures are combined in the flood model and the process used to ensure that multiple flood mitigation measures are correctly combined.

Please refer to the last section of Disclosure 2. Combined mitigation vulnerabilities are graphically compared to the unmitigated structure as well as that structure with individual mitigations implemented to ensure an expected logical relationship.

6. Describe how flood mitigation measures affect the uncertainty of the vulnerability. Identify any assumptions.

Each of the mitigation measures implemented in the model involves assumptions regarding the precise nature of the mitigation measure, its influence on additional cost (both installation and repair), and the level of protection provided. For example, wet floodproofing has a very broad definition. Disclosure 2 discusses the interpretation employed in this model in terms of physical mitigation as well as its influence on cost, repair and vulnerability. Therefore, both the interpretation and implementation of any given mitigation or combination introduce uncertainty.

ACTUARIAL FLOOD STANDARDS

AF-1 Flood Modeling Input Data and Output Reports

A. Adjustments, edits, inclusions, or deletions to insurance company or other input data used by the modeling organization shall be based upon generally accepted actuarial, underwriting, and statistical procedures.

Modifications to insurance company or other input data is based on acceptable actuarial, underwriting and statistical procedures.

B. All modifications, adjustments, assumptions, inputs and input file identification, and defaults necessary to use the flood model shall be actuarially sound and shall be included with the flood model output report. Treatment of missing values for user inputs required to run the flood model shall be actuarially sound and described with the flood model output report.

All inputs, including the identification of the input file and any modifications to the inputs necessary to run the flood model are actuarially sound and described in the model output report. This includes the treatment of missing values.

Disclosures

1. Identify insurance-to-value assumptions and describe the methods and assumptions used to determine the property value and associated flood losses. Provide a sample calculation for determining the property value.

Modeler-Defined Input File

The exposures in this file were sourced from:

- NFIP's 2012 exposure file for Florida,
- The 2019 exposures of a manufactured home insurer whose policies include flood coverage, and
- Post-2012 construction for frame and masonry owners policies located in coastal ZIP codes as reported to the modeler by the Florida OIR for 2019 stress testing.

Properties from the latter two sources were assumed to be insured to value. The NFIP policies were matched to county tax assessor (TA) databases in order to determine the current property value. For unmatched exposures the building limit was assumed to be the property value.

Sample Calculation NFIP exposures:

Property Value = Max (TA database value, policy limit)

Sample Calculation Manufactured Home Insurer and Stress Testing Policies:

Property Value = Building Limit.

Vulnerability Calibration

Vulnerability calibration was based on NFIP claims for Florida. The claim records contain a building value field which is populated at time of claim. The contents value was estimated by applying the ratio of building value to building limit to the contents limit.

Sample Calculation:

Property Value = Reported Property Value on NFIP Claim Record.

Contents Value = (Property Value/Building Limit) x Contents Limit.

Model Validation

Model validation was based on NFIP 2004 exposures and claims. The NFIP policies were matched to county tax assessor databases in order to determine the current property value, and detrended by 3% per year to adjust for the change in value between 2019 and 2004. The property value was assumed to be the larger of the detrended tax assessor value and the policy limit. For unmatched exposures the building limit was assumed to be the property value.

Sample Calculation:

Property Value = Max (TA database value/1.56, policy limit).

Insurance Companies

The model assumes that insurance companies writing voluntary flood coverage will provide the property value as required in the input specifications.

Sample Calculation:

Property Value = Property Value as provided in the exposure input record.

2. Identify depreciation assumptions and describe the methods and assumptions used to reduce insured flood losses on account of depreciation. Provide a

sample calculation for determining the amount of depreciation and the actual cash value (ACV) flood losses.

The vulnerability assumptions were calibrated using NFIP loss data which is a mix of ACV and Replacement Cost, but primarily Replacement Cost on buildings and ACV on contents. There is no depreciation assumption applied to modeled ACV losses.

Sample calculation: ACV Building Loss = Modeled Building Loss - \$0 Depreciation.
ACV Contents Loss = Modeled Contents Loss - \$0 Depreciation.

3. Describe the different flood policies, contracts, and endorsements as specified in s. 627.715, F.S., that are modeled.

The model provides inputs for the following options in the cited statute:

- Replacement cost on contents
- Water intrusion from outside the structure other than Flood
- Additional Living Expenses/Time Element Coverage
- Supplemental Flood Coverage for jewelry, fine art or other specified personal effects
- Excess Flood Coverage (excess over an underlying flood policy).

Losses are currently modeled for Additional Living Expenses/Time Element Coverage.

4. Provide a copy of the input form(s) used by the flood model with the flood model options available for selection by the user for the Florida flood model under review. Describe the process followed by the user to generate the flood model output produced from the input form. Include the flood model name and version identification on the input form. All items included in the input form submitted to the Commission should be clearly labeled and defined.

**Florida Public Flood Loss Model: Release 1.0
Input Data File Format Specifications**

Personal Residential Policies

Input files containing personal residential policies to be processed through the Florida Public Flood Loss Model should adhere to the format specifications contained in this document.

Observe the following when preparing the input file:

- (a) Provide one policy per line in a comma-separated values file (.csv).
- (b) Do not use comma within the fields' values (e.g., as thousand separators or within addresses).
- (c) Include the name of each field in the first line of the file.
- (d) For fields that require a code, enter the code that most closely represents the data value.

(e) Only include policies with flood coverage.

Each policy should contain a total of 35 attributes. Always provide all 35 attributes.

- 1. Policy Coverage Type** The type of coverage for each policy. Encode the data to one of the following:

This policy includes coverage for:	Code
Primary flood only	1
Excess flood only	2

- 2. Policy ID** A unique identifier for this policy in the data file. An alphanumeric text.

- 3. ZIP Code** The ZIP Code where this building is located. A 5-digit number.

- 4. Latitude** The latitude where this building is located. Format: YY.YYYYYY. If not known, enter UNKNOWN.

- 5. Longitude** The longitude where this building is located. Format: XX.XXXXXX. If not known, enter UNKNOWN.

- 6. County** The name of the county where the building is located.

- 7. Address** The street address of the building.

- 8. City** The name of the city where the building is located.

- 9. Year Built** The year in which the building was built. A 4-digit number or UNKNOWN.

- 10. Year Retrofitted** The 4-digit year when the building was retrofitted (brought up to code).

If only the year of roof replacement is known, enter the 4-digit year when the roof was replaced followed by R (i.e. if the roof was replaced in 1999, enter 1999R).

If not retrofitted enter NA. If not known enter UNKNOWN.

- 11. Residence Type** The type of the residence covered by the policy. Encode the data to one of the following:

Value	Code
Single family residence, townhouse, or rowhouse	1
Condo unit	2
Rental unit in a multi-family building	3
Other or Unknown	4

12. Construction Type The construction type of the building. Encode the data to one of the following:

Value	Code
Frame, Timber, Wood	1
Masonry	2
Manufactured home – not tied-down	3
Manufactured home – partially tied-down	4
Manufactured home – tied-down	5
Manufactured home – unknown	6
Other	7
Unknown	8

13. Elevation Encode the data to one of the following:

Value	Code
Slab on-grade	1
Crawlspace – open	2
Crawlspace – closed	3
Elevated	4
Unknown	5

14. First Floor Elevation The elevation (ft.) of the first floor of the building with respect to ground elevation. If not known, enter UNKNOWN.

15. Number of Stories Number of stories in the building (e.g., 1, 2, 3, etc.) or UNKNOWN.

16. Elevated or Protected Utility As a mitigation measure, indicate whether the utilities are elevated or protected.

Value	Code
No	0
Protected or elevated by 1 foot	1
Protected or elevated by 2 feet	2
Protected or elevated by 3 feet	3
Unknown	4

17. Floodproofing	As a mitigation measure, indicate whether the building is floodproofed.																		
	<table border="1"> <thead> <tr> <th>Value</th> <th>Code</th> </tr> </thead> <tbody> <tr> <td>No</td> <td>0</td> </tr> <tr> <td>Wet floodproofed by 1 foot</td> <td>1</td> </tr> <tr> <td>Wet floodproofed by 2 feet</td> <td>2</td> </tr> <tr> <td>Wet floodproofed by 3 feet</td> <td>3</td> </tr> <tr> <td>Dry floodproofed by 1 foot</td> <td>4</td> </tr> <tr> <td>Dry floodproofed by 2 feet</td> <td>5</td> </tr> <tr> <td>Dry floodproofed by 3 feet</td> <td>6</td> </tr> <tr> <td>Unknown</td> <td>7</td> </tr> </tbody> </table>	Value	Code	No	0	Wet floodproofed by 1 foot	1	Wet floodproofed by 2 feet	2	Wet floodproofed by 3 feet	3	Dry floodproofed by 1 foot	4	Dry floodproofed by 2 feet	5	Dry floodproofed by 3 feet	6	Unknown	7
Value	Code																		
No	0																		
Wet floodproofed by 1 foot	1																		
Wet floodproofed by 2 feet	2																		
Wet floodproofed by 3 feet	3																		
Dry floodproofed by 1 foot	4																		
Dry floodproofed by 2 feet	5																		
Dry floodproofed by 3 feet	6																		
Unknown	7																		
18. Location of Unit	The story in which the unit is located (e.g., 1, 2, 3, etc.) or UNKNOWN. Only applicable to units in a multi-family building; e.g., condo or rental units. Enter NA for all other policy types.																		
19. Building or Unit Area	The total square feet of the insured unit or of all floors of the insured building. If not known, enter UNKNOWN.																		
20. Building or Unit Value	The dollar amount value of the insured building or unit. If not known, enter UNKNOWN.																		
21. Contents Value	The dollar amount value of the insured contents. If not known, enter UNKNOWN.																		
22. Building Coverage	The building coverage amount in dollars. Enter 0 if none.																		
23. App. Coverage	The appurtenant structure coverage amount in dollars. Enter 0 if none.																		
24. Contents Coverage	The contents coverage amount in dollars. Enter 0 if none.																		
25. ALE Coverage	The additional living expenses (ALE) coverage amount in dollars. Enter 0 if none.																		
26. Structure Deductible	The flood structure deductible amount in dollars (convert percentages to dollar amounts).																		
27. Contents Deductible	The flood contents deductible amount in dollars (convert percentages to dollar amounts).																		
28. Building Settlement Option	The settlement option on the building. Encode the data to one of the following:																		
	<table border="1"> <thead> <tr> <th>Value</th> <th>Code</th> </tr> </thead> <tbody> <tr> <td>Replacement Cost</td> <td>R</td> </tr> <tr> <td>Actual Cash Value</td> <td>A</td> </tr> </tbody> </table>	Value	Code	Replacement Cost	R	Actual Cash Value	A												
Value	Code																		
Replacement Cost	R																		
Actual Cash Value	A																		

29. Contents Settlement Option The settlement option on the contents. Encode the data to one of the following:

Value	Code
Replacement Cost	R
Actual Cash Value	A

30. Form The policy form number or prefix, if applicable. Otherwise enter N/A.

31. Program Code Use one uppercase letter to represent each company program.

32. Territory Code Use the territory codes reflected in your rate manual.

33. Increased Cost of Compliance Whether the policy includes Increased Cost of Compliance coverage.

Value	Code
Does not include coverage	0
Includes coverage	1
Coverage does not apply	NA

34. Water Intrusion Other than Flood Whether the policy includes coverage for water intrusion other than flood.

Value	Code
Does not include coverage	0
Includes coverage	1
Coverage does not apply	NA

35. Supplemental Flood Coverage Whether the policy includes supplemental flood coverage for jewelry, fine art, or other specified personal effects.

Value	Code
Does not include coverage	0
Includes coverage	1
Coverage does not apply	NA

Example data file:

PolicyCoverageType,PolicyID,ZIPCode,Latitude,Longitude,County,Address,City,YearBuilt,YearRetrofitted,ResidenceType,ConstructionType,Elevation,FirstFloorElevation,NumberOfStories,ElevatedOrProtectedUtility,FloodProofing,LocationOfUnit,BuildingOrUnitArea,BuildingOrUnitValue,ContentsValue,BuildingCoverage,AppCoverage,ContentsCoverage,ALCoverage,StructureDeductible,ContentsDeductible,BuildingSettlementOption,ContentsSettlementOption,Form,ProgramCode,TerritoryCode,ICC,WaterIntrusion,SupplementalFloodCoverage1,ABC100,33143,28.04747,-80.66522, Miami-Dade,123 MainStreet,Miami,1981,NA,1,2,1,2,1,0,0, NA, UNKNOWN,160000,50000,160000,0,20000,8000,1000,1000,R,R

The user submits an exposure file as specified above. The model run is executed by Computer Science staff at Florida International University. No other options are available to the user.

- 5. Disclose, in a flood model output report, the specific inputs required to use the flood model and the options of the flood model selected for use in a personal residential property flood insurance rate filing. Include the flood model name and version identification on the flood model output report. All items included in the flood model output report submitted to the Commission should be clearly labeled and defined.**

Flood Output Report

Florida Public Flood Loss Model: Release 1.0

Data Processing Results: <Company Name>

Report Content:

- Original Number of the policies in data set
- Process steps to formalize the data set
- Numbers of policies which are excluded due to specified reason
- Numbers of: Construction Types, Territory Codes, Policy Forms, Program Codes, etc.

- Coverage limits for building, appurtenant structure, content, additional living expense
- Distribution of deductibles
- Number of records that change values due to missing or illogical values
- Number of records for a county whose name is changed due to inconsistencies with the zip codes

- Number of policies to generate the estimated losses
- Number of files in the report

The results are aggregated by different combinations of counties, ZIP Codes, policy forms, program codes, territory codes, elevation codes, first floor elevation ranges, floodproofing codes, as applicable.

There will be files in the report for personal residential policies with names as below:

<CompanyName>_PERSONAL_Loss_ConstType.xls
<CompanyName>_PERSONAL_Loss_County.xls
<CompanyName>_PERSONAL_Loss_PolicyForm.xls
<CompanyName>_PERSONAL_Loss_ProgramCode.xls
<CompanyName>_PERSONAL_Loss_TerritoryCode.xls
<CompanyName>_PERSONAL_Loss_Zipcode.xls
<CompanyName>_PERSONAL_Loss_ElevationCode.xls

<p><CompanyName>_PERSONAL_Loss_FirstFloorElevationRange.xls <CompanyName>_PERSONAL_Loss_FloodproofingCode.xls</p> <p><CompanyName>_PERSONAL_Loss_ConstType_PolicyForm.xls <CompanyName>_PERSONAL_Loss_ConstType_ProgramCode.xls <CompanyName>_PERSONAL_Loss_ConstType_TerritoryCode.xls <CompanyName>_PERSONAL_Loss_ConstType_ElevationCode.xls <CompanyName>_PERSONAL_Loss_ConstType_FirstFloorElevationRange.xls <CompanyName>_PERSONAL_Loss_ConstType_FloodproofingCode.xls</p> <p><CompanyName>_PERSONAL_Loss_County_ConstType.xls <CompanyName>_PERSONAL_Loss_County_PolicyForm.xls <CompanyName>_PERSONAL_Loss_County_ProgramCode.xls <CompanyName>_PERSONAL_Loss_County_TerritoryCode.xls <CompanyName>_PERSONAL_Loss_County_ElevationCode.xls <CompanyName>_PERSONAL_Loss_County_FirstFloorElevationRange.xls <CompanyName>_PERSONAL_Loss_County_FloodproofingCode.xls</p>
<p><CompanyName>_PERSONAL_Loss_Zipcode_ConstType.xls <CompanyName>_PERSONAL_Loss_Zipcode_PolicyForm.xls <CompanyName>_PERSONAL_Loss_Zipcode_ProgramCode.xls <CompanyName>_PERSONAL_Loss_Zipcode_TerritoryCode.xls <CompanyName>_PERSONAL_Loss_Zipcode_ElevationCode.xls <CompanyName>_PERSONAL_Loss_Zipcode_FirstFloorElevationRange.xls <CompanyName>_PERSONAL_Loss_Zipcode_FloodproofingCode.xls</p> <p><CompanyName>_PERSONAL_Loss_ProgramCode_TerritoryCode_ElevationCode.xls <CompanyName>_PERSONAL_Loss_ProgramCode_TerritoryCode_FirstFloorElevationRange.xls <CompanyName>_PERSONAL_Loss_ProgramCode_TerritoryCode_FloodproofingCode.xls</p> <p><CompanyName>_PERSONAL_Loss_ProgramCode_County_ElevationCode.xls <CompanyName>_PERSONAL_Loss_ProgramCode_County_FirstFloorElevationRange.xls <CompanyName>_PERSONAL_Loss_ProgramCode_County_FloodproofingCode.xls</p> <p><CompanyName>_PERSONAL_Loss_ProgramCode_Zipcode_ElevationCode.xls <CompanyName>_PERSONAL_Loss_ProgramCode_Zipcode_FirstFloorElevationRange.xls <CompanyName>_PERSONAL_Loss_ProgramCode_Zipcode_FloodproofingCode.xls</p>

6. Explain the differences in data input and flood model output required for coastal and inland flood modeling.

There is no difference in exposure input requirements between coastal and inland areas. The model output does not vary between coastal and inland areas.

7. Describe actions performed to ensure the validity of insurer or other input data used for flood model inputs or for validation/verification.

There is extensive pre-processing of exposure inputs to identify invalid coding or missing information. Exposures may be dropped or missing values assigned (e.g. year-built) based on county statistics. During pre-processing addresses are geocoded if latitude/longitude coordinates are not provided, and first floor elevation, if unknown, is assigned based on construction type and elevation code.

A flowchart of exposure pre-processing is available for review.

8. Disclose if changing the order of the flood model input exposure data produces different flood model output or results.

If exposure inputs having missing or invalid items are randomly assigned during pre-processing based on available statistics, changing the order of the input data could impact the model output.

9. Disclose if removing or adding policies from the flood model input file affects the flood model output for the remaining policies.

If exposure inputs having missing or invalid items are randomly assigned during pre-processing based on available statistics, adding or removing policies from the input file could impact the model output.

AF-2 Flood Events Resulting in Modeled Flood Losses

- A. Modeled flood loss costs and flood probable maximum loss levels shall reflect insured flood related damages from both coastal and inland flood events impacting Florida.***

Modeled flood losses are produced for both coastal and inland flood events impacting Florida.

- B. The modeling organization shall have a documented procedure for distinguishing flood-related losses from other peril losses.***

The procedure for distinguishing flood-related losses from other peril losses is documented.

Disclosures

- 1. Describe how damage from flood model generated floods (originating either inside or outside of Florida) is excluded or included in the calculation of flood loss costs and flood probable maximum loss levels for Florida.***

No events in the stochastic set of events are excluded from the calculation of flood loss costs and probable maximum loss levels, but based on the hydrological state and inundation depth at a particular location, the damage ratio may be zero.

- 2. Describe how wind losses associated with coastal and inland flooding are treated in the calculation of flood loss costs and flood probable maximum loss levels for Florida.***

Wind losses are not included in the calculation of flood loss costs and flood probable maximum loss levels.

- 3. Describe how the flood model considers the correlation and potential overlap of flood losses associated with coastal and inland flooding.***

If both coastal and inland flooding impact a location for a single storm, the model determines separate damages for each, and selects the larger damage.

- 4. Other than coastal and inland flooding, state whether any other types of flooding events are modeled. If so, describe how damage resulting from these flood type events is treated in the calculation of flood loss costs and flood probable maximum loss levels for Florida.***

Only coastal and inland flooding are modeled and included in flood loss costs and flood probable maximum loss levels.

5. Describe which non-flood water losses are considered flood losses from water intrusion. Describe how water intrusion losses are considered in the calculation of flood loss costs and flood probable maximum loss levels for Florida.

In accordance with s. 627.715, F.S. the model input record allows for the option of “water intrusion from outside the structure other than Flood. This option will not be included in flood loss costs and flood probable maximum loss levels unless elected, and is not included in the loss costs and probable maximum loss levels reported in this submission’s forms.

AF-3 Flood Coverages

A. The methods used in the calculation of personal residential structure flood loss costs shall be actuarially sound.

The model's calculation of personal residential structure loss costs is actuarially sound.

B. The methods used in the calculation of personal residential appurtenant structure flood loss costs shall be actuarially sound.

The model's calculation of personal residential appurtenant structure loss costs is actuarially sound.

C. The methods used in the calculation of personal residential contents flood loss costs shall be actuarially sound.

The model's calculation of personal residential contents loss costs is actuarially sound.

D. The methods used in the calculation of personal residential time element flood loss costs shall be actuarially sound.

The model's calculation of personal residential time element loss costs is actuarially sound.

Disclosures

1. Describe the methods used in the flood model to calculate flood loss costs for residential structure coverage associated with personal residential properties.

The model includes a set of vulnerability matrices for personal residential buildings. The matrices specify the expected percent damage for a given hydrological state and inundation depth.

For each building in a policy portfolio the applicable matrix for that building is determined by the building's characteristics.

This percent damage to the building is determined for each event in the stochastic set. The resulting damages, adjusted for policy limits, deductibles and demand surge, are aggregated across all events to calculate the average annual loss and loss cost per \$1,000 of exposure.

2. Describe the methods used in the flood model to calculate flood loss costs for appurtenant structure coverage associated with personal residential properties.

For appurtenant structures that are not rated as a separate building by the NFIP (e.g. a guest house), a set of vulnerability matrices is applied to determine expected percent damage for a given hydrological state and inundation depth.

This percent damage to the appurtenant structure is determined for each event in the stochastic set. The resulting damages, adjusted for policy limits, deductibles and demand surge, are aggregated across all events to calculate the average annual loss and loss cost per \$1,000 of exposure.

The standard NFIP policy does not include appurtenant structure coverage, beyond 10% of the building limit that can be applied to a detached garage. The model only calculates losses for this coverage if the exposure input record indicates appurtenant structures is included by providing a specific limit.

3. Describe the methods used in the flood model to calculate flood loss costs for contents coverage associated with personal residential properties.

A set of vulnerability matrices is applied to determine expected percent contents damage for a given hydrological state and inundation depth.

This percent damage to the contents is determined for each event in the stochastic set. The resulting damages, adjusted for policy limits, deductibles and demand surge, are aggregated across all events to calculate the average annual loss and loss cost per \$1,000 of exposure.

4. Describe the methods used in the flood model to calculate flood loss costs for time element coverage associated with personal residential properties.

A set of vulnerability matrices is applied to determine expected percent time element loss for a given hydrological state and inundation depth.

This percent loss is determined for each event in the stochastic set. The resulting losses, adjusted for policy limits, deductibles and demand surge, are aggregated across all events to calculate the average annual loss and loss cost per \$1,000 of exposure.

The standard NFIP policy does not include time element coverage. The model only calculates losses for this coverage if the exposure input record indicates time element is included by providing a specific limit.

AF-4 Modeled Flood Loss Cost and Flood Probable Maximum Loss Level Considerations

A. Flood loss cost projections and flood probable maximum loss levels shall not include expenses, risk load, investment income, premium reserves, taxes, assessments, or profit margin.

The model does not include expenses, risk load, investment income, premium reserves, taxes, assessments, or profit margin in the calculation of loss costs and probable maximum loss levels.

B. Flood loss cost projections and flood probable maximum loss levels shall not make a prospective provision for economic inflation.

The model does not make a prospective provision for economic inflation in the calculation of loss costs and probable maximum loss levels.

C. Flood loss cost projections and flood probable maximum loss levels shall not include any explicit provision for wind losses.

The model does not include any explicit provision for wind losses in the calculation of loss costs and probable maximum loss levels.

D. Damage caused from inland and coastal flooding shall be included in the calculation of flood loss costs and flood probable maximum loss levels.

Damage caused from inland and coastal flooding is included in the model's calculation of loss costs and probable maximum loss levels.

E. Flood loss cost projections and flood probable maximum loss levels shall be capable of being calculated from exposures at a geocode (latitude-longitude) level of resolution including the consideration of flood extent and depth.

The model allows for loss cost and probable maximum loss calculations at the geocode level of resolution including the consideration of flood extent and depth.

F. Demand surge shall be included in the flood model's calculation of flood loss costs and flood probable maximum loss levels using relevant data and actuarially sound methods and assumptions.

Demand surge is included in the model's calculation of loss costs and probable maximum loss levels. The methods and assumptions underlying the demand surge factors are actuarially sound.

Disclosures

1. Describe the method(s) used to estimate annual flood loss costs and flood probable maximum loss levels. Identify any source documents used and any relevant research results.

To estimate annual loss costs and probable maximum loss levels, losses are estimated for individual policies in the portfolio for each event in a stochastic set. Damages are estimated separately by coverage.

The estimated damages for each policy's coverages are capped by policy limits, reduced by applicable deductibles and increased to allow for the effect of demand surge on claim costs.

The modeled insured losses can then be summed across all properties in a ZIP code or across all ZIP codes in a county to obtain expected aggregate loss. The losses can also be aggregated by policy form, construction type, rating territories, etc.

Finally, modeled losses are divided by the number of years in the simulation and by the total amount of insurance to estimate annual loss costs.

To estimate probable maximum loss on an "annual aggregate" basis modeled losses for events occurring in the same year of the simulation are summed to produce annual losses. Probable maximum loss levels are calculated from the ordered set of annual losses as described in Standard AF-6, Disclosure # 6.

To estimate probable maximum loss on an "annual occurrence" basis the ordered set consists of the largest loss in each year of the simulation.

The following source was used in the research:

Wilkinson, M. E. (1982). Estimating Probable Maximum Loss with Order Statistics. *Casualty Actuarial Society, LXIX*, pp. 195-209.

2. Identify the highest level of resolution for which flood loss costs and flood probable maximum loss levels can be provided. Identify all possible resolutions available for the reported flood output ranges.

Loss costs and probable maximum loss levels can be calculated at the policy level, or for policies aggregated by territory, Zip code, county, or any characteristic provided with the exposures.

3. Describe how the flood model incorporates demand surge in the calculation of flood loss costs and flood probable maximum loss levels. Indicate if there are any differences in the manner that demand surge is incorporated for coastal and inland flooding.

Demand surge factors by county and coverage are calculated for each event in the stochastic set based on the size of the event in terms of modeled losses. These factors are applied to modeled losses which then flow into the loss costs and probable maximum loss levels. There is no difference in the manner in which demand surge is incorporated for coastal vs. inland flooding.

4. *Provide citations to published papers, if any, or modeling-organization studies that were used to develop how the flood model estimates demand surge.*

Demand surge factors are based on a study performed by the modeler relating the size of an event (in terms of losses) to the historical increase in construction costs after a hurricane. The study relied on the Marshall & Swift/ Boeckh construction cost indices for Florida Zip codes and hurricanes occurring between 1992 and 2007.

5. *Describe how economic inflation has been applied to past insurance experience to develop and validate flood loss costs and flood probable maximum loss levels.*

For validation testing NFIP 2004 exposures were matched to county tax assessor databases in order to determine the property value. The property values were detrended at 3% per year in order to approximate the property value in 2004.

AF-5 Flood Policy Conditions

A. The methods used in the development of mathematical distributions to reflect the effects of deductibles, policy limits, and flood policy exclusions shall be actuarially sound.

The methods used by the model to reflect the impact of deductibles, policy limits, and flood policy exclusions are actuarially sound.

B. The relationship among the modeled deductible flood loss costs shall be reasonable.

Testing of this requirement is incomplete

C. Deductible flood loss costs shall be calculated in accordance with s. 627.715, F.S.

The model allows for the dollar amount and percentage deductibles specified in the statute. Annual deductibles are not modeled.

Disclosures

1. Describe the methods used in the flood model to treat deductibles, policy limits, policy exclusions, loss settlement provisions, and insurance-to-value criteria when projecting flood loss costs and flood probable maximum loss levels. In particular, specify the loss settlement options available for manufactured homes.

To estimate annual loss costs and probable maximum loss levels, damages are modeled for individual policies in a portfolio for each event in a stochastic set. Damages are estimated separately by coverage.

The estimated damages for each policy's coverages are capped by policy limits and reduced by applicable deductibles.

The treatment of insurance-to-value criteria is discussed in detail under Standard AF-1, disclosure #1.

Standard NFIP policy exclusions such as additional living expense coverage are not modeled unless a limit is provided in the exposure input for a policy. Similarly, damage to property outside an insured building is not modeled unless an appurtenant structure limit is provided for a policy.

The model's vulnerability assumptions were calibrated using NFIP loss data which is a mix of ACV and Replacement Cost, but primarily Replacement Cost on buildings and ACV on contents.

There are no adjustments to individual policies, those for manufactured homes or otherwise, based on settlement option.

2. Provide an example of how insurer flood loss (flood loss net of deductibles) is calculated. Discuss data or documentation used to validate the method used by the flood model.

Flood losses net of deductibles are calculated as per the example provided.

Example:

(A)		(B)	(C)	(D)=(A)*(C)	(E)=(D)-(B)
Structure Value	Policy Limit	Deductible	Damage Ratio	Zero Deductible Flood Loss	Flood Loss Net of Deductible
\$100,000	\$90,000	\$1,500	2%	\$2,000	\$500

3. Describe how the flood model treats annual deductibles.

Annual deductibles are not modeled.

AF-6 Flood Loss Outputs and Logical Relationships to Risk

A. The methods, data, and assumptions used in the estimation of flood probable maximum loss levels shall be actuarially sound.

Testing of this requirement is incomplete.

B. Flood loss costs shall not exhibit an illogical relation to risk, nor shall flood loss costs exhibit a significant change when the underlying risk does not change significantly.

Testing of this requirement is incomplete.

C. Flood loss costs cannot increase as the structure flood damage resistance increases, all other factors held constant.

Testing of this requirement is incomplete.

D. Flood loss costs cannot increase as flood hazard mitigation measures incorporated in the structure increase, all other factors held constant.

Testing of this requirement is incomplete.

E. Flood loss costs shall be consistent with the effects of major flood control measures, all other factors held constant.

Testing of this requirement is incomplete.

F. Flood loss costs cannot increase as the flood resistant design provisions increase, all other factors held constant.

Testing of this requirement is incomplete.

G. Flood loss costs cannot increase as building code enforcement increases, all other factors held constant.

Testing of this requirement is incomplete.

H. Flood loss costs shall decrease as deductibles increase, all other factors held constant.

Testing of this requirement is incomplete.

- I. The relationship of flood loss costs for individual coverages (e.g., personal residential structure, appurtenant structure, contents, and time element) shall be consistent with the coverages provided.***

Testing of this requirement is incomplete.

- J. Flood output ranges shall be logical for the type of risk being modeled and apparent deviations shall be justified.***

Testing of this requirement is incomplete.

- K. All other factors held constant, flood output ranges produced by the flood model shall in general reflect lower flood loss costs for personal residential structures that have a higher elevation versus those that have a lower elevation.***

Testing of this requirement is incomplete.

- L. For flood loss costs and flood probable maximum loss level estimates derived from and validated with historical insured flood losses or other input data and information, the assumptions in the derivations concerning (1) construction characteristics, (2) policy provisions, and (3) contractual provisions shall be appropriate based on the type of risk being modeled.***

Testing of this requirement is incomplete.

Disclosures

- 1. Provide a completed Form AF-1, Zero Deductible Personal Residential Standard Flood Loss Costs. Provide a link to the location of the form [insert hyperlink here].***

Form AF-1 is not complete at this time.

- 2. Provide a completed Form AF-2, Total Flood Statewide Loss Costs. Provide a link to the location of the form [insert hyperlink here].***

Form AF-2 is not complete at this time.

- 3. Provide a completed Form AF-3, Personal Residential Standard Flood Loss Costs by ZIP Code. Provide a link to the location of the form [insert hyperlink here].**

Form AF-3 is not complete at this time.

- 4. Provide a completed Form AF-4, Flood Output Ranges, using the modeling-organization-specified, predetermined, and comprehensive exposure dataset. Provide a link to the location of the form [insert hyperlink here].**

Form AF-4 is not complete at this time.

- 5. Provide a completed Form AF-6, Flood Probable Maximum Loss for Florida. Provide a link to the location of the form [insert hyperlink here].**

Form AF-6 is not complete at this time.

- 6. Describe how the flood model produces flood probable maximum loss levels.**

Probable Maximum Loss (PML) on an Annual Aggregate Basis

Probable maximum loss is produced non-parametrically using order statistics of simulated annual losses.

The model produces N simulated annual losses, represented by X_1, X_2, \dots, X_N . The data are ordered so that $X_{(1)} \leq X_{(2)} \leq \dots \leq X_{(N)}$.

Let $k = (N) * (1 - \text{Annual Exceedance Probability})$.

If k is an integer, then the estimate of the PML is the k th order statistic, $X_{(k)}$, of the simulated losses. If k is not an integer, then let k^* = the smallest integer greater than k , and the estimate of the PML is given by $X_{(k^*)}$.

Probable Maximum Loss on an Annual Occurrence Basis

Probable maximum loss on an annual occurrence basis is determined similarly to probable maximum loss on an annual aggregate basis. The set of N losses, X_1, X_2, \dots, X_N , consists of the largest event loss in each simulated year, ordered from smallest to largest.

- 7. Provide citations to published papers, if any, or modeling-organization studies that were used to estimate flood probable maximum loss levels.**

Wilkinson, M. E. (1982). Estimating Probable Maximum Loss with Order Statistics. *Casualty Actuarial Society, LXIX*, pp. 195-209.

FPFLM V1.0 Feb. 29, 2020

8. Explain any differences between the values provided on Form AF-6, Flood Probable Maximum Loss for Florida, and those provided on Form SF-2, Examples of Flood Loss Exceedance Estimates (Coastal and Inland Combined).

Form AF-6 is not complete at this time.

9. Provide an explanation for all flood loss costs that are not consistent with the requirements of this standard.

Testing for compliance with this standard is incomplete.

COMPUTER/INFORMATION FLOOD STANDARDS

CIF-1 Flood Model Documentation

A. Flood model functionality and technical descriptions shall be documented formally in an archival format separate from the use of letters, slides, and unformatted text files.

The Florida Public Flood Loss Model (FPFLM) formally documents the model functionality and technical descriptions in the primary document repository, an archival format separate from the use of letters, slides, and unformatted text files. The primary document repository uses standard software practices to formally describe the model's requirements and complete software design and implementation specifications. All documentation related to the model is maintained in the project's primary document repository, a central location that is easily accessible.

B. The modeling organization shall maintain a primary document repository, containing or referencing a complete set of documentation specifying the flood model structure, detailed software description, and functionality. Documentation shall be indicative of current model development and software engineering practices.

The FPFLM maintains a primary document repository to satisfy the aforementioned requirements. In addition, the FPFLM maintains a user manual, designed for the end user, which provides a high-level introduction and a step-by-step guide to the entire system. All the documents are available for inspection on the project's primary document repository. Current software engineering best practices are used to render all the documents more readable, self-contained, consistent, and easy to understand. Every component of the system is documented with standard use case, class, data flow, sequence diagrams, etc. The diagrams describe in detail the structure, logic flow, information exchange among submodules, etc. of each component and increase the visibility of the system. The diagrams describing the component functionality and structure also make each component of the system reusable and easily maintainable.

C. All computer software (i.e., user interface, scientific, engineering, actuarial, data preparation, and validation) relevant to the flood model shall be consistently documented and dated.

The primary document repository contains all of the required documentation organized in chapters and sections linked to one another on the basis of their mutual relationships. Thus, the entire document can be viewed as a hierarchical referencing scheme in which each module is linked to its sub-module, which ultimately refers to the corresponding codes.

D. The modeling organization shall maintain a table of all substantive changes in the flood model since this year's initial submission.

This table is maintained and documented and will be available for review.

E. Documentation shall be created separately from the source code.

The aforementioned primary document repository, created and maintained according to the requirements specified in this standard, is separate from source code and source code documentation.

F. The modeling organization shall maintain a list of all externally acquired currently used flood model-specific software and data assets. The list shall include (1) asset name, (2) asset version number, (3) asset acquisition date, (4) asset acquisition source, (5) asset acquisition mode (e.g., lease, purchase, open source), and (6) length of time asset has been in use by the modeling organization.

We created and maintain a list of all the externally acquired currently used flood model-specific software and data assets. The list will be available for review.

CIF-2 Flood Model Requirements

The modeling organization shall maintain a complete set of requirements for each software component as well as for each database or data file accessed by a component. Requirements shall be updated whenever changes are made to the flood model.

The FPFLM is divided into several major modules, each of them providing one or more inputs to other modules. Requirements of each of the modules, including input/output formats, are precisely documented. In addition to maintaining a detailed documentation of each module of the system using standard software practices, several other documents are maintained as part of a large-scale project management requirement, including a quality assurance document, a system hardware and software specification document, a training document, a model maintenance document, a testing document, a user manual, etc. Moreover, detailed documentation has been developed for the database consisting of the schema and information about each table. Additionally, information about the format for each data file (in the form of an Excel or text file) accessed by different programs is documented. Whenever changes are made to a model, the corresponding requirements documentation is updated to reflect such changes.

Disclosure

- 1. Provide a description of the documentation for interface, human factors, functionality, documentation, data, human and material resources, security, and quality assurance.***

The user interface, functionality requirements, and material resources of each of the modules are described in the relevant module documentation using formal modeling languages and representations. Database schema, table formats, security, software and hardware specifications, and training plans are separately documented for the whole system in the primary document repository. A separate software testing and quality assurance document describes the system quality, performance, and stability concerns. Additionally, a user manual and a human resource management document are maintained.

CIF-3 Flood Model Architecture and Component Design

- A. The modeling organization shall maintain and document (1) detailed control and data flowcharts and interface specifications for each software component, (2) schema definitions for each database and data file, (3) flowcharts illustrating flood model-related flow of information and its processing by modeling organization personnel or consultants, and (4) system model representations associated with (1)-(3). Documentation shall be to the level of components that make significant contributions to the flood model output.**

Interface specifications for each of the software modules are included in the module's documentation. Diagrams are presented at various levels of the model documentation. High-level flowcharts are used to illustrate the flow of the whole system and the interactions among modules. More detailed diagrams are used in module-level descriptions.

The database schema is documented in the primary document repository. A detailed schema representation of the active database is documented with additional information such as database maintenance, tuning, data loading methodologies, etc. to provide a complete picture of the database maintained for the project.

Additionally, business process diagrams are used to illustrate the flow of model-related information and its processing by modeling organization personnel and consultants.

- B. All flowcharts (e.g., software, data, and system models) shall be based on (1) a referenced industry standard (e.g., Unified Modeling Language (UML), Business Process Model and Notation (BPMN), Systems Modeling Language (SysML)), or (2) a comparable internally-developed standard which is separately documented.**

Diagrams documenting the FPFLM are created according to standards International Organization for Standards (ISO) 5807, Business Process Model and Notation (BPMN) 2, and Unified Modeling Language (UML) 2.

Data flowcharts, program flowcharts, system flowcharts, program network charts, and system resources charts are created according to ISO 5807. Flowcharts illustrating model-related flow of information and its processing by team members follow BPMN 2. Other diagrams for both behavioral and structural object-oriented design documentation such as use case and class diagrams follow UML 2.

CIF-4 Flood Model Implementation

A. The modeling organization shall maintain a complete procedure of coding guidelines consistent with current software engineering practices.

The FPFLM has developed and followed a set of coding guidelines that is consistent with accepted software engineering practices. These guidelines include policies for coding style, version control, code revision history maintenance, etc. Developers involved in the system development adhere to the instructions in these documents.

B. The modeling organization shall maintain a complete procedure used in creating, deriving, or procuring and verifying databases or data files accessed by components.

The FPFLM uses a PostgreSQL databases to store, pre-process, and post-process model input and output data. The procedures for creating and using these databases is formalized in the form of stored procedures, which are documented in-line and in the primary document repository. Data files are generated by different modules and used as data interfaces between modules. Several data verification steps are undertaken to ensure their correctness. These steps are formalized in the form of Linux shell scripts and documented as part of the primary document repository.

C. All components shall be traceable, through explicit component identification in the flood model representations (e.g., flowcharts) down to the code level.

Traceability, from requirements to the code level and vice versa, is maintained throughout the system documentation.

D. The modeling organization shall maintain a table of all software components affecting flood loss costs and flood probable maximum loss levels with the following table columns: (1) component name, (2) number of lines of code, minus blank and comment lines, and (3) number of explanatory comment lines.

The FPFLM primary document repository includes a table of all software components affecting flood loss costs and flood probable maximum loss levels with the required columns.

E. Each component shall be sufficiently and consistently commented so that a software engineer unfamiliar with the code shall be able to comprehend the component logic at a reasonable level of abstraction.

Computer code comments are consistently used throughout all of the model's codebase to ease the understanding of its logic. These code-level comments include a summary of important changes, names of developers involved in each modification, function headers, and in-line comments to explain potentially ambiguous software code.

F. The modeling organization shall maintain the following documentation for all components or data modified by items identified in Standard GF-1, Scope of the Flood Model and Its Implementation, Audit 6:

- 1. A list of all equations and formulas used in documentation of the flood model with definitions of all terms and variables.**
- 2. A cross-referenced list of implementation source code terms and variable names corresponding to items within F.1 above.**

Tables mapping the equations and formulas used in the model's documentation to the source code terms and variable names are provided in the glossaries to the model's documentation, thus combining F.1 and F.2 into a single table. These tables enhance the model's documentation and include the equations and formulas for each module (not just the modified ones from the prior year's submission).

Disclosure

- 1. Specify the hardware, operating system, other software, and all computer languages required to use the flood model.**

The user-facing part of the system consists of a collection of Linux command line scripts written in Bash and Python. These interface scripts call the core components, which are written in C++, MATLAB, Python, and Scala. The core programs are run on either an HPC or Spark cluster. The details of the FPFLM hardware infrastructure are included in the primary document repository.

CIF-5 Flood Model Verification

A. General

For each component, the modeling organization shall maintain procedures for verification, such as code inspections, reviews, calculation crosschecks, and walkthroughs, sufficient to demonstrate code correctness. Verification procedures shall include tests performed by modeling organization personnel other than the original component developers.

The FPFLM software verification is done in three stages:

1. Code inspection and verification by the code developer.
2. Inspection of the input and validation of the output by the system modeler.
3. Review and extensive testing of the code by modeler personnel who are not part of the original component development.

The first level of verification includes code-level debugging, walking through the code to ensure a proper flow, inspection of internal variables through intermediate output printing and error logging, use of exception handling mechanisms, calculation crosschecks, and verification of the output against sample calculations provided by the system modeler.

In the second level of the verification, the modeler is provided with sample inputs and corresponding outputs. The modeler then conducts black-box testing to verify the results against his or her model. Finally, each component is rigorously tested by modeler personnel not responsible for original component development.

B. Component Testing

- 1. The modeling organization shall use testing software to assist in documenting and analyzing all components.***

Component testing and data testing are done in the third level of verification. The system is rigorously checked for the correctness, precision, robustness, and stability of the whole system. Calculations are performed outside the system and compared against the system-generated results to ensure the system correctness. Extreme and unexpected inputs are given to the system to check the robustness. Wide series of test cases are developed to check the stability and the consistency of the system.

- 2. Unit tests shall be performed and documented for each component.***

Unit testing is done at the first and third levels of verification. The developer tests all the units as the unit is developed and modified. Then all the units are tested again by the external testing team. Both black-box and white-box tests are performed and documented in a separate testing document.

3. Regression tests shall be performed and documented on incremental builds.

Regression testing is performed for each module. In this kind of testing methodology, the modules that have undergone some changes and revisions are retested to ensure that the changes have not affected the entire system in any undesired manner.

4. Aggregation tests shall be performed and documented to ensure the correctness of all flood model components. Sufficient testing shall be performed to ensure that all components have been executed at least once.

Aggregation testing is performed at all three levels of verification. Aggregation testing is performed by running each major module as a complete package. It is ensured that all components have been executed at least once during the testing procedure. All the test cases executed are described in the software testing and verification documentation.

C. Data Testing

1. The modeling organization shall use testing software to assist in documenting and analyzing all databases and data files accessed by components.

The FPFLM uses a PostgreSQL database to store the required data. Data integrity and consistency are maintained by the Relational Database Management System itself. Moreover, different queries are issued and PL/SQL is implemented to check the database. PostgreSQL has a very robust loader, which is used to load the data into the database. The loader maintains a log that depicts if the loading procedure has taken place properly and completely without any discrepancy. Data files are manually tested using commercial data manipulation software such as Microsoft Excel and Microsoft Access.

2. The modeling organization shall perform and document integrity, consistency, and correctness checks on all databases and data files accessed by the components.

All the tests are well documented in a separate testing document.

Disclosures

1. State whether any two executions of the flood model with no changes in input data, parameters, code, and seeds of random number generators produce the same flood loss costs and flood probable maximum loss levels.

The model produces the same loss costs and probable maximum loss levels if it is executed more than once with no changes in input data, parameters, code, and seeds of random number generators.

2. Provide an overview of the component testing procedures.

The FPFLM software testing and verification is done in three stages.

[A] Code inspection and the verification by the code developer.

The code developer performs a sufficient amount of testing on the code and does not deliver the code until he or she is satisfied with the correctness and robustness of the code. The first level of verification includes code-level debugging, walking through the code to ensure proper flow, inspection of internal variables through intermediate output printing and error logging, use of exception handling mechanisms, calculation crosschecks, and verification of the output against sample calculations provided by the system modeler.

[B] Verification of results by the person who developed the system model.

Once the first level of testing is done, the developer sends the sample inputs and the generated results back to the modeler. Then the system modeler double-checks the results against his or her model. The code is not used in the production environment unless approved by the modeler.

[C] Review and extensive testing of the code by modeler personnel other than the original component developers. The system is rigorously checked by modeler personnel (testers) other than the original component developers for the correctness, precision, robustness, and stability of the whole system. Calculations are performed outside the system and compared against the system generated results to ensure the system correctness. Extreme and unexpected inputs are given to the system to check the robustness. Wide series of test cases are developed to check the stability and the consistency of the system. Unit testing, regression testing, and aggregation testing (both white-box and black-box) are performed and documented.

Any flaw in the code is reported to the developer, and the bug-corrected code is again sent to the tester. The tester then performs unit testing again on the modified units. Additionally, regression testing is performed to determine if the modification affects any other parts of the code.

3. Provide a description of verification approaches used for externally acquired data, software, and models.

The verification approaches used for externally acquired data, software, and models are documented in the primary document repository.

CIF-6 Flood Model Maintenance and Revision

- A. The modeling organization shall maintain a clearly written policy for flood model review, maintenance, and revision, including verification and validation of revised components, databases, and data files.**

The primary document repository contains a clear policy for model review, maintenance, and revision.

- B. A revision to any portion of the flood model that results in a change in any Florida personal residential flood loss cost or flood probable maximum loss level shall result in a new flood model version identification.**

Whenever a revision results in a change in any Florida residential flood loss cost or probable maximum loss level, a new model version identification will be assigned to the revision. Verification and validation of the revised units are repeated according to the model's verification procedures.

- C. The modeling organization shall use tracking software to identify and describe all errors, as well as modifications to code, data, and documentation.**

The FPFLM uses Subversion to identify and describe all errors as well as modifications to code, data, and documentation.

- D. The modeling organization shall maintain a list of all flood model versions since the initial submission for this year. Each flood model description shall have a unique version identification and a list of additions, deletions, and changes that define that version.**

A list of all model versions since the initial submission is maintained as part of the model's documentation. Each model revision has a unique version number and a list of additions, deletions, and changes that define that version. The unique model version will consist of the scheme "V[major].[minor]." The terms "[major]" and "[minor]" are positive integers that correspond to substantial and minor changes in the model, respectively. A minor change in the model would cause the minor number to be incremented by one, and similarly, a major change in the model would cause the major number to be incremented by one with the minor reset to zero. The rules that prompt changes in the major and minor numbers are described in Disclosure 2.

Disclosures

- 1. Identify procedures used to review and maintain code, data, and documentation.**

The FPFLM's software development team employs version control software for all software development. In particular, the FPFLM uses Subversion, an accepted and effective system for managing simultaneous development of files. Subversion maintains a record of the changes to each file and allows the user to revert to a previous version, merge versions, and track changes. This software is able to record the information for each file, the date of each change, the author of each change, the file version, and the comparison of the file before and after the changes.

2. Describe the rules underlying the flood model and code revision identification systems.

The model identification system consists of the scheme "V[major].[minor]." The terms "[major]" and "[minor]" are positive integers that correspond to major and minor changes in the model, respectively. A minor change causes the minor number to be incremented by one, and similarly, a major change causes the major number to be incremented by one with the minor number reset to zero. The rules that prompt major or minor changes in the model are the following:

Any of the following events will trigger a change in the major number:

- Major updates in any of the main modules of the FPFLM: major modification of the Storm Forecast Module, Wind Field Model, Wind Speed Correction Module, Storm Surge Module, Waves Module, Inland Flood Module, Vulnerability Module, or Insured Loss Module.
- Addition or removal of options affecting how input data is processed by the model.
- Addition or removal of attributes in the model's input data specification.

Any of the following events will trigger a change in the minor number:

- Minor changes to the Storm Forecast Module, Wind Field Model, Wind Speed Correction Module, Storm Surge Module, Waves Module, Inland Flood Module, Vulnerability Module, or Insured Loss Module: minor updates such as a change in the Holland B parameter or any change to correct deficiencies that do not result in a new algorithm for the component.
- Updates to correct errors in the computer code: modifications in the code to correct deficiencies or errors such as a code bug in the computer program.
- Changes in the probability distribution functions using updated or corrected historical data, such as the updates of the HURDAT2 database: each year the model updates its HURDAT database with the latest HURDAT2 data released by the National Hurricane Center, which is used as the input in the Storm Generation Model.
- Updates of the ZIP Code list: every two years the ZIP Codes used in the model must be updated according to information originating from the United States Postal Service.
- Updates in the validation of the vulnerability matrices: the incorporation of new data, such as updated winds and insurance data, may trigger a tune-up of the vulnerability matrices used in the Insurance Loss Module.

- Modification to the set of valid values for any of the attributes in the model's input data specification.

If any change results in a change in loss costs estimates or probable maximum loss level, there will be at least a change in the minor revision number.

CIF-7 Flood Model Security

The modeling organization shall have implemented and fully documented security procedures for (1) secure access to individual computers where the software components or data can be created or modified, (2) secure operation of the flood model by clients, if relevant, to ensure that the correct software operation cannot be compromised, (3) anti-virus software installation for all machines where all components and data are being accessed, and (4) secure access to documentation, software, and data in the event of a catastrophe.

The FPFLM maintains a set of security procedures to protect data and documents from deliberate and inadvertent changes. These procedures include both physical and electronic measures. A set of policies identifies different security issues and addresses each of them. All the security measures are properly documented in the primary document.

Disclosure

1. Describe methods used to ensure the security and integrity of the code, data, and documentation.

Electronic measures include the use of different authorization levels, special network security enforcement, and regular backups. Each developer is given a separate username and password and assigned a level of authorization so that even a developer cannot change another developer's code. The users of the system are given usernames and passwords so that unauthorized users cannot use the system. External users are not allowed direct access to any of the data sources of the system. The network is extensively monitored for any unauthorized actions using standard industry practices.

Any sensitive or confidential data (insurance data, for example) are kept on an unshared disk on a system that has user access control and requires a login. Screen locks are enforced whenever the machine is left unattended. In addition, for system security and reliability purposes, we also deploy a development environment besides the production environment. Modifications to the code and data are done in the development environment and tested by in-house developers. The final production code and data can only be checked into the production environment by the authorized personnel. The models resulting from the FPFLM project can only be used by the authorized users. Authorized user accounts are created by the project manager. Regular backups of the server are taken and stored in two ways: physically and electronically. Backups are performed daily and are kept for six weeks. Nightly backups of all UNIX data disks and selected Windows data disks (at user requests) are performed over the network onto LT02 and LT03 tapes. The tape drives have built-in diagnostics and verification to ensure that the data is written correctly to the tapes. This ensures that if the tape is written successfully, it will be readable, provided no physical damage occurred to the tape. A copy of each backup is placed in a secure and hurricane-protected building. Additionally, the application server and the database server are physically secured in a secure server room with alarm systems. In case of disasters, we have implemented a set of preparation procedures and recovery plans as outlined in "FIU SCIS Hurricane Preparation Procedures."

APPENDICES

Expert Review Letter

February 4, 2020
Arthur Taylor
Physical Scientist and SLOSH modeling POC,
U.S Department of Commerce, NOAA, NWS, Meteorological Development Lab.
1325 East West Highway,
Silver Spring, MD 20910
Arthur.taylor@noaa.gov

Introduction

My review of the Coastal and Estuarine Storm Tide (CEST) model, which is the storm surge component of Florida International's (FIU) submission to the Florida Commission on Hurricane Loss Projection Methodology to meet the "2017 Hurricane Standards Report of Activities", is based on an examination of the submission draft provided to me in December as well as previous literature reviews of CEST.

GF-1 Scope of the Flood Model and Its Implementation

The intent of section GF-1 is to describe the model. FIU's response describes the model's underlying mathematics. It then answers the practical questions of: what type of computational grid; what are the boundary conditions; how are the pressure gradient and bottom friction resolved; and how it handles wetting and drying. It continues by describing how the bathymetric and topographic data are gathered and processed into a computational grid. This is followed by a description of the wind-field and how it is modified to account for terrain effects. In short, FIU's response from section 1 to 3 provides a good overview of the model.

FIU's response also contains a section 4 which describes the specific implementation of the CEST model for Florida in the form of 4 sets of computational grids that when combined cover the Florida coastline. Each set has a coarse, intermediate, and fine grid resolution. The reason for the different types of grid resolutions is to allow FIU to make an informed choice between run-time and accuracy. Their current choice of the intermediate resolution grids is reasonable based on run-time. This section is useful for detailing their implementation choices.

MF-1 Flood Event Data Sources

The intent of section MF-1 is to describe the data sources of the model as well as describe what observational data sources were used to calibrate or validate the model. FIU's response, from the storm surge model perspective, reiterated the bathymetry and topography information that was more fully covered in the GF-1 section.

It then covered the observational systems used for validation. The high water marks and NOS tide gauges are the established methods for observing storm surge. A third type of observation to consider would be the USGS's more recent efforts of pre-position storm surge sensors in the path of the storm. As this is a recent development, the data may not be available for the test storms.

MF-2 Flood Parameters (Input)

The intent of section MF-2 is to define and defend the model parameters (e.g. constants), as well as the grid cell size used by the model. FIU's response very thoroughly describes the model parameters and how they were derived. Section 4 from GF-1, which details the experiments used to choose the grid cell size, is repeated here and does a good job explaining why the intermediate grids were chosen.

MF-3 Wind and Pressure Fields for Storm Surge

The intent of section MF-3, from a storm surge perspective, is to make sure the computational area is large enough. If it isn't, then the model will miss the initial set-up of the storms. FIU's response focuses on a test of different size basins using Dennis-2005, Ivan-2004, and Ike-2008 as case-studies.

Dennis-2005 is a good test case, particularly for Florida, as it caused a coastally trapped wave to propagate along the west side of Florida. To properly capture it, the computational domain needs to somehow (via a large grid or via nesting) include the entire west coast of Florida. This is borne out in FIU's experiment with the basins AP3, AP4, AP6, AP7 and EGM3. AP3 and AP4 were not broad enough to capture the initial set-up, so did not perform well. EGM3, while broad, was not fine enough to calculate the surge near the stations. AP6 and AP7 were broad enough to capture the storm and fine enough at the stations so they performed the best.

Ivan-2004 is also a good test case as it went through an area that is highly susceptible to waves and was on the western side of the AP3, AP4, AP6, AP7 basins. As one would expect, AP7 performed the best, since it had the longest time to react to Ivan-2004 and yet was finer in resolution than EGM3. It is interesting that EGM3 performed better than AP6, which indicates that capturing the correct initial water condition is more important than having higher resolution.

Ike-2008 made landfall in Texas, so it is not a good choice for Florida. That said, the experiment does emphasize that basins can be too small to capture a storm. A general rule of thumb is that a basin needs to be 2.5 times the size of the storm. HGL5 and HGL6 satisfy that while also being finer in resolution than EGM3.

MF-4 Flood Characteristics (Outputs)

The intent of section MF-4 is to make sure the model results are consistent with the historic records. FIU's response references separated document for calibration and verification of Historical Hurricanes required by Flood Standard. I'm familiar enough with CEST to be confident that the verification of Historical Hurricanes agree well the historic record within reason.

MF-5 Flood Probability Distributions

The intent of section MF-5 is to make sure the probability distributions are reasonable. CEST is a diagnostic storm surge model, so doesn't directly have probabilities associated with it. Given a reasonable approximation to a storm's winds it can predict coastal flooding, but a different part of the proposal would deal with probability distributions associated with how those winds are selected.

That said, the section does ask about modeling of tropical and non-tropical events. FIU took this to mean 'tropical storm' strength events and did a study of TS-Fay-2008. They found that TS-Fay didn't create much flooding and concluded that Tropical Storm strength events normally doesn't induce significant surge. Before they conclude that, they could also review the impacts of TS-Gordon-2018, TS-Andrea-2013, TS-Lee-2011, and TS-Hermine-2010.

Summary

I am pleased to report that the issues that I have raised have received their attention and I believe that the model meets all the standards set forth by the commission.

FPFLM V1.0 Feb. 29, 2020

Sincerely,

A handwritten signature in black ink that reads "Arthur Taylor". The signature is written in a cursive style with a large, sweeping initial "A" and a long, horizontal flourish extending to the right.

Arthur Taylor

February 15, 2007
Gary M. Barnes
Professor, Department of Meteorology
School of Ocean and Earth Science and Technology
University of Hawaii at Manoa

Introduction

My review of the State of Florida Public Hurricane Model is based on a three day visit to Florida International University in December, and an examination of the submission draft provided to me in February. I have had full access to the meteorological portion of the model, access to the draft for the Florida commission, and access to prior submittals to the commission from several other groups in order to establish a sense of what is desired by the commission. I am pleased to report that the issues that I have raised have received their attention and I believe that the model meets all the standards set forth by the commission. Ultimately this model, when linked to engineering and actuarial components, will provide objective guidance for the estimation of wind losses from hurricanes for the state of Florida. It does not address losses from other aspects of a tropical cyclone such as storm surge, or fresh water flooding. I now offer specific comments on each of the six meteorological standards established by the commission to ascertain this model's suitability.

M-1 Official Hurricane Set

The consortium of scientists working on the Public model have adopted HURDAT (1900-2006) to determine landfall frequency and intensity at landfall. The NWS report by Ho et al. (1987), DeMaria's extension of the best track, H*Wind analyses (Powell & Houston, 1996, 1998; Powell et al. 1996, 1998) and NOAA Hurricane Research Division aircraft data are used to estimate the radius of maximum winds (RMW) at landfall. The strength of HURDAT is that it is the most complete and accessible historical record for hurricanes making landfall or passing closely by Florida. HURDAT weaknesses include the abbreviated record and questionable intensity estimates for those hurricanes early in the record, especially those that remain offshore. Evidence for the shortness of record is the impact of the last few hurricane seasons on landfall return frequency. The meteorological team has scrutinized the base set developed by the commission and made a number of adjustments to the dataset based on refereed literature and the HURDAT record. I have looked at several of these adjustments in detail and find the corrections to be an improvement over the initial base set.

M-2 Hurricane Characteristics

The model has two main components. The track portion of the model produces a storm with either an initial location or genesis point and an intensity that is derived from an empirical distribution derived from HURDAT (2006). Storm motion and intensity is then initialized by using a Monte Carlo approach, drawing from probability density functions (PDFs) based on the historical dataset to create a life for a bogus hurricane. Examination of the PDFs reveals that they are faithful to the observed patterns for storms nearing Florida, and the evolution of any particular hurricane appears realistic.

The second component of the meteorological model is the wind field generated for a given hurricane, which only comes into play when the hurricane comes close enough to place high winds over any given ZIP Code of Florida. To generate a wind field the minimum sea-level pressure (MSLP) found in the eye, the RMW at landfall, and a distant environmental pressure (1013 mb) are entered into the Holland (1980) B model for the axisymmetric pressure distribution around the hurricane. The behavior of the RMW is based on a variety of sources that include Ho et al. (1987), DeMaria's extension of the best track data, H*wind analyses, and aircraft reconnaissance radial wind profiles. The B coefficient is based on the extensive aircraft dataset acquired in reconnaissance and research flights over the last few decades. RMW and B use a random or error term to introduce variety into the model. The Holland pressure field is used to produce a gradient wind at the top of the boundary layer. The winds in the boundary layer are estimated following the work proposed by Ooyama (1969) and later utilized by Shapiro (1983) which includes friction and advection effects. These boundary layer winds are reduced to surface winds (10 m) using reduction factors based on the work of Powell et al. (2003). Maximum sustained winds and 3 second gusts are estimated using the guidance of Vickery and Skerlj (2005). Once the hurricane winds come ashore there are further adjustments to the wind to account for local roughness as well as the roughness of the terrain found upstream of the location under scrutiny. The pressure decay of the hurricane is modeled to fit the observations presented by Vickery (2005).

Gradient balance has been demonstrated to be an accurate representation for vortex scale winds above the boundary layer by Willoughby (1990) and is a fine initial condition. The slab boundary layer concept of Ooyama and Shapiro has been shown to produce wind fields much like observed once storm translation and surface friction come into play. The reduction to 10 m altitude is based on Powell et al. (2003); they use the state of the art Global Positioning System sondes to compare surface and boundary layer winds.

Perhaps the most questionable part of the wind portion of the model is the reliance on the estimates of the RMW at landfall. The scatter in RMW for a given MSLP is large; larger RMWs coupled with the B parameter control the size of the annulus of the damaging winds. The typical length of an aircraft leg from the eye is about 150 km so the choice of the B parameter is based on a small radial distance in the majority of hurricanes. The collection of quality wind observations over land in hurricanes remains a daunting task; therefore the actual response of the hurricane winds to variations in roughness is less certain. Applying roughness as a function of ZIP Code is a coarse approximation to reality. However, this is the approach chosen by the commission, and given the data limitations, a reasonable course to take.

M-3 Landfall Intensity

The model uses one minute winds at 10 m elevation to determine intensity at landfall and categorizes each hurricane according to the Saffir-Simpson classification. The model considers any hurricane that makes landfall or comes close enough to place high winds over Florida. Multiple landfalls are accounted for, and decay over land between these landfalls is also estimated. Maximum wind speeds for each category of the Saffir-Simpson scheme are reasonable as is the worst possible hurricane the model generates. Simulations are conducted for a hypothetical 60,000 years. Any real climate change would alter results, but maybe not as much as have an actual record of order of 1,000 years to base the PDFs on.

M-4 Hurricane Probabilities

Form M-1 demonstrates that the model is simulating the landfalls very well for the entire state, region A (NW Florida) and region B (SW Florida). There are subsections of the state where the historical and the simulated landfalls have a discrepancy. In region C (SE Florida) the observations show an unrealistic bias toward Category 3 storms. This is likely due to an overestimate of intensity for the hurricanes prior to the advent of aircraft sampling or advanced satellite techniques. The historical distribution for region C also does not fit any accepted distributions that we typically see for atmospheric phenomena. This discrepancy is probably due to the shortness of the historical record. I note that other models also have difficulty with this portion of the coast. I believe the modeled distribution, based on tens of thousands of years, is more defensible than the purported standard. Regions D (NE Florida) and E (Georgia) have virtually no distribution to simulate, again pointing to a very short historical record. There is no documented physical reason why these two regions have escaped landfall events. Perhaps a preferred shape of the Bermuda High may bias the situation, but this remains speculative.

M-5 Land Friction and Weakening

Land use and land cover are based on high resolution satellite imagery. Roughness for a particular location is then based on HAZUS tables that assign a roughness to a particular land use. There are newer assessments from other groups but the techniques were not consistently applied throughout the state, nor are the updated HAZUS maps for 2000 available yet. Winds at a particular location are a function of the roughness at that point and conditions upwind. A pressure decay model based on the work of Vickery (2005) produces weakening winds that are reasonable approximations of the observed decay rates of several hurricanes that made landfall in Florida in 2004 and 2005.

The maps (Form M-2) of the 100 year return period maximum sustained winds shows the following trends: (1) a reduction in the sustained winds from south to north, (2) a reduction of winds from coastal to inland ZIP Codes, and (3) the highest winds in the Keys and along the SE and SW coasts. The plotting thresholds requested by the commission partially obfuscate the gradients in wind speed, but Form M-2 produced with finer contours highlights the above trends clearly. The open terrain maps look logical; the actual terrain maps are perhaps overly sensitive to

the local roughness. Convective scale motions, which cannot be resolved in this type of model, would probably be responsible for making the winds closer to the open terrain results.

M-6 Logical Relationships of Hurricane Characteristics

The RMW is a crucial but poorly measured variable. Making RMW a function of intensity and latitude explains only a small portion of the variance (~20%). Examination of aircraft reconnaissance radial profiles shows that RMW is highly variable. Currently there are no other schemes available to explain more of the variance. Form M-3 reflects the large range of RMW. Note that only the more intense hurricanes (MSLP < 940 mb) show a trend, and only with the upper part of the range. Even open ocean studies of the RMW show such large scatter.

Tests done during my visits show that wind speed decreases as a function of roughness, all other variables being held constant. The evolution of the wind field as a hurricane comes ashore is logical.

Summary

The consortium that has assembled the meteorological portion of the Public Model for Hurricane Wind Losses for the State of Florida is using the HURDAT with corrections based on other refereed literature. These data yield a series of probability density functions that describe frequency, location, and intensity at landfall. Once a hurricane reaches close enough to the coast the gradient winds are estimated using the equations by Holland (1980), then a sophisticated wind model (Ooyama 1969, Shapiro 1983) is applied to calculate the boundary layer winds. Reduction of this wind to a surface value is based on recent boundary layer theory and observations. Here the consortium has exploited other sources of data (e.g., NOAA/AOML/HRD aircraft wind profiles and GPS sondes) to produce a surface wind field. As the wind field transitions from marine to land exposure changes in roughness are taken into account. Form M-1 (frequency and category at landfall as a function of coastal segment) and Form M-2 (100 year return maximum sustained winds for Florida) highlight the good performance of the model.

I suspect that the differences between the historical record and the simulation are largely due to the shortness and uncertainty of the record. If the consortium had the luxury of 1000 years of observations agreement between the record and the simulation would be improved. I believe that the meteorological portion of the model is meeting all the standards established by the commission. Tests of the model against H*Wind analyses and the production of wind speed swaths go beyond the typical quality controls of prior models and demonstrate that this model is worthy of consideration by the commission.

Form GF-1: General Flood Standards Expert Certification

Form GF-1: General Flood Standards Expert Certification

Purpose: This form identifies the signatory or signatories who have reviewed the current submission for compliance with the General Flood Standards (GF-1 – GF-5) in accordance with the stated provisions.

I hereby certify that I have reviewed the current submission of Florida Public Flood Loss Model
(Name of Flood Model)

Version 1.0 for compliance with the 2017 Flood Standards adopted by the Florida Commission on Hurricane Loss Projection Methodology and hereby certify that:

1. The flood model meets the General Flood Standards (GF-1 – GF-5);
2. The disclosures and forms related to the General Flood Standards section are editorially and technically accurate, reliable, unbiased, and complete;
3. My review was completed in accordance with the professional standards and code of ethical conduct for my profession;
4. My review involved ensuring the consistency of the content in all sections of the submission; and
5. In expressing my opinion I have not been influenced by any other party in order to bias or prejudice my opinion.

SHAHID HAMID
Name

PhD Economics (Financial)
Professional Credentials (Area of Expertise)

S. Hamid
Signature (original submission)

2/29/2020
Date

Signature (response to deficiencies, if any)

Date

Signature (revisions to submission, if any)

Date

Signature (final submission)

Date

An updated signature and form are required following any modification of the flood model and any revision of the original submission. If a signatory differs from the original signatory, provide the printed name and professional credentials for any new signatories. Additional signature lines shall be added as necessary with the following format:

Signature (revisions to submission)

Date

Note: A facsimile or any properly reproduced signature will be acceptable to meet this requirement.

Include Form GF-1, General Flood Standards Expert Certification, in a submission appendix.

Form GF-2: Meteorological Flood Standards Expert Certification

I hereby certify that I have reviewed the current submission of Florida Public Flood Loss Model Version 1.0 for compliance with the 2017 Flood Standards adopted by the Florida Commission on Hurricane Loss Projection Methodology and hereby certify that:

1. The flood model meets the Meteorological Flood Standards (MF-1 – MF-5);
2. The disclosures and forms related to the Meteorological Flood Standards section are editorially and technically accurate, reliable, unbiased, and complete;
3. My review was completed in accordance with the professional standards and code of ethical conduct for my profession; and
4. In expressing my opinion I have not been influenced by any other party in order to bias or prejudice my opinion.

Yuepeng Li
Name

PhD, Storm Surge/Coastal Flooding
Professional Credentials (Area of Expertise)



Signature (original submission)

02/20/2020
Date

Signature (response to deficiencies, if any)

Date

Signature (revisions to submission, if any)

Date

Signature (final submission)

Date

An updated signature and form are required following any modification of the flood model and any revision of the original submission. If a signatory differs from the original signatory, provide the printed name and professional credentials for any new signatories. Additional signature lines shall be added as necessary with the following format:

Signature (revisions to submission)

Date

Note: A facsimile or any properly reproduced signature will be acceptable to meet this requirement.

Include Form GF-2, Meteorological Flood Standards Expert Certification, in a submission appendix.

Form GF-3: Hydrological and Hydraulic Flood Standards Expert Certification

I hereby certify that I have reviewed the current submission of Inland (Freshwater) Flood Model Version 1.0 for compliance with the 2017 Flood Standards adopted by the Florida Commission on Hurricane Loss Projection Methodology and hereby certify that:

1. The flood model meets the Hydrological and Hydraulic Flood Standards (HHF-1 – HHF-4);
2. The disclosures and forms related to the Hydrological and Hydraulic Flood Standards section are editorially and technically accurate, reliable, unbiased, and complete;
3. My review was completed in accordance with the professional standards and code of ethical conduct for my profession; and
4. In expressing my opinion I have not been influenced by any other party in order to bias or prejudice my opinion.

Omar I. Abdul-Aziz
Name

Ph.D. in Civil Engineering (Water Resource)
Professional Credentials (Area of Expertise)


Signature (original submission)

02/29/2020
Date

Signature (response to deficiencies, if any)

Date

Signature (revisions to submission, if any)

Date

Signature (final submission)

Date

An updated signature and form are required following any modification of the flood model and any revision of the original submission. If a signatory differs from the original signatory, provide the printed name and professional credentials for any new signatories. Additional signature lines shall be added as necessary with the following format:

Signature (revisions to submission)

Date

Note: A facsimile or any properly reproduced signature will be acceptable to meet this requirement.

Include Form GF-3, Hydrological and Hydraulic Flood Standards Expert Certification, in a submission appendix.

Form GF-4: Statistical Flood Standards Expert Certification

I hereby certify that I have reviewed the current submission of Florida Public Flood Loss Model Version 1.0 for compliance with the 2017 Flood Standards adopted by the Florida Commission on Hurricane Loss Projection Methodology and hereby certify that:

1. The flood model meets the Statistical Flood Standards (SF-1 – SF-5);
2. The disclosures and forms related to the Statistical Flood Standards section are editorially and technically accurate, reliable, unbiased, and complete;
3. My review was completed in accordance with the professional standards and code of ethical conduct for my profession; and
4. In expressing my opinion I have not been influenced by any other party in order to bias or prejudice my opinion.

Wensong Wu
Name

PhD in Statistics
Professional Credentials (Area of Expertise)



Signature (original submission)

2/29/2020
Date

Signature (response to deficiencies, if any)

Date

Signature (revisions to submission, if any)

Date

Signature (final submission)

Date

An updated signature and form are required following any modification of the flood model and any revision of the original submission. If a signatory differs from the original signatory, provide the printed name and professional credentials for any new signatories. Additional signature lines shall be added as necessary with the following format:

Signature (revisions to submission)

Date

Note: A facsimile or any properly reproduced signature will be acceptable to meet this requirement.

Include Form GF-4, Statistical Flood Standards Expert Certification, in a submission appendix.

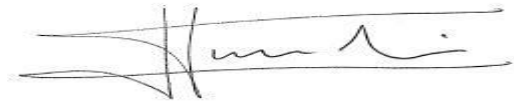
Form GF-5: Vulnerability Flood Standards Expert Certification

I hereby certify that I have reviewed the current submission of Florida Public Flood Loss Model Version 1.0 for compliance with the 2017 Flood Standards adopted by the Florida Commission on Hurricane Loss Projection Methodology and hereby certify that:

- 1. The flood model meets the Vulnerability Flood Standards (VF-1 – VF-4);
- 2. The disclosures and forms related to the Vulnerability Flood Standards section are editorially and technically accurate, reliable, unbiased, and complete;
- 3. My review was completed in accordance with the professional standards and code of ethical conduct for my profession; and
- 4. In expressing my opinion I have not been influenced by any other party in order to bias or prejudice my opinion.

Jean-Paul Pinelli
Name

PhD, P.E, Structural/Wind Engineer
Professional Credentials (Area of Expertise)



Signature (original submission)

2/20/2020
Date

Signature (response to deficiencies, if any)

Date

Signature (revisions to submission, if any)

Date

Signature (final submission)

Date

An updated signature and form are required following any modification of the flood model and any revision of the original submission. If a signatory differs from the original signatory, provide the printed name and professional credentials for any new signatories. Additional signature lines shall be added as necessary with the following format:

Signature (revisions to submission)

Date

Note: A facsimile or any properly reproduced signature will be acceptable to meet this requirement.

Include Form GF-5, Vulnerability Flood Standards Expert Certification, in a submission appendix.

Form GF-6: Actuarial Flood Standards Expert Certification

Form GF-7: Computer/Information Flood Standards Expert Certification

Form GF-7: Computer/Information Flood Standards Expert Certification

Purpose: This form identifies the signatory or signatories who have reviewed the current submission for compliance with the Computer/Information Flood Standards (CIF-1 – CIF-7) in accordance with the stated provisions. Florida Public Flood

I hereby certify that I have reviewed the current submission of Loss Model
(Name of Flood Model)

Version 1.0 for compliance with the 2017 Flood Standards adopted by the Florida Commission on Hurricane Loss Projection Methodology and hereby certify that:

1. The flood model meets the Computer/Information Flood Standards (CIF-1 – CIF-7);
2. The disclosures and forms related to the Computer/Information Flood Standards section are editorially and technically accurate, reliable, unbiased, and complete;
3. My review was completed in accordance with the professional standards and code of ethical conduct for my profession; and
4. In expressing my opinion I have not been influenced by any other party in order to bias or prejudice my opinion.

Shu-Ching Chen
 Name

Ph.D. in Electrical and Computer Engineering
M.S. in Computer Science
 Professional Credentials (Area of Expertise)

[Signature]
 Signature (original submission)

2/28/2020
 Date

 Signature (response to deficiencies, if any)

 Date

 Signature (revisions to submission, if any)

 Date

 Signature (final submission)

 Date

An updated signature and form are required following any modification of the flood model and any revision of the original submission. If a signatory differs from the original signatory, provide the printed name and professional credentials for any new signatories. Additional signature lines shall be added as necessary with the following format:

 Signature (revisions to submission)

 Date

Note: A facsimile or any properly reproduced signature will be acceptable to meet this requirement.

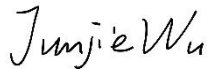
Include Form GF-7, Computer/Information Flood Standards Expert Certification, in a submission appendix.

Form GF-8: Editorial Review Expert Certification

I hereby certify that I have reviewed the current submission of Florida Public Flood Loss Model Version 1.0 for compliance with the “Process for Determining the Acceptability of a Computer Simulation Flood Loss Model” adopted by the Florida Commission on Hurricane Loss Projection Methodology in its *Flood Standards Report of Activities as of November 1, 2017*, and hereby certify that:

1. The flood model submission is in compliance with the Notification Requirements and General Flood Standard GF-5, Editorial Compliance;
2. The disclosures and forms related to each flood standards section are editorially accurate and contain complete information and any changes that have been made to the submission during the review process have been reviewed for completeness, grammatical correctness, and typographical errors;
3. There are no incomplete responses, charts or graphs, inaccurate citations, or extraneous text or references;
4. The current version of the flood model submission has been reviewed for grammatical correctness, typographical errors, completeness, the exclusion of extraneous data/information and is otherwise acceptable for publication; and
5. In expressing my opinion I have not been influenced by any other party in order to bias or prejudice my opinion.

Junjie Wu
Name



Signature (original submission)

M.S. Computer Engineering
Professional Credentials (Area of Expertise)

2/29/2020

Date

Signature (response to deficiencies, if any)

Date

Signature (revisions to submission, if any)

Date

Signature (final submission)

Date

An updated signature and form are required following any modification of the flood model and any revision of the original submission. If a signatory differs from the original signatory, provide the printed name and professional credentials for any new signatories. Additional signature lines shall be added as necessary with the following format:

Signature (revisions to submission)

Date

Note: A facsimile or any properly reproduced signature will be acceptable to meet this requirement.

Include Form GF-8, Editorial Review Expert Certification, in a submission appendix.

Form HHF-1: Historical Event Flood Extent and Elevation or Depth Validation Maps

A. Provide color-coded contour or high-resolution maps with appropriate base map data illustrating modeled flood extents and elevations or depths for the following historical Florida flood events:

- Hurricane Andrew (1992)
- Hurricane Ivan (2004)
- Hurricane Jeanne (2004)
- Hurricane Wilma (2005)
- Tropical Storm Fay (2008)
- Unnamed Storm in East Florida (May 2009)
- Unnamed Storm in Panhandle (July 2013)
- Storm chosen by modeling organization

For any storms where sufficient data are not available, the modeling organization may substitute an alternate historical storm of their choosing.

A separated document with storm surge simulation of Andrew (1992), Frances (2004), Ivan (2004), Jeanne (2004), Katrina (2005), Wilma (2005), and also tropical storm Fay (2008) is provide. Unnamed Storm in East Florida (May 2009) and Unnamed Storm in Panhandle (July 2013) are not simulated, since they are mainly rainfall events.

For simulating historical inland flood events following historical storms have been addressed:

- Hurricane Katrina (2005) instead of Hurricane Andrew (1992)
- Hurricane Ivan (2004)
- Hurricane Jeanne (2004)
- Hurricane Wilma (2005)
- Tropical Storm Fay (2008)
- Unnamed Storm in East Florida (May 2009)
- Unnamed Storm in Panhandle (July 2013)
- Hurricane Dennis (2005) as Storm chosen by modeling organization

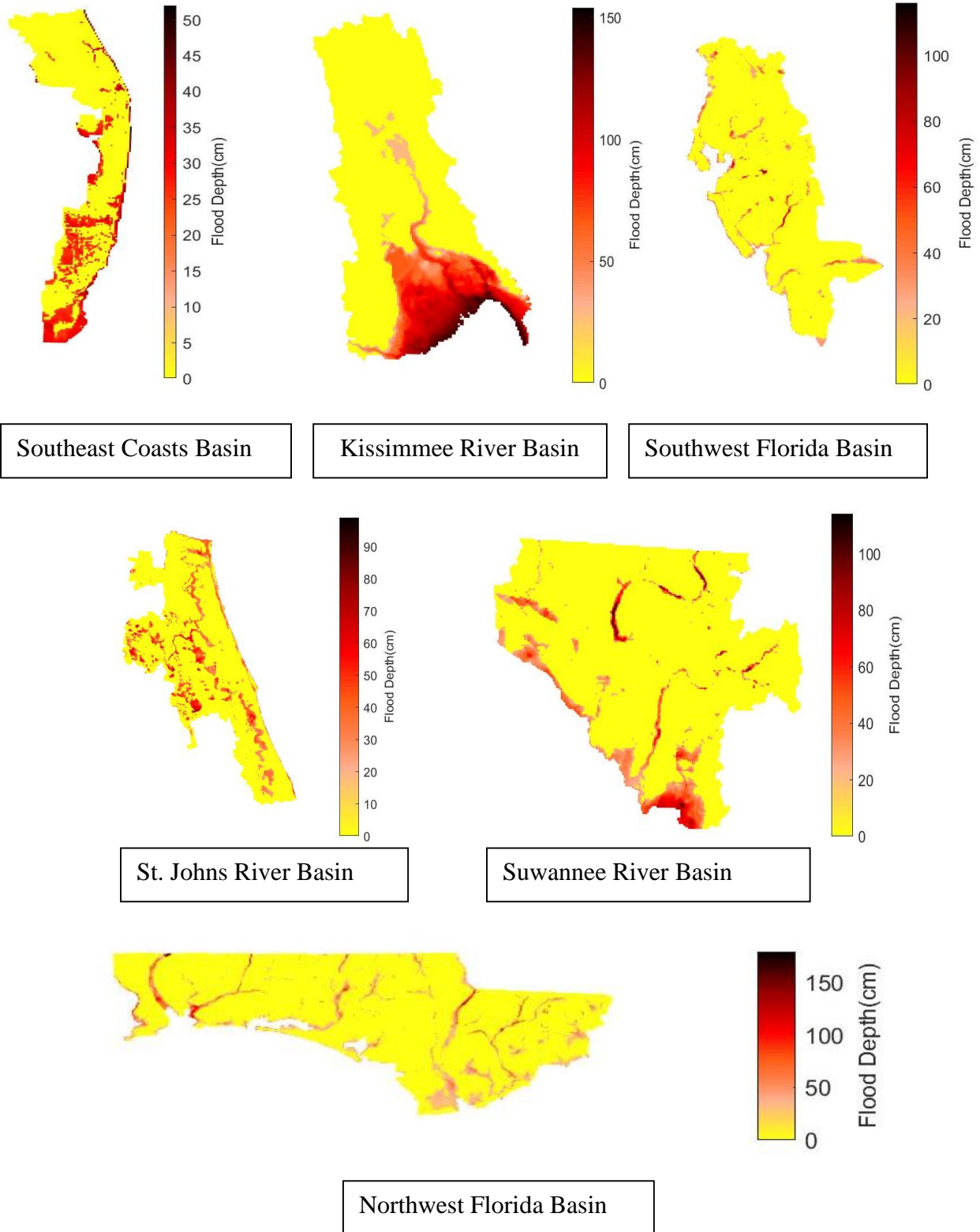


Figure 65. Flood maps for six inland basins during hurricane Katrina (2005).

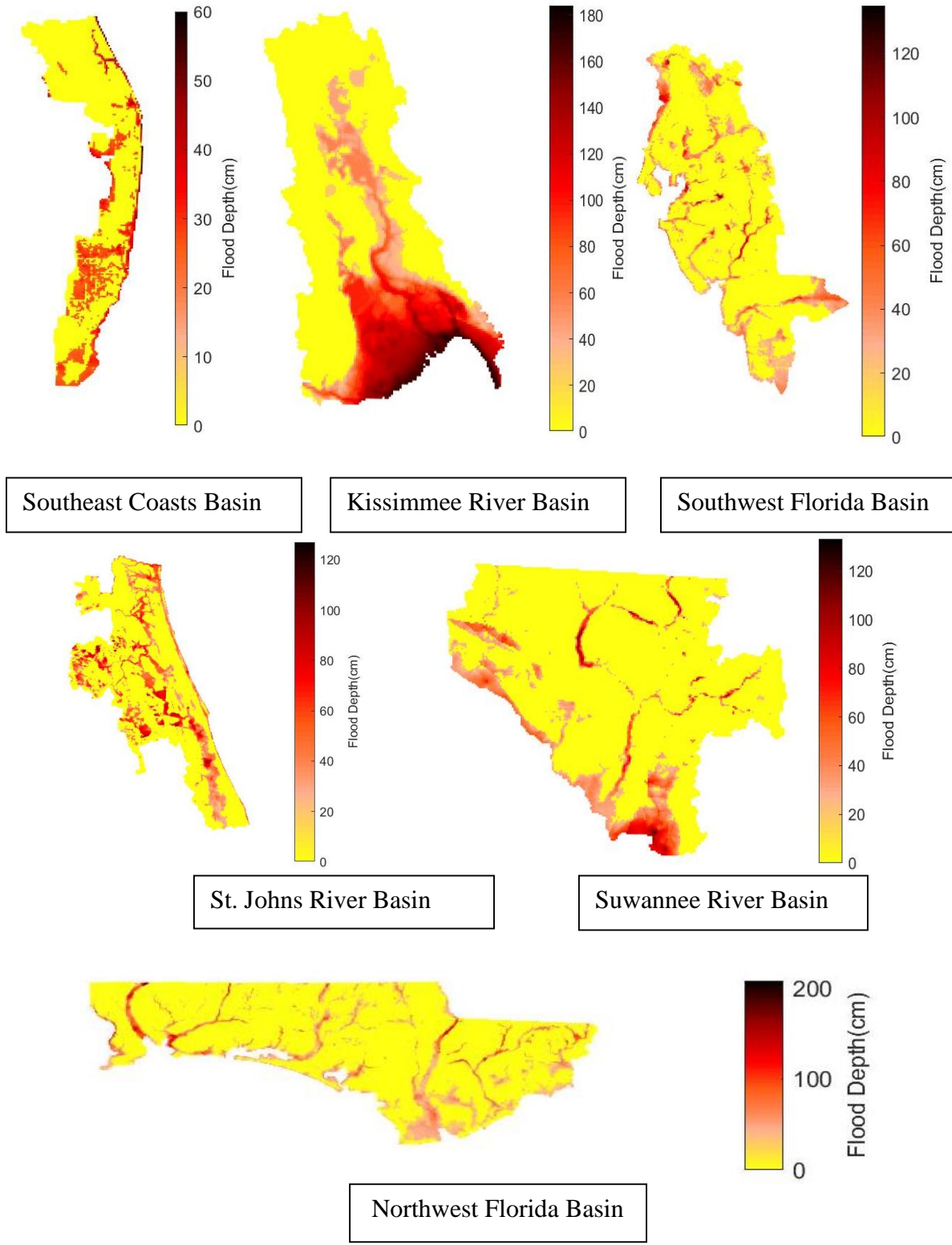


Figure 66. Flood maps for six inland basins during hurricane Ivan (2004).

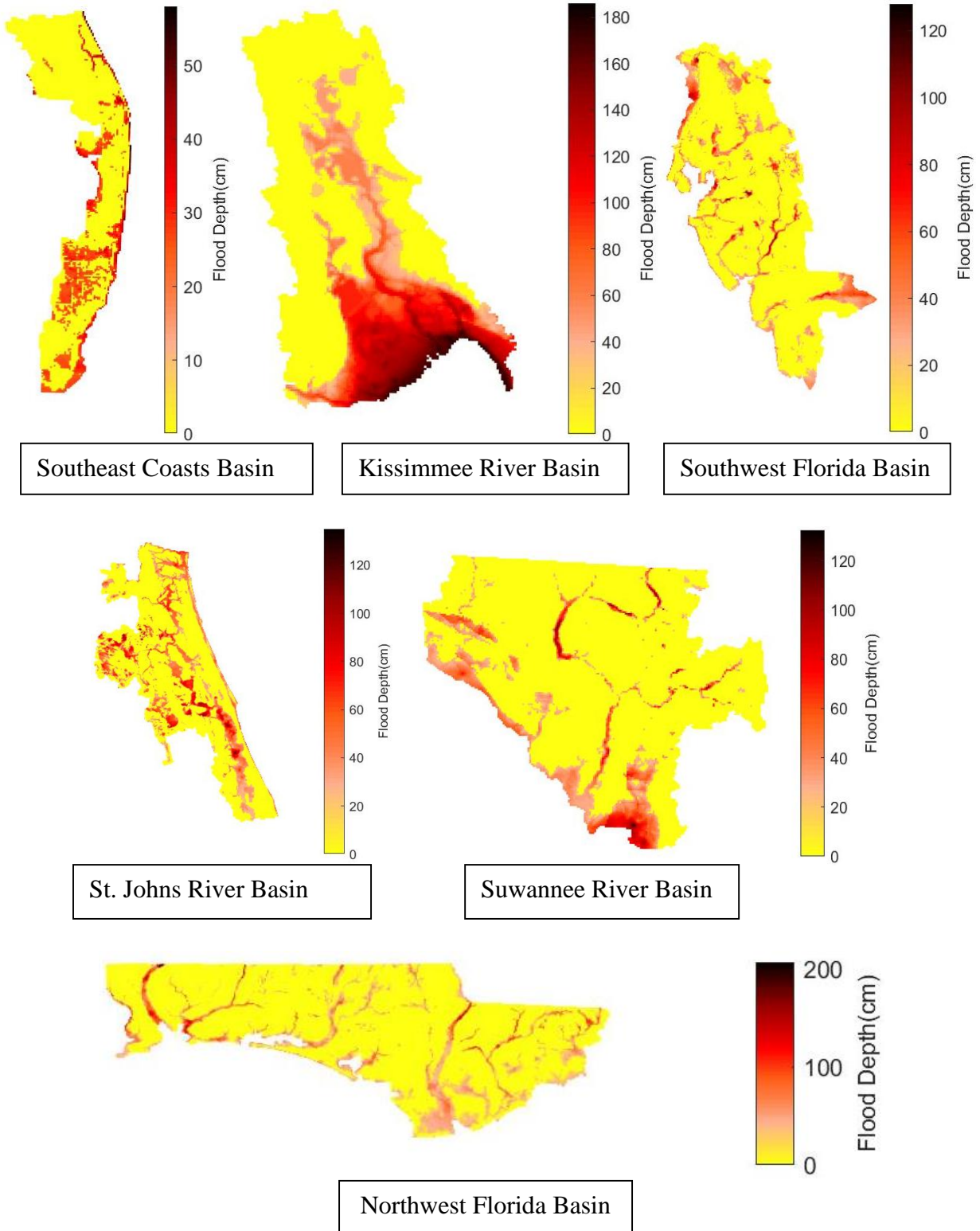


Figure 67. Flood maps for six inland basins during hurricane Jeanne (2004).

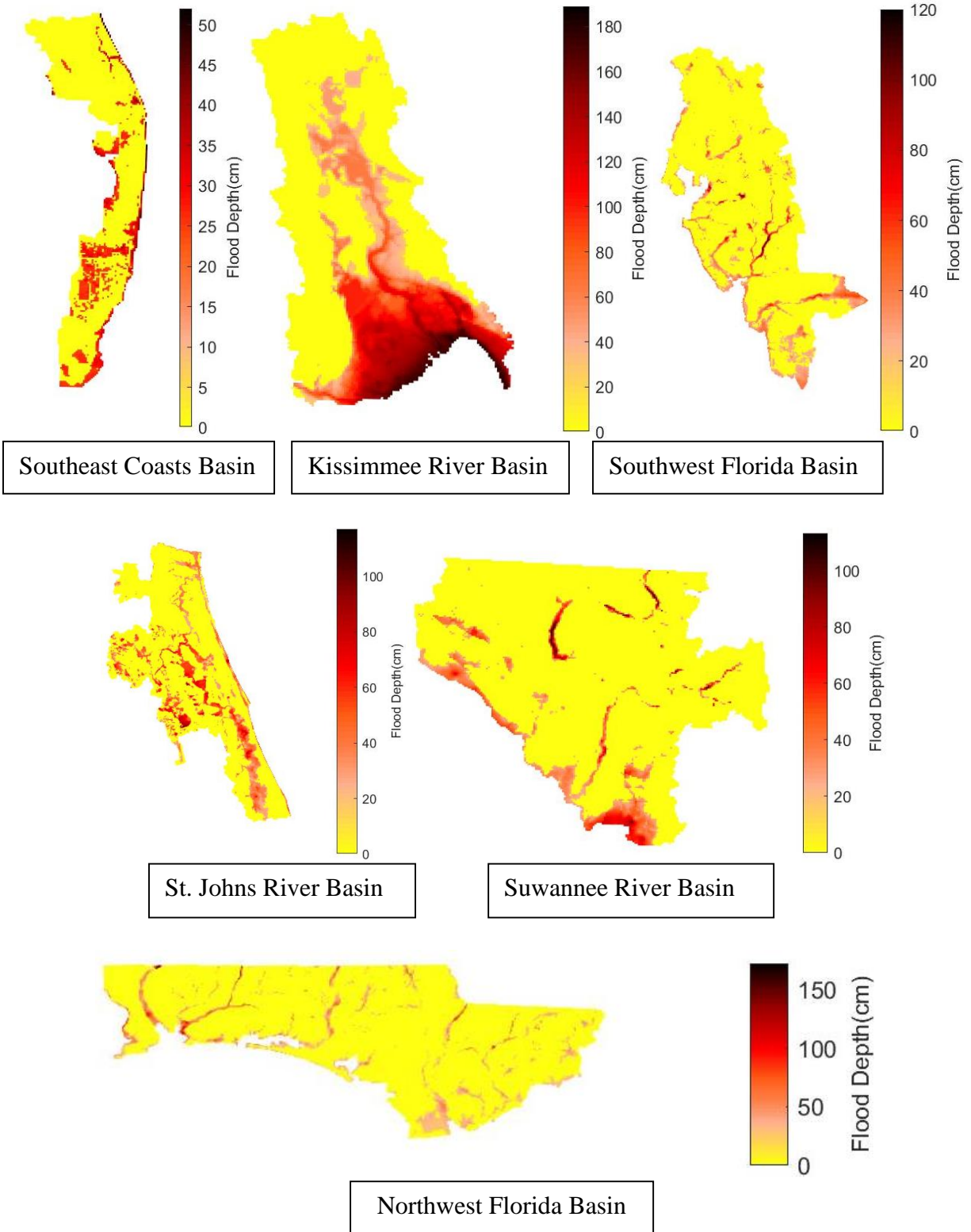


Figure 68. Flood maps for six inland basins during hurricane Wilma (2005).

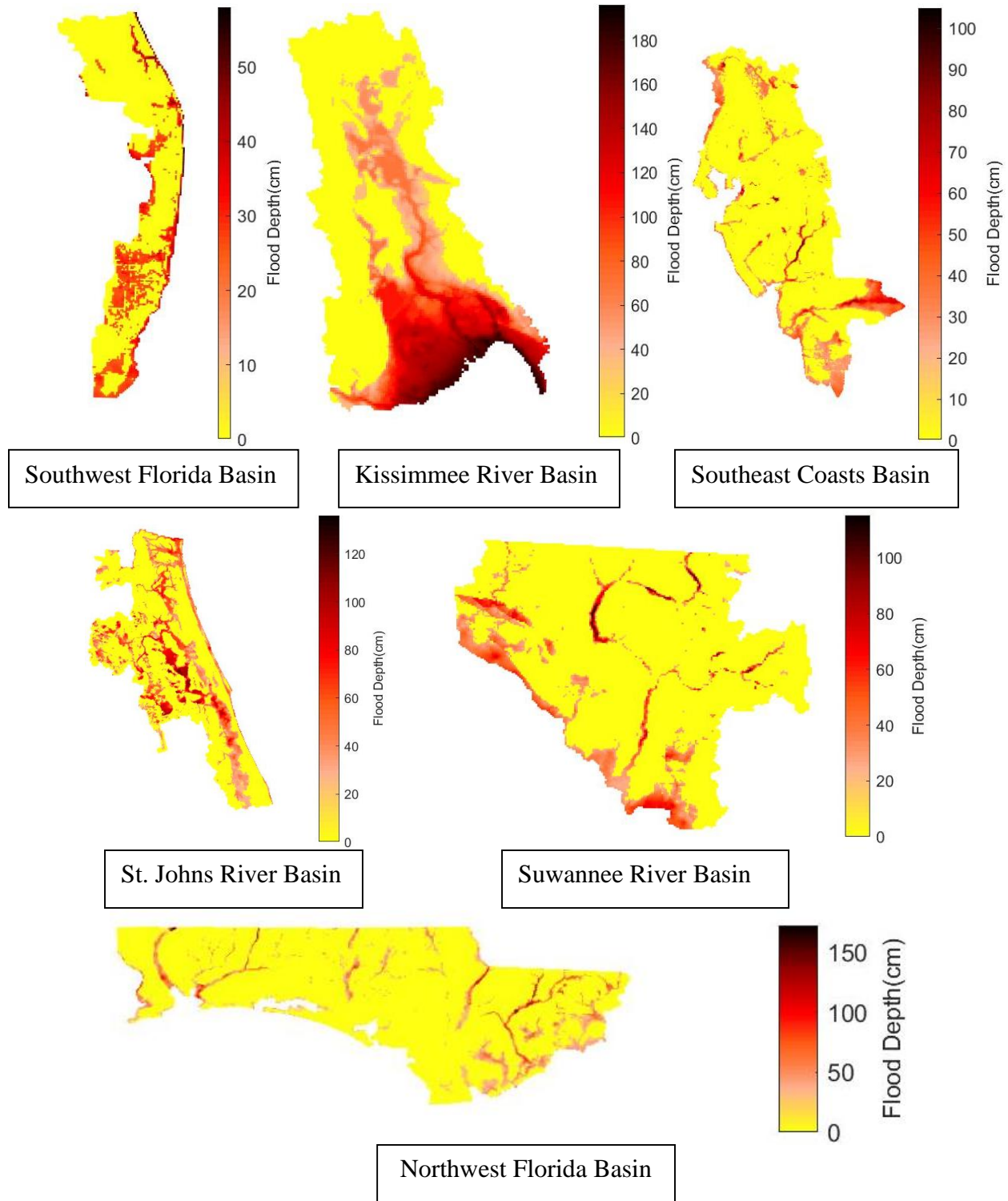


Figure 69. Flood maps for six inland basins during tropical storm Fay (2008).

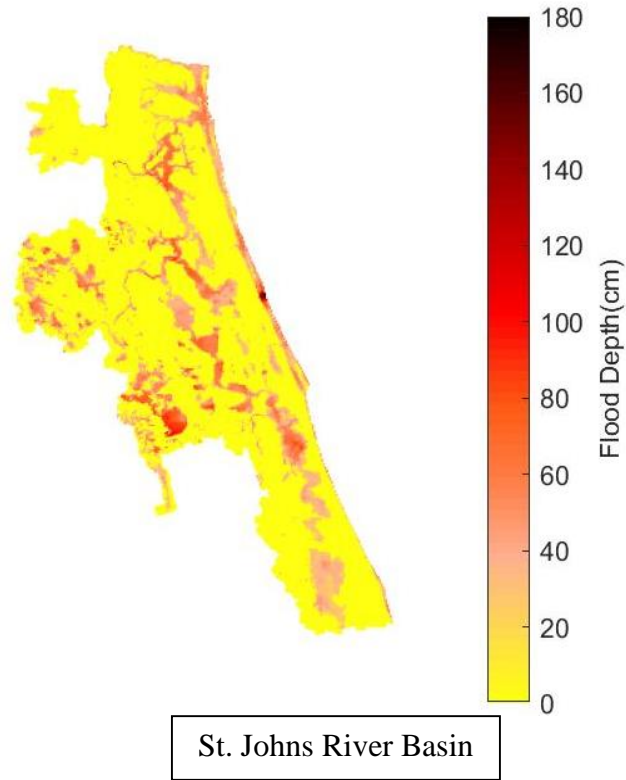


Figure 70. Flood map for East Florida during unnamed storm May (2009).



Figure 71. Flood map for Panhandle during unnamed storm July (2013).

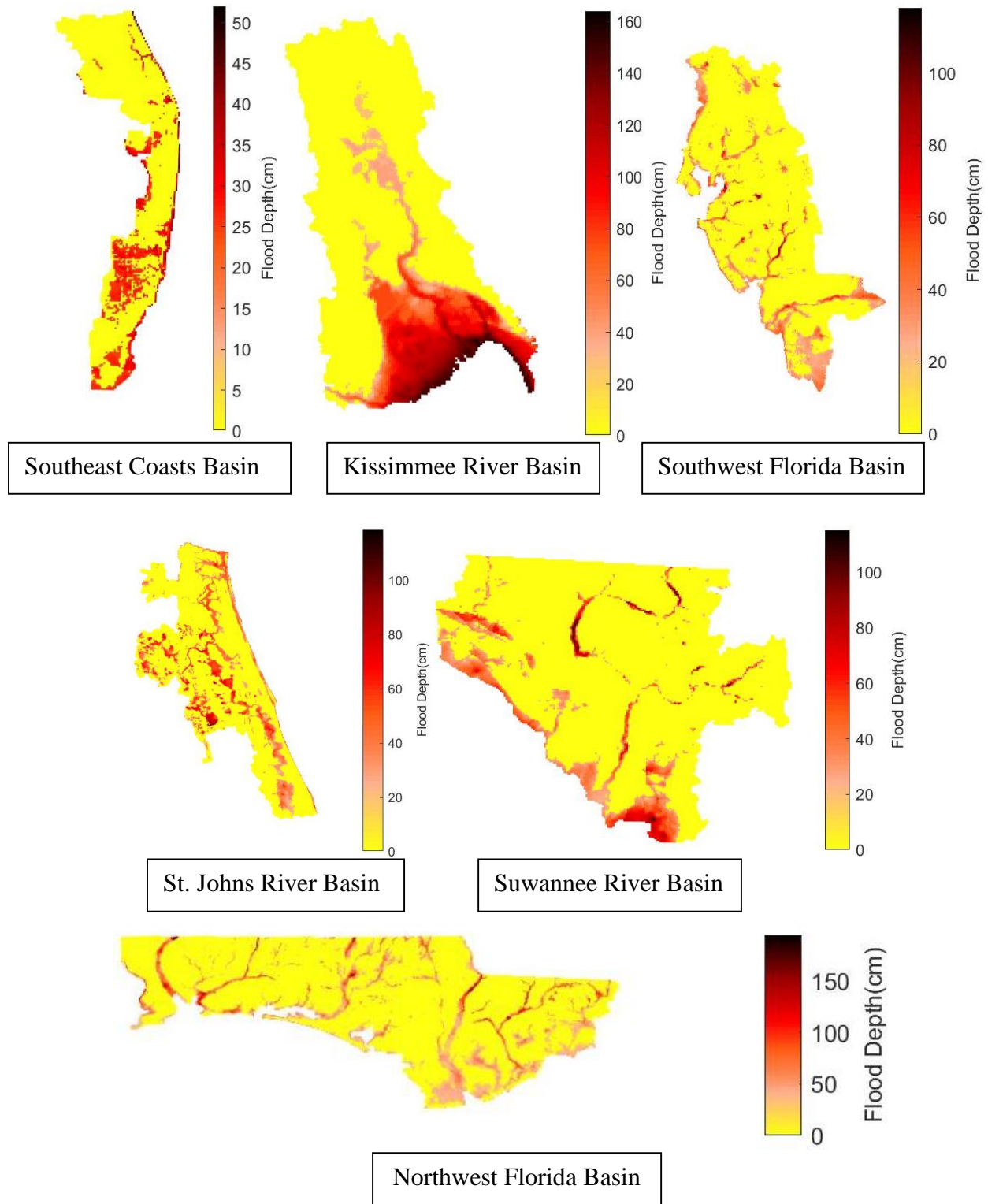


Figure 72. Flood maps for six inland basins during hurricane Dennis (2005).

- B. Plot the locations and values associated with validation points (e.g., maximum flood elevations or depths from observations such as gauge data, high-water marks) on each contour or high-resolution map for the historical events.

See the separated storm surge validation document.

The appropriate database for investigating the consistency of observed and model predicted flood depths and extents during the historical hurricane events is not available.

C. Provide sources of the validation data.

There are 3 type data are used to validate the storm surge model.

1. Time series at NOAA tide and current gauges, (<https://tidesandcurrents.noaa.gov/>),
2. Inundation maps or debris line, (<https://www.fema.gov/hurricane-ivan-surge-inundation-maps>)
3. High Water Mark (HWM) collected by different agents like FEMA, URS, or USGS.

For the historical hurricanes data, the following reports are used to calibrate or validate the coastal surge model.

Mitchell H.Murray (1992). Storm-Tide Elevations Produced by Hurricane Andrew Along the Southern Florida Coasts. U.S Geological Survey Open-File Report 96-116.

URS Group, Inc. 200 Orchard Ridge Drive Suite 101 Gaithersburg, MD 20878 (2005). Hurricane Frances Rapid Response Florida Coastal High Water Mark (CHWM) Collection FEMA-1545-DR-FL.

NOAA National Oceanic and Atmospheric Administration(2004). Hurricane FRANCES Preliminary water Levels report.

Mobile District Engineering Division Hydrology and Hydraulics Branch (2004). Tide Gage Data for Hurricane Ivan.

NOAA National Oceanic and Atmospheric Administration(2004). Hurricane IVAN Preliminary Water Levels Report.

URS Group, Inc. 200 Orchard Ridge Drive Suite 101 Gaithersburg, MD 20878 (2004). Hurricane Ivan Rapid Response Alabama and Mississippi Coastal High Water Mark (CHWM) Collection FEMA-1549-DR-AL & 1550-DR-MS.

URS Group, Inc. 200 Orchard Ridge Drive Suite 101 Gaithersburg, MD 20878 (2004). Hurricane Ivan Rapid Response Florida Coastal High Water Mark (CHWM) Collection FEMA-1551-DR-FL.

URS Group, Inc. 200 Orchard Ridge Drive Suite 101 Gaithersburg, MD 20878 (2004). Hurricane Jeanne Rapid Response Florida Riverine High Water Mark (RHWM) Collection FEMA-1561-DR-FL.

NOAA National Oceanic and Atmospheric Administration (2004).Hurricane Jeanne Preliminary Water Levels Report.

URS Group, Inc. 200 Orchard Ridge Drive Suite 101 Gaithersburg, MD 20878 (2006). Final Coastal High Water Mark Collection for Hurricane Wilma in Florida FEMA-1609-DR-FL, Task Order 460.

NOAA National Oceanic and Atmospheric Administration (2005).Hurricane Wilma Preliminary Water Levels Report.

Thomas J. Smith III, Gordon H. Anderson, and Ginger Tiling (2005). A Tale of Two Storms: Surges and Sediment Deposition from Hurricanes Andrew and Wilma in Florida's Southwest Coast Mangrove Forests.

Lars E. Soderqvist and Michael J. Byrne (2005). Monitoring the Storm Tide of Hurricane Wilma in Southwestern Florida.

The database for validating the model predicted flood depths during historical Florida flood events is not available.

D. Indicate the resolution of the flood model elevation or depth grid used on each contour or high-resolution map.

The resolutions of the grids are changed according to the location, since CEST employ orthogonal curvilinear grid. The finer grid will locate at the coast and land with the coarser grid on the open ocean.

The roughly resolution for 4 grids at coastal region are:

1. Apalachicola Bay basin, AP8, resolution is around 200 – 350 meters;
2. Tampa Bay basin, TP3, resolution is around 200 – 400 meters;
3. South Florida basin, HMI41, resolution is around 100 – 300 meters;
4. Florida Atlantic basin, EJX7, resolution is around 200 – 600 meters;

The resolution of inland flood maps for historical flood events in 1km X 1km.

E. Demonstrate the consistency of the modeled flood extent and elevation or depth with observed flood extent and elevation or depth for each historical event.

See the separated storm surge validation document.

The modeled and historical flood depths have been evaluated only for Hurricane Jeanne (2004) (FEMA, 2005), while for the other historical storms observed flood depths due to inland flooding are not available.

F. Explain any differences between the modeled flood extent and elevation or depth and the historical floods observations. Include an explanation if the differences are impacted by major flood control measures.

See the separated storm surge validation document.

The high water mark observations fall within the inland flood model predicted flood boundaries for hurricane Jeanne (2004). The average observed flood depths during hurricane Jeanne (2004) was 73 cm, while the average modeled flood depth was 41cm.

G. If additional assumptions are necessary to complete this form, provide the rationale for the assumptions as well as a detailed description of how they are included.

For the storm surge model, there is no assumption to complete this form.

Additional assumptions were not made to complete this form.

H. Include Form HHF-1, Historical Event Flood Extent and Elevation or Depth Validation Maps, in a submission appendix.

See the separated storm surge validation document.

Form HHF-2: Coastal Flood Characteristics by Annual Exceedance Probability

- A. Define one study area subject to coastal flooding within each of the five Florida geographic regions identified in *Figure 115*. The extent of each study area shall be determined by the modeling organization and shall be large enough to encompass at least one county. The modeling organization shall create the underlying grid for this form.

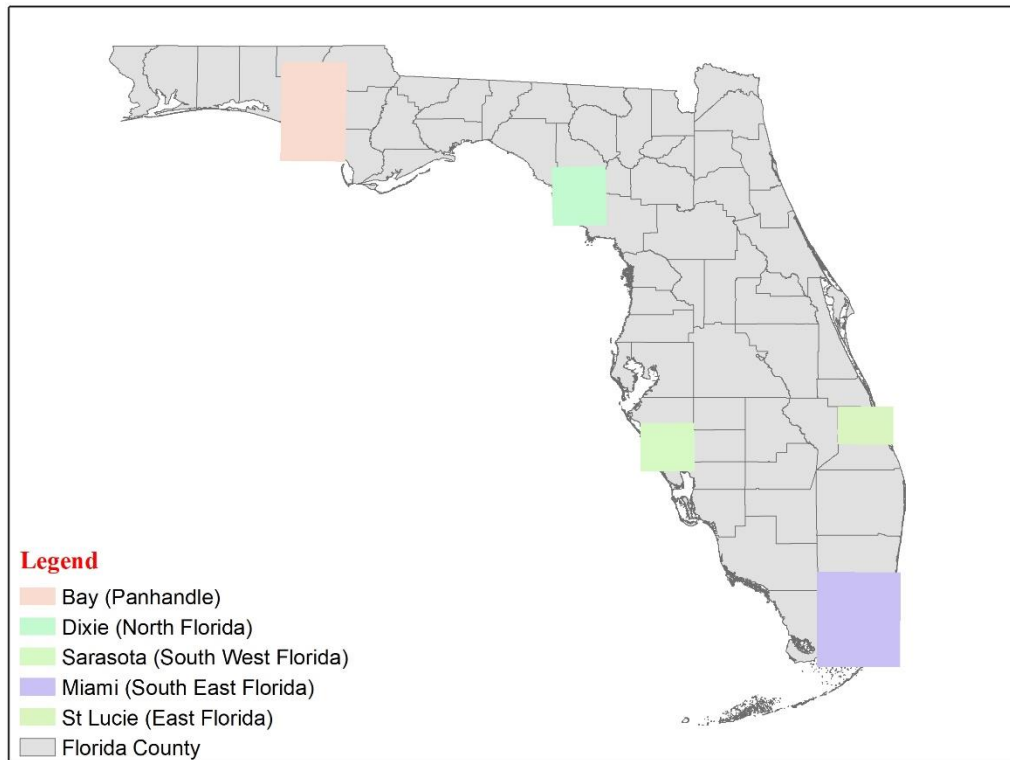


Figure 73. Five grids generated for five Florida geographic regions.

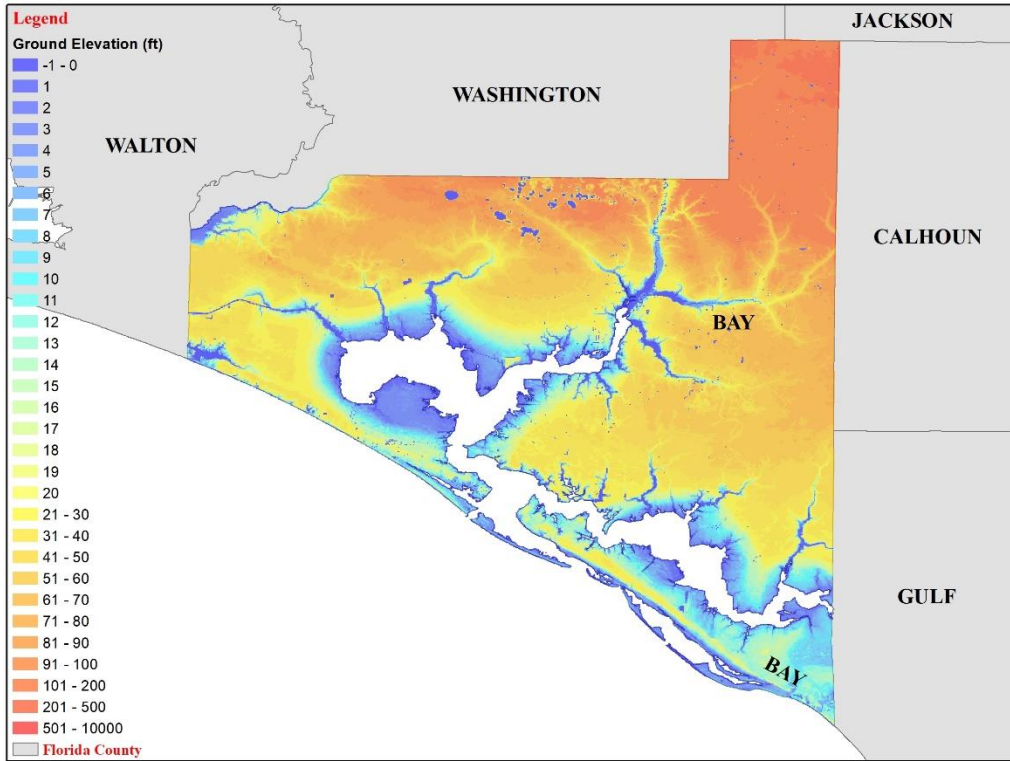


Figure 74. High resolution (100 meters) ground elevation at Bay County for Panhandle grid.

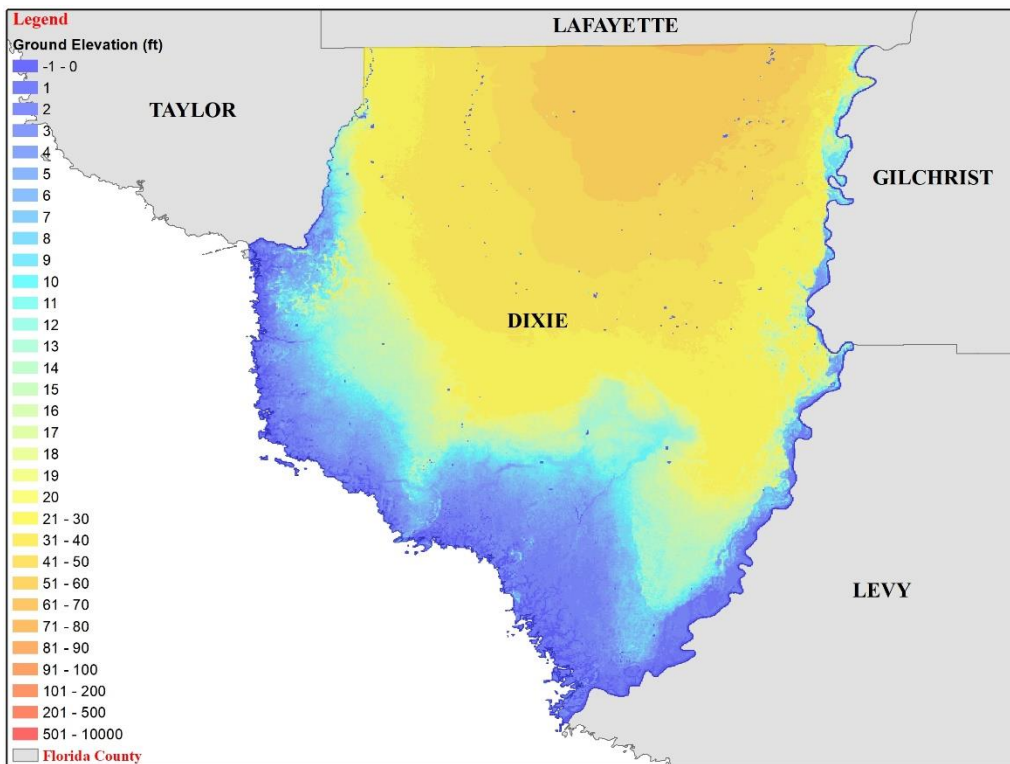


Figure 75. High resolution (100 meters) ground elevation at Dixie County for North Florida grid.

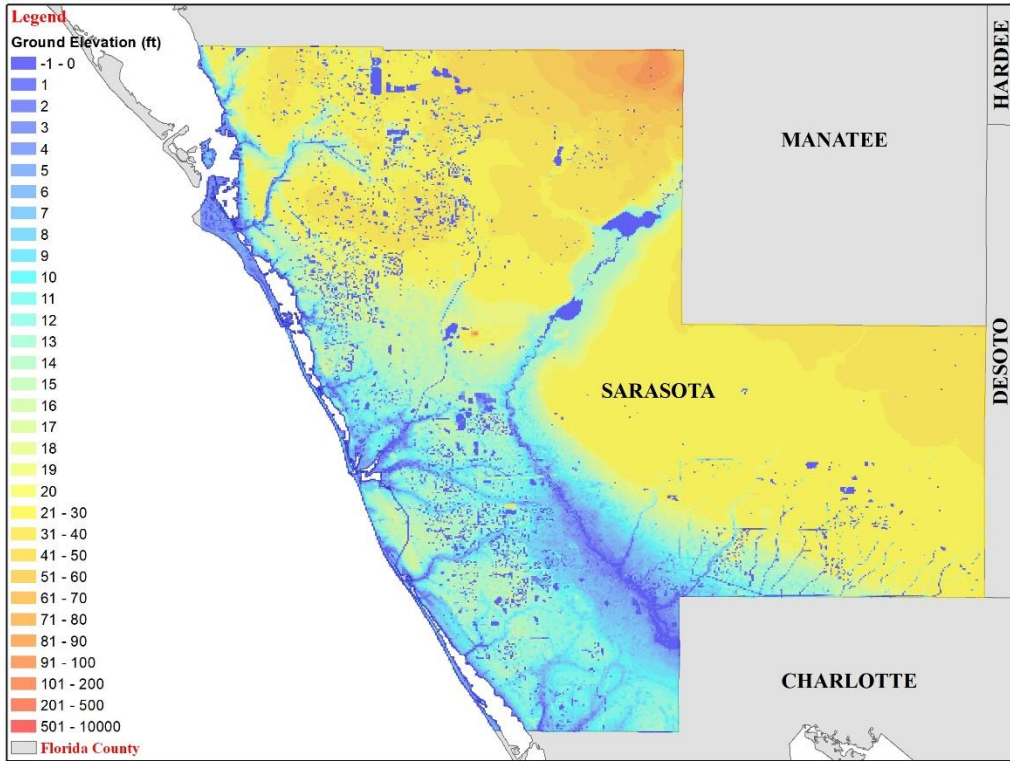


Figure 76. High resolution (100 meters) ground elevation at Sarasota County for South West Florida grid.

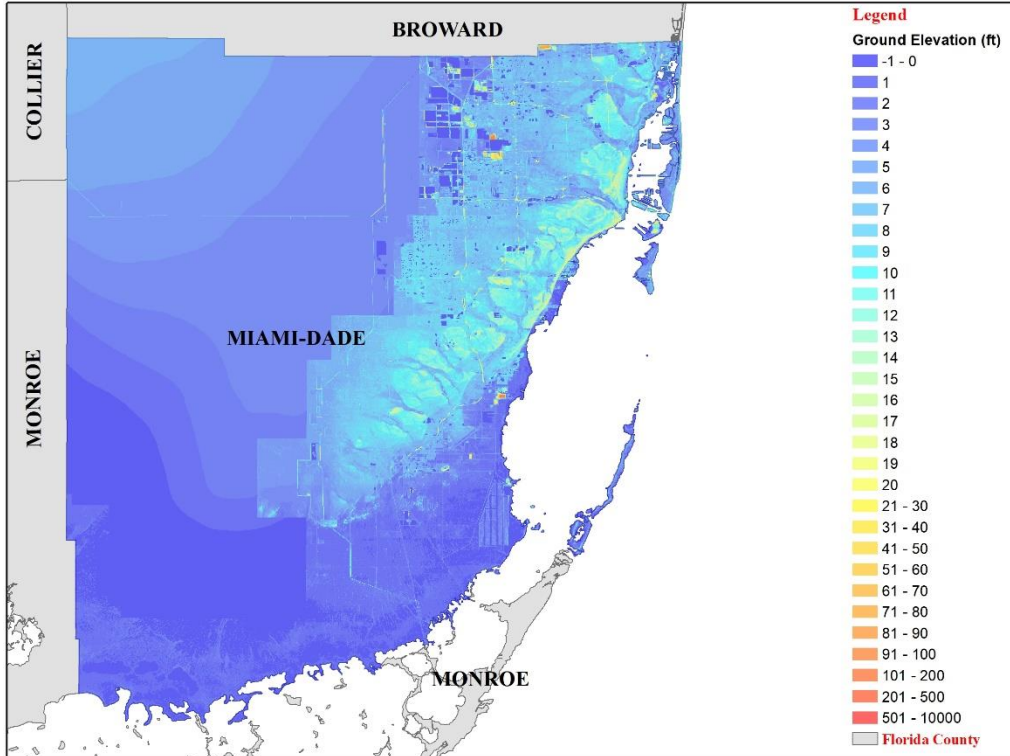


Figure 77. High resolution (100 meters) ground elevation at Miami-Dade County for South East Florida grid.

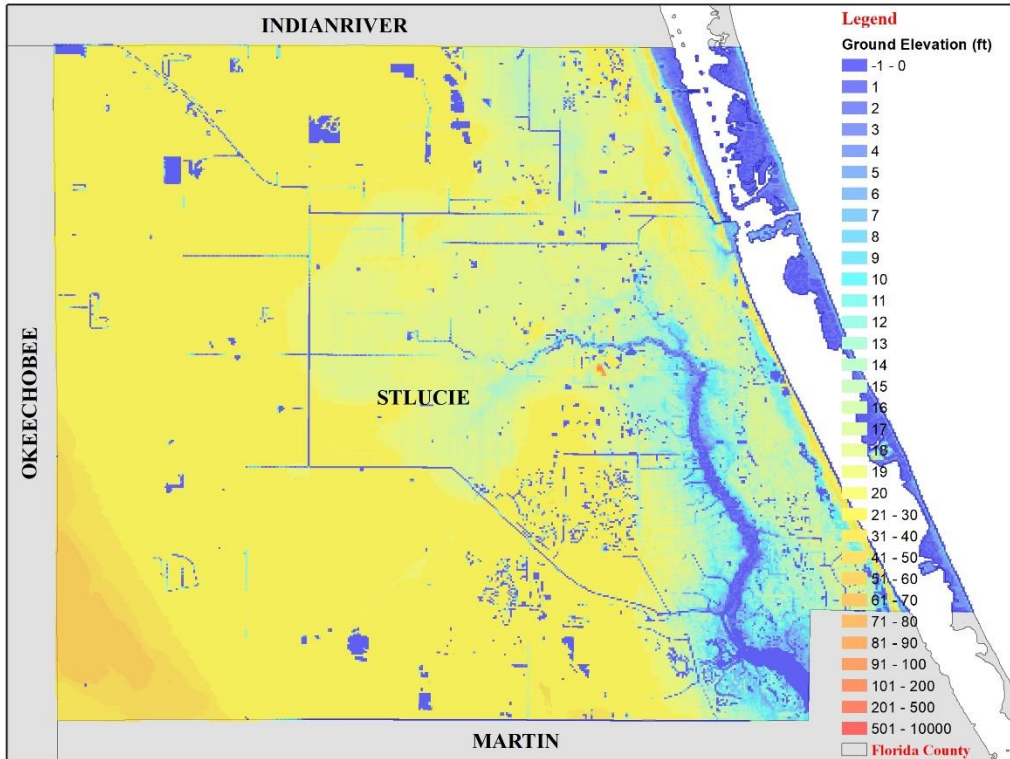


Figure 78. High resolution (100 meters) ground elevation at St. Lucie County for east Florida grid.

- B. Provide, for each study area, color-coded contour or high-resolution maps showing the modeled flood extent and elevation or depth corresponding to 0.01 annual exceedance probability. Flood extent and elevation or depth shall incorporate waves or wave proxies, if modeled. For locations subject to both coastal and inland flooding, this information should reflect only coastal flooding.

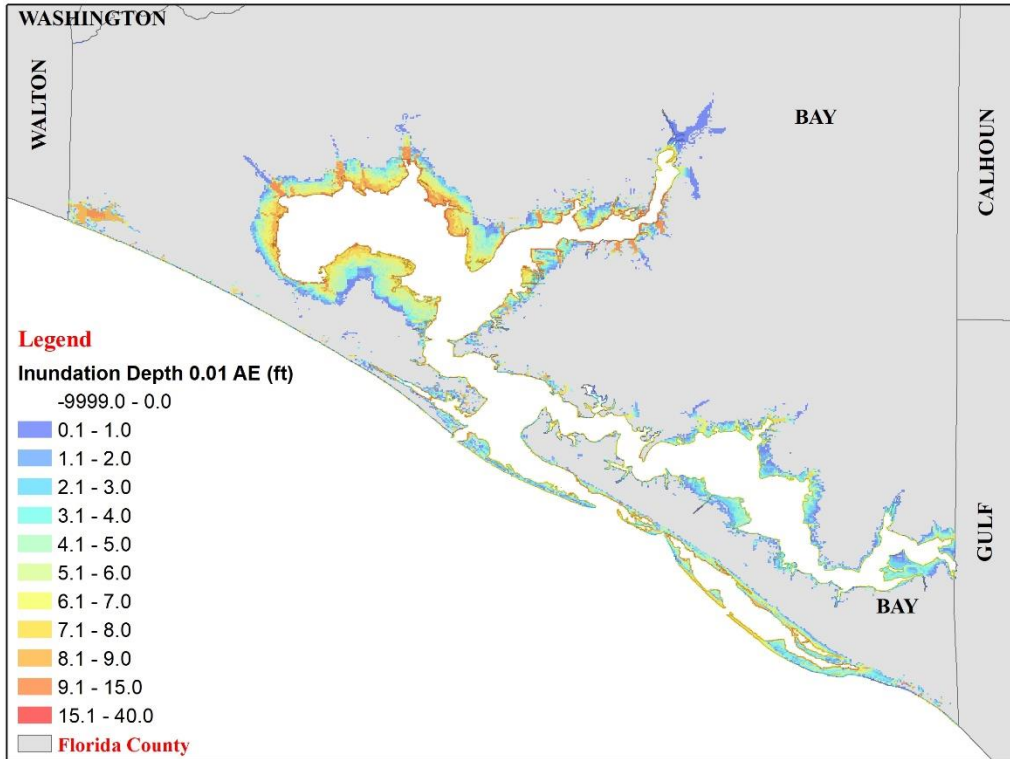


Figure 79. Color-coded contour showing the modeled flood extent and inundation depth corresponding to 0.01 annual exceedance probability at Bay County (Panhandle).

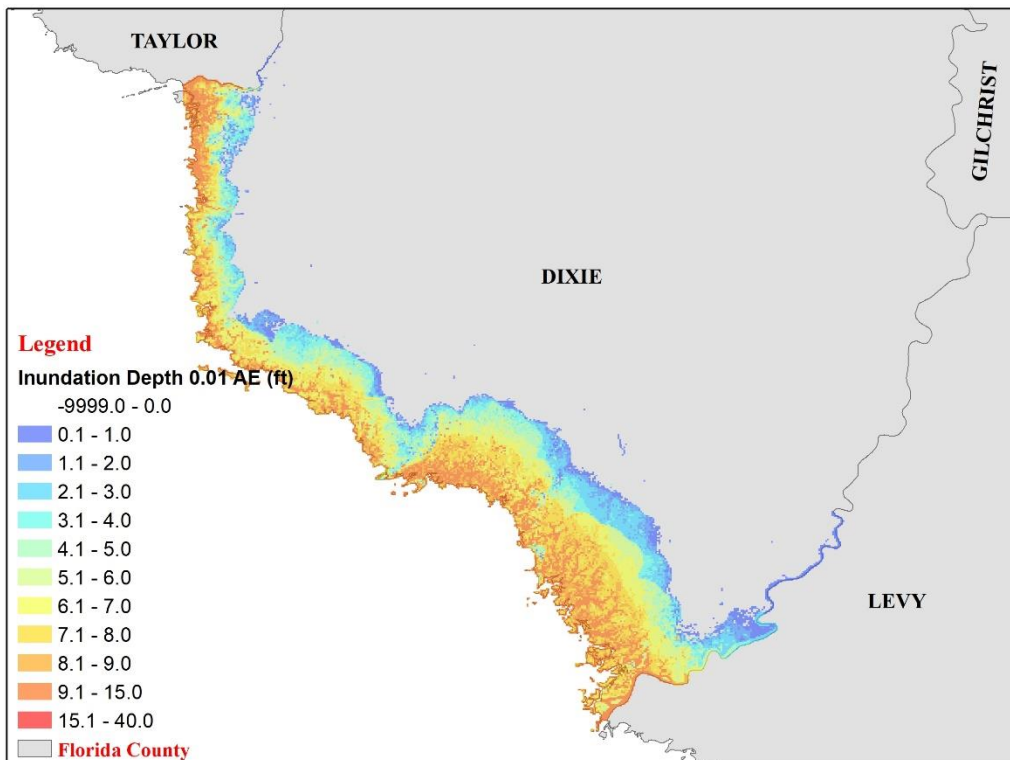


Figure 80. Color-coded contour showing the modeled flood extent and inundation depth corresponding to 0.01 annual exceedance probability at Dixie County (North Florida).

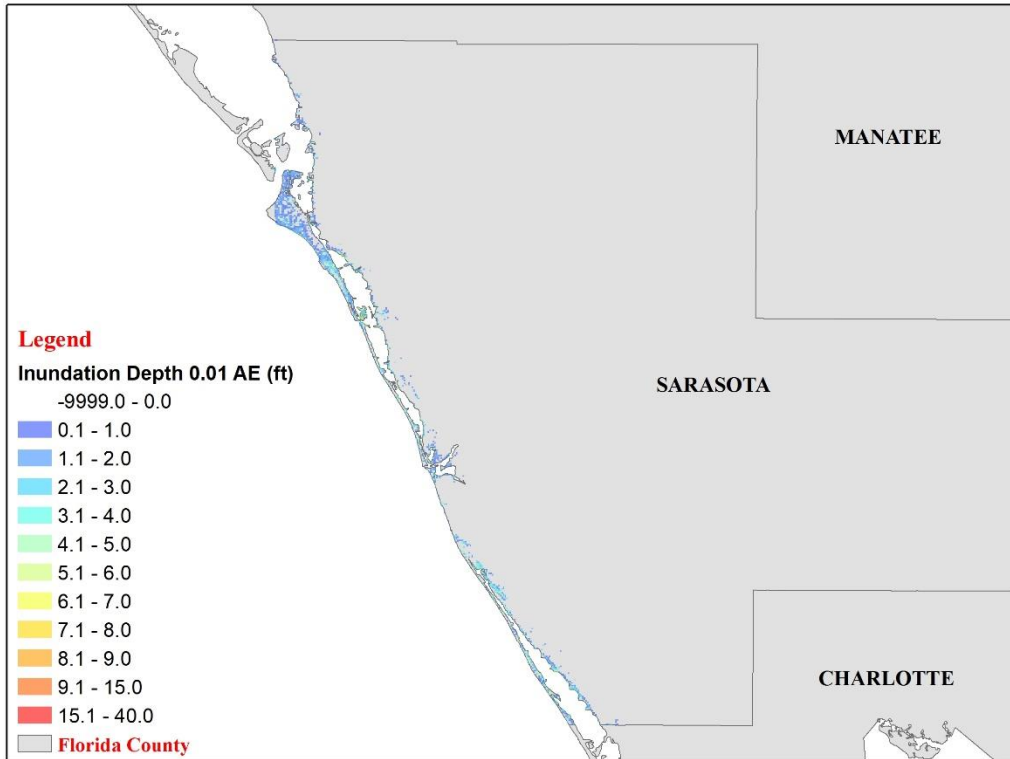


Figure 81. Color-coded contour showing the modeled flood extent and inundation depth corresponding to 0.01 annual exceedance probability at Sarasota County (South West Florida).

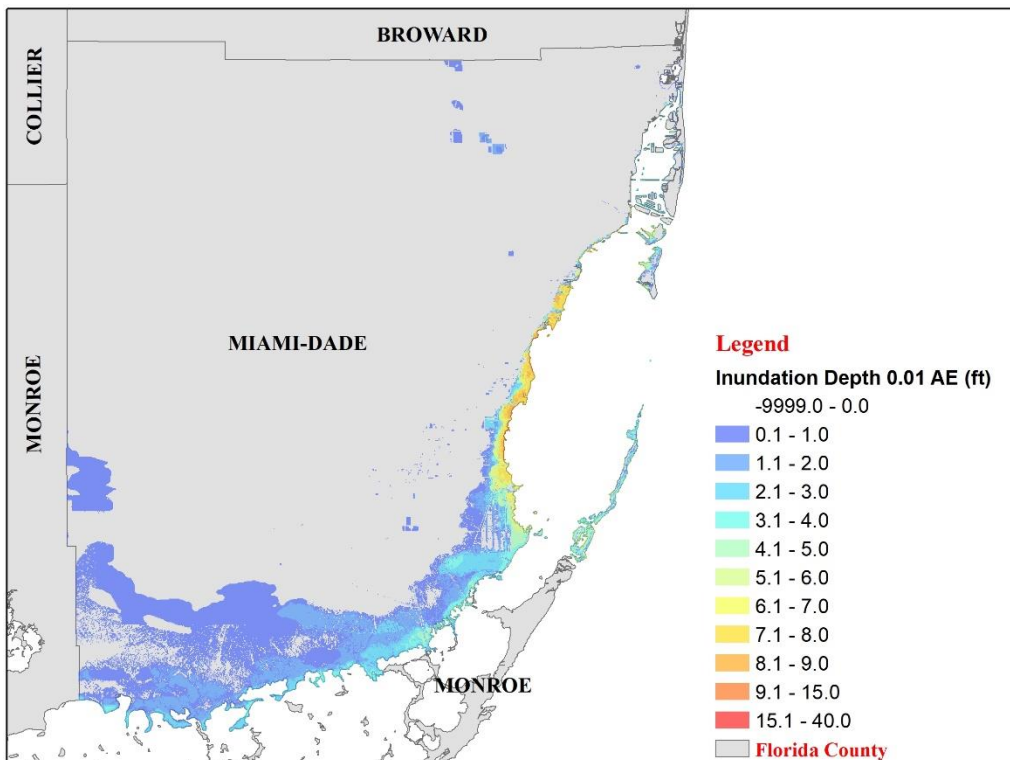


Figure 82. Color-coded contour showing the modeled flood extent and inundation depth corresponding to 0.01 annual exceedance probability at Miami-Dade County (South East Florida).

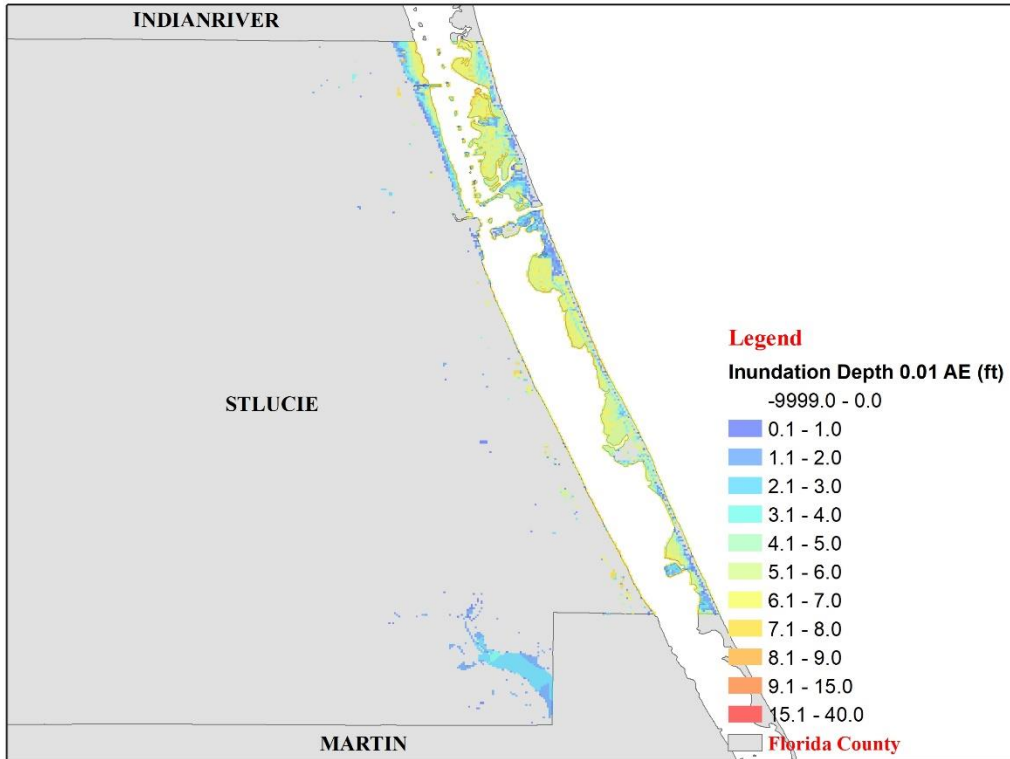


Figure 83. Color-coded contour showing the modeled flood extent and inundation depth corresponding to 0.01 annual exceedance probability at St. Lucie County (East Florida).

C. Include Form HHF-2, Coastal Flood Characteristics by Annual Exceedance Probability, in a submission appendix.

Form HHF-3: Coastal Flood Characteristics by Annual Exceedance Probabilities (Trade Secret Item)

- A. Provide, for each study area defined in Form HHF-2, Coastal Flood Characteristics by Annual Exceedance Probability, the following information. For locations subject to both coastal and inland flooding, this information should reflect only coastal flooding.
1. Study area color-coded contour or high-resolution maps showing modeled flood extent and elevation or depth corresponding to the 0.1, 0.02, 0.01, and 0.002 annual exceedance probabilities. Flood extent and elevation or depth shall incorporate waves or wave proxies, if modeled.

Bay County (Panhandle)

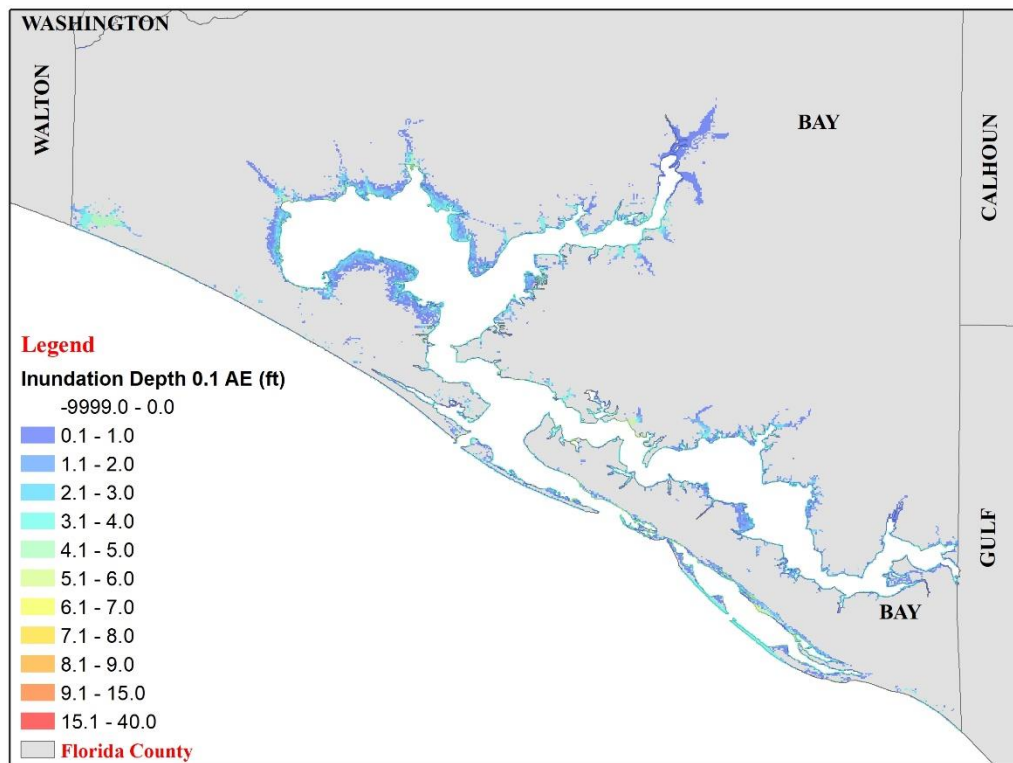


Figure 84. Modeled flood extent and inundation depth corresponding to 0.1 annual exceedance probability at Bay County (Panhandle).

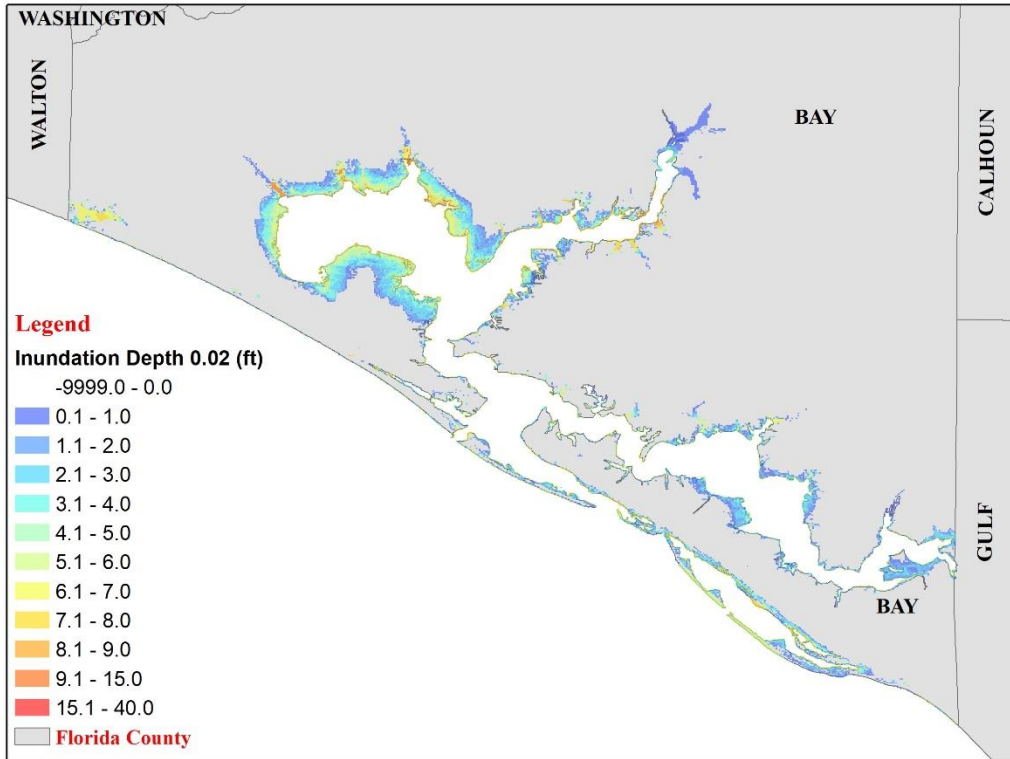


Figure 85. Modeled flood extent and inundation depth corresponding to 0.02 annual exceedance probability at Bay County (Panhandle).

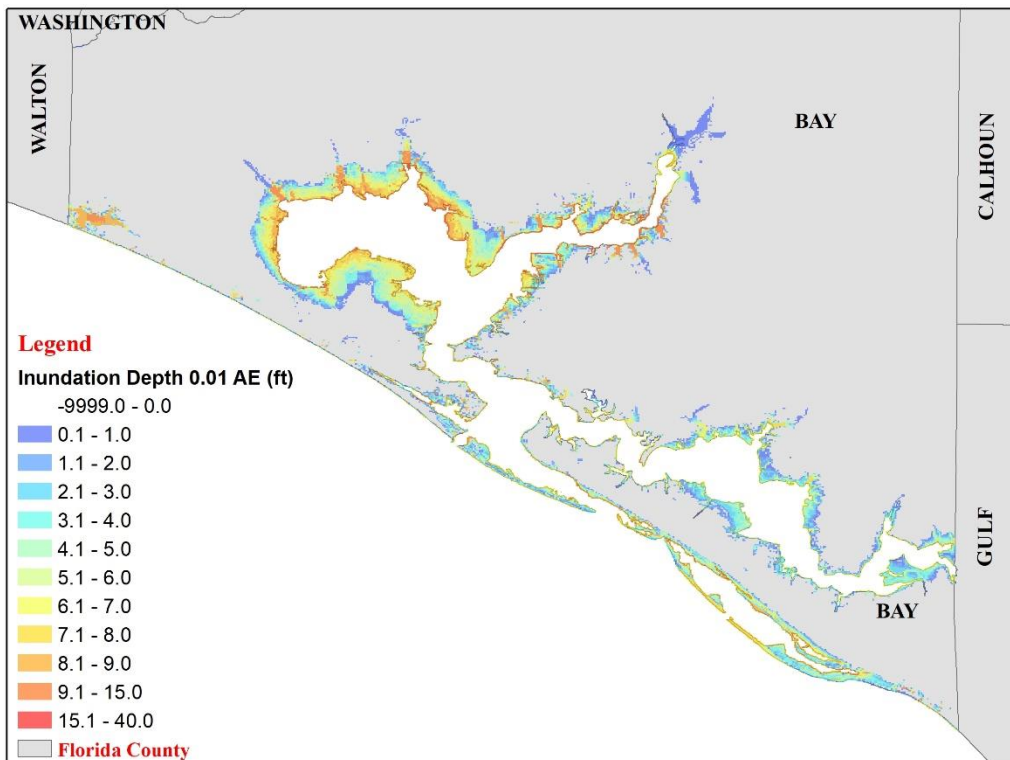


Figure 86. Modeled flood extent and inundation depth corresponding to 0.01 annual exceedance probability at Bay County (Panhandle).

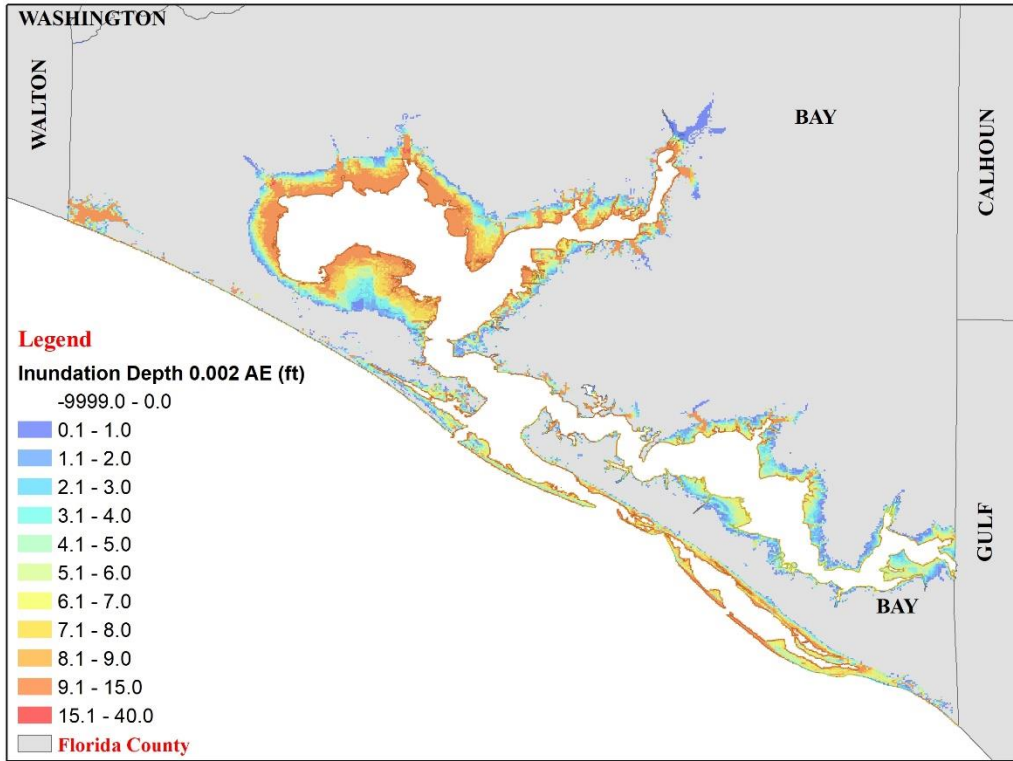


Figure 87. Modeled flood extent and inundation depth corresponding to 0.002 annual exceedance probability at Bay County (Panhandle)

Dixie County (North Florida)

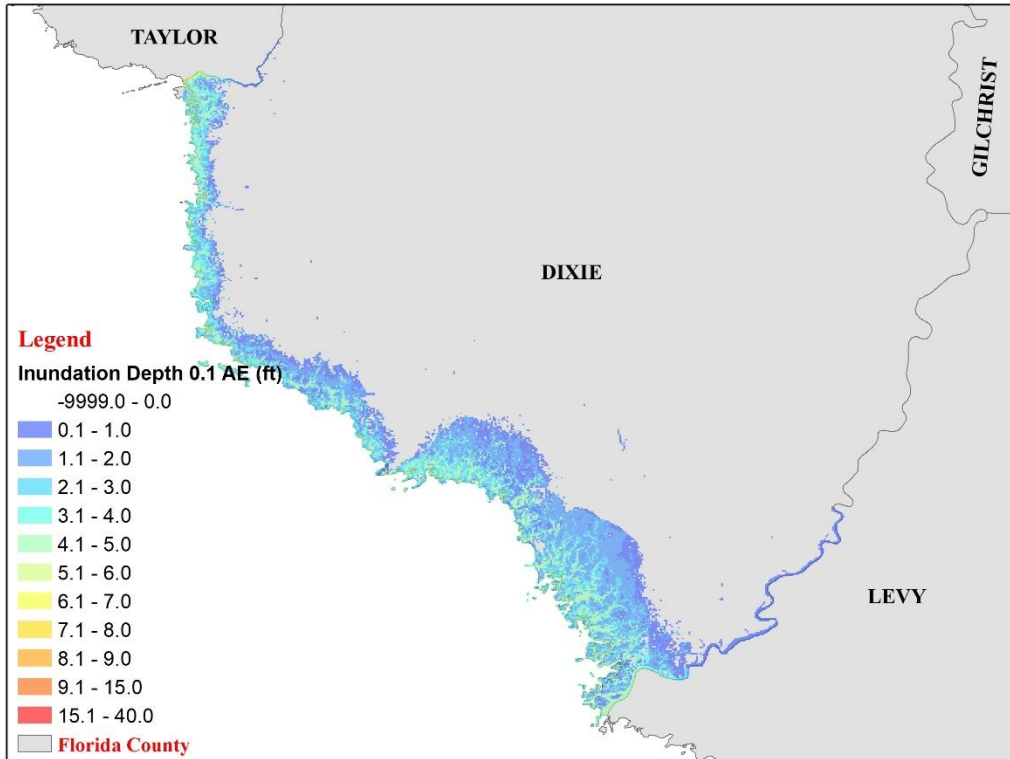


Figure 88. Modeled flood extent and inundation depth corresponding to 0.1 annual exceedance probability at Dixie County (North Florida).

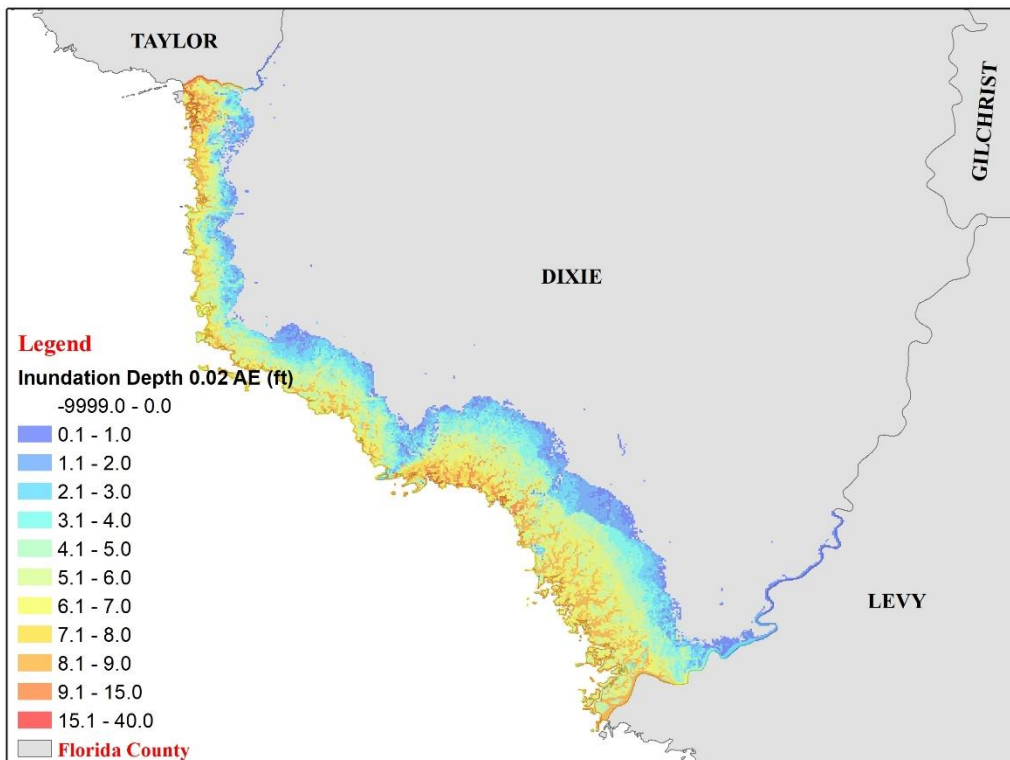


Figure 89. Modeled flood extent and inundation depth corresponding to 0.02 annual exceedance probability at Dixie County (North Florida).

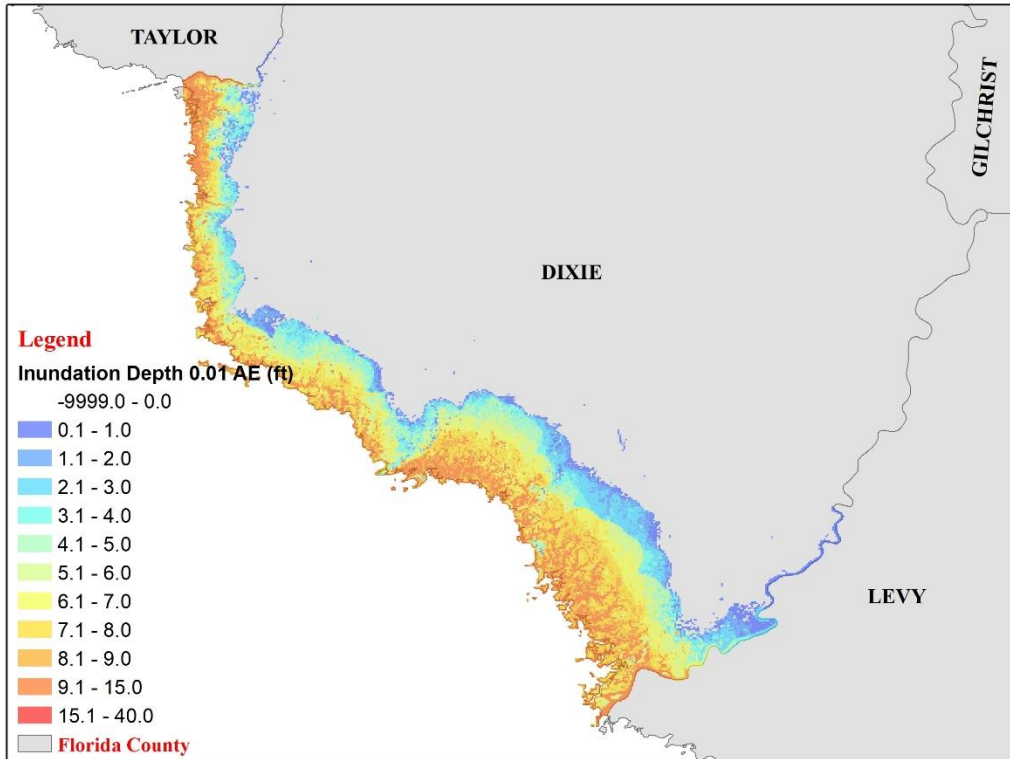


Figure 90. Modeled flood extent and inundation depth corresponding to 0.01 annual exceedance probability at Dixie County (North Florida).

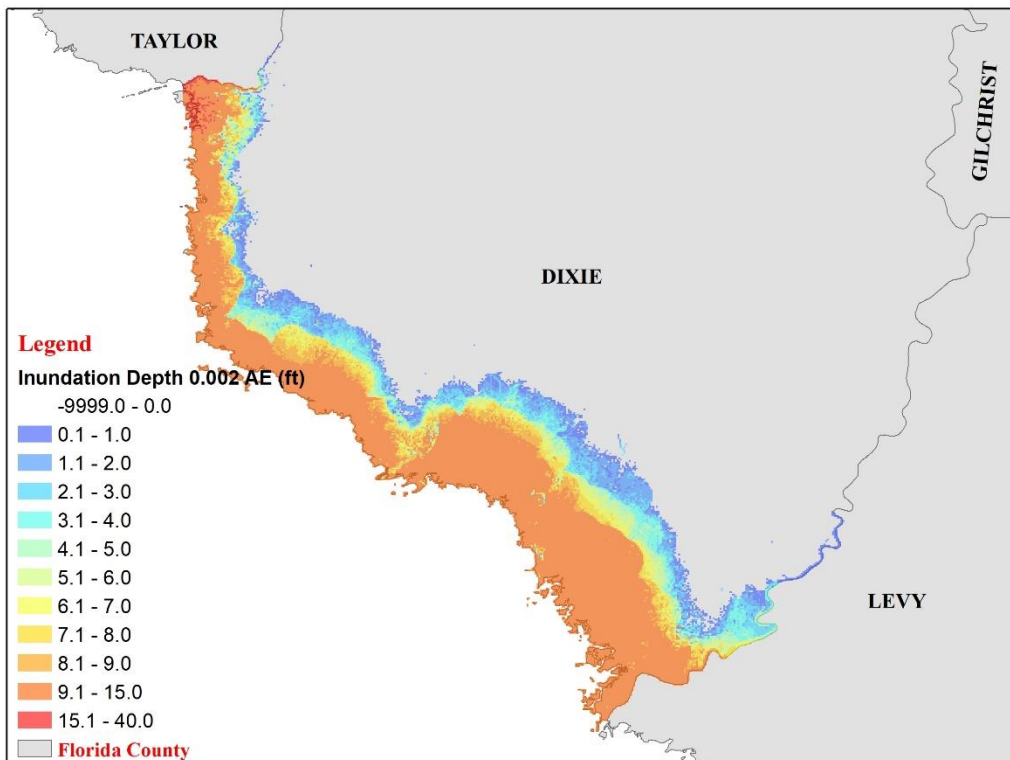


Figure 91. Modeled flood extent and inundation depth corresponding to 0.002 annual exceedance probability at Dixie County (North Florida).

Sarasota County (South West Florida)

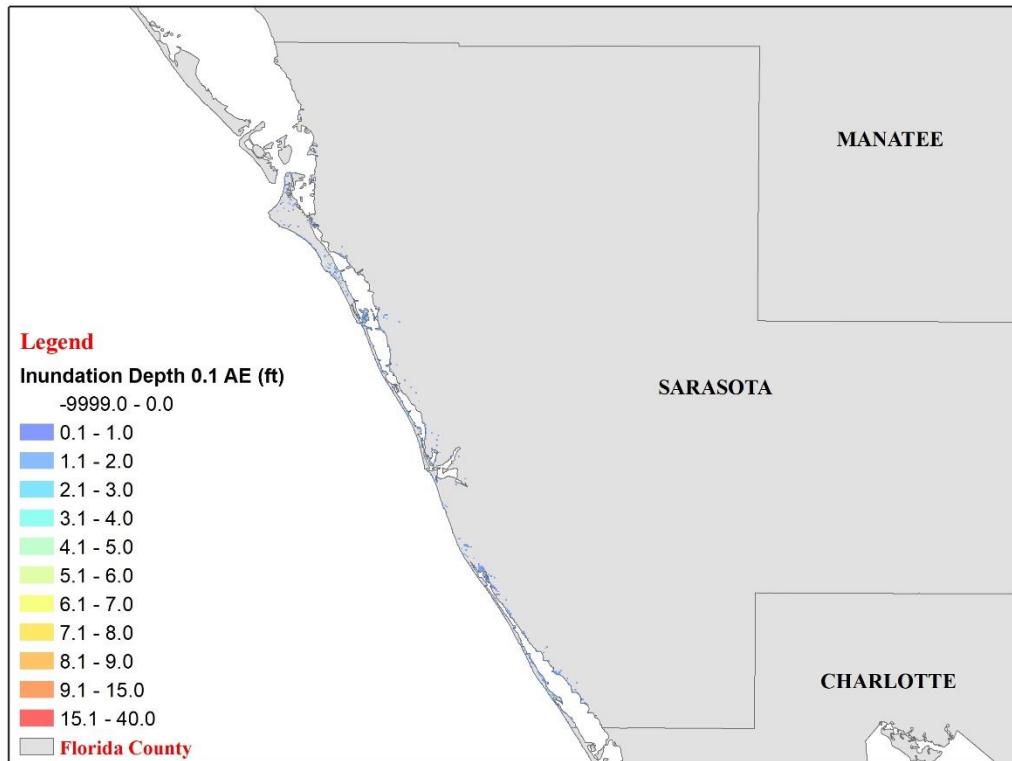


Figure 92. Modeled flood extent and inundation depth corresponding to 0.1 annual exceedance probability at Sarasota County (South West Florida).

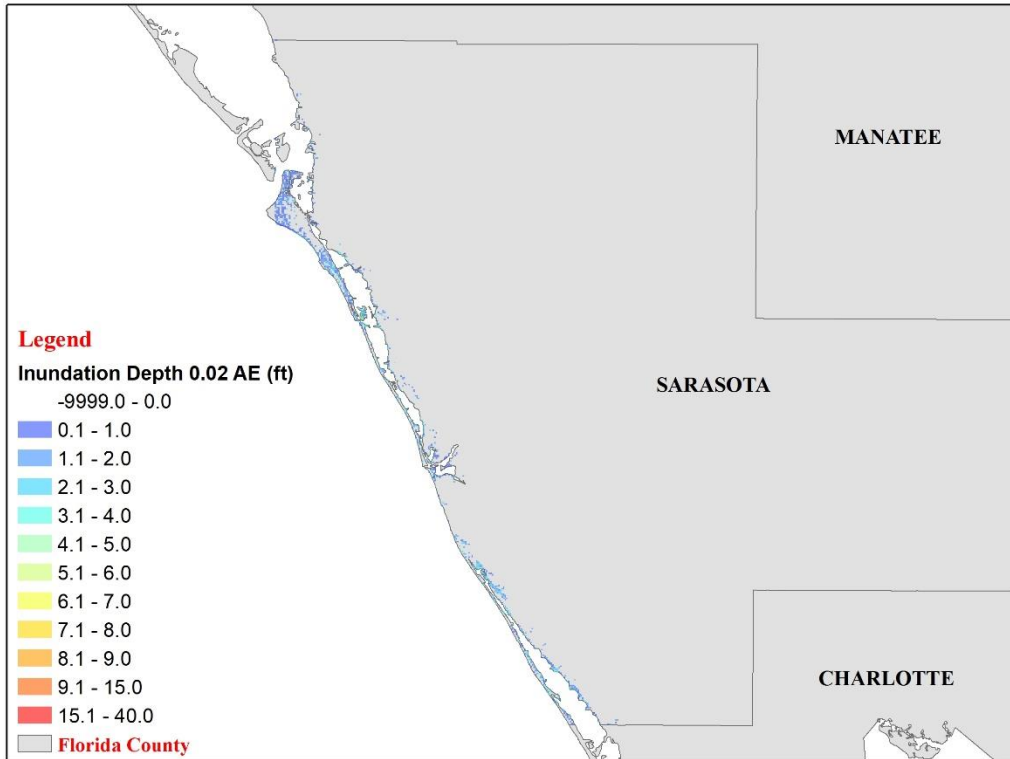


Figure 93. Modeled flood extent and inundation depth corresponding to 0.02 annual exceedance probability at Sarasota County (South West Florida).

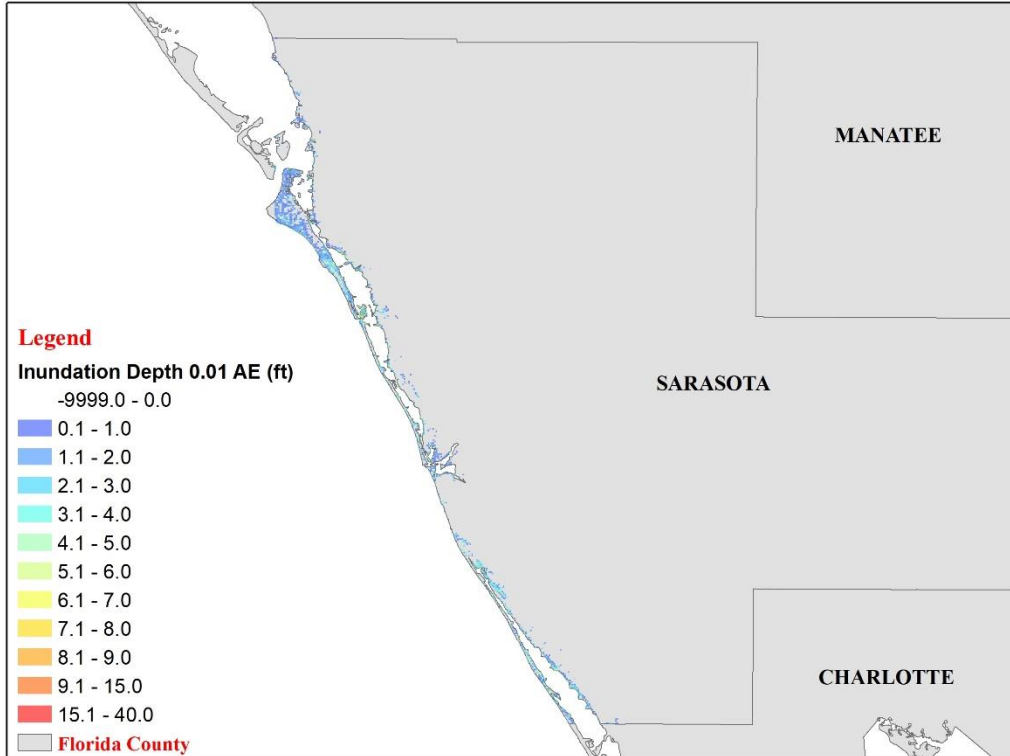


Figure 94. Modeled flood extent and inundation depth corresponding to 0.01 annual exceedance probability at Sarasota County (South West Florida).

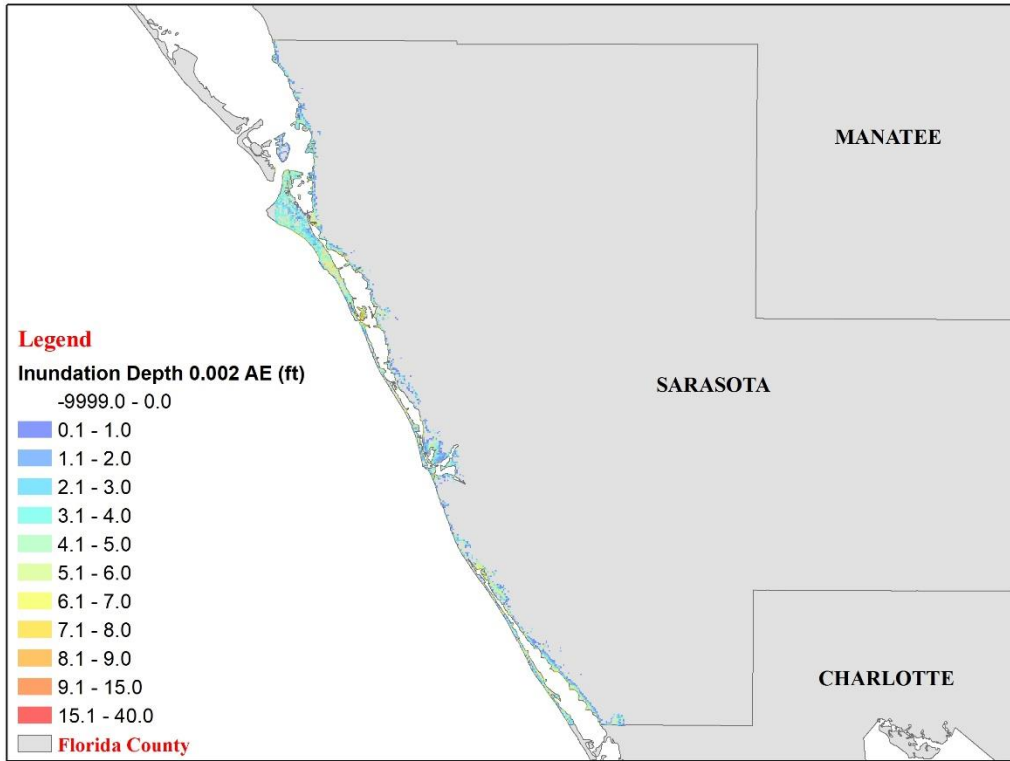


Figure 95. Modeled flood extent and inundation depth corresponding to 0.002 annual exceedance probability at Sarasota County (South West Florida).

Miami-Dade County (South East Florida)

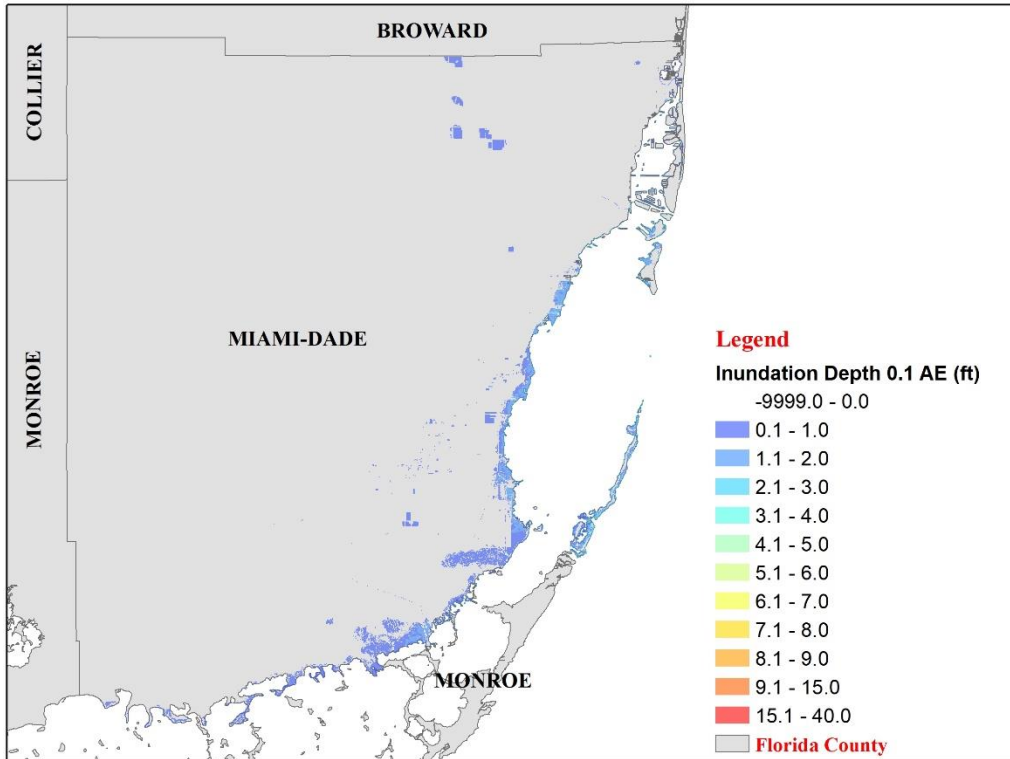


Figure 96. Modeled flood extent and inundation depth corresponding to 0.1 annual exceedance probability at Miami-Dade County (South East Florida).

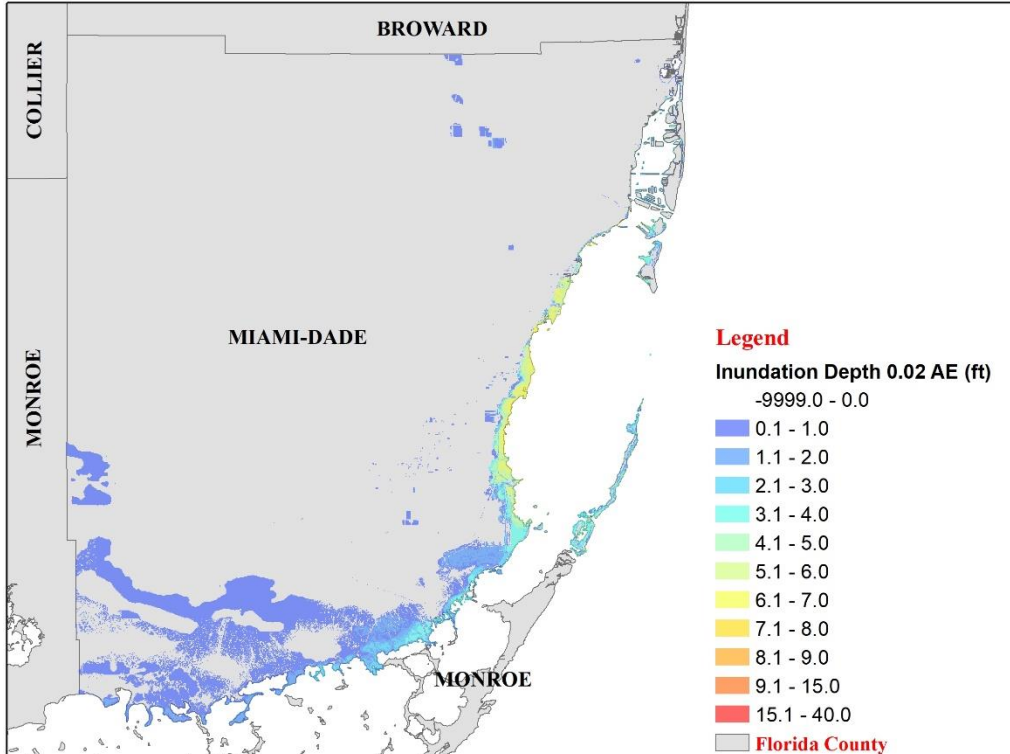


Figure 97. Modeled flood extent and inundation depth corresponding to 0.02 annual exceedance probability at Miami-Dade County (South East Florida).

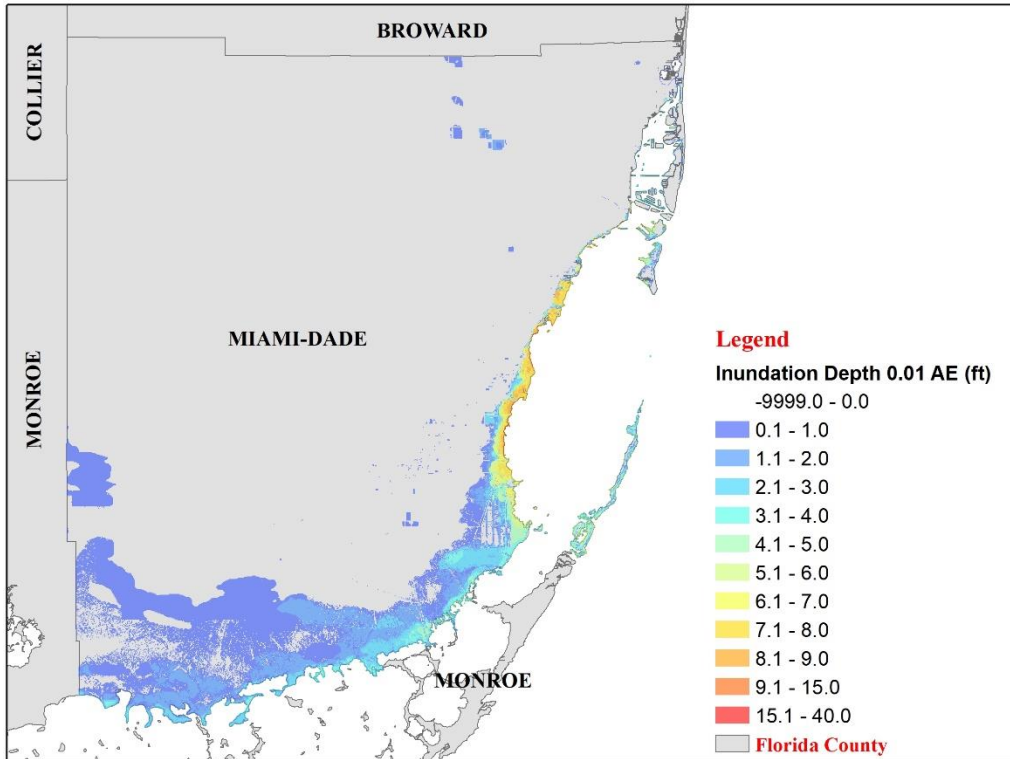


Figure 98. Modeled flood extent and inundation depth corresponding to 0.01 annual exceedance probability at Miami-Dade County (South East Florida).

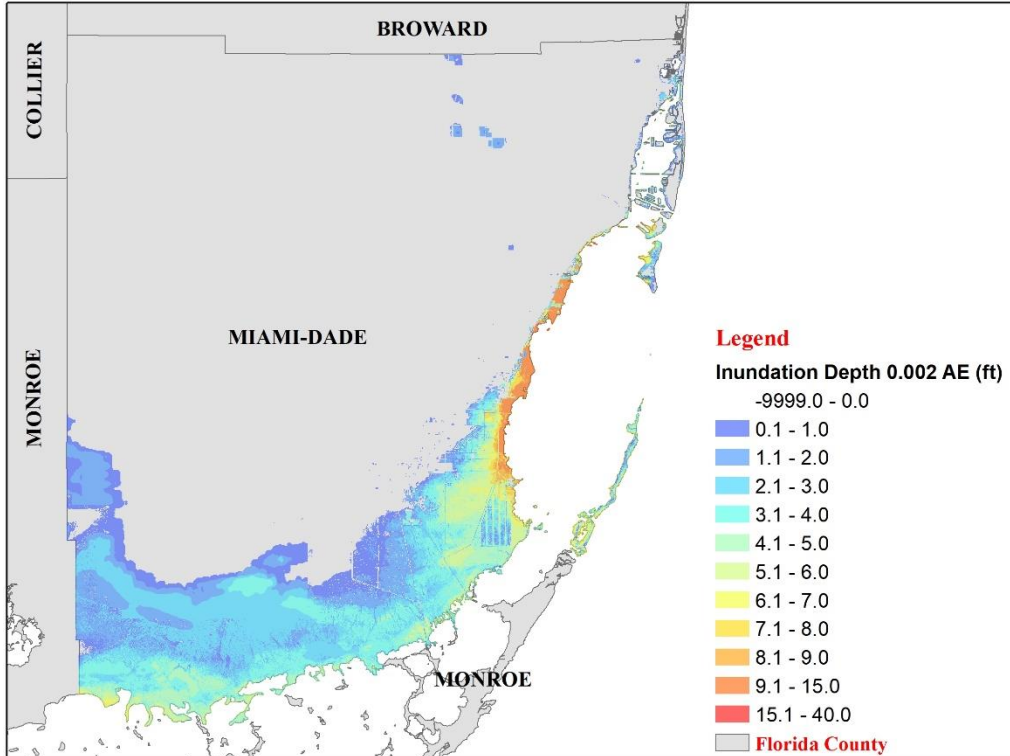


Figure 99. Modeled flood extent and inundation depth corresponding to 0.002 annual exceedance probability at Miami-Dade County (South East Florida).

St. Lucie County (East Florida)

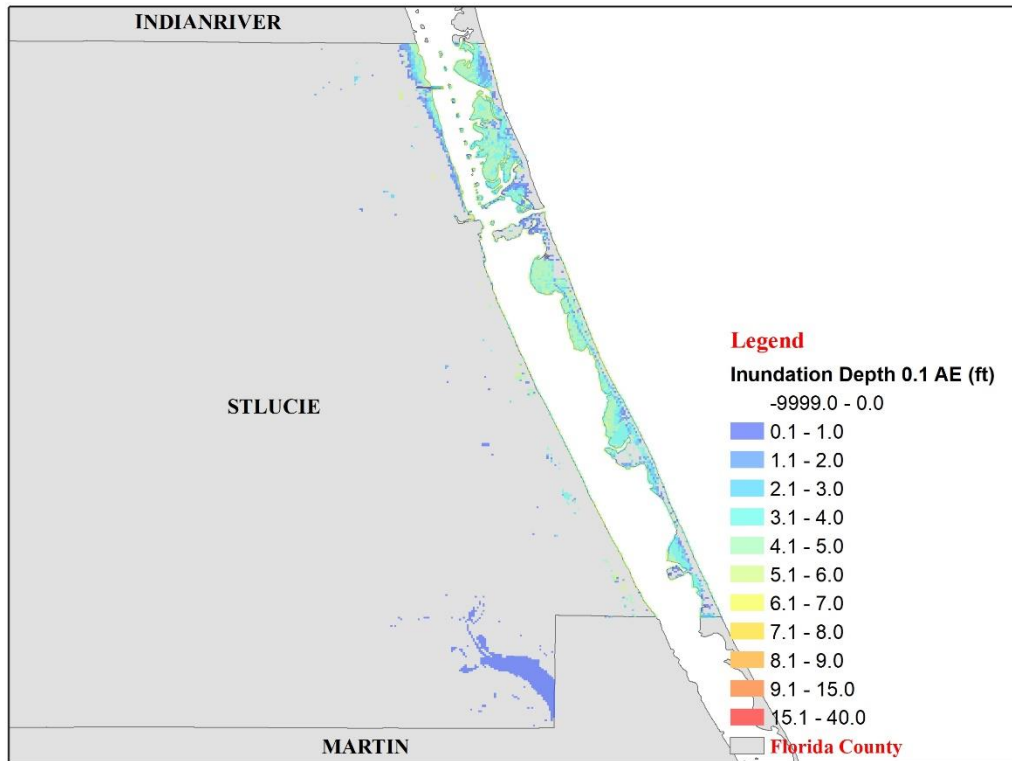


Figure 100. Modeled flood extent and inundation depth corresponding to 0.1 annual exceedance probability at St. Lucie County (East Florida).

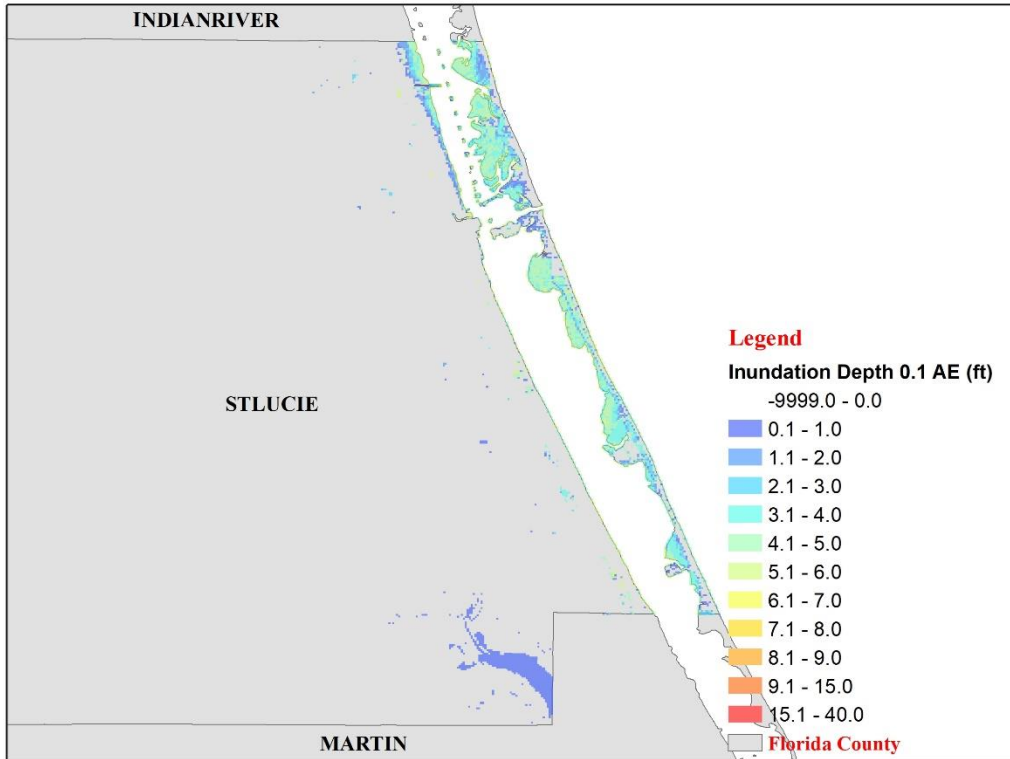


Figure 101. Modeled flood extent and inundation depth corresponding to 0.02 annual exceedance probability at St. Lucie County (East Florida).

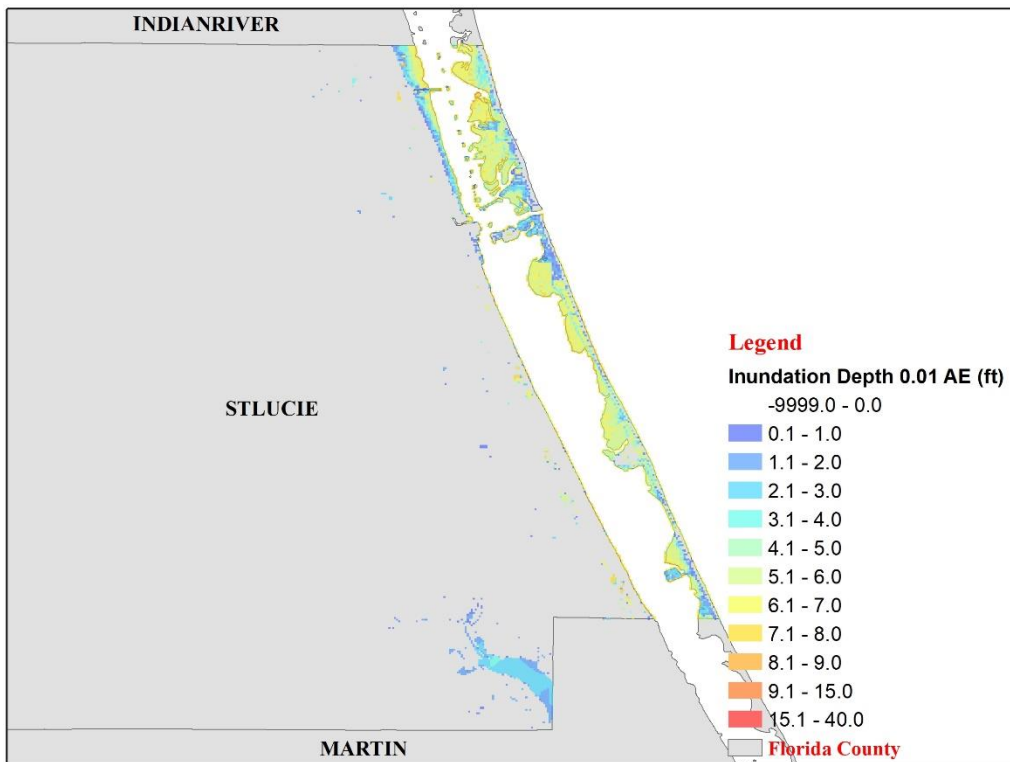


Figure 102. Modeled flood extent and inundation depth corresponding to 0.01 annual exceedance probability at St. Lucie County (East Florida).

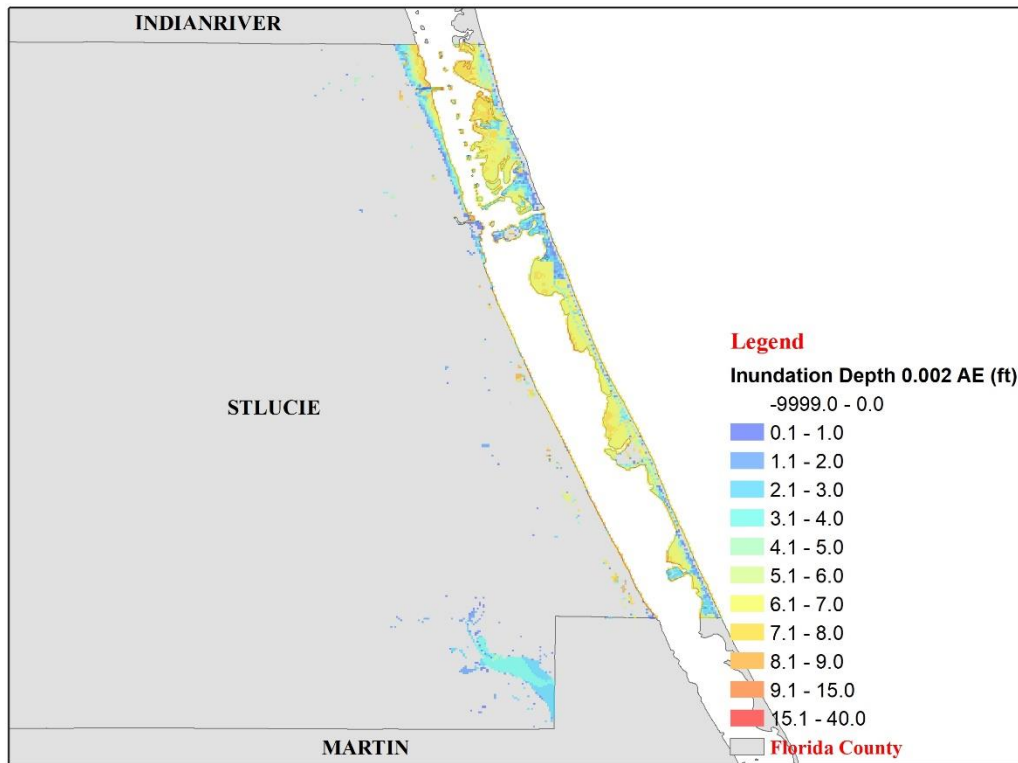


Figure 103. Modeled flood extent and inundation depth corresponding to 0.002 annual exceedance probability at St. Lucie County (East Florida).

2. Graphs and tables showing flood model results at 10 or more locations within the study area and representative of the range of flood conditions in the study area. The following flood characteristics shall be included for the 0.1, 0.02, 0.01, and 0.002 annual exceedance probabilities:
 - a. Stillwater flood elevations,
 - b. Coastal wave heights or wave proxies,
 - c. If the flood vulnerability model requires explicit representation of flood-induced erosion effects, the erosion depth (original ground elevation minus eroded ground elevation),
 - d. If the flood vulnerability model requires explicit representation of flow velocity effects, the flow velocities, and
 - e. If the flood vulnerability model requires explicit representation of flood inundation duration effects, the duration of flood inundation.



Figure 104. Selected 10 locations within the study area.

Location	County	GE	0.1 AE	0.02 AE	0.01 AE	0.002 AE	Max	Lat	Lon
1	Bay	4.3	0.0	1.6	3.6	7.2	12.4	30.268453	-85.97809
2	Bay	0.0	2.3	7.1	8.6	12.0	17.2	30.167547	-85.78490
3	Bay	0.0	3.1	5.4	6.5	8.4	11.0	30.115206	-85.60291
4	Bay	0.0	2.6	5.0	6.2	8.5	11.0	30.122054	-85.56856
5	Bay	1.7	1.1	3.5	5.1	7.8	11.7	30.152790	-85.65948
6	Bay	0.0	3.6	7.5	9.2	12.3	15.5	30.239580	-85.67597
7	Bay	0.1	2.7	7.0	8.9	12.3	15.9	30.273598	-85.64953
8	Bay	4.6	0.0	3.2	5.2	8.7	12.6	30.295038	-85.81352
9	Bay	3.6	0.0	4.8	7.0	10.3	14.0	30.293567	-85.85097
10	Bay	5.7	0.0	1.1	2.0	5.2	10.6	30.183207	-85.82006
11	Dixie	0.0	4.9	9.6	11.1	15.8	27.9	29.671267	-83.38909
12	Dixie	4.4	0.0	2.1	3.4	7.9	21.9	29.595578	-83.38421
13	Dixie	2.3	1.5	5.4	7.0	10.6	26.4	29.437471	-83.29496
14	Dixie	0.4	3.4	7.5	9.0	12.7	28.5	29.443872	-83.28995
15	Dixie	0.0	4.0	8.1	9.7	13.3	29.3	29.440353	-83.28472
16	Dixie	3.8	0.0	4.0	5.6	9.3	25.2	29.440282	-83.28884
17	Dixie	1.9	1.8	6.0	7.9	11.6	28.3	29.398385	-83.20548
18	Dixie	1.1	2.2	6.5	8.1	11.7	28.4	29.327108	-83.15041
19	Dixie	0	3.9	8.2	10.0	13.9	30.7	29.33726	-83.1362
20	Dixie	3.6	0.0	0.0	0.6	4.0	17	29.341375	-83.10437
21	Sarasota	3.8	0.0	0.1	0.5	2.9	11.5	27.28341	-82.56426
22	Sarasota	0.2	2.3	4.3	5.5	8.3	17	27.24321	-82.52633
23	Sarasota	0.4	2.2	4.0	4.9	7.6	17.3	27.203718	-82.50560
24	Sarasota	0.9	1.5	3.0	3.9	6.3	15.4	27.121962	-82.46920
25	Sarasota	1.1	1.2	3.0	3.9	6.3	15.3	27.110292	-82.46299
26	Sarasota	1.8	0.7	2.4	3.4	5.7	12.2	26.987276	-82.39893
27	Sarasota	0.8	1.6	3.5	4.6	6.8	14.2	26.981107	-82.38374

28	Sarasota	2.0	0.1	1.9	3.0	5.1	11.6	27.022316	-82.41549
29	Sarasota	3.8	0.0	0.5	1.7	4.6	14.2	27.220909	-82.5018
30	Sarasota	0.8	0.0	1.7	2.7	5.8	16.1	27.353995	-82.54807
31	Miami	2.1	0.0	0.0	1.0	6.0	11.1	25.560292	-80.32750
32	Miami	1.55	0.2	5.6	7.5	9.9	15.6	25.596346	-80.31336
33	Miami	5.5	0.0	0.8	2.5	5.1	14.7	25.649448	-80.27719
34	Miami	5.5	0.0	0.4	2.1	4.7	16.4	25.705285	-80.24795
35	Miami	5.0	0.0	1.0	2.7	5.4	16.6	25.728689	-80.23384
36	Miami	3.0	0.0	2.1	3.5	6.0	18.0	25.76186	-80.18976
37	Miami	1.7	0.0	0.0	0.0	1.4	16.6	25.784164	-80.14273
38	Miami	3.0	0.0	0.0	0.0	1.1	12.5	25.859991	-80.13919
39	Miami	3.0	0.0	0.0	1.3	2.4	11.7	25.909602	-80.13084
40	Miami	6.4	0.0	0.0	0.9	4.0	7.2	25.583728	-80.31841
41	St.Lucie	5.2	0.0	0.3	0.7	1.5	6.0	27.305172	-80.22035
42	St.Lucie	5.7	0.0	0.1	0.5	1.1	6.0	27.410157	-80.26918
43	St.Lucie	4.3	0.0	1.4	1.8	2.4	7.6	27.447258	-80.28613
44	St.Lucie	3.9	0.6	2.0	2.4	3.0	8.4	27.46719	-80.30010
45	St.Lucie	3.0	1.2	2.6	3.0	3.8	9.1	27.498821	-80.30706
46	St.Lucie	2.5	1.3	2.5	2.9	3.8	11.4	27.509835	-80.34445
47	St.Lucie	3.6	1.0	2.7	3.2	3.9	8.1	27.529559	-80.31598
48	St.Lucie	3.2	1.3	2.7	3.1	3.8	10.2	27.488127	-80.33547
49	St.Lucie	4.3	0.0	1.2	1.5	3.1	10.6	27.456477	-80.32453
50	St.Lucie	3.4	1.1	2.6	3.0	3.0	11.4	27.433874	-80.31759

Table 46. Flood model results at 10 locations within five study area (unit is feet).

Form HHF-4: Inland Flood Characteristics by Annual Exceedance Probability

- A. Define one study area subject to inland flooding within each of the five Florida geographic regions identified in *Figure 4*. The extent of each study area shall be determined by the modeling organization and shall be large enough to encompass at least one county. The modeling organization shall create the underlying grid for this form.

The defined study areas within each region is enlisted in Table 47:

Region	County
Southeast Florida	Broward
South Florida	Brevard
North Florida	Duval
Southwest Florida	Hillsborough
Panhandle	Leon

Table 47. Chosen counties within each study area.

The five counties were further discretized into a number of 1km X 1km grids.

- B. Provide, for each study area, color-coded contour or high-resolution maps showing the modeled flood extent and elevation or depth corresponding to the 0.01 annual exceedance probability. Flood extent and elevation or depth shall incorporate the effects of flood-induced erosion, if modeled. For locations subject to both inland and coastal flooding, this information should reflect only inland flooding.

The modeled flood extents and depths corresponding to the 0.01 annual exceedance probability are as follows:

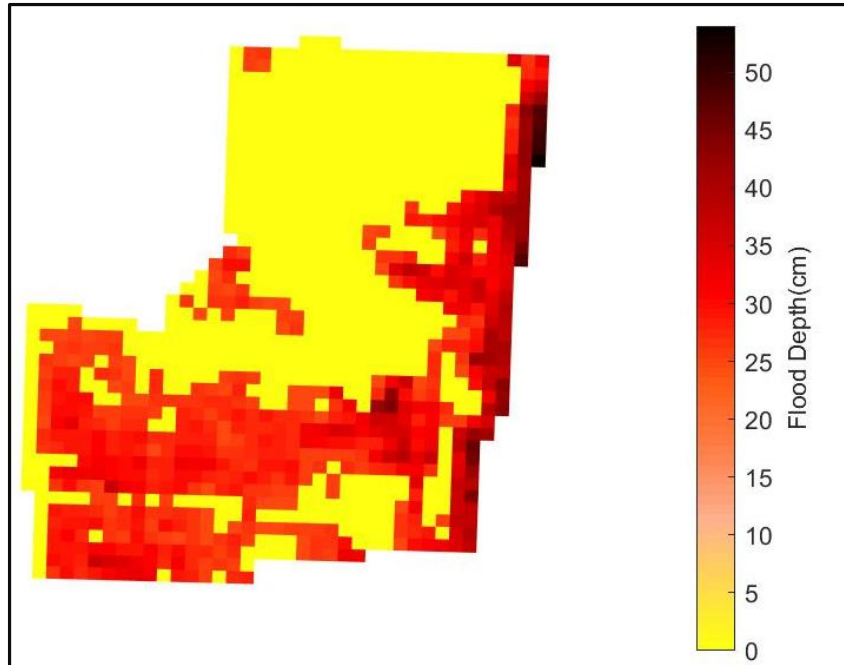


Figure 105. Modeled flood extent and depths in Southeast Florida Region (Broward County) for 0.01 exceedance probability.

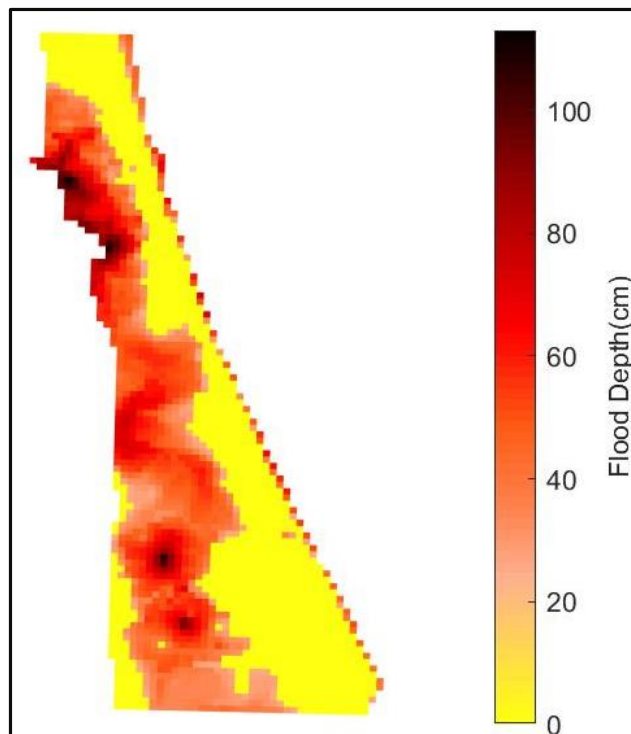


Figure 106. Modeled flood extent and depths in East Florida Region (Brevard County) for 0.01 exceedance probability.

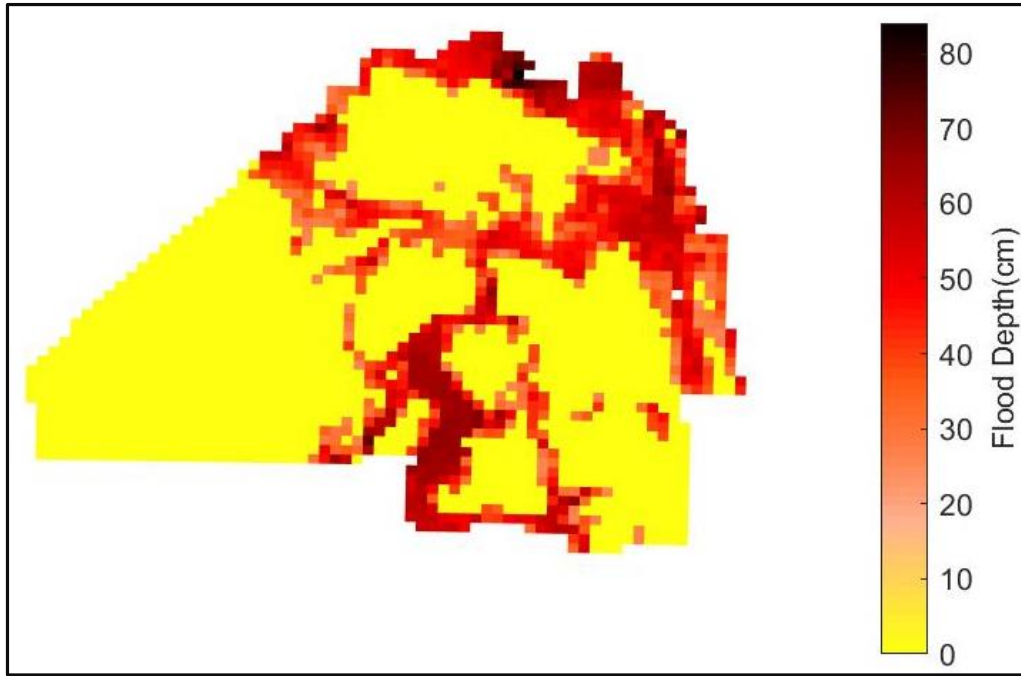


Figure 107. Modeled flood extent and depths in North Florida Region (Duval County) for 0.01 exceedance probability.

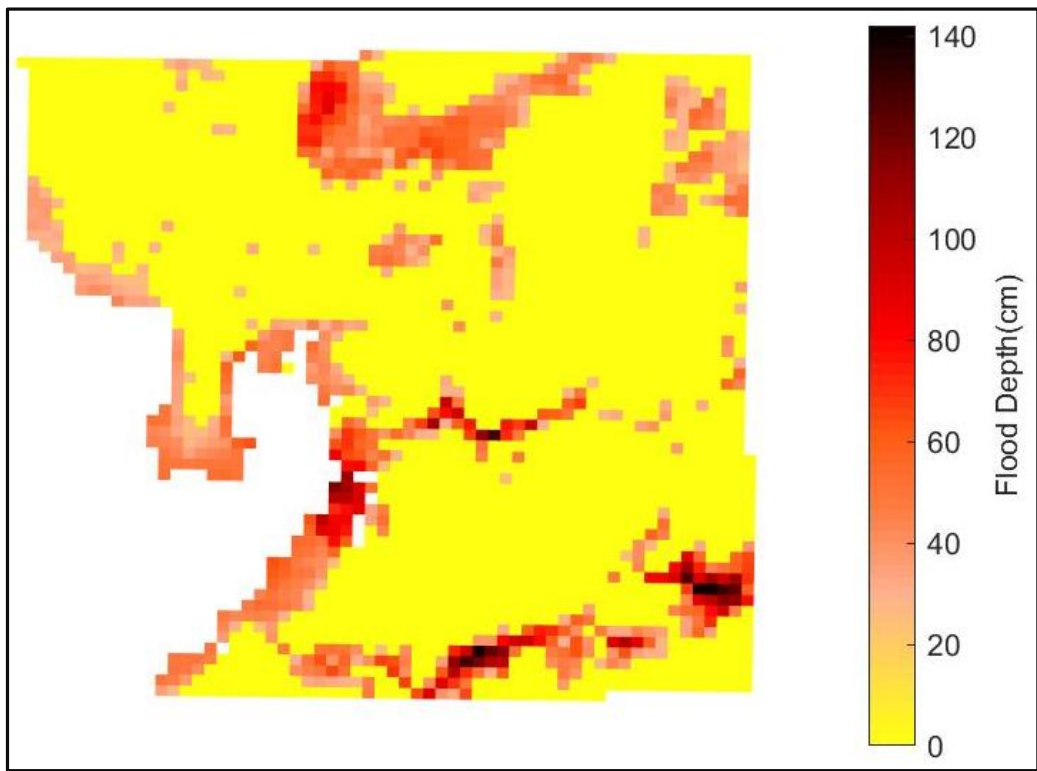


Figure 108. Modeled flood extent and depths in Southwest Florida Region (Hillsborough County) for 0.01 exceedance probability.

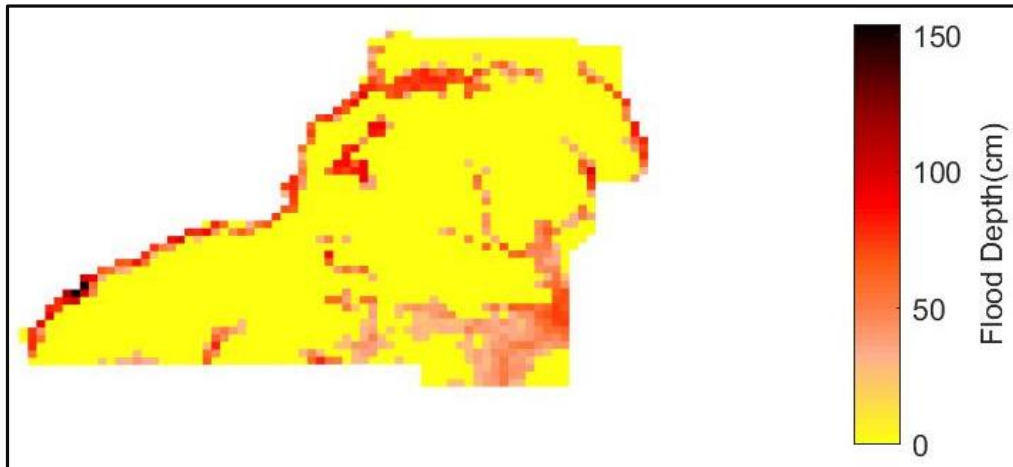


Figure 109. Modeled flood extent and depths in Panhandle Region (Leon County) for 0.01 exceedance probability.

- C. Include Form HHF-4, Inland Flood Characteristics by Annual Exceedance Probability, in a submission appendix.

Form HHF-5: Inland Flood Characteristics by Annual Exceedance Probabilities (Trade Secret Item)

- A. Provide, for each study area defined in Form HHF-4, Inland Flood Characteristics by Annual Exceedance Probability, the following information. For locations subject to both inland and coastal flooding, this information should reflect only inland flooding.
1. Study area color-coded contour or high-resolution maps showing modeled flood extent and elevation or depth corresponding to the 0.1, 0.02, 0.01, and 0.002 annual exceedance probabilities. Flood extent and elevation or depth shall incorporate the effects of flood-induced erosion, if modeled.

The flood maps corresponding to the 0.1, 0.02, 0.01, and 0.002 annual exceedance probabilities for the Southeast Florida (Broward County), East Florida (Brevard County), North Florida (Duval County), Southwest Florida (Hillsborough County), and Panhandle (Leon County) regions are given below:

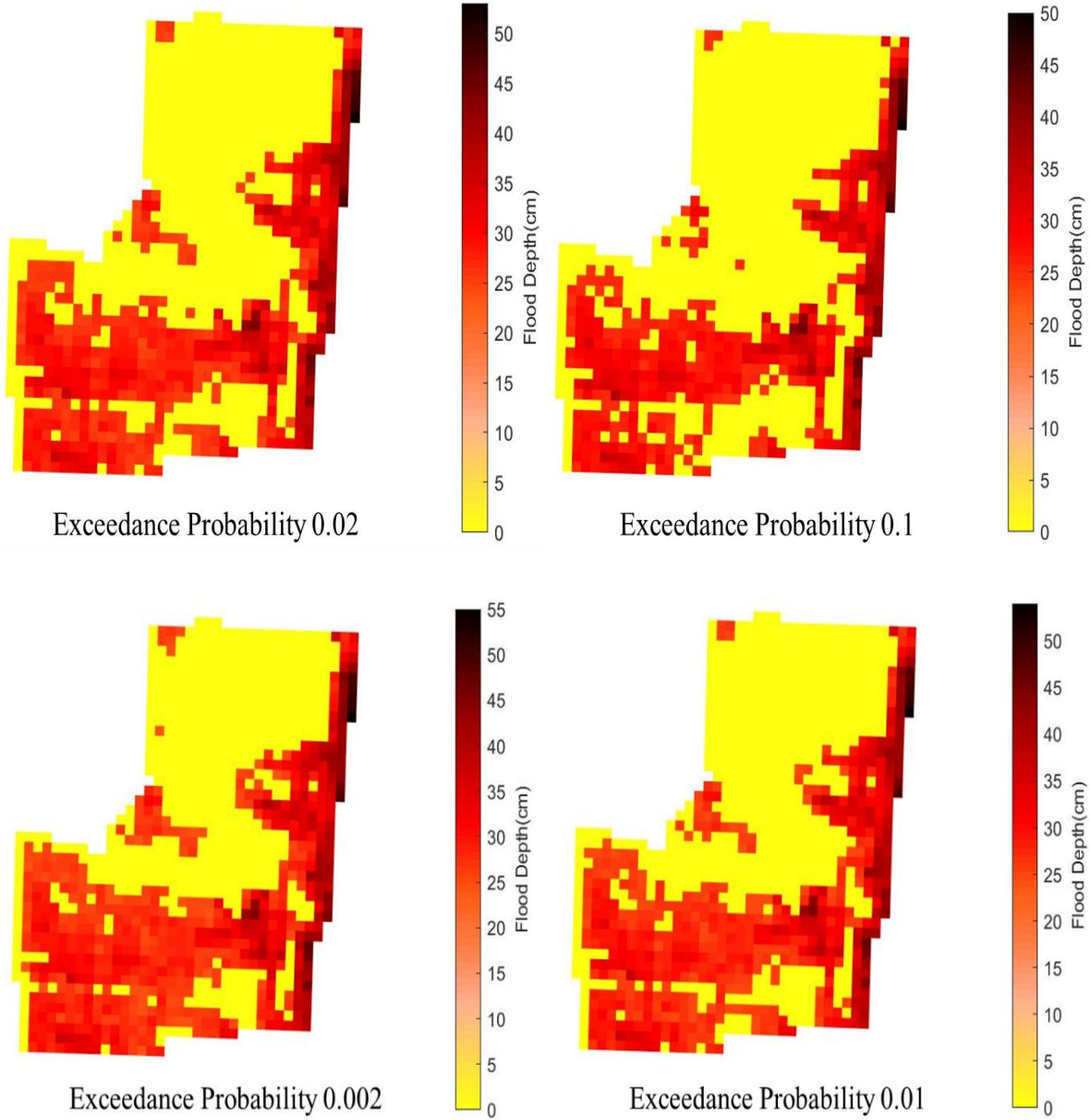


Figure 110. Flood maps for Southeast Florida Region (Broward County) corresponding to 0.1, 0.02, 0.01, and 0.002 annual exceedance probabilities.

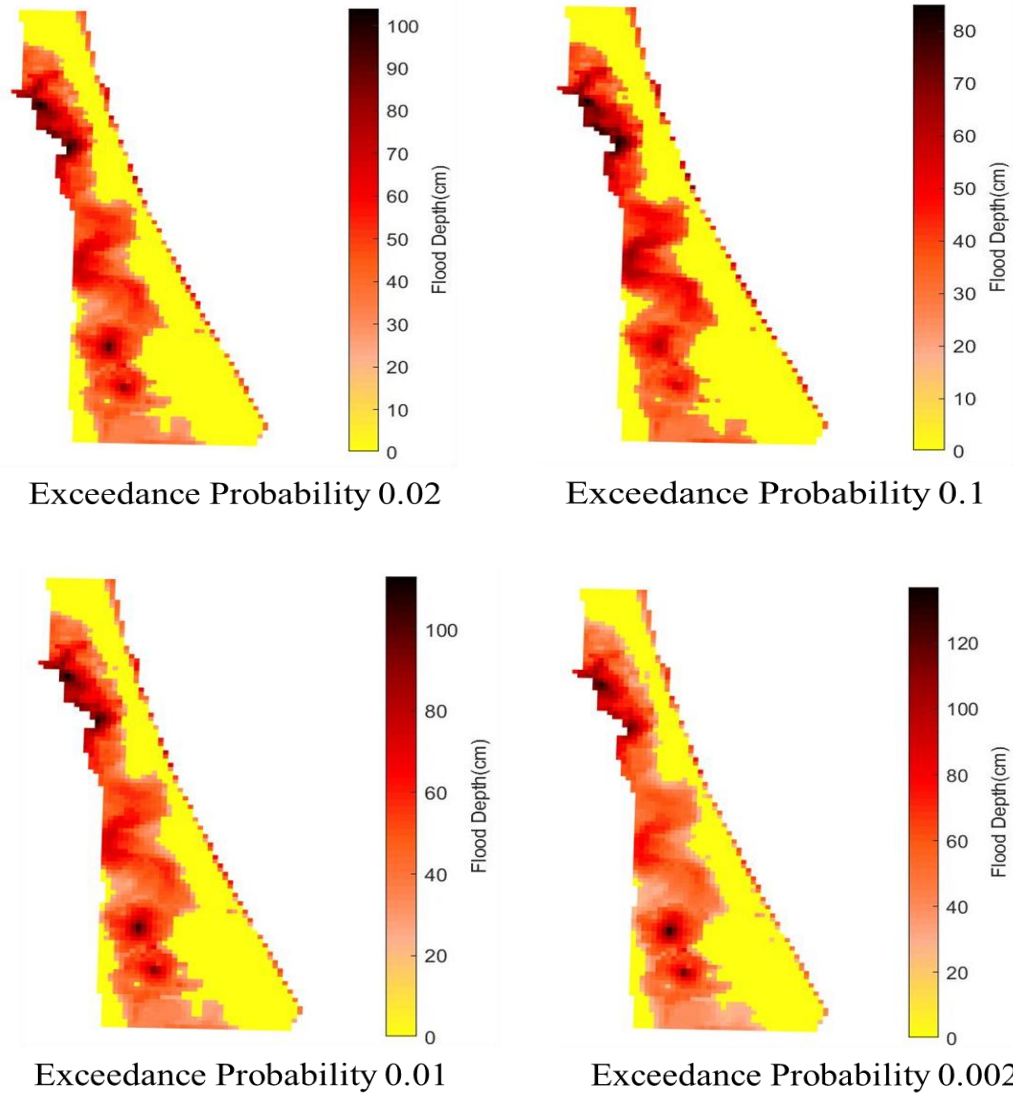


Figure 111. Flood maps for East Florida Region (Brevard County) corresponding to 0.1, 0.02, 0.01, and 0.002 annual exceedance probabilities.

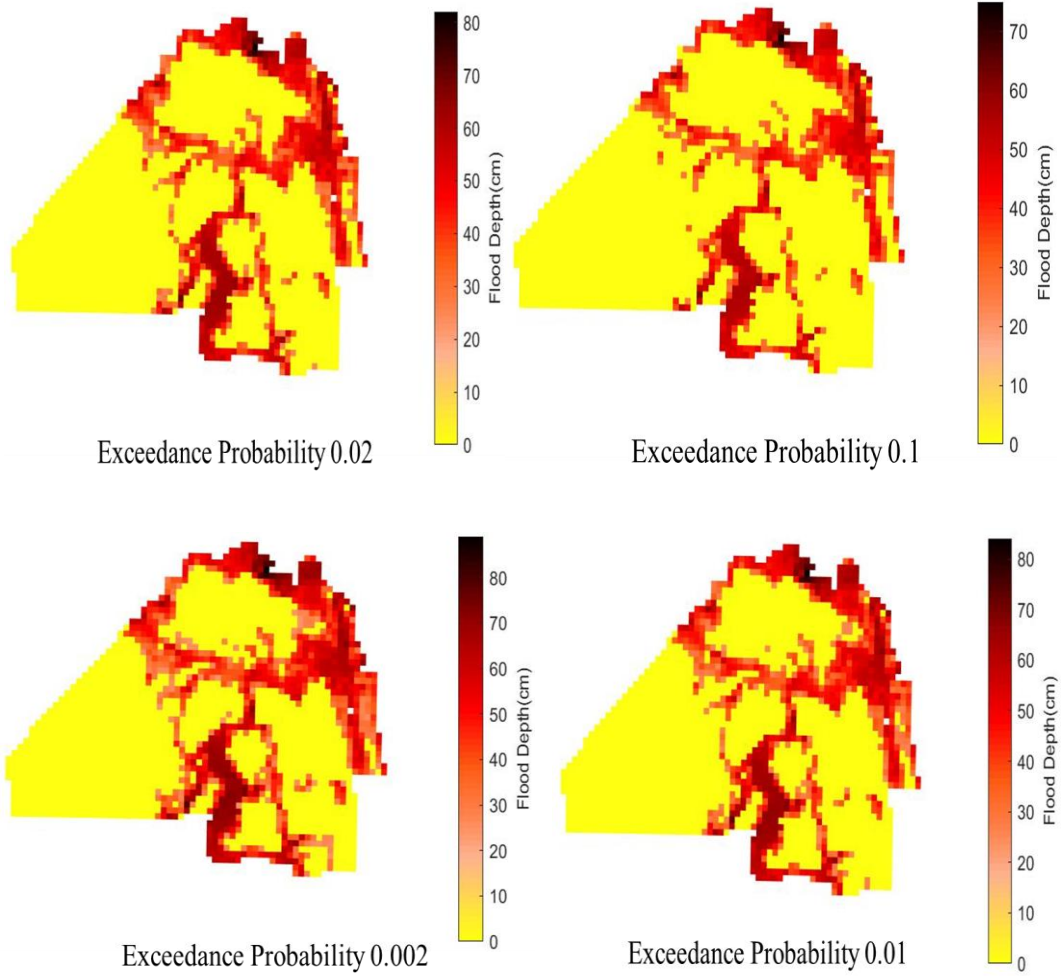


Figure 112. Flood maps for North Florida Region (Duval County) corresponding to 0.1, 0.02, 0.01, and 0.002 annual exceedance probabilities.

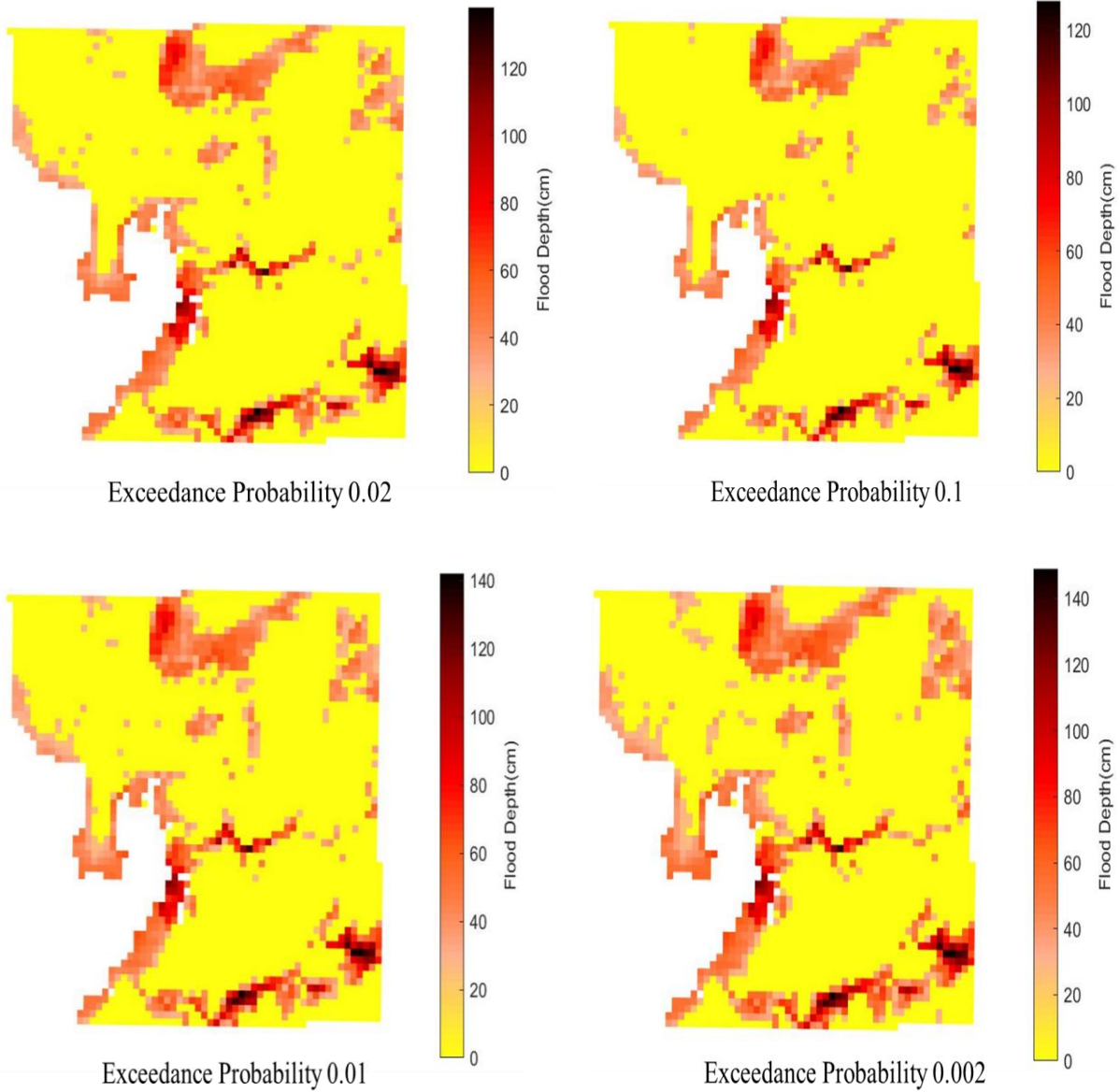


Figure 113. Flood maps for Southwest Florida Region (Hillsborough County) corresponding to 0.1, 0.02, 0.01, and 0.002 annual exceedance probabilities.

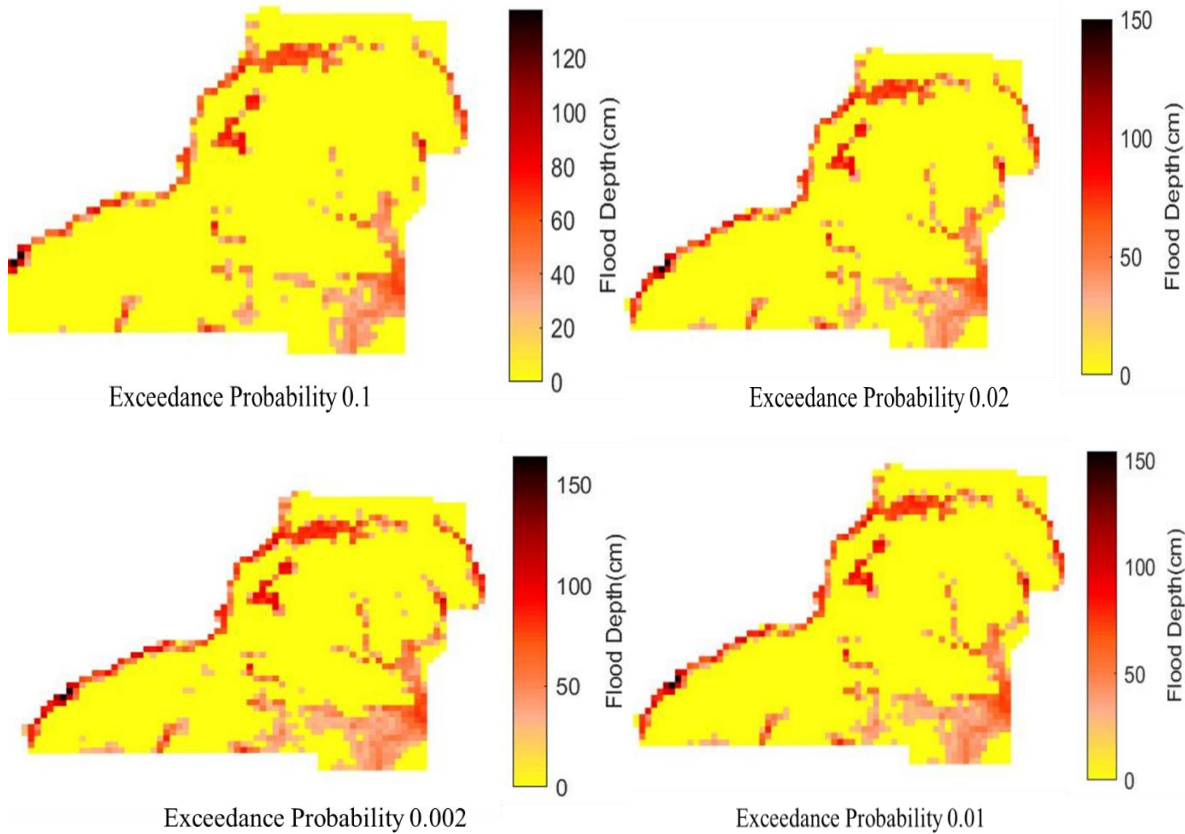


Figure 114. Flood maps for Panhandle Region (Leon County) corresponding to 0.1, 0.02, 0.01, and 0.002 annual exceedance probabilities.

2. Graphs and tables, based on the underlying gridded data, showing flood model results at 10 or more locations within the study area and representative of the range of flood conditions in the study area. The following flood characteristics shall be included for the 0.1 0.02, 0.01, and 0.002 annual exceedance probabilities:

- a. Flood elevations,

Flood elevations based on the underlying gridded data are tabulated in Table 48:

Region	Longitude	Latitude	Flood Elevations (m NAVD 1988) for Exceedance Probability 0.1	Flood Elevations (m NAVD 1988) for Exceedance Probability 0.02	Flood Elevations (m NAVD 1988) for Exceedance Probability 0.01	Flood Elevations (m NAVD 1988) for Exceedance Probability 0.002
Southeast Florida	-80.357	26.045	2.077	2.080	2.082	2.085
Southeast Florida	-80.079	26.253	1.679	1.705	1.714	1.730
East Florida	-80.822	28.636	2.357	2.410	2.430	2.473
East Florida	-80.936	28.584	1.866	2.059	2.146	2.336

North Florida	-81.753	30.194	5.211	5.290	5.320	5.381
North Florida	-81.590	30.552	1.386	1.453	1.481	1.532
Southwest Florida	-82.408	27.654	4.704	4.783	4.811	4.869
Southwest Florida	-82.082	27.731	24.166	24.266	24.304	24.382
Panhandle	-84.189	30.328	7.915	7.968	7.990	8.030
Panhandle	-84.658	30.381	15.178	15.305	15.346	15.437

Table 48. Flood elevations from underlying grids within each region.

b. Flood depths,
Flood depths based on the underlying gridded data are tabulated in Table 49:

Region	Longitude	Latitude	Flood Depths (cm) for Exceedance Probability 0.1	Flood Depths (cm) for Exceedance Probability 0.02	Flood Depths (cm) for Exceedance Probability 0.01	Flood Depths (cm) for Exceedance Probability 0.002
Southeast Florida	-80.357	26.045	24.607	24.895	25.028	25.349
Southeast Florida	-80.079	26.253	49.696	52.332	53.177	54.809
East Florida	-80.822	28.636	24.610	29.849	31.868	36.184
East Florida	-80.936	28.584	84.662	103.977	112.660	131.689
North Florida	-81.753	30.194	24.676	32.612	35.625	41.683
North Florida	-81.590	30.552	74.285	81.051	83.811	88.894
Southwest Florida	-82.408	27.654	24.608	32.439	35.270	41.034
Southwest Florida	-82.082	27.731	127.369	137.358	141.154	148.938
Panhandle	-84.189	30.328	24.591	29.878	32.071	35.992
Panhandle	-84.658	30.381	137.149	149.921	153.997	163.080

Table 49. Flood depths from underlying grids within each region.

- c. If the flood vulnerability model requires explicit representation of flood-induced erosion effects, the erosion depth (original ground elevation minus eroded ground elevation),

The flood vulnerability model requires only flood depth information at the policy locations, therefore, flood induced erosion was not considered in inland flood modeling.

- d. If the flood vulnerability model requires explicit representation of flow velocity effects, the flow and flow velocities, and

The flood vulnerability model requires only flood depth information at the policy locations, therefore, flood velocities were not used in the estimation of flood damage.

- e. If the flood vulnerability model requires explicit representation of flood inundation duration effects, the duration of flood inundation.

Flood vulnerability model takes flood depths only into account to compute inland flood damage.

State of Florida By Region



Figure 115. State of Florida By Region.

Form SF-1: Distributions of Stochastic Flood Parameters (Coastal, Inland)

Please note that this form gives the distribution of the stochastic wind parameters as the model for flooding and surge is deterministic.

Stochastic Flood Parameter (Function or Variable)	Classification: Coastal or Inland	Functional Form of Distribution	Data Source	Year Range Used	Justification for Functional Form
Holland B Error term	Both	Normal	Willoughby and Rahn (2004)	1977-2000	The Gaussian Distribution provided a good fit for the error term. See Standard S-1, Disclosure 1.
Rmax	Both	Gamma	Ho et al. (1987) , supplemented by the extended best track data of DeMaria (Penington 2000), NOAA HRD research flight data, and NOAA-HRD H*Wind analyses (Powell et al. 1996, 1998).	1901-2012	Rmax is skewed, nonnegative and does not have a long tail. So the gamma distribution was tried and found to be a good fit. We limit the range of Rmax to the interval (4, 120). See Standard S-1, Disclosure 1.
Pressure decay Term	Both	Normal	Vickery (2005)	1979-1996	From Vickery (2005)
Storm initial location perturbation	Both	Uniform	N/A	N/A	Plausible variations in initial storm locations are assumed to be uniform
Storm initial motion perturbation	Both	Uniform	N/A	N/A	Plausible variations in initial storm motion are assumed to be uniform
Storm change in motion and intensity distributions	Both	Empirical	HURDAT	1900-2017	Sampling from historical data See Standard G-1, Disclosure 2 for details

Form SF-2: Examples of Flood Loss Exceedance Estimates (Coastal and Inland Combined)

- A. Provide estimates of the annual aggregate personal residential insured flood losses for various probability levels using a modeling-organization-specified, predetermined, and comprehensive exposure dataset justified by the modeling organization. Provide the total average annual flood loss for the loss exceedance distribution. If the modeling methodology does not allow the flood model to produce a viable answer for certain return periods, state so and why.
- B. Include Form SF-2, Examples of Flood Loss Exceedance Estimates (Coastal and Inland Combined), in a submission appendix.

Part A

Return Period (Years)	Annual Probability of Exceedance	Estimated Flood Loss Modeling Organization Exposure Dataset
Top Event	N/A	<u>\$23,111,003,598</u>
10,000	0.0001	<u>\$12,919,512,938</u>
5,000	0.0002	<u>\$10,584,208,352</u>
2,000	0.0005	<u>\$8,230,378,121</u>
1,000	0.0010	<u>\$6,231,934,694</u>
500	0.0020	<u>\$4,675,158,380</u>
250	0.0040	<u>\$3,369,852,487</u>
100	0.0100	<u>\$1,946,091,874</u>
50	0.0200	<u>\$1,316,941,577</u>
20	0.0500	<u>\$790,411,775</u>
10	0.1000	<u>\$535,246,191</u>
5	0.2000	<u>\$283,298,648</u>

Part B

Mean (Total Average Annual Flood Loss)	<u>\$199,711,005</u>
Median	<u>\$21,950,480</u>
Standard Deviation	<u>\$500,898,705</u>
Interquartile Range	<u>\$226,891,014</u>
Sample Size	<u>50000</u>

Form VF-1: Coastal Flood with Damaging Wave Action

- A. Sample personal residential exposure data for 8 reference structures as defined below and 26 flood depths (0-25 feet at 1-foot increments) are provided in the file named “VFEventFormsInput17.xlsx.”

Model the sample personal residential exposure data provided in the file versus the flood depths, and provide the damage ratios summarized by flood depth and construction type. Estimated Damage for each individual flood depth is the sum of ground up loss to all reference structures in the flood depth range, excluding demand surge.

Personal residential contents, appurtenant structures, or time element coverages are not included.

Reference Structures

Wood Frame	Masonry	Manufactured Home
#1 One story Crawlspace foundation Top of foundation wall 3 feet above grade	#4 One story Slab foundation Top of slab 1 foot above grade Unreinforced masonry exterior walls	#7 Manufactured post 1994 Dry stack concrete foundation Pier height 3 feet above grade Tie downs Single unit
#2 Two story Slab foundation Top of slab 1 foot above grade 5/8” diameter anchors at 48” centers for wall/slab connections	#5 Two story Slab foundation Top of slab 1 foot above grade Reinforced masonry exterior walls	#8 Manufactured post 1994 Reinforced masonry pier foundation Pier height 6 feet above grade Tie downs Single unit
#3 Two story Timber pile foundation Top of pile 8 feet above grade Wood floor system bolted to piles	#6 Two story Concrete pile foundation Concrete slab Top of pile 8 feet above grade Reinforced masonry exterior walls	

- B. Confirm that the structures used in completing the form are identical to those in the above table for the reference structures.

The modelers do confirm that the structures used in completing the form are identical to those in the table provided.

- C. If additional assumptions are necessary to complete this form, provide the rationale for the assumptions as well as a description of how they are included.

The form was filled for the case of coastal flood with severe waves.

- D. Provide a plot of the flood depth versus estimated damage/subject exposure data.

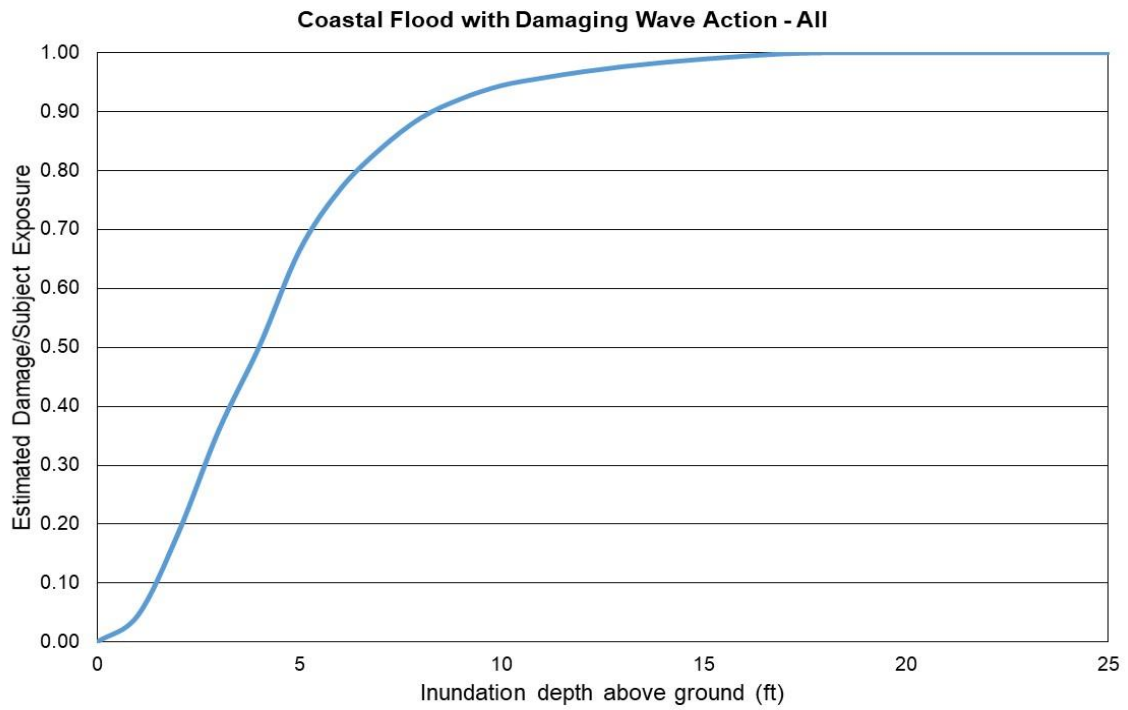


Figure 116. Coastal flood estimated damage vs inundation depth. All reference structures combined.

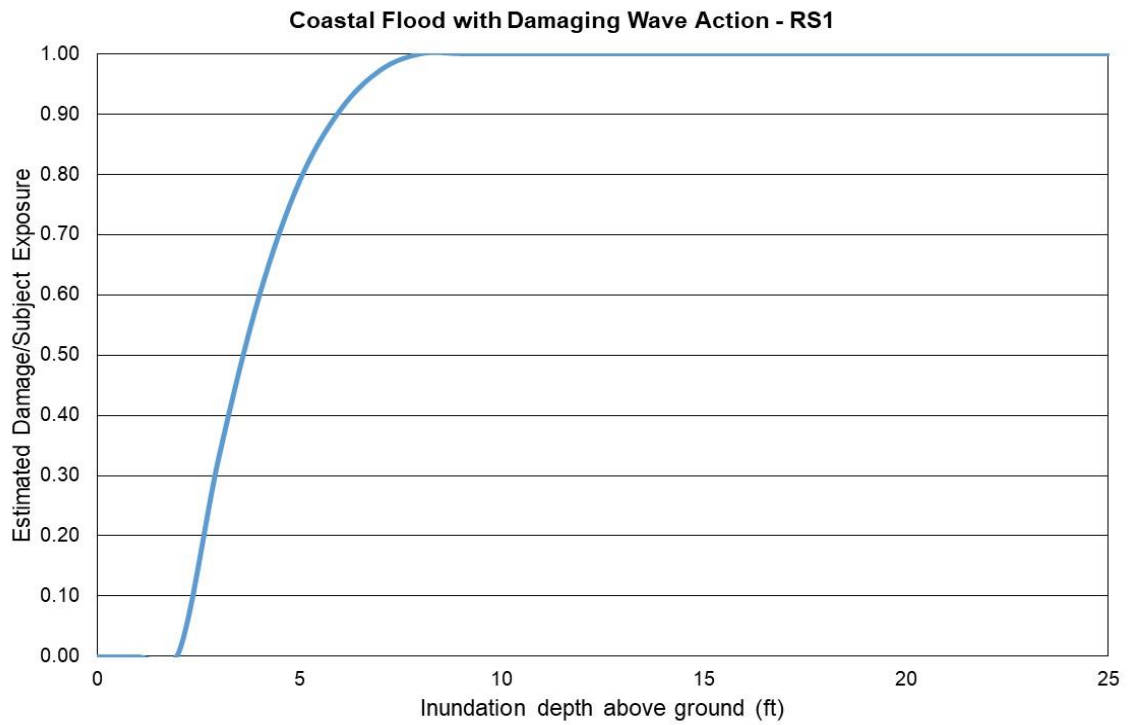


Figure 117. Coastal flood estimated damage vs inundation depth, Reference Structure 1.

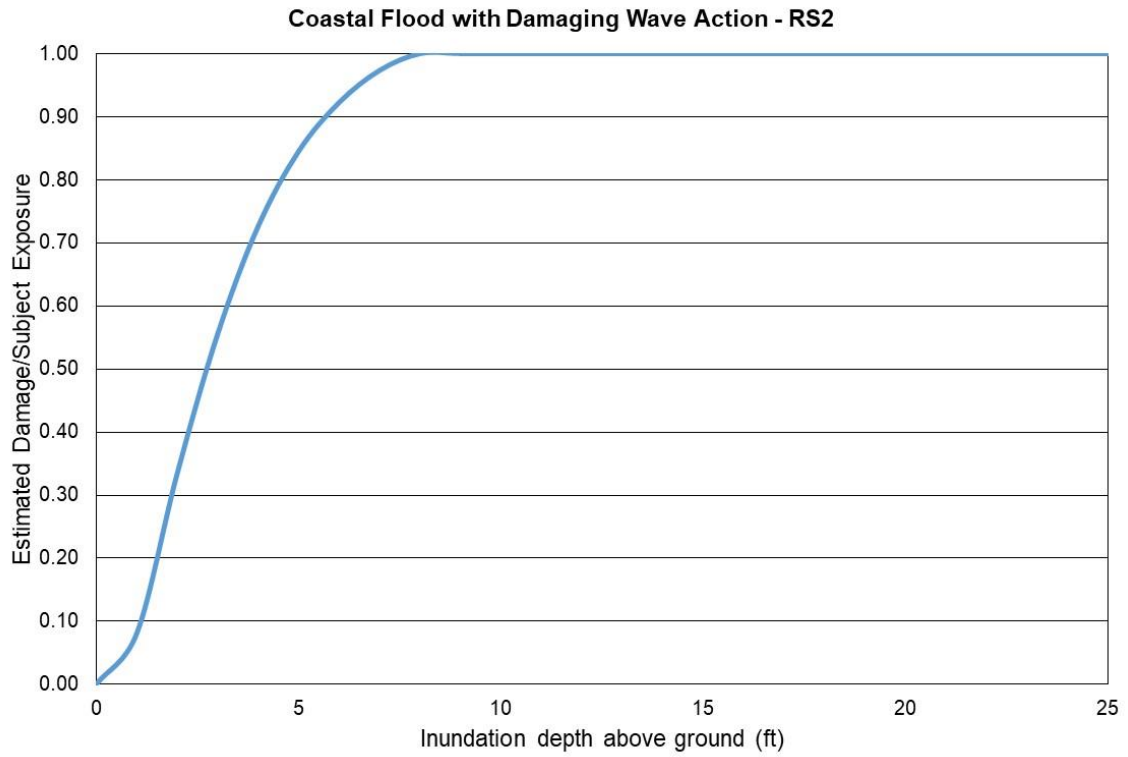


Figure 118. Coastal flood estimated damage vs inundation depth, Reference Structure 2.

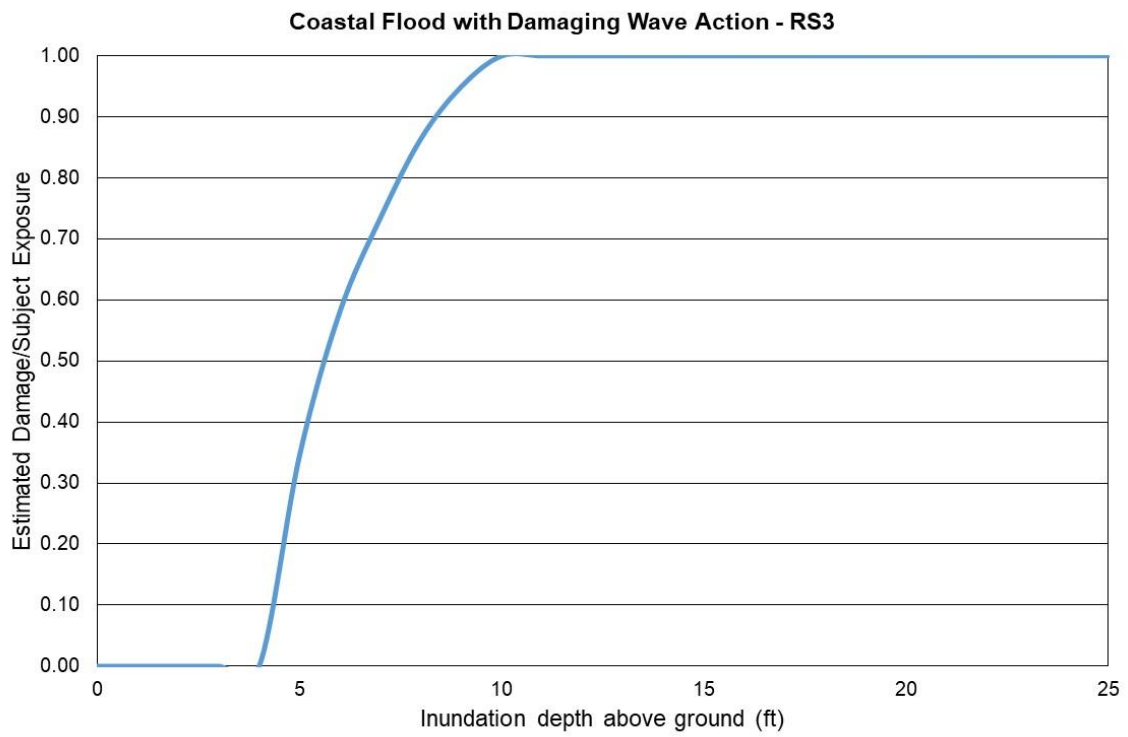


Figure 119. Coastal flood estimated damage vs inundation depth, Reference Structure 3.

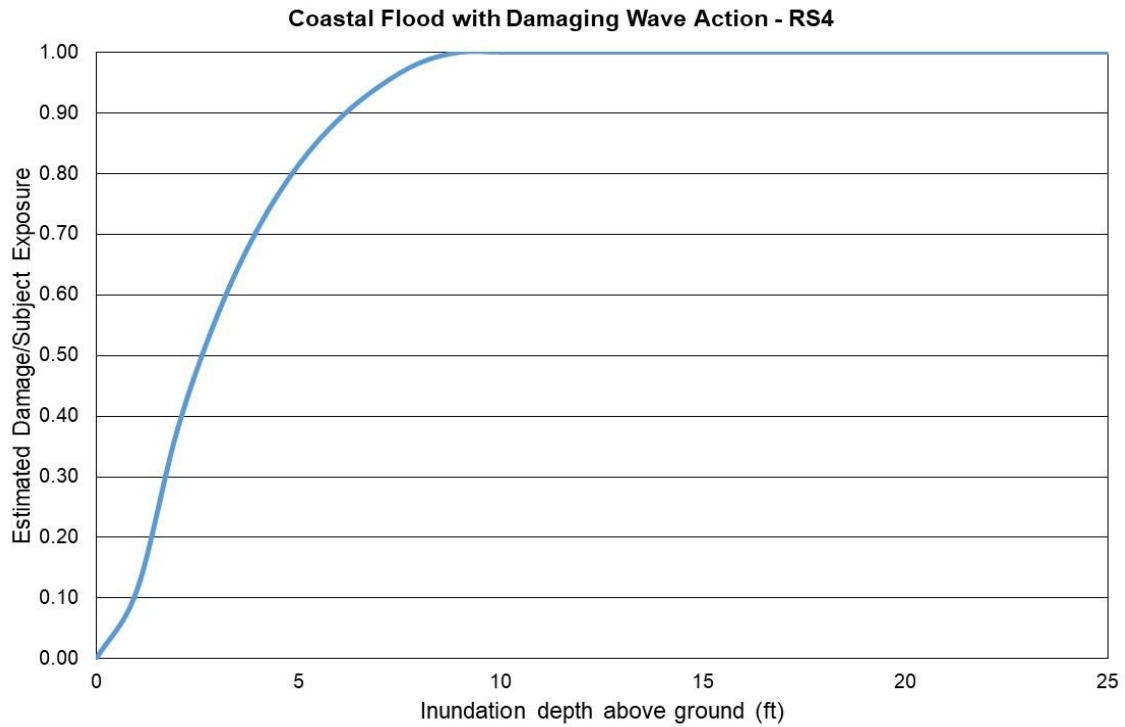


Figure 120. Coastal flood estimated damage vs inundation depth, Reference Structure 4.

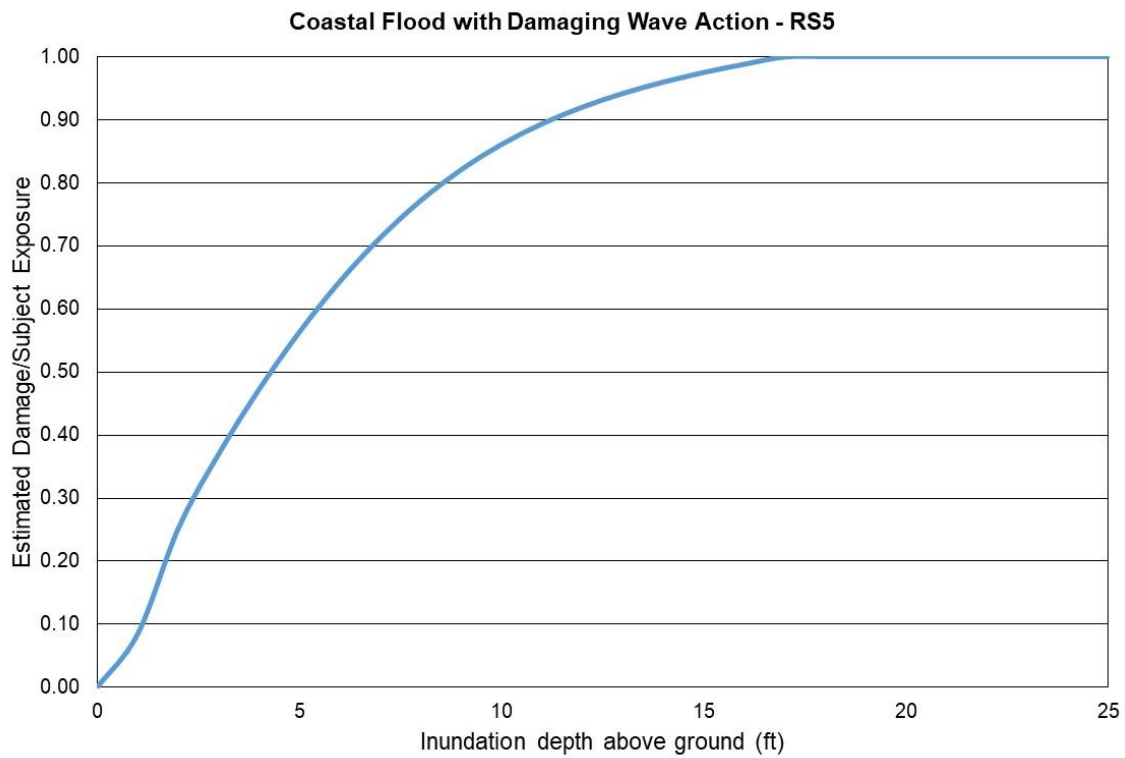


Figure 121. Coastal flood estimated damage vs inundation depth, Reference Structure 5.

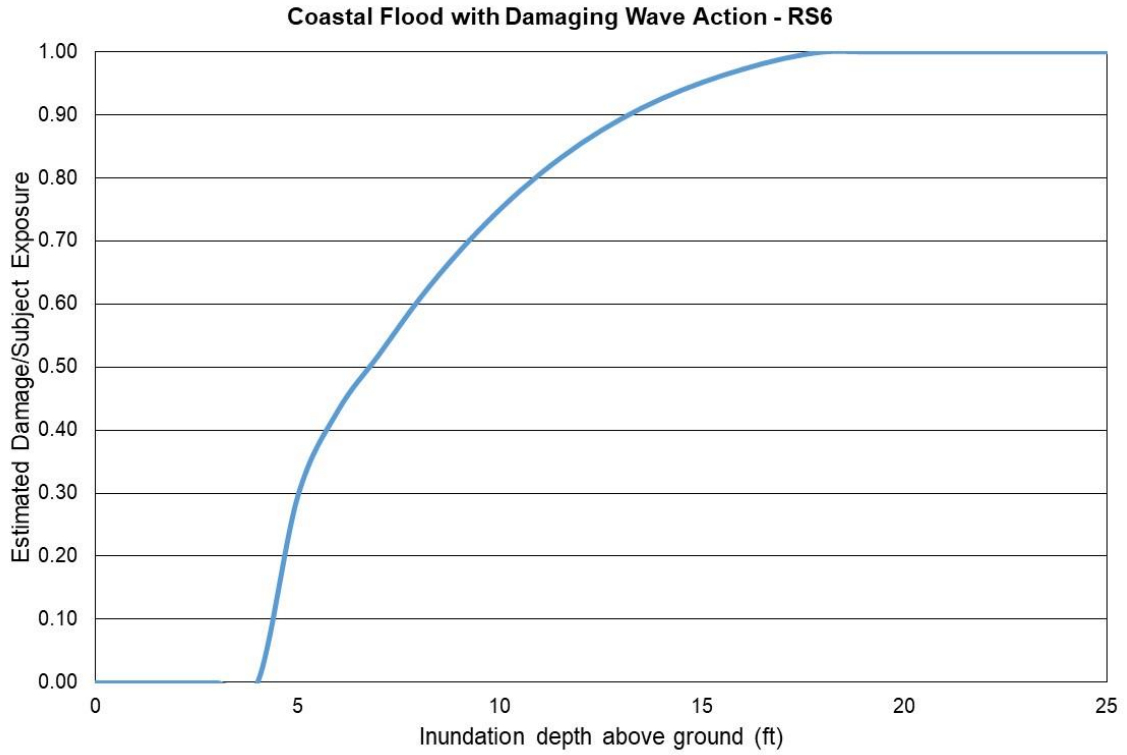


Figure 122. Coastal flood estimated damage vs inundation depth, Reference Structure 6.

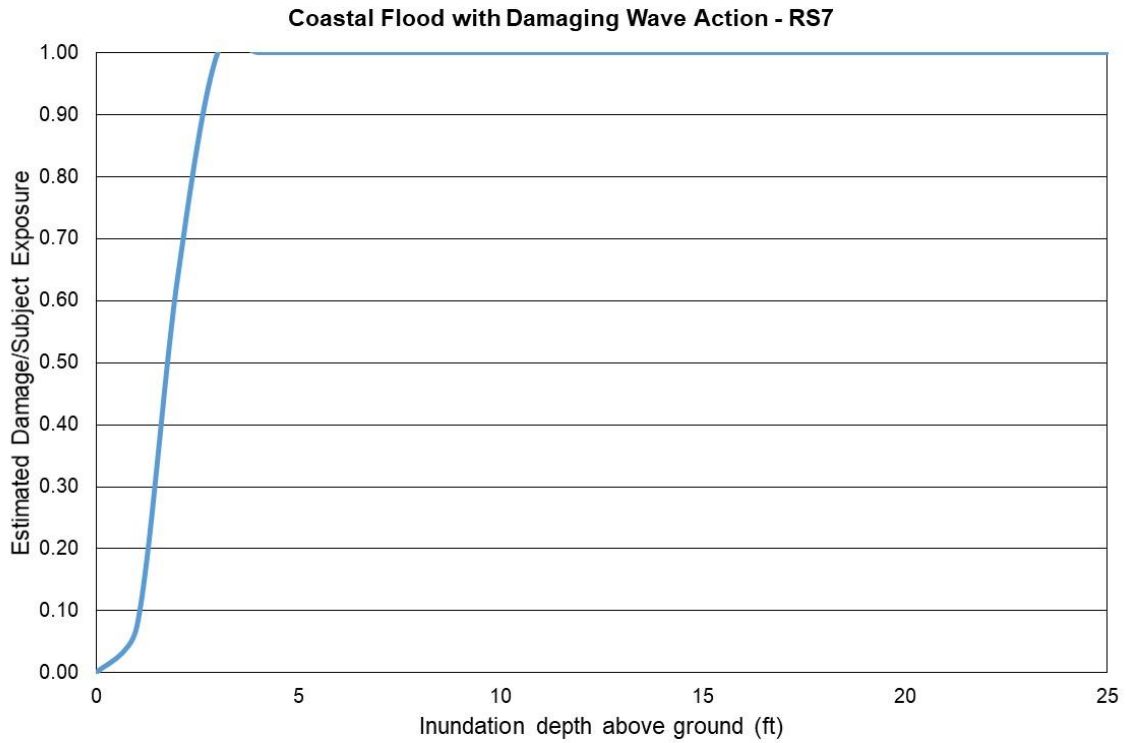


Figure 123. Coastal flood estimated damage vs inundation depth, Reference Structure 7.

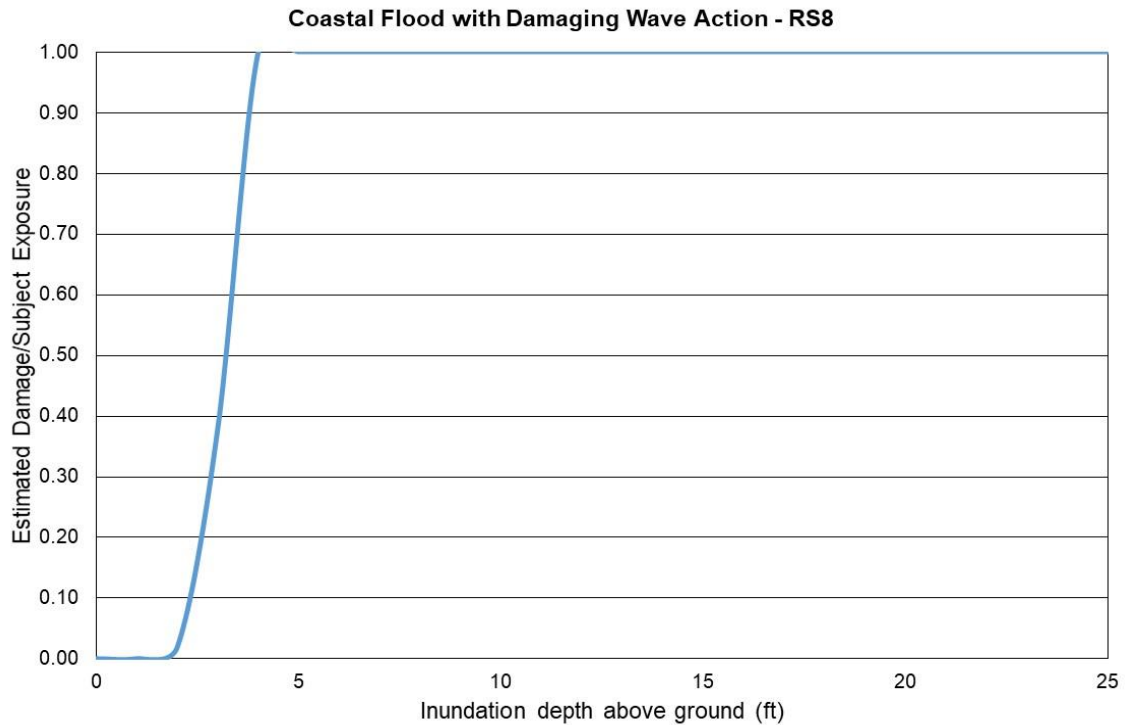


Figure 124. Coastal flood estimated damage vs inundation depth, Reference Structure 8.

E. Include Form VF-1, Coastal Flood with Damaging Wave Action, in a submission appendix.

Form VF-1: Coastal Flood with Damaging Wave Action

All reference structures combined

<u>Flood Depth (Feet) Above Ground Level</u>	<u>Estimated Damage/ Subject Exposure</u>
0	0.00
1	0.04
2	0.18
3	0.36
4	0.50
5	0.66
6	0.77
7	0.84
8	0.89

9	0.92
10	0.94
11	0.96
12	0.97
13	0.98
14	0.98
15	0.99
16	0.99
17	1.00
18	1.00
19	1.00
20	1.00
21	1.00
22	1.00
23	1.00
24	1.00
25	1.00

Reference structure 1

Flood Depth (Feet) Above Ground Level	Estimated Damage/ Subject Exposure
0	0.00
1	0.00
2	0.01
3	0.33
4	0.60
5	0.79
6	0.91
7	0.97
8	1.00
9	1.00

10	1.00
11	1.00
12	1.00
13	1.00
14	1.00
15	1.00
16	1.00
17	1.00
18	1.00
19	1.00
20	1.00
21	1.00
22	1.00
23	1.00
24	1.00
25	1.00

Reference structure 2

Flood Depth (Feet) Above Ground Level	Estimated Damage/ Subject Exposure
0	0.00
1	0.08
2	0.33
3	0.56
4	0.73
5	0.85
6	0.92
7	0.97
8	1.00
9	1.00
10	1.00
11	1.00

12	1.00
13	1.00
14	1.00
15	1.00
16	1.00
17	1.00
18	1.00
19	1.00
20	1.00
21	1.00
22	1.00
23	1.00
24	1.00
25	1.00

Reference structure 3

Flood Depth (Feet) Above Ground Level	Estimated Damage/ Subject Exposure
0	0.00
1	0.00
2	0.00
3	0.00
4	0.00
5	0.35
6	0.58
7	0.73
8	0.86
9	0.95
10	1.00
11	1.00

12	1.00
13	1.00
14	1.00
15	1.00
16	1.00
17	1.00
18	1.00
19	1.00
20	1.00
21	1.00
22	1.00
23	1.00
24	1.00
25	1.00

Reference structure 4

Flood Depth (Feet) Above Ground Level	Estimated Damage/ Subject Exposure
0	0.00
1	0.11
2	0.38
3	0.57
4	0.71
5	0.81
6	0.89
7	0.94
8	0.98
9	1.00
10	1.00
11	1.00

12	1.00
13	1.00
14	1.00
15	1.00
16	1.00
17	1.00
18	1.00
19	1.00
20	1.00
21	1.00
22	1.00
23	1.00
24	1.00
25	1.00

Reference structure 5

Flood Depth (Feet) Above Ground Level	Estimated Damage/ Subject Exposure
0	0.00
1	0.08
2	0.25
3	0.37
4	0.47
5	0.56
6	0.64
7	0.71
8	0.77
9	0.82
10	0.86
11	0.89

12	0.92
13	0.94
14	0.96
15	0.97
16	0.99
17	1.00
18	1.00
19	1.00
20	1.00
21	1.00
22	1.00
23	1.00
24	1.00
25	1.00

Reference structure 6

Flood Depth (Feet) Above Ground Level	Estimated Damage/ Subject Exposure
0	0.00
1	0.00
2	0.00
3	0.00
4	0.00
5	0.30
6	0.43
7	0.52
8	0.61
9	0.68
10	0.75
11	0.81

12	0.85
13	0.89
14	0.93
15	0.95
16	0.97
17	0.99
18	1.00
19	1.00
20	1.00
21	1.00
22	1.00
23	1.00
24	1.00
25	1.00

Reference structure 7

Flood Depth (Feet) Above Ground Level	Estimated Damage/ Subject Exposure
0	0.00
1	0.07
2	0.63
3	1.00
4	1.00
5	1.00
6	1.00
7	1.00
8	1.00
9	1.00
10	1.00
11	1.00

12	1.00
13	1.00
14	1.00
15	1.00
16	1.00
17	1.00
18	1.00
19	1.00
20	1.00
21	1.00
22	1.00
23	1.00
24	1.00
25	1.00

Reference structure 8

Flood Depth (Feet) Above Ground Level	Estimated Damage/ Subject Exposure
0	0.00
1	0.00
2	0.02
3	0.38
4	1.00
5	1.00
6	1.00
7	1.00
8	1.00
9	1.00
10	1.00
11	1.00

12	1.00
13	1.00
14	1.00
15	1.00
16	1.00
17	1.00
18	1.00
19	1.00
20	1.00
21	1.00
22	1.00
23	1.00
24	1.00
25	1.00

Form VF-2: Inland Flood by Flood Depth

- A. Sample personal residential exposure data for 8 reference structures as defined below and 26 flood depths (0-25 feet at 1-foot increments) are provided in the file named “VFEventFormsInput17.xlsx.”

Model the sample personal residential exposure data provided in the file versus the flood depths, and provide the damage ratios summarized by flood depth and construction type. Estimated Damage for each individual flood depth is the sum of ground up loss to all reference structures in the flood depth range, excluding demand surge.

Personal residential contents, appurtenant structures, or time element coverages are not included.

Reference Structures

Wood Frame	Masonry	Manufactured Home
#1 One story Crawlspace foundation Top of foundation wall 3 feet above grade	#4 One story Slab foundation Top of slab 1 foot above grade Unreinforced masonry exterior walls	#7 Manufactured post 1994 Dry stack concrete foundation Pier height 3 feet above grade Tie downs Single unit
#2 Two story Slab foundation Top of slab 1 foot above grade 5/8” diameter anchors at 48” centers for wall/slab connections	#5 Two story Slab foundation Top of slab 1 foot above grade Reinforced masonry exterior walls	#8 Manufactured post 1994 Reinforced masonry pier foundation Pier height 6 feet above grade Tie downs Single unit
#3 Two story Timber pile foundation Top of pile 8 feet above grade Wood floor system bolted to piles	#6 Two story Concrete pile foundation Concrete slab Top of pile 8 feet above grade Reinforced masonry exterior walls	

- B. Confirm that the structures used in completing the form are identical to those in the above table for the reference structures.

The modelers do confirm that the structures used in completing the form are identical to those in the table provided.

- C. If additional assumptions are necessary to complete this form, provide the rationale for the assumptions as well as a description of how they are included.

No assumptions were made filling this form.

- D. Provide a plot of the flood depth versus estimated damage/subject exposure data.

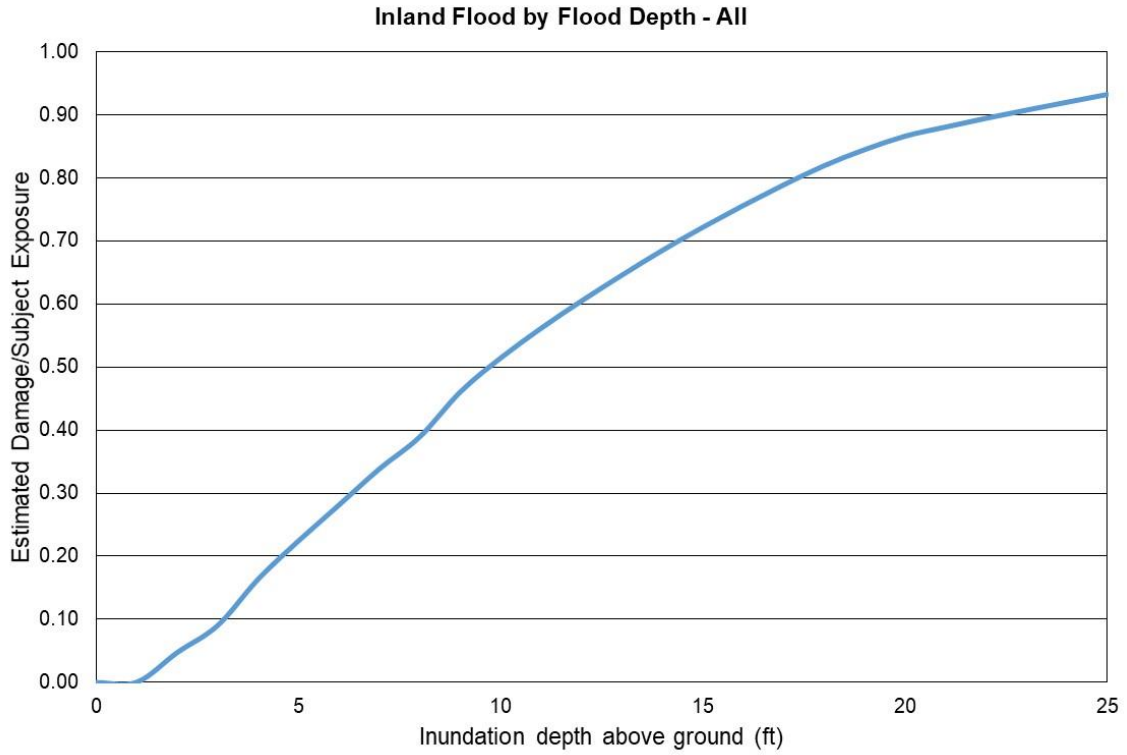


Figure 125. Inland flood estimated damage vs inundation depth – All reference structures combined.

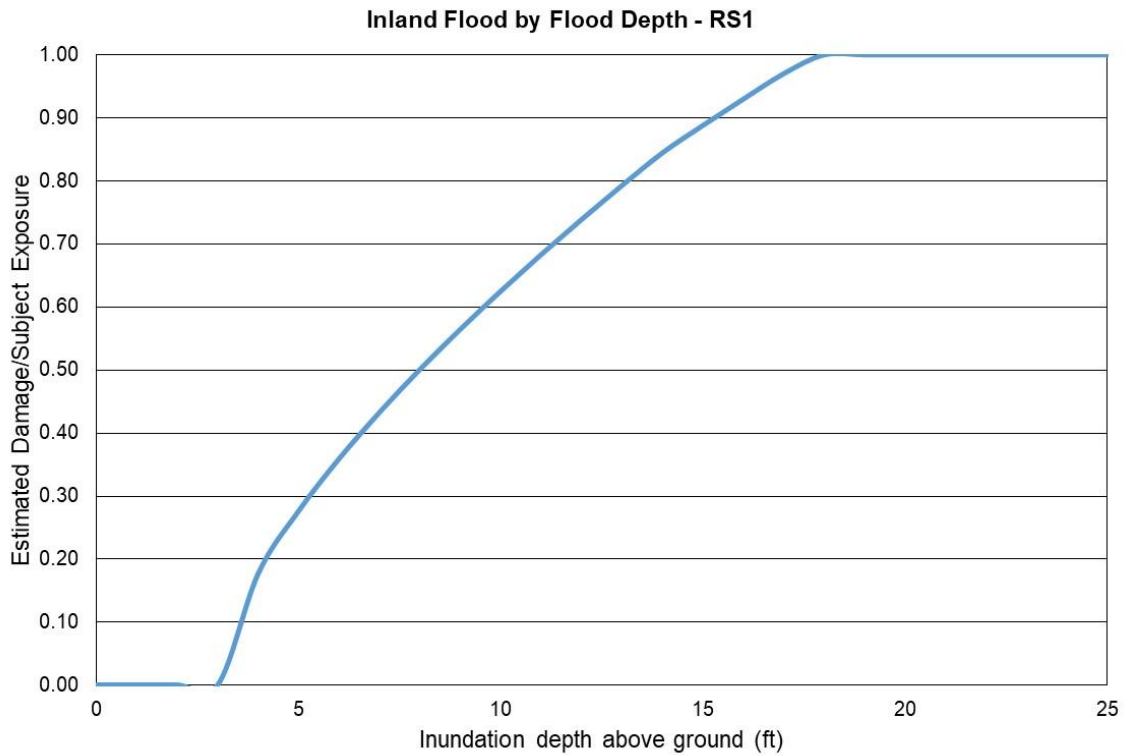


Figure 126. Inland flood estimated damage vs inundation depth, Reference Structure 1.

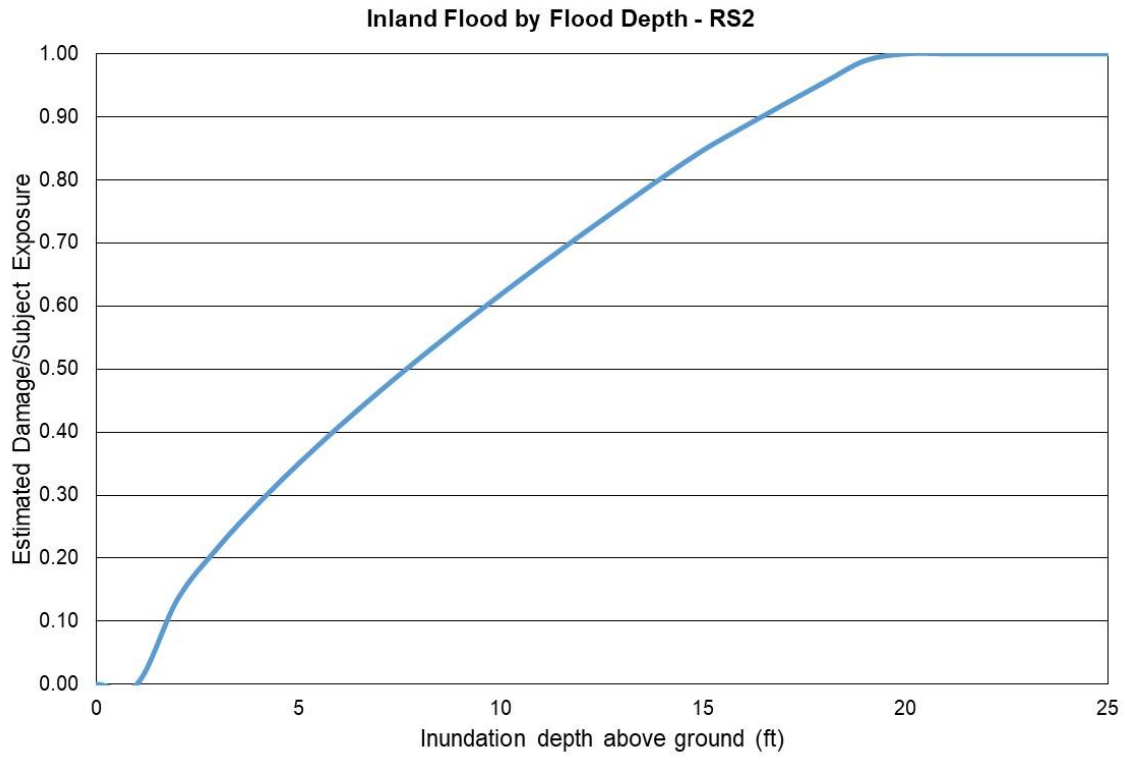


Figure 127. Inland flood estimated damage vs inundation depth, Reference Structure 2.

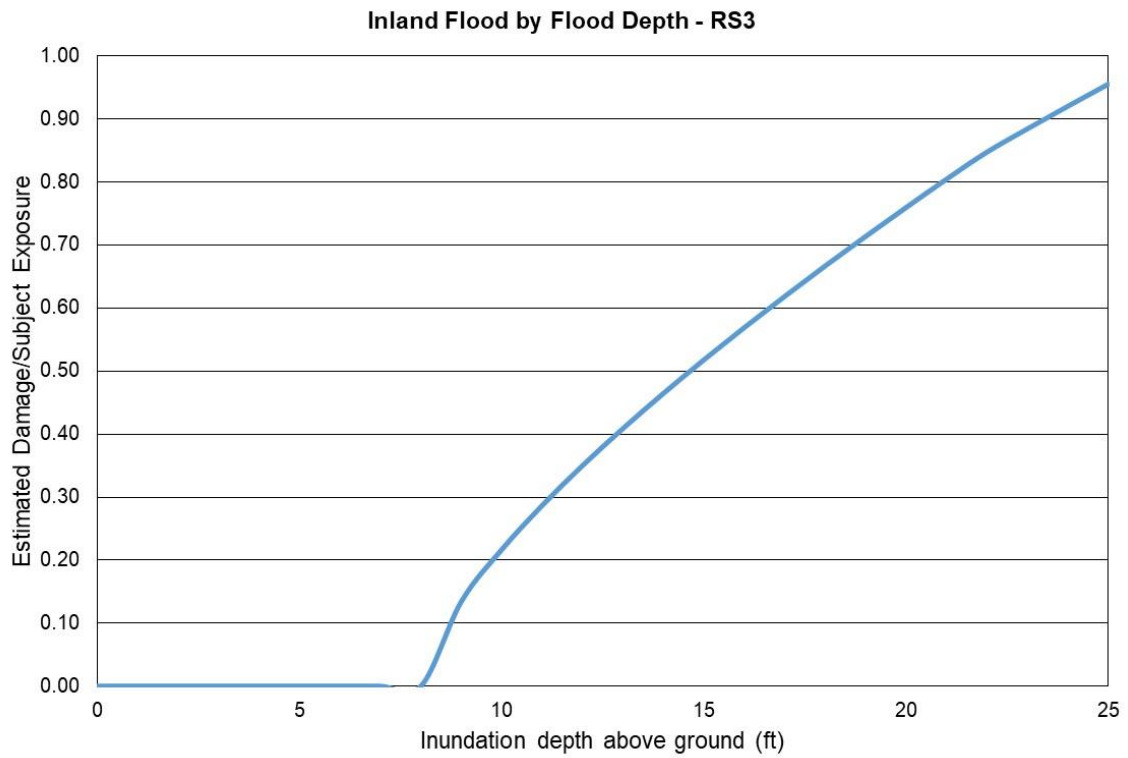


Figure 128. Inland flood estimated damage vs inundation depth, Reference Structure 3.

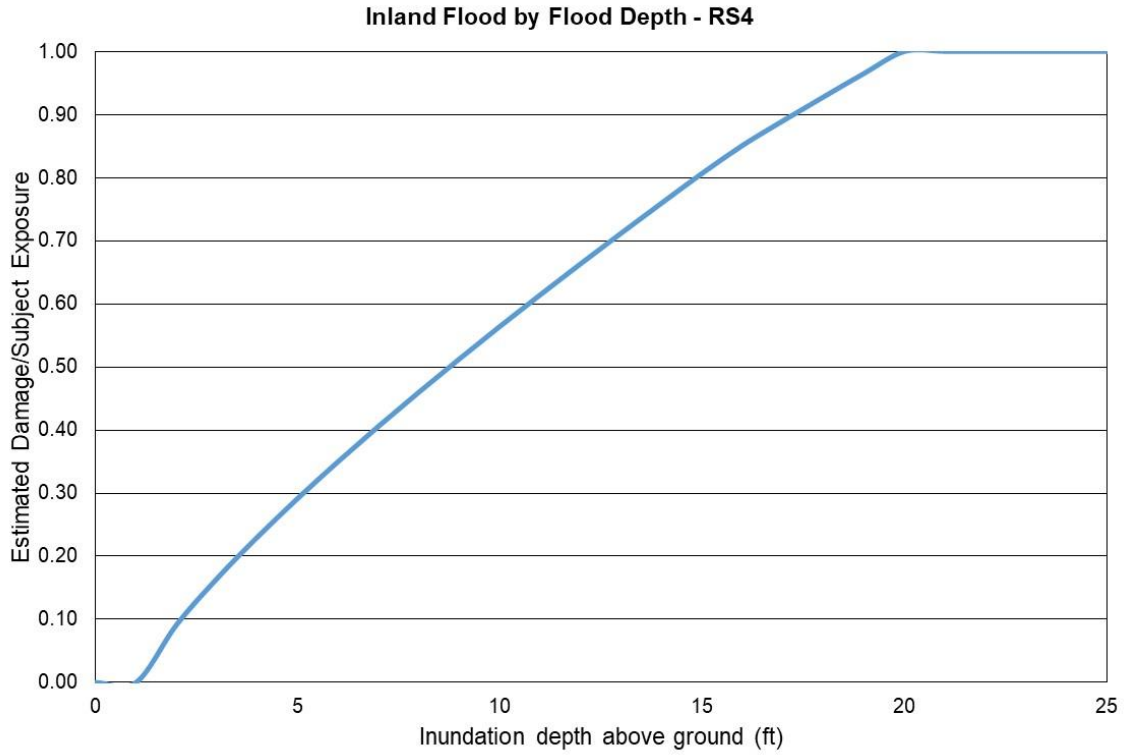


Figure 129. Inland flood estimated damage vs inundation depth, Reference Structure 4.

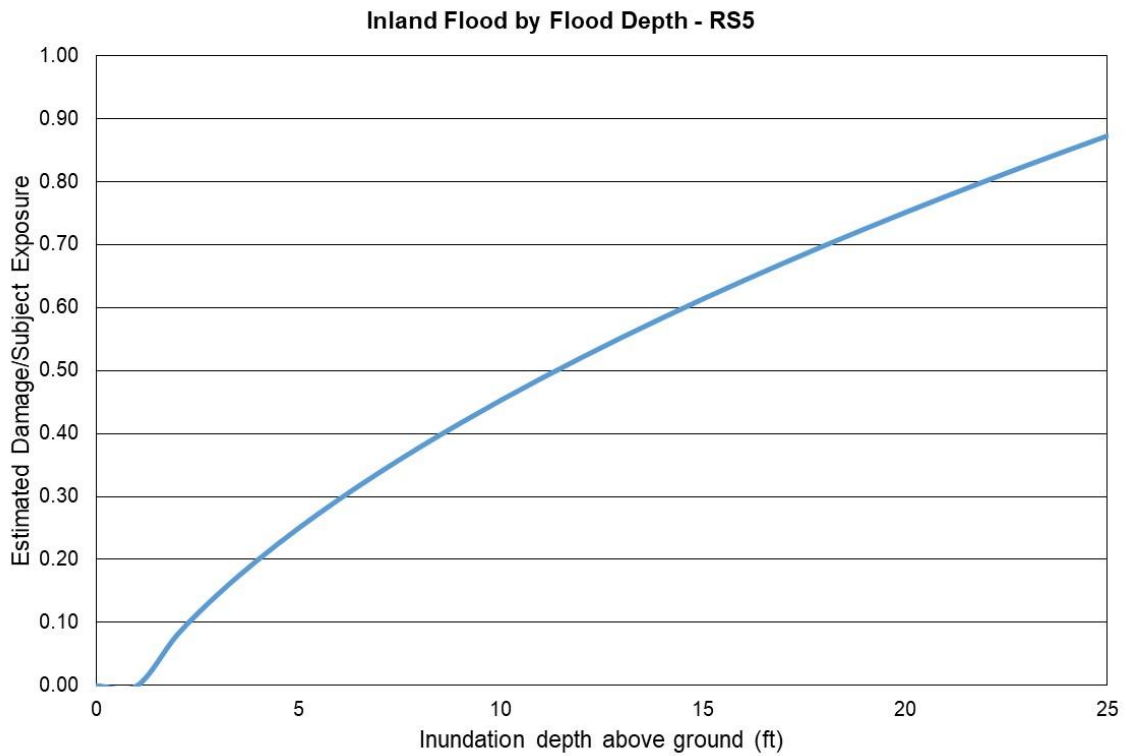


Figure 130. Inland flood estimated damage vs inundation depth, Reference Structure 5.

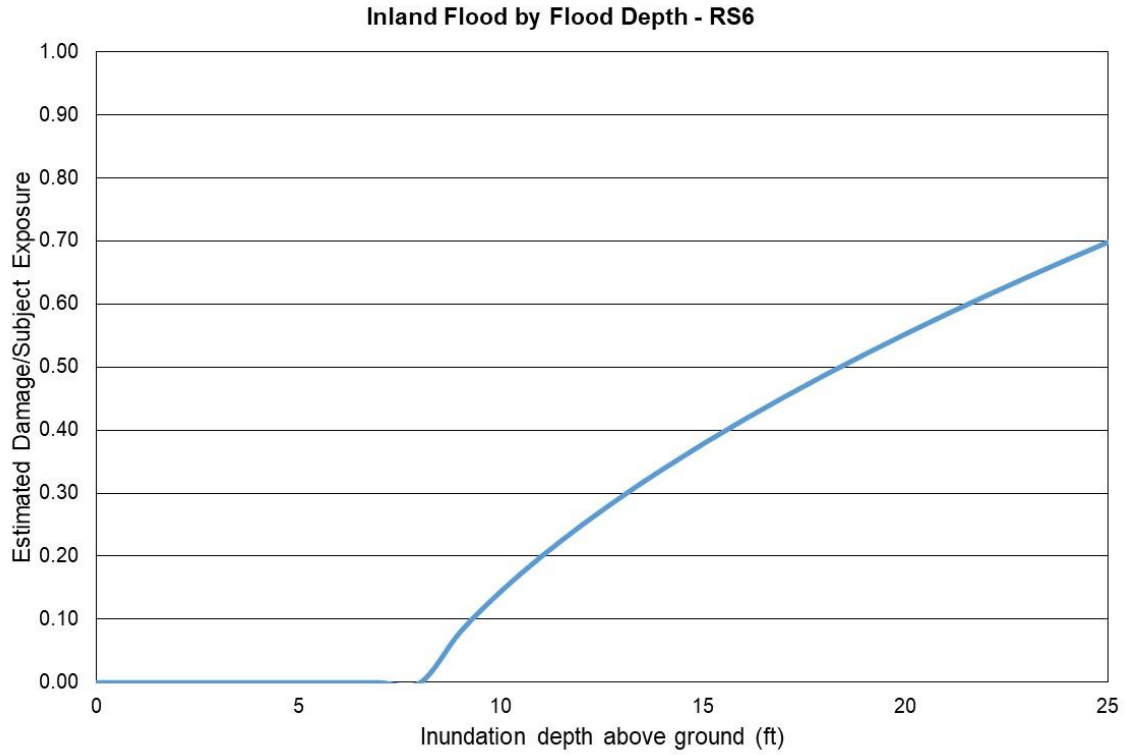


Figure 131. Inland flood estimated damage vs inundation depth, Reference Structure 6.

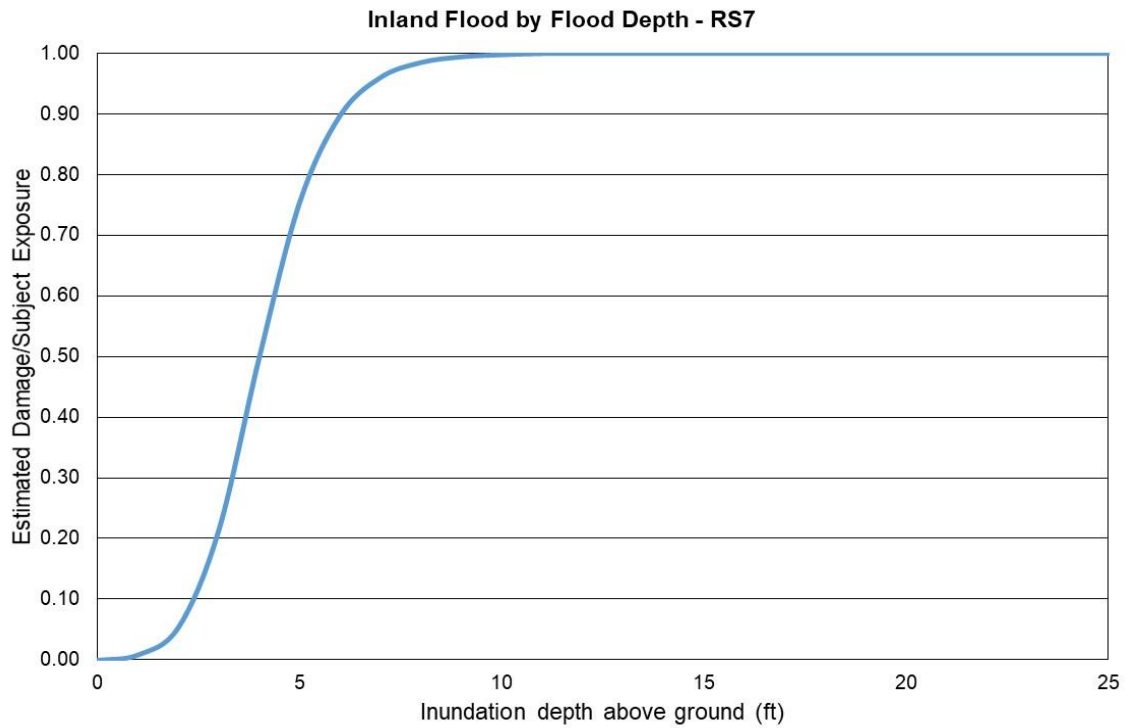


Figure 132. Inland flood estimated damage vs inundation depth, Reference Structure 7.

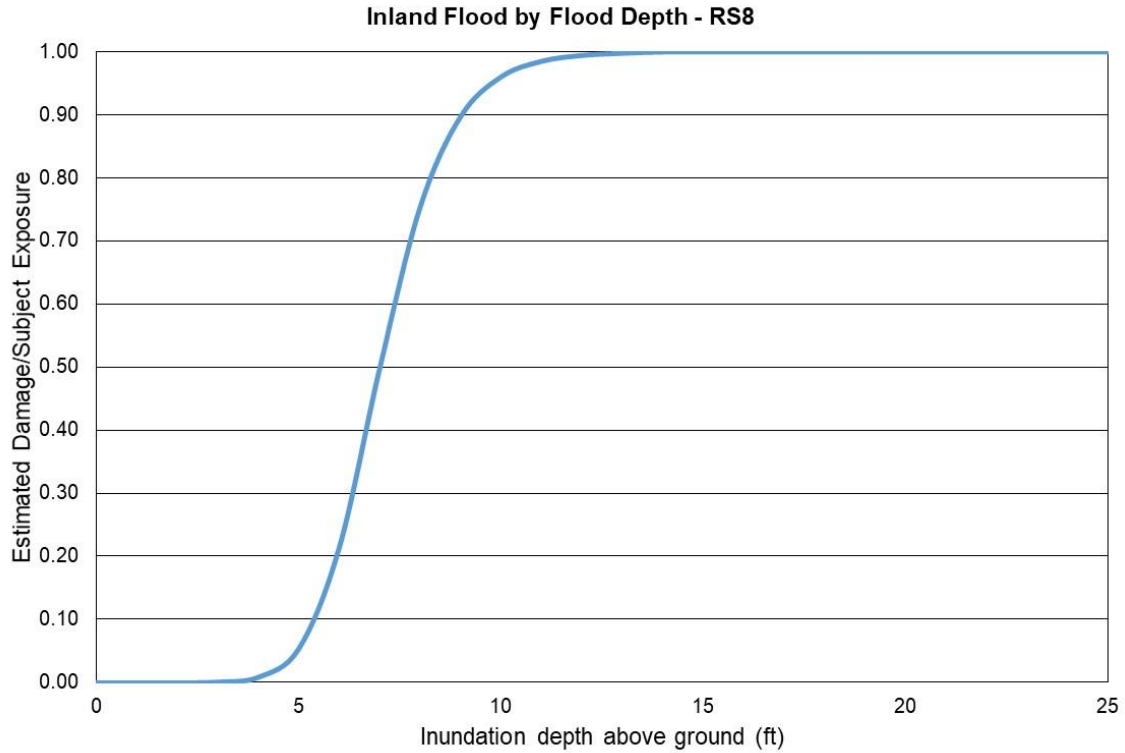


Figure 133. Inland flood estimated damage vs inundation depth, Reference Structure 8.

E. Include Form VF-2, Inland Flood by Flood Depth, in a submission appendix.

Form VF-2: Inland Flood by Flood Depth

All reference structures combined.

<u>Flood Depth (Feet) Above Ground Level</u>	<u>Estimated Damage/ Subject Exposure</u>
0	0.00
1	0.00
2	0.05
3	0.09
4	0.16
5	0.22
6	0.28
7	0.34
8	0.39

9	0.46
10	0.51
11	0.56
12	0.60
13	0.65
14	0.69
15	0.72
16	0.76
17	0.79
18	0.82
19	0.84
20	0.87
21	0.88
22	0.89
23	0.91
24	0.92
25	0.93

Reference structure 1

Flood Depth (Feet) Above Ground Level	Estimated Damage/ Subject Exposure
0	0.00
1	0.00
2	0.00
3	0.00
4	0.18
5	0.28
6	0.36
7	0.43
8	0.50
9	0.56

10	0.62
11	0.68
12	0.74
13	0.79
14	0.84
15	0.89
16	0.93
17	0.97
18	1.00
19	1.00
20	1.00
21	1.00
22	1.00
23	1.00
24	1.00
25	1.00

Reference structure 2

Flood Depth (Feet) Above Ground Level	Estimated Damage/ Subject Exposure
0	0.00
1	0.00
2	0.13
3	0.22
4	0.29
5	0.35
6	0.41
7	0.46
8	0.52
9	0.57
10	0.62

11	0.67
12	0.71
13	0.76
14	0.80
15	0.85
16	0.88
17	0.92
18	0.96
19	0.99
20	1.00
21	1.00
22	1.00
23	1.00
24	1.00
25	1.00

Reference structure 3

Flood Depth (Feet) Above Ground Level	Estimated Damage/ Subject Exposure
0	0.00
1	0.00
2	0.00
3	0.00
4	0.00
5	0.00
6	0.00
7	0.00
8	0.00
9	0.13
10	0.22

11	0.29
12	0.35
13	0.41
14	0.46
15	0.52
16	0.57
17	0.62
18	0.67
19	0.71
20	0.76
21	0.80
22	0.85
23	0.88
24	0.92
25	0.96

Reference structure 4

Flood Depth (Feet) Above Ground Level	Estimated Damage/ Subject Exposure
0	0.00
1	0.00
2	0.09
3	0.16
4	0.23
5	0.29
6	0.35
7	0.41
8	0.46
9	0.51
10	0.56

11	0.61
12	0.66
13	0.71
14	0.76
15	0.81
16	0.85
17	0.89
18	0.93
19	0.97
20	1.00
21	1.00
22	1.00
23	1.00
24	1.00
25	1.00

Reference structure 5

Flood Depth (Feet) Above Ground Level	Estimated Damage/ Subject Exposure
0	0.00
1	0.00
2	0.08
3	0.14
4	0.20
5	0.25
6	0.30
7	0.34
8	0.38
9	0.42
10	0.45

11	0.49
12	0.52
13	0.55
14	0.58
15	0.61
16	0.64
17	0.67
18	0.70
19	0.72
20	0.75
21	0.78
22	0.80
23	0.82
24	0.85
25	0.87

Reference structure 6

Flood Depth (Feet) Above Ground Level	Estimated Damage/ Subject Exposure
0	0.00
1	0.00
2	0.00
3	0.00
4	0.00
5	0.00
6	0.00
7	0.00
8	0.00
9	0.08
10	0.14

11	0.20
12	0.25
13	0.30
14	0.34
15	0.38
16	0.42
17	0.45
18	0.49
19	0.52
20	0.55
21	0.58
22	0.61
23	0.64
24	0.67
25	0.70

Reference structure 7

Flood Depth (Feet) Above Ground Level	Estimated Damage/ Subject Exposure
0	0.00
1	0.01
2	0.05
3	0.21
4	0.50
5	0.75
6	0.90
7	0.96
8	0.99
9	0.99
10	1.00

11	1.00
12	1.00
13	1.00
14	1.00
15	1.00
16	1.00
17	1.00
18	1.00
19	1.00
20	1.00
21	1.00
22	1.00
23	1.00
24	1.00
25	1.00

Reference structure 8

Flood Depth (Feet) Above Ground Level	Estimated Damage/ Subject Exposure
0	0.00
1	0.00
2	0.00
3	0.00
4	0.01
5	0.05
6	0.21
7	0.50
8	0.75
9	0.90
10	0.96

11	0.99
12	0.99
13	1.00
14	1.00
15	1.00
16	1.00
17	1.00
18	1.00
19	1.00
20	1.00
21	1.00
22	1.00
23	1.00
24	1.00
25	1.00

Form VF-3: Flood Mitigation Measures, Range of Changes in Flood Damage

A. Provide the change in the personal residential reference building damage ratio (not loss cost) for each individual flood mitigation measure listed in Form VF-3, Flood Mitigation Measures, Range of Changes in Flood Damage, as well as for the combination of the flood mitigation measures.

See Forms VF-3 below for both coastal and inland flood.

B. If additional assumptions are necessary to complete this form, provide the rationale for the assumptions as well as a detailed description of how they are included.

In the case of coastal flood, we filled the form for the case of coastal flood with severe waves, to ensure maximum differentiation between coastal and inland flood results.

C. Provide this form in Excel format without truncation. The file name shall include the abbreviated name of the modeling organization, the flood standards year, and the form name. Also include Form VF-3, Flood Mitigation Measures, Range of Changes in Flood Damage, in a submission appendix.

Reference Structures

Wood Frame	Masonry
One story Crawlspace foundation Top of foundation wall 3 feet above grade	One story Slab foundation Top of slab 1 foot above grade Unreinforced masonry exterior walls
Two story Timber pile foundation Top of pile 8 feet above grade Wood floor system bolted to piles	

D. Place the reference structures at the following locations, with latitude and longitude referenced to the World Geodetic System of 1984 (WGS84) datum, and provide the aggregated results.

Gulf of Mexico
Latitude: 27.9957517
Longitude: -82.8277373

St. Johns River
Latitude: 29.3768881
Longitude: -81.6190223

E. Provide the ground elevation used from the flood model elevation database for both reference points.

Gulf of Mexico
Latitude: 27.9957517
Longitude: -82.8277373

St. Johns River
Latitude: 29.3768881
Longitude: -81.6190223

Ground elevation: 1.91 m

Ground elevation: 1.65 m

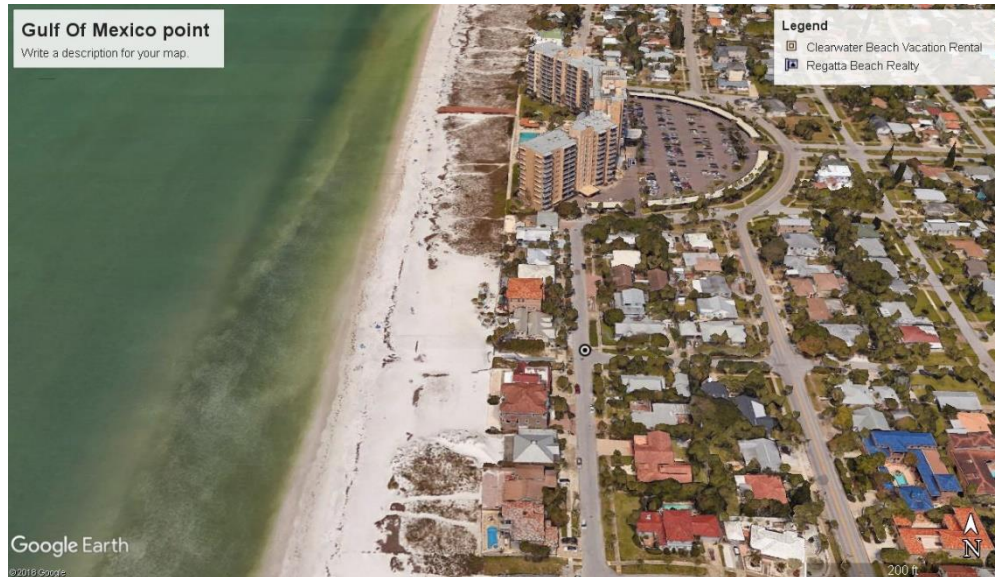


Figure 134. Gulf of Mexico location.

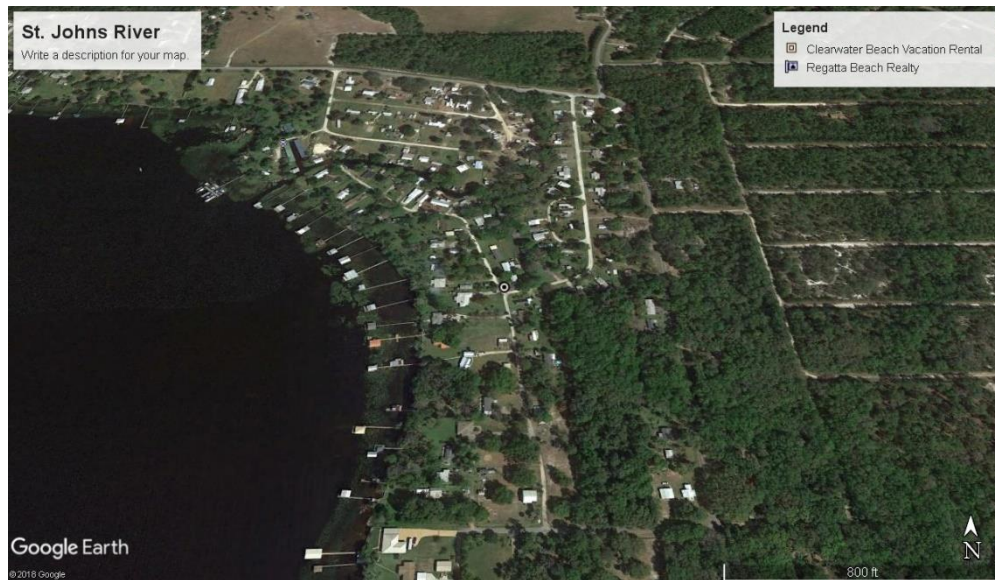


Figure 135. St. Johns River location.

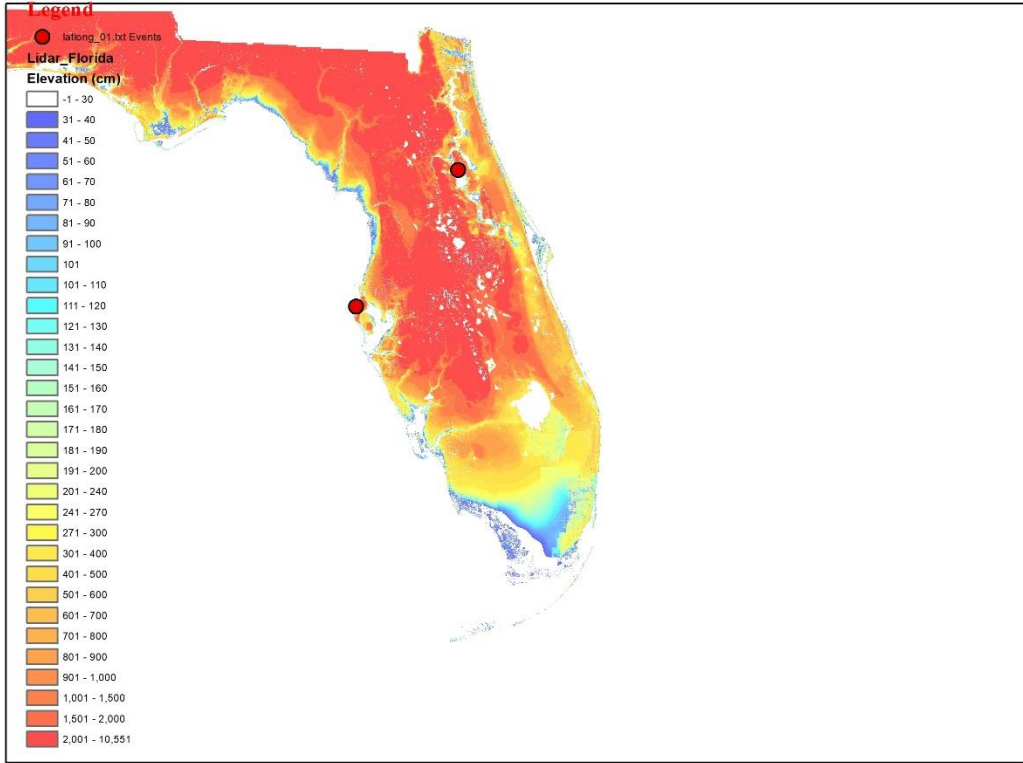


Figure 136. Elevations for the costal and inland locations from a Digital Elevation Map.

COASTAL

INDIVIDUAL FLOOD MITIGATION MEASURES		PERCENTAGE CHANGES IN DAMAGE ((REFERENCE DAMAGE RATIO - MITIGATED DAMAGE RATIO) / REFERENCE DAMAGE RATIO) * 100											
		TWO-STORY WOOD FRAME STRUCTURE					MASONRY STRUCTURE						
		FLOOD DEPTH (FT) ABOVE GROUND					FLOOD DEPTH (FT) ABOVE GROUND						
		7	9	11	13	15	1	3	5	7	9		
	REFERENCE STRUCTURE	—	—	—	—	—	—	—	—	—	—	—	—
ELEVATE STRUCTURE	Elevate Floor 1 Foot	10%	4%	0%	0%	0%	—	—	—	—	—	—	—
	Elevate Floor 2 Feet	23%	10%	0%	0%	0%	—	—	—	—	—	—	—
	Elevate Floor 3 Feet	43%	15%	2%	0%	0%	—	—	—	—	—	—	—
UTILITY EQUIPMENT	Elevate or Protect 1 Foot	8%	0%	0%	0%	0%	24%	0%	0%	0%	0%	0%	0%
	Elevate or Protect 2 Feet	9%	3%	0%	0%	0%	24%	0%	0%	0%	0%	0%	0%
	Elevate or Protect 3 Feet	9%	5%	0%	0%	0%	24%	12%	0%	0%	0%	0%	0%
FLOODPROOFING	Wet 1 Foot	21%	1%	0%	0%	0%	42%	1%	1%	1%	1%	0%	0%
	Wet 2 Feet	28%	8%	0%	0%	0%	42%	1%	1%	1%	1%	0%	0%
	Wet 3 Feet	32%	13%	0%	0%	0%	42%	25%	1%	1%	1%	0%	0%
	Dry 1 Foot	—	—	—	—	—	58%	1%	1%	1%	1%	0%	0%
	Dry 2 Feet	—	—	—	—	—	58%	1%	1%	1%	1%	0%	0%
	Dry 3 Feet	—	—	—	—	—	58%	28%	1%	1%	1%	0%	0%
FLOOD OPENINGS		ONE-STORY WOOD FRAME STRUCTURE											
		FLOOD DEPTH (FT) ABOVE GROUND											
		1	3	5	7	9							
	Flood Openings in Foundation Walls	0%	11%	5%	3%	0%	—	—	—	—	—	—	—
FLOOD MITIGATION MEASURES IN COMBINATION		PERCENTAGE CHANGES IN DAMAGE ((REFERENCE DAMAGE RATIO - MITIGATED DAMAGE RATIO) / REFERENCE DAMAGE RATIO) * 100											
		TWO-STORY WOOD FRAME STRUCTURE					MASONRY STRUCTURE						
		FLOOD DEPTH (FT) ABOVE GROUND					FLOOD DEPTH (FT) ABOVE GROUND						
		7	9	11	13	15	1	3	5	7	9		
Elevate Utility Equipment 2 Feet Above Floor and Wet Floodproof Structure to 2 Feet		30%	9%	0%	0%	0%	59%	1%	1%	1%	1%	0%	0%

INLAND

INDIVIDUAL FLOOD MITIGATION MEASURES		PERCENTAGE CHANGES IN DAMAGE ((REFERENCE DAMAGE RATIO - MITIGATED DAMAGE RATIO) / REFERENCE DAMAGE RATIO) * 100											
		TWO-STORY WOOD FRAME STRUCTURE					MASONRY STRUCTURE						
		FLOOD DEPTH (FT) ABOVE GROUND					FLOOD DEPTH (FT) ABOVE GROUND						
		7	9	11	13	15	1	3	5	7	9		
	REFERENCE STRUCTURE	—	—	—	—	—	—	—	—	—	—	—	—
ELEVATE STRUCTURE	Elevate Floor 1 Foot	0%	100%	24%	14%	10%	—	—	—	—	—	—	
	Elevate Floor 2 Feet	0%	100%	53%	30%	21%	—	—	—	—	—	—	
	Elevate Floor 3 Feet	0%	100%	100%	47%	32%	—	—	—	—	—	—	
UTILITY EQUIPMENT	Elevate or Protect 1 Foot	0%	16%	0%	0%	0%	0%	0%	0%	0%	0%	0%	
	Elevate or Protect 2 Feet	0%	16%	0%	0%	0%	0%	18%	0%	0%	0%	0%	
	Elevate or Protect 3 Feet	0%	16%	16%	0%	0%	0%	18%	0%	0%	0%	0%	
FLOODPROOFING	Wet 1 Foot	0%	45%	0%	0%	0%	0%	0%	0%	0%	0%	0%	
	Wet 2 Feet	0%	45%	0%	0%	0%	0%	38%	0%	0%	0%	0%	
	Wet 3 Feet	0%	45%	45%	0%	0%	0%	38%	0%	0%	0%	0%	
	Dry 1 Foot	—	—	—	—	—	0%	0%	0%	0%	0%	0%	
	Dry 2 Feet	—	—	—	—	—	0%	43%	0%	0%	0%	0%	
	Dry 3 Feet	—	—	—	—	—	0%	43%	0%	0%	0%	0%	
FLOOD OPENINGS		ONE-STORY WOOD FRAME STRUCTURE											
		FLOOD DEPTH (FT) ABOVE GROUND											
		1	3	5	7	9							
	Flood Openings in Foundation Walls	0%	0%	6%	5%	4%	—	—	—	—	—		
FLOOD MITIGATION MEASURES IN COMBINATION		PERCENTAGE CHANGES IN DAMAGE ((REFERENCE DAMAGE RATIO - MITIGATED DAMAGE RATIO) / REFERENCE DAMAGE RATIO) * 100											
		TWO-STORY WOOD FRAME STRUCTURE					MASONRY STRUCTURE						
		FLOOD DEPTH (FT) ABOVE GROUND					FLOOD DEPTH (FT) ABOVE GROUND						
		7	9	11	13	15	1	3	5	7	9		
Elevate Utility Equipment 2 Feet Above Floor and Wet Floodproof Structure to 2 Feet		0%	52%	0%	0%	0%	0%	44%	0%	0%	0%	0%	

Form VF-4: Coastal Flood Mitigation Measures, Mean Coastal Flood Damage Ratios and Coastal Flood Damage/\$1,000 (Trade Secret Item)

A. Provide the mean coastal flood damage ratio (prior to any insurance considerations) to the reference structure for each individual flood mitigation measure listed in Form VF-4, Coastal Flood Mitigation Measures, Mean Coastal Flood Damage Ratios and Coastal Flood Damage/\$1,000 (Trade Secret Item), as well as the percent coastal flood damage for the combination of the flood mitigation measures.

See Form VF-4 below.

B. Provide the coastal flood damage/\$1,000, rounded to three decimal places, for the reference structures and for each individual flood mitigation measure listed in Form VF-4, Coastal Flood Mitigation Measures, Mean Coastal Flood Damage Ratios and Coastal Flood Damage/\$1,000 (Trade Secret Item), as well as the coastal flood damage/\$1,000 for the combination of the flood mitigation measures.

See Form VF-4 below.

C. If additional assumptions are necessary to complete this form, provide the rationale for the assumptions as well as a detailed description of how they are included.

In the case of coastal flood, we filled the form for the case of coastal flood with severe waves, to ensure maximum differentiation between coastal and inland flood results.

D. Provide a graphical representation of the personal residential structure vulnerability functions for the reference and fully mitigated structures.

Reference Structures

Wood Frame	Masonry
One story Crawlspace foundation Top of foundation wall 3 feet above grade	One story Slab foundation Top of slab 1 foot above grade Unreinforced masonry exterior walls
Two story Timber pile foundation Top of pile 8 feet above grade Wood floor system bolted to piles	

Reference and mitigated structures are fully insured personal residential building structures with a zero deductible structure only policy.

See Figure 137 through Figure 145 Because there are too many vulnerability curves to plot in one figure, for the sake of clarity, the mitigations were divided in four sets for the one-story masonry and the two-story frame structures, and the last figure corresponds to the one-story frame structure.

In each figure, there are two horizontal axes: the upper axis represents the inundation depth in meters and the lower axis represents the inundation depth in feet.

- E. Place the reference structures at the following location, with latitude and longitude referenced to the World Geodetic System of 1984 (WGS84) datum.

Gulf of Mexico

Latitude: 27.9957517

Longitude: -82.8277373

- F. Provide the ground elevation used from the flood model elevation database for the reference point.

Gulf of Mexico

Latitude: 27.9957517

Longitude: -82.8277373

Ground elevation: 1.91 m

INDIVIDUAL FLOOD MITIGATION MEASURES		MEAN COASTAL FLOOD DAMAGE RATIO										COASTAL FLOOD DAMAGE PER \$1,000									
		TWO-STORY WOOD FRAME STRUCTURE					MASONRY STRUCTURE					TWO-STORY WOOD FRAME STRUCTURE					MASONRY STRUCTURE				
		FLOOD DEPTH (FT) ABOVE GROUND																			
		7	9	11	13	15	1	3	5	7	9	7	9	11	13	15	1	3	5	7	9
	REFERENCE STRUCTURE	—	—	—	—	—	—	—	—	—	—	—	—	—	—	—	—	—	—	—	
ELEVATE STRUCTURE	Elevate Floor 1 Foot	66%	91%	100%	100%	100%	—	—	—	—	—	\$66	\$91	\$1.00	\$1.00	\$1.00	—	—	—	—	
	Elevate Floor 2 Feet	57%	86%	100%	100%	100%	—	—	—	—	—	\$56	\$85	\$1.00	\$1.00	\$1.00	—	—	—	—	
	Elevate Floor 3 Feet	42%	80%	98%	100%	100%	—	—	—	—	—	\$41	\$80	\$980.77	\$1.00	\$1.00	—	—	—	—	
UTILITY EQUIPMENT	Elevate or Protect 1 Foot	68%	95%	100%	100%	100%	9%	57%	81%	94%	100%	\$67	\$94	\$1.00	\$1.00	\$1.00	\$85.05	\$56	\$81	\$94	\$1.00
	Elevate or Protect 2 Feet	67%	92%	100%	100%	100%	9%	57%	81%	94%	100%	\$66	\$91	\$1.00	\$1.00	\$1.00	\$85.05	\$56	\$81	\$94	\$1.00
	Elevate or Protect 3 Feet	67%	90%	100%	100%	100%	9%	50%	81%	94%	100%	\$66	\$90	\$1.00	\$1.00	\$1.00	\$85.05	\$50	\$81	\$94	\$1.00
FLOODPROOFING	Wet 1 Foot	58%	94%	100%	100%	100%	7%	56%	81%	94%	100%	\$57	\$93	\$1.00	\$1.00	\$1.00	\$65.13	\$56	\$80	\$93	\$1.00
	Wet 2 Feet	53%	87%	100%	100%	100%	7%	56%	81%	94%	100%	\$52	\$87	\$1.00	\$1.00	\$1.00	\$65.13	\$56	\$80	\$93	\$1.00
	Wet 3 Feet	50%	82%	100%	100%	100%	7%	43%	81%	94%	100%	\$50	\$82	\$1.00	\$1.00	\$1.00	\$65.13	\$42	\$80	\$93	\$1.00
	Dry 1 Foot	—	—	—	—	—	5%	56%	81%	94%	100%	—	—	—	—	—	\$47.53	\$56	\$81	\$93	\$1.00
	Dry 2 Feet	—	—	—	—	—	5%	56%	81%	94%	100%	—	—	—	—	—	\$47.53	\$56	\$81	\$93	\$1.00
	Dry 3 Feet	—	—	—	—	—	5%	41%	81%	94%	100%	—	—	—	—	—	\$47.53	\$40	\$81	\$93	\$1.00
FLOOD OPENINGS		ONE-STORY WOOD FRAME STRUCTURE										ONE-STORY WOOD FRAME STRUCTURE									
		FLOOD DEPTH (FT) ABOVE GROUND																			
		1	3	5	7	9						1	3	5	7	9					
	Flood Openings in Foundation Walls	0%	29%	75%	95%	100%	—	—	—	—	—	\$-	\$294.02	\$750.21	\$948.36	\$1,000.00	—	—	—	—	—
FLOOD MITIGATION MEASURES IN COMBINATION		MEAN COASTAL FLOOD DAMAGE RATIO										COASTAL FLOOD DAMAGE PER \$1,000									
		TWO-STORY WOOD FRAME STRUCTURE					MASONRY STRUCTURE					TWO-STORY WOOD FRAME STRUCTURE					MASONRY STRUCTURE				
		FLOOD DEPTH (FT) ABOVE GROUND																			
		7	9	11	13	15	1	3	5	7	9	7	9	11	13	15	1	3	5	7	9
Elevate Utility Equipment 2 Feet Above Floor and Wet Floodproof Structure to 2 Feet		51%	87%	100%	100%	100%	5%	56%	81%	94%	100%	\$510.78	\$866.31	\$1,000.00	\$1,000.00	\$1,000.00	\$45.85	\$562.54	\$809.11	\$937.03	\$1,000.00

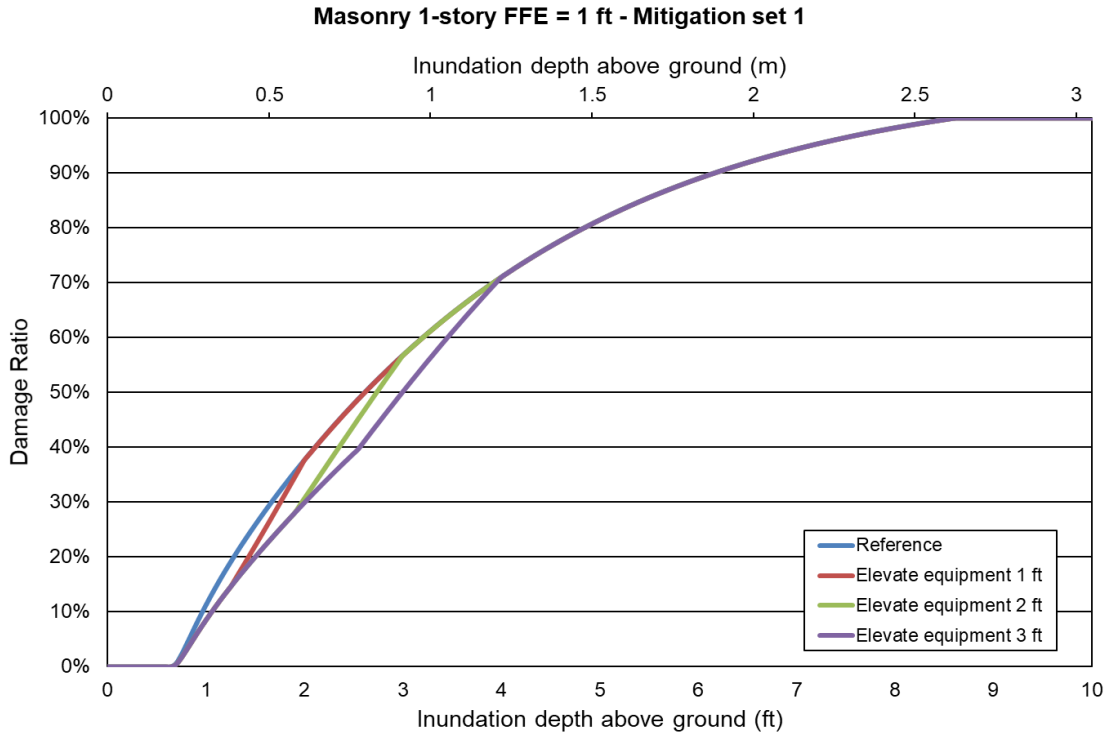


Figure 137. Mitigation measure: elevate equipment. One-story masonry home.

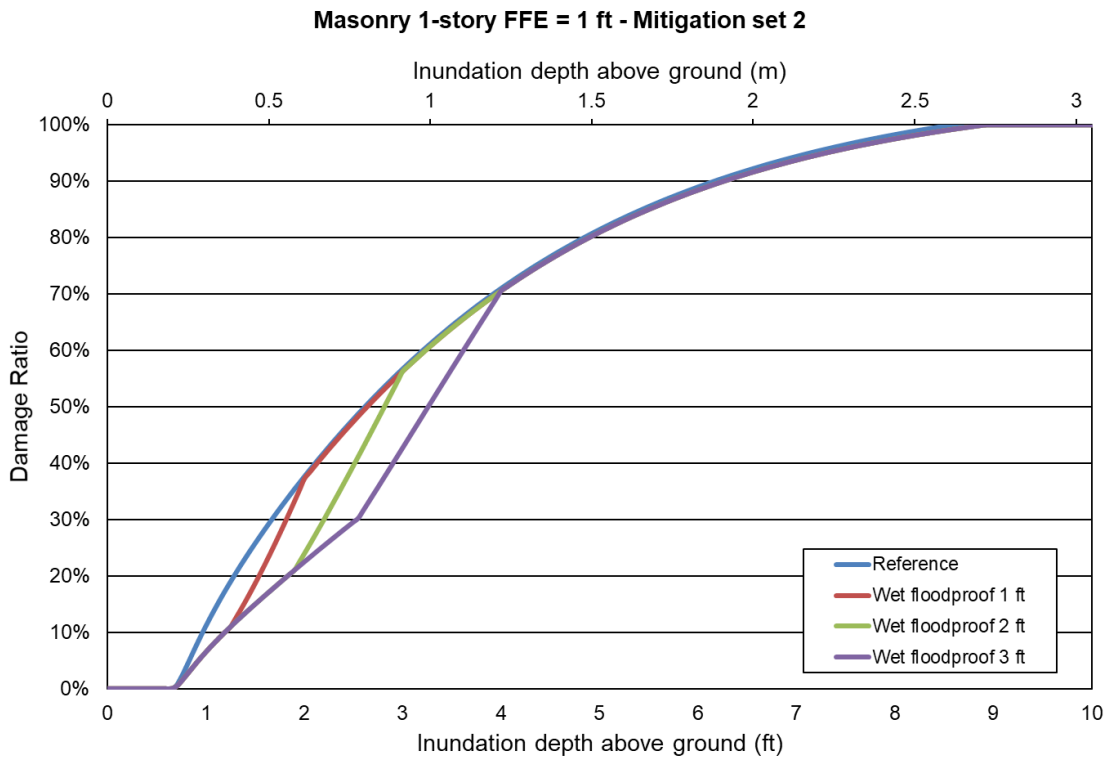


Figure 138. Mitigation measure: wet floodproof. One-story masonry home.

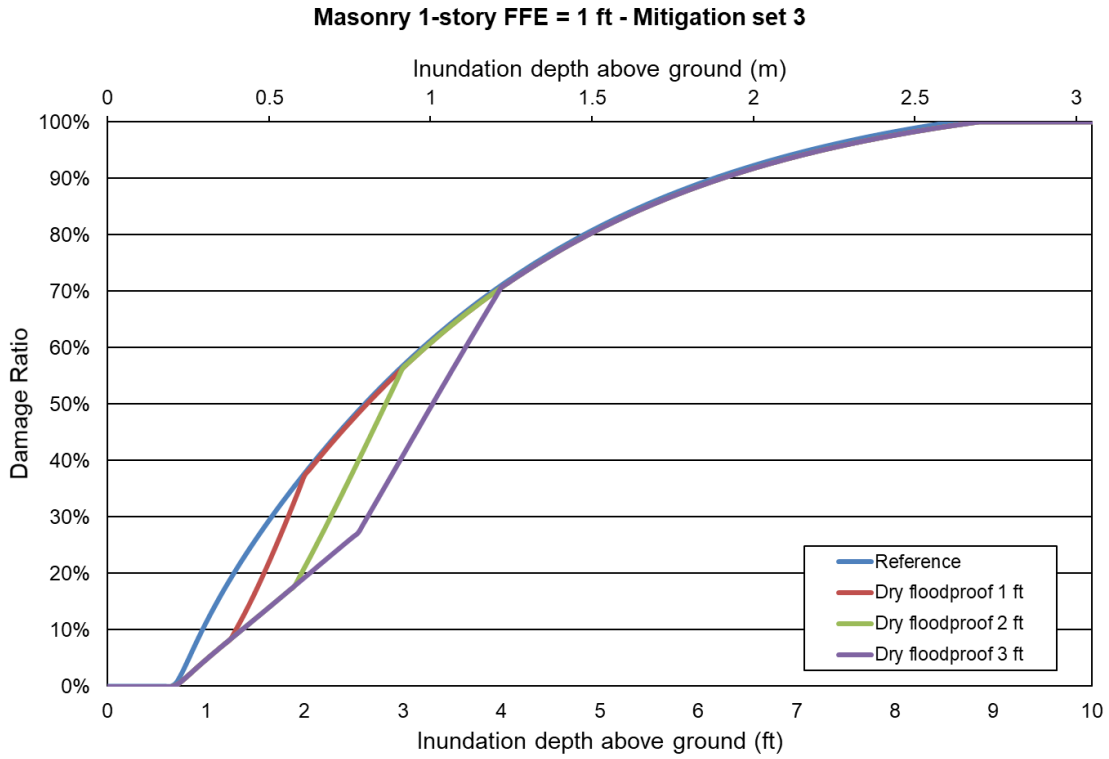


Figure 139. Mitigation measure: dry floodproof. One-story masonry home.

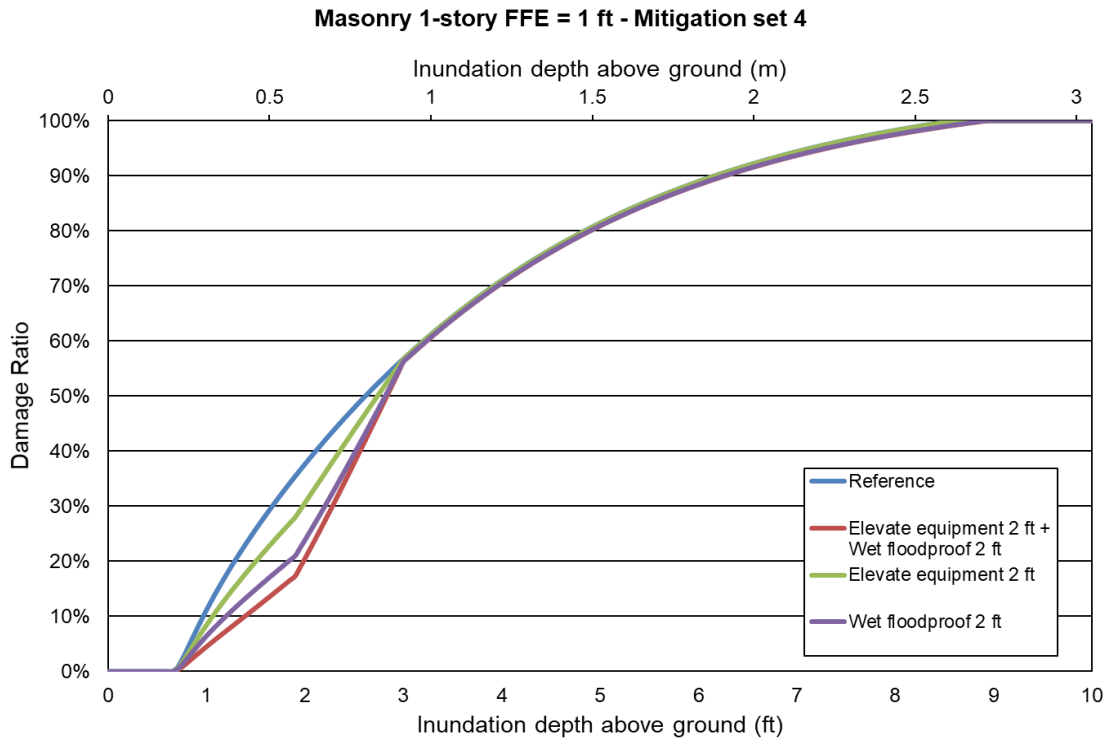


Figure 140. Mitigation measure: combined vs individual. One-story masonry home.

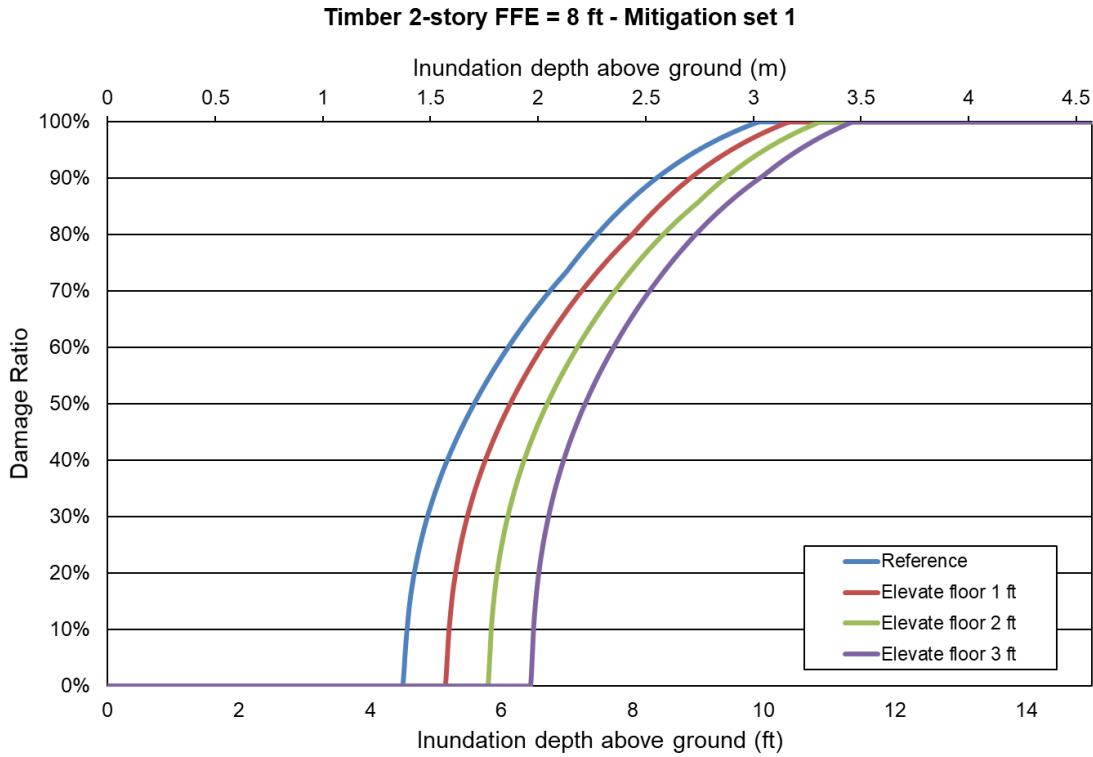


Figure 141. Mitigation measure: elevate floor. Two-story frame home.

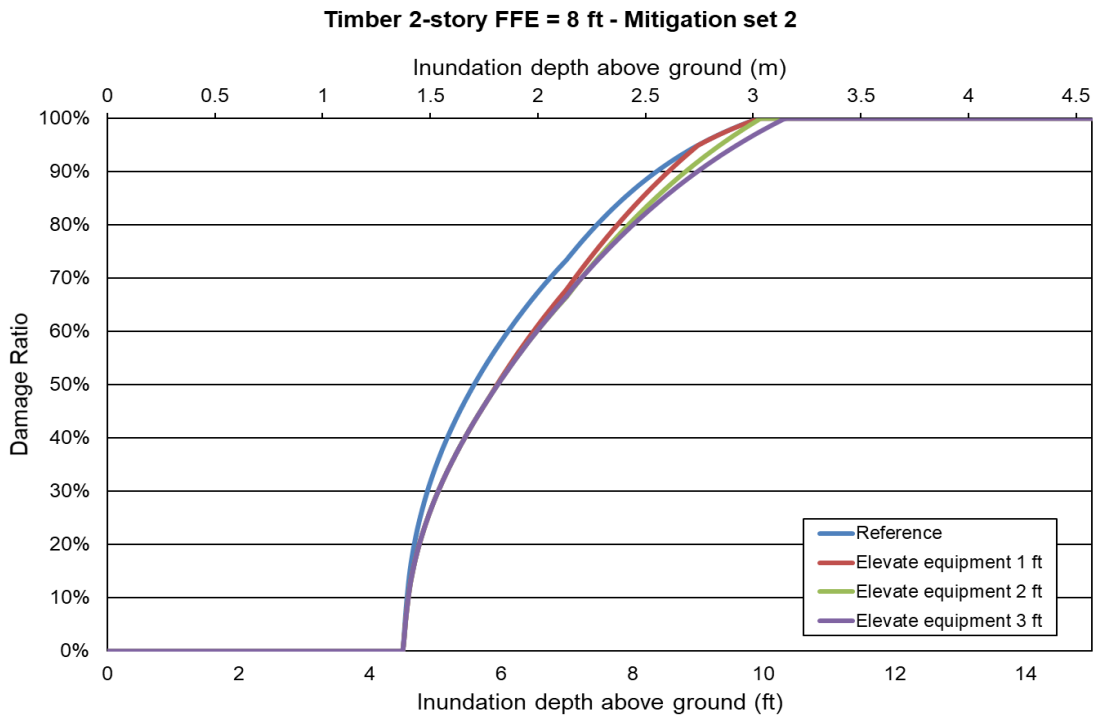


Figure 142. Mitigation measure: elevate equipment. Two-story frame home.

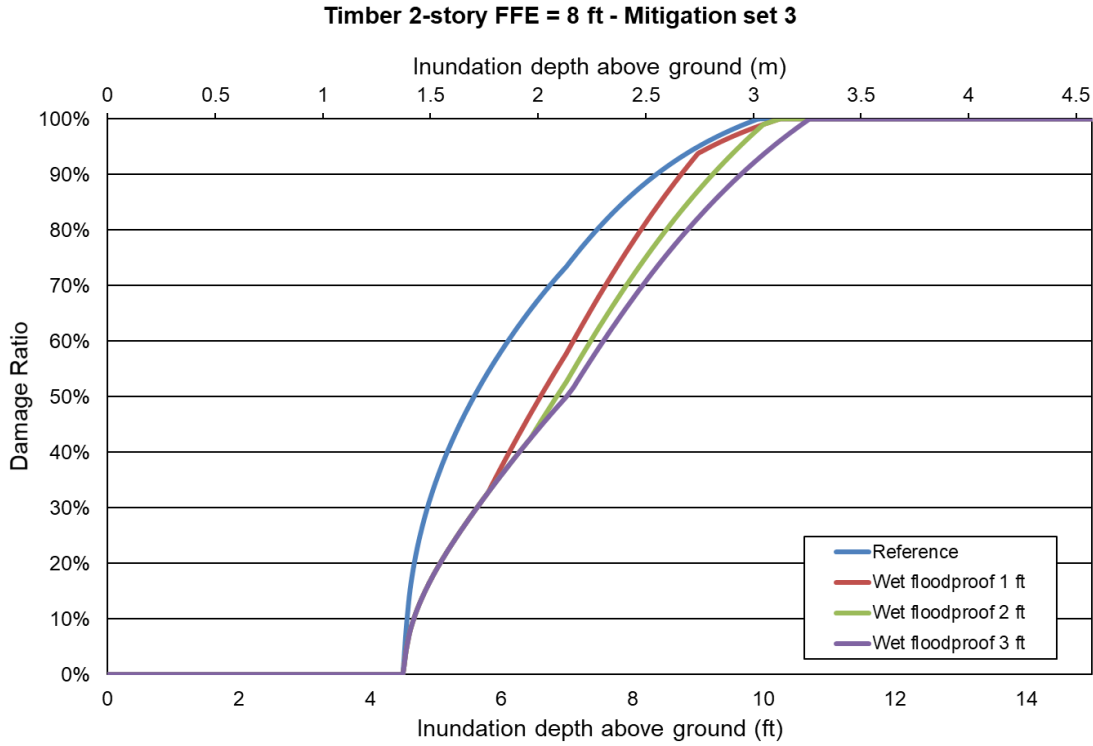


Figure 143. Mitigation measure: wet floodproof. Two-story frame home.

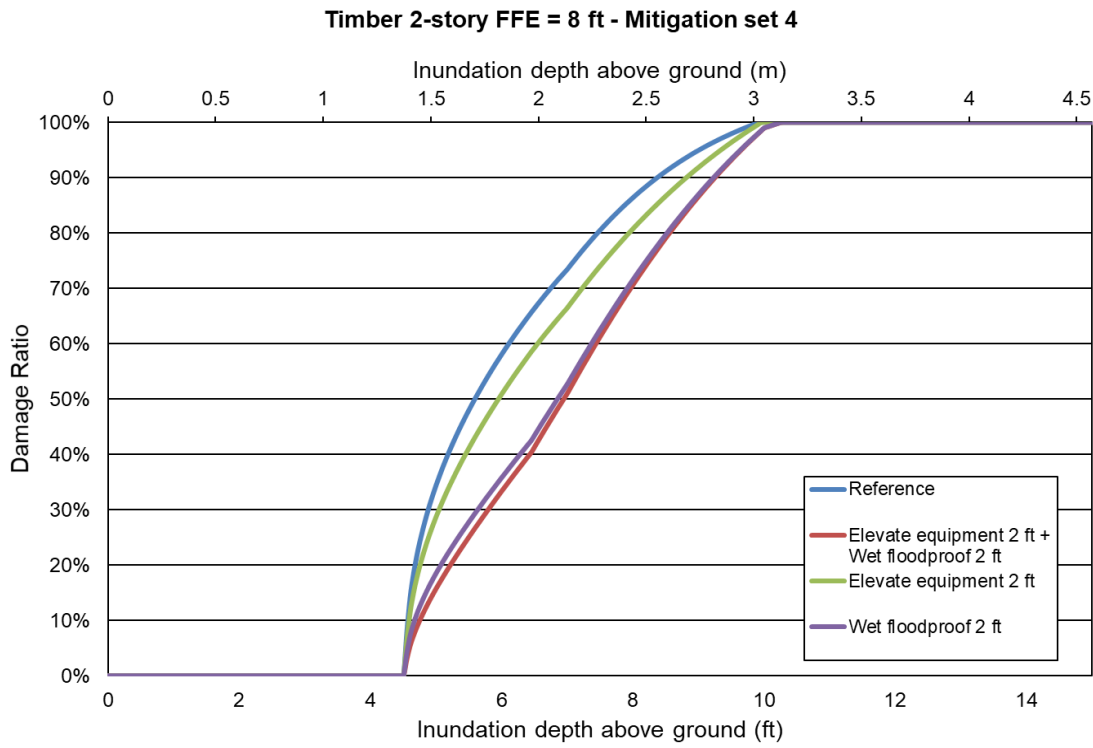


Figure 144. Mitigation measure: combined vs individual. Two-story frame home.

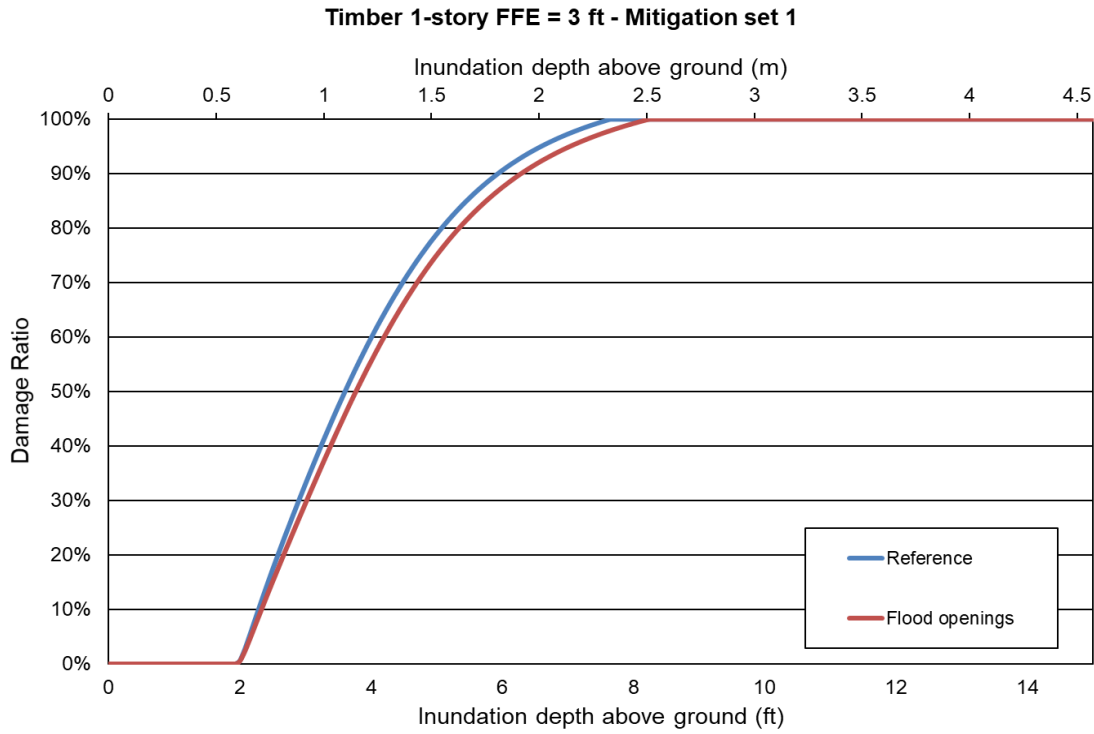


Figure 145. Mitigation measure: flood openings. One-story frame home.

Form VF-5: Inland Flood Mitigation Measures, Mean Inland Flood Damage Ratios and Inland Flood Damage/\$1,000 (Trade Secret Item)

A. Provide the mean inland flood damage ratio (prior to any insurance considerations) to the reference structure for each individual flood mitigation measure listed in Form VF-5, Inland Flood Mitigation Measures, Mean Inland Flood Damage Ratios and Inland Flood Damage/\$1,000 (Trade Secret Item), as well as the percent inland flood damage for the combination of the flood mitigation measures.

See Form VF-5 below.

B. Provide the inland flood damage/\$1,000, rounded to three decimal places, for the reference structures and for each individual flood mitigation measure listed in Form VF-5, Inland Flood Mitigation Measures, Mean Inland Flood Damage Ratios and Inland Flood Damage/\$1,000 (Trade Secret Item), as well as the inland flood damage/\$1,000 for the combination of the flood mitigation measures.

See Form VF-5 below.

C. If additional assumptions are necessary to complete this form, provide the rationale for the assumptions as well as a detailed description of how they are included.

Not applicable.

D. Provide a graphical representation of the personal residential structure vulnerability functions for the reference and fully mitigated structures.

Reference Structures

Wood Frame	Masonry
One story Crawlspace foundation Top of foundation wall 3 feet above grade	One story Slab foundation Top of slab 1 foot above grade Unreinforced masonry exterior walls
Two story Timber pile foundation Top of pile 8 feet above grade Wood floor system bolted to piles	

Reference and mitigated structures are fully insured personal residential building structures with a zero deductible structure only policy.

See Figure 146 through Figure 154 Because there are too many vulnerability curves to plot in one figure, for the sake of clarity, the mitigations were divided in four sets for the one-story masonry and the two-story frame structures, and the last figure corresponds to the one-story frame structure. In each figure, there are two horizontal axes: the upper axis represents the inundation depth in meters and the lower axis represents the inundation depth in feet.

- E. Place the reference structures at the following location, with latitude and longitude referenced to the World Geodetic System of 1984 (WGS84) datum.

St. Johns River

Latitude: 29.3768881

Longitude: -81.6190223

- F. Provide the ground elevation used from the flood model elevation database for the reference point.

St. Johns River

Latitude: 29.3768881

Longitude: -81.6190223

Ground elevation: 1.65 m

INDIVIDUAL FLOOD MITIGATION MEASURES		MEAN INLAND FLOOD DAMAGE RATIO										INLAND FLOOD DAMAGE PER \$1,000									
		TWO-STORY WOOD FRAME STRUCTURE					MASONRY STRUCTURE					TWO-STORY WOOD FRAME STRUCTURE					MASONRY STRUCTURE				
		FLOOD DEPTH (FT) ABOVE GROUND																			
		7	9	11	13	15	1	3	5	7	9	7	9	11	13	15	1	3	5	7	9
	REFERENCE STRUCTURE	—	—	—	—	—	—	—	—	—	—	—	—	—	—	—	—	—	—	—	
ELEVATE STRUCTURE	Elevate Floor 1 Foot	0%	0%	22%	35%	46%	—	—	—	—	—	\$-	\$-	\$21 6.63	\$35 0.12	\$46 4.71	—	—	—	—	
	Elevate Floor 2 Feet	0%	0%	13%	29%	41%	—	—	—	—	—	\$-	\$-	\$13 4.22	\$28 6.75	\$40 9.03	—	—	—	—	
	Elevate Floor 3 Feet	0%	0%	0%	22%	35%	—	—	—	—	—	\$-	\$-	\$-	\$21 6.63	\$35 0.12	—	—	—	—	
UTILITY EQUIPMENT	Elevate or Protect 1 Foot	0%	11%	29%	41%	52%	0%	16%	29%	41%	51%	\$-	\$11 2.50	\$28 6.75	\$40 9.03	\$51 7.88	\$-	\$16 4.48	\$29 1.87	\$40 6.31	\$51 3.13
	Elevate or Protect 2 Feet	0%	11%	29%	41%	52%	0%	13%	29%	41%	51%	\$-	\$11 2.50	\$28 6.75	\$40 9.03	\$51 7.88	\$-	\$13 4.14	\$29 1.87	\$40 6.31	\$51 3.13
	Elevate or Protect 3 Feet	0%	11%	24%	41%	52%	0%	13%	29%	41%	51%	\$-	\$11 2.50	\$24 0.34	\$40 9.03	\$51 7.88	\$-	\$13 4.14	\$29 1.87	\$40 6.31	\$51 3.13
FLOODPROOFING	Wet 1 Foot	0%	7%	29%	41%	52%	0%	16%	29%	41%	51%	\$-	\$74. 26	\$28 6.75	\$40 9.03	\$51 7.88	\$-	\$16 4.48	\$29 1.87	\$40 6.31	\$51 3.13
	Wet 2 Feet	0%	7%	29%	41%	52%	0%	10%	29%	41%	51%	\$-	\$74. 26	\$28 6.75	\$40 9.03	\$51 7.88	\$-	\$10 2.61	\$29 1.87	\$40 6.31	\$51 3.13
	Wet 3 Feet	0%	7%	16%	41%	52%	0%	10%	29%	41%	51%	\$-	\$74. 26	\$15 8.66	\$40 9.03	\$51 7.88	\$-	\$10 2.61	\$29 1.87	\$40 6.31	\$51 3.13
	Dry 1 Foot	—	—	—	—	—	0%	16%	29%	41%	51%	—	—	—	—	—	\$-	\$16 4.48	\$29 1.87	\$40 6.31	\$51 3.13
	Dry 2 Feet	—	—	—	—	—	0%	9%	29%	41%	51%	—	—	—	—	—	\$-	\$93. 48	\$29 1.87	\$40 6.31	\$51 3.13
	Dry 3 Feet	—	—	—	—	—	0%	9%	29%	41%	51%	—	—	—	—	—	\$-	\$93. 48	\$29 1.87	\$40 6.31	\$51 3.13
FLOOD OPENINGS		ONE-STORY WOOD FRAME STRUCTURE										ONE-STORY WOOD FRAME STRUCTURE									
		FLOOD DEPTH (FT) ABOVE GROUND																			
		1	3	5	7	9							1	3	5	7	9				
		Flood Openings in Foundation Walls	0%	0%	26%	41%	54%	—	—	—	—	—	\$-	\$-	\$259.0	\$411.8	\$539.8	—	—	—	—
FLOOD MITIGATION MEASURES IN COMBINATION		MEAN INLAND FLOOD DAMAGE RATIO										INLAND FLOOD DAMAGE PER \$1,000									
		TWO-STORY WOOD FRAME STRUCTURE					MASONRY STRUCTURE					TWO-STORY WOOD FRAME STRUCTURE					MASONRY STRUCTURE				
		FLOOD DEPTH (FT) ABOVE GROUND																			
		7	9	11	13	15	1	3	5	7	9	7	9	11	13	15	1	3	5	7	9
	Elevate Utility Equipment 2 Feet Above Floor and Wet Floodproof Structure to 2 Feet	0%	6%	29%	41%	52%	0%	9%	29%	41%	51%	\$-	\$64.71	\$286.75	\$409.03	\$517.88	\$-	\$92.05	\$291.87	\$406.31	\$513.13

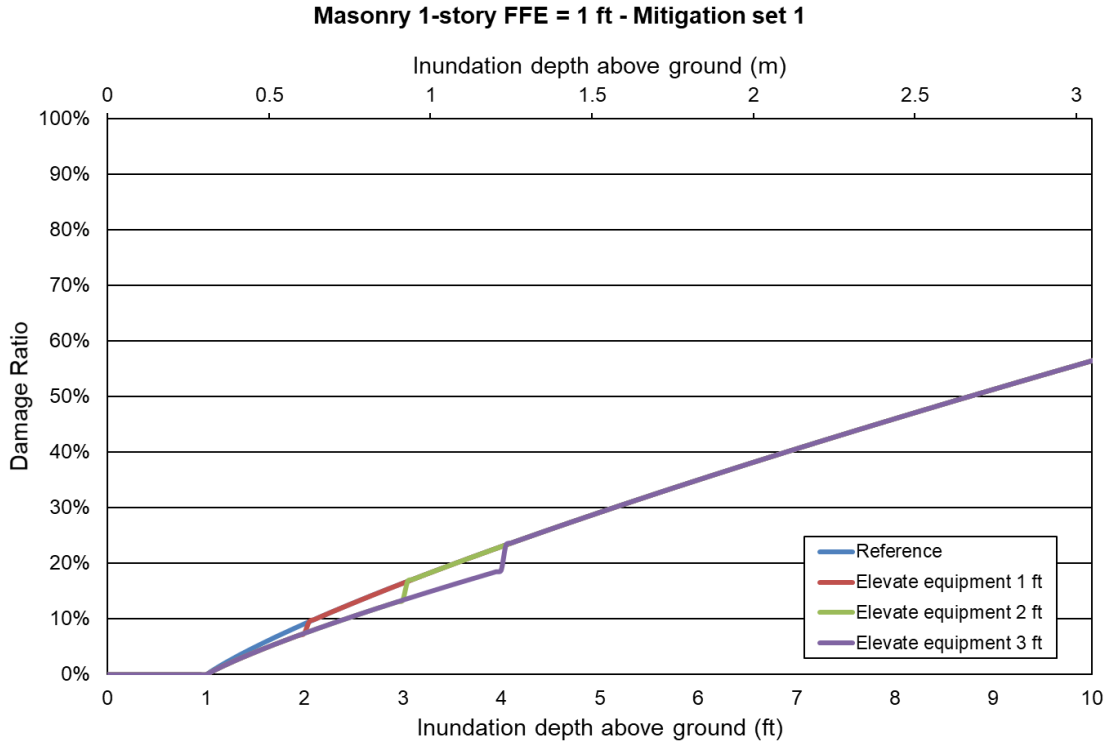


Figure 146. Mitigation measure: elevate equipment. One-story masonry home.

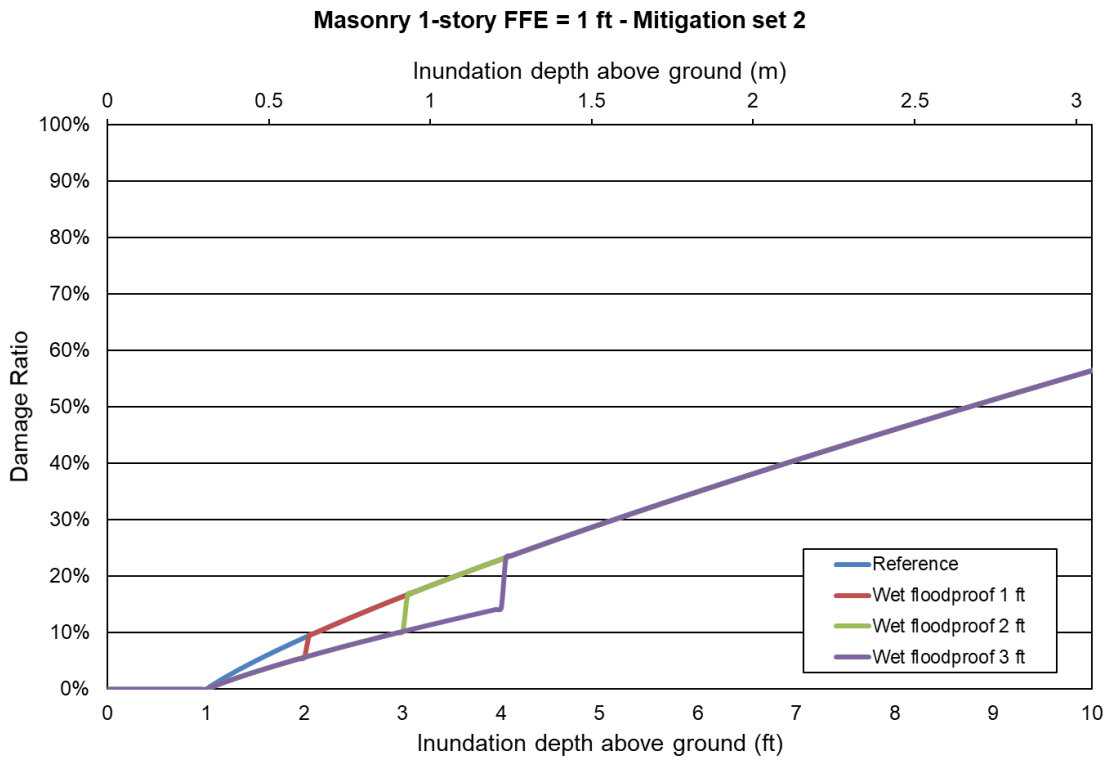


Figure 147. Mitigation measure: wet floodproof. One-story masonry home.

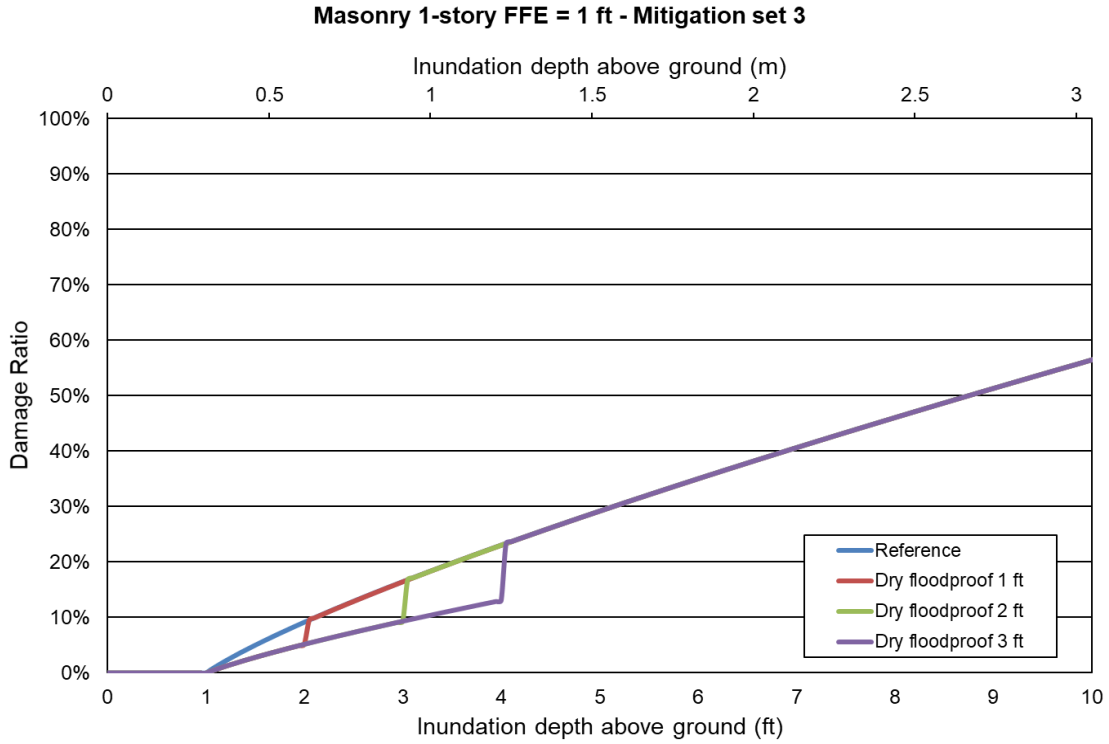


Figure 148. Mitigation measure: dry floodproof. One-story masonry home.

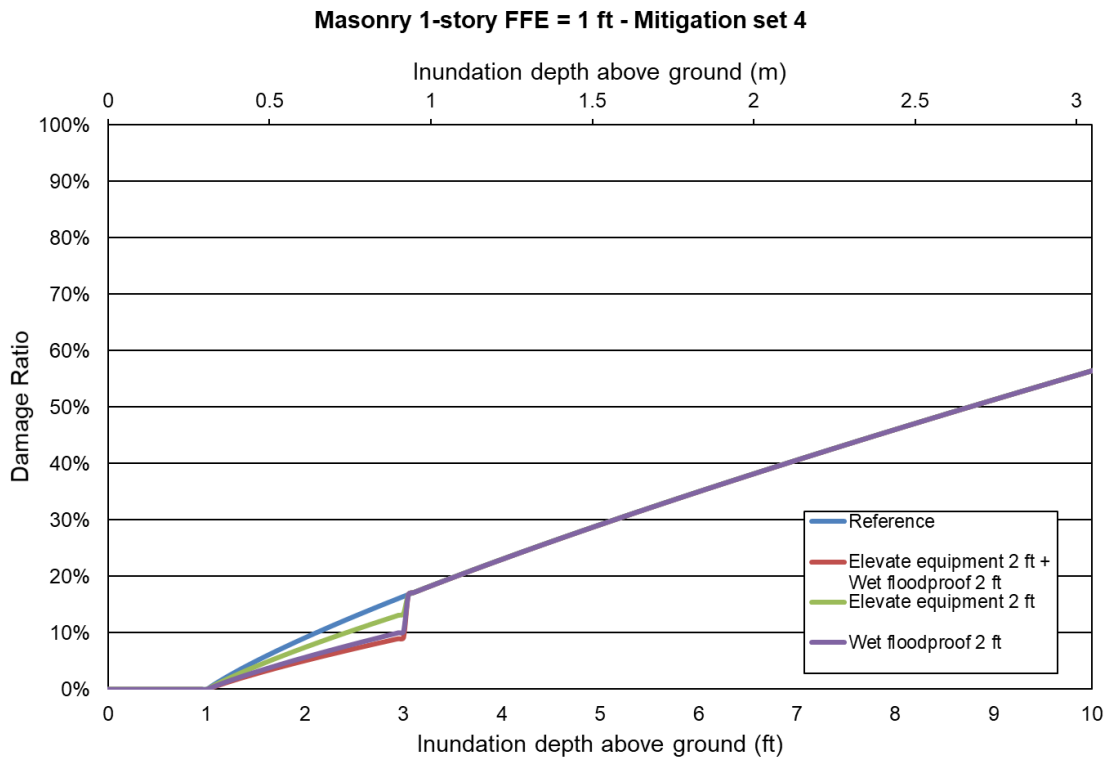


Figure 149. Mitigation measure: combined vs individual. One-story masonry home.

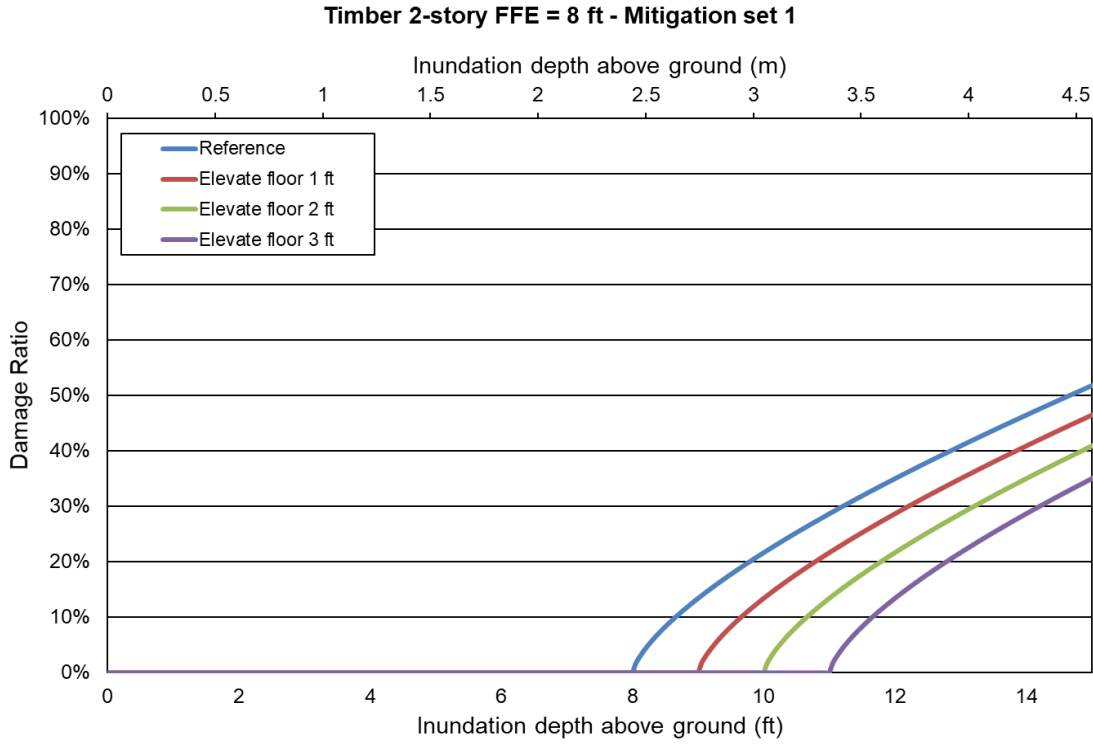


Figure 150. Mitigation measure: elevate floor. Two-story frame home.

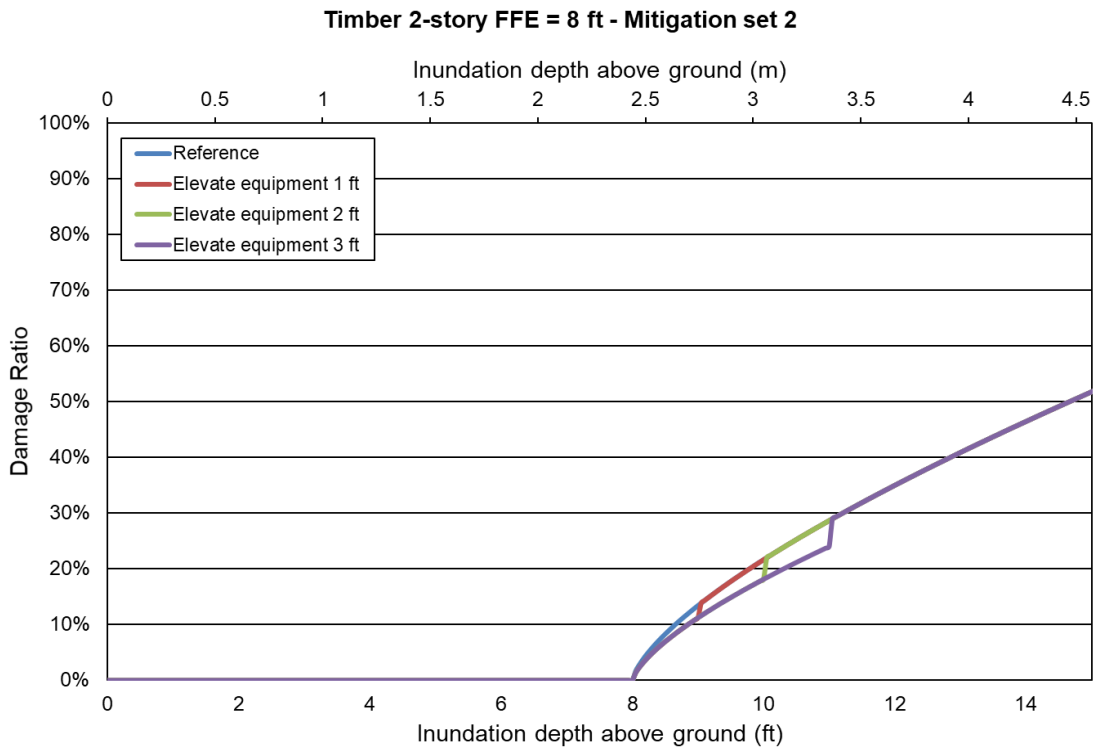


Figure 151. Mitigation measure: elevate equipment. Two-story frame home.

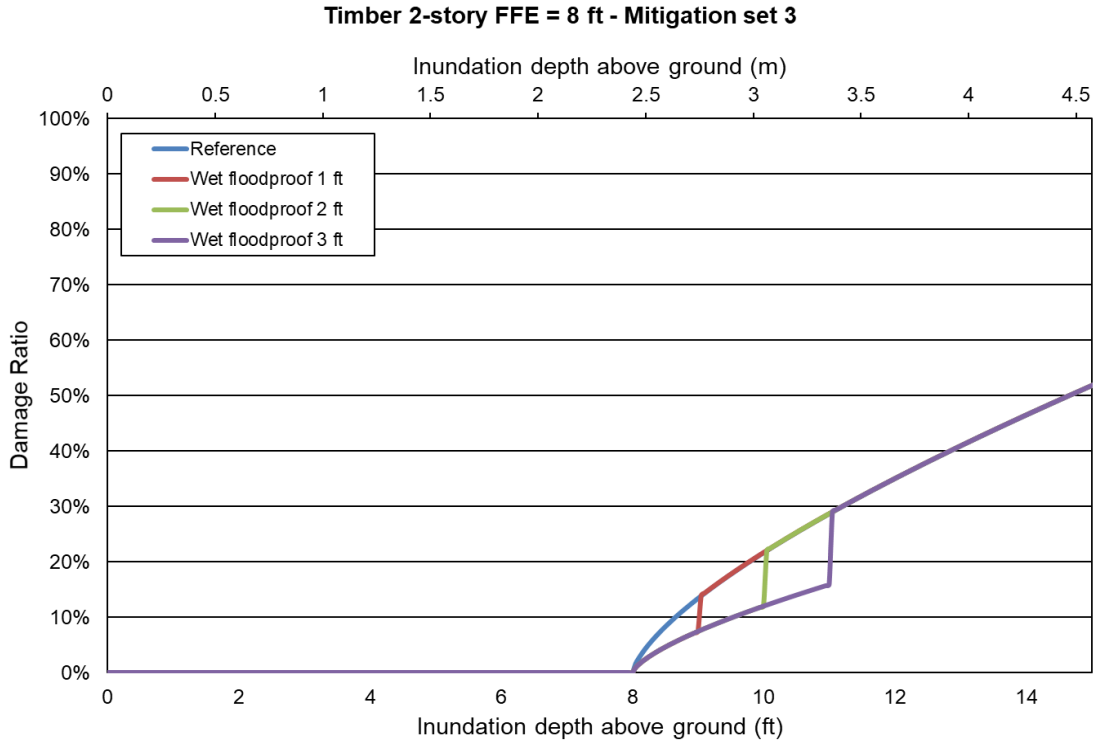


Figure 152. Mitigation measure: wet floodproof. Two-story frame home.

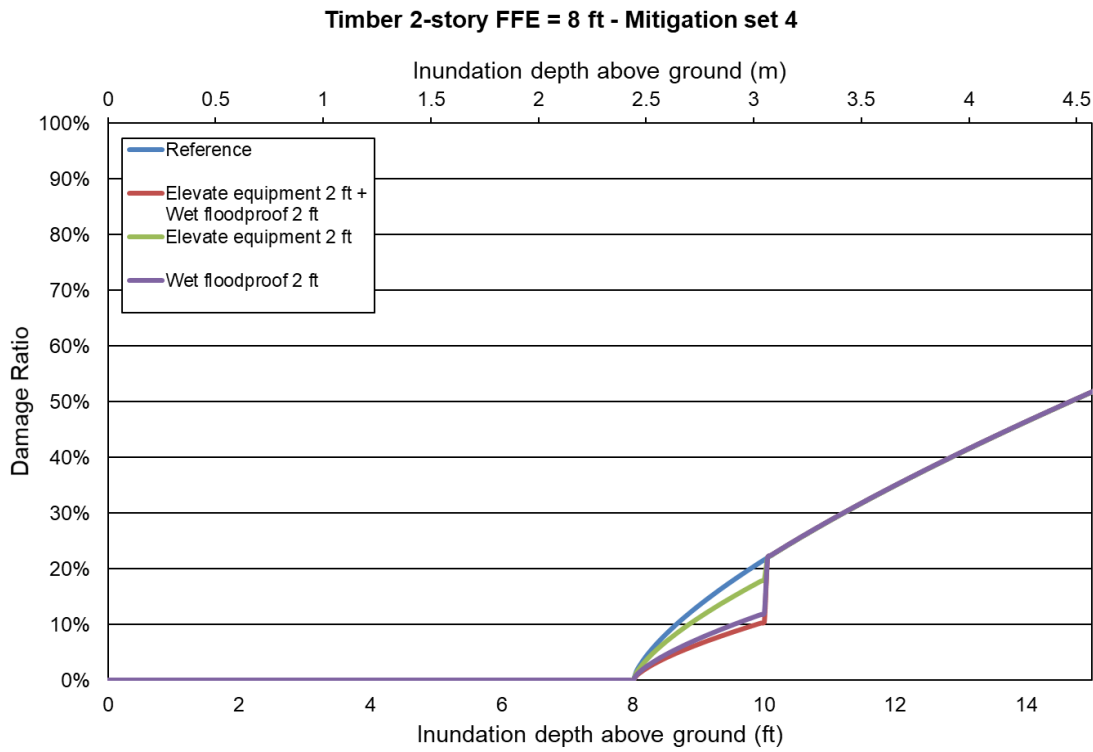


Figure 153. Mitigation measure: combined vs individual. Two-story frame home.

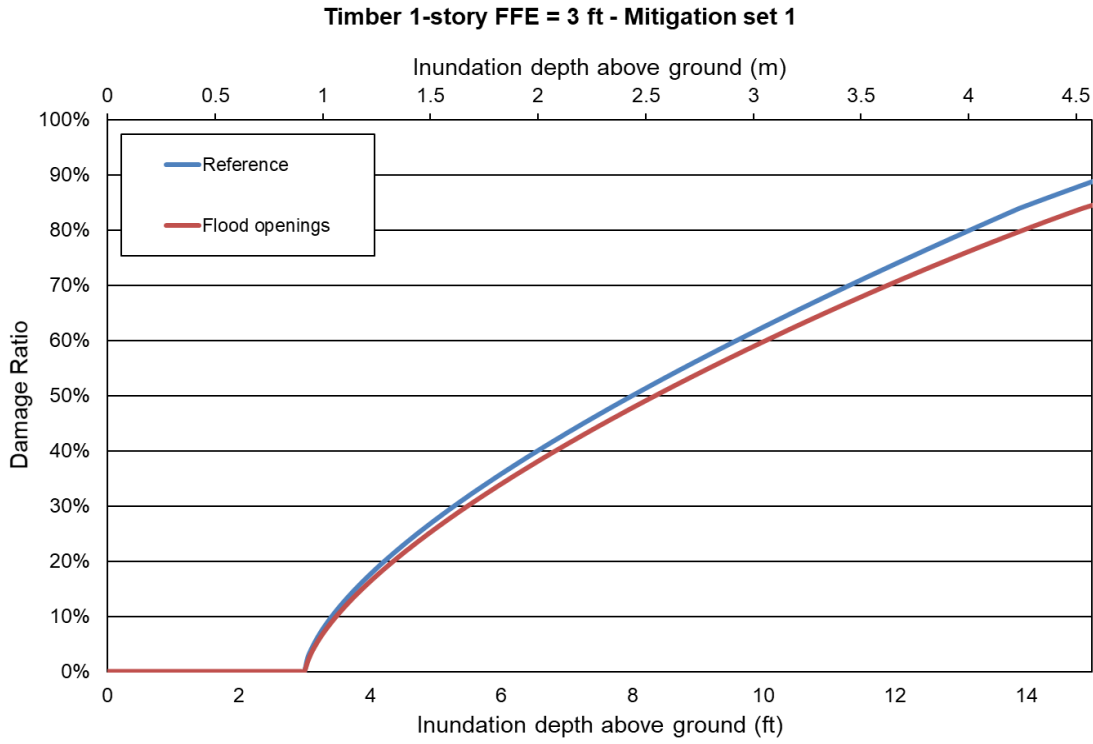


Figure 154. Mitigation measure: flood openings. One-story frame home.

Form AF-1: Zero Deductible Personal Residential Standard Flood Loss Costs

Form AF-2: Total Flood Statewide Loss Costs

Form AF-3: Personal Residential Standard Flood Loss Costs by ZIP Code

Form AF-4: Flood Output Ranges

Form AF-5: Logical Relationship to Flood Risk (Trade Secret Item)

Form AF-6: Flood Probable Maximum Loss for Florida

List of Acronyms

Florida International University
Florida Public Flood Loss Model 1.0
Feb. 29, 2020

Acronym	Full Name
ACV	Actual Cash Value
ACV S/ACV C	Structure Actual-Cash-Value, Contents Actual-Cash-Value
ACV S/RC C	Structure Actual-Cash-Value, Contents Replacement-Cost
AFRES	Air Force Reserves
ALE	Additional Living expenses
AOML	Atlantic Oceanographic and Meteorological Laboratory
AP	Appurtenant
APA	American Psychological Association
ASCE	American Society of Civil Engineers
ASHARE	American Society of Heating, Refrigeration and Air Conditioning
CDFs	Cumulative Distribution Functions
CDO	Cost of Damage to Openings
CLR	Commercial Low-rise Model
CNL	C Numerical Library
COV	Coefficient of Variation
CP	Central Pressure
CPTA	County Property Tax Appraiser
CR	Commercial Residential
CVS	Concurrent Versions System
DA	Damage Array
DR	Damage Ratio
EDR	Expected Damage Ratio
EDV	Expected Damage Value
EIDR	Expected Interior Damage Ratio
EL	Equilibrium Layer
EPR	Expected Percentage Reduction
ERS	European Remote Sensing
ESDU	Engineering Sciences Data Unit

Acronym	Full Name
FBC	Florida Building Commission
FDFS	Florida Department of Financial Services
FEMA	Federal Emergency Management Agency
FFP	Far Field Pressure
FHCF	Florida Hurricane Catastrophe Fund
FPFLM	Florida Public Hurricane Loss Model
GOES	Geostationary Operational Environmental Satellite
GPS	Global Positioning System
HRA	High Risk Accounts
HRD	Hurricane Research Division
HUD	Housing and Urban Development
HURDAT	Hurricane Database
HVHZ	High Velocity Hurricane Zone
IBHS	Insurance Institute for Business and Home Safety
IBL	Internal Boundary Layer
ID	Interior Damage Ratio
IMSL	International Mathematical and Statistical Library
ISO	Insurance Services Office
JDBC	Java Database Connectivity
JNI	Java Native Interface
JSP	Java Server Pages
LB	Low-rise Commercial Residential Building
M00	Base Medium Model
M01	Retrofitted Medium Model (Re-roof and Re-nailed decking)
M10	Modified Medium Model. Weaker Decking Connection
MBL	Mean Boundary Layer
MFR	Multi-Family Residential Building
MH	Manufactured Home
MHB	Mid and High-rise Building
MPH	Miles Per Hour
MRLC	Multi-resolution Land Characteristics Consortium
NAHB	National Association of Home Builders
NCEP	National Centers for Environmental Prediction
NFIP	National Flood Insurance Program
NHC	National Hurricane Center
NLCD	National Land Classification Database
NOAA	National Oceanic and Atmospheric Administration
NWS	National Weather Service
OIR	Florida Office of Insurance Regulation
OSB	Oriented Strand Board
PBL	Planetary Boundary Layer
PDF	Probability Density Function
Pmin	Minimum Central Pressure
PML	Probable Maximum Loss
PR	Personal Residential
PRB	Personal Residential Single-Family Home Buildings
R2W	Roof to Wall Connections
R-CLIPER	Tropical Cyclone Rainfall Climatology and Persistence Model
RC S/ACV C	Structure Replacement-Cost, Contents Actual-Cash-Value
RC S/RC C	Structure Replacement-Cost, Contents Replacement-Cost
RES	Residential Building Model
Rmax	Radius to Maximum Winds

Acronym	Full Name
S00	Base Strong Model Inland
S00-OP	Base Strong Model with Metal Shutters
S02	Strong Inland Model with Metal Roof
S02-OP	Strong Inland Model with Metal Roof and Metal Shutters
S01	Modified Strong Model for HVHZ
SBC	Standard Building Code
SFBC	South Florida Building Code
SFMR	Stepped Frequency Microwave Radiometer
SQL	Structured Query Language
SSM/I	Special Sensor Microwave Imager
SV S/RC C	Structure Stated-Value, Contents Replacement-Cost
SV S/SV C	Structure Stated-Value, Contents Stated-Value
TE	Time Element
TECDO	Total Expected Cost of Damage to Openings
TRMM	Tropical Rainfall Measuring Mission
UML	Unified Modeling Language
USGC	United States Geological Survey
USPS	United States Postal Service
VT	Translational Velocity
W00	Base Weak Model
W01	Retrofitted Weak Model (Re-roof and Re-nailed Decking)
W10	Modified Weak Model. Stronger Decking Connection
WBDR	Wind-borne Debris Region
WDR	Wind Driven Rain
WDR1	Wind Driven Rain variable #1
WDR2	Wind Driven Rain variable #2
WSC	Wind Speed Correction
WMD	Water Management District